Institut für Verbrennungskraftmaschinen und Thermodynamik
Institute of Internal Combustion Engines and Thermodynamics

Technische Universität Graz
Graz University of Technology

8th International Conference

TUNNEL SAFETY AND VENTILATION

- New Developments in Tunnel Safety -

25. - 26. April 2016

Graz University of Technology

Redaktion / Editor:
P. Sturm / S. Minarik

I m p r e s s u m:

Verlag der Technischen Universität Graz
Technikerstraße 4
A-8010 Graz
Tel.: +43 316 873 6157
Fax: +43 316 873 6671
E-Mail: verlag@tugraz.at
UID(VAT) ATU 57477929

Reports of the Institute of Internal Combustion Engines and Thermodynamics,
Graz University of Technology, Vol. 100

Herausgeber/Publisher: Univ.-Prof. Dr. H. Eichlseder

ISBN: 978-3-85125-464-8

ORGANISATION

A.Univ.-Prof. Dr. Peter STURM
Mrs. Sabine MINARIK
Graz University of Technology
Institute of Internal Combustion
Engines and Thermodynamics
A-8010 Graz, Inffeldgasse 21a, Austria

Tel.: +43/316-873 30200
Tel.: +43/316-873 30231
Fax.: +43/316-873 10 30231
E-Mail: minarik@tugraz.at
Homepage: www./ivt.turgraz.at

PREFACE

Ladies and Gentlemen, Dear Participants,

In 2002, the Institute of Internal Combustion Engines and Thermodynamics organized an International Conference on Tunnel Safety and Ventilation. The aim of that conference was to provide a forum for information exchange among operators, users, technicians, scientists and companies involved in the design, construction and equipping of road and rail tunnels. The success of the 2002 conference led to the organization of biennial follow up meetings.

Each conference has been accompanied by an exhibition, and each year, like the conference itself, the exhibition has grown. The success of the exhibitions has forced us to leave the confines of our University campus and to move to the roomier facilities of the trade fair centre.

Our interests and focus have also changed and this is reflected in our topics. The first conferences were strongly influenced by the tunnel incidents of the late 1990's and related safety issues. Nowadays road tunnel operation, the conflict between the needs for upgrading existing road tunnels and requirements given in a legal framework dominate.

Traffic is increasing, at both a national as well as an international level. Thus, while in densely populated areas there is much greater demand for sub-surface transportation, in rural areas there is an increasing need to upgrade the road infrastructure. The implementation of the EU Directive on the minimum safety requirements for tunnels in the trans-European road network (2004/54/EC) forced many of the tunnel operators to upgrade the existing tunnels.
Many of the existing tunnels (i.e. those 20 to 30 years old), are currently being refurbished and upgraded by the addition of a second tunnel tube. The upgrading process as well as the construction of second tubes constitutes a big challenge in practice, as – in contrast to new tunnel construction – several prevailing structures and systems act as constraints and have to be taken into consideration in planning. There is also the additional need to ensure that traffic flow can be maintained throughout the construction period.

The question of tunnel safety is a highly controversial field. It is often claimed that several new techniques are now on the market and that these can help improve safety due to quicker and more reliable detection, more efficient installations and/or additional equipment. However, such 'improvements' often result in significant increases in complexity, as well as in the cost of operation and maintenance of the new safety equipment.

Cost benefit analyses combined with risk assessment studies provide a valuable tool when attempting to deal with questions of safety at an acceptable cost level. The time is now right for us to discuss what safety standards are required in our tunnels and at what price. We hope that the present conference will be of some value in such a discussion.

This conference wouldn't be the "Graz" conference without the related exhibition. Many companies have put a lot of effort into presenting their latest developments and technologies. Conference participants now have the chance to get into contact with leading companies in the electro-mechanical tunnel business, to establish new contacts, and also to strengthen existing ones.

Another exciting and distinguishing aspect of the “Graz” conference is the accompanying technical visit. Contrary to former events where a life live fire test was performed, this time the construction site of the second bore of the Gleinalm tunnel will be the location for a visit. In fact the conference returns to the location in which in 2002 a test with a water shield installation was performed in order to demonstrate tunnel safety installations. While at that time the tunnel consisted in a single bore with bi-directional traffic, this time we have to see the final construction activities of the second bore, which shall be put in operation in 2017. Many thanks to the tunnel operator ASFiNAG. Special thanks to Mr. Gerhard Ruhdorfer and Mr. Herwig Moser for organizing this visit.

We wish to extend a special thank you to our scientific committee for its valuable work in defining the objectives of this conference, and in selecting the presentations.

We also extend our professional thanks to the authors for their hard work in preparing abstracts, papers, posters, and of course their presentations.

And finally, we wish to offer our sincere thanks to all the people in the background who have been working to ensure that this will be a smooth, enjoyable and effective conference for us all.

It is my pleasure to welcome you all on behalf of the conference scientific committee and to wish you all a successful meeting and a sound basis for fertile networking in the future.

Peter J. Sturm

Graz, April 2016

ON THE ROAD TO SAFER TUNNELS

[1]F. Zumsteg, [1]U. Steinemann, [2]M. Eisenlohr
[1]US+FZ Consulting Engineers, Lenzburg/Wollerau CH
[2]Swiss Federal Roads Office (FEDRO), Bern CH

ABSTRACT

The fatal fire events around the turn of the millennium led to the amplified efforts to make tunnels safer. Due to the strong traffic increase and as a result of increased social claims and expectations, the pressure has increased prominently for higher tunnel safety with corresponing bigger investment and maintenance efforts. The legal pressure for the identification of persons responsible for incidents also contributes to it. This is reflected on the extent of the requirements in standards and guidelines and has an effect on the inventiveness of manufacturers and engineers as well as on the complexity of the systems in tunnels.

Keywords: tunnel safety, ventilation, complex systems

1. INTRODUCTION

With regard to ongoing developments we recapitulate successful innovations of the tunnel equipment with their benefit and cost in this paper as well as illutions and dilusions. It turns out that man as the element of uncertainty often limits the use of the systems.

In theory many of the developments are plausible. In reality, however, difficulties lead to necessary modifications and compromises.

2. MEANING OF TECHNICAL ACHIEVEMENTS

A topic at this year's SWISSBAU was: Is modern technology our rescue or do we have to rescue ourselves from it? The following examples show that this question also has significance for the tunnel equipment. Besides technology in an incident the often unpredictable human behaviour is decisive for success or failure.

2.1. Fire and smoke detection

Thermal detection is the standard of fire identification in many places. Today thermal linear sensors are used in all Swiss tunnels with a length over 600 m. With sufficient temperature or sufficient temperature rise the sensors react quickly and locat a fire exactly. An experience of the years well before 2000 was that the turbidity measurements often detected a fire in the Gotthard road tunnel earlier than the thermal sensor although turbidity sensors were mounted at intervals of more than 1 km. Only in 2005, thus 25 years after the opening of the Gotthard tunnel, the Swiss Federal Roads Office FEDRO published a draft for the guideline Fire Detection [1] which prescribes the smoke detection. Today smoke detectors are used in Switzerland in most tunnels at intervals of 100 m, in special cases even at intervals of 50 m.

As engineers we have to ask the question how it was possible that this change was carried out so late. The fact that smoke represents the primary peril for the tunnel users seems obvious today.

The specifications in [1], which were accompanied by the further development of smoke detectors led to the euphoric feeling to have solved the problem of the smoke and therefore fire detection. There was even the hope to be able to go without supplementary systems. Fortunately such simplifications were not introduced immediately because the real time evaluation of the smoke signals proved to be more complicated than expected. Ventilation systems with point extraction by controllable dampers need a precise indication of the fire location. Otherwise the operation of the exhaust air can endanger the tunnel users additionally by transferring the smoke at remarkable speed through the driving space. Moving and pulsating smoke sources confront the developers of the software with fiddly questions. Moreover, it cannot be excluded that a smoke detector is faulty. Again and again, at the check of the functionality of the systems in the tunnel one discovers new scenarios and sequences which show that a reliable fire locating detection takes its time even with smoke detectors. At a smoke test recently carried out with an initially moving smoke source we had to notice that the automatic ventilation mode yielded a place discrepancy between fire place and location of detection of 300 m. It can be stated that smoke detection leads to a quick alerting and in the large majority of all cases to an exact determination of the fire location. The thermal linear sensor installed furthermore ensures a system redundancy, offers the possibility of a manual justification of the ventilation operation and can serve the advancing fire brigade as a useful basis for their attack.

2.2. Congestion detection for a correct ventilation reaction in the case of a fire

Smoke extraction right downstream the incident or longitudinal ventilation blowing the smoke in driving direction through the tunnel are means to keep smoke away from people in a tunnel with one-directional and initially free flowing traffic. Since the ventilation operation shall happen automatically and in general without a manual intervention, the set value of the flow corresponds to the approaching air flow of at least the critical velocity according to the design fire.

With a fire within congested traffic the above mentioned ventilation operation is unreasonable. The attempt to grasp congestion reliably to determine the appropriate ventilation operation proves to be very difficult. On the one hand, the question arises how congestion has to be defined for this need for multi-lane tunnels and, subsequently, whether the recordings at certain cross-sections suffice, e.g. in front of the exit portal, or whether a recording is indispensable over the total tunnel length. The complexity of the system and particularly the interpretation of the recorded signals are very high for the latter.

A pragmatic approach consists in putting the focus onto the phase of self-rescue. An approaching flow speed lowered to 1.5 m/s allows people in the congestion downstream to escape. A transverse system operates at full extraction capacity and a symmetrical flow toward the fire is installed in the case of traffic congestion (cf. section 2.4).

2.3. General behaviour rules and alerting of the tunnel users

The quick alerting of the persons in the tunnel is a prerequisite for their adequate behaviour. While the alerting concerns persons mainly who do not have any view on the event, behaviour instructions are for everyone of importance. The experience shows that the behaviour of the persons can be chaotic despite of quick alerting and correct information. The aim is therefore "giving the people a fair chance for the escape". The safety means such as detection, alerting, ventilation and positioning of emergency exits have to interact properly.

With regard to adequate alerting the opinions differ considerably although their investment is low in comparison with systems like ventilations or fire extinguishing systems. The temporal optimization of the processes of ventilation scenarios deals with time spans of 10 seconds. If one can encourage persons to escape on foot, we can win several minutes. The results of the thorough research and the positive experiences with loudspeakers, e.g. in Holland and in

Germany, should be perceived also in other countries and the use of loudspeakers should be considered.

The general information of the road users about the behaviour is of great importance for a fire incident in a tunnel. The fatal fire events around the turn of the millennium have led to considerable reinforcements of these activities and the appreciation of the road users of these requests has increased at the same time.

2.4. Arrangement of emergency exits

Thirty years ago the necessity of emergency exits for tunnels with transverse ventilation was questioned. With the understanding that transverse ventilation alone cannot ensure the safety of the tunnel users in a fire incident, the knowledge of the importance of short distances of the emergency exits grew. In the year 1980 the Gotthard road tunnel was opened to the traffic and it is equipped with emergency exits at intervals of 250 m. With this it fulfills the Swiss norm [2] presently in effect. Due to the civil engineering costs, exponents warned until the year 2004 of the "inflation of emergency exits".

Short and steep bi directional tunnels for wich ventilation in the case of a fire is not suitable, [3] [4], are today planned with emergency exit intervals of down to 60 m. Short distances of the emergency exits are a substantial motivation due to their visibleness and obvious accessibility to begin the escape besides the theoretically calculable shorter escape time. With difficult tunnel geometries and for cut and cover tunnels short emergency exit distances often offer an effective and - regarding investment and maintenance - favourable measure for the achievement of the requested safety standard.

2.5. Doors and ventilation of emergency exits

A general principle is to open emergency exit doors in escape direction and sometimes by means of a crash bar. This principle was and partly still is applied so stringently that certain doors were no more openable with physical strength against the excess pressure in the incident ventilation operation.

The pursued methods of resolution are:

- opening aid for wing doors with external power
- opening aid for wing or sliding doors with mechanical strength transmission (e.g. tunnel Flüelen, CH)
- double doors with different opening directions (RABT [5])
- sliding doors (FEDRO [6]).

Figure 1: Sliding door seen from pressurized safety tunnel to the deriving space

The approach to use sliding doors as it is pursued as consistently as possible in Switzerland gives cause to serious discussions. Altogether, the advantages predominate, however, clearly: The escape routes including the safety galleries can robustly be ventilated and well designed sliding doors with the dimension B x H = 1.25 m x 2.1 m can be opened with 60 N at a pressure load over the door well up to 300 Pa (Figure 1). The various experiences during the last 10 years with constructional lacks have led to mature door constructions by now.

It is plausible that railway tunnels are equipped with motor-driven openings of the escape doors due to a high number of persons approaching the door and the consequently large area of the doors.

2.6. Automatically controlled dampers for smoke extraction

In the year 1987 the Rosenbergtunnel was opened in the city of St Gallen. It was the first Swiss tunnel with automatically controlled ventilation dampers in the intermediate ceiling. However, until the year 2000 most transvers ventilated tunnels in Switzerland had no controllable dampers but distributed exhaust openings. Reasons against controllable dampers were doubts about sensors needed for the determination of the fire location, the complexity of the facilities and the so-called "mechanized intermediate ceiling" with its maintenance effort. Moreover, there was the expectation that smoke is generally warm, rises to the ceiling and can be extracted from there even over longer distances. This assumption arose from fire tests which were not able to cover the reality extensively due to lacking disturbancies of the air flow. In the meantime the experiences show that the stability of stratified smoke hardly ever meets this expectation in a real fire scenario. A chaotic event like a vehicle fire in a tunnel is mastered only with a massive use of ventilation.

An earlier argument cannot be wiped off the table, though: Inadequately maintained extraction dampers can be more dangerous for persons than the earlier distributed exhaust openings in the case of a fire in the tunnel. In theory it may seem as a trifle. In practice, however, the maintenance of the dampers is not always sufficient. Reasons for it can be: lacking appreciation of the danger of a malfunction and missing financial and personnel resources subsequently. No country is known where this is not a issue.

2.7. Frequency controlled fans

Speed controlled fans make the life easy for the ventilation designer. He can fix the desired volume flow exactly even without big risk of calculation errors. Frequency converters are additional electronic and thus failure-prone components which have a considerably shorter life cycle in comparison with fans and cables. Due to the required coordination of frequency converter, cable and motor a partial replacement represents an increased risk with regard to the fault-free operation of the safety facilities ventilation.

With few exceptions only one reason stands for speed control for exhaust air fans which are operated only in the fire case: the limitation of the starting current. This is required for weak power supplies.

Usually large axial fans are tested sequencially to safe peak energy costs. It has to be noted that axial speed controlled fans working in parallel have to be tested contiguously to guaranty a proper start-up.

A more important use can arise from speed control for jet fans. But even here theory promises more than what practice with all unpredictabilities can offer.

The demand of FEDRO in [7], to use frequency converters only if power supply or aerodynamic reasons require it makes sense.

2.8. Manual interventions in the ventilation control

Manual interventions in the ventilation operation during a fire require a detailed knowledge of the complete system as well as the current situation in the tunnel. While due to their computational simulations the designer of the ventilation systems and the developer of the ventilation programmes regard a manual intervention as feasible, this is understandably enough a hot potato for most operators who are multiple charged particularly in a first phase of the incident. In certain areas of Switzerland operators explicitly wish that the possibility for manual interventions is omitted. In general, automatic operation cannot be activated any more after a switchover to hand operation without endangering the persons in the tunnel. An operator should manually intervene only according to 4 eye principle and preferably according to on-site demand.

A meaningful approach is to offer ergonomically clear manual transitions to pre-programmed scenarios, e.g. to shift the extraction point or to change to the appropriate traffic mode.

2.9. Complexity of systems, open and closed-loop control

Computer simulations of ventilation controls can mislead to implementing complicated and strongly differentiated procedures. It does not increase the safety of the tunnel users if under special conditions a dedicated ventilation scenario is assigned to a 60 m long portal near section. In the example mentioned here with only one single smoke detector in the concerning section the scenario would not have been testable. A basic principle must be:

What is not properly testable must be avoided.

The inclusion of experienced operators in the conception of controls has proved of value. This might lead to more intensive discussions, in general, however, to more robust systems which operators understand even without very effortful training and without support of the developers. This is of special importance under the aspect of the fluctuation of personnel.

2.10. Safety and availability during refurbishments

It is essential that during the renewal of existing tunnel systems the safety standard does not fall below the minimal specifications. This requirement is plausible particularly for older systems with considerable safety backlog demand. It can be drastic, however, for the sequence of the refurbishment.

One has to consider whether a short phase with partial fulfilment of an individual system can be accepted to be able to quickly obtain a higher safety level. For short work phases and hardly assignable states, quantitative risk analysis is not suitable for this evaluation.

2.11. Thermal requirements on components

High thermal requirements give the impression that the feasible gets implemented. If high requirements seem necessary, concept and layout of the components have to be analysed. In general, the temperature resistance of 250°C over 2 hours of the ventilation components, like exhaust air or jet fans, suffices to cover the effective requirements of the rescue phases. The results in the bast publication [12] for fireloads up to 50 MW confirm widly the indications in the directive [9].

2.12. Risk analyses

The request of the EU in the guideline [7], article 13, for the creation of national methodologies for a risk analysis was also heard in Switzerland. The corresponding FEDRO guideline [8] was put into effect in 2014. The target to use gainfully the limited means is plausible. The requirements to master fire incidents in tunnels are high today. Hopefully these requirements are not increased further purely due to new technical developments of safety facilities for mastering the rare fire events with serious consequences.

Certain refurbishing concepts show a great and not plausible discrepancy between the approaches according to standards, like [9], and according to quantitative risk analysis, QRA, like [8]. While the disadvantage of the application of the standard requirements is the not object-specific distinction of safety facilities, crucial points of the QRA are:

- Missing basic data and statistics due to the few events.
- Difficulty of parameter definitions, two exemples:
  The economic costs, in [8] with CHF 21 per person and hour, drive up the congestion consequence and affect the result strongly.
  Non-zero escape velocities in dense smoke overestimate the benefit of emergency exits and reduce the fatality rate.
- Complexity of the methodology, versatility across the trades: The methodology requests the knowledge in all trades, the ability to carry out an assessment coordinated integrally and the critical questioning of the results.

The plausibility of the results of the QRA must in any case be checkable and be checked. Parameters must, if necessary, be analysed and adapted. This can be required also object-specifically which means that one leaves the official specifications and with that the legally stable terrain what sacrifices a great advantage of the method.

An example of an implausible result from the QRA is the long permitted distance of emergency exits in railway tunnels. From events in vehicular tunnels it is known that an initially moving smoke source leads to an extensive area with smoke and therefore represents a considerable peril. A train fire in a tunnel starts almost always from an initially moving smoke source and even in the self rescue phase the smoked area is mutual. Moreover, the fleeing people's density in a rail tunnel is much higher than in a road tunnel.

2.13. Geometry of lay-by niches

In the fatal bus crash in the tunnel Sierre of March 13th, 2012, 28 persons, among them 22 children, were killed. The accident started an intense discussion about the shape and arrangement of lay-by niches. Should the end walls be at an angle or can it be right-angled? Depending on the incident scenario the one or other solution proves to be more favourable. It is not possible in the end to realize the optimal safeguard for all scenarios. As long as a man steers the vehicle, the variety of his reactions is unfathomable.

2.14. Kerb height in tunnels

There is a great disagreement with regard to the kerb height. Kerb heights of 12 to 18 cm are commonly realized with a lowering in front of emergency exits. Quoted reasons are the safety of pedestrians on their way to the next emergency exit, the high intake capacity of the slit gutters, the protection of signals on the margin of the clearance profile and the function of spur keeping. The latter was often specified as a main reason. One can doubt whether this goal really is accomplished. In the outline of the new RABT a kerb height of 3 cm is provided on both sides of the complete tunnel length. Thus it becomes easily walkable especially for handicapped persons but at the same time it is also drivable. The low frequency of walking persons on the kerb while traffic is running makes it difficult to give reasons for higher kerbs. The experience will have to show which consequences this modification in Germany will have. A direct transferability of statistics from other countries is hardly possible.

2.15. Developments on the vehicles

The predominant number of accidents arises from a human misconduct. Safety facilities, like seat belts, crush zones or ABS, is a matter of course today. Distance and lane hold systems are already just as ordinary. Further developments, such as self steering cars are in the test phase and will contribute prominently to the diminution of accidents within a few years. The more complex the systems the higher their maintenance needs. The developpement leads to a shift of responsibilities from the individual vehicle driver to the system manufacturers and the servicing shops.

Reports about spontaneous fires of electric vehicles because of short circuits or battery problems have lowered the hopes concerning a positive effect, on the fire frequency and fire load of electric cars already. The initial fire performance is possibly smaller but the cargo load which is decisive in great events remains the same. In a fire where large batteries are involved a new danger from poisonous substances can arise. However, the already approved vehicle-bound extinguishing systems are desirable for a wider use.

2.16. Measures against recirculation

According to [9] recirculation of polluted air between exit and entry portal has to be reduced with measures like portal offset or partition walls at twin-tube road tunnels. In reality it looks differently.

Figure 2: Naturally ventilated tunnel with portals in a deep cut and with potential recirculation of smoke and polluted air

Sometimes the local situation is taken into account too little, architecture is placed over the function or this requirement simply gets forgotten. It has to be stated that a recirculation is unwanted in normal and in emergency operation and shall be reduced with suitable measures. Passive measures against recirculation work without further technology and without time delay.

2.17. Cross border harmonization of safety measures

International activities have already achieved a considerable degree of harmonization in the area of signalization of the safety facilities and partly of safety requirements. One of such basic documents represents [10]. The World Road Association, PIARC, has created substantial bases in all sorts of areas. The report [11] stands as a fundamental document in the field of ventilation. Further coordinations are necessary particularly at areas like Europe in which one can pass through several countries within a few hours. The facilities which directly concern the tunnel users like the way of the alerting, the behaviour instructions, the driving education or the signalling, are most important. Moreover, it would be useful to harmonize issues such as adequate information of the tunnel users, handicapped person suitability, detection systems, kerb heights and emergency door opening concepts.

3. CONCLUSION

The examples in this paper show that there is no direct road to safer tunnels. New theoretical findings and technical developments prove in practice to be demanding, delicate on disturbances and intensive in maintaining.

The specifications and requirements in standards and guidelines should permit a sufficient flexibility for an object-specific distinction, however without disturbing the uniformity of the systems to such an extent that the understanding of the operation is afflicted. This is a balancing act which cannot be avoided. As a principle, simple and checkable systems should guarantee a proper interaction with the other facilities. The simplicity of the systems has to be stressed according to servicing effort and corresponding servicing costs. If servicing and maintenance are inadequate, safety systems can mutate to hazards.

Steep tunnels are still planned with ventilations whose positive safety effect is overestimated clearly. It lays in the responsibility of the engineers to show and explain the bounds of the feasibility to the builder-owner. An attempt to solve this problem consists in giving passive systems increased weight such as emergency exits and structural design which reduce smoke recirculation. Higher investment costs relativize with reference to the life cycle.

4. LITERATURE

[1] Swiss Federal Roads Authority: Directive 13004, Branddetektion in Strassentunneln, V2.10, 2007

[2] Standard SIA 197/2, Design of tunnels – road tunnels, 2004

[3] Zumsteg F., Steinemann U., Berner M.: Ventilation and distance of emergency exits in steep bi-directional tunnels, Conference "Tunnel Safety and Ventilation", Graz 2006

[4] Bettelini M., Seifert N.: On the safety of short road tunnels, Conference "Tunnel Safety and Ventilation", Graz 2010

[5] Richtlinien für die Ausstattung und den Betrieb von Strassentunneln, RABT, 2006

[6] Swiss Federal Roads Authority: Directive 13011, Road tunnel doors and gates, V1.05, 2009

[7] Swiss Federal Roads Authority: Fachhandbuch 23001, Betriebs- und Sicherheits-ausrüstungen

[8] Swiss Federal Roads Authority: Directive 19004, Risikoanalyse für Tunnel der Nationalstrassen, V1.01, 2014

[9] Swiss Federal Roads Authority: Directive 13001, Lüftung der Strassentunnel, V2.03, 2008

[10] Council of the European Union, EU: Directive on Minimum Safety Requirements for Tunnels in the Trans-European Road Network, 2004/54/EG

[11] PIARC: Fire and smoke control in road tunnels, PIARC Committee on road tunnels C5, Report 05.05.B, 1999

[12] Bundesanstalt für Strassenwesen bast: Forschungsprogramm Strassenwesen, Anforderung an die Temperaturbeständigkeit von lüftungstechnischen Bauteilen, FE 15.0514/2011/ERB, 24.5.2013

DISASTER MANAGEMENT REQUIRES A STRONG AND WELL-ESTABLISHED SAFETY CULTURE

André Stein;

Ponts et Chaussées, Luxembourg

ABSTRACT

In most cases, large differences in pressure exist between the portals of long road tunnels as they often connect areas exhibiting different meteorological situations. While the forces resulting from the pressure gradient are taken into account in design and planning of new tunnels, problems may arise when existing tunnels require upgrading. In most cases such tunnels are ventilated by a transverse ventilation system or a system with massive point extraction. These requires an exact control of the air or smoke flow in the case of an emergency and hence an enormous technical effort to achieve the ventilation goals. This paper focuses on the problem of pressure gradients in long alpine tunnels, the technical solutions available, and on what needs to be considered when designing such installations in tunnels undergoing upgrading.

Keywords: ventilation design, transverse ventilation system, long tunnels, pressure gradients

INTRODUCTION

In general, long road and rail tunnels often connect regions exhibiting different meteorological conditions. This is certainly the case where long mountain ridges are traversed, but is also common elsewhere. Pressure gradients have a large influence on ventilation design as they act as additional forces on the air column inside the tunnel.

Summary:

Everyone knows that instructions concerning an adequate reaction in emergencies are essential for all safety areas. For instance, an instruction manual, an alarm and emergency response plan, and brief usage instructions, among others, are required to guarantee an adequate response.

One of several paradoxes of the procedural rules is that they may encourage people to become command receivers and / or misuse them in order to avoid personal responsibility. These days, however, it is a well-known fact that disaster management requires flexibility, creativity, and above all the spirit of initiative, because disasters never follow a predictable scenario.

Another common problem is that usage instructions are static and thus not really suitable in terms of the selected approach to deal with unforeseen technical incidents / human behaviour. To put it in a nutshell, usage instructions can be an obstacle that stands in the way of efficient disaster management. It is sometimes necessary to choose between two evils and thereby even to disobey instructions in order to prevent a worse scenario from happening.

Usage instructions are indispensable but require a strong, stable, yet intuitive safety culture within the emergency services and tunnel management in order to enable the most effective disaster management.

1. PREVENTING DISASTERS

Human errors and technical malfunctions are inevitable in a road tunnel. Our goal must be to prevent a catastrophic escalation of a primary event, even if a chain of unfortunate circumstances significantly worsened the initial situation. According to the author, to make this happen we need more than an alarm and emergency response plan or an instruction manual.

The nature of disasters is such that their spatial and temporal courses are not possible to predict. Their management requires flexibility, creativity, spirit of initiative, resolution and sense of responsibility among all employees of emergency services and tunnel management in addition to significant expertise.

Plans and instruction manual - an obstacle?

In an organised, "proper" safety culture, there is always the risk that people will acquire a behaviour that sounds like this: "I follow the instructions and therefore I'm safe. I am relieving myself of any responsibility as I do only what the internal emergency plan tells me to do." Such conduct is extremely inappropriate when dealing with disasters, because, despite all the uncertainties with respect to big incidents in tunnels, one thing is clear: an efficient disaster management requires measures that are different from the ones we could anticipate beforehand.

The author believes that reducing the preventive operational planning is not an option and that plans and instruction manuals can only be interpreted as "help for self-help", since they contain no set-in-stone absolute truths for all those involved. Self-efficacy of disaster helpers is essential. This means that people have to be convinced that they can manage their mission using their own professional competence.

It takes confidence not only in yourself, but also in your colleagues, superiors, and the organisation.

2. THE FOCUS IS ON PEOPLE

Too long have we tried to achieve safety through purely technical solutions, too little importance was attributed to the education and training of people, which are designed to prevent an incident in the tunnel from bringing about catastrophic consequences.

Technical competence is important and actually relatively easy to achieve, but influencing people in the right way is much harder. The real question is: "How do people handle the issue of safety and how deep is their understanding of the risks that go hand-in-hand with a tunnel incident?" It is also crucial how the staff of the emergency services cooperate with each other. In this context, we start talking about safety culture.

3. SAFETY CULTURE

Safety culture is the way and manner in which an organisation deals with safety issues.

Standards, values, goals, interests and behaviours of all stakeholders reveal a certain, better or worse, safety culture.

Commonly, there are 5 types of safety cultures:

- **Emerging** → basic safety culture
- **Managing** → reactive safety culture
- **Involving** → planned safety culture
- **Cooperating** → proactive safety culture
- **Continually improving** → resilient, intuitional safety culture

4. A BETTER SAFETY CULTURE WILL REQUIRE A TOP/DOWN APPROACH

Changing the safety culture of an organisation is a lengthy and difficult process, which does not only affect the behaviour of its employees. The change has to start upstream, with personal values and beliefs. This will only become possible if the process of change will be given the highest priority at all levels of management. Change management is first of all a top/down approach, where the management tier leads by example.

Table 1 represents how management deals with the safety topic.

Table 1: Behaviour of the management within a specific safety culture.

	Behaviour of the management
basic safety culture	There is no need for action without legal provisions. We are not talking about the incident, and thereby we avoid problems.
reactive safety culture	Safety is guaranteed. If we come across a problem, we will act.
planned safety culture	We are very well organised, and we can deal with any situation.
proactive safety culture	We analyse all incidents, and we are always looking for ways to improve ourselves.
resilient, intuitional safety culture	I lead by example, I'm aware of my people's problems, I discuss their problems with them and encourage them to be proactive in all their safety concerns.

The change in the safety culture requires not only the leadership of the management, but also involvement of the staff, an open dialogue, and transparency within the organisation at all times (Diagram 1). Staff must be encouraged to take an interest in safety issues and also apply their knowledge in practice. It is crucial that everyone concerns themselves with workspaces and safety problems of others.

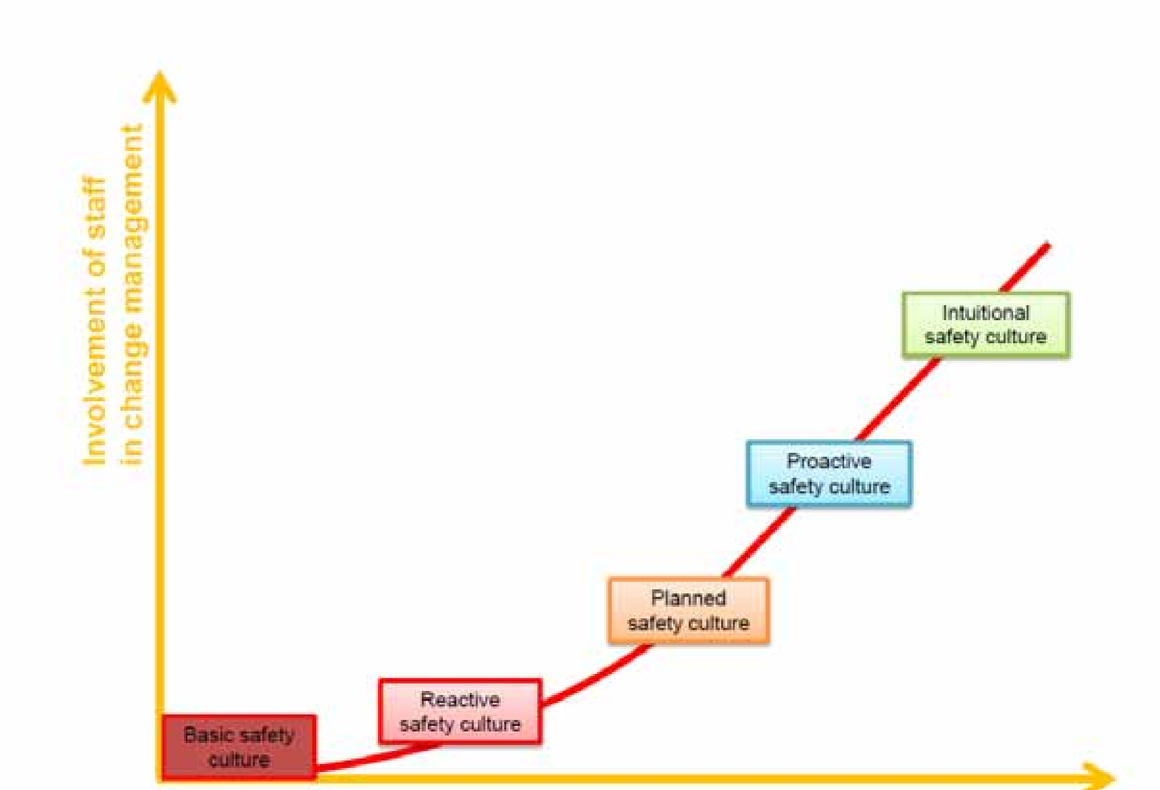

Diagram 1

5. RESILIENT ORGANISATION

The issue of making the disaster management system work through a strong and well-established safety culture is inextricably linked with the issue of a "resilient organisation". What it essentially comes to is that an organisational structure (for example, a fire department) is established in such a way that in unfavourable conditions (e.g. a certain leader is not present, a task group is late, emergency personnel are faced with a technical breakdown, etc.) it proves to be resilient, acts quickly and efficiently.

A resilient organisation is only possible within a stable and strong safety culture and requires from its employees:

- an ability to have a realistic assessment of the situation through individual attention
- acceptance of the situation
- strong analytical capabilities
- willingness to take responsibility and independent capacity to act
- self-efficacy and self-confidence
- esprit de corps
- confidence in the support of the organisation
- ability to manage emotions
- creativity

This is a lengthy process that can only be achieved if the leadership of the management always stays in motion.

ON THE AERODYNAMIC CHARACTERISTICS OF PARTLY OPEN GALLERIES IN CASE OF FIRE

*T. Stammwitz, **S. Rigert, ***N. P. Hoj, **M. Bettelini
*Swiss Road Authority FEDRO, Thusis, Switzerland
**Amberg Engineering Ltd., Regensdorf-Watt, Switzerland
***HOJ Consulting, Brunnen, Switzerland

ABSTRACT

Galleries completely or partly opened on one side are very common in the Alpine area, where they provide protection against natural dangers (avalanches, landslides and falling rocks) while allowing for a fair level of natural lighting and ventilation. The strong natural ventilation does also influence smoke propagation. However, from a normative point of view, galleries often fall into a grey zone, treated neither as open road nor as closed tunnel, engendering uncertainties about the required safety equipment.

The effect of the side openings ("windows") of galleries on smoke propagation is investigated based on CFD simulations and on experience from a real fire event. The results are evaluated especially in terms of need for safety equipment, particularly emergency exits, and compared to fully closed tunnels. The results show, that requirements on self-rescue facilities for partly open galleries are generally lower than for tunnels. On the other hand, steep galleries coupled to tunnels do not show the tendency to mitigate the effects of incidents.

Keywords: gallery, fire safety, smoke propagation ventilation design

1. INTRODUCTION

This papers deals with the operational safety of galleries in case of fire, from the point of view of self-rescue and intervention. The primary focus is on road infrastructures but the main findings and conclusions apply also for galleries on railway networks.

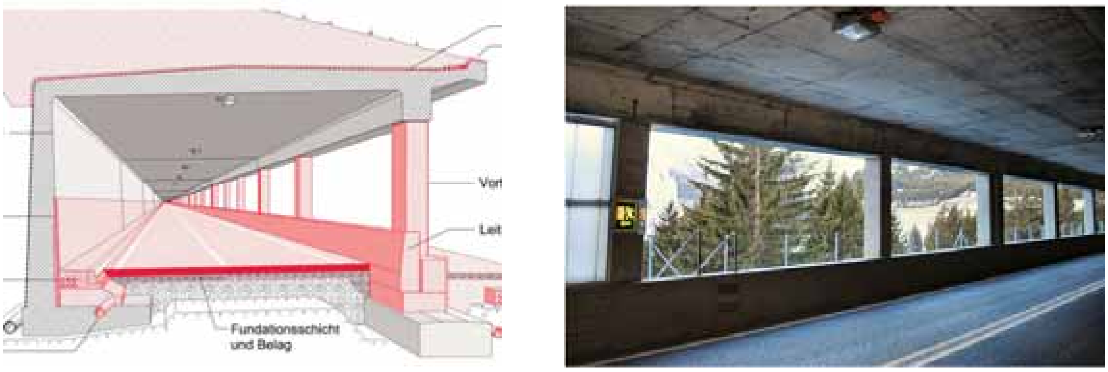

Figure 1: Typical Swiss protection gallery investigated in this paper

Galleries are a very common feature of roads and railway lines in the Alpine area. Schellenberg (2009) reviews more than 350 existing protective galleries in Switzerland. About 300 are located on the national, cantonal or local road network, while about 50 are part of the railway network. The primary function of galleries is generally protection against natural dangers, particularly avalanches, landslides, falling rocks or mudflow. The typical structure of protection galleries is presented in Figure 1. In most cases, they are entirely closed on the top and on one side while they are partially or entirely open on the opposite side. Galleries are frequently combined with tunnels, for offering an optimum compromise between protection of the infrastructure, investment and operating cost. Galleries are particularly interesting because of the high level of natural lighting and ventilation. Noise-protection galleries in urbanized areas could be structurally different but share many common elements in terms of smoke propagation and requirements on safety facilities.

A large body of literature is available on the structural behavior of galleries in case of rock fall and avalanche. Knowledge on smoke propagation and the resulting conditions for self-rescue and intervention is very limited. Mayer et al. (2012) investigated the requirements for certain safety equipment in galleries with lateral openings and ceiling openings based on quantitative risk analysis. They concluded, that the influence of emergency exits on the risk level is reduced with lateral openings, especially if the inner clearance is increased or if the ceiling is inclined towards the lateral opening.

Most current regulations do not distinguish between tunnels and galleries. The European directive 2004/52/EC defines “tunnel length” as ”the length of the longest traffic lane, measured on the fully enclosed part” and NFPA 502 defines a road tunnel as “an enclosed roadway for motor vehicle traffic with vehicle access that is limited to portals”. The French regulation (2000) is an exception because it provides explicit guidance on this subject: the national regulation on road-tunnel safety is not applicable to enclosures with openings larger than 1 m^2 per lane and m length. Most protection galleries have significantly larger openings.

The lack of specific regulations, coupled with poor physical understanding of smoke propagation in partly enclosed traffic infrastructures, result in significant uncertainties concerning the level of safety facilities required for user protection in galleries, particularly emergency exits. These issues, largely related to smoke propagation shall, be addressed here. This paper focusses on galleries with comparatively large side openings, of the order of at least 1/3 of the side surface or more (Figure 1). Most existing galleries fall into this category.

2. THEROETICAL INVESTIGATION OF KEY PARAMETERS

In normal operating conditions, the combined effect of vehicle motion (piston effect and pressure fluctuations) and external wind generally allow for an excellent air exchange in galleries. An entirely different situation arises in case of fire, where the exchange with the exterior is dominated by thermal effects and where much of the smoke should be expelled through the side openings over a short distance, for ensuring a proper level of safety.

A simple model about the thermal exchange over the sidewall can be used for illustrating the underlying physics. Consider an enclosure opened on one side subject to an arbitrary temperature difference. The air velocity through the opening can be expressed as

$$u = \sqrt{\frac{2}{\rho_i} \cdot (p_i - p_o)} \approx \sqrt{2 \cdot g \cdot y \cdot \left(\frac{T_i}{T_o} - 1\right)}$$

where the symbols denote: y = vertical coordinate, p = pressure, ρ = air density, T = air temperature, g = gravitational acceleration, i = inside, o = outside.

This simple approximation shows, that a substantial air exchange through the side openings can be expected in case of fire, with air speeds of the order of 2-3 m/s or more. Further significant differences compared to tunnel fires are:

- The airflow available for combustion in the case of galleries is virtually unlimited and fires are most likely to be fuel limited.

- The longitudinal airflow below the smoke layer in direction to the fire plume, which tends to destabilize the smoke layer, is limited.
- The "stack" effect, generating a longitudinal airflow, is limited by the loss of buoyancy due to the smoke leaving the gallery and due to the openings, which prevent the creation of a longitudinal pressure difference.
- The potential for using mechanical ventilation is very limited (creation of longitudinal pressure difference is not possible) and cannot be seen as efficient safety measure in open galleries.

The physics of smoke propagation in galleries is largely determined by the key geometric parameters (width, height, open height, lateral and longitudinal slope) and by the vertical thermal gradients.

3. APPROACH AND CASE STUDIES

3.1. Approach

The authors investigated a number of real-life galleries in the past few years, covering a wide range of relevant parameters. While not systematic, these investigations are quite representative for two-lane galleries in the Alpine room. All investigations were carried out based on CFD simulations carried out using the commercial software package FDS. FDS (http://www.nist.gov/el/fire_research/fds_smokeview.cfm), combined with its own visualization tool, is considered by many tunnel specialist as the preferred software for investigating tunnel fires and smoke propagation.

All case studies presented herein refer to existing infrastructures and are based on real investigations carried out by and for the responsible road authority. The identification and localization of the different objects is immaterial.

3.2. Small longitudinal slope

An existing urban gallery is used as prototype for illustrating the simplest situation, a gallery with small longitudinal and characterized by the following parameters:

- Length: ca. 200 m
- Slope: 0.6%
- Width: 9.5 m (2 lanes)
- Height: 5.7 m
- Average side-opening height: 3.7 m.

A HGV fire on the inner lane with idealized HRR curve was considered, which rises linearly to 30 MW within 5 minutes. The gallery structure and smoke propagation in absence of wind are illustrated in Figure 2. Smoke stratification and visibility conditions within the gallery are excellent during all the phases of the fire.

Galleries are frequently exposed to wind. A specific investigation was therefore carried out with an external wind of 1.4 m/s orientated at 45° with respect to the tunnel axis. The results are presented in Figure 3. They show that external wind does not change the previous conclusion. Although the wind does generate some turbulence around the pillars of the openings, the visibility conditions are deteriorated only locally, close to the burning vehicle. Self-rescue conditions are pretty good over a long time period. It was concluded that the initially planned emergency exits are not needed.

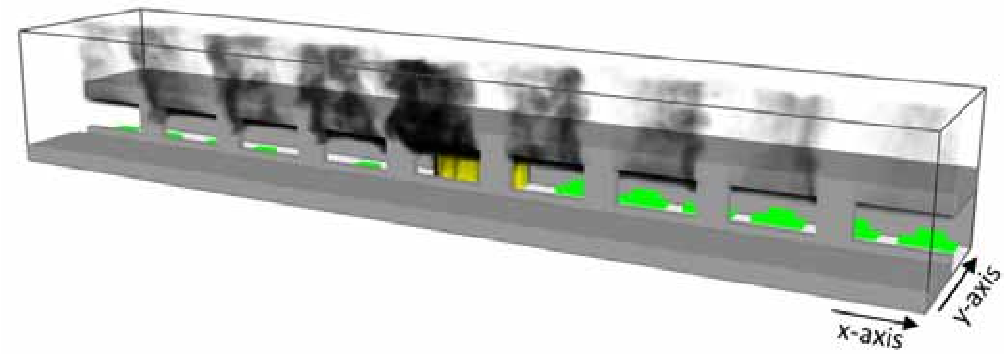

Figure 2: Smoke propagation and visibility in the gallery 4 minutes after start of fire (no wind).

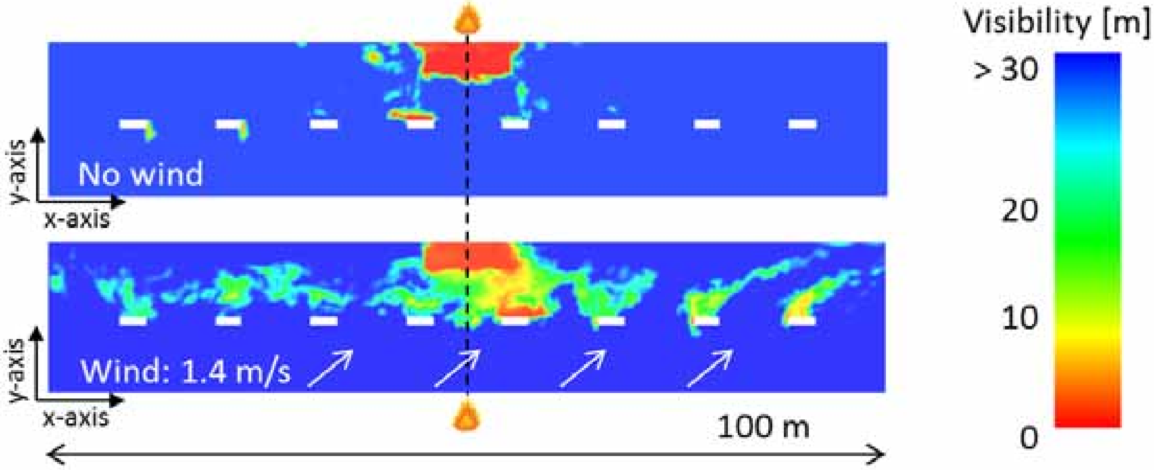

Figure 3: Visibility conditions in the gallery at 2 m height for a 30 MW fire, 4 minutes after start of fire, for different wind situations (white rectangles are pillars)

3.3. Large longitudinal slope

Particularly in mountainous areas, longitudinal slopes in excess of 3% are frequently encountered. Many existing galleries even exceed the now commonly accepted threshold of 5%. The influence of longitudinal slope is well known for closed tunnels. The difference between tunnel and a partly open gallery shall be illustrated based on a gallery characterized by the following parameters (Figure 1):

- Length: ca. 600 m
- Slope: 6.1%
- Width: 9.5 m (2 lanes)
- Height: 5.7 m
- Average side-opening height: 3.7 m.

Further assumptions are: all vehicles at rest, vanishing initial air velocity, no external wind.

The results are presented in Figure 4, which shows the visibility conditions computed for two geometrically identical structures, the gallery presented in Figure 1 and the tunnel resulting if the sidewall is completely closed. The openings in the gallery prevent the development of a strong stack effect with a high longitudinal velocity and allow smoke to leave the gallery over the side openings. A significant fraction of the buoyancy flux is lost and the stack effect is significantly reduced, as shown in Figure 4. The stratified layer is stabilized and the propagation velocity of the smoke front is reduced. Compared to a closed tunnel, the self-rescue conditions are significantly better.

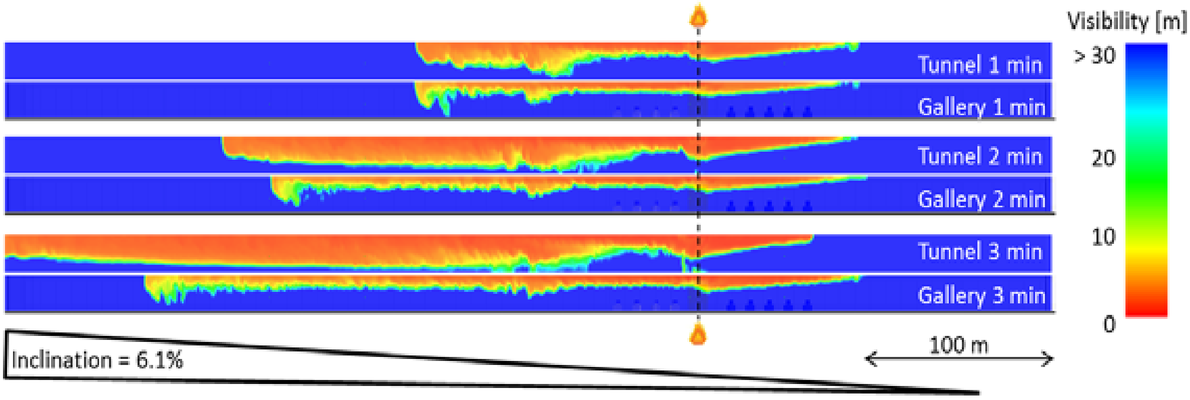

Figure 4: Smoke propagation in tunnel and gallery with identical shape (6.1% slope)

The openings do not only allow smoke to leave the gallery, they also reduce the longitudinal velocity towards the fire source in the "fresh air" layer below the smoke layer. The smoke layer is thus much more stable, even if the temperature in the smoke layer decreases. This effect is characterized by the specific Froude number, which is defined as:

$$\mathrm{Fr} = \frac{u_{avg}^2}{\sqrt{g \cdot H \cdot \Delta T_{cf} / T_{avg}}}$$

According to Nyman and Ingason (2012), a stratified smoke layer is expected for Fr < 0.9. Due to the vanishing longitudinal velocity in the gallery (no generation of longitudinal pressure difference) in the fresh air layer below the smoke layer, the Froude number is obviously smaller than in the tunnel, or in other words, smaller temperature differences between smoke layer and fresh air layer are possible without loss of stratification.

A further advantage is, that local disturbance and mixing of the smoke layer with the lower fresh air layer has no impact on self-rescue conditions further away. Usually these disturbances are convected towards the fire source. The missing longitudinal air velocity prevents the transport of such disturbances.

3.4. Interaction between tunnel and gallery

Techno-economical project optimization in mountainous areas frequently leads to road sections with continuous sequences of tunnels and galleries without entirely open sections in between. Galleries are also very common at the ends of tunnels, as a compromise between safety and excavation cost. The slope is frequently high to very high and frequently exceeds 5% in existing infrastructures. The situation is investigated based on the following real-life example: a tunnel, which is coupled to a gallery at the upper portal, both with a longitudinal slope of 6.1%. The properties of the gallery are in fact identical to the one presented in chapter 3.3. The tunnel has a length of about 550 m and is not ventilated mechanically.

Due to the thermal effect and to the tunnel slope, airflow towards the upper portal with high velocity is generated, destroying smoke stratification. The configuration with a gallery tends to have a slightly higher longitudinal velocity in the beginning due to the shorter tunnel and smaller friction losses (Figure 5), and thus a slightly faster smoke propagation. At the boundary Gallery – Tunnel, smoke is already distributed over the whole tunnel cross section. Looking at the further development of the smoke propagation, the positive effect of the gallery can be observed. The smoke propagation velocity is slowed down and smoke density is lower in the gallery if compared to a geometrically identical tunnel. However, the differences between gallery and tunnel are small and self-rescue conditions are not improved in a manner that would lead to a reduction of the required safety equipment. The loss of stratification in the tunnel cannot be reversed and the high smoke propagation velocity is mainly based on the longitudinal airflow driven by the stack effect in the tunnel.

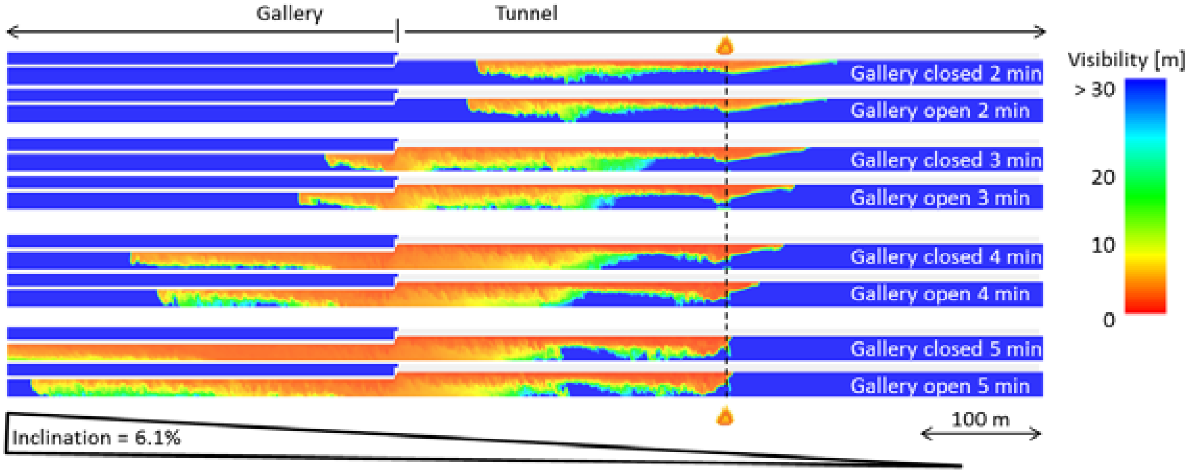

Figure 5: Smoke propagation in case of fire in the tunnel with adjacent gallery, slices called tunnel are fully closed in the gallery section too.

3.5. Fire position in relation to open side and influence of aspect ratio

The fire position has been identified as a possible influence factor for smoke propagation and characteristics of the smoke layer, especially in wide galleries. An example where the focus has been laid on temperature distribution and development shows that the influence of fire position (close to the open side or close the sidewall) can be neglected. If the fire is placed close to the open side, the conditions are slightly less favorable, due to the local disturbances at the closed sidewall.

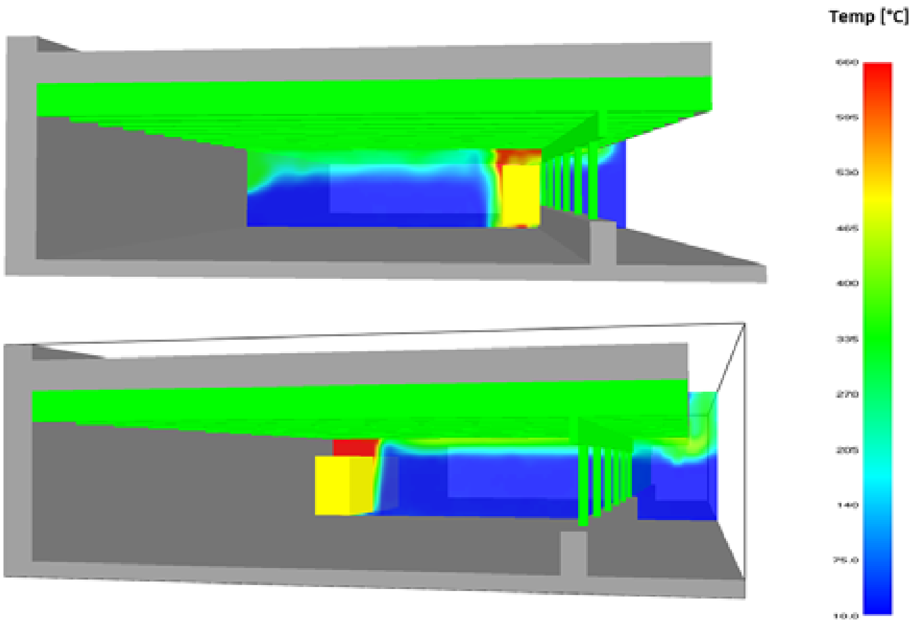

Figure 6: Different fire positions in a wide gallery (temperature distribution)

4. FINDINGS FROM REAL EVENTS

Two fires confirm and further illustrate the findings from the simulations presented in the previous chapters. The first example is a bus fire, which occurred in the year 2002 in a 2.2 km long combined system consisting of tunnels and galleries with 5.7 to 6% longitudinal slope. The fire occurred in a 231 m long tunnel, whose upper portal is directly connected to a 432 m long gallery. The upper part of the gallery during the fire is presented in Figure 7. The available documentation and direct witness reports indicate a considerable amount of smoke being released through the side openings of the gallery. Nevertheless, a large amount of optically unstratified smoke was expelled at high speed through the upper portal of the gallery. Intervention was only possible through the lower portal. This confirms the simulation results presented in chapter 6, showing that in case of fires in a tunnel with adjacent gallery, the gallery has only limited influence on the smoke propagation and stratification.

Figure 7: Smoke propagation during a bus full fire (2002). View of the upper gallery portal and image of the bus after the fire in the inlay at the left lower corner.

A full fire of a medium-size personal car occurred in the year 2015 at the lower end of the same tunnel-gallery system, consisting of a 424 m long gallery connected through its upper portal to a 541 m long tunnel equipped with longitudinal ventilation with jet fans. The intervention services reported a variable level of smoke stratification within the gallery and very bad visibility at the interface between the tunnel and the gallery. After fire detection, the jet fans in the tunnel were operated towards the gallery (lower tunnel portal) for protecting the tunnel against smoke propagation. This clearly shows that the interface between tunnels and galleries is extremely important and needs to be investigated in detail.

5. DISCUSSION OF FINDINGS AND PRACTICAL IMPLICATIONS FOR DESIGN AND OPERATION

Smoke propagation in case of fire in galleries was analyzed for a variety of configurations using CFD and the most important observations could be confirmed on a real fire. The main findings and conclusions are as follows:

- In case of small longitudinal slope, and excellent exchange with the exterior is observed also in case of external wind, resulting in good visibility and favorable conditions for self-rescue and intervention.

- Larger gallery aspect ratios and different fire locations within the gallery do not change in a significant manner the previous conclusion.
- In case of fires in galleries with large longitudinal slope, a reduced stack effect, slower smoke propagation and fair stratification are observed compared to the corresponding tunnel configurations. This virtually corresponds to a smaller heat-release rate, because a significant part of the buoyancy is “lost” through the sidewalls. Again, this results in favorable conditions for self-rescue and intervention.
- Fires in a tunnel continuing at its upper portal with a gallery represent a major safety problem. The “stack effect” results in a large longitudinal air velocity within the tunnel, with full loss of optical stratification at the lower portal of the gallery. Under these conditions, loss of stratification within the gallery cannot be prevented. The propagation speed of the smoke front is much higher than in case of a fire with identical characteristics but located in the gallery.
- Significant smoke destratification can occur at the interface between tunnels (frequently protected against smoke penetration by mechanical ventilation generating airflow towards the fire) and galleries with longitudinal slope, where the gallery is located at the upper portal of the tunnel. Simulation and real fires showed that these locations are critical for both self-rescue and intervention.
- Fires in galleries are most likely to be fuel controlled, because of the virtually unlimited availability of air. Proper liquid collection is required at least in case of transportation of liquid fuels.

It should be noted that most simulations were carried out considering idealized conditions, ignoring e.g. vehicle motion or external wind. The experience gained from smoke propagation within different types of galleries allows drawing some conclusions about the need of emergency exits. Galleries, which are not coupled with a tunnel, show improved characteristic compared to tunnels. The distance between emergency exits can be reduced or emergency exits can even be completely eliminated. Careful investigation is required in case of galleries coupled to tunnels. In case the tunnel has a large longitudinal slope, the side openings of galleries do not influence smoke propagation in way that would allow reducing emergency exits.

The specific characteristics of galleries have a profound impact on safety design, which should be based on specific analysis and regulations rather than on rules developed for tunnels.

6. REFERENCES

French Regulation (2000) Instruction technique relative aux dispositions de sécurité dans les nouveaux tunnels routiers (conception et exploitation), Annexe No 2 à la circulaire interministérielle no 2000-63 du 25 août 2000 relative à la sécurité dans les tunnels du réseau routier national.

Mayer, G., Sistenich, C., Zimmermann, U., Zulauf, C., (2012) Risk analyses of the safety level of galleries, 6th International Conference ‘Tunnel Safety and Ventilation’, Graz.

Nyman, H., Ingason, H., (2012) Temperature stratification in tunnels. Fire Safety Journal 48:30-37.

Schellenberg, K., (2009) On the Design of Rockfall Protection Galleries, Institute of Structural Engineering, Swiss Federal Institute of Technology Zurich, January 2009.

INCIDENT TESTED: RESCUE, EVACUATION AND FIRE PROTECTION AT THE KORALM TUNNEL 2

A REVIEW OF THE FIRE EVENT IN 2015 AND THE PRACTICAL IMPLEMENTATION OF THE CONCEPT IN THE EVENT OF AN INCIDENT

S. Fehleisen, ÖBB-Infrastruktur AG
J. Frießnegg; ARGE KAT2, Austria

1. ABSTRACT

As a new high-speed railway connection between Graz and Klagenfurt, the Koralm Railway represents a crucial component in the context of the Baltic-Adriatic Corridor. With a length of about 33 kilometres, the Koralm Tunnel--the centrepiece of this new line--will become one of the longest traffic tunnel constructions in the world.

In the tunnel construction phase, the construction lot "Koralm Tunnel 2" represents the longest of the three main construction lots. Apart from excavator driving and drill-and-blast driving, two tunnel boring machines are also being used on this 20 kilometre length. The length as well as the complexity already pose specific challenges for the construction phase in terms of safety, rescue and evacuation, and fire prevention.

With the starting of the construction in 2011, the implementation of the rescue, evacuation and fire protection concept specified in the tender was also initiated by the contractor in cooperation with the client and the emergency services.

In February 2015, the emergency management had to be put into real action on account of a fire in an standby generator on one of the two tunnel boring machines. The fire could be brought under control successfully and all persons were rescued and evacuated from the tunnel unharmed. The professional and calm handling of the incident showed how significant prior emergency drills and coordination are.

Keywords: tunnel safety, evacuation and fire protection for underground construction, long tunnels, tunnel fire

2. INTRODUCTION

The construction of the Koralm Railway is carried out over several phases, with some sections being worked on simultaneously. Apart from the 33 kilometre long Koralm Tunnel--which is the centrepiece of the Koralm Railway--and other smaller stations and stops, two new intercity stations will be built near the two tunnel portals. Presently, the work is completed or under construction for 90 percent of the Koralm Railway projects. The Koralm Railway will be fully operational by 2023 as a continuous double-tracked, electrified high-speed railway line with maximum speed of up to 250 kilometres per hour (ÖBB, 2012a).

3. THE KORALM TUNNEL 2 CONSTRUCTION LOT (KAT2) AND ITS REQUIREMENTS IN TERMS OF RESCUE, EVACUATION AND FIRE PROTECTION

The nearly 33 kilometre long Koralm Tunnel is designed as a twin-tube, single-track tunnel and passes under the Koralpe mountain massif with a maximum overburden of circa 1,200 metres.

Both traffic tubes are linked via cross passages every 500 metres and run at an axis-centre distance of 23-50 metres. The tunnel tubes will be excavated to have a diameter of ten metres.

As additional safety system, a refuge room with emergency station facing the traffic tubes is built approximately in the middle of the tunnel (ÖBB, 2012b). Two ventilation shafts will be provided for air circulation in both tubes in case of fire, during maintenance activities and in the event of breakdowns.

Measures for further investigation and research were undertaken in preparation of the main phase, which formed the basis for the detailed planning of the three main construction lots of the Koralm Tunnel: KAT1, KAT2 and KAT3 (Figure 1).

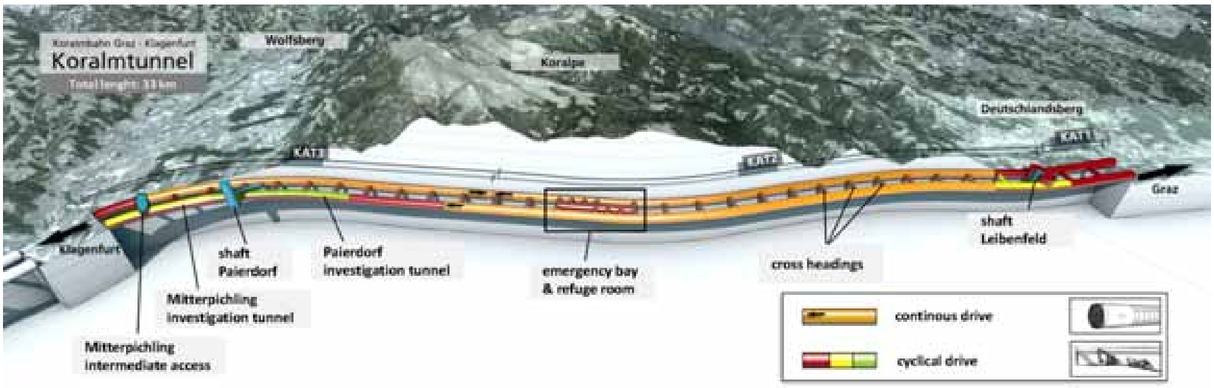

Figure 1: Construction lots division and tunnelling types (Source: ÖBB)

The construction work on the Koralm Tunnel began in 2008 with construction lot KAT1; the preliminary structural work has already been completed. Implementation of construction lot KAT2 followed in year 2011. In January 2014, the construction of the third tunnel construction lot KAT3 started from the western portal.

For the construction of the Koralm Tunnel, both cyclical (excavator and drill-and-blast driving) and continuous (mechanised) tunnelling techniques are being used. In total, three tunnel boring machines are being used, two in Styria and one in Kärnten in the construction lot KAT3.

3.1. Construction lot KAT2 at a glance

In January 2011 began the implementation of the longest of the three tunnel construction lots in the Western Styrian region of Deutschlandsberg with 4,500 meters cyclical drive. Since early 2013, both tunnel boring machines of KAT2 have been running from Kärnten towards the boundary line of the third construction lot KAT3.

By year 2017, up to 17 kilometre length of tunnel has to be excavated by the machine. After that, 39 cross passages and the over 900 metre long refuge room will be built using cyclical tunnelling. This will be followed by the concreting phase and completion of the preliminary structure by 2019. At present, around 600 people are directly employed in the construction lot KAT2.

The long tunnelling lengths, the complexity as well as the long construction periods gave rise to safety-related parameters, which had to be appropriately taken into consideration in the planning phase itself (ÖBB, 2009):

- Entrance access via ventilation and construction shaft
- Two tunnelling activities operating in parallel with two tunnel boring machines
- Continuous segment lining
- Long tunnelling lengths, up to 17 kilometres from the construction shaft in the western direction

- Providing adequate quantities of air and ensuring tolerable temperatures at the work sites
- Occupational safety and fire protection
- Emergency exits for self-rescue: the distance between the heading face and the last cross passage that can be used as emergency exist can be up to six kilometres
- Evacuation routes for third-party rescue; only rail-bound from the point of mechanised tunnelling

These parameters, especially due to the long tunnelling lengths, made it necessary to include requirements and considerations in safety planning with regard to the layout of emergency exits, which was beyond the usual extent of planning until this point.

3.2. Rescue, evacuation and fire protection in the planning phase

During the tender planning phase itself there was a fire in a small excavator that was tunnelling the Paierdorf exploratory tunnel (KAT3 zone) in 2008; luckily, the fire only caused damage to property.

The findings of the evaluation were incorporated into the rescue, evacuation and fire protection planning in the call for tenders for KAT2 (and KAT3). As a result, a detailed concept became available as guideline for specifying minimum standards, which with the award of the contract also became part of the construction contract (ÖBB, 2009). This concept was prepared jointly with the planning coordinator as well as an engineering consultancy for occupational safety and fire protection, which was called in additionally.

In a nutshell, the concept rests on three main pillars (ÖBB, 2009):

- Structural fire protection
- Technical fire protection, and
- Organisational fire protection

The aim was and remains to avoid incidents in advance through preventative measures and/or to reduce risks through measures that lower the probability of occurrence. Here, self-rescue with all its requirements and exigencies always remains in the foreground.

The individual points of the rescue, evacuation and fire protection concept are outlined in the following (ÖBB, 2009).

3.3. Implementation of measures during the construction phase

3.3.1 Preventative measures for structural fire protection

Structural fire protection involves specifications with regard to e.g. the design and organisation of permanent assembly stations, workshops and storage areas below ground, as well as fire compartments below and above ground. In particular, the set of measures for emergency and escape exits deals with the minimum requirements for this part of the concept.

3.3.2 Preventative measures for technical fire protection

The measures refer to technical fire protection for the most part. These include devices like fire detection and alarm systems in sections with higher risk of fire, equipment for immediate fire-fighting and first response, special fire extinguishers, special fire extinguishing systems at exposed locations, as well as protective equipment, emergency vehicles and special fire-fighting equipment.

Following are examples of the technical measures:

- Safety centre KAT2

The safety centre was planned as a control and monitoring location, where all warning and communications systems converge. From here, the coordination happens for the ventilation and the emergency exits and the entire electronic personnel identification system below ground as well as the vehicle access above ground are monitored. Emergency services are alerted only by the safety centre. It has an emergency power back-up, is available round the clock and is connected to a control room from where all actions and measures are coordinated in an emergency situation.

- Communication systems

Upon mutual agreement between client, contractor and emergency services an analogous radio system based on a 70-centimetre band was installed below ground. It not only connects to the emergency hotline of rescue services, the radio channels are also available as ‘construction radio’ to the workers on site and on the tunnel railway.

- Refuge chambers on the tunnel boring machines

In the concept, there was also a provision for refuge containers on both sides of the tunnelling machines. The specifications given in the tenders were appropriately adjusted to or expanded in accordance with the construction phases by the contractor consortium. Thus, the supply of breathing air in these refuge chambers was extended to 18 hours for 15 people.

- Rescue trains for the construction phase

In the planning phase itself, the refuge chambers on the tunnel boring machines were considered to be inadequate given the long tunnelling lengths. Therefore, four rescue trains permanently on standby were provided for the mechanised tunnelling phase. These rescue trains (Figure 2), as priority measure in terms of self-rescue, are intended as shelter or as means to exit the tunnel in emergency situations. A rescue train is always on standby to enter the tunnel for third-party rescue.

Figure 2: One of the four rescue trains at KAT2 (Source: ÖBB)

The four units are designed to carry 25 persons and with eight hours supply of breathing air. These four trains are driven by diesel engines. Measuring equipment, first-aid implements, means of lighting and communication, as well as fire-fighting and rescue equipment are all part of the train fittings.

An additional platform vehicle was designed for transporting the special fire-fighting equipment, which along with a high-pressure mist extinguisher system including power blowers also carries a generator, a portable fire pump with hose reel and a tank unit (4,000 litres).

3.3.3 Organisational fire protection

- Measures at the construction site

Organisational fire protection is a crucial component of the concept which should not be underestimated. It requires a significant amount of effort in terms of planning, implementation, coordination, sensitisation and communication. The guidelines and specifications for this have been considered in the tenders; the implementation, however, depends mainly on the dedication and commitment of the people on site. Therefore, apart from internal trainings in first aid and first response, additional restrictive regulations and rules of conduct have been prepared and implemented by the contractor consortium (ARGE KAT2, 2015).

Further specifications involve training of 'pilots below ground', who in an emergency situation enter the area along with the third-party rescue team. Fifteen employees of the construction company are presently trained as breathing apparatus wearers and accompany the emergency services personnel of the portal fire brigade in emergency situations. Emergency and contingency plans were prepared in parallel for each construction phase and for various scenarios, and allocated to the appropriate areas of responsibility within emergency management.

- Measures outside the construction site

Although self-rescue is the main focus of the concept, preliminary coordination and preventative emergency planning with third-party rescue teams is indispensable.

Apart from fire drills and site inspections, emergency management and its on-site implementation were evaluated in detail and appropriately updated at the beginning of the construction work.

In addition, trainings for incident commanders on site are an integral component of regular fire drills. The objective of these trainings is to optimise cooperation, identify weak points in the communication flow and interfaces, as well as to gain better knowledge and understanding of the processes and requirements of other institutions.

4. THE UNDERGROUND FIRE EVENT IN 2015

In February 2015, a fire in a standby generator below ground became the 'worst case scenario' for emergency preparedness.

At around 12:50 in the afternoon, the safety centre was informed by an employee below ground about a fire in the northern tunnel boring machine. The origin of the fire was a standby generator on the upper deck of the machine, which at the time was less than eleven kilometres away from the construction shaft KAT2 and was shut down for maintenance work.

The standby generator on fire--which had a power output of 130 kilovolt-ampere--was located 150 metres away from the heading face and was used for supplying power to lighting systems and auxiliary systems as well as for ventilation during the extension of high voltage power supply every 500 metres of excavation.

The standby generator, which at this point had been in operation only for 20 hours, had several safety and fire-fighting mechanisms (automatic shutdown and self-extinguishing devices) installed in it.

4.1. The sequence of the fire event

The fire was detected by the persons present in the tunnel, who were standing less than 15 metres away from the standby generator. A rapid spreading of smoke was caused by the ventilator units.

Upon detecting the fire, the safety centre KAT2 was alerted by mobile phone. At this point, 25 persons were present in the area of the northern tunnel boring machine. A part of them could be brought to safety by means of the tunnel railway for personnel, a few reached the safe south tube on foot. Seven persons were unable to escape due to the smoke and had to withdraw into the refuge containers in the front part of the machine.

4.2. Rescue and evacuation measures and emergency management

After the fire was discovered and the safety centre was informed, the emergency services was alerted by the safety centre and the internal alerting was carried out according to the alarm plan. Simultaneously, a team of incident commanders was formed. The operating officer-in-charge of the construction company coordinated with representatives of the client and the emergency services to take appropriate actions at the construction site.

The immediate actions taken were:

- Switching off the ventilation in the affected tube and starting up the ventilators as per the ventilation concept (supplying fresh air to the south tube)
- Evacuation of both tunnel tubes
- Ascertaining the number of persons present in the tunnel using the electronic personnel identification system
- Contacting the persons in charge below ground to clarify the situation
- Identifying the persons at the ventilator shaft above ground and comparing with the lists from the electronic personnel identification system

A crew of the construction company entered the safe south tube on a rescue train in order to clarify the situation and to clear the smoke in the north tube.

When no more smoke was perceived at the level of the last cross passage excavated towards the north tube, the incident commanders decided that a fire brigade crew with breathing gear and a construction site 'pilot below ground' should go towards the machine by a rescue train (Figure 3).

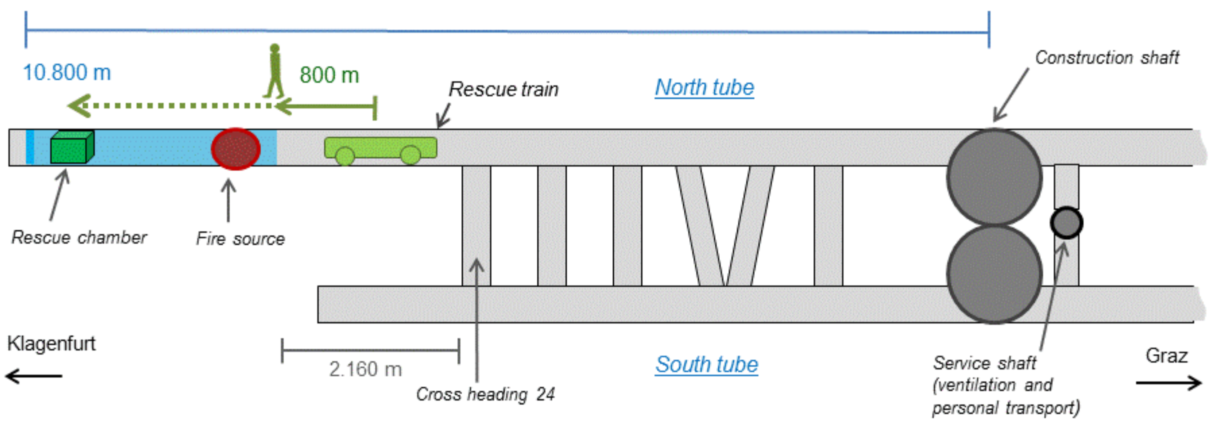

Figure 3: Diagrammatic representation of the course of action for rescuing the people (Source: ÖBB)

In clear visibility, the rescue train could pull in up to 800 metres before the northern tunnel boring machine. The last metres towards the tunnel boring machine had to be covered on foot by the crew with breathing gear because of the smoke in the tunnel tube.

On reaching the machine, the emergency services personnel made their way till the refuge chamber, where the seven persons found unharmed took their oxygen self-rescuers and were led to the rescue train by the crew.

In under two hours the rescued persons could be handed over to Red Cross above ground for a precautionary medical examination.

During the rescue operation below ground, further measures such as blockades and monitoring the access to the construction site equipment areas, creating reserves and withdrawal zones, as well as attending to media, etc. were coordinated by the incident commanders.

After the fire was out, the damages caused by it had to be ascertained: the area surrounding the standby generator had been severely damaged; however, the fire event remained limited to the area where the machine was installed.

The actual cause of the fire could not be established by the experts because of the heavy damage to the standby generator; a technical fault was suspected.

Figure 4: Standby generator after the fire (Source: ARGE KAT2)

5. SUMMARY

From the very beginning, a lot of importance was given in particular to the cooperation of the project partners on site with each other as well as with the external emergency service personnel. It was clear to all that to deal with a complicated incident--which cannot be excluded at a tunnelling site like KAT2, given the scale of the project--it is essential to have the knowledge about the relevant practices and processes.

To sum up the fire event, the following points may be noted: the rescue and evacuation concept had functioned successfully, the cooperation between the incident commanders and all persons involved was exceptionally professional. At the same time, the impact which such an incident may involve could also be reduced.

The approach to incorporate minimum standards for rescue, evacuation and fire protection into the tender planning phase aimed to set out a clear path for fulfilling the safety objectives and to achieve the ability to act in an emergency situation. The details, however, could be defined only in the course of specific work preparation by the contractor company. It is important to define threats, risks and application limits as well as to specify clear responsibilities. This again calls for awareness and acknowledgement of the time and operational effort required for this purpose.

To arrive at reasonable solutions with acceptable effort and expenditure requires involvement and commitment on part of the client, contractor as well as the external rescue services and public authorities. The open exchange of experiences and perceptions has a positive impact on the cooperation and breaks down bias amongst all parties involved. The fact that a safety officer appointed by the contractor and a site coordinator for the client are always available on site from the very beginning has significantly contributed to high implementation quality.

The fire event and its professional and calm handling showed how significant prior emergency drills and coordination are. Quick and appropriately reliable communication and decision-making channels cannot be planned as part of a technical rescue and evacuation concept; instead, they are based on sincere cooperation and a culture of open discussion, which is preceded by one important thing: Commitment to the task and to the safety of all the people on site.

LIST OF FIGURES

BIBLIOGRAPHY

ARGE KAT2 (2015): *Rettungs- und Brandschutzkonzept* [Concept for rescue, evacuation and fire protection] KAT2. Construction phase 2c. Deutschlandsberg.

ÖBB-Infrastruktur (2009): Koralm Tunnel construction lot KAT2. Tender documents - OHS plan, technical terms of contract Appendix 17. ÖBB-Infrastruktur AG. Vienna

ÖBB-Infrastruktur AG (2012a): *Durchbruch in die Zukunft. Der Koralmtunnel.* [Breaking through to the future - The Koralm Tunnel] 1st Edition, p. 9-11. ÖBB-Infrastruktur AG. Vienna

ÖBB-Infrastruktur AG (2012b): *Durchbruch in die Zukunft. Der Koralmtunnel.* [Breaking through to the future - The Koralm Tunnel] 1st Edition, p. 49-65. ÖBB-Infrastruktur AG. Vienna

ABBREVIATIONS

KAT1, KAT2, KAT3	Main construction lots of the Koralm Tunnel
ÖBB	*Österreichische Bundesbahnen* [Austrian Federal Railways]
ARGE KAT2	Construction consortium Koralm Tunnel 2 (contractor)

PRELIMINARY VENTILATION AND COOLING DURING THE CONSTRUCTION OF THE BRENNER BASE TUNNEL

A. Busslinger (*), R. Insam (**)
(*) HBI Haerter AG, Switzerland
(**) BBT SE, Austria

ABSTRACT

With a length of more than 55 km, the Brenner Base Tunnel (BBT) connecting Austria and Italy will be one of the world's very long tunnels in the future. During the construction phase, climatic conditions need to be maintained fulfilling the occupational health requirements, assuring the functionality of the machinery and allowing the intended construction processes.

In view of the extended construction time of the BBT lasting several years and the long tunnel sections of more than 10 km, a sound planning of the preliminary ventilation and cooling systems is required. The proposed paper shall address the related requirements, the design methodology, the simulation tools and the results of the design process.

In addition to the general methodology for the assessment of the tunnel environmental conditions, particular aspects shall be highlighted such as the heat and emission sources during the construction phase. The concepts for ventilation and cooling as well as the performance data of their key components shall be presented. As another topic, the impact of tunnel logistics and the need for flexible enlargement of the underground ventilation and cooling network shall be addressed.

Keywords: Brenner Base Tunnel, temporary ventilation, temporary cooling, climate simulation, occupational health

1. INTRODUCTION

The BBT represents the key element of the planed railway link between Munich and Verona and therefore of the European high performance railway network (cf. Figure 1). With its length of more than 55 km (64 km including all existing tunnel connections) this tunnel system will be amongst the world's longest traffic tunnels.

Since construction of the BBT will last over several years and many of the underground construction sites stretch across more than 10 km a sophisticated design of the temporary ventilation and cooling systems is inevitable.

2. DESIGN OBJECTIVES

Underground working sites are subject to mandatory regulations regarding occupational medicine. Particularly the maximum concentrations of diesel engine emission must not be exceeded. Accordingly country-specific guidelines of minimum fresh air supply depending on the number of employees and the engaged diesel power are defined. In addition maximum air speed and temperature limits at work sites must be kept. Beside these the preliminary ventilation has to cope with specific objectives relating to (fire) incidents, e.g. the provision of smoke free escape routes and the extraction of smoke during fire fighting.

Generally the preliminary ventilation and cooling systems shall restrain the construction progress on the smallest possible scale while keeping a high level of flexibility (to changed boundary conditions) and availability all through the construction period.

Last but not least the impact on the ambient (emissions, noise, etc.) has to be minimised.

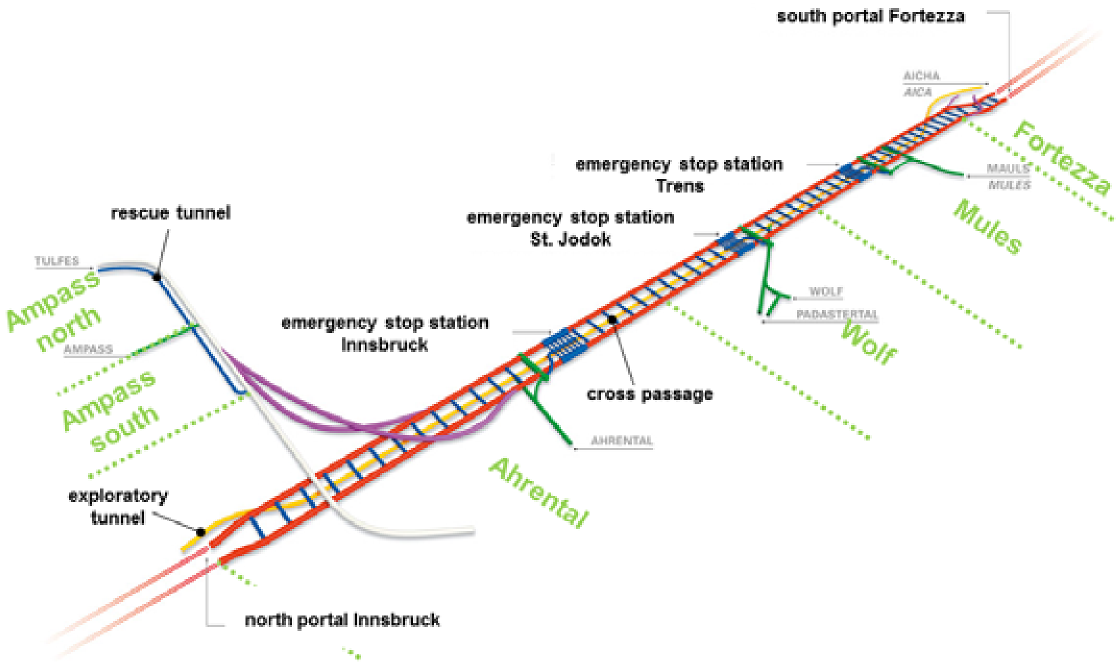

Figure 1: Schematic overview Brenner Base Tunnel incl. sections of temporary ventilation and cooling (green).

3. BASE DATA

The fundamental base data of the ventilation and cooling design are the construction cycle and the corresponding construction methods as well as the accompanying tunnel logistics.

3.1. Construction schedule

The schedule of a tunnel project concentrates the most important parameters influencing the ventilation and cooling design. Particularly it defines the interaction of construction activities within a single lot but as well between different construction lots.

Roughly operation of the BBT is foreseen for 2026. To reach this goal tunnel construction is carried out at the portal Fortezza as well as at the intermediate attacks in Ampass, Tulfes, Ahrental, Wolf and Mules. The typical civil construction sequence includes the excavation of the exploratory tunnel, the main and connection tunnels as well as the tunnel lining. The following considerations are based on the construction schedule of 2012. However the schedule is updated periodically in relation to the current boundary conditions.

3.2. Construction method

The tunnel construction method and particularly the excavation technique with the associated diesel power and heat emission is an essential design basis of the ventilation and cooling system.

In the BBT the drill and blast method is mainly applied to excavate the access tunnels, the emergency stop stations and cross passages as well as some parts of the main tunnels and the exploratory tunnel. TBMs will excavate the longest sections of the main and exploratory tunnels.

3.3. Logistics

Beside the actual construction the tunnel logistics and particularly all transport activities heavily affect the ventilation and cooling requirements. Major tunnel projects as the BBT imply numerous transports of personnel and material (concrete, steel support, muck, etc.). Substantial fresh air need is caused by diesel powered transport (e.g. trucks and trains) whereas electric conveyer belts (e.g. for mucking) may be neglected in this regard. Most of the mucking in the main tunnels of the BBT will be carried out with conveyor belts. However the tunnel logistics of the BBT is especially governed by the limited available space at the portals.

4. METHODOLOGY

Figure 2 roughly describes the procedure of the preliminary ventilation and cooling design. Based on occupational medical guidelines for underground work (partly regulated by law, cf. BauV 1994 and D.P.R. 1956) the fresh air requirements are defined. Here the substantial input parameters are the number of employees and the amount of diesel power on site. The cooling power requirements are calculated considering the resulting fresh air supply, heat emissions from machinery and additional factors (heat of surrounding rock and latent heat as well as heat exchange between air, rock, cooling flow and air ducts, meteorology at portals, etc.). However this calculation calls for adequate simulation tools (e.g. the numerical code BAUKLIMA of HBI Haerter).

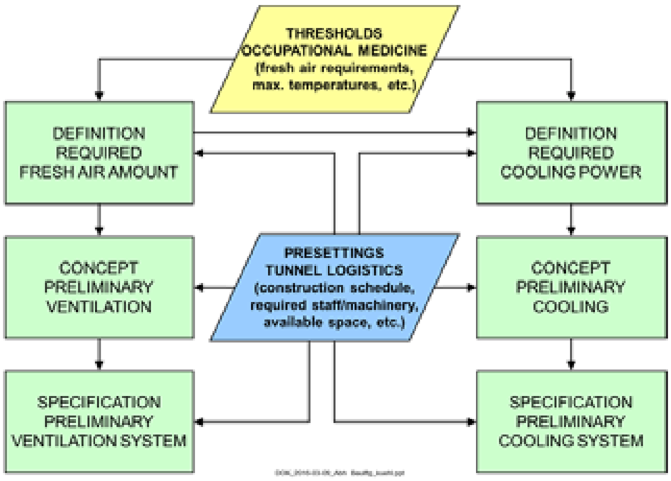

Figure 2: General methodology of preliminary ventilation and cooling design.

The required fresh air amount, its distribution in the individual tunnel sections and the boundary conditions given by the tunnel logistics (available space and time for temporary installations, etc.) determine the concept of the preliminary ventilation (positions and number of ventilation elements). Hence each ventilation component (fans, ducts, air barriers, air locks, etc.) can be specified in depth. This specification is performed with appropriate codes and typically based on the approved guideline of the Swiss society of engineers and architects (SIA, cf. SIA 1998).

The calculated cooling power requirement, its individual application and the above mentioned prerequisites of tunnel logistics apply for the conception of the preliminary cooling (position and number of cooling elements). Hereafter the cooling components (air cooling machines, pipes, pumps, cooling towers, pressure exchange systems, etc.) are specified in detail. This again is carried out mostly with special computer codes. According to Figure 2 the tunnel logistics hold a central role in the design of preliminary ventilation and cooling.

5. CONCEPTS FOR THE BRENNER BASE TUNNEL

As introduced the construction schedule of the BBT includes excavation from many portals. On behalf of the preliminary ventilation and cooling 6 construction lots (and 11 phases) are distinguished (cf. Figure 1). The definition of these lots depends on the civil contract sections e.g. the intermediate attacks at Ampass, Ahrental, Wolf, Mauls and Fortezza. To ensure a continuous construction operation each lot and phase owns its individual ventilation and cooling concept. Here the excavation process typically calls for the most powerful ventilation and cooling.

5.1. Ventilation

All ventilation concepts of the BBT own the following, general characteristics:

- Each lot gets its individual concept, e.g. after breakthrough to neighbouring lots main tunnels will be separated again by air locks or barriers to prevent negative interaction of ventilation systems.
- The maximum ventilation power respectively the maximum number of installations depends on the peak performance construction activity and maximum tunnel length (e.g. highest simultaneous power of machinery).
- Every available opening to the ambient (portals of main tunnels, exploratory tunnel, escape tunnel, access tunnels) is employed for air supply or removal.
- The fresh air requirements in every tunnel section and at any time are achieved.
- There is no substantial obstruction of the tunnel construction due to tunnel ventilation (positioning of air ducts, fans, air locks, etc.).

Consequently the defined ventilation concepts consist in 3 fundamental methods:

- Fresh air ducts: Fresh air is supplied via air ducts to the tunnel face or at work sites. Waste air (loaded with diesel and heat emissions) is released to the ambient at the portals via the tunnel cross section.
- Air circulation: Fresh air flows through the first of two parallel tunnel tubes to the tunnel face or at work sites. Via continuously excavated cross passages fresh air is conducted to the second tunnel face whereas waste air is emitted to the second tunnel tube. Hence the whole waste air is removed to the portal and ambient via the second tunnel tube.
- Linking air duct sections: In order to supply fresh air in long and narrow tunnel headings without parallel tubes (e.g. exploratory tunnels) fresh air duct sections can be linked by interconnected fans (booster stations). This allows for comparably smaller fresh air duct diameter due to reduced pressure loads.

The introduction of every ventilation concept of the BBT is beyond the scope of this paper. The concept of the construction lot Wolf (centre part of BBT, cf. Figure 1) is described exemplarily. Figure 3 illustrates the ventilation concept during the most intense construction phase (excavation of the emergency stop station and 4 main tunnel headings).

The main fan power in the ventilation cavern relates to this increased fresh air requirements. The emergency stop station tunnel faces receive fresh air via ducts. The headings of the main tunnels north and south are fed with air circulation systems. Nearly the whole amount of waste air is released at the portals of the access tunnel Wolf as well as of the tunnels

Padastertal. Additionally a minimum of fresh air supply is provided for the exploratory tunnels connecting the lots Ahrental (mucking) and Mules (no activity). Special interest was given to the main fan positions inside the tunnel. The current concept provides a minimum noise impact to the ambient.

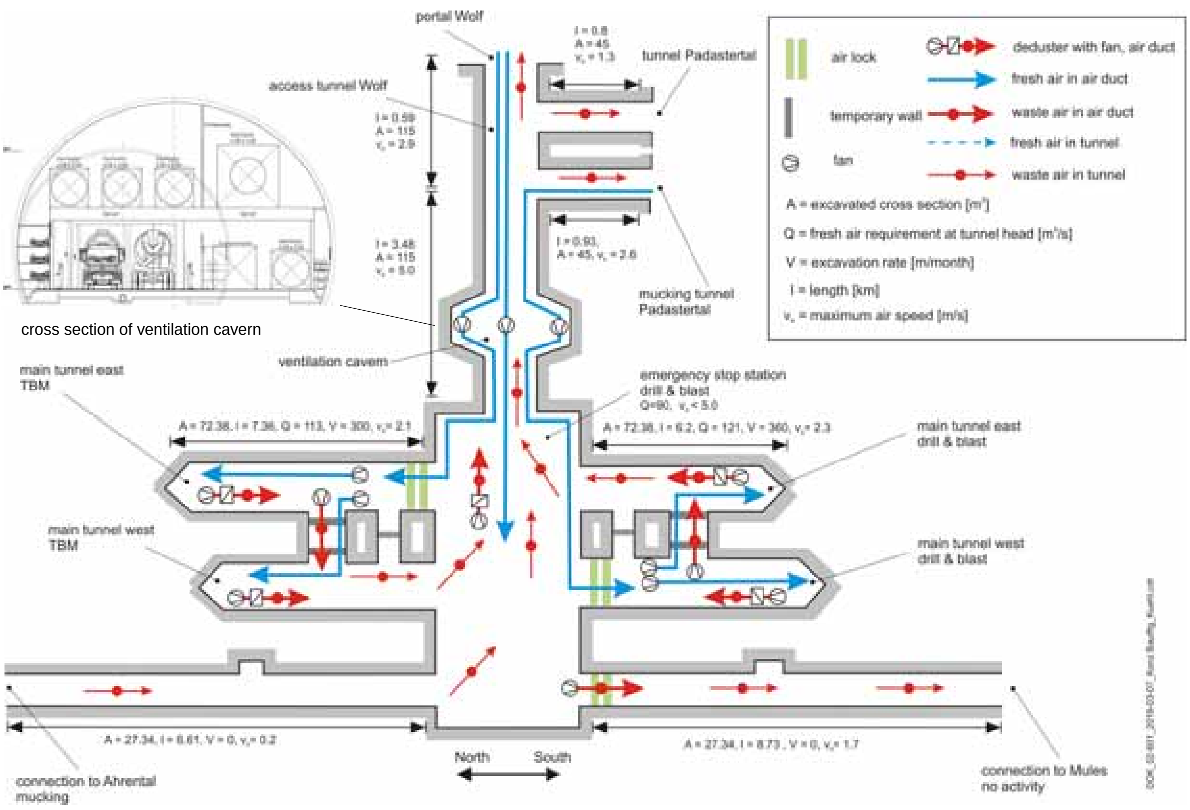

Figure 3: Ventilation concept construction lot Wolf.

5.2. Cooling

The preliminary cooling concepts of the BBT are based on the following principles:

- Local heat removal (e.g. decentral cooling): Air cooling machines are placed next to the main heat sources (e.g. at tunnel faces with main technical heat loss). Heat exchange between tunnel air and cooling water is stimulated.
- Heat transport: The heated cooling water is piped to the tunnel portal. The system of cooling pipes is split in 2 parts, the cooling water flow (supply of cold water) and the cooling water return flow (removal of warm water).
- Heat disposal: The collected tunnel heat must be released at the portals. Cooling towers (or adequate measures) establish the heat exchange between warm cooling water and ambient air.

With no major input and output of water the above defined method is called a closed circuit. This bears the following advantages:

- Comparably small water requirement
- Low impact on the ambient (e.g. no cold water removal from and warm water release to rivers)
- Widely independent from environmental impact (e.g. water shortage)

Figure 4 depicts a typical preliminary cooling concept of the BBT using the example of the construction lot Wolf. Cooling installations are generally not required if the cooling effect of the ventilation (supply of cold air) satisfies the according needs.

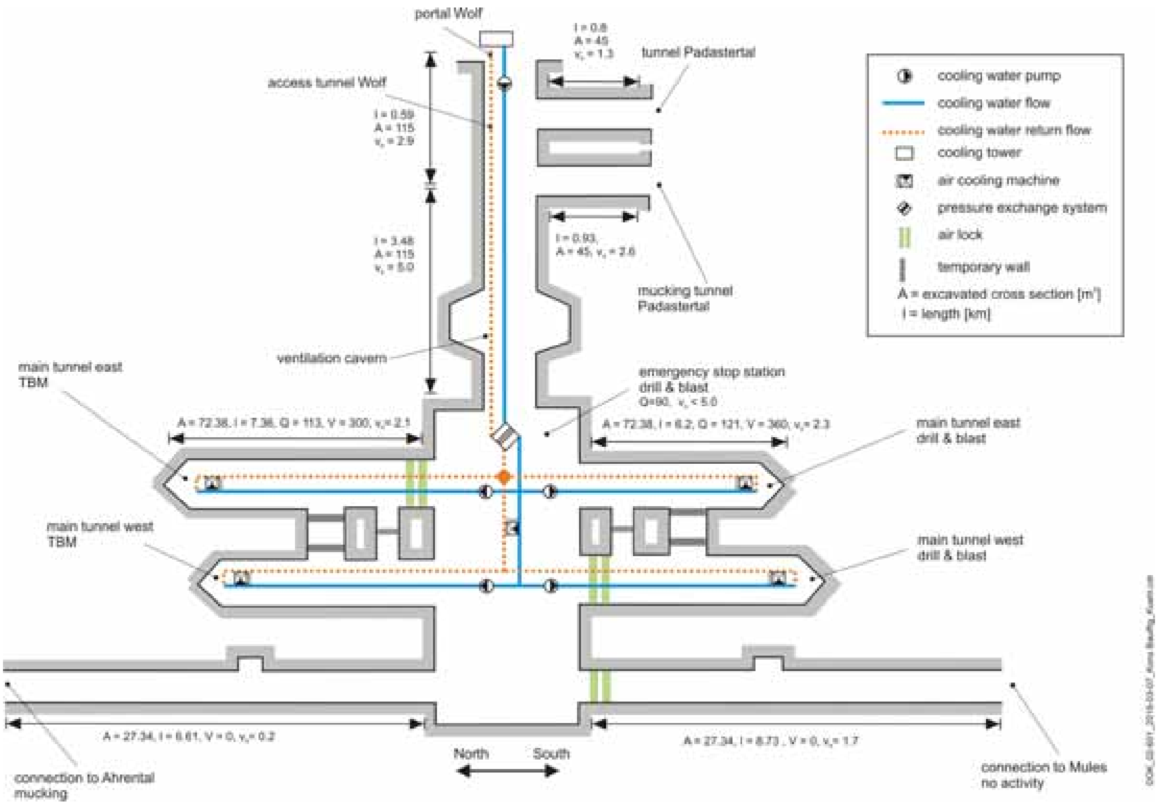

Figure 4: Cooling concept construction lot Wolf.

Cooling systems are provided for the excavations of the emergency stop station as well as for the main tunnel headings to the north and the south. The piping network consists in a primary circuit from the cooling towers at the portal to the access tunnel foot and a secondary circuit from the access tunnel foot to the tunnel faces with the air cooling machines. These circuits are driven by water pumps and separated by a pressure exchange system due to the essential altitude difference between portal and tunnel level.

6. SPECIFICATION/PERFORMANCE DATA

6.1. Ventilation

Based on the ventilation concepts particularly fans and air ducts must be specified. Usually a simulation tool with the background of SIA 1998 is adopted for this purpose.

Figure 5 exemplarily gives the relation of fan power and fan flow rate to the air duct diameter of the longest exploratory tunnel heading in Wolf. Based on the defined fresh air demand at the tunnel face different specifications are possible. While increasing the duct diameter the required fan power and flow rate can be reduced. This increase of course is strongly limited by the available space in the tunnel cross section (e.g. space requirements of transport).

The current project proposes a total of 56 main fans (in caverns or at portals), 16 auxiliary fans (at tunnel faces), about 200 km of air duct, 172 air barriers and 8 air locks for the civil construction phase of the BBT. However this number may change within executive planning.

The main fans exhibit a maximum electric power demand of about 25 MW and deliver a maximum fresh air flow of about 2’100 m^3/s to the underground.

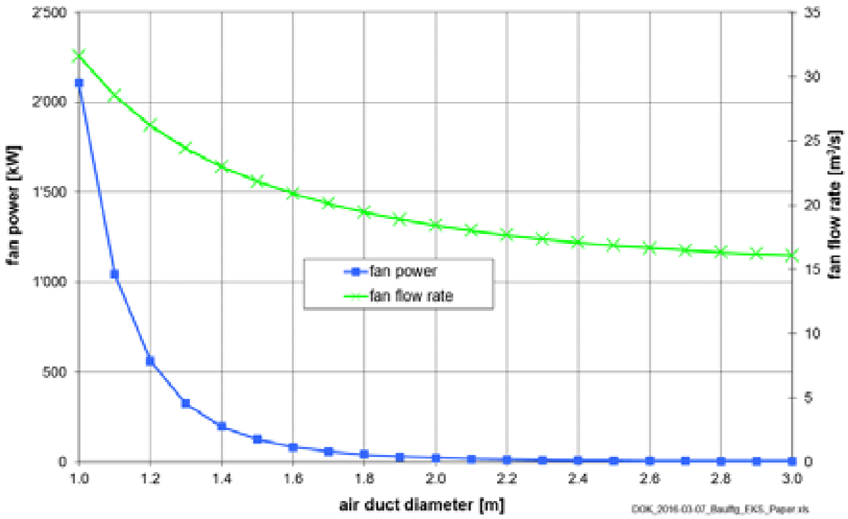

Figure 5: Calculated, possible fan power and flow rate vs air duct diameter for a given fresh air supply at tunnel face (12.5 m^3/s), ventilation of exploratory tunnel section (about 8 km), construction lot Wolf (first construction phase).

6.2. Cooling

The specification of the preliminary cooling system initiates from the mentioned cooling concepts. The main requirements for the air cooling machines, the piping network, the water pumps and cooling towers are based on tunnel climate simulations (e.g. with the numerical code BAUKLIMA of HBI Haerter). Figure 6 illustrate the calculated air temperatures along parts of the tunnel system using the example of the construction lot Wolf.

The code BAUKLIMA provides the demand and distribution of cooling power in each tunnel heading in order to fulfil the climate threshold value. Beside other parameter it considers the excavation rate and the heat emissions of all machinery (given by tunnel logistics) as well as the thermal relation between ventilation and cooling (e.g. heat exchange of air duct and cooling pipes with the tunnel air) and the heat transport in the surrounding rock. Particularly it is obvious that additional cooling must be involved mainly at tunnel faces while the rock acts as a substantial heat sink along tunnel sections.

The current concepts and specification of the preliminary cooling result in a total number of 6 cooling towers (at access tunnel portals), 94 circulation pumps, about 300 km of cooling pipe (primary and secondary circuit), 228 air cooling machines (air to water heat exchanger incl. cooling machine and fan) and 1 pressure exchange system for the civil construction phase of the BBT. This order of magnitude may change with the executive planning. The power demand of the air cooling machines sums up to a total of about 50 MW providing the underground with a cooling power of about 70 MW.

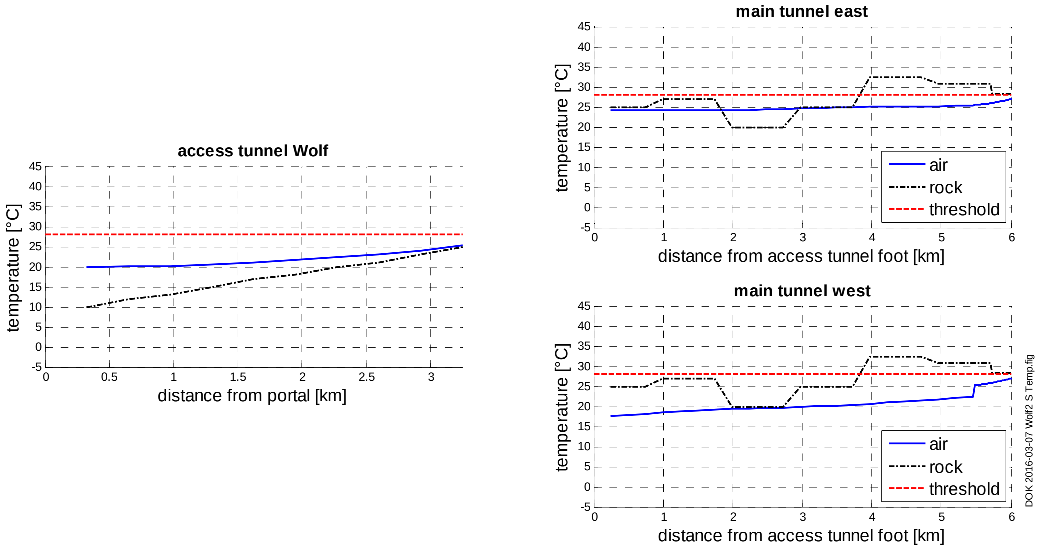

Figure 6: Calculated temperature along access tunnel and main tunnels south, construction lot Wolf.

7. CONCLUSIONS

The conception and specification of the preliminary ventilation and cooling of the BBT revealed the following main findings:

- The planed bundling of excavation methods and tunnel headings leads to substantial fresh air supply to the underground whereas the related accessibility is limited.
- Currently no major additional excavation is required for ventilation and cooling (e.g. no additional shafts and tunnels).
- Only a diligent analysis of construction sections and phases ensures an uninterrupted operation of ventilation and cooling.
- Beside the guidelines of occupational medicine the presettings of the tunnel logistics form a main basis of ventilation and cooling design.
- In order to specify and verify the preliminary ventilation and cooling systems adequate simulation tools must be used (e.g. the code BAUKLIMA) particularly considering the interaction of ventilation and cooling.
- A module based design of ventilation and cooling rather allows for changes in the construction schedule (e.g. can be adapted easier) than a fixed or centralised solution.
- Changes of the tunnel logistics relating to the preliminary ventilation and cooling must be continuously checked.

8. REFERENCES

BauV (1994): Verordnung des Bundesministers für Arbeit, Soziales und Konsumentenschutz über Sicherheit und Gesundheitsschutz auf Baustellen und auf auswärtigen Arbeitsstellen (Bauarbeiterschutzverordnung BauV), StF: BGBl. Nr. 340/1994

D.P.R. (1956): Decreto del president della repubblica (D.P.R.) 20 marzo 1956, n. 320 Norme per la prevenzione degli infortuni e l'igiene del lavoro in sotterraneo

SIA (1998): Preliminary ventilation of underground structures, Swiss society of engineers and architects SIA, guideline no. 196, 1998

THE VENTILATION AND COOLING OF LONG RAILWAY TUNNELS DURING EQUIPMENT: EXPERIENCES AND CHALLENGES ON THE EXAMPLE OF THE GOTTHARD BASE TUNNEL

S. Gehrig, T. Melchior
Pöyry Switzerland Ltd, Zurich, Switzerland

ABSTRACT

The Gotthard Base Tunnel is the longest railway tunnel built to date. The tunnel will be opened for traffic in the year 2016. For construction purposes, the tunnel was subdivided into several sections. Upon completion of the shell construction, the sections were subsequently handed over to the Railway Systems General Contractor responsible for installation of the railway infrastructure systems. These installation works required the equipment of the construction site with temporary systems, such as ventilation and cooling. The overburden with a maximum of 2'500 m and elevated rock temperatures of up to 44°C, the extraordinary length of the tunnel as well as the step-wise growing of the equipment site and the fast-moving line construction constituted demanding boundary conditions, leading to special requirements to the temporary ventilation and cooling system in order to provide an acceptable tunnel climate. The authors conducted the design of this system and accompanied the implementation and operation. The system was devised in such a way that it could grow and move with the construction process. Along with the design specification and condition-adaptable ventilation and cooling concepts, an outline of the experiences gained and challenges encountered during the planning and operation of the ventilation and cooling system, e.g. integration of permanent infrastructure installations into the system or on-site observations concerning tunnel climate objectives, is presented in this paper.

Keywords: long tunnels, equipment site, ventilation, cooling, Gotthard base tunnel

1. INTRODUCTION

The new Gotthard Base Tunnel is the world's longest railway tunnel and will be opened for traffic in 2016. Between 2007 and 2015 the railway infrastructure systems, including the slab track, the catenary, the electric power supply, cables, telecommunication and radio systems, safety and automation systems, and control systems, were installed. The tunnel owner, AlpTransit Gotthard Ltd. (ATG), assigned this task to a single general contractor, the Transtec Gotthard Consortium (TTG). Besides the aforementioned permanent systems, installation of temporary construction-site systems such as electric power supply, lighting and communications was required. For the removal of pollutants and to provide an acceptable climate for the work force, a temporary ventilation and cooling was necessary. The authors conducted the design of the ventilation and cooling system and accompanied the implementation and operation. This paper presents the challenges faced and the experiences gained by the authors and their client TTG during this task.

2. BOUNDARY CONDITIONS

2.1. The Tunnel

The railway tunnel consists of two single-track, 57 km long tubes connected by four cross-overs and 178 cross connections (Figure 1). The cross sectional area of the tubes is slightly greater than 40 m^2. The overburden reaches 2'500 m in the middle of the tunnel. Two multi-function stations (MFS) divide the whole tunnel into three sections of almost equal length: the northern (Erstfeld - Amsteg - Sedrun), central (Sedrun - Faido) and southern section (Faido - Bodio). Each MFS contains technical rooms for the railway system equipment and two emergency stations equipped with a smoke extraction (Figure 1). The MFS Faido is accessed by a 2.7 km long adit equipped with a fresh and a waste air channel, covering a difference in height of 340 m. The MFS Sedrun is accessed by two 780 m deep vertical shafts. Shaft I serves as fresh-air duct and shaft II is used as exhaust air duct under operating conditions. Ventilation stations for the operation phase are located at the entrance portal of the adit in Faido and within the shaft canopy region in Sedrun. In Amsteg, a third simple adit gives access to technical rooms and the tunnel. The tunnel connects Erstfeld in the canton of Uri (north of the Alps) to Bodio in the canton of Ticino (south of the Alps).

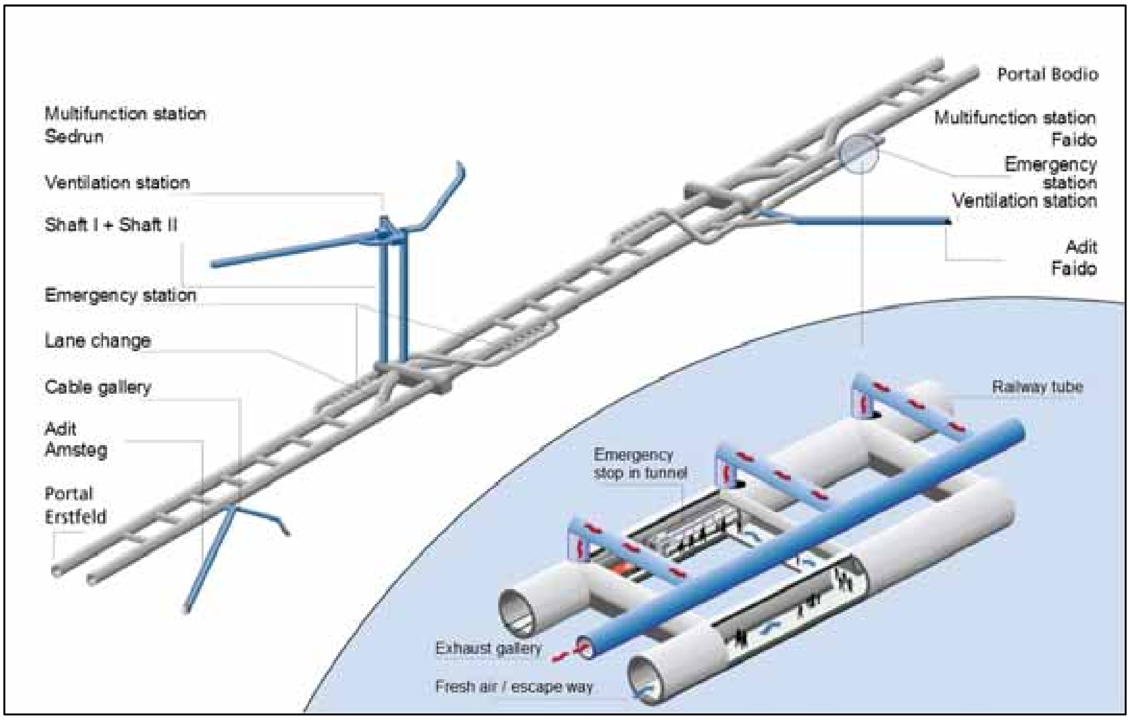

Figure 1: View of the Gotthard Base Tunnel (courtesy of AlpTransit Gotthard Ltd.)

2.2. The Equipment Work

Construction of the tunnel structure in the different sections was performed simultaneously by three different constructors. Upon completion of the main construction works, and before installation of the railway infrastructure systems, the tunnel was equipped with the technical infrastructure systems, including, amongst others, doors, gates, HVAC systems and the operational tunnel ventilation. Thereafter the various tunnel sections were handed over stepwise to the rail systems contractor TTG starting with the south-west tube between Faido and Bodio in 2010, followed by the east and west tubes in the north between Erstfeld and Sedrun in 2011 and 2012, the east and west tubes in the central section between Sedrun and Faido in 2012 and 2013, and finally the south east tube in 2014. Equipment of the tunnel with the railway systems overlapped with some of the structure construction phases. While in the inner tunnel sections construction of the tunnel structure was still in progress, the railway infrastructure systems in the outer sections were already being installed. Due to the tight time schedule, installation of tunnel and railway infrastructure systems sometimes took place simultaneously in the same tunnel section. This led the GBT construction site to be characterised by a multitude of activities of several contractors in different levels of completion at the same time and sometimes even at the same place.

From the point of view of the temporary ventilation and cooling, these simultaneities required an intense coordination with all parties working within or outside the domain of the consortium for the definition of the time schedules, the ventilation / cooling concepts and the installation sites for the temporary equipment. The complication in the ventilation and cooling system design was posed by the fact that it had to grow stepwise as the various tunnel sections were handed over to TTG.

2.3. The Machines Deployed

The main transports and heavy-duty works had to be done with diesel engine driven vehicles and machines. First the temporary installations as well as power and communication cables were installed using tyred vehicles (200 to 300 kW each). Thereafter, the slab track was installed. It was the most power consuming process that involved a rail train (1’500 kW), a sleeper train (1’500 kW), a 450 m long concrete carrier train (3’000 kW), and several smaller diesel driven machines assisting the trains (e.g. 300 kW welding machine, 30 kW concrete shuttles, etc.). In order to keep the emissions level as low as possible, once at-site, the concrete carrying train machinery could be driven electrically using the temporary power supply. Installation of the remaining systems, such as the catenary, was carried out by trains driven with somewhat smaller locomotives (approx. 700 kW) and rail cars (up to 450 kW).

The requirements to the diesel engines were very strict: They had to comply with the EU guideline 2004/26, status June 2004, and be additionally equipped with an oxidising catalyst for CO and HC, a selective catalytic reduction system for NOx and a particle filter according to the VERT list [1].

2.4. The Heat Sources

The rocks surrounding the GBT tunnel are the main heat source/sink. Along the length of the tunnel, the rocks almost approach ambient conditions in the close proximity of the tunnel portals and attain the core temperatures of almost 44 °C in the central region of the tunnel characterised by high overburden. This heat load can reach up to 11 MW per tube. However this figure varies strongly depending on the ventilation strategy and transient phenomena. During intensive work phases, the concrete curing process for laying the slab track and other machines used in the GBT can add up to 0.4 and 1.7 MW of heat load respectively per tube.

2.5. The Requirements to the Ventilation and Cooling

The main goal of a tunnel equipment site ventilation is to provide salubrious working conditions by removing pollutants (e.g. diesel emissions, dust particles), and introducing fresh air to the working sites. Considering the extreme thermal conditions, additional tunnel cooling becomes inevitable. Temporary ventilation system may be adapted to provide sufficient ventilation in case of an emergency such as fire. The dilution of natural gas is not an issue in the GBT, as such gas sources are not found therein. The ventilation had to comply to the SIA guideline 196 [2] which demands the provision of 2 m^3 of fresh air per minute per nominal diesel engine power for normal transports and 4 m^3 of fresh air per minute per nominal diesel engine power for heavy duty stationary engines. Moreover the air velocity in the tubes have to remain within a working band of 0.3 $m \cdot s^{-1}$ to 5 $m \cdot s^{-1}$, thereby limiting the volume flow of the system to 200 $m^3 \cdot s^{-1}$ at the most (based on the mean tunnel cross sectional area). This was in accordance with the maximum installed diesel power per ventilation line.

Further the climatic design goal for the cooling system prescribed by the owner was a maximum of 28 °C dry-bulb temperature in the working section. In practice however, the temperature limits set by SUVA guidelines [3] were followed which prescribe that up to a wet bulb globe temperature (WBGT) of 28°C no limit on the type of activity is necessary. Between a WBGT of 28° and 30°, only light works should be permitted. Above a WBGT of 30°C no work should be allowed. In addition to the thermal and flow conditions, the air quality (emissions, dust and hazardous gases) need to be monitored.

3. THE EQUIPMENT SITE VENTILATION SYSTEM

The main fans of the equipment site ventilation system had to be designed to cope with large pressure differences between portals crossing the alps, strong buoyancy effects, especially at the shafts in Sedrun, and the piston effect of trains used on the equipment site. The maximum speed of trains was limited to 40 km/h during the equipment phase. The equipment site ventilation stations were always equipped with two parallel operating reversible fans (approx. 600 kW each), thus reducing the risk of a non-ventilated tunnel section. The fans had 2 stages; they were fully reversible, designed to convey each 100 $m^3 \cdot s^{-1}$ and driven by a frequency converter. As the tunnel was handed over stepwise to TTG, the ventilation system was successively extended, featuring a total of 8 main fans in its final phase.

In the early phases, circulation ventilation systems were installed in the outer tunnel sections, with fans being positioned in cross connections. These fans sucked in the fresh air from one portal and exhausted the air via the neighbouring portal. Lock gates were installed at the boundaries towards the inner tunnel sections in order to avoid interference with the tunnel constructors' ventilation systems. The northern circulation system was extended to about halfway through the tunnel by the time the first part of the central section was handed over to TTG. Fans that were previously installed in cross sections were moved to the emergency stations in the MFS Sedrun and two new fans were added to the system. Each emergency station was equipped with two fans, one in the exhaust gallery and one in the escape way. As the temporary ventilation system should not cause an obstruction to the installation of the permanent infrastructure, the installation of the fans in the emergency stations proved to be the best trade-off. This however required the installation of gates in the tunnel tubes, one per emergency station. The design of these gates demanded a significant coordination effort, as they had to allow the installation process in the tunnel cross section (slab track, catenary, handrails, …) and at the same time reduce air flow leakages to a minimum. Additional gates and locks were installed in the galleries of the MFS. Further various components of the permanent technical infrastructure, such as the escape doors in the emergency stations, were integrated into the control system of the construction site ventilation.

With the handing over of the second part of the central tunnel section, TTG became responsible for the ventilation of the complete GBT. The MFS Faido was equipped with ventilation components similar to the MFS Sedrun. Thereafter each tube was ventilated with a longitudinal mode of ventilation (portal to portal as shown in Figure 2).

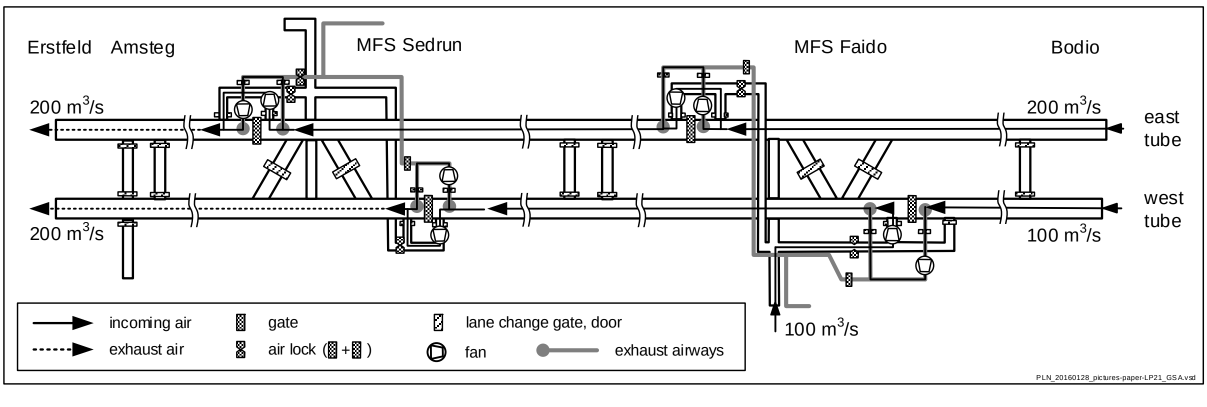

Figure 2: Whole tunnel ventilation system in its greatest extension

In its greatest extension, the ventilation system counted 8 main fans and 25 gates in the tubes and the MFS. It used numerous doors and gates from the permanent installations. Auxiliary structures, for example the shaft head in Sedrun or various galleries in the MFS, were ventilated by smaller fans, partially using flexible air ducts, not shown in Figure 2. At this stage the system was very versatile: as the fans were reversible, it was possible to reverse the main flow direction in the tunnel tubes. Further it was possible to inject fresh air in the tunnel tubes through the adits in Sedrun and Faido, which proved to be very helpful when occasional temperature peaks occurred. Additionally each section of the tunnel could be ventilated separately. This flexible system allowed for quick adjustments to effectively ventilate the fast moving equipment site.

4. THE EQUIPMENT SITE COOLING SYSTEM

4.1. System Choice

TTG had the requirement to reuse as far as possible the cooling systems of the constructors. This led the system choice to a cooling water cycle with mine air coolers (MAC) common for underground construction sites. In such a system, the tunnel air is chilled on the working site using the coolers. These yield there waste heat to the water cycle, which brings it above ground. There the hot water is cooled down in open cooling towers near wet-bulb temperature and re-injected in the cycle again. The temperature of the transported water ranges between 20 °C to 38 °C with a temperature difference over the condenser of the MACs between 10 °C to 12 °C. The installed MACs had a net refrigeration capacity of 420 kW each.

4.2. Constitution of the Cooling System

Respecting the technical and time constraints, the cooling mechanism was sub-divided into a) “cooling GBT north” – i.e. from Erstfeld to Sedrun – and b) “cooling GBT south” – i.e. from Sedrun to Bodio (cf. Figure 3).

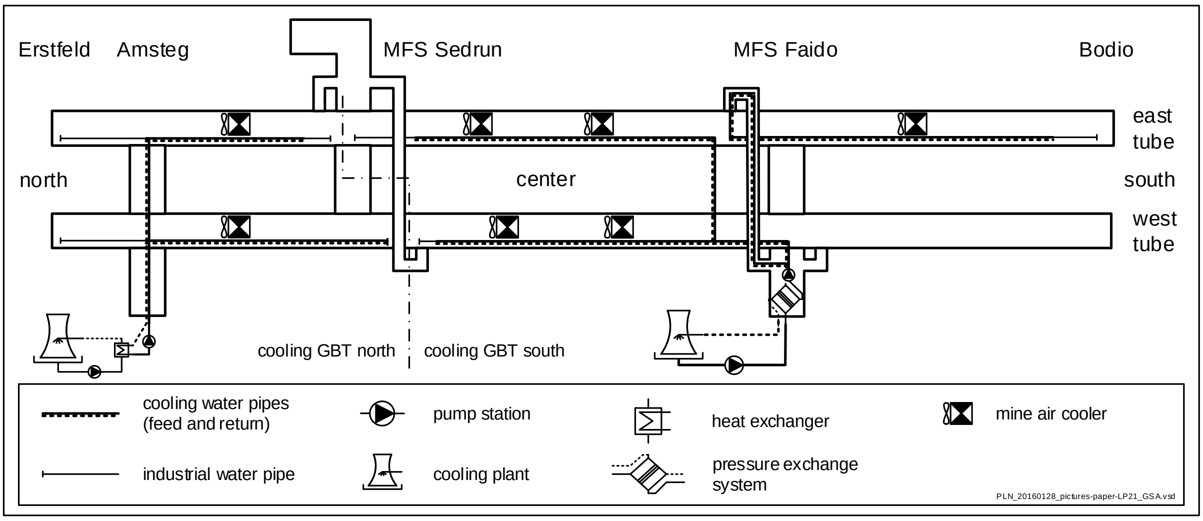

Figure 3: Equipment site cooling of the GBT. The number of MACs represented does not correspond to the reality

In the preliminary cooling phases, the south-west part of the tunnel was cooled and fed with industrial water acquired by the extension of the tunnel constructor’s cooling system from Faido. Once it came to the cooling GBT north, a completely new system was built as the constructor’s cooling system needed to be totally dismantled. This builder had severe problems with clogging pipes, which was attributed to bad water quality. For this reason the newly devised system had two water cycles separated by a plate heat exchanger above ground. The open primary cycle disposed the waste heat directly to the atmosphere in cooling towers. The closed secondary cycle ramified back into the tunnel. It was equipped with a combined air eliminator/dirt separator so as to remove oxygen and dirt from the cycle. These measures remediated the problems seen with the previously installed cooling system.

In the final stage, the already installed cooling system in the south was taken over and adapted to TTG's needs. The backbone of this open system was the primary cycle with its cooling plant located above ground level and its pressure exchange system in the MFS Faido. The later allows to pass water from the primary cycle at high pressure (PN40) to the secondary cycle at low pressure (PN25) and back. It was necessary because of the great height difference along the adit.

The refrigeration, cooling and pump capacities are listed in Table 1.

Table 1: Refrigeration and cooling capacity of the equipment site cooling GBT

Parameter	Cooling GBT north	Cooling GBT south
Max. requested refrigeration capacity in tunnel, MW	8.4	11.8
Max. requested cooling capacity in tunnel, MW	11.4	16.0
Cooling capacity available at cooling plant, MW	11.4	21.0
Pump capacity available at cooling plant, $m^3 \cdot h^{-1}$	800	1'120
Max. number of MACs includable	20	28

The water pipes in the tunnel tubes were mainly DN 400 plain steel pipes without corrosion protection. Both feed and return lines were installed on the outer kerbside in a very tight clearance gauge. In order to allow for maintenance, these lines were fitted with gate valves at intervals of about 2.5 km. The MACs were mounted at the tunnel wall above the pipes. Connections to the water cycle and the temporary power supply were provided at every second cross connection. The coolers were distributed and relocated according to the refrigeration need of the sites.

5. EXPERIENCES AND CHALLENGES DURING DESIGN AND OPERATION

The following sections present some of the challenges faced and the experiences gained by the authors and their client during the planning and the operation of the ventilation / cooling.

5.1. High coordination effort

The consortium counted thirty lots. Sixteen more relevant lots were counted outside of the consortium. At first, the existence of any possible interfaces among the lots was investigated. A total of 24 lots were identified to have an interface with the lot "equipment ventilation and cooling". For each of these lots, the interfaces were described in a document that had to be regularly revised as the project proceeded. The lots directly relevant to the ventilation/cooling were the northern, central and southern constructors, TTG's temporary power supply and logistics and several permanent lots inside TTG: In order to dimension the equipment ventilation/cooling, their working processes had to be thoroughly analysed and catalogued. Conflicts between temporary ventilation/cooling components, operating machines and permanent installations had to be recognized and solved both temporally and spatially. The time dedicated to these coordination efforts amounts about half the total planning time.

5.2. Integration of permanent equipment into the temporary ventilation

As the equipment phase of GBT lasted several years, permanent equipment like doors, gates and the ventilation of the tunnel and the cross connection might remain unused for a long time until the beginning of the tunnel operation. For certain equipment and devices such as electromechanical equipment, a regular maintenance is necessary. This was the case e.g. for the ventilation of the cross connections, where ATG licensed TTG to not only use the equipment but even to embed them into its temporary tunnel control system. In general it is advisable to integrate permanent ventilation elements into the temporary ventilation where available in order to reduce additional maintenance and avoid the installation of parallel temporary systems.

5.3. Ventilation supports cooling

The ventilation system was dimensioned based on the fresh air requirements per kW nominal diesel power prescribed by SIA196. During operation, the concentration of the pollutants CO, NO and NO_2 were monitored and compared to the legal occupational exposure limits (OEL). It was found that these concentrations were far below the OEL most of the time, except for short episodes that could be related to some processes of the slab track or the use of engines not conforming to the requirements. The ventilation design based on SIA 196 contains therefore a large reserve with respect to the OEL. The ventilation was nevertheless not oversized, as the experience with the climatic requirements has shown: The high flow rate resulting from the requirements on emission dilution supported a lot the cooling, especially in the central section. The effect was strong, as was noticed “in absentia” during longer interruptions of the ventilation at the transition from one ventilation system to another. During the joint operation of the ventilation and the cooling, the operating goal of 28°C WBGT could be easily kept most of the time. The dry cooling was then not used to capacity. Thus the ventilation was slightly oversized with respect to the OEL but well sized with respect to cooling.

5.4. Sizing of the cooling

The cooling was designed for 28 °C dry-bulb temperature but operated following the WBGT index. The design requirement arose from the SUVA guideline [3], which rests on the assumption of a frequent relative humidity of 100%. Actually, the tunnel is sealed against water seepage for its complete length. As a result, the measured humidity in the central tunnel section was very low i.e. about 30% (median value). Air at this relative humidity and 28° WBGT has a dry-bulb temperature of about 38 °C. This difference in assumed and actual relative humidity explains clearly the oversizing in cooling system. In the central tunnel section, the design specified at most 17 MACs running simultaneously to temperate the climate. In practice, 10 to 15 MACs were observed to suffice the cooling demand.

5.5. Climatic conditions during transition periods

Periods of transition between project and ventilation phases often came along with a loss of control on the air flows and local overheating that could not be avoided. The following examples show this. At the beginning of the equipment work, the ventilation and cooling have first to be built in and commissioned. The teams mounting the temporary equipment in the central section therefore had to work in a very hot environment. At the end of the equipment, the ventilation and cooling have inevitably to give way to final works. This forced TTG to dismantle the ventilation and the cooling before the end of the equipment.

5.6. Design of cooling water cycle

The southern secondary water cycle remained opened to atmospheric air and had only gross filtering means. The northern secondary cycle was not only closed but also equipped with an air eliminator/dirt separator. This difference in design led in the south to rusty incrustations growing to a few centimetres on the pipes’ surface whereas in the north, no major corrosion was observable. This difference is attributed to the abundance resp. the lack of dissolved oxygen in the cooling water. These incrustations are detrimental during operation as they increase the flow resistance in the hydraulic system. In order to resell the temporary installation, a proper treatment becomes inevitable for the case of corrosion affected parts thereby impacting the cost/price ratio.

5.7. Alternative cooling concepts

One of the main factor in deciding about the cooling system was the availability and re-use of a partly/fully working cooling system installed in earlier construction phases. Although it appears to be a cost efficient methodology, several factors challenge the use of an already installed construction site cooling system. For example:

a) Several disruptions of the cooling GBT south were related to the age of its backbone.

b) The equipment phase of the tunnel grows at a faster speed over the complete length of the tunnel compared to construction phase which is more localized. This feature led to the fact that either additional MACs were employed or they were displaced often.

c) Almost 25-30% of the cooling capacity needed in the retained solution arose from the heat input of the MAC's compressors themselves.

d) MACs need a power supply thereby demanding appropriate sizing and placement of the cables and transformers along the complete length of the tunnel beforehand. This in-turn adds to the heat load.

An efficient cooling methodology could have been one with a chilled water cycle instead of a cooling water cycle: The water is chilled down to 1-4 °C with an efficient central refrigeration plant above ground and then pumped into the tunnel. There it gets the air cooled down as it flows through the pipes. This system is realised e.g. for the in-operation cooling of the Channel Tunnel. The application of this system was discarded for GBT mainly due to the prohibitive price and space requirements of insulated steel pipes. Recent developments by a Polish company showed the use of plastic pipes with pressure specification up to PN 40 at diameters up to DN 400 with reasonably good insulation level. This new type of pipe system in combination with conventional steel pipes would allow to build chilled water cycles that insulate at low space requirement and effectively cool the intended locality.

6. CONCLUSION

This paper presented the challenges faced and the experiences gained by the authors and their client during the planning and the operation of the equipment site ventilation/cooling of the GBT. Design specifications including various concepts employed to improve the flexibility of the system are presented. This paper outlines that the systems devised and used were capable to adapt to an environment with parallel running processes. Furthermore, some of the experiences gained and challenges encountered during the planning and operation of the ventilation and cooling system are also highlighted.

7. ACKNOWLEDGEMENTS

The authors would like to pay their gratitude towards the company AlpTransit Gotthard Ltd. and the Transtec Gotthard Consortium for authorising to publish the content of this paper.

8. BIBLIOGRAPHY

[1] VERT-Filterliste, Geprüfte und erprobte Partikelfilter-Systeme für die Nachrüstung von Dieselmotoren, Bundesamt für Umwelt, Wald und Landschaft (BUWAL), Bern, Dezember 2005.

[2] Schweizerischer Ingenieur- und Architekten-Verein, SIA 196, Baulüftung im Untertagebau, Zürich, 1998

[3] SUVA, Schweizerische Unfallversicherungsanstalt, Abteilung Arbeitsmedizin, Arbeitsmedizinische Prophylaxe bei Arbeiten im Untertagebau im feucht-warmen Klima, März 2003, Bestellnr. 2869/26.d

INVESTIGATING DIFFERENT OPERATIONAL SCENARIOS FOR THE PROPOSED EMERGENCY VENTILATION SYSTEM IN FURKA TUNNEL

Rehan Yousaf, Tom Melchior
Poyry Switzerland Ltd.

ABSTRACT

Furka tunnel is a 15.4 km long tunnel located at about 1500 m above sea level connecting the Cantons of Uri and Wallis in Switzerland. As part of the tunnel refurbishment project namely "Update Furka", the operators "Matterhorn Gotthard Bahn (MGB)" have to adapt the tunnel to the actual operational and safety standards e.g. constructing evacuation pavement, handrails, installing lighting and signals inside the tunnel etc. to be completed by the year 2022. During the complete renovation phase, the tunnel shall be un-interruptedly used by passenger and vehicle transport trains. Given economical and topological constraints, a longitudinal ventilation of the tunnel in case of emergency was proposed and put forward to the Federal Office of Transport (FOT), the authority with jurisdiction (AHJ) for approval. This paper presents different operational scenarios i.e. types of trains, their running combination in the tunnel network, different portal conditions, ventilation strategies varying from one fire scenario to the other etc., investigated for the proposed longitudinal emergency ventilation system.

Keywords: ventilation design, piston effects, smoke propagation, evacuation, numerical simulations

1. INTRODUCTION

Furka tunnel is mainly considered as a single tube single track tunnel with the exception at two crossing junctions which allow the presence of up to four simultaneous trains. One of the crossing junction namely "Geren", that runs for a length of about 900 m is a single track twin tube section whereas the crossing junction "Rotondo" is a single tube double track section comprising 915 m of length. The cross sectional area and shape of the tunnel varies along the length of the tunnel as shown in the Figure 1.

An originally planned access gallery "Bedretto" is located approx. mid-way of the tunnel. This gallery however is non-accessible at present. Two axial fans are installed in the niche, half way of the tunnel near to this gallery. A door is installed at the axial fan niche. In case of a fire emergency, the door is closed and the air is pushed via the fans in one or the other direction of the tunnel. A defined longitudinal flow due to piston effect of trains cannot be guaranteed due to travelling of trains in opposite directions, stopping at cross connections and specific geometrical conditions of the tunnel. The tunnel is planned to be subdivide into 8 blocks in terms of the control strategy, thereby allowing an intentional interrupting of the power supply in one or more blocks in case of a fire.

The tunnel is used by "Regional trains (RE)", "Vehicle transport trains (A)" and special trains namely "Glacier Express (GEX)" with maximum speeds of 65, 80 and 65 km/h respectively. Considering the standard train time table, a maximum of 2 trains can be present in the tunnel for about 83 % of time. All the "A trains" running through the Furka tunnel are equipped with two locomotives i.e. at front and rear of the train.

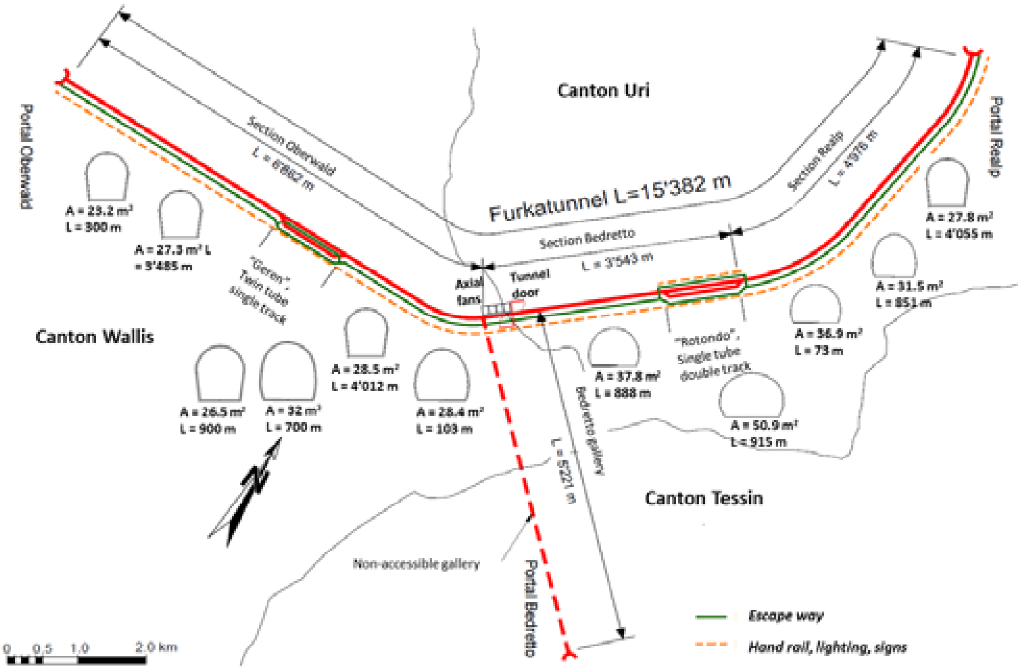

Figure 1: Diagrammatic layout of Furka tunnel

2. GOAL AND OBJECTIVES

The investigations undertaken during the course of this project are aimed to:

a) Provide a proof of the proper functionality of the proposed ventilation system
b) Highlight the short comings in the evacuation process in case of a fire emergency
c) Evaluate the aero- thermodynamic conditions for the critical most scenario using 1- and 3-dimensional "Computational Fluid Dynamics (CFD)" simulation
d) Provide recommendations for the detailed rescue planning

In order to attain the above mentioned goals, both 1- and 3D numerical simulation were conducted to investigate the air flow, smoke propagation and temperature distribution for different operational scenarios.

3. METHODOLGY

As starting point for the investigation, a distance vs time plot was devised. This plot is based on the normal and emergency operational concepts including the self- and assisted rescue phases. A 1-D network model for the complete tunnel was generated using the software IDA Tunnel [1]. For each of the investigated scenarios, the 1-D simulations provide the temporal and spatial information about the flow velocity and smoke propagation. As 1-D simulations cannot capture the effect of thermal stratification and back-layering effects, a transient 3-D simulation was carried out using the 3-D CFD software STAR CCM+ [2] for the worst scenario (based on the 1-D simulation results).

4. FIRE SCENARIO AND EMERGENCY VENTILATION

For the current project, the emergency ventilation is activated only for a stationed fire on a train/transported vehicle. In principal any train on fire has to follow the directive of "driving out of the tunnel". Nevertheless, in case of an accidental still stand of the emergency train, the position of fire on the train elects the ventilation strategy i.e. a) if the fire located at front of the train, the emergency ventilation impels the flow in the direction of travel, b) if the fire is located at the rear of the train, the emergency ventilation impels the flow in the direction opposite to direction of travel. The heavy vehicles being prone to high fire loads, can only be parked in the front or rear of the vehicle transport train section whereas the passenger cars are parked in the middle section of the train. Considering the above facts, the probability that a fire breaks out in the middle of the train, leading to a train still stand inside the tunnel is very low. Considering the tunnel geometry, fire possibilities and the train time table, different fire emergency scenarios were investigated during the course of the project. For the current paper only two major scenarios (and their variations) are presented as shown in Table 1.

Table 1: Definition of different emergency scenarios

Nr.	Scenario	Description
1	Standard	Five different operational variations considering standard geometrical section (single tube single track) with 1 or two trains in the tunnel system, with positive as well as negative influence of portal pressure on tunnel air flow.
2	Low air flow	Emergency in the section Geren in tube with smaller cross sectional area (does not form ventilation design basis)

For all the above mentioned cases, the fire is considered to take place on a truck located on the vehicle transport train.

5. ASSUMPTIONS AND BOUNDARY CONDITIONS

The following sections give an overview of the different assumptions and boundary conditions used for the investigation.

5.1. Numerical Modelling

For a 1-D investigation, the simulation covered two hours of normal traffic flow in order to account for proper initial flow field. The simulated flow velocities were compared with the actual measurements to validate and calibrate the numerical model. For the 3D simulation, only a part of the tunnel (critical section Geren) is modelled with boundary conditions taken from the 1-D simulations so as to correctly predict the air/smoke movement and the presence/absence of thermal stratification. For the 3-D flow simulation, the turbulence was resolved using a “Two-Layer-k-ε” turbulence model on a computational mesh of about 4 M cells. Radiation effects were modelled using the “Discrete Transfer Radiation”, with air as participating media for radiative heat transfer.

5.2. Tunnel geometry

A detailed 3-D scan was conducted for the complete tunnel and the data was mathematically analyzed to subdivided the tunnel into 10 segments (in terms of area) with 3 different tunnel profiles i.e. horse shoe, elliptical and circular (see Figure 1). The tunnel lining is very rough thereby requiring experimental investigations of the wall roughness in the tunnel. A value of 0.066 was found for the wall roughness coefficient.

5.3. Climatic conditions

Based on the meteorological data [3], a portal pressure of ± 200 Pa (95%-value) was used. Simulations were conducted for different ambient temperatures i.e. for an yearly average temperature of 5°C, summer with 20°C and winter with -15°C. In order to account for the thermal gradient in the tunnel wall, the tunnel was modelled as semi-infinite wall with a core temperature of 20°C (based on an iterative simulation approach by taking into account the long term temperature measurements).

5.4. Train data

Train data relevant for the investigation is presented in Table 2. The data is obtained either from previously conducted experimental work or from the train manufacturers.

Table 2: Outline of train data used in numerical simulations

<table>
<tr><th>Train type:</th><th>Vehicle transporting</th><th>Regio.</th><th>Fire fighting</th><th>Paramedic</th><th>Evacuation</th></tr>
<tr><td>Train length [m]</td><td>263.7</td><td>105.4</td><td>19.2</td><td>19.4</td><td>69.2</td></tr>
<tr><td>Cross-section area Locomotive [m^2]</td><td>9.1</td><td>9.1</td><td rowspan="2">8.0</td><td rowspan="2">8.6</td><td>9.1</td></tr>
<tr><td>Cross-section area of coach [m^2]</td><td>3.0</td><td>8.6</td><td>8.6</td></tr>
<tr><td>Coach parameter [m]</td><td>14.0</td><td>13.3</td><td>15.0</td><td>14.0</td><td>13.3</td></tr>
<tr><td>Hydraulic resistance coefficient. c_f [-]</td><td>0.0286</td><td>0.0075</td><td>0.013</td><td>0.013</td><td>0.0075</td></tr>
<tr><td>Head and tail loss coeff. $\zeta_h+\zeta_t$ [-]</td><td>2.6</td><td>1.3</td><td>1.3</td><td>1.3</td><td>1.3</td></tr>
</table>

5.5. Axial fan

In order to correctly estimate the flow conditions in the tunnel, the fan characteristic curve as provided by the manufacturer was implemented in the IDA tunnel software. The tunnel door was modelled to allow air leakage as a function of pressure difference (10.5 m^3 s^{-1} for a pressure difference of 5’500 Pa, varying linearly down to zero with zero pressure difference).

5.6. Fire and smoke

The fire is assumed to grow linearly from 0 to 30 MW in 5 minutes and remains constant for the simulation time. In 1-D simulations, the fire is modelled as a moving source of heat and smoke. As 3-D simulations are carried out for a still standing train, the fire and smoke sources are modelled as stationary volumetric source (1 MW m^{-3}). In order to account for the thermal and smoke propagation effects in 3-D simulation prior to the still-stand of the train, a fictive minute is simulated to match the actual gradient of heat and smoke release rates. The boundary conditions for this fictive minute are taken from the results of 1-D simulations. The heat release rate was assumed to be 36 kJ g^{-1} with a smoke yield factor of 0.052. Based on the guidelines [4], the mass specific extinction coefficient (k_m) of 7600 m^2 kg^{-1} is used. The transport equations solved by the 3-D CFD simulation gives the mass concentration (m) of smoke which in turn is converted into visibility using the formula $ibility\ [m] = \frac{8}{m \times k_m}$, where 8 is an experimentally obtained coefficient for light emitting signs [5].

5.7. Timeline

Considering the beginning of fire as start time "t_A", it is assumed that the fire remains undiscovered for about half a minute. It takes another half minute in case of a truck fire to reach the fire power of 3 MW, at which the locomotive is assumed to be out of order for driving the train out of the tunnel (t_B). The train comes to rest with a deceleration rate of 0.62 m s^{-2} at time t_C. Communication with the personal on board the train and fire localization is considered to take another 2 minutes before the driver contacts the tunnel control centre thereby reaching at a time t_D. The contact and reporting time of another 0.5 minute leads to a time t_E where the tunnel control centre signals a stop for any train approaching the tunnel and a reduction in speed, down to 40 km h^{-1} of train(s) leaving the tunnel. At the same time t_E, the tunnel door starts to get closed. Ventilation is started once tunnel door is closed. Within 40 minutes from the time of alarm, fire-fighting trains enter the tunnel (t_F), followed by paramedic trains at time t_G and evacuation train at time t_H. The times where an evacuation and paramedic train runs back out of the tunnel are named as t_I and t_J respectively. A typical time line with one emergency train (fire located in front) and an opposing train is shown in Figure 2. Trains represented by dotted lines enter the tunnel only upon the instructions of the officer in-charge and the entry times may vary depending upon the conditions.

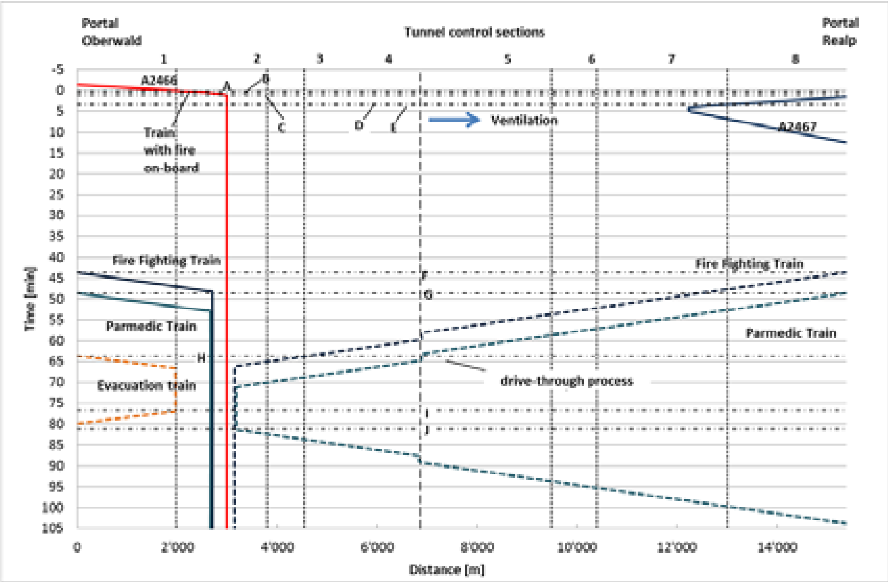

Figure 2: Typical time line showing train movements in the tunnel network

Once started, the emergency ventilation fans are assumed to reach their full capacity within 1 minute. The tunnel door is assumed to take 1 minute to completely open or close. In case trains have to pass through the door, additional 15 and 45 seconds are assumed for the approval and “drive-through” processes respectively. Depending upon the scenario under investigation, different trains along with their position in the tunnel can be plotted on the time line chart.

6. RESULTS

The time line chart for each of the investigated scenario and variation served as input for the simulation. The time line notation shown in Figure 2 is used consequently to explain the simulation results. The effect of fire, train movements, ventilation etc. on airflow and smoke spread in the tunnel are shown from the point of ignition of fire until the first 15 minutes that are crucial for initial self-rescue phase.

6.1. Standard Scenario

For a standard scenario, different variations were investigated i.e.

- Variation 1 (V1): 1 emergency train with fan adverse portal pressure and fire at front.
- Variation 2 (V2): Same as V1 but with fan assisting portal pressure.
- Variation 3 (V3): Additional train with fan adverse portal pressure and fire at front.
- Variation 4 (V4): Same as V3 but with fan adverse portal pressure and fire at rear (i.e. reverse ventilation direction).
- Variation 5 (V5): Operational improvements to V3.

The results of the 1-D simulation variations V1 to V5 are shown in Figure 3 and Figure 5 as velocity curves and as smoke contours for a visibility level of 10 m in Figure 4 and Figure 6.

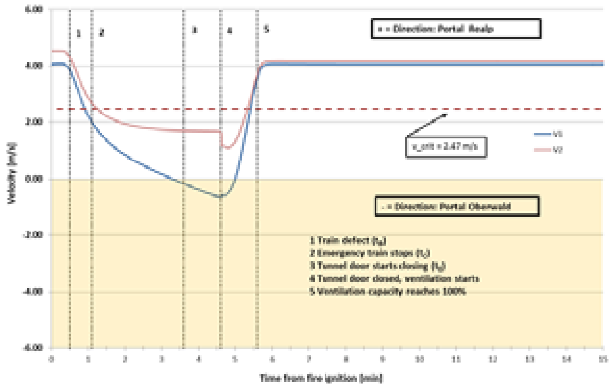

Figure 3: Air velocity in tunnel at 2'500 m from portal Oberwald for standard scenario variation 1 & 2.

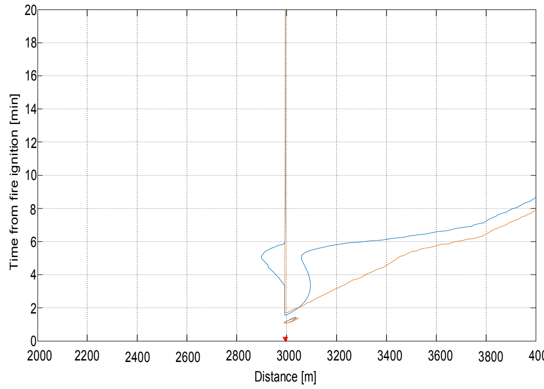

Figure 4: Smoke contour for standard scenario variation 1 & 2.

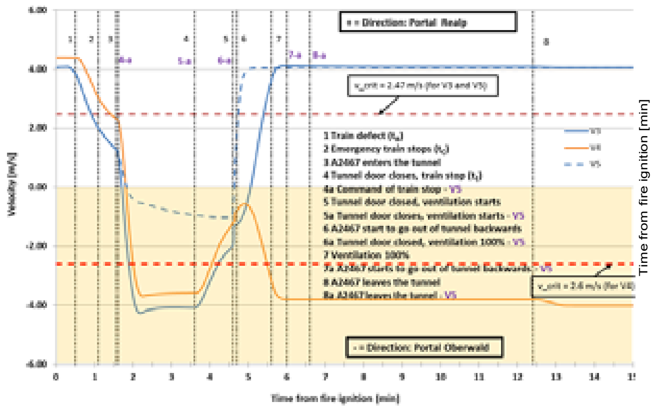

Figure 5: Air velocity in tunnel at 2'500 m from portal Oberwald for standard scenario variation 3, 4 and 5.

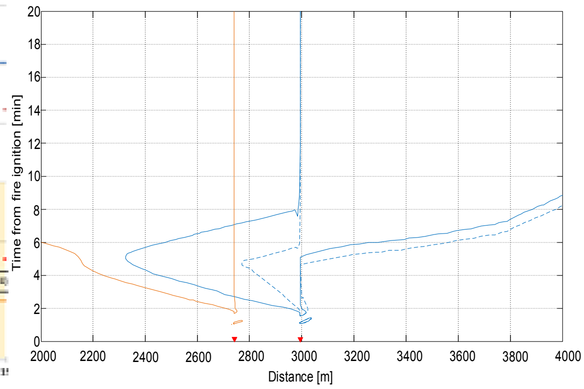

Figure 6: Smoke contour for standard scenario variation 3, 4 and 5.

An air flow reversal is observed for variation 1 due to portal pressure difference, with velocity falling well below the critical velocity limit (between pt. 1 and 4). This flow reversal causes the smoke to travel towards the rear of the train. Once the tunnel door is closed and axial fan is started (pt. 4), the air (as well as the entrained smoke) is pulled back towards the front of the train blowing the smoke and hazardous gases downstream of fire (see Figure 4). On the contrary to variation 1, simulation results of variation 2 with a fan assisted portal pressure of 200 Pa does not show any flow reversal after the emergency train has come to rest. Considering the fact that the critical velocity is not reached, a certain level of back-layering is expected. Such back-layering effects are not depicted by the 1-D simulation results.

With fire position as in variations 1 and 2 (approx. 3000 m from portal Realp), results of variation 3 show the effect of a vehicle transport train "A2467" entering from the portal Realp (pt. 3 in Figure 5) (travelling opposite to the emergency train). The result of this train movement has a pronounced negative effect as it propagates the smoke to almost 700 m upstream of fire (seen as solid blue line in Figure 6).

In variation 4, the fire is located at the rear of the train. For such a case, the air needs to be pushed out via the portal Oberwald. The non-emergency train "A2467", which enters the portal Realp (pt. 3 in Figure 5) creates a positive impact on the ventilation goal. Once it stops (pt. 4 in Figure 5), the flow velocity falls rapidly below the critical velocity. After the tunnel door is closed and ventilator is started (pt. 5 in Figure 5), the standing train A2467 starts to drive against the fan’s flow direction causing a further decrease in flow velocity in tunnel (pt. 6 in Figure 5). Once the fan is running at its full capacity (pt. 7 in Figure 5), a flow velocity higher than required critical velocity towards portal Oberwald is achieved. A slight increase in this flow velocity is observed as the train A2467 leaves the portal Realp (pt. 8 in Figure 5).

Based on the results of simulation variations 1-4, two operational improvements were devised i.e. a) the driver contacts the control centre as soon as the train comes to a stop and the control centre sends out a “stop-signal” for the rest of the trains within 0.5 minutes, b) the ventilation fans should be started simultaneously with the closing of the tunnel door. The effect of these operational changes are simulated in variation 5. The results show that even though, a complete flow reversal could not be avoided, the extent to which the smoke gets propagated is decreased (from 700 m to 200 m) upstream of fire (see Figure 6).

6.2. Low air flow scenario

This scenario is a replica of standard scenario variation 4 with the exception that the train on fire comes to a stop inside the section “Geren” in the smaller cross section tube. The results are plotted for air velocity upstream of fire in the twin tube single track as well as inside the single track single tube section before the tunnel section “Geren” for the first 25 minute after the breakout of fire (see Figure 7). The results show that even after the train “A2467” has left the tunnel and the fans run at their full capacity, the required critical velocity cannot be achieved in the double tube section. This would lead to a constant back-layering phenomena.

A 3-D CFD simulation was performed to evaluate the intensity of this back-layering. CFD results in Figure 8 show the temperature profile (in train vicinity) whereas Figure 9 show visibility profiles (complete length of Geren section of tunnel) at a longitudinal plane (5.6 and 8 minutes after the start of fire).

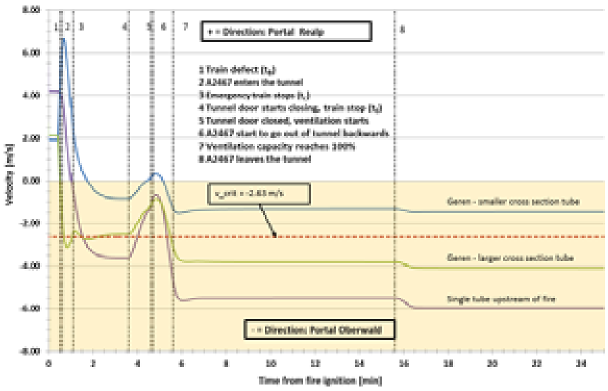

Figure 7: Velocity profiles upstream of fire in case of emergency train in Geren.

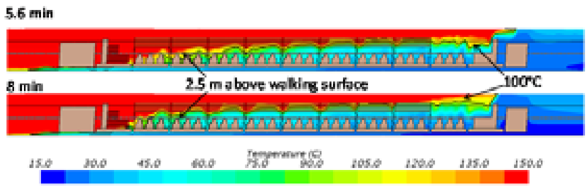

Figure 8: Temperature profile along the length of the burning train.

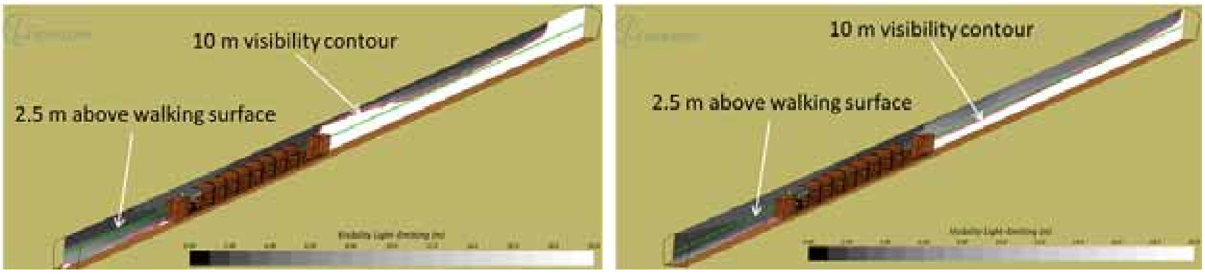

Figure 9: Visibility profile along the length of Geren tunnel section at 5.6 min (left) and 8 min (right) after the start of fire.

Based on simulation results, the times 5.6 and 8 minutes represent the stretches where the visibility level is still acceptable (visibility equals 10 m at 2.5 m above walkway) and not any more acceptable (below 10 m at 2.5 m above walkway) respectively. The red contour line represent the 10 m visibility limit whereas the green line marks the height of 2.5 m above the walking surface (Figure 9). Based on simulation results, a steady state is seen to be reached 20 minutes from the time of fire ignition as shown in Figure 10.

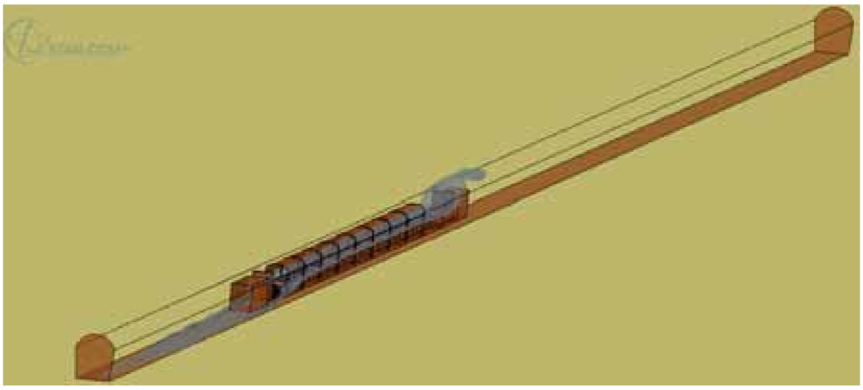

Figure 10: Visibility of 10 m represented as iso-surface, 20 minutes after start of fire.

7. CONCLUSIONS

Based on the analysis of variation 1 and 2 of the standard scenarios, it can be seen that the portal pressure plays a vital role on the initial flow in the tunnel after the train(s) have stopped and the ventilation system is not fully in operation. Possible worst case can arise if this portal pressure gets overlapped by the presence of another moving train in the system.

In the absence of the operational measures i.e. early stopping of train and simultaneous start of ventilation and closing of tunnel door, the smoke could easily extend to around 700 m upstream of fire as seen in variation 3 of the standard scenario. The escape conditions in the absence of operational measures will not get immediately better with the start of the fans, instead escape conditions can get more intensified and prolonged for the initial rescue phase as the fans will pull back the smoke along the tunnel from upstream of the fire towards downstream.

Considering the fact that the hydraulic resistance is far more in the smaller cross section tube (Geren section), majority of the fan generated flow would enter the bigger cross section tube of the Geren tunnel section. In case of a fire in the smaller tube, a critical scenario of low air flow shows that the critical velocity cannot be achieved without constructional measures or change in fan size and/or efficiency as such implementations are tied with high costs. Based on the results of “low air flow” scenario, one can conclude that a certain level of back-layering would prevail. It can however be seen that due to the presence of certain air flow, the strong smoke is restricted to regions in closed vicinity of train thereby allowing a better chance of evacuation when compared to a tunnel without a ventilation system.

8. REFERENCES

[1] IDA Tunnel, www.equa.se/en/tunnel.
[2] STAR-CCM+®, CD-adapco, www.cd-adapco.com.
[3] http://www.meteoschweiz.admin.ch/home/klima/gegenwart/klima-verlauf.html.
[4] VSWKI BT101-04: „Rauch- und Wärmeabzugsanlagen – Teil 4: Ingenieurverfahren zur Bemessung von Entrauchungsanlagen – Grundlagen“, 2011-09.
[5] SFPE Handbook of Fire Protection Engineering, 3rd Edition 2002, NFPA, Quincy, Massachusetts, USA.

EGRESS WAY VENTILATION FOR ESCAPE ROUTES IN TUNNELS – THE DESIGN OF OVERPRESSURE SYSTEMS

J.W. Huijben, M.E. Huijben
Tunnel Safety Consults, The Netherlands
E. Thesing
PhiTech Solutions, The Netherlands

ABSTRACT
Escape routes like corridors, cross connections, adjacent tunnel tubes and stairwells should be kept smoke-free during a tunnel fire. Ventilation systems are often used to keep the smoke out of the escape routes. In practice, current tunnel-design projects show that principals and designers have difficulties in choosing applicable systems, and setting realistic requirements and boundary conditions. A worldwide overview of laws, standards and recommendations show that there is little information on these systems. There are hardly any publications on this subject, not even on other applications such as in buildings; especially high-rise buildings. So far. no proven calculation methods and validated boundary conditions have been found. A research project has been launched to collect and develop knowledge on egress way ventilation systems. The first results are presented in this paper.

Keywords: escape routes, egress way ventilation systems, tunnel fires, tunnel ventilation

1. INTRODUCTION

Similar to other buildings tunnels have escape routes to provide safe escape in case of fire and other severe circumstances. In some cases the tunnel tube itself is the escape route but more common is the use of cross connections to the other tube if present of the use of escape corridors alongside the tunnel tube or stairwells to the surface. The purpose is to provide a safe area to road users as soon as they left the tunnel tube during an incident and, when fitting in the action plans, to provide safe access to the tunnel tube for emergency services. So between tunnel tube and the safe area escape doors are placed and often the escape routes are pressurized to keep them smoke free.

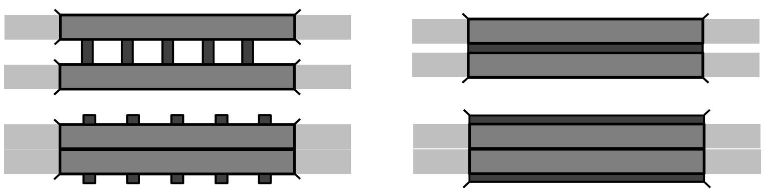

Figure 1: Arrangements of escape routes

Such pressurisation systems will provide a safe escape route granted that it complies with these aspects:

- It must be possible to open the escape doors (the differences in air pressure over an escape door should be limited)
- The escape route must be kept free of smoke and hazardous gases (minimum air flow through an open escape door)
- The airflow may not counteract the evacuation (limitation of the air velocity)

In case of cross connections or stairwells adjacent to the tunnel tubes the possibility of keeping the escape routes smoke free is mainly directed by the tunnel ventilation system. The reason is the high capacity of tunnel ventilation compared to the pressurisation system of escape routes which capacity is smaller just because of the available space for these systems. For the design of these pressurisation systems reliable calculation methods are in use.
The design of overpressure systems for escape corridors alongside tunnel tubes is more difficult. Depending the location and size of the incident more or less escape doors to the corridor can be opened simultaneously which has its influence on the capacity of the system. Often it is only possible to supply air at one or both ends of the escape corridor which requires transport of air over long distances. Pressure differences over escape doors can be very different from door to door and are even dependent on the fire location and fire size and functionality of the tunnel ventilation system. This leads to the question how to control the overpressure system in a dynamic situation where doors are opened and closed.
In practice tunnel design projects show that clients and designers have difficulties in choosing applicable systems and setting realistic requirements and boundary conditions. A worldwide overview of laws, standards and recommendations show that there is little information about these systems. There are hardly any publications on this subject for tunnels and not that much on other applications as in buildings, especially high rise buildings. For tunnels no proven calculation methods and validated boundary conditions have been found so far.
These facts concluded in launching a research project, to collect and develop knowledge on pressurisation systems for escape corridors. The goal of this research project is to provide realistic boundary conditions for pressure differences over escape doors and for the minima and maxima of air velocities in opened escape doors and escape corridors. Another goal is to find design solutions and methods for controlling the system. The results will be collected in a recommendation on overpressure systems for escape routes in tunnels providing possible solutions and calculation models.

The research project contains the following steps:

- Collecting information from publications, recommendations, standards and national laws
- Collecting information on existing systems in use and their functionality
- Definition of realistic boundary conditions
- Definition of a design model based on results of measurements in tunnels & CFD analysis
- Recommendation on control systems for overpressure systems in escape corridors

2. COLLECTED INFORMATION FROM REGULATIONS

Information has been collected from documents dealing with tunnels but also from documents dealing with pressurisation systems in buildings, especially for high rise buildings. An analysis was made of Dutch standards and regulations related to pressurisation equipment in tunnels and the operation of these systems. Dutch regulation for high-rise buildings and stairwells were included as additional input. Several foreign standards have been analyzed as well, to find out how the subject is handled in other countries. Useful standards from Europe and US were included, in order to get a complete picture of global legislation, and its mutual similarities and differences.
The regulations and standards for tunnels taken in account are the Dutch law suit WARVW/RARVW, the Dutch standard for highway tunnels (LTS 1.2), the German standard RABT 2006, the French interministerial circular n° 2000-63, the Austrian standard, the Swiss guideline FEDRO 2003 and the USA standard NFPA 502. As far as known standards, guidelines and laws on tunnels published by other countries do not contain conditions for pressurisation systems. An overview of the results is shown in table 1.

Table 1: Overview of prescriptions for pressurisation of escape routes in tunnels

country	document	pressure difference door [Pa]	Air velocity door [m/s]	Nr. of simultaneous open doors	Air velocity corridor [m/s]	Door open force [N]
NL	RARVW	≥ 10	n/a	30%, min. 3	n/a	≤ 100
NL	LTS 1.2	n/a	≤ 6,5	30%, min. 3	≤ 2 (fire ≤ 25MW) ≤ 5 (fire > 25MW	Additional force 15 nominal; Add. Force 20 for first 10 cm
DE	RABT2006	n/a	n/a	n/a	n/a	≤ 100
F	CIRC2000	≥ 80	n/a	n/a	n/a	n/a
A	RVS	n/a	≥ 2,5	n/a	n/a	≤ 100
S	FEDRO2003	≥ 50	≥ 3,0 ≥ 1,5 ≥ 1,5	1 3 adjacent 2 unfavourable	n/a	n/a
US	NFPA502	n/a	≥ 0,75 ≤ 11	n/a	≤ 11	67 (release latch) 133 (opening)

Likewise conditions for overpressure systems in buildings were derived from the European standard EN 12101-6 (2005) and several other publications. The results are shown in table 2.

Table 2: Overview of prescriptions for pressurisation of escape routes in buildings

country	document	pressure difference door [Pa]	Air velocity door [m/s]	Nr. of simultaneous open doors	Air velocity corridor [m/s]	Door opening force [N]
EU	EN12101-6	≥ 50 ≥ 10	≥ 0,75 Not given	1, other closed Doors opened	n/a	≤ 100
other	several	≥ 50	≥ 0,75		n/a	≤ 100

The following conclusions can be drawn from the literature study regarding pressurisation systems:

- Most standards include design requirements for dimensions of escape doors. These standards often contain requirements to "*prevent smoke and heat from reaching the escape routes behind emergency exit*", like stated in the EU 2005-54.
- Requirements for the minimum of pressure difference through an escape door vary from 10 Pa onto 50 Pa.
- There are no requirements to the maximum differential pressure across an escape door. This may seem sensible when a limit is set to the maximum opening force of an escape door. However, high pressure in the escape corridor could result in high air flows through open escape doors. This would create dynamic behavior of air between the escape route and the tunnel tube, which are completely unknown at the time. In addition, none of the standards indicate whether it is static or total pressure and where it needs to be measured exactly. In buildings it is reasonable to calculate with static pressure but in tunnels due to air movement through the tunnel tube and escape corridors it is not clear at first sight.
- Only the NFPA502 sets a minimum and maximum value for the air speed through an escape door. Some other give a minimum, which differs from the standard for buildings. The Dutch LTS sets a maximum but not a minimum.
- Aside from the US and the Netherlands, no requirements are set for the maximum air velocity in the escape corridor. In the Netherlands, the LTS prescribes a limit of 2.0 m/s for tunnel fires smaller than 25 MW, and 5 m/s for tunnel fires above 25 MW. In the US this value increases to 11.0 m/s.
- The Number of open emergency doors is only prescribed in the Dutch and Swiss standards.

- There appears to be an international agreement for the opening force of doors. In many cases this is prescribed as 100N for the opening force of the door. Although most standards prescribe a maximum opening force with ventilation enabled, the Dutch LTS and the US NFPA prescribes a maximum opening force required when unlocking the door.

The variety of boundary conditions raises the question which are right, reasonable and reachable.
Research done by Li et al at the Southwest Jiaotong University, China (2009) shows that the minimum air velocity through an open door with dimensions of 2,1 m height should be in the range of 0,5 – 0,8 m/s which is good order with the standard EN 12101-6.

3. COLLECTED INFORMATION FROM PRACTICE

Static and total pressure vary along the length of a tunnel tube. Wall friction losses, pressure losses due to traffic, stack effects and the influence of longitudinal ventilation result in certain pressure lines as illustrated in Figure 2 for a particular tunnel. In this figure the static pressure is given because the static pressure is the actuating force on the air flow through open doors. The pressure can be an overpressure in the direction to the escape corridor, but downstream the fire the pressure is negative and in the direction of the tunnel tube because of stack effects in the tunnel tube. The figure is given for a certain fire location, other locations result in different pressure behavior. Also the influence of the fire size is illustrated.

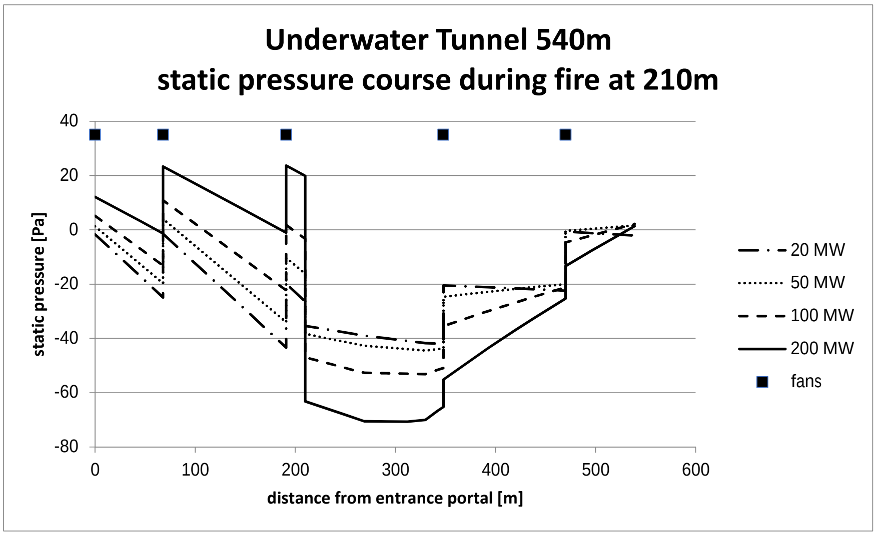

Figure 2: Pressure in an underwater tunnel during fire

Measurements on sliding escape doors searching for the influence of pressure differences on the opening force of sliding doors were done by Rijkswaterstaat (Wim Janssen et al, The Netherlands). This resulted in a behavior as given in Figure 3. It can be seen that door opening forces easily exceed a limit of 100 N if pressure differences are higher than 50 Pa. However pressure differences higher than 50 Pa are to be expected based on results as shown in Figure 2. It is also known that poor maintenance on doors result in excessive opening forces. Measurements on rotating doors show that pressure differences can result in not being able to open the door during incidents – so sliding doors are normally recommended for tunnels.

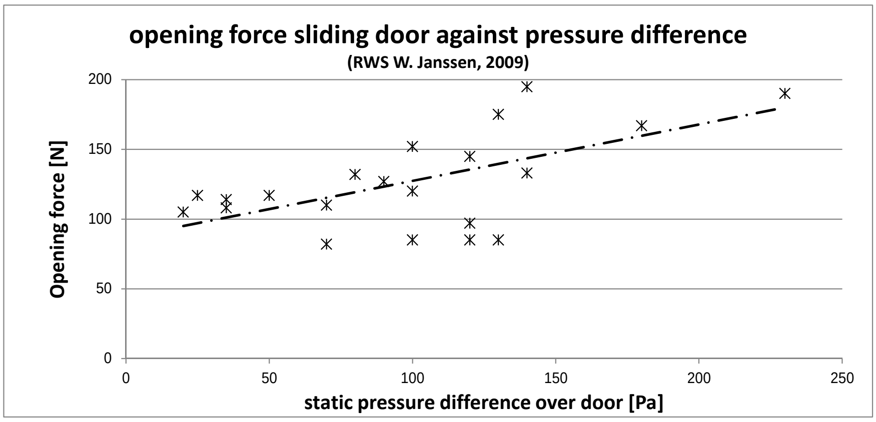

Figure 3: Opening force sliding door due to pressure difference

Measurements of air velocities in escape routes show that air velocities in escape corridors can easily be in the range of 3 – 7 m/s and air velocities in the opening of escape doors are up to 10 m/s depending the which door is opened.

4. PRESSURISATION SYSTEMS FOR LONGITUDINAL ESCAPE CORRIDORS

Systems commonly used in Dutch road tunnels are as shown hereafter. These corridors are mainly between the tunnel tubes as shown in Figure 4. Between the tunnel tubes is a "middle tube" containing in the upper part a service corridor for cabling and installations and in the lower part the escape corridor. Typical lengths of Dutch tunnels are between 500m and 2000m, some are longer. The floor of the service corridor can be completely closed but can also be of an open structure to combine service corridor and escape corridor to one aerodynamic space.

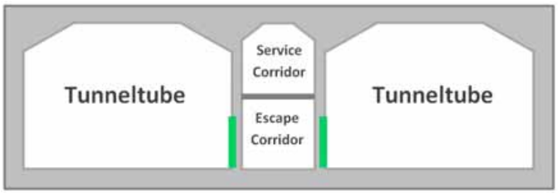

Figure 4: Schematic presentation of cross section of a common Dutch road tunnel

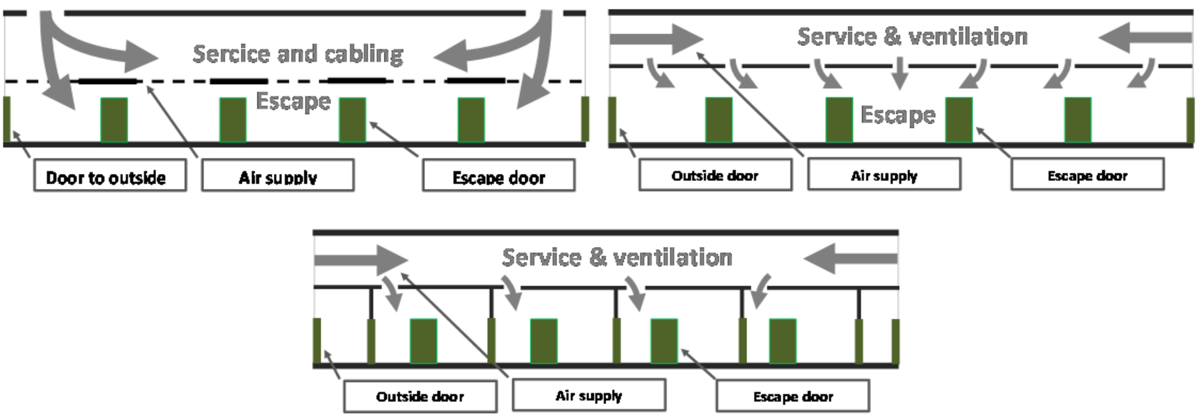

Figure 5: Schematic presentation of possible air supply into the escape corridor

In case of underwater tunnels it is only possible to supply air to the “middle tube” at both ends of the tunnel. Due to the use of longitudinal tunnel ventilation it depends on the location of the air intake air if supply can be provided at both ends or only at one end of the middle tube. Tunnels in urban areas are just below ground level and depending on the use of the space on top of the tunnel air intakes somewhere along the tunnel are possible. This has resulted in tow type of air supply as shown in Figure 5.

Other solutions of air supply to the escape corridor are using a specific ventilation duct allowing for higher transportation speeds.
By means of controlling the air velocities in the escape corridor it would be preferable to partition the corridor in compartments, the best in one compartment per escape door. However this is often not preferable in an escape corridor because that would hinder the escaping process. So we have to deal somehow with air flows through the escape corridor.

5. CALCULATION METHODS

There are two existing methods often used to calculate the air pressure and air flow in escape corridors in road tunnels.
One method is a model as used in designing mechanical ventilation duct systems. This model considers the tunnel and the escape routes as air ducts. In the calculation escape door between tunnel tube and escape corridor are examined as a T-component as shown in Figure 6. For T-components in ventilation ducts pressure drop figures are known from literature.

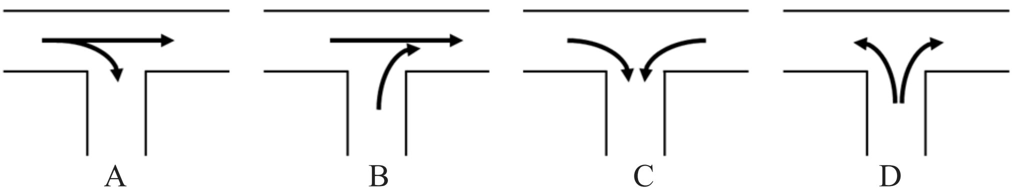

Figure 6: Escape door considered as T-part of an air duct

Another method is using the calculation methods of pressurising systems for staircases in buildings. With this method an escape door in a tunnel is considered equal as the door of a staircase. The most used formulae for flow through an emergency door is

$$[\text{Volume Flow Door}] = 0{,}83 * [\text{Door Cross section}] * [\text{pressure difference}]^{(1/n)}$$

n = 2 for large openings en n = 1,6 for small openings.

Both calculation models are an approximation of reality, but the results of the research done by Li et al at the Southwest Jiaotong University, China (2009) show that better calculation methods are needed.

Preliminary attempts in our research project using CFD has been done and show results for the relation between pressure difference and the square of the air velocity in de door opening are as shown in Figure 7. The air velocity in the escape corridor has influence on the amount of flow through an open escape door.

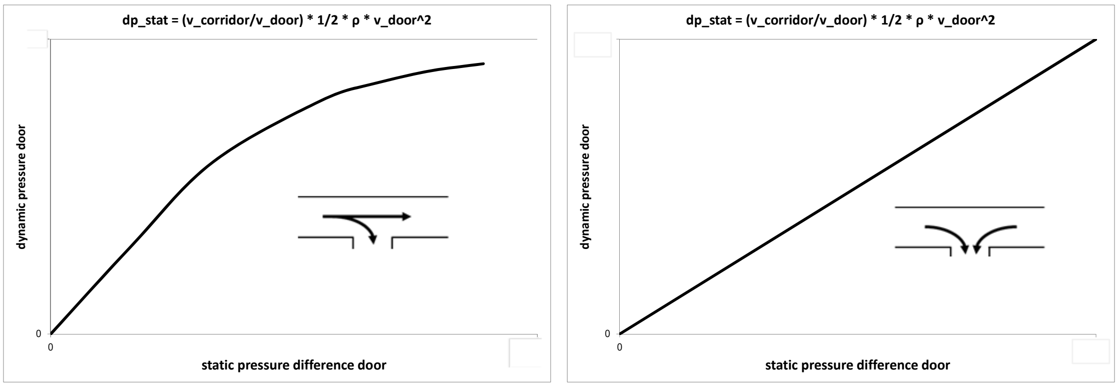

Figure 7: Escape door considered as T-part of an air duct

6. CONTROL SYSTEM

In buildings are systems in use to control the pressure in staircases and shafts by pressure measurements in the shaft and pressure relief valves. Sometimes measurement of the pressure difference over each emergency door is used. The same types of systems are also in use for escape corridors in tunnels.

It is desirable to maintain an certain pressure in the escape corridor during normal tunnel operation. This in order to prevent debris and dirt flowing into the escape corridor. Because all doors are closed a relatively small volume flow is required related to leakages of the structure.

During an emergency opening and closing of doors requires a dynamic control system which controls the deliverance of an air flow adjusted to the actual need and maintaining pressures on a certain level. The length of corridors, the number of doors and the large variety of possible pressure differences over escape doors makes it difficult to find a reliable control system based on pressure differences. And maintaining a minimum pressure level in the escape corridor itself may result in high velocities through open doors. Other control systems take in account the number of doors opened or even which doors are open.

It is considered as wise to use pressure relief valves. In an emergency situation a door may suddenly be opened requiring immediate air flow in the escape corridor. This can only be reached if the fan – which can be at a large distance from the open door – is already delivering air flow with an initial pressure. With all doors closed this air flow is relieved via the valve to the outside. When other doors are opened, the fan accelerates and increases airflow until the desired pressure in the corridor is reached.

Although, if one of the exit doors gets closed after the fan has reached its operating point, there may be a pressure peak in the corridor that can reach rather high values. This pressure peak can cause the exit doors to be clamped into the rabbet. To prevent these pressure peaks a pressure relief valve is needed in every ventilation compartment. The pressure relief valve will open at an adjustable pressure. The required pressure to open the valve can be determined by calculations.

The peaks in excess pressure are mainly caused by the inertia of the fan and to a lesser extent by the electronic control. The use of a pressure relief valve, the end of each compartment in the escape corridor, this problem could best avoided.

7. CONCLUSION AND RECOMMENDATIONS

The definition of the boundary conditions for pressurisation systems in escape corridors alongside tunnel tubes differ from country to country and even differ with the boundary conditions set for buildings. Also it is not clear if the actual boundary conditions can be met in practice – it seems that the conditions are exceeded very easily. The establishment of realistic and reachable boundary conditions is needed. Existing calculation methods do not fit well for the situation. This conclusion is supported by research results reported in literature. Validated calculation models, based on measurements and simulation models, will improve the reliability of such systems in real emergency situations providing the desidered level of safety. Because the functionality of pressurisation system in escape corridors in strongly related to tunnel ventilation design recommendations are desirable. Ideas about the functionality of control systems, which can handle the variety of scenario's of number and location of simultaniously opened doors, must be developed.

8. REFERENCES

1. NEN 6092 (1995) - Brandveiligheid van gebouwen - Eisen en bepalingsmethode voor overdrukinstallaties in trappehuizen
2. NPR 6095-1 (2012) - Smoke and heat control systems: Guidelines on design and install-lation of smoke and heat exhaust installations and smoke control systems in car parks
3. NPR 6095-1 (2012) - Smoke and heat control systems: Guidelines on design and installation of pressurisation installations
4. NEN EN12101-6 (2005) - Smoke and heat control systems: Specification for pressure differential systems
5. NFPA 502 - Standard for Road Tunnels, Bridges, and other Limited Access Highways
6. FEDRO guideline for tunnels, GR 2003
7. AHREA Handbook, HVAC Systems and Equipment, Chapter 19, 2012
8. AHREA Handbook, HVAC Applications, Chapter 53, 2015
9. Verificatie en validatie overdruksystemen MTK wegtunnels, Beschrijving methodiek. Den Boer & Van Oerle, Peutz, 2014
10. Overdrukinstallatie voor trappenhuizen in het ministerie van Veiligheid en Justitie en Binnenlandse Zaken en Koninkrijksrelaties te Den Haag – TVVL Magazine, 2013
11. System Air documentation on pressure differential systems in stairways, (2013)
12. Theoretical and Experimental Study of Critical Velocity for Smoke Control in a Tunnel Cross-Passage, Ying Zhen Li, Bo Lei, Haukur Ingason, Fire Technology, April 2013, Volume 49
13. Applying the EU Directive On Existing Tunnels With Transverse Ventilation, Huijben & Rikkelman, Lyon, 2011
14. NCHRP Synthesis 415: Design Fires in Road Tunnels, Igor Y. Maevski; Transportation Research Board, 2011
15. Gluren bij de buren – Wim Janssen, Rijkswaterstaat, 2009
16. Small scale experiments on critical velocity in a tunnel cross-passage – Li, Lei, Xu, Deng, School of Mechanical Engineering, Southwest Jiaotong University, China, 2009
17. Onderzoek vluchtgang ventilatie Coentunnel - Metingen, S&T Engineering, juli 2008
18. TVVL Magazine - thema nummer Hoogbouw, 2007
19. Tunnel Ventilation and Safety in Escape Routes, Hartman & Huijben, 2006
20. Ventilation of Protected Areas in Road Tunnels, Zumsteg, Steinemann, Wildi, Graz, 2004
21. V2BO advies - hoogbouw: eisen en richtlijnen brandveiligheid – Leersum, 2003
22. Rookbeheersing door overdrukventilatie en rook- en warmteafvoerinstallatie, Bosma & Scheffrahn, Van Andel, 1998

COMPARING PIARC EMISSIONS WITH AUSTRALIAN TUNNEL MEASUREMENTS

C. Stacey, M. Meissner, P. Ridley,
Stacey Agnew Pty Ltd, Australia

ABSTRACT

For the last two decades or so, Australian road tunnel ventilation design has relied on the emissions data published by PIARC, with little retrospective examination to ensure that the estimation method is current or to ‘calibrate’ the method for future projects. Accurate, short term measurements in the M5 East tunnel were compared against the results from an IDA Tunnel model which used the PIARC prediction data, extrapolated to 2015, and applied to the observed traffic and airflows. For the M5 East geometry, when the modelled traffic flow and the observed traffic had closely the same behaviour, the carbon monoxide emissions were over-estimated by the PIARC method, with a factor of 0.6 to 0.85 to be applied to the prediction. The PIARC method predicts the total oxides of nitrogen (NO_X) rather than nitrogen dioxide (NO_2) directly. The fraction of the NO_X which is NO_2 was estimated following data from Carslaw and Rhys-Tyler. The NO_X predictions were then seen to be slightly low, requiring to be increased by a factor of 1.2 or 1.3 relative to the Australian method. The approach used for predicting the ratio NO_2:NO_X was found to reproduce the observed ratio well.

Keywords: ventilation design, emission data, nitrogen dioxide.

1. INTRODUCTION

All recent road tunnels in Australia have had their in-tunnel and external pollution assessed during design using the emission estimation methods given by PIARC (Road Tunnels: Vehicles, Emissions and Air Demand for Ventilation. Document 2012R05EN, 2012). The base PIARC figures were published in 2012, using data on the Australian fleet collected earlier. The data and methods are referred to here as “PIARC” or “PIARC 2012”. This report examines the accuracy of the PIARC pollution models when extrapolated to 2015, using recent real-time operating data and measurements from the M5 East tunnel in Sydney.

The uncertainty in estimates of future emissions comes from both the uncertainty as to the current accuracy of models, and the uncertainty involved in the extrapolation of trends. The purpose of the comparison against recorded 2015 data is to give confidence in the current prediction, such that one source of uncertainty in estimating future emissions is greatly reduced.

The PIARC 2012 document gives a detailed estimation method and also a simplified approach, tailored (at the time) to the Australian fleet. This paper compares both methods to the measured data.

1.1. Limitations

The location of CSIRO monitoring equipment and the ventilation system of the M5 East tunnel mean that the Westbound tunnel between the Duff St supply point and the Western crossover dominate the pollution levels measured. This effectively limits the range of assessment to gradients in the range -1% to +6%. Refer to the shaded region of Figure 2.

2. TUNNEL SCHEMATIC AND MODEL PARAMETERS

A dynamic model of the M5 East tunnel was constructed using the software package IDA Tunnel (EQUA AB, 2016), which is written specifically to simulate ventilation networks with traffic, pollution and thermodynamic behaviours. Model parameters were based on available drawings and technical information available from the tunnel operator. The overall schematic of the tunnel is shown in Figure 1, with the alignment of the westbound tube shown in Figure 2 (the eastbound tube runs beside the westbound tube). The tunnel is unusual in having air exchange effected near the middle of each tube, with crossover fans near the portals (segments 15 and 16 in Figure 1). The crossover fans take air that would otherwise leave the exit portal, and direct that air into the adjacent traffic tube.

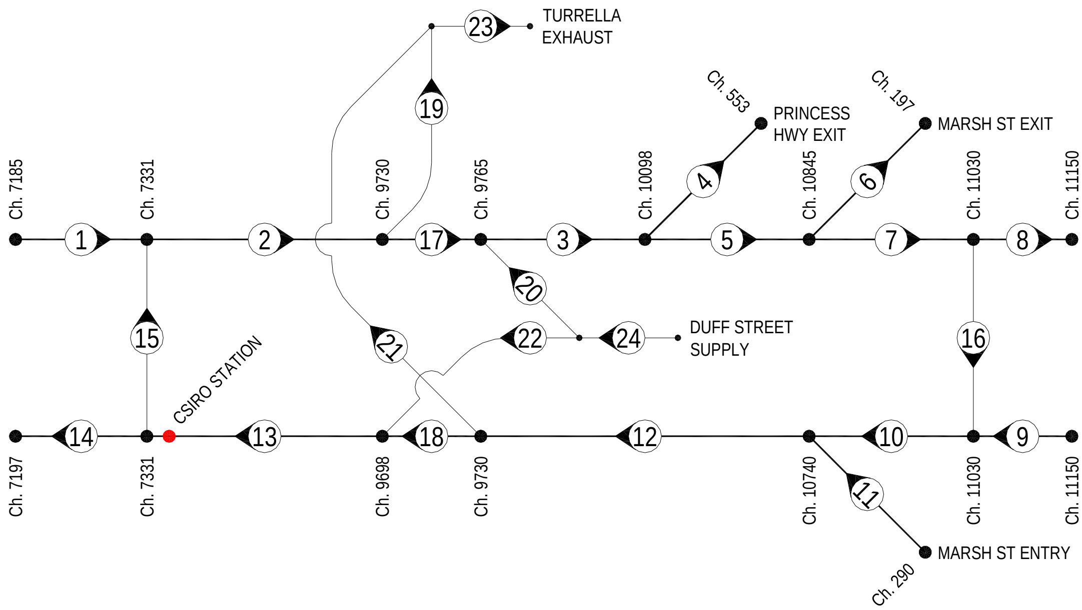

Figure 1: Tunnel ventilation schematic.

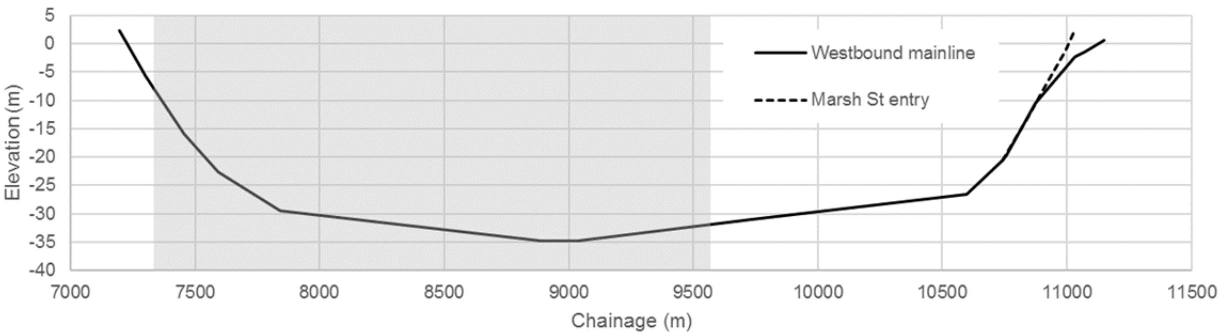

Figure 2: Westbound vertical alignment.

For the purposes of this work, calibration of the vehicle and tunnel aerodynamic properties has not been performed. Since the objective is to understand pollution emissions, it is more important to duplicate the observed dilution as closely as possible. To ensure that the simulated air flows transporting pollutants along the tunnel are closely matched to actual flows, the tunnel airflows have been driven by jet fans in the simulation to match the time-varying in-tunnel air flow measurements.

3. IN-TUNNEL MEASUREMENTS AND OPERATING DATA

Data from a number of sources were used as inputs to the dynamic model and for comparison of the simulated results. The primary source of input data to the model was obtained from the tunnel SCADA system.

Traffic loop data were used as vehicle flow inputs into the model at vehicle entrances and traffic diverges. Traffic loops are positioned at various locations through the tunnel and discriminate vehicles into three categories (small, medium and large) based on the vehicle length. Vehicle flows were aggregated across all lanes as IDA Tunnel does not provide the capability to simulate separate conditions for each lane in multiple-lane sections.

Airflow sensors are positioned through the tunnel system and in ventilation supply and exhaust airways, providing a record of the network airflow conditions. Data were provided at random non-concurrent times and this was pre-processed by interpolating each sensor at concurrent 3-minute intervals. Noise in the signal was addressed by applying a least squares fit at each time-slice to ensure that continuity was preserved in the network airflow figures. The calibration status of airflow sensors is unknown, however the technique applied would avoid sensitivity to any one aberrant sensor.

In-tunnel pollution measurements used for comparison against the simulated results were provided by the CSIRO. Measurement of NO, NO_2, CO, CO_2 and $PM_{2.5}$ were completed by the CSIRO on the 26^{th} and 27^{th} March 2015 in the westbound tunnel immediately upstream of the western end cross-over fan installation, see Figure 1. The results on the two days were similar, with only those from the 26^{th} March presented here for brevity.

4. VEHICLE FLOW MODEL CALIBRATION

It is difficult to model traffic behaviours in the unstable flow region at the transition from free-flowing to congested flow. The IDA Tunnel parameters were adjusted, seeking to replicate the observed speed-flow relationship, noting also that the data only give speed at discrete locations.

From 9 am up until approximately 11:30 am on the 26^{th} March 2015, there was good correlation between the simulated and measured traffic speed. Beyond that time, the model diverged from the measured conditions despite our calibration efforts. Pollution results have been interpreted only where both speed is well correlated with measurements.

5. POLLUTION MODEL PARAMETERS

5.1. Traffic mix

Automated traffic network survey data collected during the period November to December 2014 were analysed to obtain overall fleet characteristics. Vehicles were categorised into a PIARC category based on the “Vehicle Type Description” in the data. The registration information also included vehicle build date, allowing the fleet age distribution to be compiled.

5.2. PIARC 2012 – Euro classification

Data from the Australian Government (Department of Infrastructure and Regional Development, 2016) on the introduction date of vehicle standards was used to estimate the proportion of vehicles in each Euro classification based on the age distribution profile shown in Figure 3. Due to the nature of the estimation method and available data, there is some uncertainty inherent in this methodology. Firstly, new model and existing model vehicles have differing years of implementation. Secondly, for the proportion of vehicles which are imported by global manufacturers, actual implementation of engine emissions standards may occur ahead of the legislated requirement.

Euro standards have been adopted for each vehicle category in accordance with Table 1.

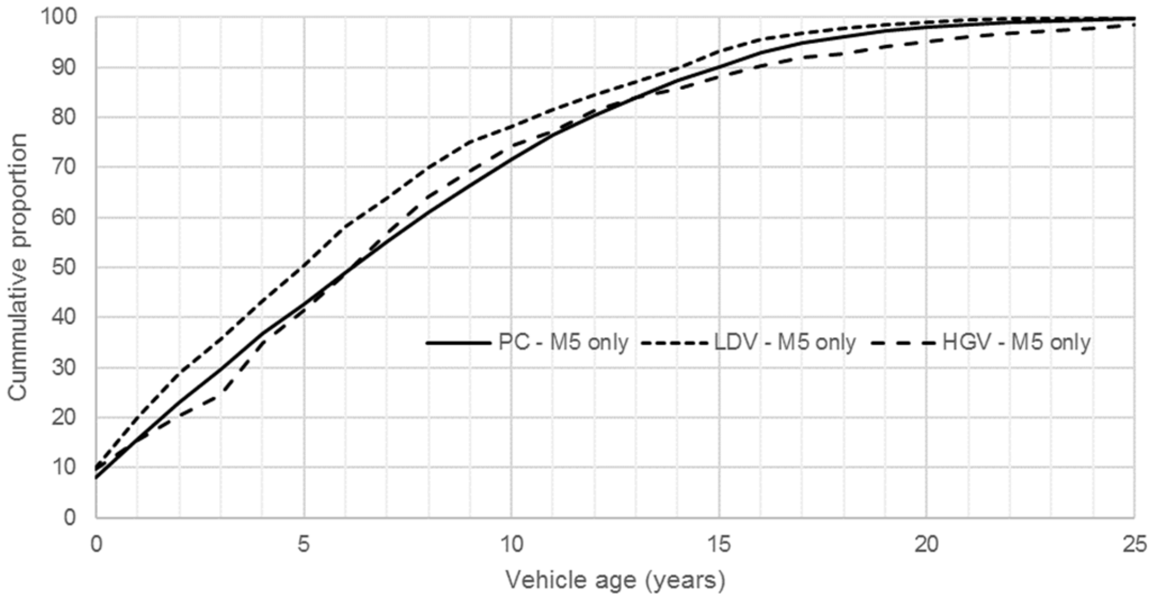

Figure 3: Traffic survey data vehicle age distribution.

Table 1: Assumed average year of implementation for Euro standards in Australia.

Category	Pre-Euro	Euro 1	Euro 2	Euro 3	Euro 4	Euro 5	Euro 6
PC – Petrol/Diesel	-	n/a	2003	2005	2009	2015	2017
LDV – Petrol	-	n/a	2003	2005	2009	2015	2017
LDV – Diesel	-	n/a	2002	2005	2007	2015	2017
HGV – Diesel	-	1996	2000	2003	2007	2010	2017

5.3. PIARC 2012 – Australia

Table 2 below shows the key parameters adopted in developing the pollution generation tables in accordance with PIARC 2012, based on PIARC's Australian fleet appendix (Appendix 3.1). Typical average fleet parameters are based on the traffic survey data outlined in Section 5.1.

5.4. NO2 emissions

PIARC tables give NO_X generation rates as a function of vehicle speed and road gradient. Since NO_2 is typically the dominant design pollutant, the mass ratio NO_2:NO_X is a key parameter in the PIARC method. It is highly desirable to have tables of NO_2 evolution rather than its proxy NO_X, which bundles together the NO and NO_2.

NO_2:NO_X mass ratios for the various vehicle classes were calculated using the fleet age profile. The vehicle classes are then further subdivided into Euro classes defined in Section 5.2. The input data for the estimates of NO_2 ratio come from (Carslaw & Rhys-Tyler, 2013) who used remote sensing of travelling surface vehicle's emissions (measured immediately after the vehicle tailpipe) to determine the ratio of vehicle pollutants NO_2, NO_X and NH_3 to CO_2 emissions.

It is considered that applying Carslaw and Rhys Tyler's surface vehicle data to a tunnel scenario is valid. NO from the exhaust is converted to NO_2 in the presence of ozone (O_3) when it enters the atmosphere. However, in a tunnel environment (remote from the entry portal), where the ozone has been depleted, NO_2 levels should be unaffected by the further conversion of NO to NO_2. Ozone reactions are also catalyzed by any surfaces and so tunnel walls and fittings also eliminate ozone from the ingested air flow. Efforts to identify NO to NO_2 conversion by ozone just inside tunnel entry portals have not been able to show NO_2:NO ratios different from the tailpipe ratios seen later in the tunnel[1]. Hence readings taken at the tailpipe of a vehicle (prior to any atmospheric conversion of NO to NO_2) should allow reasonable estimation of the resulting NO_2 in a tunnel.

Another issue which increases the uncertainty of the rate of NO_2 generation is that the evolution of pollutants is a function of the vehicle operating power. The work by Carslaw and Rhys Tyler does not attempt to quantify this relationship.

NO_2 emissions for each of the three vehicle classes, are predicted from PIARC NO_X tables multiplied by the appropriate NO_2:NO_X mass ratio predicted from the Carslaw Rhys-Tyler data.

Table 2: Parameters applied with the PIARC emission factors and CO_2 model.

Vehicle Category	**PC**	**LDV**	**HGV**
% Diesel in Category	7.3%	46.3%[2]	100.0%
Vehicle Mass (kg)[3]	1,650	3,150	15,500
Idle heat release (W)[3]	10,000	15,000	35,000
Overall thermal efficiency (%)[3]	31%	31%	31%
Frontal Area (m^2) [3]	2.5	4.0	7.1
Drag Coefficient[3]	0.32	0.53	0.46
Coefficient of rolling resistance[3]	0.02	0.02	0.01
PIARC Australian emission factors			
Future Years (ft) factor CO - gasoline	0.59	0.69	0.73
Future Years (ft) factor CO - diesel	0.67		
Mass factor CO	n/a	n/a	0.80
Future Years (ft) factor NOx - gasoline	0.55	0.72	0.74
Future Years (ft) factor NOx - diesel	0.84		
Mass factor NOx	n/a	n/a	0.80
Future Years (ft) factor Opacity - diesel	0.00	0.64	0.73
Mass factor Opacity	n/a	n/a	0.80
Factor non-exhaust particulate matter	1.0	1.0	1.0
Carslaw - Rhys Tyler NO_2:NO_x ratios			
Petrol	2.7%	2.7%	n/a
Diesel	26.1%	26.5%	18.4%

[1] Sturm P., Personal communication, October 2015.

[2] PIARC 2012 Australian appendix only provides emissions tables assuming a fixed proportion of diesel vehicles in both LDV (50%) and HGV (100%0 categories.

[3] Used only for the purposes of estimating vehicle CO_2 emissions.

5.5. CO_2 emissions

Vehicle characteristics were used to estimate the vehicle CO_2 emissions on the basis of vehicle speed and road gradient, adopting an average CO_2 production rate of 0.0681 g/J for petrol engines and 0.0750 g/J for diesel engines. Aerodynamic drag has been calculated assuming conditions of zero wind velocity, which will over-estimate the drag.

6. RESULTS

The figures below compare simulated results using pollution generation tables based on PIARC 2012 with in-tunnel measurements on 26th March 2015. Two results are provided for each pollution model, with the fleet mix treated differently to address the uncertainty in vehicle types. In the first approach, vehicle flows reported by tunnel traffic loops are unaltered, with small, medium and large vehicles simulated as PC, LDV and HGV respectively. In the second approach, vehicle flows reported by the tunnel traffic loops are adjusted ('adj' added to trace name) such that the daily total vehicles in small and medium are redistributed to match the PC and LDV proportions as per the automated traffic network survey;

- Small (adj) = small × 0.95
- Medium (adj) = medium + 0.05 × small

Scaling factors were applied to emissions tables for each pollutant, to achieve a better match between simulated and measured data. No attempt has been made to calibrate individual vehicle categories separately and the same scaling factor has been applied to PC, LDV and HGV emissions tables for each pollutant. The resulting scaling factors are shown in Table 3.

Similarly, parameters within the heat and CO_2 emissions model were adjusted until a more appropriate fit to measured data was obtained, the resulting factors are incorporated in Table 2.

Table 3: Global 2015 calibration factors for PIARC emissions models in M5 East.

	Australia	Australia (adj)	Euro	Euro (adj)
NO_X	1.3	1.2	1.4	1.3
NO_2:NO_X ratio	1.0	1.0	1.0	1.0
CO	0.85	0.75	0.75	0.6
Total particulates	1.0	1.0	1.25	1.25

With the above scaling factors applied, the simulated and measured results are compared in the plots below. Calibration of the CSIRO sensors was performed between 9:45 am and 9:55 am.

The following observations are made based on the calibration necessary to fit the curves.

- NO_X is underestimated by PIARC's methodologies, while CO is overestimated.
- The simulated ratio of NO_2:NO_X is consistent with measured values, indicating that the data from Carslaw and Rhys Tyler are directly applicable to the Australian fleet.
- The combined effects of exhaust and non-exhaust particulate emissions is estimated with reasonable accuracy based only on tailpipe emissions, with the Australian methodology slightly under-predicting and the Euro methodology slight over-predicting.
- CO_2 is slightly over-predicted by the approach developed for this study. Correcting the vehicle air speed may correct that. The close match gives confidence that the fleet mass is well reflected in the model.

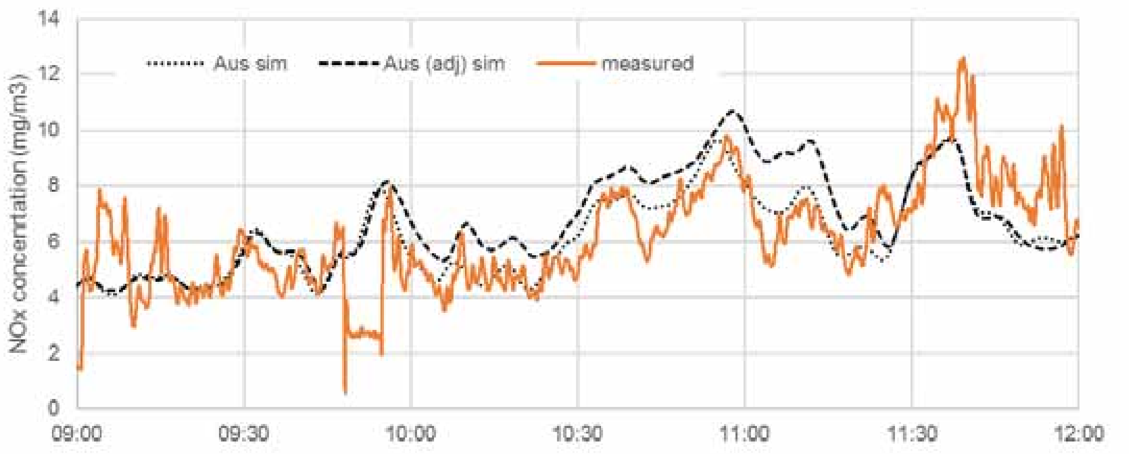

Figure 4: Comparison of calibrated NO_X model, 26th March 2015.

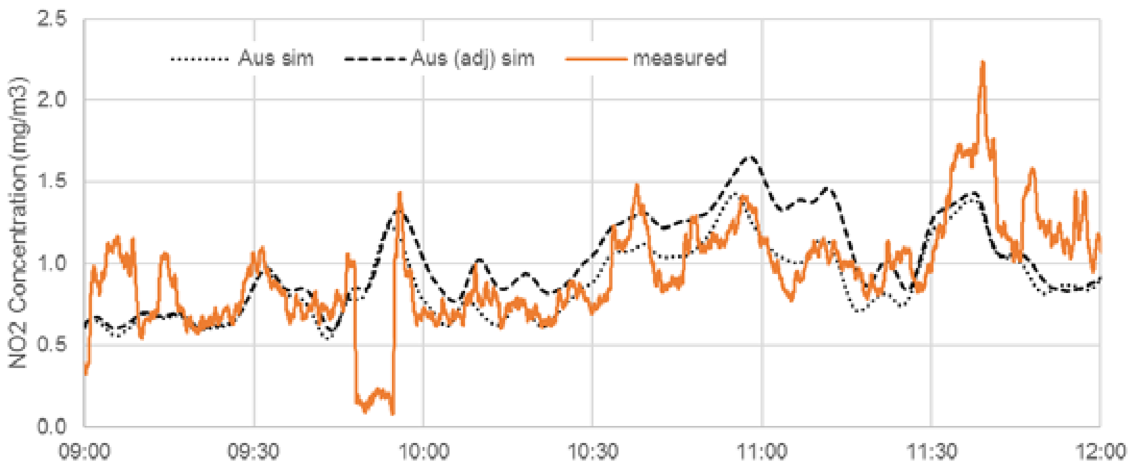

Figure 5: Comparison of calibrated NO_2 model, 26th March 2015.

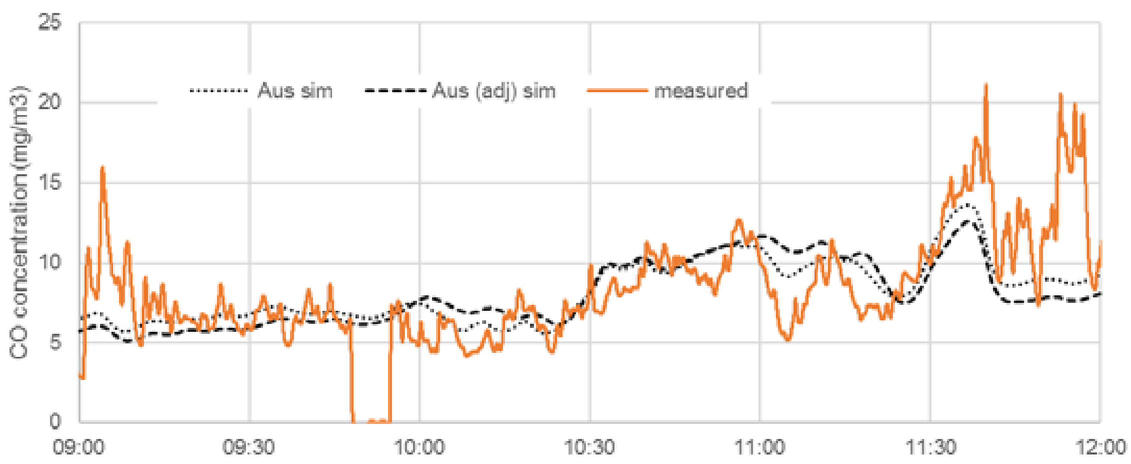

Figure 6: Comparison of calibrated CO model, 26th March 2015.

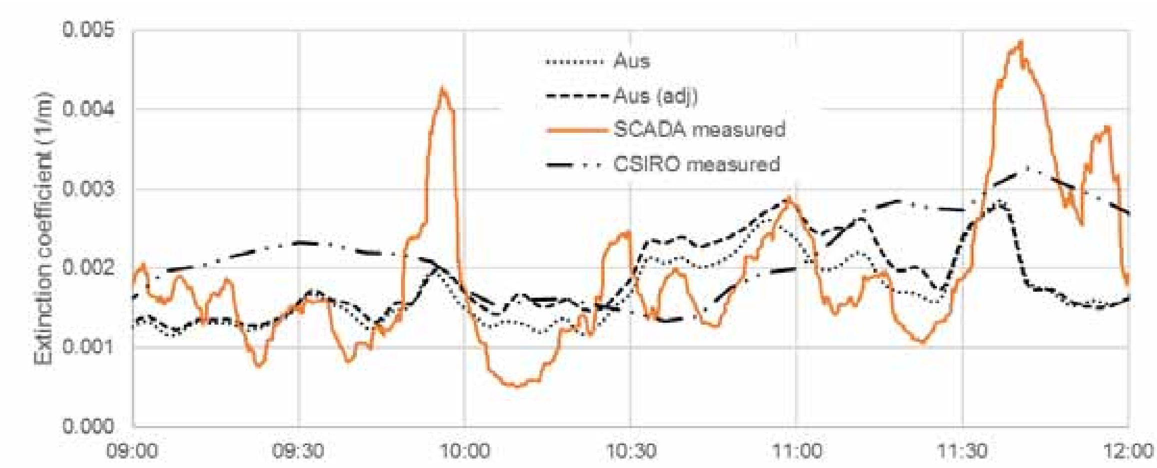

Figure 7: Comparison of calibrated particulate matter model, 26th March 2015.

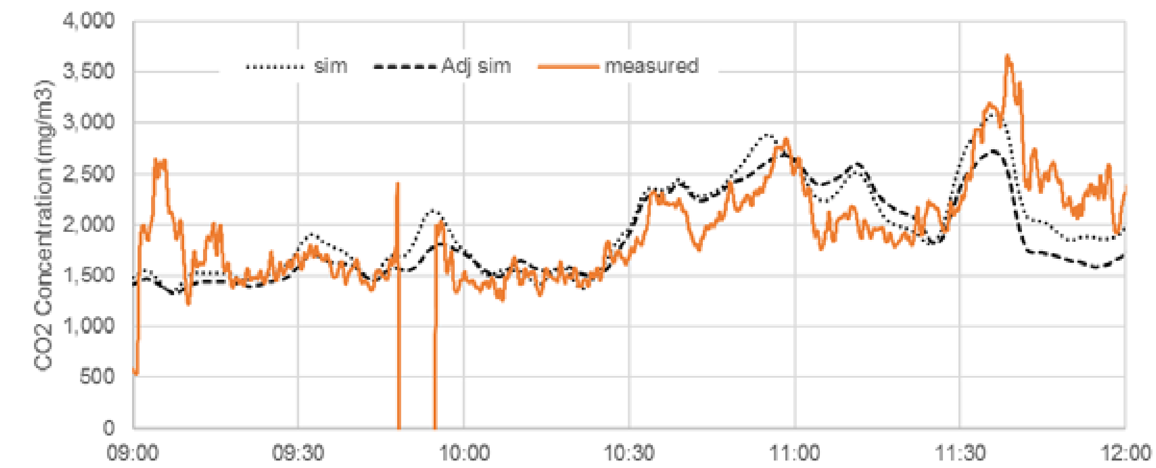

Figure 8: Comparison of calibrated CO_2 model, 26th March 2015.

ACKNOWLEDGEMENTS

The authors thank Dr Brendan Halliburton and CSIRO for the detailed site measurements, and NSW Roads and Maritime Services for permission to publish.

REFERENCES

Carslaw, D., & Rhys-Tyler, G. (2013). New insights from comprehensive on-road measurements of NOx, NO_2 and NH_3 from vehicle emission remote sensing. *Atmospheric Environment*, 339-347.

Department of Infrastructure and Regional Development. (2016, March 15). *Vehicle Emissions Standards*. Retrieved from https://infrastructure.gov.au/roads/environment/emission/index.aspx

EQUA AB. (2016, March 15). *IDA Tunnel*. Retrieved from EQUA AB: http://www.equa.se/en/tunnel

PIARC. (2012). *Road Tunnels: Vehicles, Emissions and Air Demand for Ventilation. Document 2012R05EN*. PIARC Technical Committee C4 Road Tunnels Operation.

INVESTIGATIONS ON SMOKE PROPAGATION WITH LONGITUDINAL VENTILATION BY MEANS OF A MODEL TUNNEL

[1]A. Klein, [2]W. Jessen, [1]M. Oeser, [2]W. Schröder, [3]C. Sistenich;
[1]Institute of Highway Engineering, RWTH Aachen University, D
[2]Institute of Aerodynamics Aachen, RWTH Aachen University, D
[3]Federal Highway Research Institute (BASt), Bergisch Gladbach, D

ABSTRACT

To examine the operation of longitudinal ventilation systems for road tunnels especially with regard to emergency ventilation, a small scale model tunnel has been developed in the scope of a research project. Key features of this 1:18-scale model tunnel with a two-lane cross section either of rectangular or horseshoe shape are working jet fans and the possibility to investigate the influence of standing or moving vehicles on the flow. The smoke plume of a fire was modelled isothermally by injecting a helium-air mixture through a circular hole in the road surface with respect to a similar buoyancy effect. The helium-air mixture has been seeded with tiny particles in order to apply the particle-image velocimetry (PIV) technique to determine the resulting flow fields and corresponding velocity distributions.

In this paper, the results of investigations on the influence of standing vehicles on the smoke propagation with longitudinal ventilation inside the model tunnel are presented. The propagation of smoke along the tunnel axis depends on the traffic situation and ventilation velocity. The interaction of the ventilation flow by jet fans and the modeled smoke plume showed the generation of the backlayering effect along the tunnel ceiling depending on the jet velocity. With an analysis of mean velocities at different time intervals the formation of the backlayer and its propagation opposite to the ventilation direction has been shown in detail.

Keywords: longitudinal ventilation, model tunnel, isothermal experiments, PIV, backlayer

1. INTRODUCTION

1.1. Overall scope and goals of the research project

The main goals of this project were the development and the construction of a model tunnel that allows the investigation of flows in a road tunnel as realistic as possible in order to enable its application for the evaluation of ventilation concepts. Experimental investigations were carried out in this model tunnel with regard to enhancing tunnel safety and to both optimize longitudinal ventilations systems and tunnel design. In parallel, these experiments were transferred into computational fluid dynamics models.

In order to achieve the above mentioned goals the main parameters with influence to smoke propagation and stratification were covered, e. g. the tunnel slope, cross-section geometry, standing and moving traffic and operation of jet fans.

1.2. Design of the model tunnel

Within this research project a model tunnel with a scale of 1:18 and a length of 12 meters was built in modular construction that can be extended for future investigations. It consisted of two-lane cross-sections for unidirectional and bidirectional traffic (RQ 26t and 10,5t according to the German standard RABT 2006 [1]) with either a rectangular or horseshoe profile (**Figure 1**). The tunnel elements are made out of transparent materials (PMMA, PA) and MDF resting on a substructure (aluminum profiles) that allows the adjustment of the slope. The construction allows a wide variety of different tunnel design features like an adjustable road level for the rectangular profile, the installation of emergency alcoves or suspended tunnel ceilings for the horseshoe profile.

Beside the consideration of standing vehicles the use of a modified slot car system enables also the investigation of moving traffic i. e. the piston effect on smoke propagation.

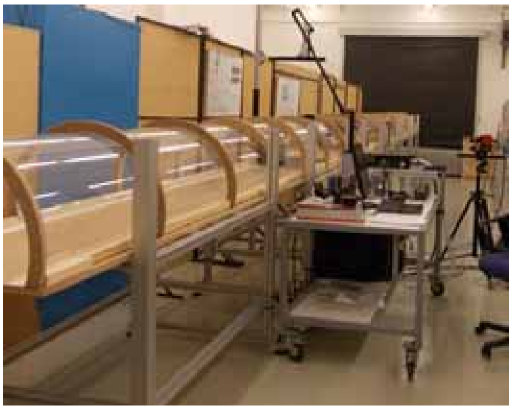

Figure 1: Setup of the model tunnel with rectangular (left) and horseshoe (right) profile

1.3. Isothermal modelling of tunnel fires

In most of the past investigations a downscaled combustion of e. g. propane or ethanol was used to model a tunnel fire (Ingason/Werling 1999 [2], Wu/Bakar 2000 [3], Roh et al. 2007 [4]). In order to transfer measured velocities v_M from the model into real scale (v_R), the conservation of the Froude number that represents the ratio between inertia forces to gravitational forces is required:

$$Fr = \frac{v_M}{\sqrt{g \cdot L_M}} \overset{!}{=} \frac{v_R}{\sqrt{g \cdot L_R}} \quad \Rightarrow \quad v_R = v_M \cdot \sqrt{\frac{L_R}{L_M}}$$

where g is the gravitational acceleration and L_M and L_R are characteristic values of length.

For this investigation, an isothermal approach was chosen that modelled the buoyancy forces related to a fire by the injection of a helium-air mixture. This approach has been successfully implemented by Vauquelin (2008) [5] in investigations dealing with the determination of critical velocities as well as smoke stratification and smoke extraction.

From the Froude similarity the following correspondence for the heat release rate Q between model and real scale can be derived:

$$Q_R = Q_M \cdot \left(\frac{L_R}{L_M}\right)^{\frac{5}{2}}$$

The composition and the volume flows of the helium-air-mixtures used in this project can be associated with convective heat release rates Q_C in a range from 0.73 to 2.91 kW (1–4 MW in real scale).

While a strict conservation of the Reynolds number is not possible in this reduced scale the flow velocities were chosen high enough to ensure a turbulent flow in the model tunnel.

1.4. Design of model jet fans

Based on high-performance impellers for model aircrafts, jet fans with three different diameters and performance features were constructed. These impellers were mounted into aluminum cylinders that match the scaled geometry of real jet fans with sound absorbers. Jet fans with fan wheel diameters of 28 mm, 40 mm and 50 mm were manufactured representing real diameters of 500 mm, 710 mm and 900 mm, respectively (**Figure 2**). After calibrating the jet exit velocity by using the PIV technique the required jet velocity can be adjusted with a potentiometer continuously in a range from 2 to 30 m/s.

Depending on the ventilation cases investigated, these fans are installed either into haunches, niches or underneath the ceiling of the model tunnel.

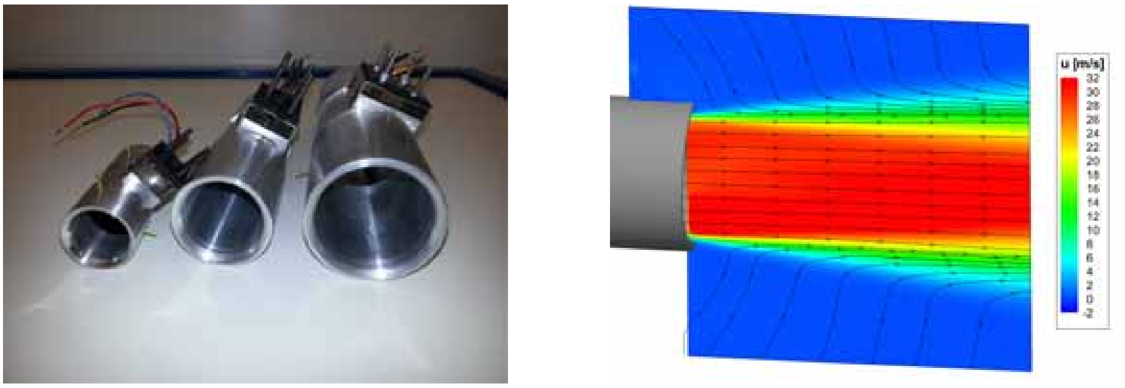

Figure 2: left: final construction of the modelled jet fans with three different fan wheel diameters (28 mm, 40 mm and 50 mm); right: velocity distribution downstream of the fan outlet in the x-y-plane from calibration

1.5. Measurement technique and experimental setup

The velocity and vorticity distributions are measured by the PIV method. The PIV is a laser-optical, nonintrusive measurement technique for flow diagnosis that enables the planar measurement of unsteady flow fields. The principle of PIV is based on illumination and tracking of tracer particles that are added to the flow and follow the flow structure. A detailed description of the PIV technique can be found in publications such as Adrian [6] and Raffel et al. [7].

Figure 3 shows a sketch of the helium-air injection into the model tunnel with 1–2 µm particles of solvent di-ethyl-hexyl-sebacat (DEHS) added to the flow by a seeding generator. All investigations described in this paper were carried out with a seeded helium-air mixture representing a convective heat release rate Q_C of 2 MW.

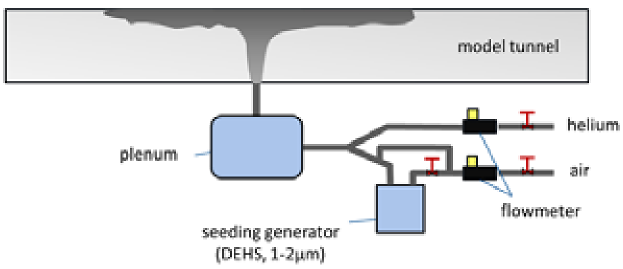

Figure 3: Sketch of the helium-air mixture injection into the model tunnel

With the experimental setup, a fire incident with ensuing traffic congestion in a unidirectional tunnel with horseshoe profile was considered. The outlet for the helium-air mixture was located in the middle of the tunnel. Upstream of this outlet a congestion consisting of heavy goods vehicles on the right lane and passenger cars on the left lane was established (both vehicle types to scale, **Figure 4** left). Additional experimental series were performed without vehicles as a reference. Four model jet fans with a fan wheel diameter of 40 mm were installed in groups of two in the calotte area (**Figure 4** right) with a distance from floor level of 285 mm (≙ 5.13 m) and a lateral spacing of 190 mm (≙ 3.42 m) with respect to the jet fan axis.

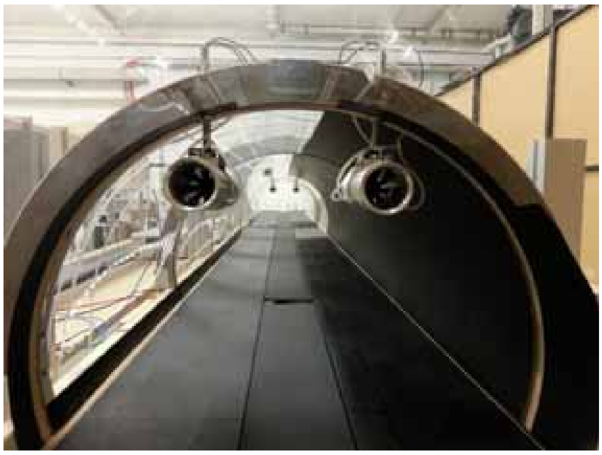

Figure 4: left: modelled congestion with standing HGV on the right lane and passenger cars on the left lane; right: Installation of jet fans in the model tunnel

The PIV measuring plane was located at the injection hole in the *x*-*y*-symmetry plane of the model tunnel as shown in Figure 5.

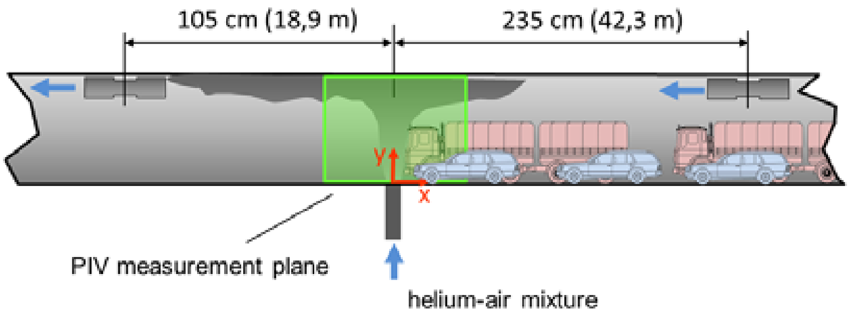

Figure 5: Location of the PIV measuring plane between the jet fan groups in the symmetry axis

2. EXPERIMENTAL RESULTS

2.1. Influence of standing vehicles on tunnel flow with mechanical ventilation

The experiments were performed with two different jet exit velocities $u_j = 3.7$ m/s and 5.0 m/s, respectively. Figures 6a and 6b show the visualization at four consecutive time steps t_1–t_4 and the corresponding velocity distributions for a jet exit velocity of $u_j = 3.7$ m/s without any vehicles in the model tunnel. The rising plume of the emanating helium-air mixture is visualized through the seeded tracer particles that are illuminated by the pulsating laser. The follow-up behavior of the tracer particles ensures that the particles remain in the helium-air plume and enable a clear distinction between the plume and air in the tunnel.

In the beginning at time step $t_1 = 2$ s, the helium-air plume is rising towards the tunnel ceiling with a slight inclination to the left due to the ventilation from the jet fans. At time step $t_2 = 15$ s, the helium-air mixture close to the ceiling has started to flow opposite the ventilation direction indicating the backlayering process. This process continues at time step $t_3 = 21$ s showing an advanced wedge-shaped propagation of the helium-air mixture further upstream leaving the measurement plane. Later at $t_4 = 45$ s, the backlayering of the helium-air mixture has clearly grown in size and is distributed in the upper two thirds of the tunnel height.

The development of the flow field is illustrated with the corresponding velocity distributions averaged over three time intervals in Figure 6b. The velocity distribution of the absolute velocity u_{abs} for the time interval of the first 2 seconds shows that the backlayering has not started yet. For the consecutive interval of 6 seconds (Figure 6b center) the streamlines indicate the generation of a vortex with clockwise rotation close to the tunnel ceiling where the ventilation flow impinges on the helium-air plume. The helium-air mixture is entrained into this growing vortex and transported opposite to the ventilation direction along the tunnel ceiling. About 40 seconds later the vortex has clearly grown and the recirculation stretches far beyond the measurement plane opposite to the ventilation direction. For the latter velocity distribution of u_{abs} the time interval was set to 10 seconds (Figure 6b right).

a)

b)

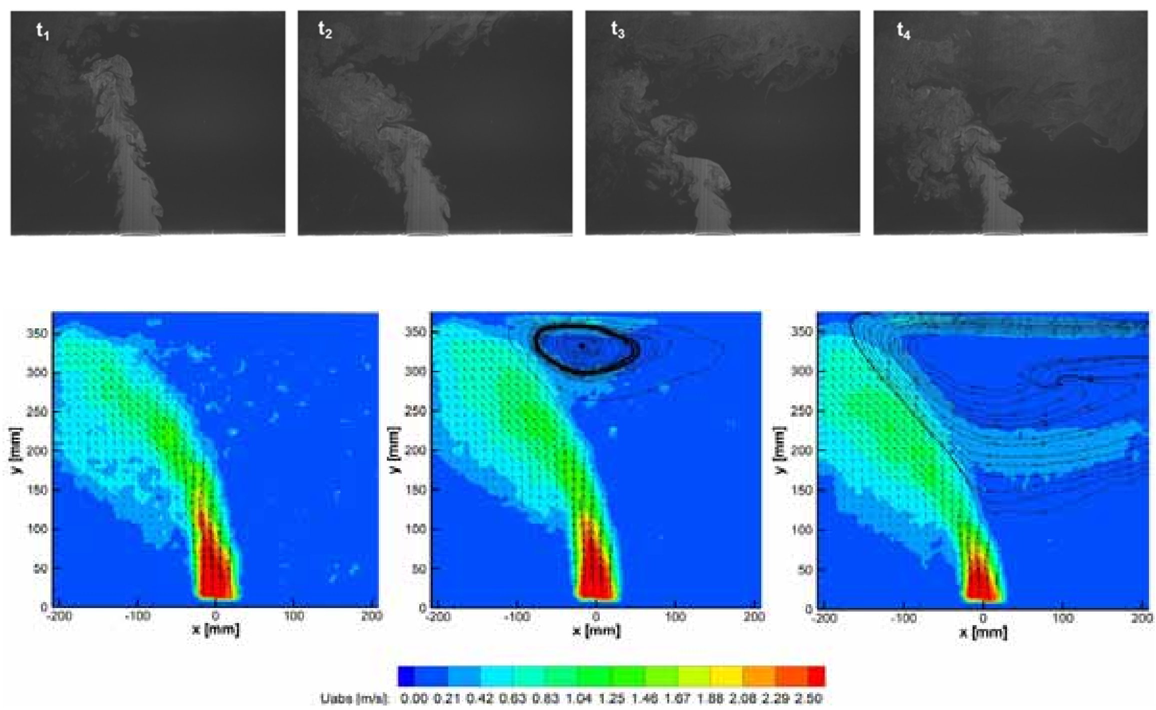

Figure 6: a) Visualization of the spread of the helium-air mixture at four time steps without standing vehicles, jet velocity $u_j = 3.7$ m/s; b) corresponding velocity distributions

With traffic congestion in the tunnel the process described above tends to appear more pronounced due to the partial blockage of the tunnel cross section (Figure 7a). The generation of the backlayer seems to be accelerated ($t_1 = 1$ s, $t_2 = 3$ s). At $t_3 = 8$ s the size has grown and the helium-air backlayer covers already half of the cross section and stretches beyond the area depicted. Later at $t_4 = 39$ s the helium-air propagation opposite the ventilation direction has further continued.

The corresponding velocity distributions for u_{abs} and streamlines derived from two averaged time intervals are plotted in **Figure 7**b. Contrary to the case without vehicles the generation of the vortex starts already during the first 2 seconds of the measurement (**Figure 7**b left). The velocity distribution in **Figure 7**b (right) has been averaged over a time interval of 10 seconds about 40 seconds after the start of the measurement. The recirculation zone is covering the whole tunnel height so that the helium-air mixture is distributed down to the floor level. In comparison to the velocity distributions of the empty tunnel the plume seems to be bended less by the ventilation.

a)

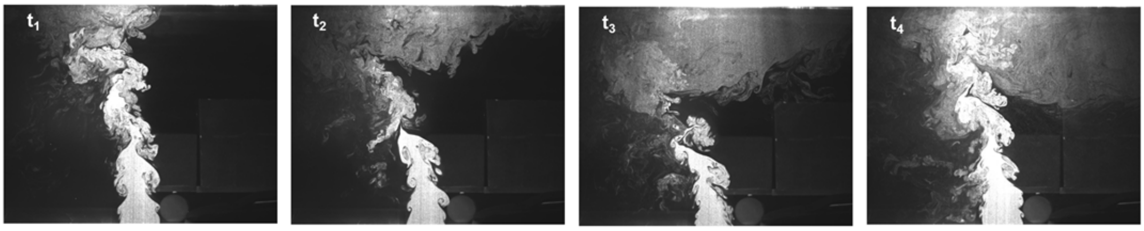

b)

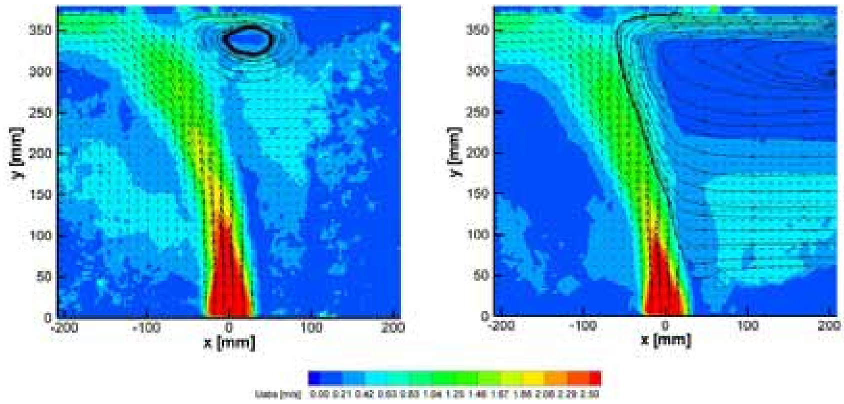

Figure 7: a) Visualization of the spread of the helium-air mixture at four time steps with standing vehicles, jet velocity u_j = 3.7 m/s;
b) corresponding velocity distributions

An increase of the jet exit velocity up to 5.0 m/s leads to a visibly more bended helium-air plume in ventilation direction. For both investigated traffic configurations no backlayering effect has been observed. The ventilation velocity seems to be high enough to blow the helium-air plume completely downstream of the modelled fire (Figure 8).

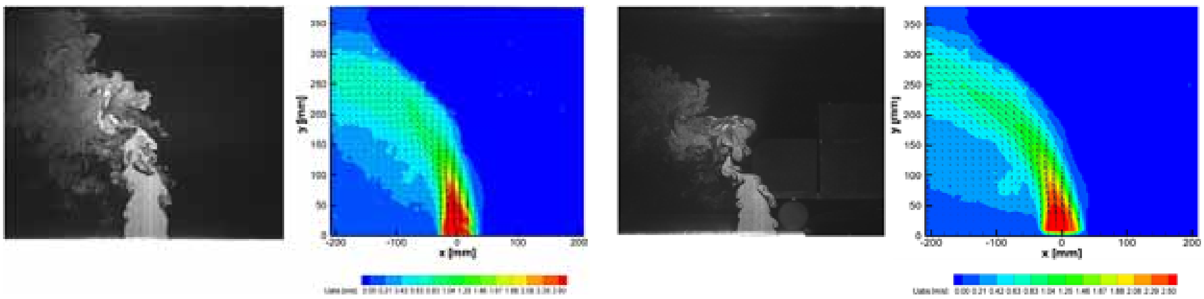

Figure 8: Visualization of the spread of the helium-air mixture and corresponding velocity distributions, jet velocity u_j = 5.0 m/s; left: without standing vehicles, right: with standing vehicles

3. NUMERICAL RESULTS

The CFD (computational fluid dynamics) simulations have been performed with the FDS (Fire Dynamics Simulator) V6 that is known for its frequent application in tunnel fire studies. The FDS simulations have been conducted for the same isothermal scenarios as described above using a helium-air mixture injection into a model tunnel. Additionally, FDS has been applied to an exothermal approach with down-scaled propane fires showing only insignificant differences between both approaches regarding smoke propagation velocities and layer thicknesses.

The velocity distributions for u_{abs} resulting from the FDS simulation using a helium-air mixture show a good agreement with the experimental results. The observed development of a backlayer depending on the presence of standing vehicles and the jet exit velocity has been confirmed (**Figure 9**). The velocity values and the size of the recirculation area match very well with those resulting from the PIV measurements (**Figure 7**b right).

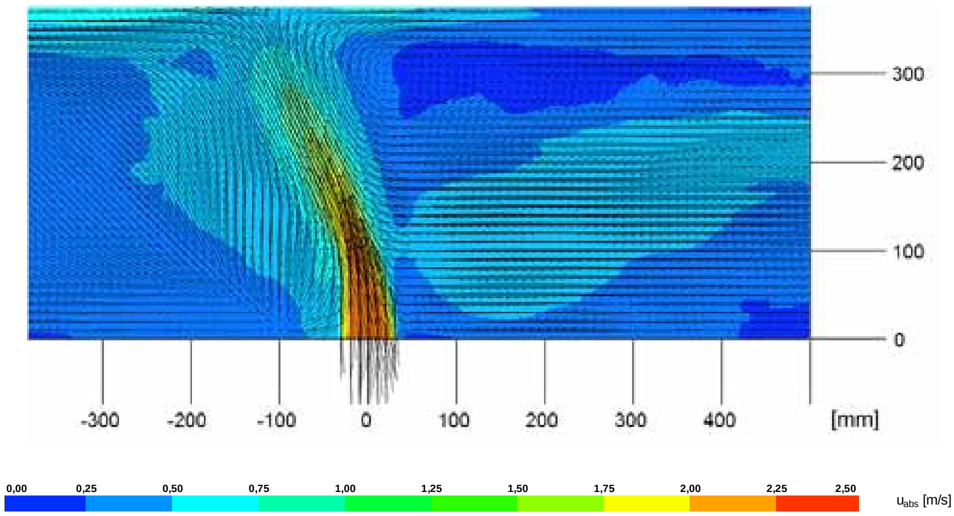

Figure 9: Velocity distribution with standing vehicles, jet velocity u_j = 3.7 m/s, simulated for the injection of a helium-air mixture ($Q_{C, equiv.}$ = 2 MW)

4. CONCLUSIONS

The impact of longitudinal ventilation on the smoke propagation in case of a tunnel fire has been investigated experimentally and numerically in a small scale model tunnel using an isothermal approach by injecting a helium-air mixture. The influence of the traffic situation and the ventilation velocity has been considered evaluating the propagation of the helium-air mixture.

The results show the influence of standing vehicles in the tunnel compared to an empty tunnel lead to an accelerated development of the backlayering effect at lower ventilation velocities. Increasing the ventilation velocity prevents the formation of backlayer in both cases. This effect should be taken into consideration when the longitudinal distance between jet fan groups is defined. Future research on the model tunnel will include the variation of jet fan velocities and heat release rates.

The application of the nonintrusive PIV technique with regard to investigations on smoke propagation in a model tunnel gave valuable insight into the interaction between the ventilation flow and the plume that is relevant for the development of the backlayer phenomena.

Further results obtained in the project prove that small-scaled investigations of flow in a road tunnel can be performed reasonably. For example the velocities of smoke propagation corresponded to literature values with respect to the smaller scale and the heat release rates. It can therefore be assumed that the model tunnel can be used for scientific purposes as well as for the dimensioning of ventilation systems especially in circumstances differing from the technical standard.

5. ACKNOWLEDGEMENTS

The results presented in this paper originate from the research and development project “Investigations on the optimization of longitudinal ventilation systems for road tunnels based on the development of a model tunnel” (FE 15.0539/2011/ERB). This project was supported by the German Federal Ministry of Transportation and Digital Infrastructure (BMVI) and conducted by the Federal Highway Research Institute (BASt). After the completion of the project the model tunnel is now situated at the BASt.

6. REFERENCES

[1] RABT 2006: “Richtlinien für die Ausstattung und den Betrieb von Straßentunneln”, Ausgabe 2006. Forschungsgesellschaft für Straßen- und Verkehrswesen, Köln 2006

[2] Ingason, H., Werling, P.: “Experimental Study of Smoke Evacuation in a Model Tunnel“. FOA Defence Research Establishment, Report No. FOA-R--99-01267-311--SE, Tumba/Sweden, 1999

[3] Wu, Y., Bakar, M.Z.A: “Control of smoke flow in tunnel fires using longitudinal ventilation systems - a study of the critical velocity.” Fire Safety Journal 35 (2000), pp. 363-390

[4] Roh et al.: “Critical velocity and burning rate in pool fire during longitudinal ventilation”. Tunnelling and Underground Space Technology 22 (2007), pp. 262–271

[5] Vauquelin, O.: “Experimental simulations of fire-induced smoke control in tunnels using an ‘air-helium reduced scale model’: Principle, limitations, results and future”. Tunnelling and Underground Space Technology 23 (2008), pp. 171–178

[6] Adrian, R. J.: “Particle-Imaging Techniques for Experimental Fluid Mechanics”. Annu. Rev. Fluid Mech., 23 (1991), pp. 261–304

[7] Raffel, M., Kompenhans, J., Willert, C. E.: “Particle Image Velocimetry”. Springer-Verlag, New York, 2007

TUNNEL COMPLEX BLANKA IN PRAGUE – TESTING OF THE OPERATIONAL SAFETY AND FIRE VENTILATION SYSTEM

[1]J. Zápařka, [1]L. Šajtar, [1]J. Pořizek, [2]J. Šulc,
[1]Satra spol. s r.o., Czech republic
[2]CTU in Prague, Faculty of Electrical Engineering, Department of Control Engineering

ABSTRACT

This contribution presents the process of testing of the equipment of the 5, 5 km long "Tunnel complex Blanka", before opening for the testing operation in September 2015.

The tunnel complex includes in each tube two exits and two entry ramps, thus dividing each tube into three tunnels. All the tunnels are unidirectional, with occurrence of traffic congestions. The safety concept is based on quick reaction and on control of the direction and velocity of the longitudinal flow in the tunnel. For the means of the fire detection and correct localization, there are installed smoke detectors along the whole length of tunnel complex, thus dividing the whole complex into 125 fire detection sections, which correspond to certain types of system reaction.
The height and width of the cut and cover cross-section didn't allow duct for smoke extraction along the whole length of the tunnel complex. So there are combinations of driven sections, with smoke extraction by few remotely controlled dampers and duct underneath the roadway, than cut and cover sections with massive single point extraction and also exit ramps and portal sections, with longitudinal smoke extraction.
There is 2nd Phase of the fire ventilation, for the safe access of the fire-fighters, which ensures minimally critical velocity and thus clear access from the upstream side of the fire.
Besides the complex testing of the technical equipment, there was payed close attention to the training of operators, and then testing of their coordination, especially with fire brigades, police and medics.
By the time of the conference, there is first experience with testing operation, so some preliminary results are also presented.

Keywords: fire ventilation system, tunnel system testing, commission testing, testing operation

1. INTRODUCTION

The tunnel complex Blanka is city tunnel with recent traffic intensity 75.000 veh /24h. The tunnel complex is located on the Inner City Ring Road and after its completion, the traffic intensity is expected over 100.000 veh /24h. The traffic consists of 95% of personal vehicles and there is 12 ton limit for trucks. Besides the main entry and exiting portals, there are entry and exiting ramps, so separating and merging lanes are involved along the tunnel, widening the tunnel locally from 2 continues lanes into three.
The emergency situations have been evaluated on basis of 30 MW design fire, peaking in 10th minute from the start. Critical for the design and dimensioning were sections of the tunnel with 5% longitudinal down-grade.
After opening for operation, the first half of year gives first results from the standard operational ventilation. Special requirements were demanded for the portal and ramp emissions. Ventilation system had to provide such mode of operation, that all the pollution would leave the tunnel through the stacks. For this purpose was designed expert system, that is able to keep the portals in negative pressure by the means of jet fans and machine rooms, using energetically most effective way.

2. SYSTEM TESTING

The system testing of the entire tunnel complex was conducted in three stages. At first the individual elements and equipment was tested for function and performance. During this period was controlled dimensioning and performance of fans and dampers. Also ability to extract smoke through the extraction point was tested by hot and cold smoke. This can be seen on Figures 1 and 2. After completion of the first stage starts verification of automatic operation, when all states, and transitions between them, have to be tested. Only after that can be tested the whole tunnel emergency system, when relationships between the complexes were verified. Regarding the operational safety the focus was on following:

2.1. Fire and smoke detection

The fire and smoke in the tunnel can be detected by several means. The only fully automatic detection, that doesn't require confirmation of the operator, is liner heat detection along the whole length of the tunnel. Smoke can be detected by CCTV cameras or by smoke detectors. There is smoke detector for each of 125 detection sections. The affected detection section is offered for confirmation to the operator. Also near the cross-passages are alarm push-bottoms.

2.2. Detection of moving smoking vehicle

The detection system has to ensure reliable identification of the fire location even in the case, when the smoke source at the beginning moves along the tunnel and stops after a while and only than flares up. During these tests, the detection algorithm was optimized, in order to show on screen, increased level of opacity travelling through the tunnel and when the smoke source stops, to offer specific detection section for the operator to confirm and thus start the emergency sequence.

2.3. Pre-ventilation

This mode was implemented in order to make sure, that in the period between beginning of the fire and alarm confirmation that starts the fire ventilation, the longitudinal flow doesn't reverses direction against the standard traffic direction. This mode is initiated by smoke detection and starts to act only when the velocity plummets under 1,2 m/s.

2.4. Smoke control

The objective for the fire ventilation in urban tunnel with congested traffic is to protect persons trapped in the tunnel on both sides of the fire, by maintaining low longitudinal airflow velocity in the direction of traffic and by extracting the smoke by the machine-room. Typical extraction in the driven sections is through 3 dampers, 80-90 meters apart. One opened damper upstream and two dampers down-stream from the fire. In the case of design fire intensity, the smoke builds up on both sides of the fire in few minutes.

After arrival of fire brigades, save access to the fire is provided by increase of the longitudinal flow up to at least critical velocity, which ensures spreading of the smoke only down-stream from the fire. Also extraction of the smoke is to the maximum capacity through 3 dampers opened down-stream from the fire.

During the thorough system testing and optimisation, hundreds of tests were done.

3. TESTS FOR COMMISSIONING

From those 125 possibilities of detecting sections of fire location in the tunnel, 8 were picked for commissioning tests. Alarm was initiated by several means: by heating of the linear detection cable, by initiating the smoke detector, through CCTV video-detection or by alarm push-buttons. It also included initiation by moving smoking vehicle that stopped in the tunnel after a while as seen on Figure 3. After initiation all the equipment including ventilation had to perform according to the design.

Besides equipment reaction, the cooperation of tunnel operators and rescue units was tested according to the emergency procedures. These procedures were based on fire load of design intensity. In the Figure 3, next to the picture from the tests, is seen fire development with expected smoke propagation, to compare with smoke propagation of aerosol during the tests. By purple colour is visualised smoke temperature of 60°C.

The strategy for fire-fighting is based on accessing the fire through the first cross-passage up-stream from the fire.

Figure 1: Hot smoke extraction

Figure 2: Cold smoke extraction

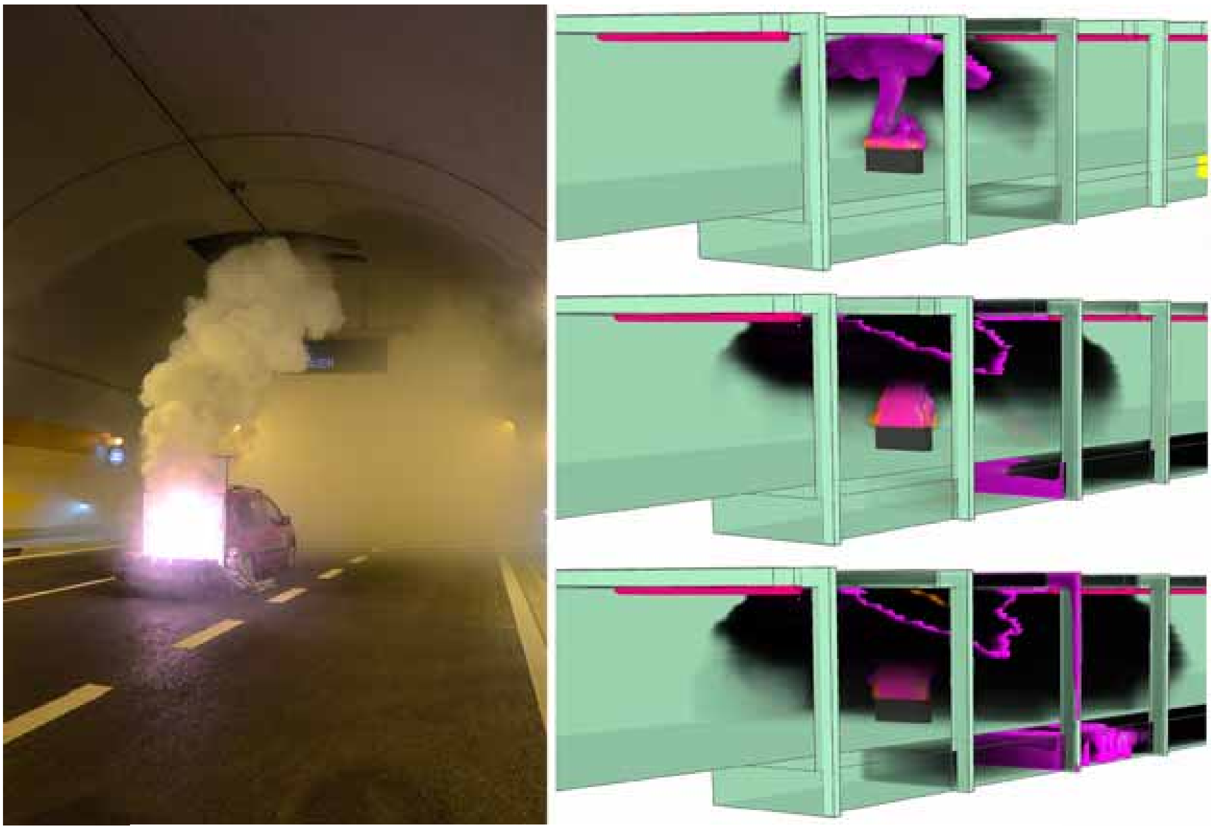

Figure 3: Aerosol and CFD solution for design fire of 30 MW

4. TESTING OPERATION

Only after opening for operation the detection system can be optimized. Main focus has been kept on decreasing the number of false alarms mostly from CCTV video-detection. Alarms from video-detection or smoke detection, have to be confirmed by the operator, so it doesn't start the emergency sequence automatically.

The standard operational ventilation system was gradually being put into operation in the last quarter of 2015. At the first stage of operation, various power levels were tested and the relevant faults remedied.

Connected to the tunnel control system, a robust stand-alone controller is responsible for control and regulation of the entire ventilation system. The controller is sending its commands to the individual fans and associated plant. Due to the number of actuators and segmentation of the tunnel complex, the ventilation system control is complicated. The control is unique in terms of its design and working principle. Values of all the actuating variables are set and then returned by feedback on the basis of contemporary traffic conditions, nature of traffic and air pollution levels and thanks to incessant numeric analysis of the one-dimensional mathematical & physical model of the ventilation system. Number, direction of running and power of jet fans and fans in the plant rooms have been determined for fulfillment of all the conditions and utmost economy of operation. In this way, the controller will distribute necessary capacity to be shared among four plant rooms and – depending on the air pollution level inside the tunnel and growths in traffic density – will select an adequate level of the service ventilation intensity. The jet fans provide smooth control of the direction and value of airflow longitudinal velocity inside the tunnel.

At present, operation of the service ventilation can be considered as well stabilized and the conditions are met during the daytime at which there are no natural pollutant exhausts from the tunnel complex exit portals due to the piston effect, as it was required within the construction permit procedure.

Figure 4 provides information about location of measuring points of volume flow and pollution in the machine-rooms (red – extraction machine-room; orange – transfer machine-room from exiting into entry tube) and outside the tunnel around the portal (purple and blue).

Figure 4: Measuring points by the portal, expected increase of pollution produced by the tunnel [1].

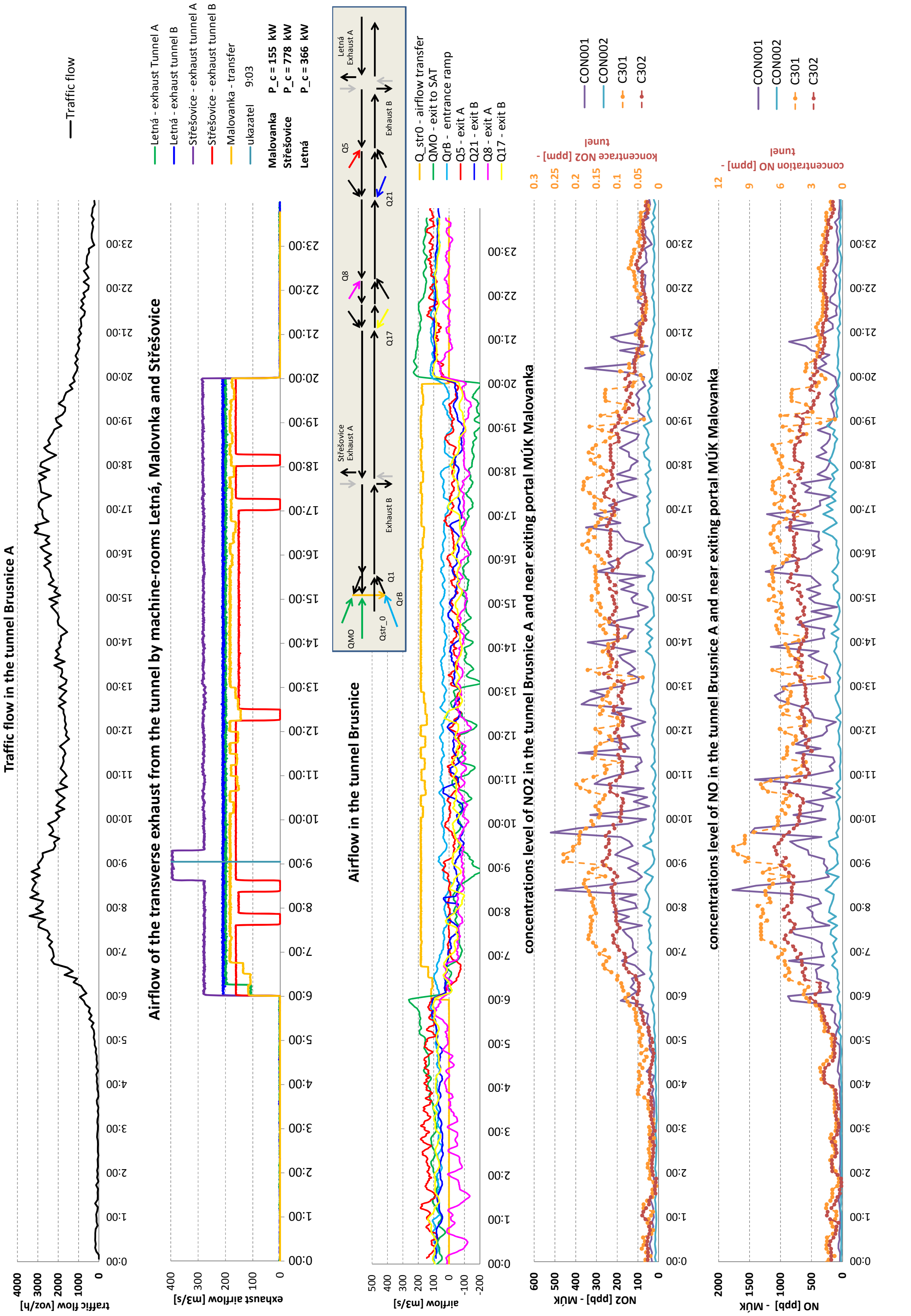

Figure 5: Measured values: Traffic intensity, extracted volume, airflow at the portals and ramps, concentration levels of NO_2 and NO (outside the tunnel scale no the left in ppb and inside the tunnel scale on the right in ppm, for inside the tunnel [2].

This year witnessed beginnings of detail pollution level measurements around the exit portals, exhaust stacks, and surface roads. Nitrogen oxides, suspended particles (PM10 and PM2.5 fractions) will be measured, along with the Benzo[a]pyrene (BaP) analysis and the measurements will be taken from the total of 8 locations at various levels of the tunnel service ventilation output.

5. CONCLUSION

The tests of the fire ventilation and emergency equipment before tunnel opening met the design performance expectations. During the testing operation, majority of false alarms have been eliminated.

Regarding the normal, standard operation, it can be concluded that the main efficiency and economy indications of the ventilation system designed, match the expected requirements, according to which the design of the system itself and its operation methods was drawn up. With growing morning traffic the forced ventilation system is activated, which then – all day long until evening when the traffic density drops again – efficiently prevents polluted air exhausts through the exit portals without exceeding the permissible levels of pollution inside the tunnel. The most part of the total daily summary of the pollutants produced inside the tunnel is extracted and exhausted through the stacks.

6. REFERENCES

[1] J. Maňák; Dispersal study; Rozptylová studie pro emise znečišťujících látek z dopravy pro alternativní umístění a výšky výdechu; April 2008, Prague

[2] J. Pořízek: Partial report from testing operation; Dílčí zpráva vyhodnocení zkušebního provozu; February 2016, Prague.

TUNNELS CORROSION AND SEVERAL PROBLEMS IN FANS IN ROAD TUNNELS OF A-67 HIGHWAY

[1]F. Collazos-Arias, [2]P. Pascual-Muñoz, [3]L. Ayres
[1]Ministry of Development, Spain
[2]University of Cantabria, Spain
[3]Imesapi, Spain

ABSTRACT

This paper focuses on the problem of pressure gradients in long alpine tunnels, the technical solutions available, and on what needs to be considered when designing such installations in tunnels undergoing upgrading. This paper analyses the recent experiences concerning the thorough inspection of tunnel fans as part of the plan of general maintenance of the A-67 highway in the North of Spain. In this inspection, several problems arose in 12 fans of 4 different tunnels such as defects on engines and impellers or corrosion in different elements from the fans and their anchors. In response to this, the manufacturing company issued a report in which they basically attribute such problems to the corrosive environment in the tunnels due to the spread of salt and brine in areas close to the openings, which is then dragged inwards by the vehicles. In view of the serious risk for the road safety due to having many fans down and not being able to foresee the evolution of the rest of them, a decision was made to declare the maintenance works as an emergency. It should be considered that many fans got unhooked from their anchors at the ceiling, even though none of them fell down on the road because it was fastened by the safety chain. On the other hand, some of the blades broke down and fell on the road, luckily without accidents. With some operation problems and increasing repair costs, the fans kept on working in the tunnels until recently, when a rapid degradation caused that 38 out of the 122 fans in the five tunnels became out of broken blades by friction with the casing, broken startup systems, high vibrations, etc. Corrosion in many elements, including the anchors, also appeared. Those 38 fans were replaced by stainless steel fans to comply with the corrosive environment in the tunnels, which is due to their height above the sea level and the road treatments with salt and brine close to their openings. Besides, a revision and a total repair was carried out in the rest of the fans: anchors, casings, blades, engines, instrumentation and electrical wiring.

Keywords: ventilation design, long tunnels, corrosion.

1. INTRODUCTION

In the Highway Cantabria- Meseta, in the Community of Cantabria, in the North of Spain, the section comprised between Reinosa and Torrelavega (Figure 1) the tunnels of Lantueno, Somaconcha, Pedredo, Gedo and Riocorvo are found, whose geometric characteristics are in Table 1.

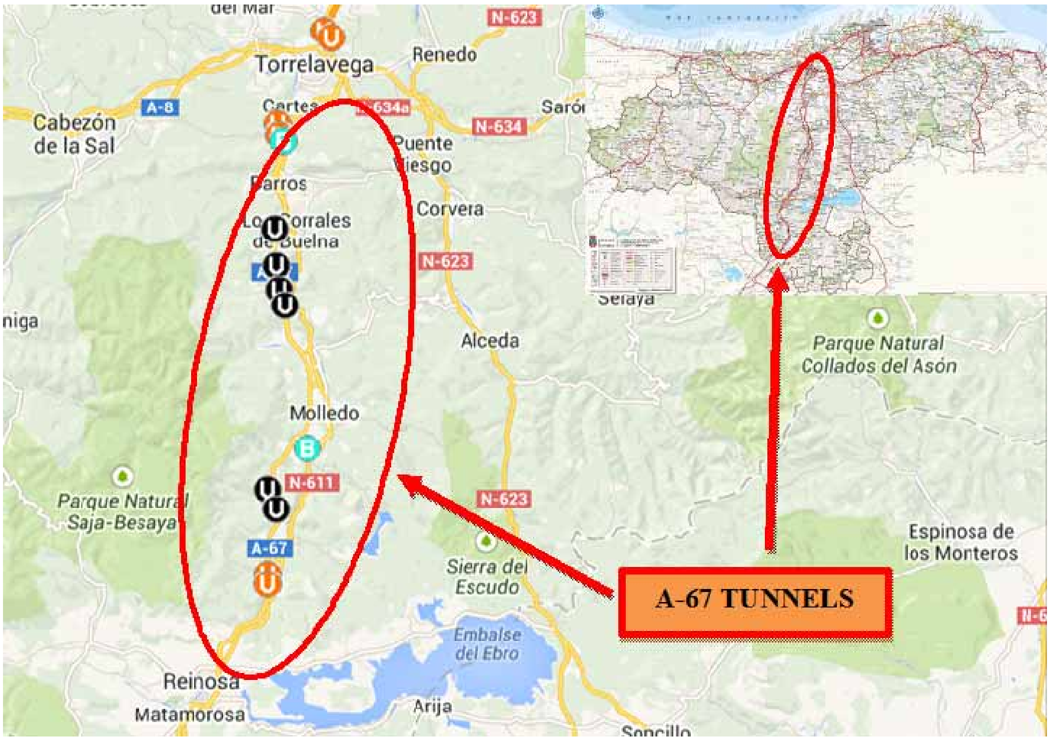

Figure 1: Map of Highway A-67 tunnels

Table 1: Characteristic's road tunnels A-67

Name of the tunnel	Length [m]	Tube (numbers of fans)	Direction	Pk.	Pk.	Height [m]
Riocorvo	660	Tube 1 (6)	Palencia	174+038	173+378	110
	685	Tube 2 (6)	Santander	173+378	174+063	
Gedo	2.453	Tube 1 (22)	Palencia	166+883	164+430	200
	2.431	Tube 2 (20)	Santander	164+430	166+861	
Pedredo	1.063	Tube 1 (14)	Palencia	162+901	161+838	290
	1.061	Tube 2 (14)	Santander	161+838	162+899	
Somaconcha	1.500	Tube 1 (8)	Palencia	148+305	146+805	650
	1.573	Tube 2 (16)	Santander	146+805	148+378	
Lantueno	732	Tube 1 (6)	Palencia	142+632	141+900	750
	694	Tube 2 (6)	Santander	141+938	142+632	

These tunnels start with the highway design at 110 m height up to 750 m height in a length of 35.000 m as it may be appreciated it in Figure 2.

Figure 2: Longitudinal section and orthophotos of the A-67 from kp 118 to kp 175

The sections where the tunnels are set were put into service from May 2003 to January 2008. Lately, a series of problems and incidents have occurred in the mentioned tunnels, which are specified next.

Concerning ventilation the problems were:

- Corrosion of different parts of the fans.
- Break of blades. Break of contactors.
- Break and corrosion of anchors.
- Vibrations in the fans.

Concerning other equipment the problems were:

- Break of the OTS optical controller for fire detection.

Following, the events recently happened in the highway are summarised. Mid 2011, after extensive maintenance by the Conservation departament of roads requested to the fans manufacturer, a series of problems in the 12 fans in the tunnels Lantueno, Somacocha, Gedo and Pedredo, like defects in the engines and impellers and corrosions in different pieces of the fans and anchors were detected.

The failures were repaired and the fans went on working in quite acceptable conditions until March 2013, time when problems arise again in 3 fans in the Lantueno tunnel, such as impeller break, electrical engine break and corrosion in the blades.

The fans manufacturer issues a report on 29 July 2013 in which, basically, the problems are attributed to the corrosive environment found in the tunnels due to the salt and brine spread out very closely to the tunnels openings and which are later dragged inside by the vehicles wheels, especially the Lantueno tunnel, which is the one presenting the greater problems. It is placed at the highest level of all the tunnels.

With some problems in their operation and with increasingly higher reparation costs, the fans went on working in the tunnels until a fast degradation takes place, as 38 of the 122 fans that the five tunnels gathered show such failures that they end up out of order, as blades broken by frame rubbing, start system broken down, high vibrations, damaged contactors, damaged engines, etc., apart from corrosion in many pieces, including anchors.

The most worrying fact is that some fan unhooked from its anchors to the tunnel ceiling, although it did not fall on the road thanks to the safety channel (Figure 3 and Figure 4**)** and that no blade got broken and fallen on the pavement, avoiding accidents.

It must be highlighted that the tunnels were under reduced conditions for traffic safety reasons in case of a fire, excess of CO and/or excess of opacity. Fans with excessive vibration were cancelled so that blades, or their fragments, were not sent out to the pavement.

In order to preserve the tunnels ventilation, it was considered that the 38 cancelled fans had to be replaced by other new, with a clear definition and demand of operation in the A-67 tunnels.

On the other hand, the OTS optical controller for fire detection, which in turns sends the signal to the URS, universal remote station, activates the response established in the fire protocol.

The tunnels control centre in Pedredo is surrounded by mountains. There may be powerful thunderstorms. During an operation test of the three existing OTS it was verified that they did not work since the thunderstorm had left them out of order, being necessary to check all elements likely to end up out of service like this, such as CO detectors, variable signaling panels and protect the tunnel control building, in general, from the lightning with lightning protection.

Figure 3: Break of fan support in Lantueno tunnel ceiling

Figure 4: Detail of support break in Lantueno tunnel ceiling

2. JUSTIFICATION OF THE INTERVENTION

2.1. Ventilation system.

A relation of some warnings happened in the tunnels is present in Table 2 due to reasons such as break of the fan start system, likely vibration sensor failures or excessive fan vibration, symptom preceding its break. The mentioned warnings demand the execution of immediate repairs, and in due case, the fan substitution.

Table 2: Some of the warnings happened in the tunnels.

Starter shot	Blades resting in exterior frame
Starter shot	Broken down engine
Starter shot	Dismantled fan
Starter shot	Broken down contactor
Starter shot	Fan has broken blades
Starter shot	Breakdown in electrical engine
Starter shot	Blades resting in exterior frame
Starter shot	Reading in sensor of normal vibration. Failure in intermediate equipment.
Starter shot	Reading in sensor of quite high vibration. Possible failure of vibration sensor or the fan is vibrating a lot.
Starter shot	Reading in sensor of normal vibration. Failure in intermediate equipment.

Next, some pictures of the mentioned problems are shown in **Figure** 5, 6, 7, 8 and 9.

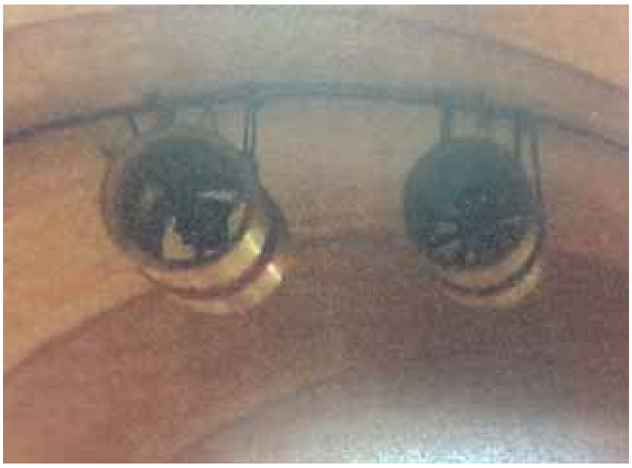

Figure 5: Blades of impeller broken. Fan V5 direction to Santander. Lantueno tunnel (18/11/2013).

Figure 6: Disassembly of fan in tunnel key of Lantueno tunnel

Figure 7: Detachment of the fastening area of the engine 1 and 2 direction Palencia Lantueno tunnel.

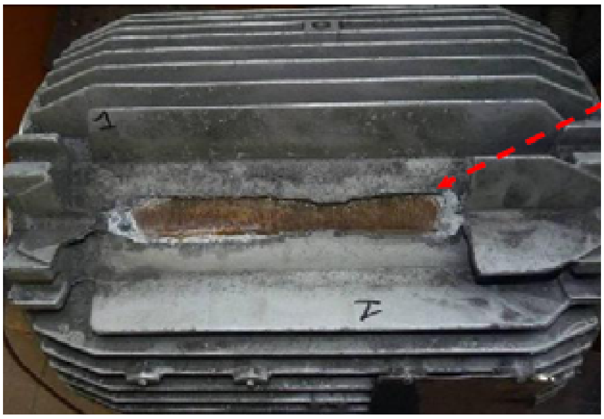

Figure 8: Break in the fastening area of engine of fan V5 direction Palencia Lantueno tunnel.

Figure 9: Iron oxides (stator corrosion) of the engine of the fan V5 direction Palencia Lantueno tunnel

2.2. Other equipment

As it has been previously mentioned, three OTS optical controller units for fire detection were out of service, with the subsequent risk for traffic safety, which implies that a fire may occur in the tunnel and that the corresponding responses are not activated.

3. TECHNICAL SOLUTIONS

A total of 38 fans were replaced by other of stainless steel, due to the corrosive surrounding where the tunnels are located for their height above the sea and the salt and brine treatments in their opening, and a revision and total repair of the remaining both in anchors, frames, blades, engines, intruments and electrical wiring.

Of the 38 replaced fans, the following characteristics are fulfilled:

- 12 units, in Lantueno tunnel, of reversible jet fans, with 3 phase engine of 30kw, 1000mm diameter IP55 and waterproofing type H for 250º for 2 hours, with stainless steel impeller. 6 units are placed in the tube direction Palencia and 6 units in the tube direction Torrelavega.
- 22 units in the Pedredo and Gedo tunnels, of reversible jet fans, with 3 phase engine of 30kw, of 1200mm diameter IP55 and waterproofing type H for 250º for 2 hours, with stainless steel impeller. Distributed in the following way: 8 units placed in Pedredo (4 units in each tube) and 14 units in Gedo (6 units in tube direction Palencia and 8 units in tube direction Torrelavega).
- 4 units in the Riocorvo tunnel, of reversible jet fan, with 3 phase engine of 37kw, of 1200mm diameter IP55 and waterproofing type H for 250º for 2 hours, with stainless steel impeller. 2 units are set in each tube.

Of the remaining 122 fans, a record and a fine-tuning were made for each ventilation equipment. At the reception of the equipment, the different elements were verified: drive and extraction mufflers (painting, scuffing, bruised and thread); the turbine (painting, impact, balancing); support (painting and impact); ferrule (painting, scuffing, bruised, terminal box, fittings); engine (painting, lubrication, wiring, fron and rear bearing, support screws) and a no-load test. And at the delivery verification a test was made in direct direction (fulfilled with a visual inspection of the engine supports, shock absorbers, electric connection, painting state, inside and outside cleaning, start time, turning sense, screws state, lubrication of equipment, screws tightening).

In relation to the instrumentation, the OTS in the technic rooms existing in the Pedredo Norte, Gedo Norte and Gedo Sur tunnels will be replaced. Both the hardware and software were replaced which rule the OTS optical controllers of fire detection with the aim to guarantee their operation.

RISK ANALYSES OF TUNNELS USING THE SWISS GUIDELINE AND METHODOLOGY FOR RISK ASSESSMENT AND RISK EVALUATION

**Niels Peter Høj, *Samuel Rigert, and *Marco Bettelini
* Amberg Engineering Ltd., Regensdorf-Watt, Switzerland
** HOJ Consulting, Brunnen, Switzerland

ABSTRACT

Significant experiences with the use of the new Swiss guideline for risk analyses of road tunnels have been gained during 2015. This paper presents the background of the methodology and illustrates its practical application. The methodology is applicable for new projects, in order to demonstrate the most efficient design options, and for existing tunnels, which may not be fully compliant with present day regulations, in order to decide on the best upgrade options.

Based on this experience, the paper illustrates how the fire risk was assessed in two tunnels. The risk was estimated in the initial condition and subsequently with different safety measures including emergency exits of different types and distances. In the first example, it was proven that the construction of emergency exits was cost efficient and recommendable. In a second case, a comparison was made between a tunnel project with a high gradient and an alternative with a longer tunnel with a more moderate gradient. Using the new methodology it could be shown that the longer tunnel did not constitute a cost efficient alternative to the steep tunnel.

Keywords: quantitative risk analysis, risk assessment, risk evaluation

1. INTRODUCTION

At the end of 2014, the Swiss Federal Roads Administration (FEDRO) issued a guideline (ASTRA 19004, 2014) on Risk Analyses for Tunnels on the National Roads network. The guideline specifies in which cases risk analyses have to be carried out, the level of detail to be applied for the analyses and risk evaluation principles. In an additional document (ASTRA 89005, 2014) FEDRO specifies in detail the methodology, which shall be used for risk assessment and risk evaluation. The methodology includes also a parametric model for ventilation, smoke propagation and emergency egress. The guideline's goal is a high reproducibility of the results of risk analyses. A third document (ASTRA 89007, 2014) specifies the format of the results and gives a template for the reporting of the risk analyses.

In the following, the methodology is briefly outlined and its application is illustrated based on two examples.

2. METHODOLOGY

The core of the risk evaluation methodology is the ALARP principle and the application of marginal costs of substitution. This means that the fatality risk shall respect predefined limits and the safety shall be improved until further improvements can be shown cost-inefficient. The guideline specifies the "weight factors" on the consequences, the limits and the procedure for proving the tolerability of the risk.

The methodology and the background for the methodology is well documented in the technical reports associated to the guideline (ASTRA 89005, 2014) and has been presented in a number of papers. In the following, some key aspects are highlighted.

- Homogeneous segments
- Bayesian probabilistic nets
  - Models for influence on risk of various tunnel design parameters / safety measures
  - A parametric model for ventilation, smoke propagation and emergency egress
- Evaluation procedures for the risk and for safety measures

A tunnel system is described by a number of parameters influencing the risk in the tunnel. These parameters (for example traffic, geometry etc.) may vary along the tunnel axis. In addition, the basic risk of events is dependent on the zones of the tunnel: entrance, interior and exit. For the quantitative analyses, each tunnel tube of the tunnel system is divided into segments, in which the parameters do not vary (the so-called homogeneous segments).

For each of the homogeneous segments, the risk is assessed by use of so-called Bayesian probabilistic nets (BPN). These nets are able to model the dependence between various risk indicators (for example the describing parameters) and the outcome. BPN can be understood as further development of logical trees (event trees, fault trees) and offers in addition to these the possibility to integrate the correlation between the risk indicators. In addition, BPN can be presented in a more compact and transparent way than logical trees with many parameters. Figure 1 presents a principle illustration of the nets applied for each homogeneous segment. The actual BPNs used in the methodology consist of a large number of nodes representing all influencing factors and intermediate results. Reference is made to ASTRA 89005 for more details. The outcome of all nets is aggregated to represent the risk assessment for each traffic direction and the entire tunnel system.

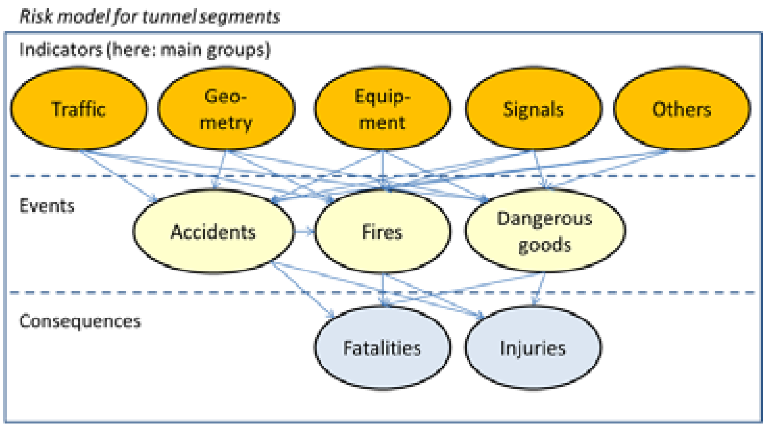

Figure 1: Bayesian probabilistic net risk model for tunnel segments (principle)

The risk assessment integrates models for the influence of a large number of relevant influencing parameters: Traffic volume, variation of traffic over time, congestion frequency, percentage of heavy vehicles, traffic speed, accident frequency, exits and entrances, horizontal radius, gradient, number and width of lanes, one-way or two-way traffic, distance between emergency exits, lighting (normal/emergency), monitoring system and ventilation.

In particular, the influence of the ventilation system and the ventilations strategy on smoke propagation has been integrated in the risk assessment model based on more than two million simulations of tunnel systems with various features. The simulations were carried out with the programs SPRINT and ODEM. (Riess et al, 2000 and 2010). Based on the simulations, response surfaces were fitted in order to achieve suitable parametric models (Riklin et al, 2014, Brandt et al, 2015). The parametric models can substitute adequately and with a high degree of accuracy individual smoke propagation and egress simulations.

Finally, the Swiss guideline and the technical documentation specify the evaluation procedures for risk acceptance and for safety measures. The procedure is based on the ALARP principle with limits of tolerability and evaluation of cost efficiency based on marginal costs of substitution (MRS).

3. APPLICATION

During 2015, significant experiences with the use of the new Swiss methodology for risk analyses of tunnels have been gained and in the following two cases are presented.

3.1. Case 1: Existing tunnel

A number of relatively short tunnels in Switzerland with bi-directional traffic did not have emergency exits and an upgrade program was started to build emergency exits and/or escape tunnels. These upgrade projects are rather costly and the question is, whether the upgrade is cost efficient or if the tunnels could be improved through other, less costly measures. In the following it is illustrated how the fire risk is estimated in a (hypothetic) existing tunnel without emergency exits.

The tunnel is located in a mountainous area with very steep gradients of 6%, has bidirectional traffic in one tube and its length is approximately 2 km. The traffic is neither extremely high nor extreme low, with 17’000 vehicles per day in 2035 and a percentage of heavy vehicles of 8%. Transport of dangerous goods is not allowed. The ventilation system is rather weak and is categorized as natural ventilation.

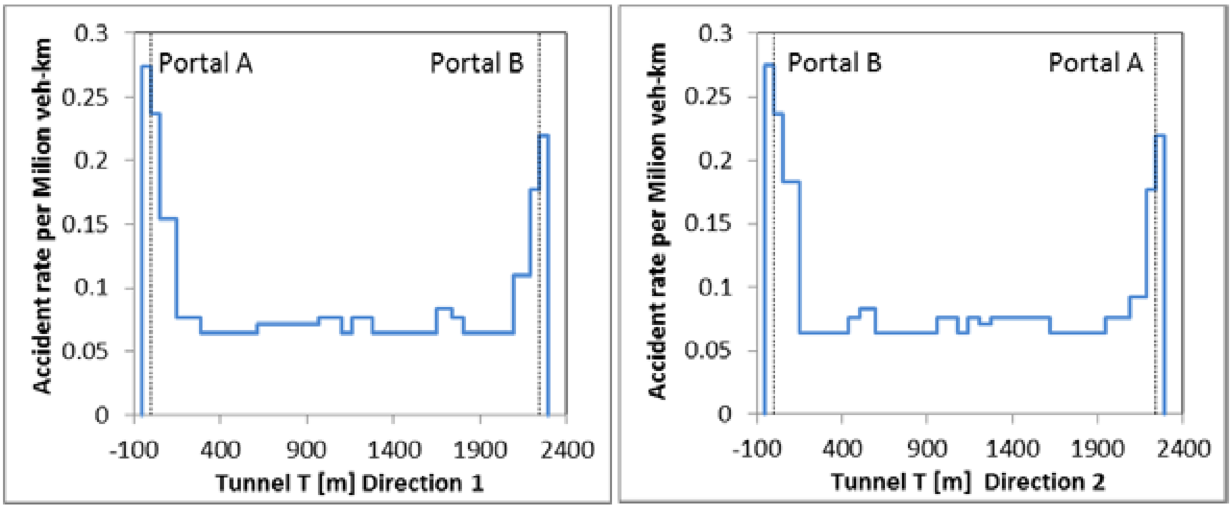

Figure 2: Case 1: Accident rates along the tunnel axis for the two directions

First, the risk is estimated for the initial condition without emergency exits. Figure 2 shows the accident rate over the length of the tunnel in direction 1 (upwards) and direction 2 (downwards). The accident rate is increased at the portals. The accident rate is rather high due to the gradient and other parameters (horizontal radius and others) result in some variation of the accident rate along tunnel length.

The fire rate is shown in Figure 3 for direction 1 (upwards) and direction 2 (downwards). It is clearly visible that the fire rate is very high, in particular in direction 1, as a result of the large upwards gradient.

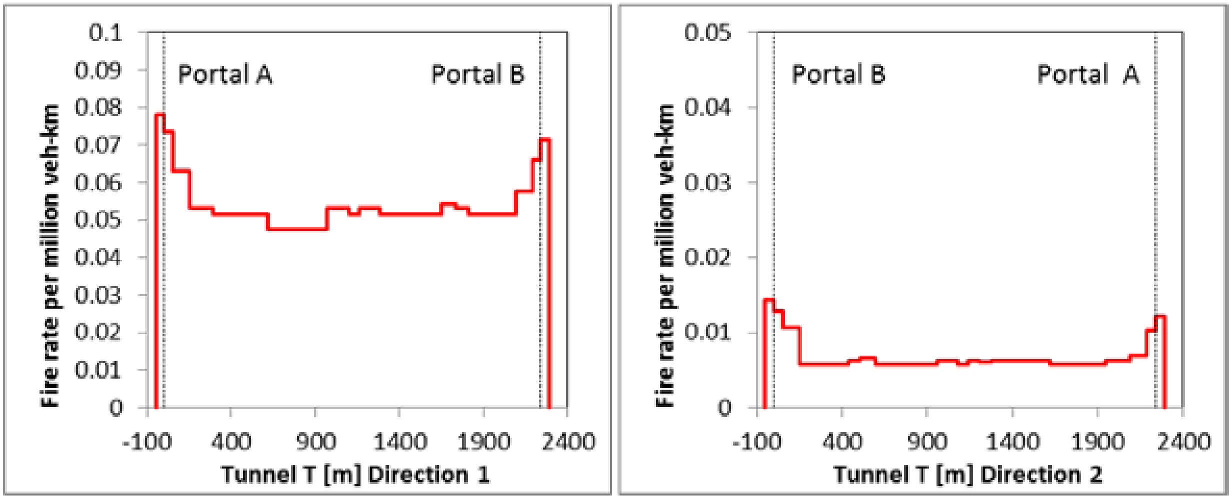

Figure 3: Case 1: Fire rates along the tunnel axis for the two directions

The fatality rate is shown in terms of fatalities per billion vehicle-km in Figure 4. The rate is very high in both directions and significantly over the defined upper tolerability limit (13 fatalities per billion veh-km). Vehicle fires are the main contributor to the fatality risk.

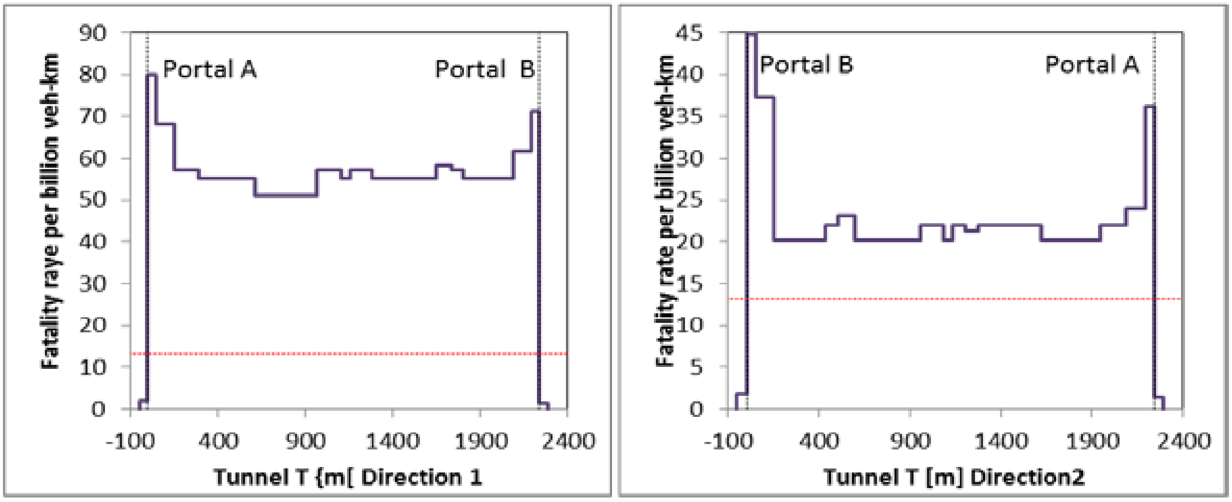

Figure 4: Case 1: Fatality rates along the tunnel axis for the two directions

For this reason, it is necessary to implement safety measures. The risk must be brought under the upper tolerability limit. Emergency exits with a distance of 300 m, 200 m and 100 m were identified as suitable safety measures to reduce the fire risk. In addition, improved lighting (in the following denoted as 5 $cd{\cdot}m^{-2}$) was investigated.

The investment and running costs of the measures were calculated and, according to the guideline, transformed into annual costs (based on the annuity factor and inflation factor given in the guideline). The costs of improving the lighting appeared to be very low, whereas the investments for emergency exits were in the magnitude of 25 MCHF, resulting in annual costs in the magnitude of 1 MCHF. The annual costs of establishing emergency exists every 100 m, 200 m and 300 m did only increase by about 10% because a major part of the investment was a parallel safety tunnel to be used for the egress.

The benefit resulting from the emergency exits every 300 m was a significantly reduced fatality risk in case of fire. With distances of 200 m and 100 m, this risk could be further reduced to approximately half and one quarter of the risk with exits at 300 m. The benefits in terms of reduced annual risk of fatalities and injuries were quantified in monetary units according to the specified weighting factors used for road traffic in Switzerland, which specifies a MRS of 5 MCHF and an equivalent of 31 injuries with 1 fatality. Based on this, the efficiency of the measures were determined as the ratio between the quantified annual benefit in monetary units and the quantified annual costs.

The efficiency of emergency exits every 300 m was 1.425, for exits every 200 m it was 1.430 and for exits every 100 m it was 1.401. The efficiency of improved lighting was 3.719. Even though the benefits arising from this measure were relatively modest, the very low annual cost made this measure the most efficient one. Following the principles of ASTRA 89005, the measures shall be introduced incrementally, starting with the most efficient measure, until further measures are no longer efficient. This is illustrated in Figure 5. In this incremental method, the efficiency of the remaining measures has to be re-evaluated after each step, because the efficiency of remaining measures is decreased by the risk reduction of already applied safety measures. This is why in the present example, each safety measure is cost efficient, but the situation changes if they are combined. Emergency exits every 200 m are efficient but if the distance was reduced to 100 m, the measure was not efficient.

Finally, it was verified that the resulting fatality rate was under the upper limit, see Figure 6. Under the assumption that all relevant measures had been identified and assessed, the risk in the tunnel would thereby be acceptable. The package with the combination of measures could be recommended for construction.

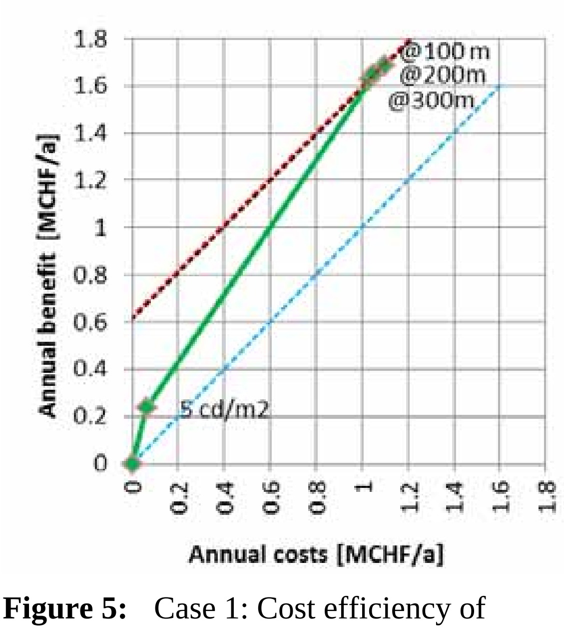

Figure 5: Case 1: Cost efficiency of combination of measures

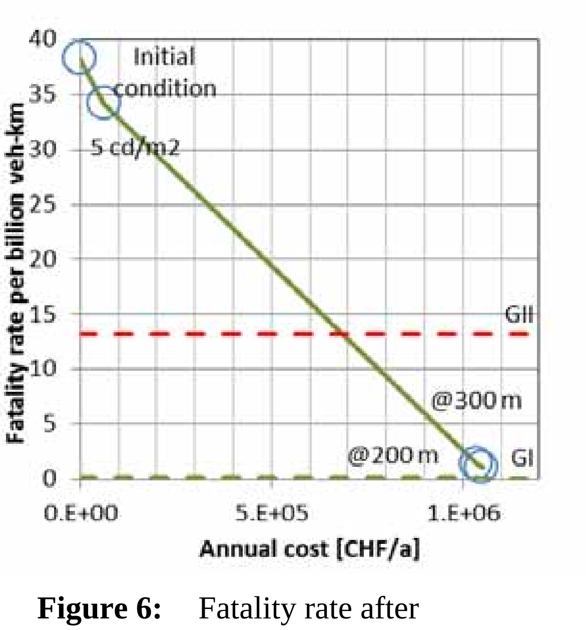

Figure 6: Fatality rate after combination of measures

3.2. Case 2: New tunnel project

In a second example, the comparison was made for a project with a very high gradient and an alternative of a longer tunnel with a more moderate gradient. The tunnel was planned with one tube and two-way traffic. The traffic was modest (8000 veh./day), the design level of the tunnel was good with a cross sectional width of 12 m, a ventilation system with smoke extraction and a modern LED lighting system providing more than 3 cd/m^2 in the tunnel interior at day time. Furthermore, the tunnel had a service- and escape tunnel with emergency exits every 275 m. These design features are in line with the Swiss regulation for road-tunnel design, SIA 197 (2004) and other national norms.

The key issue was the very high longitudinal slope. For topographical reasons and for connection to the existing road network the location of the portals was fixed. The initial project was an approximately 2000 m long tunnel with a gradient of 6.3%. This gradient is exceeding the limit of 5% for which the SIA 197/2 states: *"Due to the increased risk (accidents, smoke spread) the maximum longitudinal slope shall not exceed 5%"*.

For this reason, an alternative was proposed, with a gradient just under 5%. Since the locations of the portals were fixed, the tunnel necessarily had to be longer, as it appears from the sketch shown in Figure 7.

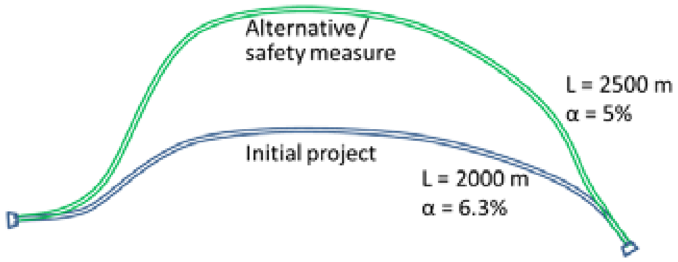

Figure 7: Alignment of the tunnel (initial project) with high gradient and alternative, which is longer with lower gradient

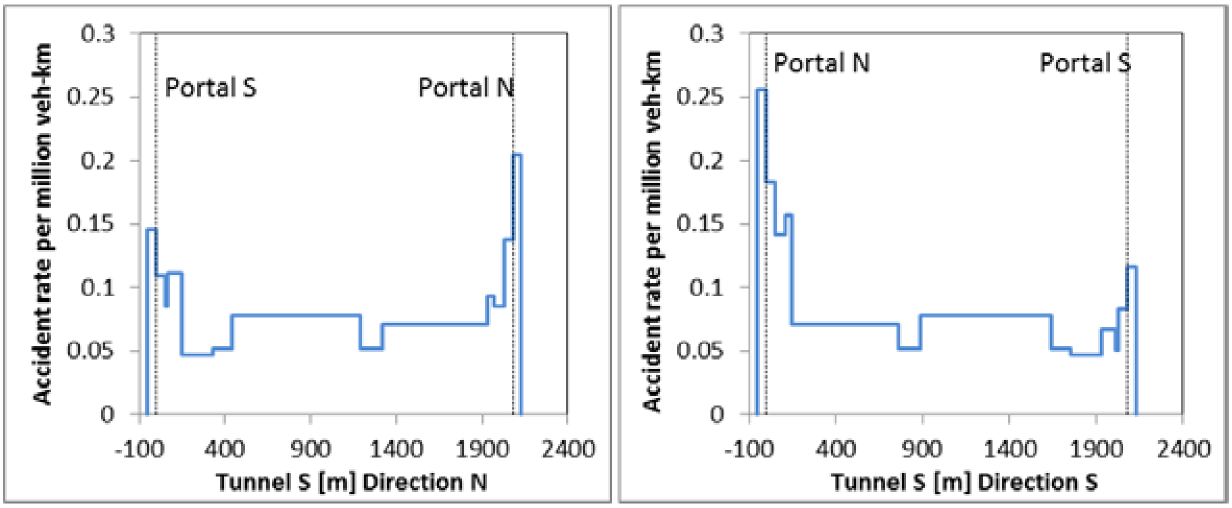

Figure 8: Case 2: Accident rates along the tunnel axis for the two directions of the initial project with gradient >5%

The risk assessment of the initial project demonstrated, as it was expected, the influence of the gradient. The accident and fire rates were increased compared to a tunnel with lower gradient. The fire rate was in particular increased in the upwards direction. The accident rate and fire rate are illustrated in Figure 8 and Figure 9.

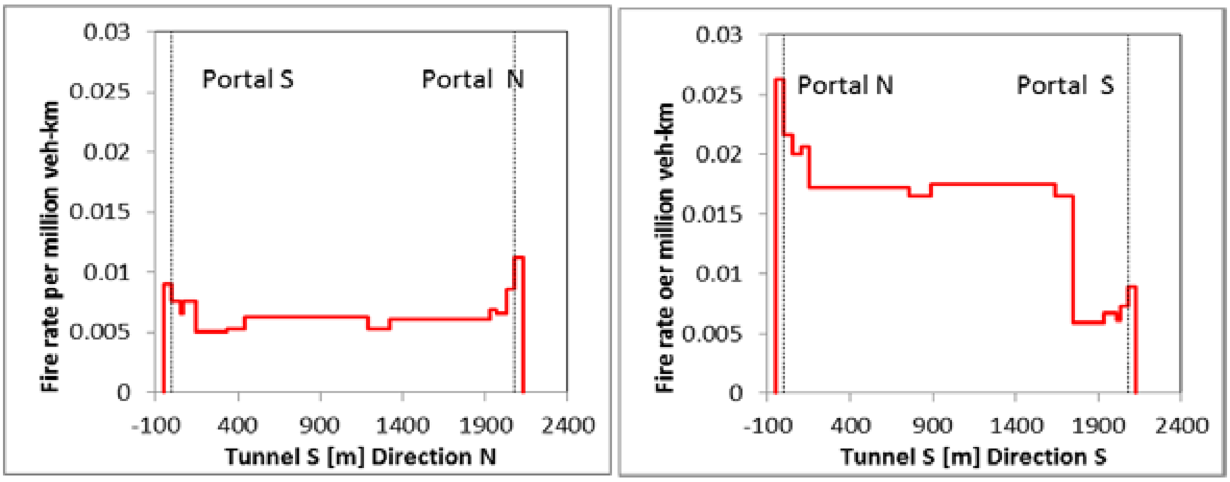

Figure 9: Case 2: Fire rates along the tunnel axis for the two directions of the initial project with gradient >5%

Because of the increased accident and fire rates, it would be expected that the fatality rate be increased. This is the case if one would compare the fatality rate of the actual project with a similar tunnel with 2% or 3%. However, the fatality risk is not increased to a level shown in Case 1, because the high design level with emergency exits, ventilation, light etc., which contribute to reduce the risk.

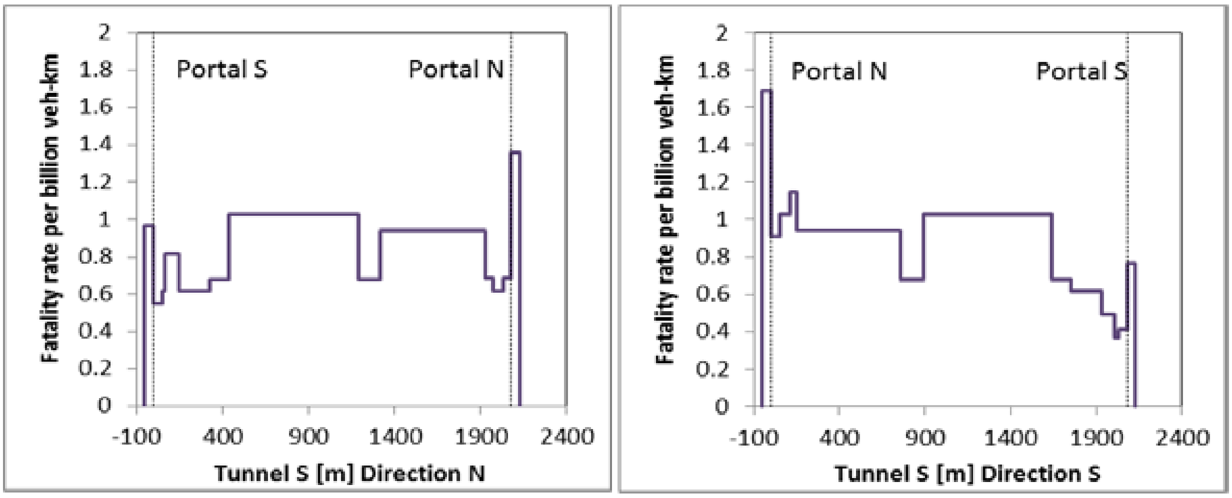

Figure 10: Case 2: Fatality rates along the tunnel axis for the two directions of the initial project with gradient >5%

It was decided to investigate the original design and its alternative from the point of view of safety. The result of the risk assessment for the alternative was a reduced fatality rate. In the initial design, the overall fatality rate was approximately 1.0 fatalities per billion vehicle km. In the alternative, the overall fatality rate could be reduced to 0.9 fatalities per billion vehicle km. In both cases, the vast majority of the fatality risk originated from accidents. The risk of fatal consequences from fires was very effectively reduced by means of ventilation and short distances between emergency exits. However, for the evaluation of the benefits of the measure, the weighted annual consequences of fatalities and injuries are decisive. In spite of the reduced rate, the 20% longer tunnel length resulted in an increased annual risk, because of the increased tunnel length. Fewer injuries from fires, approximately 5% more injuries from accidents and 10% more fatalities from accidents resulted in a total dis-benefit of approximately 5000 CHF/year.

Taking into consideration the approximately 25 MCHF additional construction cost for 500 m additional tunnel, the annual cost of the measure was estimated to about 1 MCHF. The cost efficiency of the measure was hereby -0.005, which is of course far from the cost efficiency of 1.00, where the measure is recommendable. Using the new methodology it could be shown that the longer tunnel did not (in this case) constitute a cost efficient alternative to the original design.

4. CONCLUSIONS

One year after the release of the new Swiss methodology for risk analysis, a number of significant experiences could be collected. The new approach proved to be very reliable and provided very important contributions to a number of projects.

The methodology proved to be an extremely valuable tool for deciding about project variants, and for basing decisions on a solid base. Using the methodology, reproducible results are obtained, such that projects are stabilized and responsibility is drawn away from the decision makers. Additionally, there is a strong focus on cost efficiency, which is important for tunnel owners and operators, who are interested in both, high level of safety and efficient operation.

5. REFERENCES

ASTRA 19004 (2014), Risikoanalyse für Tunnel der Nationalstrassen, 2014, Bern.

ASTRA 89005 (2014), Risikokonzept für Tunnel der Nationalstrassen / Methodik zur Ermittlung und Bewertung der Risiken in Tunnel, 2014, Bern.

ASTRA 89007 (2014), Risikoanalyse für Tunnel der Nationalstrassen: Anwendungsbeispiel, 2014, Bern.

Brandt, R; Schubert, M; Høj, N.P. (2012), On Risk Analysis pf Complex Road-tunnel systems; 6th International Conference ‘Tunnel Safety and Ventilation’ 2012, Graz.

Brandt, R., Riklin, N., Butty, V., Frey, S., Schubert, M., Høj, N. P. (2015), Gammeter, C., Gogniat, B. (2015), Quantification of Consequences of Road-Tunnel Fires ISAVFT 2015, 16th International Symposium on Aerodynamics,Ventilation & Fire in Tunnels, Seattle, 2015.

Brandt, R., Schubert, M., Høj, N.P., Gogniat, R., & Gammeter, C. (2016), Swiss guideline and methodology for risk analysis of road tunnels. 7th International symposium on Tunnel Safety and Security (ISTSS), Montréal, 2016.

Riess, I,, Brandt, R., (2010): ODEM: A One-Dimensional Egress Model for Risk Analysis, 5th Symposium Tunnel Safety and Ventilation, Graz, Mai 2010, Graz, 2010.

Riess, I., Bettelini, M, Brandt, R. (2000): Sprint – A Design Tool for Fire Ventilation, 10th Int.Conference, Aerodynamics and Ventilation of Vehicle Tunnels, bHr, 2000, Boston.

Riklin, N., Brandt, R., Butty, V., Frey, S., Schubert, M., Høj, N. P, (2014): Einfluss der Tunnellüftung auf das Risiko eines Strassentunnels, Fachbericht ASTRA N191-1345, 2014, Bern.

Schubert, M., Høj, N. P., Köhler J., Faber M. H., (2011), “Development of a best practice methodology for risk assessment in road tunnels”, Research Project ASTRA 2009/001, Report Nr. 1351, 2011, Bern.

SIA 197/2 (2004) Projektierung Tunnel, Strassentunnel Schweizer Norm, Schweizerischer Ingenieur- und Architektenverein (SIA), 2004, Zürich.

FINDINGS FROM THE NEW PIARC REPORT "EXPERIENCE WITH SIGNIFICANT INCIDENTS IN ROAD TUNNELS"

B. Kohl
ILF Consulting Engineers Austria GmbH, Austria
Member of PIARC Technical Committee C 3.3 „Road Tunnels Operations“ and leader of Working Group „Feedback from experience on road tunnel safety“

ABSTRACT

Approximately ten to fifteen years ago many countries introduced tunnel safety management systems and started paying attention to tunnel safety in a more structured way. In the new PIARC report "Experience with Significant Incidents in Road Tunnels" several contributing countries share information on lessons learned from incidents and developments in safety management and risk analysis and conclusions are drawn on topics of general interest. In the paper new incident rates for collision and fires in road tunnels are presented and relevant influencing parameters are discussed. Furthermore the paper presents interesting findings from real incident information, which completes the statistical data in an illustrative manner.

Keywords: significant tunnel incidents, tunnel fire rates, tunnel collision rates

1. MOTIVATION AND SCOPE

The World Road Association (PIARC) is a non-profit organisation established in 1909 to improve international co-operation and to foster progress in the field of roads and road transport.

The topic that is the subject of this paper was defined in the PIARC Strategic Plan 2012 – 2015 approved by the council of the World Road Association, whose members and representatives of the member national governments. The strategies for the Technical Committee TC 3.3 "Road Tunnel Operations" defined in this strategic plan include "drawing lessons from current practice regarding safety management and the analysis of road tunnel accidents and fires worldwide".

In the past 10 – 15 years, in particular since the issue of the EC Directive 2004/54/EC on minimum safety requirements for tunnels in the trans-European road network, tunnel operators in many countries introduced tunnel management systems and started paying attention to tunnel safety in a more structured way. In the cause of this process a lot of experience and data on aspects regarding tunnel safety has been collected.

Following the Technical Committee's strategic plan, the Working Group "Feedback from Experience on Road Tunnel Safety" dedicated its activities of the past working cycle 2012 – 2015 to look into the experience many countries have gained with the application of various tools for tunnel safety management and to analyse information on significant tunnel incidents. The results of these activities are presented in the report "Experience with significant incidents in road tunnels", which will be published in the PIARC virtual library in 2016.

The paper is focused on significant incidents. Significant incidents are incidents which require special attention, because they are, or have the potential to develop into, events with serious consequences to the health or life of people, to property, to infrastructure or to the environment; or are valuable for further evaluation with respect to underlying basic risk factors. Significant incidents in particular include collision and fires.

This information was evaluated statistically in order to provide new basic reference values for incident rates in order to update such quantitative information published by PIARC in earlier reports (like in PIARC doc. 05.05B “Fire and Smoke Control in Road Tunnels” from 1999 [7]).

This quantitative information is completed by a discussion of relevant influence parameters and a qualitative evaluation of a set of road tunnel incidents. Furthermore relevant aspects of data collection are presented and – following the concept of an integrated approach to road tunnel safety (PIARC 2007/R07 [10]) – it is discussed, how lessons learned can contribute to improve tunnel safety and how a more complete and specific incident data set can enhance tunnel safety management tools like risk assessment.

2. COLLISIONS WITHIN ROAD TUNNELS

2.1. Background and influencing parameters

A road tunnel is a section of road in a confined space with lateral and vertical restrictions. The specific characteristics of the tunnel system determine the distinct differences of collisions in tunnel sections in comparison to open road section.

The specific tunnel influence acts on both, occurrence as well as a consequences of tunnel collisions:

- Specific types of collisions cannot occur in tunnels, e.g. collisions caused by wind, rain, snow and other environmental influences, others have a reduced probability of occurrence in tunnels, e.g. collisions caused by lane changing or turning manoeuvres, pedestrians, wild animals, or loss of traction on a slippery road surface.
- Specific types of collisions have an increased probability of occurrence, e.g. collisions with stationary obstacles like tunnel walls or entry portals and there are causes for incidents which are unique to tunnels, such as sudden windscreen misting resulting in impaired visibility.
- The consequences of collisions in tunnels may be increased, mainly caused by space limitations (for instance collisions with the tunnel sidewall instead of with a safety barrier).
- Emergency response may be impaired, due to impeded access to an incident for the emergency services.

Based on detailed studies of collisions in tunnels and the experience and knowledge of tunnel operators and tunnel safety experts relevant influencing factors were identified and discussed, such as: Basic tunnel configuration (unidirectional or bidirectional tunnel); horizontal or vertical alignment; number and width of driving lanes; separation between driving lane and tunnel wall; presence/distance of layby’s or emergency lanes; tunnel length / tunnel zones; traffic load, composition and characteristics; intersections and ramps; speed; tunnel lighting and optical guidance for drivers; driver information and traffic management systems; technical standard of vehicles; cultural factors.

The combined influence of these parameters is complex and hence quantification of parametric influence is challenging. There is little evidence that the influence of these factors can be addressed individually, and only for a very limited number, is a quantitative approach available.

There are published studies that provide information on this topic (for instance [1], [2], [3], [4]), but great care has to be taken when comparing and discussing results from different studies, because the results are influenced by many factors, such as conditions and methods for data acquisition, quality and completeness of data, definitions and methods applied for the study as well as specific national aspects relevant for traffic safety and traffic management.

Different results have been obtained in different studies (some support each other, others seem to be contradictory), and only for very few parameters clear conclusions can be drawn:

- Tunnel length / tunnel zones: the highest collision rates are observed in the (entrance) portal area and in the entrance area, with lower rates in the interior zone and as a consequence the collision rate decreases with tunnel length [2], [4], [3].
- Speed / speed control: a higher speed has a clear negative effect on the consequences and probably also on the occurrence of tunnel collisions, hence modern electronic speed control systems have a positive influence [1], [2].
- Tunnel slope: the collision rate increases with a high tunnel gradient [12].
- Traffic composition / HGV: a higher share of HGV increases the consequences of collisions [1], [3].

For other parameters the identified influences were considered as not statistically significant. Hence it can be concluded, that further studies are required to improve the knowledge on tunnel collisions, in particular to better understand the interaction of the various influencing parameters. To provide a sound basis for such studies the specific requirements for data collection on tunnel collisions needs to be defined, covering both the incident itself as well as the boundary conditions and influencing parameters as mentioned above. Specific guidance on this topic is provided in the PIARC report [11].

2.2. Collision rates

The collision rates presented in the body of the report and in this paper are based only on the quantitative incident information immediately available to the task group members responsible for the drafting of the report. Bidirectional and unidirectional tunnels are addressed separately as far as possible to take into account the different conditions. With the available data it was possible to calculate the average collision rate for road tunnels for some countries. These rates are not necessarily representative of all tunnels of this country, but represent only a sample.

The average collision rates of various countries are presented in table 1. For some countries (*), the rates are based on very limited information (detailed information can be found in the PIARC report [11]).

Table 1: Collision rates (CR) for road tunnels in various countries [11] (collisions with casualties)

	Collision rate (C_R) [per 10^8 veh. km]	
Country	**unidirectional traffic**	**bidirectional traffic**
Austria	9.80	3.60
Argentina*	-	5,74
Denmark	3.97	-
France	8.72	5.30
Italy	12,02	-
Netherlands	5,35	-
Norway	11,60	11.72
South Korea	2,10	-
Spain	6,30	9.30
Switzerland	7,58	-
Vietnam*	-	71.98** (18.00)

** collision rate includes all collisions (number in brackets: estimation of rate for collision with causalities)

In addition in the subsequent diagrams the total number of collisions in the records is shown in relation to the corresponding traffic for various countries (including reference lines for collision rates) for both – bidirectional as well as unidirectional tunnels.

The collision rates presented in table 1 were calculated on the basis of incident statistics that cover a certain period of time, which differs from country to country. When evaluating the data it was observed that in data covering a longer period of time the collision rates were decreasing over time (see for instance [1], [2]). Hence the rates presented in table 1 represent an average value for the registered period. The reasons for this effect have not been addressed and therefore this effect cannot be discussed in more detail. It is not clear at this stage, to what extent this decrease in rates of collisions with personal injuries is due to a general increase in traffic safety or due to specific efforts to increase tunnel safety in particular.

Furthermore, the statistics on collision rates cover different types of tunnels; for instance, in Austria and Italy the data refers to motorway tunnels only, whereas in Norway all tunnel types are included. Moreover, the standard of tunnel equipment in many Norwegian tunnels is quite different to other countries, because in Norway many tunnels are located in quite remote areas.

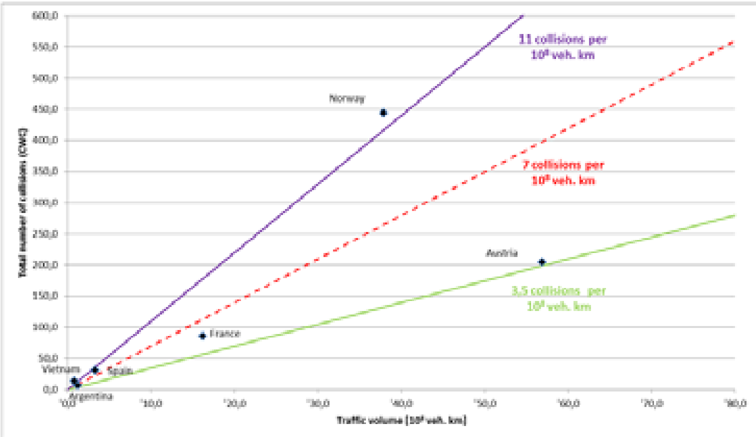

Figure 1: Total number of collisions in the records shown in relation to the corresponding traffic for various countries – reference lines for collision rates in bidirectional tunnels [11]

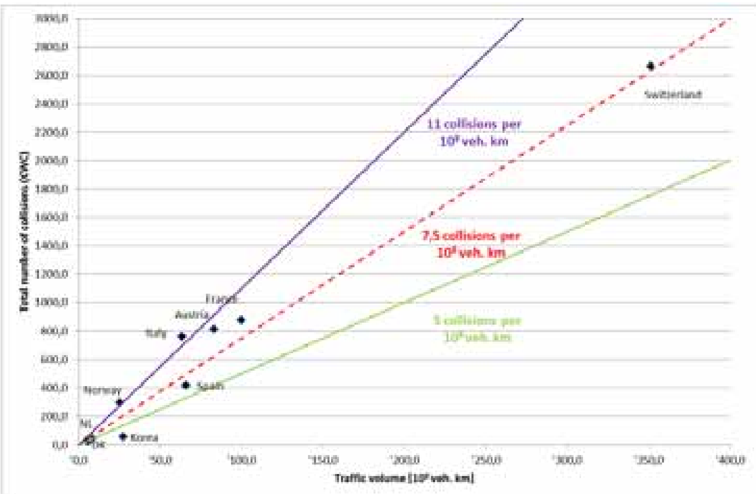

Figure 2: Total number of collisions in the records shown in relation to the corresponding traffic for various countries – reference lines for collision rates in unidirectional tunnels [11]

3. TUNNEL FIRES

3.1. Background and influencing parameters

The confined space of a tunnel provides an environment in which fires are particularly dangerous because untenable conditions may develop rapidly in case of a fire.

However, although the discussion on tunnel fires is often dominated by the extreme events which occurred in the Mont Blanc tunnel, the Tauern tunnel and the Gotthard Tunnel, in reality the majority of tunnel fires are relatively small events in comparison, which nevertheless may have the potential to develop into more serious events, depending on various influencing parameters.

In the PIARC report focus is given to updating fire rates rather than discussing the consequences of fires, because the consequences of a specific tunnel fire are very much dependent on the specific circumstances of an individual event. As tunnel fires are rare events, an entirely statistical approach to the assessment of consequences of tunnel fires is not likely to be sufficient.

The collection and use of data on the occurrence of tunnel fires require a stringent definition of events which should be considered as fires. In the context of the PIARC report a fire is defined as “an unwanted or uncontrolled combustion process characterized by heat release and accompanied by smoke, flames, or glowing”. Consequently, smoke releases without fire (i.e. either smoke without significant combustion or smoke without heat release or negligible heat release) are not addressed as fires in this report. This definition is in particular relevant for data collection and data evaluation to ensure the comparability of fire rates.

Three types of tunnel fires can be distinguished with regards to their characteristics:

- Fires resulting from vehicle defect (technical, electrical or mechanical defaults): such fires typically start in engine, exhaust system, wheels or brakes, seldom in the load. These fires in most cases are shielded fires which are likely to develop slowly in the first phase, with progressive development in later phase resulting in a fully developed fire. This type of fire development increases the opportunity to extinguish a fire (or delay its further development) either by the use of manual fire extinguishers, fixed fire-fighting systems and/or by responding fire fighters, before it is able to threaten the health and safety of people in the tunnel.
- Fires triggered by a collision: such fires are often accelerated by (limited amounts) of fuel that has leaked as a result of the collision, hence the development is typically faster.
- Flammable liquid fires, i.e. pool fires with large amounts of flammable liquids, are extremely rare occurrences, which require a large amount of flammable liquid to be released (as a consequence of a collision or by other reasons).

The majority of vehicle fires occur as a result of vehicle defects. However, fires caused by collisions can have severe consequences as they may develop more rapidly and often involve persons who are unable to escape from the burning vehicle.

In determining the likelihood of tunnel fires the following influencing factors are relevant:

- Collision rates
- Percentage of HGV traffic (because there may be a difference in the fire rates of HGVs and passenger cars)
- Gradients in the tunnel and the length of the gradient.
- Gradients on the routes leading towards the tunnel
- Combination of tunnel length and gradient

- Traffic composition / age, technical standard and maintenance of the vehicles, in particular of heavy vehicles

Up to now, statistics have been insufficient for the establishment of reliable models for quantifying the influence of these parameters on fire rates. For this reason the existing models may be regarded as expert judgements, which later may be supported by real data (see for instance [5], [6]).

The development and consequences of a fire, following ignition, is not discussed further in this paper. Reference is made to a wide range of literature existing on this topic and to the annex of the PIARC report [11], where a representative sample of characteristic tunnel fires is reported.

3.2. Fire rates

The fire rates presented in the body of the PIARC report [11] and in this paper are based only on the quantitative incident information immediately available to the task group members responsible for the report. With the available data it was possible to calculate the average fire rate for road tunnels for some countries: these rates are not necessarily representative of all tunnels of this country but represent only a sample.

The average fire rates of various countries are presented in table 2. For some countries (*), the rates are based on very limited data (detailed information can be found in the PIARC report [11]).

Table 2: Fire rates for road tunnels in various countries [11]

Country	Fire rate all vehicles [per 10^9 veh. km]
Norway	15.0
Netherlands	3.2
Austria	6.5
Germany	25.7
Italy	5.6
Spain	3.5
France	10.6
United Kingdom*	10 – 20
Czech Republic	17 - 25
Japan**	(38)
South Korea	6.4
Vietnam*	560

** rate based on data of four tunnels with fire events only (upper value)

In figure 3 the fire rates are compared with respect to numerical fire rate per billion veh.-km. Instead of presenting the fire rates graphically, the total number of fires in the recording is shown in relation to the corresponding tunnel-traffic volume for each of the countries. Hence, in figure 3, the slope of a line from (0,0) to the data point will correspond to the fire rate. The data points based on a high tunnel-traffic volume (here: Austria, France, Italy, Norway and South Korea) give more weight to the general fire rate than those with a low traffic volume.

As illustrated in figure 6, the fire rates are generally within the interval 5 – 15 fires per billion vehicle-km. The tendency is that the rates are now lower than the fire rates reported in the old PIARC report 05.05.B [7] from 1999 which were in the range of 0 - 250 per billion vehicle-km based on the individual tunnels with a weighted average of 45 per billion vehicle-km.

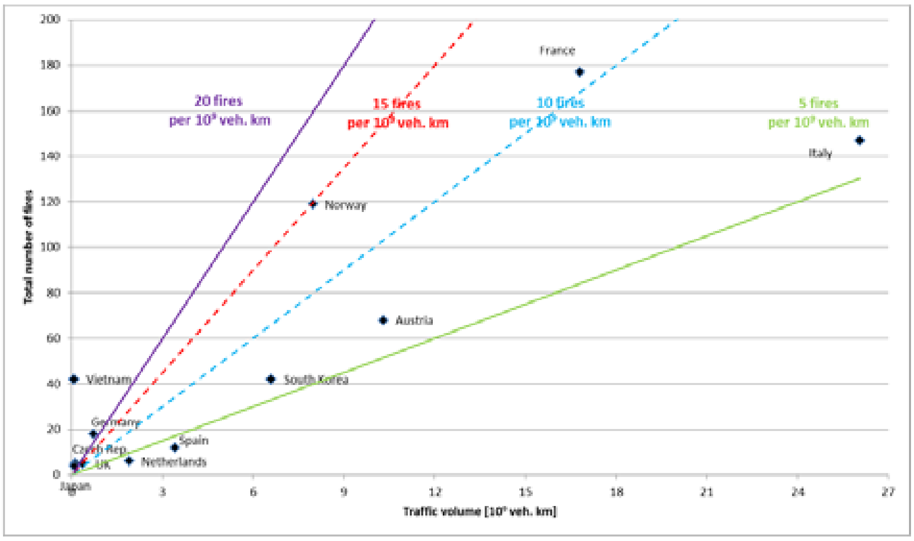

Figure 3: Total number of fires in the records shown in relation to the corresponding traffic for various countries - reference lines for fire rates [11]

In general there is a significant uncertainty associated with the recording of the fires and the resulting fire rates. Where possible the events which are "smoke without significant combustion" have been excluded from the statistical basis. Nevertheless these events may in some cases have been counted as fires, with the tendency that the fire rates presented above are upper values.

In the new PIARC report [11], in addition to the estimate of fire frequency rates, some registrations, estimates and export judgement regarding type and severity of tunnel fires are documented, relevant information can be found in this report [11] and in the underlying literature respectively ([4], [5], [6], [8], [9]).

4. FINDINGS FROM REAL INCIDENT INFORMATION

The statistical approach presented in chapter 2 (for collisions) and in chapter 3 (for fires) produces figures which can be used in risk analysis for instance. Such figures are theoretical. A more illustrative approach to the feedback from experience based on observations and findings of general interest can be very useful in addition to the statistical approach.

At the level of an individual tunnel, there are (hopefully) normally too few recordings for a sound statistical evaluation as well as for illustrative purposes. Sharing information at national or international level allows gathering a greater variety of incidents giving way for a more representative view: whereas it is established practice to do it for statistical purposes, it is only rarely done for illustrative purposes, in most cases focusing on major incidents only (like Mont-Blanc tunnel fire, St.-Gotthard tunnel fire, etc.). In this report this approach is expended to a randomly selected more representative set of different types of incidents.

It shall provide a realistic idea of incidents happening in road tunnels as well as give examples which conclusions can be drawn at object level, based on the evaluation of such individual incidents. Even if related to a specific context, it is often possible to draw conclusions of general interest based on qualitative, but detailed information of real incidents (videos, incident reports, etc.).

Therefore information on 34 real incidents – provided by tunnel operators from 16 different countries worldwide and selected on a random basis – was collected and evaluated by the working group and documented in the appendix of the report.

Without claiming to be complete a set of conclusions of general interest can be drawn for the results; regarding human behaviour, tunnel operation, emergency response and tunnel infrastructure and equipment. The most relevant findings can be summarized as follows:

Human behaviour:

- The behaviour of car drivers (driving too fast and too close, unforeseeable driving manoeuvres) seems to be the most common cause of tunnel incidents and may also cause problems in incident management (like impeding access of emergency services to the site of incident).
- In case of a fire, drivers often pass by the vehicle on fire as long as they think it is possible to do so, despite of the potential danger (heat, lack of visibility due to the smoke, etc.).
- Traffic management measures – such as closing of a lane (e.g. by red crosses) or closing of the tunnel (by traffic lights) are often neglected if not enforced by additional means (e.g. like barriers for tunnel closure.
- Evacuation instructions through broadcast, loud speakers and/or message signs are often followed by road users, when provided in an understandable manner.

Tunnel operation:

- Problems of communication between the different stakeholders involved (between operator, road users and the various rescue services) are a key issue in incident management; communication problems can be caused by various different reasons, such as language problems, unsuited or wrong application of procedures, inadequate or malfunctioning communication devices, compatibility problems of different equipment etc.
- A well trained operator, who is familiar with the systems available, is a key factor for a successful incident management; real incidents demonstrate that the actions of the operator may influence the course of an incident in both ways, positively as well as negatively. It shall be avoided to overburden operators by too many tasks at the same time.

Emergency response:

- Too reach the scene of an incident may be a key issue for the emergency services, in particular in unidirectional tunnels with high traffic loads, when they try to approach the scene in driving direction.
- In some cases the emergency services did not know or not follow the emergency procedures; hence the importance of regular on-site training is stressed.

These examples demonstrate how useful such information at international level can be for the various stakeholders involved in tunnel safety, especially to improve the installation of equipment (radio, barriers etc.) and the way they are used.

5. APPLICATION OF THE DATA

In several previous PIARC reports the role and importance of an integrated approach to tunnel safety has been discussed. In PIARC report 2007/R07 (Integrated Approach to Road Tunnel Safety [10]), a schematic representation of the proposal for an integrated approach to the safety of new and in-service tunnels is presented (see figure 4). In this figure the feedback from lessons learned to changes in the definitions of the safety features of a tunnel is illustrated.

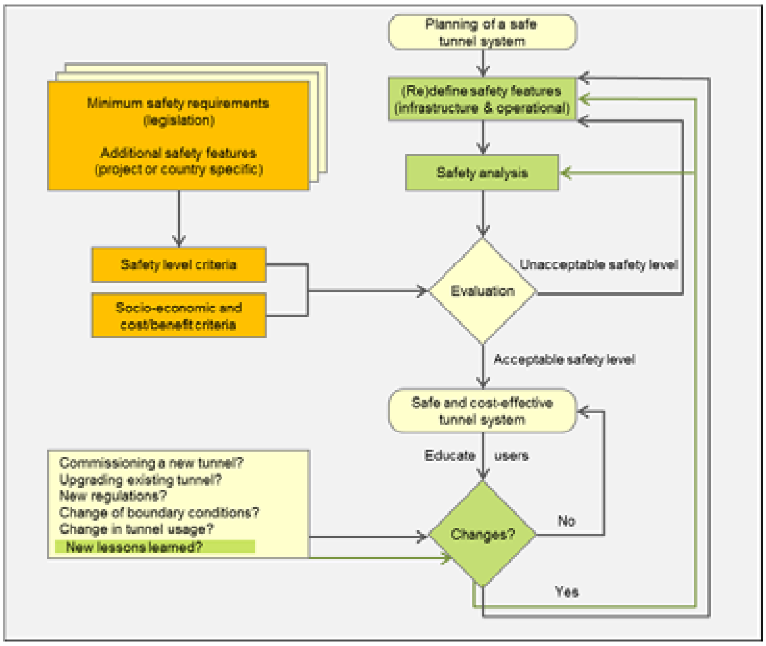

Figure 4: Integrated approach to road tunnel safety – feedback chain [10]

Learning from experience can be implemented in the tunnel safety management procedures for different topics and at different levels. For the topic specifically addressed in this paper – significant tunnel incidents – the data can be applied at two levels:

5.1. Application of the data at a local level – concerning a specific tunnel

The evaluation of the incidents which occurred in a specific tunnel may allow the detection of deficiencies in the infrastructure, equipment, signaling, emergency response, etc. and to propose and implement appropriate improvement measures. Hence this may contribute to the assessment of the acceptability of the real or scheduled safety of the specific tunnel.

Furthermore the illustrative information from incidents which occurred in other tunnels, like the one presented in chapter 4, may provide valuable input to design decisions as well as the planning of procedures and it could also contribute to a realistic planning of scenarios for emergency exercises.

5.2. Application of the data at a national or international level

The evaluation of incidents at network level allows the main incident rates of different types of tunnels to be obtained (national statistics for specific types of tunnels), thus providing data for risk analysis for tunnels in the design stage or in operation without sufficient specific data. On this basis, prioritization of improvement measures can be made – together with other relevant aspects (e.g. operational and/or financial parameters). This general assessment can be complemented with specific analyses, to study for instance the occurrence of collisions at specific locations in a tunnel (e.g. lay-bys) or the influence of specific types of equipment.

Furthermore, the data provides a basis for a reference framework to inform safety policy development by the authorities (regarding tunnels as a specific element of the whole road system). In particular quantitative reference values can be established, which may be used as a basis for the comparison of the level of safety of a given tunnel with a national or international benchmark.

In particular high quality incident data is required to support the application of risk analysis for road tunnels: the incident data along with their statistical processing and other supplementary data constitute the basis of the application of risk analysis methodologies which allow for a quantitative assessment of the risks in a tunnel. The key input data strongly depends on the risk analysis methodology and its requirements. For instance a specific quantitative risk analysis method requires as input the collision rates for all anticipated types of collisions and the implied consequences. But some qualitative risk analysis methods (scenario analysis) also require collision data in order to select the most representative scenarios and to select reliable input parameters such as response time, time to achieve the closure of the tunnel etc.

The reliability and the uncertainty of the outcomes of risk analysis are strongly influenced by the reliability and the uncertainty of the input data. When these data are applied as input for risk analysis special attention must be given to the specific conditions under which the incident data have been developed. Before the incident data can be applied to a risk analysis for a specific tunnel it has to be assessed whether the conditions of this tunnel are comparable and the necessary calibrations have been made, if required. Further, the presented incident rates usually represent "basic" values which have to be calibrated at least for the most significant influencing parameters, in order to represent applicable rates for the specific tunnel considered.

Incident rates should be used with care, and evaluation of the applicability and modification of the rates for an application for a given tunnel should be done by experts with experience in tunnel safety. When the above conditions are fulfilled, the incident rates can be applied in order to achieve safety systems for the tunnels which are balanced in relation to the risk caused by significant incidents specific for road tunnels.

6. REFERENCES

[1] CALIENDO C., DE GUGLIELMO, M. L., 2012: "Accident rates in road tunnels and social costs evaluation", SIIV- 5th International Congress- Sustainability of Road Infrastructures. In: Procedia-Social and Behavioral Sciences, Vol. 53, 166-177

[2] NUSSBAUMER C., NOSSEK G., Safety of Road Tunnels. Traffic safety in Highway and Expressway tunnels (1999 to 2009), Austrian Road Safety Board, Austria

[3] SALVISBERG U., ALLENBACH R., HUBACHER M., CAVEGN M. & SIEGRIST S. (2004), Verkehrssicherheit in Autobahn- und Autostrassentunnel des Nationalstrassennetzes, bfu-Report Nr. 51, Schweizerische Beratungsstelle für Unfallverhütung, Bern

[4] CETU/BG Pannes, accidents et incendies dans les tunnels routiers-Etude statistique à l'échelle nationale-rapport d'étude, Bron, 2015

[5] A. LENTZ, ILF; B. KOHL, ILF; Auswertung der ASFINAG-Tunnelbrandstatistik 2006-2012(Evaluation oft he ASFiNAG statistics on tunnel fires), RVS-Arbeitsausschuss 09.03.11 Tunnelrisikomodell, 2013

[6] TØI rapport 1205/2012 "Kartlegging av kjøretøybranner i norske vegtunneler 2008-2011 (Mapping of vehicle fires in Norwegian road tunnels 2008 – 2011)

[7] PIARC REPORT 05.05.B, Fire and Smoke Control in Road Tunnels, PIARC Committee on Road Tunnels (C5), 1999

[8] TNO 2012 R1 1094, De statistische kans op brand in tunnels (The statistical probability of fire in tunnels), of 22 January 2013

[9] NAM GOO KIM, JONGWOO JO, Expressway Tunnel Fire Case Analysis Effective Safety Improvement Planning, Korea Expressway Corporation

[10] PIARC TECHNICAL REPORT 2017R07, "Integrated Approach to Road tunnel Safety" PIARC Technical Committee C3.3 Road Tunnels Operation, Paris 2007

[11] PIARC TECHNICAL REPORT "Experience with Significant Incidents in Road Tunnels PIARC Technical Committee C3.3 Road Tunnels Operations, Paris 2016 – published soon

[12] CETU/BG Pannes, accidents et incendies dans les tunnels routiers-Etude statistique à l'échelle nationale-rapport d'étude, Bron, 2015

CONSEQUENCE ANALYSIS OF FALSE FIRE DETECTION IN ROAD TUNNELS

[1]T. Sakaguchi, [1]I. Nakahori, [2]B. Kohl, [2]O. Senekowitsch, [3]A.E. Vardy
[1]Sohatsu Systems Laboratory Inc., Kobe, Japan
[2]ILF Consulting Engineers, Linz, Austria
[3]Univeristy of Dundee, Dundee, Scotland, UK

ABSTRACT

Regulations for fire detection in road tunnels vary strongly around the world. For example, the required speed of fire detection in Japan is much faster than in Europe. Moreover, the minimum size of fire that must be detected at the required speed is much smaller than in Europe. These two requirements have led to the widespread adoption of different technologies for fire-detection and this, in turn, leads to different probabilities of false alarms. This paper uses both qualitative and quantitative methods of consequence analysis to assess the influence of the different regulations on overall risk for tunnel users. It is found that, for the chosen tunnel type, which is especially common in Japan, the speed of detection is less important than the choice of ventilation strategy. Also, advantages gained from high detection speeds might be outweighed by disadvantages of false alarm rates as small as one per week. These findings are not applicable to all types of tunnel. The relative importance of rapid fire detection might be significantly greater in tunnels with fixed firefighting systems, for instance.

Keywords: fire detection, false fire alarm, risk analysis, consequence analysis

1. INTRODUCTION

In modern road tunnels, the breakout of a fire is detected and monitored by one or more sensors such as flame-detectors, infrared cameras, video cameras, thermal cameras and linear temperature cables. When these detect a fire, various actions are triggered automatically – e.g. changes to the ventilation control regime, smoke extraction, activation of fixed fire-fighting systems and notifications to bodies such as emergency services. Usually, they will also include traffic control and the provision of targeted guidance to vehicle users. The use of automatic responses such as these has big potential advantages for reducing the severity of incidents and the risks for persons caught up in them. However, *automatic* triggering of such responses also has its own risks. For instance, *false* fire detection in tunnels can cause unnecessary traffic jams at tunnel portals and hence possible vehicle collisions causing injury and even fatalities. Accordingly, it is important to minimize the risk of false detection, not only to maximize the effectiveness of valid detection.

This paper presents both qualitative and quantitative assessments of risks associated with valid and false fire detection. It does so by applying formal consequence analysis to a selection of scenarios used as the basis of regulations in three countries, namely Japan, Germany and Austria. The outcomes are summarized in a manner that enables rational judgment to be made of the balance between *rapid* detection and *reliable* detection. Both are highly desirable, but neither can be maximized without compromising the other to some degree.

To ensure adequate focus on the key purposes of the paper, some potentially important factors are addressed in a simplified manner. For instance, the influence of interventions by human operators is modelled partly on published data, but also on wider experience, especially in the case of remotely-controlled tunnels. Other important factors are excluded completely. For example, only longitudinally-ventilated tunnels are considered (these are the dominant type amongst Japan's vast number of tunnels) and no account is taken of the possible availability of fixed-fire-fighting systems (FFFS). These would be included when appropriate in practical design studies, but their inclusion herein would complicate the inference of generic conclusions.

2. REGULATIONS FOR FIRE DETECTION

As fire detection plays such a critical role in tunnel emergency operations, performance criteria for fire detection systems are strictly specified in regulations. However, some strong differences exist between regulations in different countries. Herein, specific attention is paid to requirements in Japan, Germany and Austria.

In ***Japan***, a $0.5m^2$ plate, 2 litres gasoline fire must be detected within 30s (NB: the regulation does not place limits on the air speeds for which this must be achieved). Since the prescribed fire is very small, the time taken for temperatures to increase significantly except very close to the fire is such that the criterion tends to favour flame detectors (infrared detectors). Typically, such sensors are installed on tunnel walls at 50m intervals.

In ***Germany***, if the tunnel air speed is less than 6m/s, a $4.0m^2$ plate 20 litres gasoline fire must be detected in less than 60s [1]. Typically, this is achieved using a linear temperature cable installed on the center of the tunnel ceiling. In sharp contrast with Japan, flame detector-type sensors are not used in Germany.

In ***Austria***, if the tunnel air speed is less than 3m/s, a fire formed by two $1m^2$ plates, each with 10 litres methylated-spirit pools must be detected in less than 90s [2]. As in Germany, this is typically achieved using linear temperature cables on the center of the tunnel ceiling and flame-detectors are not used.

It is noteworthy that the Japanese regulation not only requires the smallest detection time (30s), but also stipulates that it must be achieved for much smaller fires that those prescribed in the European examples. The regulation applies to all expressway tunnels and national road tunnels owned and operated by the Nippon Expressways Companies (NEXCO), the Urban Highway Companies (UHC), and the Ministry of Land, Infrastructure, Transport and Tourism (MLIT).

Notwithstanding the differing characteristics of the prescribed conditions, the overall aims of the regulations in the three countries (i.e. maximizing safety) are the same. One purpose of this paper is to investigate how well the aims are achieved. For brevity, the three regulations are characterized in the remainder of the paper by 30s, 60s and 90s detection times.

For obvious reasons, the prescribed fires in each of the above cases are capable of being reproduced simply and accurately. However, it should not be assumed that pool fires are necessarily representative of typical tunnel fires. For instance, it was concluded in the ESCOTA report [3] that fire began with flame in only 1% of the actual fires for which data were collected. In most of the fires, smoke was observed before flames. This could have potentially important consequences for the effectiveness of different types of fire detection systems, especially if their effectiveness is assessed solely on the basis of gasoline or heptane fires on open plates.

3. FIRE EMERGENCY RESPONSE

When a fire breakout is detected, a series of measures follows, typically including:

- notifying operators and emergency services and providing information about the fire source
- traffic restrictions; e.g. traffic lights or barriers at the portals (and information displays)
- traffic control; e.g. emergency display boards and radio broadcasts within the tunnel, especially advising on the nearest emergency exits
- ventilation control to facilitate safe evacuation; e.g. zero-flow control in Japan, low-speed flow in the EU
- fire risk mitigation measures, such as triggering fixed firefighting systems to minimize fire growth, protect tunnel facilities and assist emergency personnel

In *supervised* tunnels in Japan, these measures are undertaken manually by human operators after confirmation of fire breakout and its scale with the aid of video cameras in the tunnel. In the large number of *non-supervised* tunnels, however, the emergency responses are initiated automatically by a fire emergency panel.

Within the EU (particulary in Autsria and Germany), the general emergency response in supervised tunnels is broadly similar to that in Japan, but the usual provision in non-supervised tunnels differs from Japan. Instead of having fully integrated emergency and alarm circuits, it is usual to have semi-integrated alarm procedures that, in most cases, notify a human operator who then acts in accordance with information from sensors.

4. MODEL FIRES IN CONSEQUENCE ANALYSES

The main purposes of this paper are (i) to illustrate the power of rigorous consequence analysis modelling for comparing alternative approaches to fire response and (ii) to use the method to make rational comparisons between the distinctively different fire response processes adopted in Japan and typical EU countries. Since this cannot realistically be done for a large number of individual tunnels, it is necessary to undertake the comparisons on the basis of selected tunnel scenarios. Once again, differences exist between the approaches adopted in Japan and the EU.

4.1. Japan: *Qualitative* Consequence Analysis

In Japan, the focus is on qualitative (not quantitative) consequence analysis when designing safety devices and equipment for either new or refurbished tunnels. A “standard” fire is defined with particular characteristics regarding smoke density distribution and heat release rate (HRR). These are based on measurements made in a series of full-scale fire tests conducted to determine smoke densities and HRR that are used in engineering design [4]. **Figure 1** illustrates smoke density distributions s*V(1/m*m3/min) measured in five different fire tests, namely a bus interior fire, a bus undercarriage fire, a passenger car interior fire, a passenger car underbody fire, and a 4m^2 plate gasoline fire. The smoke release rate adopted for a 20MW standard fire is based on the measured smoke distribution of the bus undercarriage fire. This case is used as a standard in engineering tunnel fire emergency responses in Japan and it is used in qualitative consequence analysis in Section 5.1.

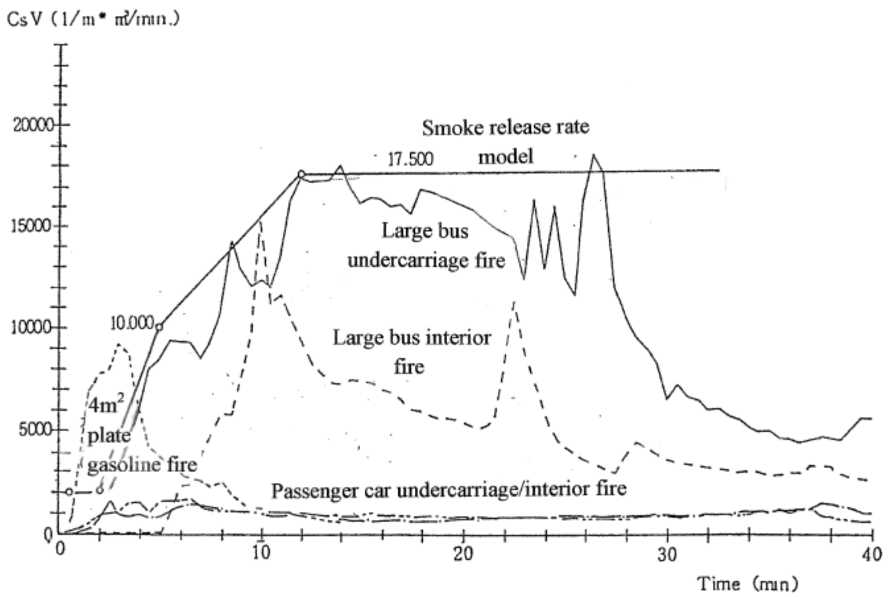

Figure 1: Measured smoke release rates and 20MW standard fire in Japan

4.2. Austria: *Quantitative* Consequence Analysis

The chosen method of quantitative consequence analysis is based on Austrian Regulations. In RVS 09.03.11, published by the Austria Society for Research on Road, Rail and Transport [5], which provides the methodical basis for Tunnel Risk Analysis in Austria, the consideration of three different model fires is officially required. One model fire, characterized with a maximum HRR of 5 MW, represents a median passenger car fire and two model fires, with maximum HRRs of 30 MW and 100 MW respectively, represent HGV fires with different cargo loads. The model fires are based on simplified assumptions, including:

- The increase of HRR in each of the three fire sizes is approximated as linear
- The fire-development times depend only on the maximum heat release rate (Table 1)
- The prescribed HRR development is independent of the longitudinal air flow velocity
- The pollution emissions rates are constant in time and depend only on the maximum HRR. They are stated in RVS 09.03.11 [5].

Table 1: Time required to reach the maximum fire load

Fire Size	5 MW	30 MW	100 MW
Timespan until full development [s]	180	300	420

4.3. Purposes of Japanese and Austrian fire models

Overall, probabilistic approaches to risk assessment are an attempt to represent a variety of tunnel fires in a realistic way through the superposition of different, albeit individually deterministic, models of fire development. The specifications of the individual models inevitably reflect the intended purposes of the regulators. In Japan, the broad purpose is to assess individual tunnel systems explicitly in their own right and the result is a simple "okay" or "not okay". In Austria, the aim is somewhat broader, nominally enabling a more quantitative outcome that, in principle, can be used to compare the relative degrees of safety of the target tunnel and any other tunnel. This is done by assessing the safety of the chosen systems with reference to a universally defined tunnel as well as to the actual tunnel.

5. CONSEQUENCE ANALYSIS - VALID FIRE DETECTION

Implications of the 30s, 60s and 90s "rules" are now assessed by applying both qualitative and quantitative methodologies to the model tunnel summarized in **Table 2**.

Table 2: Model tunnel and its characteristics

Tunnel length	2,990m
Emergency exits	6
Tunnel cross section	Vaulted, 71m^2 (8.4m diameter)
Traffic volume	25,000 vehicles/day
Traffic mix	60.4% passenger cars 39.6% HGV (incl. bus)
Traffic speed	80km/h
Traffic signals	Traffic signals at both portals
Traffic condition	Asymmetric and symmetric traffic scenarios

5.1. Qualitative Consequence Analysis

Simulations of the standard 20MW fire (**Figure 1**) followed by zero-flow ventilation control have been conducted using a tunnel safety simulator [6]. Although all three detection times have been modelled, only the 90s case is presented here because it is clearly the least safe of the three. **Figure 2(a)** shows the evolution of the longitudinal velocity along the tunnel. Immediately after the fire breaks out, but before it is detected and the zero-flow response control system is activated, the air velocity in the tunnel increases. Zero-flow conditions are achieved approximately 3½ minutes thereafter. The jet fan velocities needed to achieve zero velocity are shown in **Figure 2(b)** as a percentage of the maximum required jet fan capability. The jet fans continue to operate after zero-flow has been achieved because the chosen boundary conditions would cause a net air flow rate if the fans were switched off.

Figure 3 shows the evolution of smoke density predicted by the simulator together with possible evacuation paths from the fire location – assuming rapid responses and average evacuation speeds of 1m/s. Persons evacuating to the left are in a smoke-free environment almost immediately whereas those evacuating to the right are continually exposed to smoke. Nevertheless, the smoke density to which they are exposed is less than the value of 0.4/m that is the approximate limit of densities for which fatalities are a strong risk. Accordingly, the qualitative methodology leads to the conclusion that the tunnel is "okay" even with a 90s detection time.

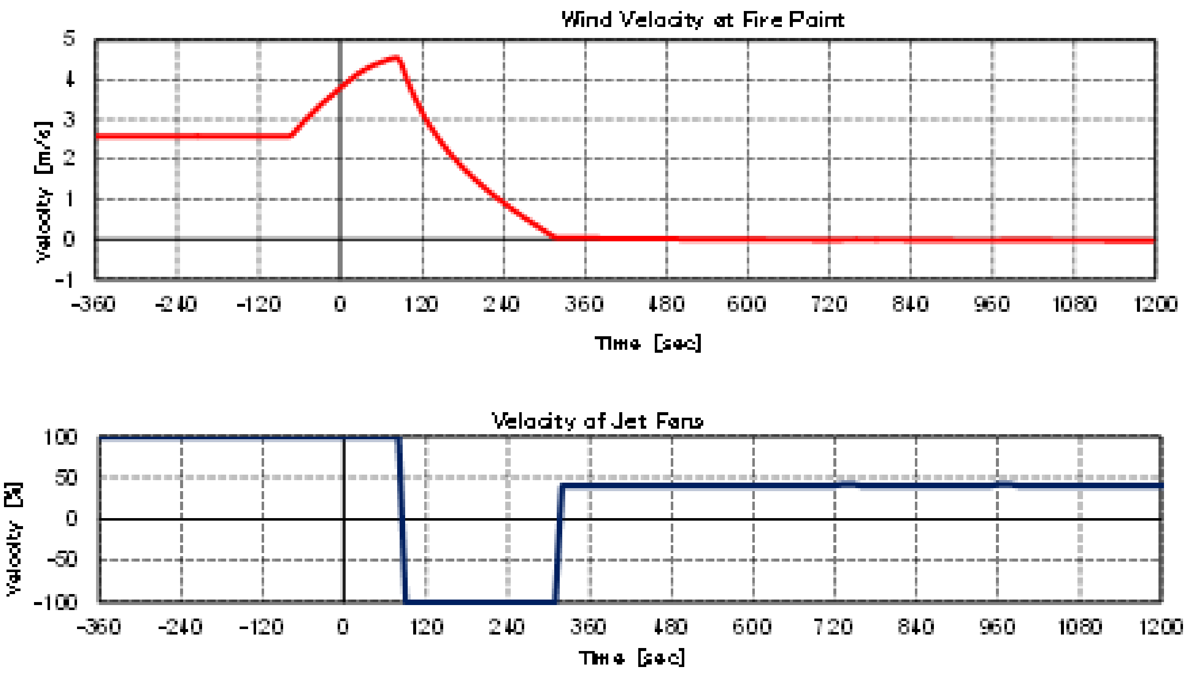

Figure 2: Air-flow velocity and output of jet-fans: 90s delay in fire detection

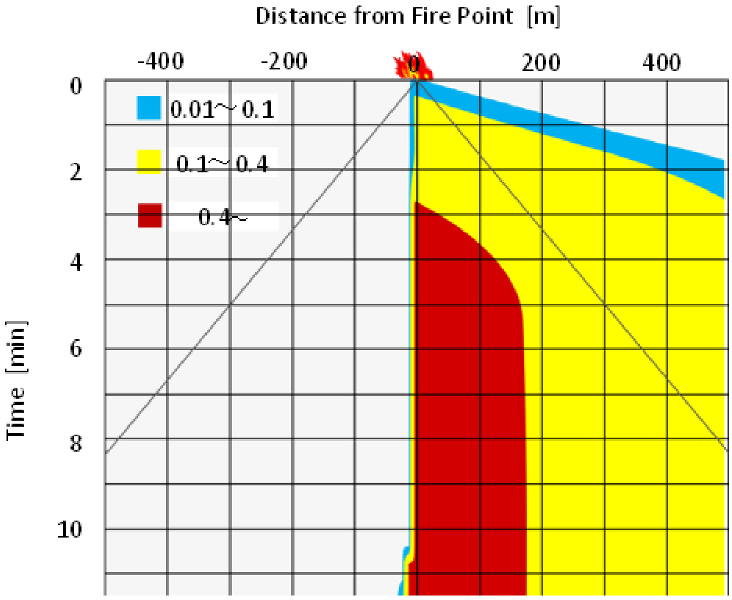

Figure 3: Smoke density and evacuation paths for a 20 MW fire (90sec detection time)

5.2. Quantitative Consequence Analysis

The Austrian methodology for carrying out tunnel risk analysis ("TuRisMo") is now used to evaluate the influence of different fire detection times, i.e. 30s, 60s and 90s, on the expected risk-value of the model tunnel specified in **Table 2**. TuRisMo uses a fully integrated quantitative approach and therefore allows for the implementation and detailed analysis of a broad variety of tunnel characteristics and safety measures. Detailed descriptions of the model and its implementation can be found in [5], [7] and [8]. One specific feature that can be taken into account when applying the Austrian tunnel risk analysis model is the composition of the emergency-response timeline. The general structure of a timeline table is depicted in **Figure 4**. Although the detailed form of the table might seem complicated, the important features for analyzing the impact of different fire detection times/rules are straightforward.

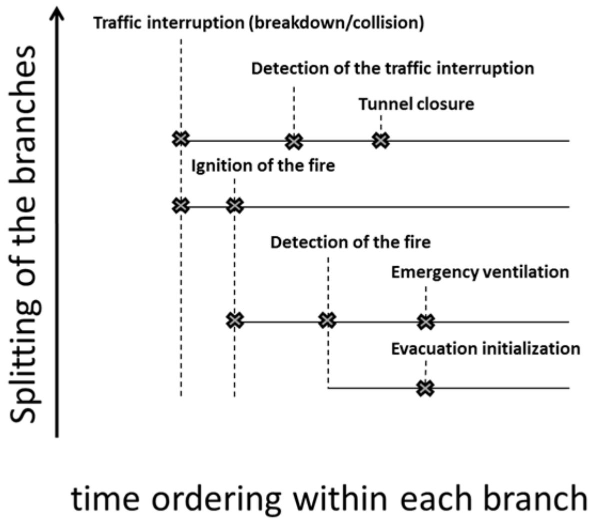

Figure 4: Time table of events for the quantitative risk analysis model

First, the detection of the traffic interruption and the detection of a possible consequential fire are separated and are considered independently of each other. Thus, for example, a variation of the fire detection time does not *a priori* imply a variation in tunnel closure times. This is because traffic interruptions such as accidents are usually detected before a consequential fire and may in themselves trigger closure of the tunnel. The following results for the model tunnel are based on an assumption of a fixed detection of the primary traffic interruption, 37 seconds after the initial incident, for all fire detection times considered.

Second, the transition from normal to emergency ventilation and the initialization of evacuation occur after the detection of a fire and therefore depend on the fire detection time. The ensuing result necessarily depends on many factors, especially the facilities available for use in the emergency response. For instance, if smoke-extraction or FFFS systems exist, their effectiveness will depend not only on their individual activation times, but also on the sequence in which they are activated in relation to each other and in relation to the time of change from routine to emergency ventilation. TuRisMo enables account to be taken of all such factors, but they are not considered herein because the necessary discussion of multiple options would detract from the primary purposes of the paper. Instead, attention is limited to the initiation of the changed ventilation regime and of the evacuation process. The risk assessment has been carried out for six cases, namely all combinations of the three detection times and two ventilation strategies. The latter are defined in **Table 3**. One is indicative of the Japanese zero-flow approach [4] and the other is indicative of a strategy that is more common in Europe [9]. The outcomes are summarized in **Figure 5**.

Table 3: Definition of two different fire emergency ventilations at the model tunnel

Model tunnel	Ventilation system	Ventilation strategy
Longitudinal Tunnel with Zero-Flow Ventilation	24 jet-fan positions with 2 jet-fans at each position	Longitudinal air velocity between 0.25m/s and -0.25m/s
Longitudinal Tunnel with Standard-Flow Ventilation	24 jet-fan positions with 2 jet-fans at each position	Longitudinal air velocity between 1.0m/s and 1.5m/s

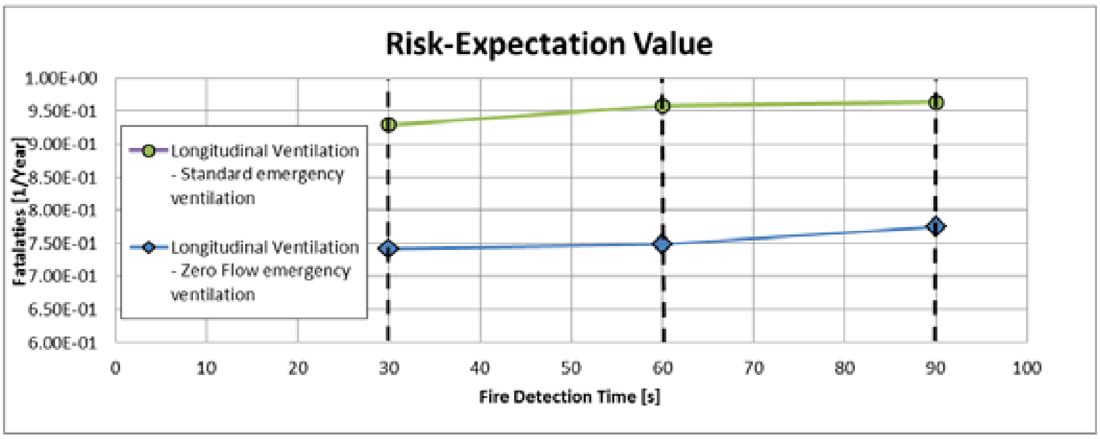

Figure 5: Dependency of the expected risk (fire risk + collision risk) value on the fire-detection time and the ventilation control strategy

By inspection, for the chosen scenario, the choice of the ventilation strategy has a much greater influence than the fire detection time. The “zero-flow” approach leads to a prediction of 20% fewer fatalities per year than the standard European strategy whereas a reduction in the detection time from 90s to 30s reduces the predicted fatality rate by only about 4%. Of course, it should not be inferred that the detection speed is unimportant in general. Indeed, it can be highly influential in other scenarios – e.g. when smoke extraction or FFFS capabilities exist. Nevertheless, the outcomes shown in Figure 5 do provide a clear demonstration that preconceptions can be very misleading. At the very least, it should not be assumed *a priori* that rapid fire detection will always have a significant influence on the eventual outcome even though it will always give some advantage. Similarly, it should not be assumed that the ventilation strategy will always have a strong influence. For example, the existence of smoke-extraction or FFFS capabilities could simultaneously increase the value of rapid fire detection and decrease the influence of the ventilation regime.

6. CONSEQUENCE ANALYSIS - FALSE FIRE DETECTION

In the preceding section, it is implicitly assumed that the information received from all sensors is valid. In practice, however, the possibility exists of false alarms and/or of the false interpretation of signals by a human operator. The false/nuisance alarm rate of a tunnel influences risk in two ways. First, tunnel users who are travelling towards the location of a falsely detected fire might have to stop inside the tunnel if it has internal traffic signals. Similarly vehicles approaching the tunnel might be stopped by external traffic signals or barriers. In both cases, this creates a risk that would not exist in the absence of the false detection, namely rear-end collisions. In tunnels with FFFS, additional risk is notionally possible through unnecessary activation. Such possibilities, whilst small in themselves, can have cumulative consequences for overall risk that change the relative advantages of alternative response strategies. Such effects can be simulated in the event tree according to RVS 09.03.11 in a direct manner. For instance:

- Rear-end collisions between stationary and late-stopping vehicles inside the tunnel define a distinct branch within the event tree, enabling false detection rates to be translated into modified probabilities for the existence of stopped cars within the tunnel.
- The corresponding risk arising for vehicles approaching the tunnel is most conveniently modelled by artificially extending the assumed length of the tunnel so that it includes the external regions in which a collision risk is incurred.

Figures 6 and **7** summarize risk analysis results for the standard European ventilation method and the zero-flow ventilation method respectively. The model tunnel is as defined in **Table 2** and a range of combinations of fire detection times and false/nuisance alarm rates is considered. These parameters are treated independently in this presentation even though they might not be independent in practice. Indeed, it is likely that an inverse relationship will exist between them because rapid detection and, especially, rapid reaction to detection, reduce the time available for reliability checks. For the chosen scenario, false alarm rates of very low frequency have an even smaller influence than that reported above for the speed of fire detection. However, the influence of more frequent false alarms is quite strong. It is therefore potentially important to take formal account of false alarms when assessing overall risk, not simply to regard them as a nuisance.

A subset of the same information is presented in a different format in **Figure 8** which shows selected combinations of the false alarm rate and the prescribed detection time. The general patterns for the two ventilation control strategies are very similar. For obvious reasons, the lowest possible risk would occur with the smallest false alarm rate and the smallest fire detection time. Assuming that these extremes are mutually exclusive, the Figure shows that, on balance, slightly lower risk will ensue from allowing an increased detection time of 90s than from allowing an increased false detection rate of one per week. Significantly greater risk will arise if the false detection rate increases significantly – e.g. to one per day.

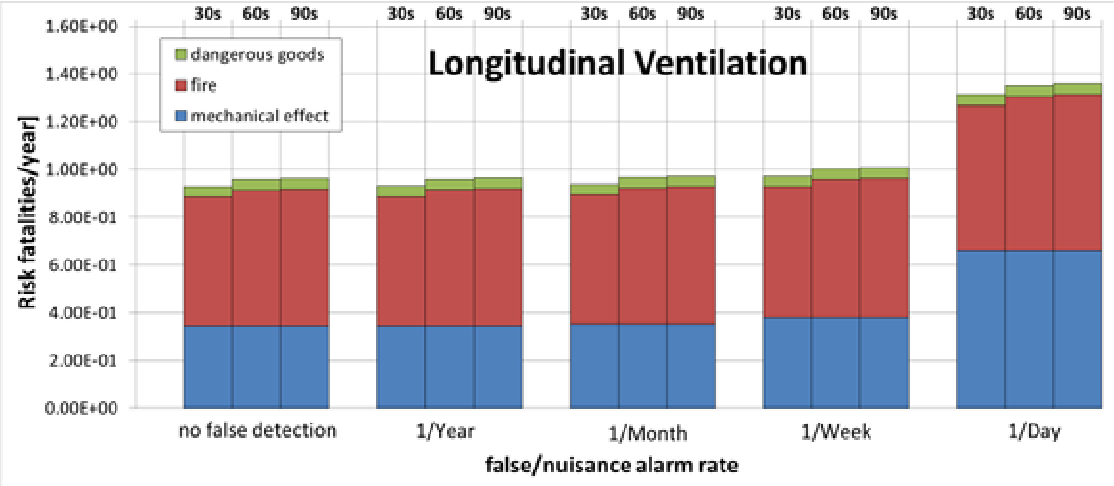

Figure 6: Risk (fire risk + collision risk) dependencies on false/nuisance alarm rate and fire detection time for standard-flow ventilation control

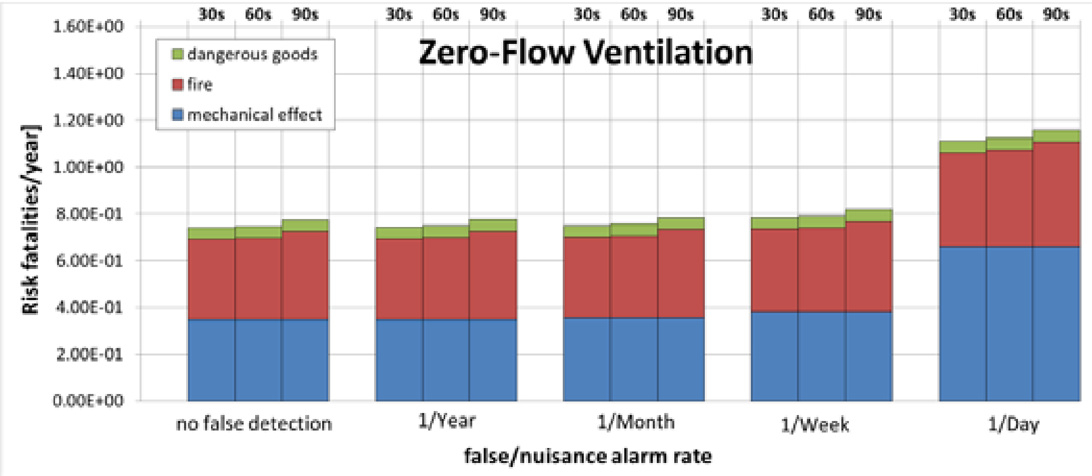

Figure 7: Risk (fire risk + collision risk) dependencies on false alarm rate and fire detection time for zero-flow ventilation control

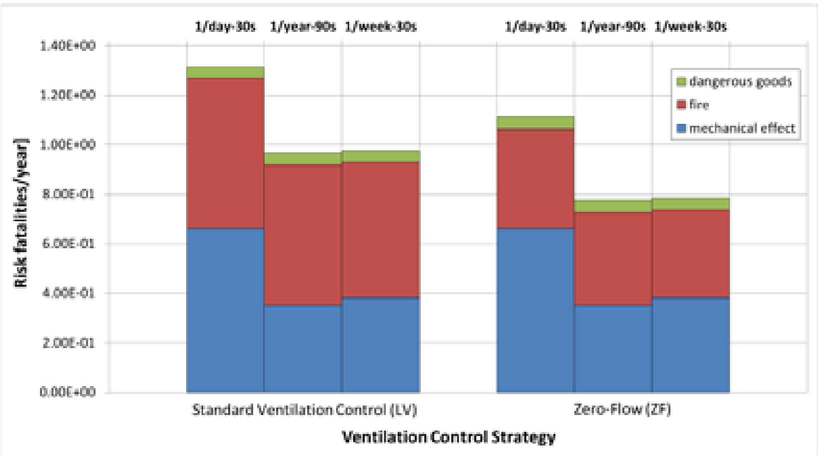

Figure 8: Comparison of selected false alarm rates and fire detection time combinations

7. CONCLUSIONS

Qualitative and quantitative consequence analyses have been used to estimate the relative influence of different requirements for fire detection rates in road tunnels in Japan (30s), Germany (60s) and Austria (90s). The analyses have been applied to the particular case of a longitudinally-ventilated tunnel with bi-directional traffic. This type of tunnel is very common in Japan although it is less common in Europe. The model tunnel does not have FFFS and there is no provision for smoke extraction within it.

For the chosen tunnel scenario, it has been found that:

• Overall risk depends much more strongly on the ventilation control strategy than on the time required for fire detection;

• Overall risk has only weak dependence on false alarms when these are significantly rarer than one per week, but it increases significantly with increasing frequency of false alarms;

• A false alarm rate of approximately one per day can be as important as the difference between emergency ventilation control for zero-flow and the corresponding control for a steady, moderate flow speed;

• In general, there is likely to be an inverse relationship between fire detection times and the frequency of false alarms. Therefore the consequences of false alarms need to be considered carefully when attempting to design fire detection systems that are both rapid and reliable.

Although these conclusions are believed to be valid for tunnels of the type considered herein, it should not be assumed that they are also valid for other types of tunnel.

8. REFERENCES

[1] German Road and Transportation Research Association, RABT 2006 –Guideline for equipment and conduction of road tunnels, Cologne 2006.

[2] FSV (Austria Society for Research on Road, Rail and Transport), Guideline RVS 09.02.22-Tunnel Equipment, Vienna 2014.

[3] Arnaudet, J. G., ESCOTA Report, ITC Tunnel Fires and Escape from Tunnels Conference, Lyon, 1999.

[4] Mizuno, A., Ohashi, H., Nakahori, I., Okubo, N., "Emergency operation of ventilation for the Kan-Etsu road tunnel", 5th ISAVVT, BHR Group, Seattle, pp.77-91, 1985.

[5] FSV (Austria Society for Research on Road, Rail and Transport), Guideline RVS 09.03.11-Methodology of Tunnel Risk Analysis, Vienna 2015.

[6] Nakahori, I., Sakaguchi, T., Kohl, B., Forster, C., Vardy, AE., "Risk assessment of zero-flow ventilation strategy for fires in bidirectional tunnels with longitudinal ventilation", 16th ISAVFT, BHR Group, Seattle, pp.501-516, 2015.

[7] Forster, C., Kohl, B., Wiesholzer, S., "Methodologies for accurate risk modeling in the context of integrated quantitative risk analysis", 16th ISAVFT, BHR Group, Seattle, pp.517-531, 2015.

[8] ILF Consulting Engineers, Federal Ministry of Transport, Innovation and Technology, Final Report 'Broadening and deepening of the Austrian tunnel risk model TuRisMo 2', 2015.

[9] FSV (Austria Society for Research on Road, Rail and Transport), Guidline RVS 09.03.31-Ventilation Systems, Vienna 2014.

[10] Maevski, I., Josephson, B., Klein, R., Haight, D., Griffith, Z., "Final testing of fire detection and fire suppression systems at Mount Baker Ridge and First Hill Tunnels in Seattle", 16th ISAVFT, BHR Group, Seattle, pp.745-754, 2015.

DEVELOPING A NEW MODEL TO PREDICT FIRE FLAME LENGTH UNDER TUNNEL CEILING BASED DIMENSIONAL AND REGRESSION ANALYSIS

B. Niknam, K. Shahriar, H. Madani
Amirkabir University of Technology, Iran

ABSTRACT

In this paper, a new model was developed to predict the length of the flame under the tunnel ceiling. Using dimensional analysis the length of the dimensionless flame under the tunnel ceiling was expressed as a function of the released heat as well as the velocity of the dimensionless flow together with tunnel's cross section blockage percentage. The coefficients of the developed function parameters were measured using the data of RuneHamar tunnel and regression analysis and it was determined that the dimensionless flame length has a linear relationship with the released dimensionless heat and the velocity logarithm of the dimensionless flow, and a second-order Relationship with reversed tunnel blockage percentage. To ensure the accuracy of the developed model, the fire data of Eureka and Memorial tunnels was analyzed using the new model and previous formulations and a favorable convergence was achieved on the relationships. In addition, the RuneHamar r T2test was modeled using FDS software; in addition the flame length obtained from the new and the simulation models, compared to previous models, was closer to reality, and had a high reliability

Keywords: Flame Length, Fire, Dimensional Analysis, RuneHamar Tunnel FireTest

1. INTRODUCTION

In recent years , Several enormous fires have taken place in road tunnels, including the fire in the of Mont Blanc tunnel between Italy and France in 1999, with 39 casualties, the fire in Taurn tunnel of Austria with 12 casualties and the fire of Gotthard tunnel in 2001 with 11 casualties [1]. The type of Truck loads has the most important role in the outcome of fire events, and this could be attributed to high energy content of the truck loads, such that the fire can easily spread along the truck load through the ventilation system. In all fire incidents mentioned above, at least 10 cargo trailers with other cars were involved in the fire. The fire started from one or two cars and then was spread to the rest of the cars after some time. The spread of fire in this manner has a very important role in the outcome of fire. Because it leads to an increase in fire intensity and decrease firefighters access to the fire point to extinguish the fire and perform rescue operations. There is a great deal of information about the behavior of the truck fires inside the tunnel but in order to evaluate the fire intensity, additional information such as fire spread manners and flame length is required. In the archives, many equations have been proposed to calculate the flame length according to maximum temperature of fire. These equations cannot be used because of low vertical height of the flame [2]. Alpert modified these equations for fires inside the tunnel and developed a new equation for calculation of the radial spread of flame under the tunnel ceiling [3].

The modified equation for fire in galleries which is very similar to fires in tunnels was proposed by Delichatsios. He used the ratio of the width to the height of the gallery to develop his model; therefore his equation cannot be used to analyse the results obtained from large-scale tests such as the fire of Runne Hummer, Memorial, Firetun and other tunnels. In 2007, Lönnermark carried out a back analysis on Alpert equation (1), and calculated the gas temperature, the heat released from the fire and flame length under the ceiling of the tunnel [5].

$$T_{\max} = T_0 + \frac{5.38\left(\frac{Q}{r}\right)^{\frac{2}{3}}}{H_f} \qquad (1)$$

In his study, Lönnermark used the tunnel height instead of height between the fire source and the ceiling of the tunnel. In Alpert equation, parameter r was used to express flame spread under the ceiling of the tunnel. Due to the limiting effect of the tunnel and the impact of ventilation system on the spread of fire, some modifications should be made on the parameters of the Alpert equation for description of flame spread mechanisms under the ceiling of the tunnel. In the first step, Lönnermark used the parameter r to calculate the length of the flame under the tunnel ceiling, to fit the best diagram to the data of RuneHamar tunnel, he had to do some modifications on the power factor of parameters. For doing so, he made use of Rew and Deaves study [6] who developed an equation to calculate the length of flame spread under the tunnel ceiling as a function of longitudinal ventilation flow rate. By performing a back analysis on the Alpert equation and combining that with the Davis and Raw equation, Lönnermark developed the following general equation to calculate the length of the flame under the tunnel ceiling.

$$L_f = \frac{k_2 Q^a u^b}{\left(T_{ft} - T_0\right)^{\frac{3}{2}} H_t^{\frac{3}{2}}} \qquad (2)$$

Lönnermark calculated The Constant coefficients of the above equation, using regression analysis on the Runehamar tunnel data and finally equation (3) was presented for calculation of the flame length.

$$L_f = \frac{1370 Q^{0.8} u^{-0.4}}{\left(T_{ft} - T_0\right)^{\frac{3}{2}} H_t^{\frac{3}{2}}} \qquad (3)$$

In Fig 1, the flame length obtained from equation 3 has been compared to the large-scale fire tests such as Memorial, Eureka and RuneHamar. According to Fig1, the flame length obtained from equation 3 is not consistent with the data of Memorial and Eureka tunnel tests, but these data are in favorable convergence with the results of RuneHamar tunnel tests. the difference in flame length obtained from equation 3 and Memorial and Eureka tests can be attributed to different fire sources and ignition mechanisms (RuneHamar: wood and plastic, Memorial: hydrocarbon fuel, Eureka: cars), lack of access to appropriate data during Eureka and Memorial tests, and the like. Although, the equation (3) is in good convergence with the Runehamar data, these are some faults in the flame length obtained from this equation.

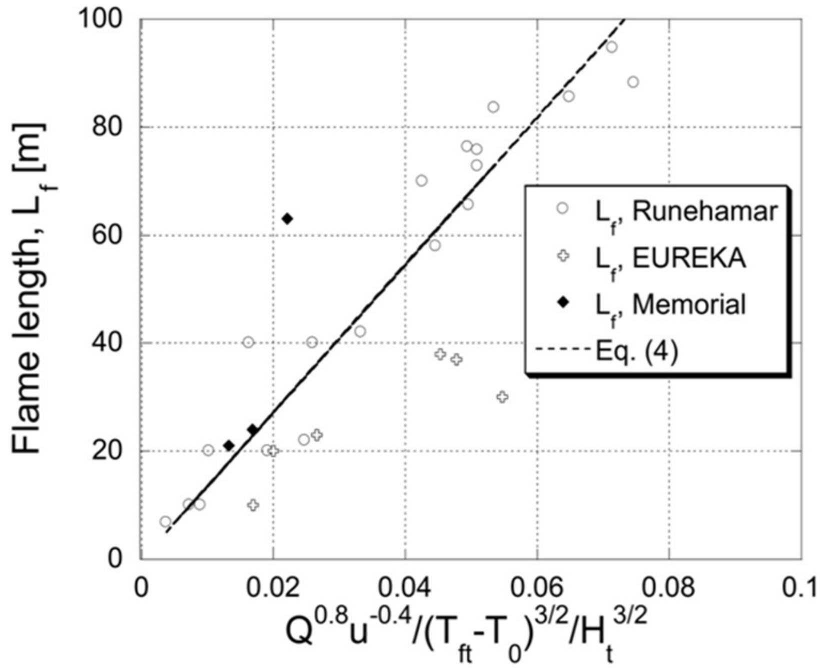

Fig.1: Comparison of flame length obtained from Lönnermark equation with large-scale fire tests [5]

Equation (3) is the last formula for calculation of the flame length under the tunnel ceiling. in this equation, the flame length is in direct relationship with the heat released from fire and is in inverse relationship with the flow rate, while, according to Carvel investigation, [7] (Table 1) increasing flow rate, leads to increased heat released from the fire. Therefore, increased flow rate will lead to greater flame length, while according to equation (3) this relationship is just the other way round, according to this equation, increased flow rate leads to reduction of flame length. On the other hand, the impact of blockage by cars and three-dimensional fire on flame length is not considered in this equation. Considering the impact of tunnel blockage by cars and three-dimensional fire on fire behavior, the present paper developed a new equation for prediction of flame length under tunnel ceiling.

Table 1: The Effect of ventilation on the Heat Release Rate from the truck fire [7]

Cross-section shape	Circular			Semicircle			Horseshoe			Rectangular		Semi-elliptical			
	)single lane(			)two- lane(			)Two-lane(			)Two-lane(		)Three-lane(			
Velocity (m/s)	Fire size (MW))														
	A	B	C	A	B	C	A	B	C	A	B	C	A	B	C
2	20	40	34	24	44	40	20	44	34	30	60	40	30	60	44
4	34	64	40	40	70	44	34	64	44	44	74	44	44	74	60
6	40	80	64	44	84	70	44	84	64	60	90	70	60	90	74
10	64	100	74	70	104	80	64	100	80	70	110	80	74	110	8

2. PROBLEM SOLVING METHOD

2.1. Dimensional Analysis

This method allows for prediction of the quality of mathematical relations between the physical parameters. In dimensional analysis, recognition of the parameters involved in the problem is one of the major necessities of the analysis. The theorem Π or Kingham theorem as a general rule, has been widely used in dimensional analysis. According to this theorem, when there is a relationship between N_1 physical variables and these variables can be represented in form of N_2 main dimensions, $N_1 - N_2$ number of dimensionless multiplication between those physical variables can be written. These dimensionless multiplications are Π sentences and are represented by $\Pi_1, \Pi_2, ..., \Pi_n$ .The relationship between these multiplications can be represented as follows [8]:

$$F(\Pi_1\Pi_2...\Pi_n) = 0 \tag{4}$$

$$\Pi_1 = f(\Pi_2\Pi_3...\Pi_n) \tag{5}$$

According to the previous research, the parameters affecting the length of the flame under the tunnel ceiling include: Fire Heat Released rate Q, longitudinal velocity of air flow u , geometry of the tunnel,A_t , cross-section of the fire A_f , tunnel height H_t, density of air ρ , ambient temperature T , heat capacity of air C_p acceleration of gravity g.The length of the flame under the tunnel ceiling can be stated as follows.

$$L_f = f(Q, C_p, T_0, g, H_t, A_t, A_f, u, \rho) \tag{6}$$

In the above equation, the flame length is presented as a function of the parameters affecting it. By changing the parameters into dimensionless parameters, equation 6 can be expressed in form of equation 7.

$$\frac{L_f}{H_t} = f\left(\frac{Q}{\rho u^3 H_t^2}, \frac{C_p T_0}{u^2}, \frac{gH_t}{u^2}, \frac{Af}{A_t}\right) \tag{7}$$

The above equation can be re-written as follows.

$$\frac{L_f}{H_t} = f\left(\frac{Q}{\rho C_p T_0 g^{\frac{1}{2}} H_t^{\frac{5}{2}}}, \frac{u^2}{gH_t}, \frac{Af}{A_t}\right) \tag{8}$$

In equation 8, the released dimensionless heat is the first phrase, the third phrase is the tunnel blockage ratio and the second phrase can also be considered as dimensionless ventilation velocity.

$$u^* = \frac{u}{\sqrt{gH_t}} \tag{9}$$

As a result, the length of the flame under the tunnel ceiling can be expressed as a function of the heat released rate, Dimensionless longitudinal velocity and tunnel blockage ratio in form of equation 10.

$$L_f^* = f\left(Q^*, u^*, \frac{Af}{A_t}\right) \tag{10}$$

2.2. Determination of impact coefficients of the parameters

The dimensionless flame length can be expressed in the form of equation 11

$$L_f^* = f\left(Q^*, u^*, \frac{Af}{A_t}\right) \rightarrow \tag{11}$$

$$L_f^* \cong f\left(\left(Q^*\right)^{\alpha}\left(u^*\right)^{\beta}\left(1-\frac{Af}{A_t}\right)^{\gamma}\right)$$

The data of in situ fire tests were used to determine the constant coefficients of equation 11. Which are discussed below .

2.2.1. Dimensionless heat released rete

The Runehamar tunnel fire test data [5] and regression analysis were used to determine the constant coefficient of, or rather the most appropriate function to express the relationship between the flame length and the dimensionless released heat. Fig.2,Fig.3 and Fig.4 show the fitted functions for the Runehamar tunnel fire test data. According to the convergence coefficient of the fitted functions, linear function is best fitted for the results obtained from the three fire test on the Runehamar tunnel. Therefore, the linear equation is the best function for expressing the relationship between the flame length and the heat released from the fire.

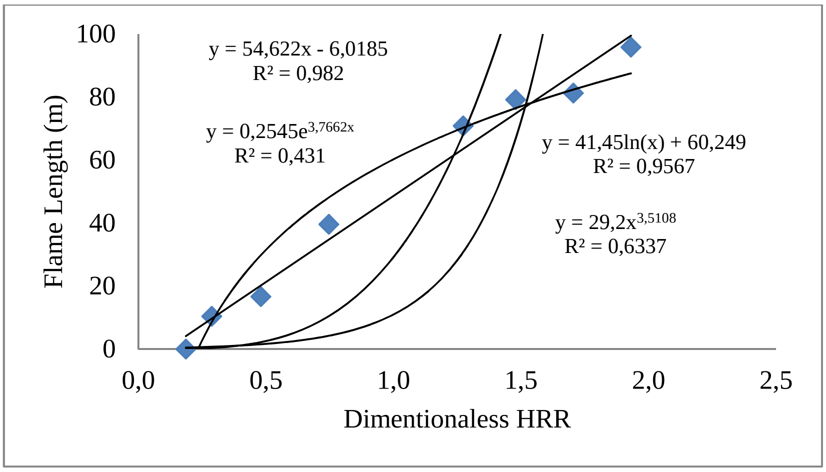

Fig. 2: Determination of the best equation for expression of the relationship between flame length and the heat released during the fire in T1 test in Runehamar tunnel.

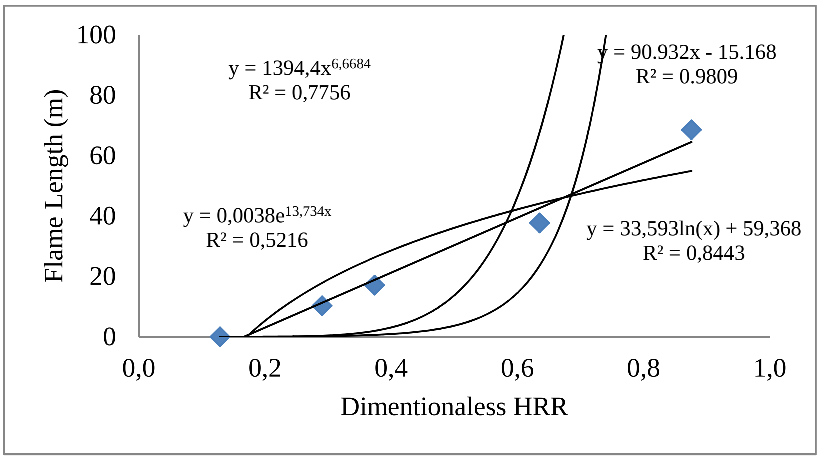

Fig. 3: Determination of the best equation for expression of the relationship between flame length and the heat released during the fire in T2 test in Runehamar tunnel.

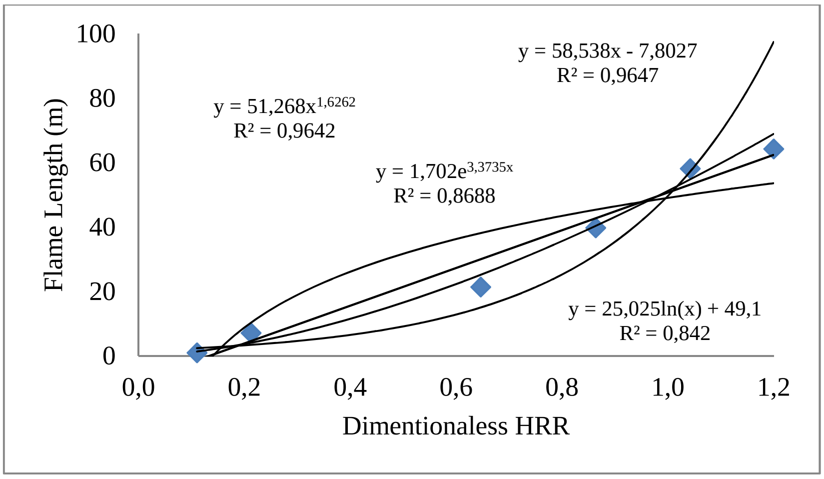

Fig. 4: Determination of the best equation for expression of the relationship between flame length and the heat released during the fire in T3 test in Rune hamar tunnel.

Table 2: The convergence coefficient of the functions fitted for the Runehamer tunnel data

Relationship between the flame length and the dimensionless heat release rate in Runehamar tunnel fire test series		
Test NO.	The type of equation	Convergence coefficient
Test T_1	Linear	0.982
	Logarithmic	0.956
	Power	0.6337
	Exponential	0.431
test T_2	Linear	0.98
	Logarithmic	0.84
	Power	0.7756
	Exponential	.0.5216
test T_3	Linear	0.9647
	Logarithmic	0.842
	Power	0.9642
	Exponential	0.8688

2.2.2. Dimensionless Velocity

The relationship between the critical velocity and flame length was determined using the T_2 test data in Runehamar tunnel. For doing so, several functions were fitted to the data. According to Fig. 5 and Table 3, logarithmic equation has the best convergence with the Runehamar tunnel data, therefore this equation is the most appropriate function for expression of the impact of dimensionless flow rate on the flame length. To ensure the accuracy of this equation, the data of Ingason experimental model [9] was also used. The data of the released temperature and flow rate during this test was available, but the flame length was not measured. According to the analyses conducted in the previous section, there is a linear relationship between the released heat from the fire and the flame length. Therefore, the function fitted for expression of the relationship between the released heat and flow rate can also be used to express the importance of the flow rate in the flame length. After regression analysis it was found out that the logarithmic function has the best convergence with the data of Ingason model and this confirms the accurate selection of the logarithmic equation to express the relationship between the flame length and the ventilation flow rate.

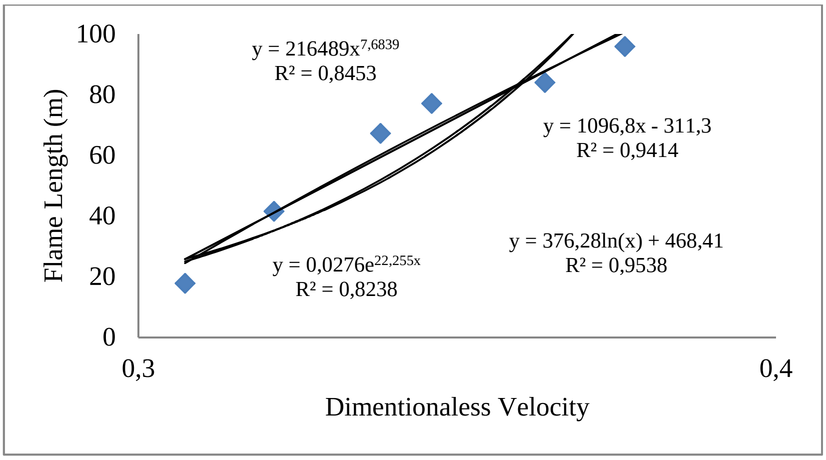

Fig. 5: Determination of the best equation for expression of the relationship between the flow rate and flame length in T1 Runehamar tunnel test

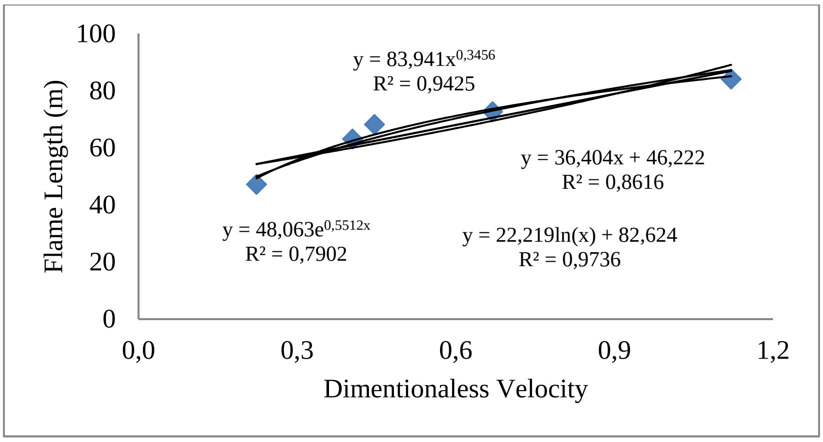

Fig. 6: Determination of the best equation for expression of the relationship between the flow rate and the released heat in the Ingason model [9]

Table 3: The convergence coefficients of the fitted models on the Runehamar tunnel [5] and Ingason model [9]

Relationship between the flame length and the dimensionless velocity in Runehamar tunnel fire test [5]		
Test NO	The type of equation	Convergence coefficient
T_2	Linear	9414.0
	Logarithmic	9538.0
	Power	8453.0
	Exponential	8238..0

Relationship between the heat release rate and the velocity in Ingason model[9]		
	The type of equation	Convergence coefficient
	Linear	8616.0
	Logarithmic	9736.0
	Power	9425.0
	Exponential	7902.0

2.2.3. The effect of tunnel blockage

In 2009, Kayli [10] developed an experimental model in a scale of 1 to 10, and investigated the effect of cars blockage on fire behavior inside tunnels, and measured flow rate and the rate of materials burning impact on the percentage of different blockages. Unfortunately no data is available about the flame length in Kayli test, but due to the linear relationship between the released heat and the flame length, the best function fitted on the released heat and the tunnel blockage will be generalized to the flame length. Fig.7. Shows the data received from the kayli tests. According to Fig. 7, the second-order contribution factor has the highest convergence coefficient with the Kayli's data; therefore, second-order contribution function is the best choice for expression of the relationship between the flame length and the percentage of tunnel blockage.

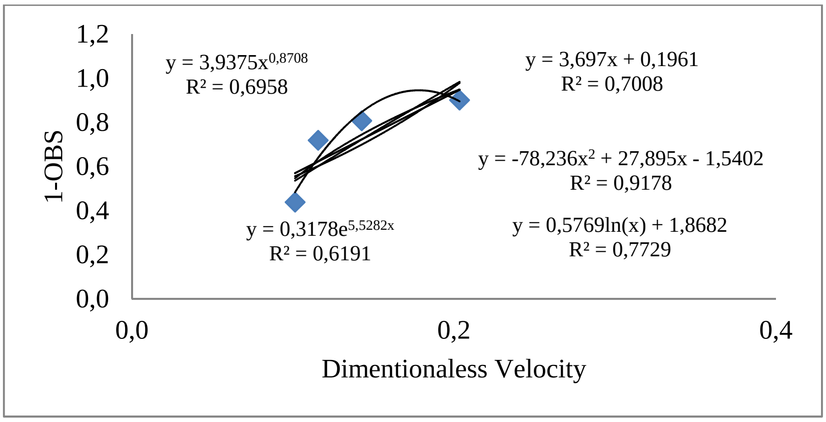

Fig. 7: Determination of the best equation for expression of the relationship between tunnel blockage and the released heat in the kayli model [10]

2.2.4. The general equation

According to dimensional analysis, the dimensionless flame length can be defined in form of equation 12.

$$L_f^* = f\left(\frac{(Q^*)\left|\ln(u^*)\right|}{\left(1-\frac{Af}{A_t}\right)^2}\right) \tag{12}$$

After regression analysis on the data of T_2 test in the Runehamar tunnel, the dimensionless flame length can be expressed in form of Equation 13.

$$L_f^* = 5.307\left(\frac{(Q^*)\left|\ln(u^*)\right|}{\left(1-\frac{Af}{A_t}\right)^2}\right)^{0.686} \tag{13}$$

Where u is the dimensionless ventilation velocity, Q is the dimensionless Heat Release Rate, A_f/A_t is the tunnel blockage ratio and L_f^* is the dimensionless flame length.

3. NUMERICAL MODELING

Using FDS software [11, 12] the T2 test of Runehamar model was modeled. Fig. 8 shows the comparison of heat released rate from the simulation and T2 test in the Runehamar tunnel. According to Fig 8 there is a favorable consistency between the simulation and the reality in the fire growth phase, but in the development phase, the simulated fire remains at its peak for a longer period of time and follows a procedure which is different from the Runehamar tunnel test, but this case, would not cause any significant error in the flame length prediction and just causes the fire flame to remain at its peak for a longer period of time. Fig 9, shows the geometry of the developed model, Runehamar tunnel, and the maximum length of the flame at the peak of the fire. According to Figure 9, the maximum flame length obtained from modelling at the released heat of 150 MW is 85 meters, while the flame length in the Runehamar tunnel, Deaves formula and equation 11 is 78 meters. At the fire peak point, there is an error of 10% between results of modelling and the results obtained in reality. But in earlier phases of fire, this error is lower at heat release of less than 40 MW and released heat within the range of 75 to 125 MW, and in some cases the length of the simulated flame is exactly consistent with flame length obtained from the Runnehamar tunnel test (Fig.10).

4. VALIDATION

Fig10 shows the comparison of the flame length obtained from T2 test of Runehamar tunnel with the flame length obtained from equation 13, Deaves formula (Equation 14) [5] and the simulation results.
According to Figure 9, Formula 13, unlike Deaves Formula, has a good consistency with the data of Runehamar tunnel test, and this could be attributed to the right choice of functions for expression of the relationship between the parameters associated with the flame length, such as released heat, the flow rate, and tunnel blockage in equation 12, while these parameters are not appropriately introduced in the calculations of equation 14, on the other hand, The impact of tunnel blockage on the behavior of the fire inside the tunnel is totally missing in the formula 14, and these cases lead to increased deviations of equation 14 from the in situ data.
To evaluate the validity of the proposed formulas, it is necessary to compare the results of equation 13 with data from other in situ fire tests. The Memorial and Eureka [12, 13] data were used for this purpose. Table 4 shows the features of Memorial and Eureka tunnel tests. The flame length obtained from Memorial and Eureka tunnel tests have considerable consistence with the results obtained from formula 13. There are slight differences between the dimensionless flame lengths obtained from the two tests. The difference between flame length in Eureka tunnel test and in equation (13) is sinusoidal, which can be attributed to unknown height of the tunnel and tunnel blockage in the test reports.

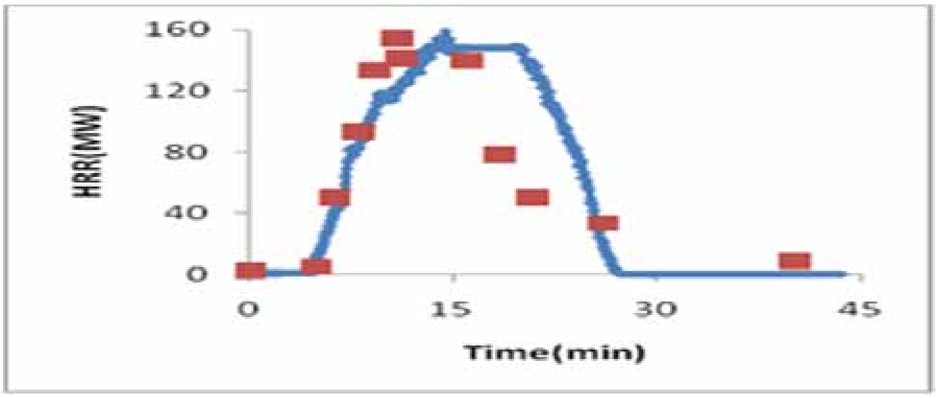

Fig. 8: The released heat from the developed model and T2 test in Runemahar tunnel

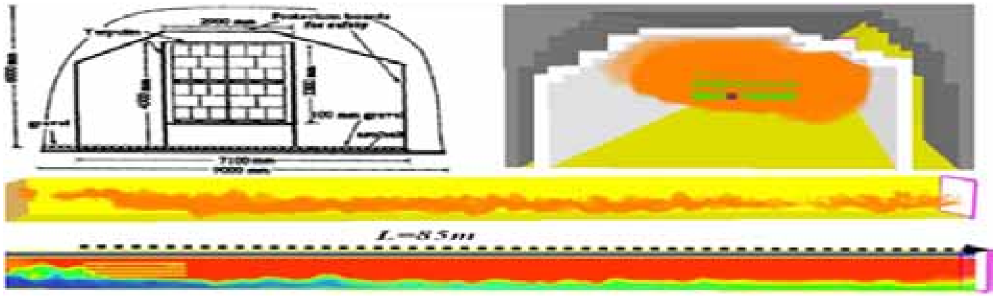

Fig. 9: The geometry of Runehamer tunnel, and the developed model and flame length at the fire peak moment

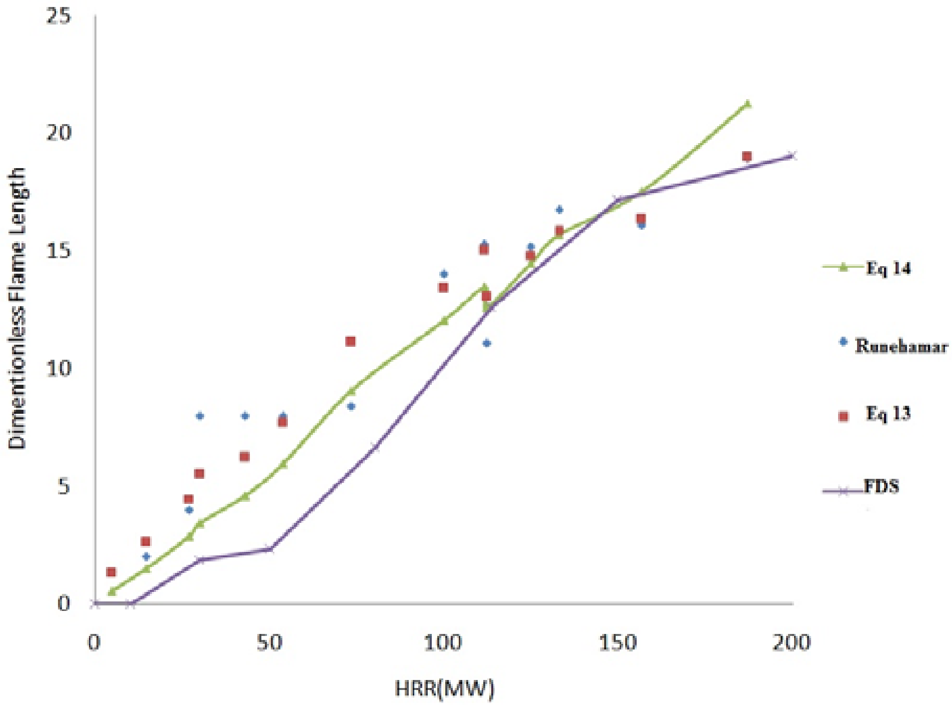

Fig. 10: Comparison of the flame length in Runehamar test, Eq 13 , Eq14 and numerical simulation

Table 4: Comparison of the flame lengths obtained from large scale tests [5,13,14] and equation 13

HRR(MW)	Runehamar [5]	Eq13	Eq14	HRR(MW)	Memorial [13]	Eq13	Eq14
5	1.35	1.31	0.51	50	4.3	98.2	86.0
14.84	2	2.62	1.48	50	65.2	33.2	1.1
27	4	4.46	2.86	100	98.7	6.3	26.2
30	8	5.48	3.44	HRR(MW)	EUREKA 499[14]	Eq13	Eq14
43	8	6.22	4.59	51	81.1	76.0	41.3
54	8	7.67	5.94	63	63.3	88.0	22.4
73.5	8.4	11.14	9.02	72	81.1	43.5	9.6
100	14	13.38	12.025	80	63.3	8.5	6.7
111.8	15.28	14.99	14.19	90	18.4	12.1	6
112.5	11.1	13.03	12.58	106	45.5	1.7	13.10
125	15.16	14.77	14.47	112	9.6	36.7	7.10
133	16.72	15.84	15.68	120	45.5	48.9	11.13
156.63	1.16	16.35	17.51	120	72.6	71.7	46.11

5. CONCLUSIONS

In this paper, a new model was introduced for predicting the length of flame under the tunnel ceiling, with consideration of the cars and fire blockage effect. The heat released by the fire, the flow rate, and tunnel blockage are the most important parameters affecting the length of the flame under the tunnel ceiling. The role and relation of dimensionless parameters including the released heat, flow rate and tunnel blockage in the flame length was determined. According to data obtained from in situ tests, the flame length has a linear relationship with released heat and the dimensionless flow rate logarithm, and also a second order with tunnel blockage The validity of the model developed using the data of Runehamar, Memorial, raperford tunnel tests was evaluated. According to the observations, the developed equation (equation 13) is considerably consistent with the actual data and this could be attributed to appropriate choice of the function to express the role of parameters in the flame length and investigation of all the parameters involved in this problem. There are minor differences between the on-dimensional flame length obtained from equation 13, Memorial and Eureka tunnel tests and this could be attributed to unknown height and blockage of tunnels and constant flow rate during the tests, and different fired loads in Rune hamar, Memorial and Eureka tunnel tests.

6. REFERENCE

[1] F. Vuilleumier, A. Weatherill, B. Crausaz, Safety aspects of railway and road tunnel: example of the Lotschberg railway tunnel and Mont-Blancroad tunnel, Tunneling and Underground Space Technology, (2002) 153–158.

[2] C.L. Beyler, Fire Plumes and Ceiling Jets, Fire Safety Journal, (1986) 53-75.

[3] R,L Alpart, ceiling jet flows, in SFPE handbook of fire protection Engineering and national fire protection association, (2002) 2-31.

[4] M.A. Delichatsios, the Flow of Fire Gases under a Beamed Ceiling, Combustion and Flame, (1981) 1-10.

[5] A Lonermark, H,Ingason, Fire Spread and Flame Length in Large-Scale Tunnel Fires, Fire Technology journal, (2006) 283-302.

[6] C. Rew and D. Deaves, Fire Spread and Flame Length in Ventilated Tunnels—A Model Usedin Channel Tunnel Assessments, Proceedings of the International Conference on Tunnel Fires and Escape from Tunnels, Lyon, France, (1999). 397–406.

[7] R.O Carvel, A,beard, variation of heat release rate with forced ventilation for vehicle fires in tunnel, fire safety journal ,(2001)569-596.

[8] H. Ingason , Model scale tunnel fire tests, SP Report 2005:49, Swedish National Testing and Research Institute,(2005).

[9] S.kayli, the influence of tunnel blockage on heat release rate of fire, Doctoral Thesis, Metu University, Turkey, (2009).

[10] Fire Dynamics Simulator, http://fire.nist.gov/fds .

[11] S.R.Lee, H.S .Ryou, An experimental study of the effect of the aspect ratio on the critical velocity in longitudinal ventilation tunnel fires, Journal of Fire Sciences ,(2004) 119–138.

[12] .Memorial Tunnel Fire Ventilation Test Program—Test Report Massachusetts Highway Department and Federal Highway Administration,(1995).

[13] .S.E. French,EUREKA 499—HGV Fire Test (Nov. 1992)—Summary Report,in Proceedings of the International Conference on Fires in Tunnels, E. Ivarson (Ed.), SP Swedish National Testing and Research Institute, Bor˚ as, Sweden ,(1994) 63–85

CFD AND ENGINEERING METHOD COUPLING FOR EVALUATING THE FIRE RELATIVE TO BATTERY TRANSPORTATION

Benjamin TRUCHOT, Guillaume LEROY and Guy Marlair
INERIS, Verneuil en Halatte, France

ABSTRACT

Using CFD fire modelling for underground infrastructure always face off the same problem that consists in defining the heat release rate and toxic gas source term. Based on a large series of experiments, standards were defined some decades ago and are currently used for safety design. The development of new energy carriers however let fire safety engineer to wonder about the applicability of those standards and the possibility to consider more realistic curves.
This paper proposes an innovative model to build the heat release rate and toxic gas emissions curve for trucks. It consists in splitting the vehicle in several interconnected elements that have their own curves. A relation can then be supposed for the propagation in order to obtain a global curve. After comparison to experimental available data, this model can be applied for designing source term including new energy carriers as batteries.
One of the main interest of such an approach consists in considering individual fire tests that could be easily managed and then considering real emission factors for the different individual component of the vehicle.

Finally, the fire and toxic gas emission curve produced by such an approach can be introduce in a CFD code, not for safety design because of the specificity of the curve but for giving a positioning regarding the applicability of standards compared to current real fires.

Keywords: electric car, HGV, CFD modelling

1. INTRODUCTION

New Energy Carrier (NEC) is nowadays in great expanding because of the well known impact of transport technologies on global warming. To ensure a mass development of those technologies, safety must be considered on the very beginning. Even several technologies exist, this paper focus on electro mobility. Some works were recently published focussed on the consequences of electric car fire in tunnel. One of the major issues for using such NEC should however be relative to transport. Consequences of fire have to be considered in case of Hazardous Goods Vehicle (HGV) that carries batteries, and compared with the commonly used standard curve for HGV.

This paper focuses on this case of fire on a HGV that carries batteries. Defining the fire curve is the first step. Data are available in the literature for a standalone battery fire, both in terms of heat release rate and in terms of toxic gas production, fire resistance of batteries were also communicating for some of them. This paper presents an engineering method that aims to compute the source terms that corresponds to fire propagation to the whole vehicle considering standalone fire curves and fire resistance available data. This model can also consider different ignition configurations, the case of a fire that stars on the lorry, brake failure for example, or the case of a fire that starts on one of the batteries. Of course, in such a case, the fire propagation to the battery loading is fully different and thus, fire consequences are also. This fire curve built with this model provides not only the heat release rate along time but also the distribution of toxic gases release rate.

Because the source term curve alone cannot be used for concluding regarding the human potential risk, the FDS fire code was used in order to predict detailed consequences on a given standard tunnel geometry on one chosen scenario using both standard and modelled fire curve. These consequences were evaluated both in terms of temperature, for the stratification process, and toxicity, for ensuring a safe evacuation.

2. BACKGROUND ON DATA USED FOR FIRE IN TUNNEL CONSEQUENCES MODELLING

The main focus of the present paper is the batteries loaded truck fire consequences in case of fire in tunnel. To provide a better understanding of the problematic, an overview of the current methods and standards used is required.

2.1. The difficult choice of the toxic properties of the design fire

As discussed in (1), different sources are available for defining the characteristics of the design fire. It is commonly admitted that a passenger car will generate less than 10 MW fire, even for a large passenger car, that a buses fire will generate around 20 MW fire and that heavy goods vehicles can lead to fire up to more than 100 MW. This heat release rate is of course directly linked, not only with the temperature curve in the vicinity of the fire, but with the smoke production too. A smoke production rate for design fire was proposed by different sources as (1) or (2). One of the main interests of those two references is to provide the quantity of carbon dioxide and monoxide and consequently an estimation of the ratio between those two values. Some values are reminded in Table 1.

Table 1: Example of design fire smoke production rate and CO/CO_2 ratio

Nature of the fire and source	Pic heat release rate [MW]	CO_2 producti on rate [kg/s]	CO production rate [kg/s]	CO_2/CO ratio
Plastic passenger car (1)	5	0.4 – 0.9	0.02 – 0.046	8 – 45
Large passenger car (2)	8	0.8	0.02 – 0.1	7.6 – 39
Lorry without dangerous goods (1)	20	1.5 – 2.5	0.077 - 0.128	12 - 32
Lorry without goods or heavy goods vehicle(2)	30	3	0.08 - 0.4	7.6 – 39
Heavy goods vehicle (1)	20 – 30	6 – 14	0.306 – 0.714	0.8 – 46
Heavy goods vehicle with combustible load (2)	100	10	0.25 – 1.3	7.6 - 39
Heavy goods vehicle with hazardous goods load (2)	200	20	0.5 - 2.6	7.6 – 39

It must be first added that, of course, CO is not the only toxic gases produced by a car fire but it gives a representation of the global toxicity (4) (5).

2.2. The impact of the load on the design fire

In the specific case of hazardous goods transport, the nature of the product in the loading could have a major influence on the smoke toxicity. This of course could change radically the conclusion of the safety study regarding the available time for people evacuation. Then, before going any further in analysing batteries impact on the toxic loaded of truck fire, the relation between toxic gases production rate, represented by the CO production, and the heat release rate has to be analysed for different categories of materials. Based on the available data for various products (9), the analysis could be achieved regarding the CO production rate, based on the CO_2/CO ratio. Common values for this ratio is typically given by (9)

3. BACK ON THE AVAILABLE EXPERIMENTAL DATA

3.1. Batteries fire

Batteries currently appear are a new king of hazardous goods that should need, in the future, a large amount of transport. Consequently, it is crucial to be able positioning batteries transportation truck fire relatively to the currently design fire.
Based on available date for batteries combustion (4), it is possible to build an equivalent CO production rate. Of course, batteries fires generate a large variety of toxic compounds as mainly hydrogen fluoride. Because of the high level of toxicity of such products, each compound has to be considered in building the toxic source term. To create an equivalent CO source term, the toxic cumulative effect from (11) is used.

3.2. Available data for other part of the truck

If batteries are a source of toxic gases in case of fire, other compounds in trucks also generate such products in case of fire. Data regarding toxic emission for cars and individual compounds were recently published (14). Those data indicate that, while carbone dioxide is the main product generated during a car fire, in terms of mass, acid gases as HCl or HF, while being produced in lower quantity, have a more important potential considering toxicity. Those gases are generated, at specific rate, by various compounds as foam in seats, plastics or also cooling system product.

3.3. Synthesis of available data

As an illustration of available data, emission factor for the different individual compounds are given in

Table **2**.

Table 2: Synthesis of toxic emission for some individual compounds

	Gasoil	Plastics	Tyres	electric cables	Batterie s
Mass of product burn [kg]	131	48	49	36	71
Emission factors [mg/g] or [g/kg]					
CO_2	2823	2034	1469	728	1 196
CO	31	20	42	9,1	5,4
HCl	-	2,2	0,2	2,1	1
HF	-	0,014	0,003	0,11	14,3
NOx	1,2	5,0	2,8	2,5	1,3

4. MODELLING FIRE PROPAGATION

4.1. Evaluation of the HRR curve

Regarding car fire, several tests were achieved (8) or more recently (4)(14) and lead to normalized fire curve for such vehicles (2). Such a curve does not however enable to predict real car fire considering these curve give just an estimation of the maximum power and duration linked with linear curve. Furthermore those curves are only provided for one “small vehicle” and one “large vehicle” while there is differences between vehicles. To make a better prediction of the heat release rate from a vehicle fire, a specific model was developed. The fire curve predicted using analytical model was then introduced in the FDS CFD fire code to evaluate the ability of this code to predict the fire consequences. Having validated the numerical approach, it was then used to model some other scenarios.

4.1.1 Mathematical modelling of a car fire

Considering total heat release rate for a vehicle is governed by the heat release of the different components, this tool enables to compute the fire curve by summing the individual heat release, considering also a propagation time. The car is split into 5 parts, namely: wheels, engine block, interior, trunk and fuel tank. The average combustion velocity and heat of combustion is then computed for each part considering the distribution between following materials.

Table 3: Used heat of combustion and combustion velocity for individual elements.

Material	□Hc (MJ/kg)	□ (g/m²/s)
Polymers	35	20
Elastomers	35	20
Oil	40	30
Battery	35	25
Tires	30	20
Fuel	42	55

Each component fire curve follows three phases: the fire growth, a steady state and a linear decrease phase. The contribution of each element is then summed. The non-combustible materials are considered as sink of energy.

4.2. Evaluation of batteries loading consequences

As detailled previouly in the present paper, consequences of the presence of batteries in the truck loading as to be considered not only in terms of HRR but in terms of toxic gases production too. The objective of the paragraph is to present the curve built with the model described hereunder for those two quantities. Hypotheses are described first.

4.2.1. Hypotheses

The considered truck was 38 tons one composed with tractor and trailer. The tractor includes about 5 tons of combustible products as tires, plastic and foams associated with the potential 600 kg of fuel. The trailer is assumed being composed mainly with non combustible materials excepted tires, around 1 000 kg, and loading, 25 000 kg. Considering that the mass of one battery can be taken equal to 250 kg, this means that about 100 of batteries can be present inside the trailer distributed as schemed on Figure 1.

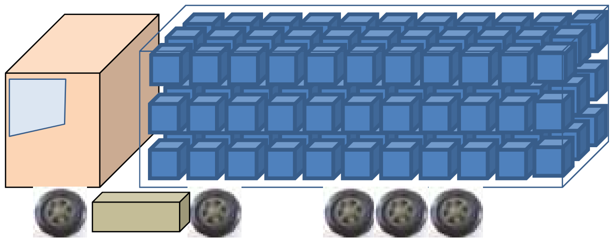

Figure 1: Schematic view of the modelled truck loaded with batteries

Even some data exist in the literature (1) (2) regarding truck fire that can be used for having a global HRR curve, propagation inside the batteries loading has to be modeled. Consequently, hypotheses are required regarding HRR for each and criteria for ignition. Based on available data in the literature concerning Li-Ion batteries, a design fire curve can be built for such a product, Figure 2.

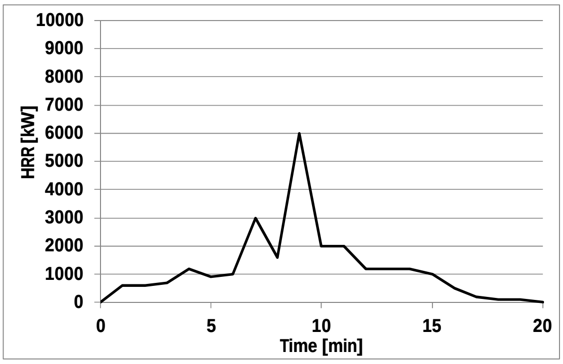

Figure 2: Design fire curve for a battery

Because defining the ignition temperature for a product as complex as a battery is quite complex, the criteria considered in the present paper is that the adjacent element fire starts when the one in fire reach 1 MW. Because of this can appear arbitrary, some parametric variations were made to evaluate its influence.

The last hypothesis is the ignition location. Two possibilities consequences were evaluated. The first case consists in a fire ignition due to a mechanical failure in the trailer, the second is a battery self ignition. Consequently, the fire propagation scheme is then highly different between those two cases.

4.2.2. HRR curve

The HRR curve obtained based on hypothesis described hereunder are given on Figure 3. Those curve are compared, on this graph, with the French standard one for truck loaded with highly flammable goods, without hazardous ones, and with the standard one for hazardous goods transportation truck (2).

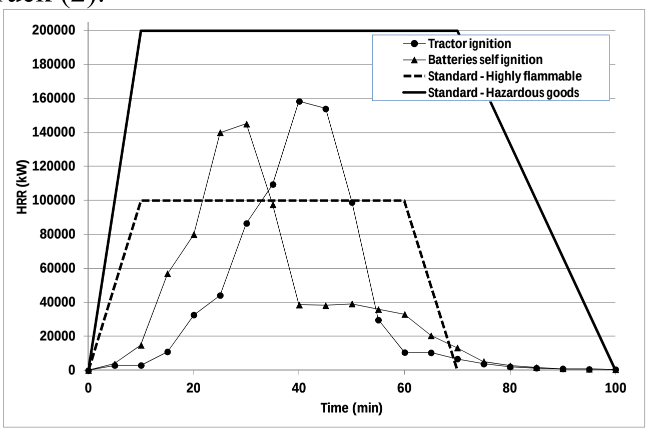

Figure 3: HRR curves for batteries loaded truck

The main conclusion of this first comparison is that the HRR for a batteries loaded truck stay under the hazardous goods one. This means that the fire design curve for hazardous goods still remain conservative.
The impact of the hypothesis regarding fire propagation was evaluated by forcing the propagation between the element after 2, 5 and 10 minutes. Results are plotted on Figure 4.

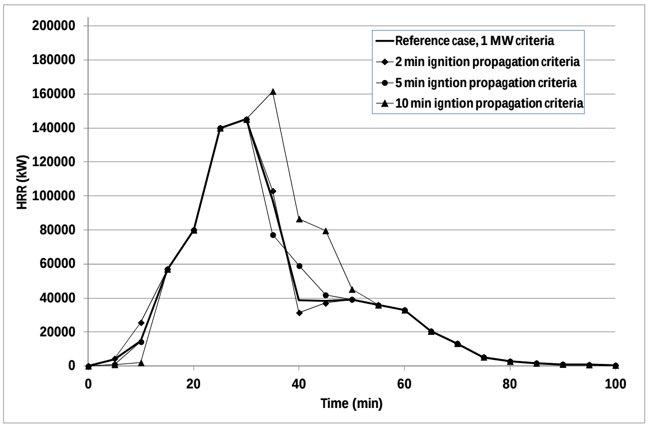

Figure 4: Parametric variation of the propagation criteria

This comparison shows that the hypothesis on the ignition criteria does not slightly influence the HRR curve. The 1 MW reference criteria is then considered in the following.

4.2.3. Toxic production rate curve

As mentioned previously, one of the key parameter for fire safety design is the toxic gases production rate. Because of the large amount of gases and their specific toxicity that are produced in case of battery fire, the equivalent rate of CO can reached around 50 (g/s)/MW considering the cumulative toxic effect as described in (11). This value is of course only valid for the battery, the emission rate to be considered for the other parts of the truck is the standard value for well ventilated fire, this means 2,56 (g/s)/MW. The emission curves for standard design fires and batteries loaded trucks are then given on Figure 5. The CO production curves for battery fires are given considering the experimental configuration, the standard curves are given for well ventilated and under ventilated fires for the purpose of comparison.

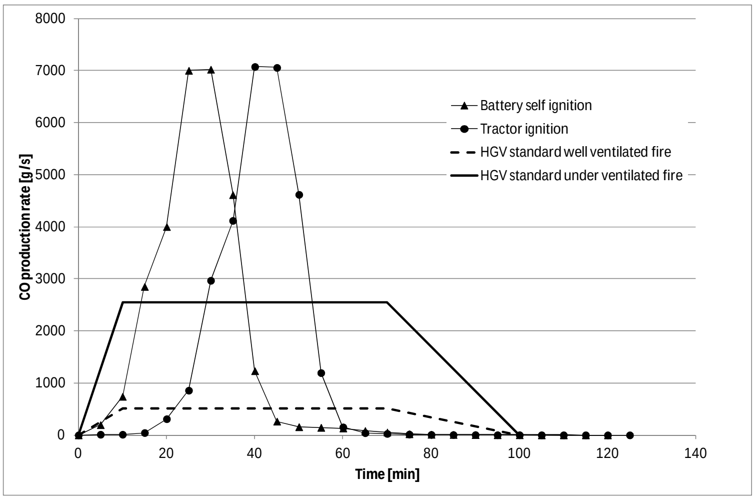

Figure 5: CO production curves for batteries loaded truck

These curves clearly indicate that, whatever the ignition source, the toxic gases production rates is clearly higher for a batteries loaded truck that for the standard case.

5. EVALUATION OF CONSEQUENCES IN CASE OF FIRE IN TUNNEL

As described in the previous paragraphs, while the HRR for a batteries transportation truck is lower than the HRR design fire curves, the toxic gases production rate is larger. An evaluation of the impact of this conclusion using a numerical modelling approach is proposed. This evaluation was managed using the Fire Dynamic Simulator (FDS) fire code developed by the National Institute for Standard and technology (NIST). This code was previously evaluated by INERIS for tunnel configuration modelling based on experimental data (12). The objective of this paragraph is not achieving a detail analysis of consequences in case of tunnel fire but to give an illustration of consequences for a given scenario.

5.1. Geometry and numerical hypotheses

The data considered in the present study is a two lanes tunnel, 10 m width and 5.5 m height, a total length of 500 m was modelled. Because of their influence on the flow, vehicles inside the tunnel were considered based on a classical congested distribution. Because of the influence of vehicles blocked inside the tunnel on smoke distribution (13), a vehicle distribution inside the tunnel was considered. Considering the integral length scale is in the order of the half diameter of the tunnel, the cell size was set lower than the twentieth of the half width. The characteristic size of the cell was then 0.2 m in each direction. A picture of the geometry is given hereafter on Figure 6.

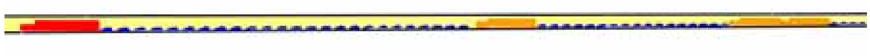

Figure 6: Picture of the numerical geometry

In such a configuration, the ventilation velocity has to be reduced to maintain the stratification during the evacuation phase. In the present simulation, a negative velocity at 1 m/s is supposed to be generated by pressure differences between tunnel portals. Then, he ventilation system is started after 1 minutes, after 2 minutes, the velocity reaches 0 and is then controlled at 1 m/s 3 minutes fire ignition.

5.2. Results representation

One of the main objectives of this simulation is to evaluate the impact of the fire of a truck that transports batteries in terms of temperature, visibility but also toxicity near the ground. As mentioned previously, a detail analysis should require numerous scenarios with different ventilation and traffic configuration. The one given in this paragraph only aims to give an illustration of how the above described experimental results can be introduced in a numerical simulation.

In such a situation, the first element to be checked is the stratification upstream and downstream the fire. Figure 7 shows the temperature distribution for both cases each minutes between the crucial 1 and 4 minutes after ignition.

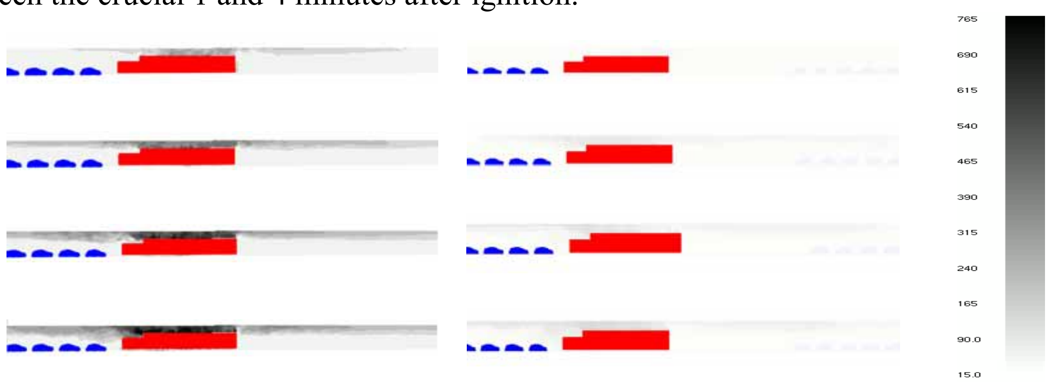

Figure 7: Temperature distribution for standard fire (left) and batteries loaded truck fire (right)

This first result shows that stratification is maintained for both fire curve hypothesis and that, considering a real curve, with a lower HRR will led to a reduced temperature under ceiling and, consequently, a lower stratification criterion.

The important factor however is the toxicity near the ground during the evacuation process. To evaluate the impact in terms of toxicity, Figure 8 gives the equivalent CO toxicity 2 m above the g round 5 minutes after ignition.

Figure 8: CO mass fraction as equivalent toxic 2 m above ground during the evacuation process for the standard curve (top) and adapted one (bottom) after 4 minutes

This results shows that whether the fire development is slower using the real curve, the toxicity near the ground is more important. This phenomenon is clearly due to the relation between thermal stratification and toxic emission factor.
While this configuration is just an example for a given scenario, geometry, ventilation, cars distribution, … it indicates that, for hazardous goods that could generate a large amount of toxic, using the standard are not necessarily a safe way in a design process.

6. CONCLUSIONS AND PERSPECTIVES

While CFD models are nowadays commonly used for fire safety, mainly in the field of tunnel safety, one of the key issue consists in determining the source term. Over the past decades a lots of work were managed in the aim of defining such source terms for several types of vehicles in different conditions. Those works led to the publication of generic fire curves. While those curve are a fundamental background for fire safety, the development of new energy carriers generates imposes fire safety engineer to wonder about the applicability of the standards.
In order to be able defining specific consequences generated by an innovative configuration, this paper details a methodology for evaluating fire consequences from the vehicle fire development, including each component, to the smoke dispersion based on a CFD approach.
This paper shows, first that the HRR proposed by the standard curve are in good accordance with what can be evaluated thanks to this model. As an example, the HRR curve of a batteries loaded truck is still under the hazardous goods 200 MW fire curve, this means that structure design based on the HGV curve still prevent for an impact from such a transportation. On top of that, as many of other curves, this model shows a propagation not so fast as predicted by the standard.

Regarding people safety, the main interest is however consisting in defining a toxic equivalent source term based on the characteristics of each element. It can then be shown that, as for recent vehicles (14), emission factor is more important than the one proposed in the standard. To evaluate the impact of a modification on tunnel safety, a CFD model was run for a given ventilation scenario. It shows, first, that considering the real HRR curve led to a limitation of under ceiling temperature in the first minutes of the fire with, as a consequence, a lower stratification phenomenon. On the opposite, because the fire development is not so fast, consequences on people are maintain in accordance with the evacuation process. This case show once more that being able evacuate rapidly the tunnel is a key issue for people safety because of the fast degradation of tenability after some minutes after ignition.
These conclusions still need to be extended to other scenarios and configuration. While the development of NEC is still a continuing process, it should be required, in the future years, to propose an evolution of the commonly used standard curves.

REFERENCE LIST

(1) AIPCR, “Fire and smoke control in road tunnels” (2005).

(2) CETU publication – “Guide to road tunnel safety documentation – booklet 4, specific hazard investigation”, September 2003.

(3) Salvi, O., Lönnemark, A., Ingason, H., Truchot, B., Leucker, R., Amberg F., Molenaar DJ, Hejnv, H., “New energy carriers in vehicles and their impact on urban infrastructures (tunnels, car parks and transport stations”. Proceedings of the 4th International symposium on tunnel Safety and security, Frankfort 2010.

(4) Lecocq, A., Bertana, M., Truchot, B. and Marlair, G., “Comparison of the Fire Consequences of an Electric Vehicle and an Internal Combustion Engine Vehicle”, FIVE 2012.

(5) Truchot,B. And Marlair G., “Investigating the risks of new energy carriers in road tunnels to enable better safety management planning” – Fire Protection and Safety in Tunnels, Bergen 2014.

(6) Truchot, B. and Marlair, G. “New energy carriers in underground infrastructures – unanswered questions and research needs”, ITA COSUF June 2014.

(7) International Standard CD 13571, “Life-threatening components of fire - Guidelines for the estimation of time available for escape using fire data”, 2010.

(8) Lonnermark, A., Blomqvist, P.; “Emissions from an automobile fire”, Chemosphere 62(7) (2006).

(9) Lecocq, A., et al, “Comparisons of fire consequences of an electrical vehicle and an internal combustion engine vehicle”, FIVE conference, Chicago (2012).

(10) Tewarson, A. “Generation of heat and fire products”, FM Technical report, May 1995

(11) ISO document 13571, “Life-threatening components of fire - Guidelines for the estimation of time available for escape using fire data” (2012).

(12) Truchot, B. et al., “ Numerical analysis of smoke layer stability”, ISAVT 2009, New Brunswick

(13) Truchot, et al. Tunnel fire safety forum 2015.

(14) Truchot, B. et al,, “An experimental evaluation of the toxic gas emission in case of vehicle fires”, ISTSS (2016), Montreal.

THE TREATMENT OF THE THROTTLING EFFECT IN INCOMPRESSIBLE 1D FLOW SOLVERS

C. Fleming, G. Clark, K. Meeks; Atkins Ltd, UK
T. Wicht; HBI Haerter, Switzerland

ABSTRACT

This paper is concerned with the throttling effect of a tunnel fire and how it is treated in one-dimensional flow solvers. We explain the primary mechanisms by which airflow is resisted by a tunnel fire. While compressible flow solvers inherently capture these mechanisms, corrections are required for incompressible solvers. In one approach, where a user-controlled parameter is required, we suggest a method for its reliable calculation.

Keywords: fire throttling effect, tunnel fire, incompressible flow solver, longitudinal ventilation system

1. INTRODUCTION

When a fire occurs in a uni-directional tunnel with a longitudinal ventilation system, the ventilation system is typically used to direct combustion products towards the exit portal, away from trapped vehicles. This aids self-rescue of tunnel users and enables fire fighters to tackle the fire from the upstream side.

A longitudinal ventilation system is typically designed to induce an airflow at such a rate as to prevent reverse stratification, or backlayering, of smoke upstream of the fire site. There are several established models for predicting the ‘critical velocity’, the velocity threshold above which backlayering does not occur (e.g. Oka and Atkinson, 1995; Kennedy et al, 1996). The ventilation system must introduce sufficient momentum to achieve the critical velocity while overcoming several sources of aerodynamic resistance, for example due to vehicle drag, wall friction, local losses, buoyancy, portal pressure differences and the momentum change across the fire. While the critical velocity reaches a plateau for heat release rates above a certain threshold (Hwang and Edwards, 2005), the aerodynamic resistance continues to increase (Vaitkevicius et al, 2015).

In this paper we examine the primary mechanisms of fire throttling, and show how they are treated in incompressible one-dimensional flow solvers. We review two models of the momentum change across the fire, and propose a method for their implementation in a particular type of flow solver.

2. ANALYSIS OF FIRE THROTTLING

2.1. Primary mechanisms

Hwang and Chaiken (1978) identified the primary mechanisms of fire-related resistance in their investigation into the interaction of fires and ventilation flow rate in mine shafts. The flow is heated as it passes through the fire, resulting in a reduction in density and increase in velocity downstream. Wall friction and local losses increase downstream of the fire, as they are proportional to density and to the square of velocity, and the latter dominates. Additionally, the fluid momentum increases as it passes the fire, presenting a corresponding resistance to the upstream flow. Hwang and Chaiken also allow for mass injection due to combustion, which is not considered in this paper.

2.2. Fire throttling in incompressible flow solvers

One-dimensional incompressible flow solvers are based on the Bernoulli equation, with additional terms to account for energy sources and losses. The flow velocity is typically calculated by balancing the pressure changes due to fans, vehicles, wall friction, local losses, buoyancy, etc. (US Department of Transportation, 2001).

2.2.1. Wall friction and local losses

Wall friction and local losses are normally determined by applying a local loss factor (*K*-factor) to the local dynamic pressure,

$$\Delta p = K \frac{1}{2} \rho u^2 \tag{1}$$

where ρ is density and u is velocity. The loss factor corresponding to wall friction is calculated as $K_\mathrm{f} = \lambda L/D$, where λ is the Darcy friction factor and L and D are the length and hydraulic diameter of the tunnel. In regions of elevated temperature, for example downstream of a fire, the density and velocity of the heated air is calculated by applying the Ideal Gas Law,

$$\rho_\mathrm{h} = \rho_\mathrm{c} \frac{T_\mathrm{c}}{T_\mathrm{h}} \tag{2}$$

$$u_\mathrm{h} = u_\mathrm{c} \frac{T_\mathrm{h}}{T_\mathrm{c}} \tag{3}$$

where T_c and T_h are the absolute temperatures (in Kelvin) upstream ('cold') and downstream ('hot') respectively. Equations 1 – 3 are combined to yield the corrected loss,

$$\Delta p = K \frac{1}{2} \rho u^2 \frac{T_\mathrm{h}}{T_\mathrm{c}} \tag{4}$$

Note that wall friction and local losses diminish with distance from the fire, as the downstream air loses heat to the tunnel walls.

2.2.2. Momentum change across the fire

As the flow passes the fire it is heated and undergoes rapid expansion. This change of velocity and density constitutes an increase in momentum, which resists the upstream flow. This mechanism is not captured in the Bernoulli equation or the usual local losses, and hence must be represented with a further loss term.

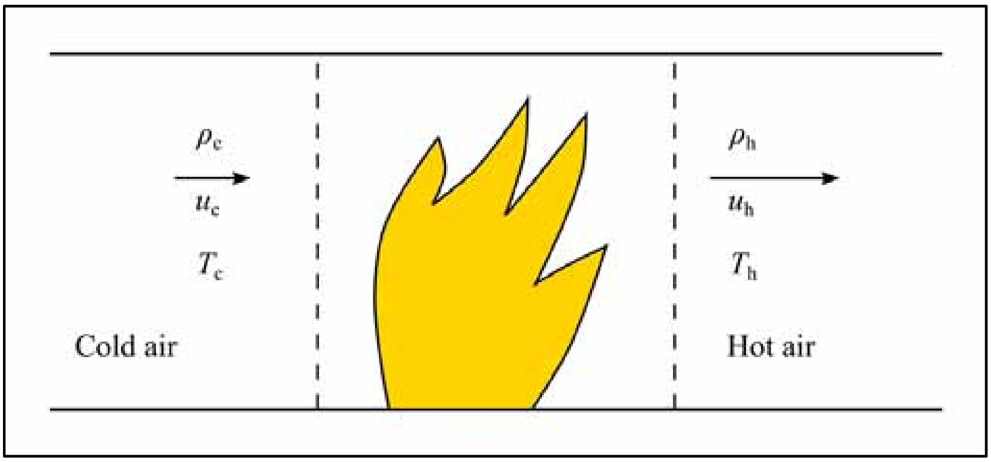

Figure 1: Diagram of the control volume around the fire, with flow from left to right

This term can be calculated following Hwang and Chaiken (1978), who consider a one-dimensional control volume containing a fire in a tunnel, with the ventilation system driving an airflow in one direction. The scenario is illustrated in figure 1, where heat is added to the flow as it passes the fire, reducing the density and increasing the velocity downstream. The resistance to the upstream flow is equivalent to the change of momentum,

$$\begin{aligned} F &= \dot{m}(u_c - u_h) \\ &= \rho_c u_c A(u_c - u_h) \end{aligned} \tag{5}$$

The downstream velocity is expressed in terms of the upstream velocity by applying a temperature correction based on the Ideal Gas Law (equation 3), yielding the pressure drop across the fire,

$$\Delta p_{\text{fire}} = \frac{F}{A} = \rho u_c^2 \left(\frac{T_h}{T_c} - 1\right) \tag{6}$$

Another method of predicting this loss term is presented by Dutrieue and Jacques (2006), who derive an empirical relationship between the fire pressure drop, heat release rate, hydraulic diameter and upstream velocity, based on a parametric study using a three-dimensional flow solver,

$$\Delta p_{\text{fire}} = \frac{Q^{0.8} u^{1.5}}{D^{1.5}} C \tag{7}$$

where C is an empirical constant with a value of 41.5×10^{-6}.

3. IMPLEMENTATION OF MOMENTUM CHANGE AT FIRE

Some incompressible flow solvers allow the user to specify the pressure change at the fire as an input value. This can be useful where additional effects, for example the deflection of the fire plume, are to be accounted for. We demonstrate how this feature can be used in one such solver, IDA Tunnel 1.1 (EQUA, 2014). We implement the Hwang and Chaiken model (equation 6) and the Dutrieue and Jacques model (equation 7), hereafter referred to as HC78 and DJ06 respectively. Predictions of flow velocity and static pressure are then compared with results from SES v4.1, which uses the HC78 model without user input.

3.1. Fire pressure change coefficient

In IDA Tunnel, the pressure change at the fire site is specified using a coefficient, C_{fire}, which acts as a constant of proportionality to the heat release rate. This coefficient can be determined by applying the HC78 or DJ06 models.

As both models require knowledge of the flow solution, they must be applied iteratively. An initial flow is simulated with $C_{\text{fire}} = 0$ Pa/MW. The value of C_{fire} is then updated by calculating the fire pressure change (via the HC78 or DJ06 model) and dividing by the heat release rate,

$$C_{\text{fire}} = \frac{\Delta p_{\text{fire}}}{Q} \tag{8}$$

The simulation is then repeated with the updated value of C_{fire}, and the procedure is continued iteratively until the terms in the fire pressure change equation (e.g. equation 6 for HC78 or equation 7 for DJ06) converge.

3.2. Solver verification

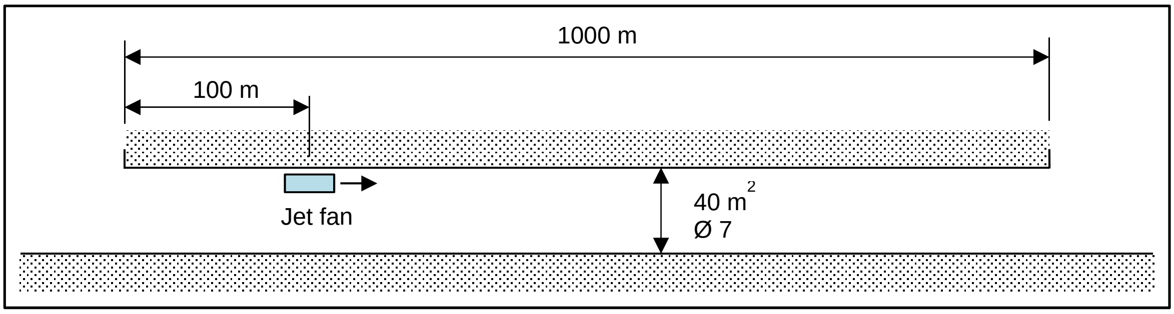

Figure 2: Diagram of the tunnel showing primary dimensions for verification simulations

Prior to evaluating the implementation of the HC78 and DJ06 models in IDA Tunnel 1.1 against SES 4.1, we consider a trivial scenario without a fire to verify agreement of the solvers. A single jet fan is simulated in an empty 1 km long tunnel, as described in figure 2 and table 1.

Adiabatic walls are specified[1] and local losses are neglected in order to isolate the pressure drop at the fire site in later simulations. The tunnel is discretised with a one-dimensional grid of 8 m long elements. In SES, two 'sections' are created: the first extending from the inlet to the 200 m point and containing the jet fan at 100 m, and the second section between the 200 m point and the exit portal.

Table 1: Model parameters for verification simulations

Ambient conditions	Temperature	10°C
	Absolute atmospheric pressure	101325 Pa
Tunnel	Length	1000 m
	Cross-sectional area	40 m^2
	Hydraulic diameter	7 m
	Gradient	0%
	Darcy friction factor	0.02
Ventilation system	Number of jet fans	1
	Position	100 m from entry portal
	Cross-sectional area	1 m^2
	Jet velocity	30 m s^{-1}
	Installation factor	1.0

Predictions of the flow velocity and the total pressure change over the downstream section (between the 200 m point and the exit portal) by IDA Tunnel and SES agree well, as shown in table 2.

Table 2: Predictions of velocity and total pressure change in the absence of a fire

Solver	Velocity [m s^{-1}]	Total pressure change ($200\text{ m} < x < 1000\text{ m}$) [Pa]
SES	3.702	19.704
IDA	3.701	19.670

[1]This required the wall heat transfer variable 'QWALSS' in the SES source code to be set to zero.

3.3. Predictions of the pressure change at the fire

A fire is now introduced in the region between 200 m and 208 m from the entry portal, so that it is downstream of the jet fan. The convective heat release rate is 20 MW, with no radiative portion and no mass generation. All other simulation conditions are consistent with the preceding verification case.

Note that the prescription of adiabatic walls is unphysical, leading to the over-prediction of wall friction and local losses (neglected here) downstream as the air is not allowed to lose heat. However, this measure eliminates differences due to the wall heat transfer models in IDA Tunnel and SES v4.1 and hence the predicted momentum change at the fire site can be compared directly.

Three cases are simulated using IDA Tunnel: firstly with the coefficient C_{fire} set to zero, and two further cases where C_{fire} is set according to the HC78 and DJ06 models as outlined in section 3.1. The method of implementation of these models in IDA is verified by comparison with an SES simulation, as this solver uses the HC78 model without user input.

Longitudinal profiles of static pressure, velocity and temperature are presented in figure 3. Note that this scenario is devised specifically for comparing predictions of the pressure drop at the fire site. The adiabatic condition at the walls and elimination of entry and exit losses mean that the numerical values reported cannot be applied to other tunnel fire cases.

No pressure drop occurs across the fire for the $C_{\text{fire}} = 0$ case. However, the increase in wall friction downstream of the fire is clearly indicated by the change in static pressure gradient at $x = 200$ m. As explained in section 2.2.1, this is because the greater downstream temperature corresponds to reduced density and increased velocity.

Predictions of static pressure, velocity and temperature by IDA Tunnel using the HC78 model agrees perfectly with SES, verifying the implementation method. Note that static pressure is only available at a single point in SES – the node at $x = 200$ m, between the upstream and downstream sections.

The DJ06 model over-predicts the pressure drop at the fire site relative to the HC78 model. The greater system resistance reduces the flow velocity, which in turn increases the heat transfer from the fire, leading to a higher downstream temperature.

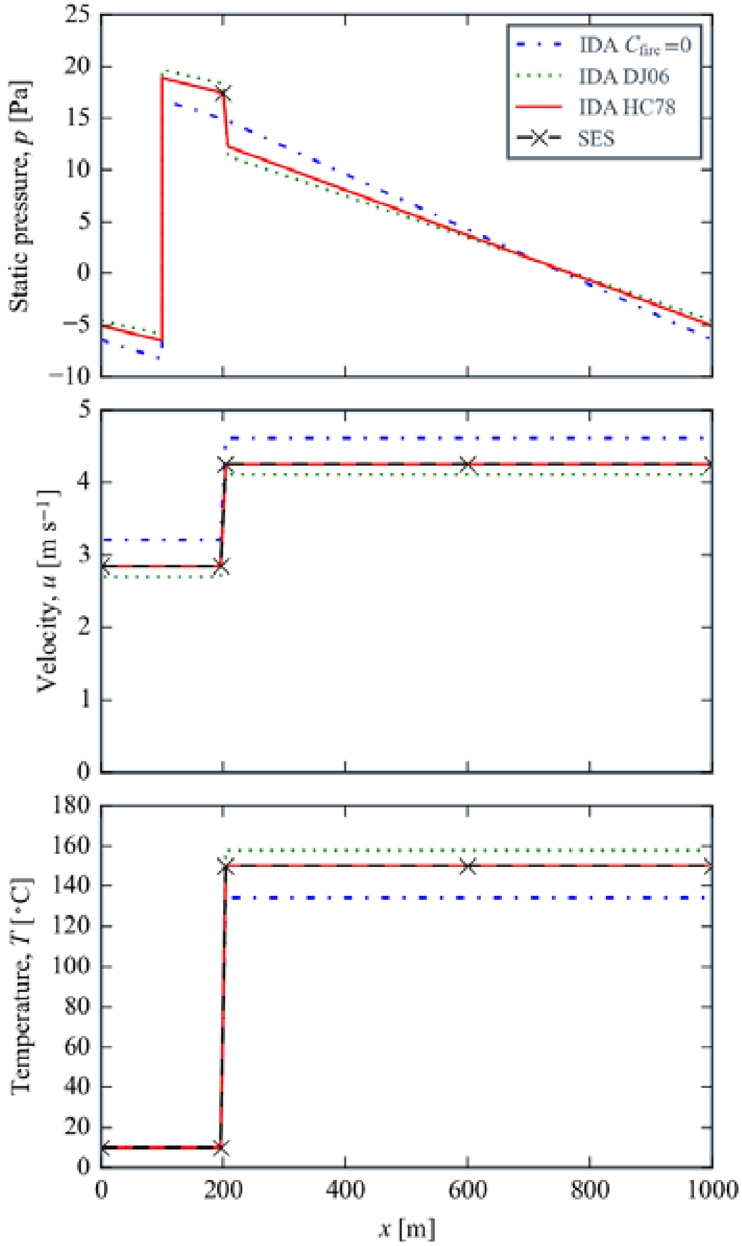

Figure 3: Predicted longitudinal profiles of static pressure, velocity and temperature using IDA Tunnel 1.1, where C_{fire} is set at zero as well as via the HC78 and DJ06 models, and using SES, which features the HC78 model

3.4. Effect of heat release rate

The implementation of the HC78 model in IDA Tunnel is now compared with SES for heat release rates of 5 MW, 20 MW, 50 MW and 100 MW. The latter two cases require two and four jet fans respectively in order to ensure critical velocity is exceeded.

The pressure change across the fire is presented in figure 4, showing good agreement in all cases. Predictions of static pressure, velocity and temperature profiles were practically identical, with maximum normalised error of 0.4% occurring for static pressure in the 100 MW case (not presented for brevity).

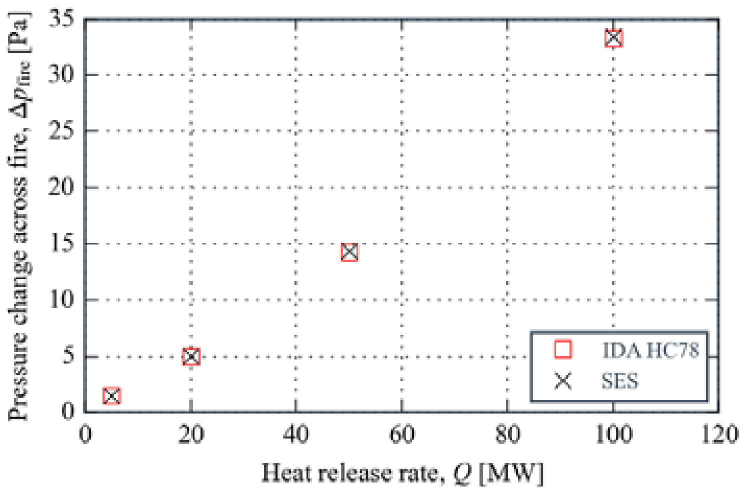

Figure 4: Comparison of the pressure change at the fire site for a range of heat release rates

3.5. Effect of wall heat transfer

The effect of wall heat transfer has been eliminated from this study in order to isolate the momentum change across the fire. Solver comparisons which incorporate wall heat transfer have not been considered due to modelling differences and are left to a future study. However, the iterative method of prescribing the pressure change at the fire site, described in section 3.1, has been found to converge well when wall heat transfer is allowed.

4. CONCLUSIONS

A fire increases the aerodynamic resistance of a tunnel through several mechanisms. The increase in velocity downstream of the fire leads to elevated wall friction and local losses, and the momentum change which occurs across the fire causes a corresponding resistance to the upstream flow.

One-dimensional incompressible flow solvers require a correction to the friction and local loss terms to account for fire throttling. An additional loss term is required to account for the momentum change across the fire.

Some flow solvers allow the user to prescribe the pressure drop at the fire. For one such solver, IDA Tunnel 1.1, we propose an iterative method for determining this term, and verify its accuracy through simplified comparisons with another flow solver, SES v4.1.

REFERENCES

Dutrieue R, Jacques E (2006) ‘Pressure loss caused by fire in a tunnel’ in Proc. 12th International Symposium on Aerodynamics and Ventilation of Vehicle Tunnels. BHR Group, UK

EQUA Simulation AB (2014) IDA Tunnel 1.1, http://www.equa.se/en/tunnel/ida-tunnel/overview

Hwang CC, Chaiken RF (1978) ‘Effect of duct fire on the ventilation velocity’ US Bureau of Mines Report of Investigations 8311, http://hdl.handle.net/2027/mdp.39015078483404

Hwang CC, Edwards JC (2005) ‘The critical ventilation velocity in tunnel fires—a computer simulation’ Fire Safety Journal, 40(3):213-44

Kennedy WD, Gonzales JA, Sanchez JG (1996) 'Derivation and application of the SES critical velocity equations' ASHRAE Trans: Research 102(2):40–4

Oka Y, Atkinson GT. (1995) 'Control of smoke flow in tunnel fires' Fire Safety J 25:305–22

U.S. Department of Transportation (2001) 'SES Version 4.1 User's Manual', formerly available from the National Technical Information Service, Springfield, Virginia 22161.

Vaitkevicius A, Collela F, Carvel R (2015) 'Investigating the Throttling Effect in Tunnel Fires' Fire Technology, pp. 1 – 10, DOI:10.1007/s10694-015-0512-z

HOW TO COMPUTE RELEVANT METEOROLOGICAL PORTAL DIFFERENCES

B. Höpperger, J. Croll

TFD Consulting Engineer e.U., Austria

ABSTRACT

A ventilation system in road tunnels must be able to handle the relevant meteorological portal pressure difference mostly based on a 95 % or 98 % quantile of hourly values from a representative year. Meteorological forces often require more than 50 % of the ventilation power in the traffic area. Unfortunately there are different theories to compute the relevant pressure difference. Also guidelines don't describe a definitive way. A variation of up to 50 % results between the theories.

In some projects it was necessary defining the way to compute the relevant portal pressure difference considering the point of view of the independent engineer as well as the point of view of the government and their experts. At the end there are different ways used in different projects depending on their actors.

The presentation will show the possible variation between the theories using on-site measurement data as well as computed data by the meteorological institute ZAMG for several long road tunnels in Austria.

Higher meteorological forces could require additional jet fans or in the worst case additional jet fan niches and therefore result in higher investment costs with a potential economic risk of several hundred thousand euros.

A possible future way of required measurement sensors and meteorological data and a suggestion how to compute the relevant quantile will be outlined achieving a standard procedure to obtain relevant portal pressure differences for the ventilation design.

Keywords: ventilation design, meteorology, portal pressure difference, wind loads, barometrical pressures, long tunnels

1. INTRODUCTION

Meteorological conditions can have a significant impact on the ventilation design of tunnel systems. Especially in mountainous regions, if mountain ridges separate the tunnel portals, barometrical pressure differences between the portal areas may alter in a range of several hundred Pascal. Besides the barometrical pressure difference, two further meteorological effects have to be considered in the design of tunnel ventilation systems. Wind pressures lower the effectiveness of the ventilation system whenever the wind direction is opposite to the direction of air extraction. Further, differences in the temperatures inside and outside the tunnel induce thermic pressures.

To get an idea of the barometrical pressure differences in relation to wind pressures, **Table 1** lists both, barometrical portal pressure differences and wind pressures, for some Austrian tunnels. Within a range of several Pascal, the listed wind pressures are much lower than the barometrical pressure differences.

Table 1: Impact of wind on portal pressure differences for some Austrian road tunnels

Name of the tunnel	Length [m]	95th-percentile of portal pressure differences [Pa]		
		Barometrical	Wind	In total
A10, Tauerntunnel	6,546	227.5	8.5 (3.6%)	236.0
A10, Oswaldibergtunnel	4,307	30.0	1.4 (4.5%)	31.4
A12, Landecker Tunnel	6,955	67.4	11.8 (14.9%)	79.2
S16, Strenger Tunnel	5,851	101.6	1.2 (1.2%)	102.8

2. REGULATIONS IN GUIDELINES

The Austrian RVS 09.02.31 [1] recommends to measure barometrical pressure, wind direction and wind speed at the (projected) portal position and if existent at the (projected) top of the shafts within a measurement period of several years. Depending on the risk level of the tunnel, either the 95th-percentile or the 98th-percentile is assessed for both, barometrical pressures and wind speeds. In case of lacking measurement data, as per RVS 09.02.31, appropriate meteorological analyses must determine the decisive meteorological impact. The regulations in the RVS 09.02.31 focus on how to evaluate portal pressure differences resulting from wind loads. It does not provide a method regarding the evaluation of barometrical pressures, e.g. how to handle vertical temperature gradients and hence how to transfer pressure data from both portals onto a common altitude.

The German RABT 2006 [3] as well focus on portal pressure differences resulting from wind loads. For the ventilation design, the 95-percentile of the wind component normal to the portal has to be considered.

As per Swiss ASTRA 13001 [2] the 95th-percentile out of period of at least one year has to be used within the ventilation design. Wind pressures and barometrical pressure differences have to be considered, each with the more unfavourable direction. Further, the pressure differences due to temperature differences inside and outside the tunnel have to be considered in the ventilation design.

Neither RABT nor ASTRA describe a detailed method for the evaluation of barometrical portal pressure differences.

3. VARIATION OF PORTAL PRESSURE DIFFERENCES USING DIFFERENT METHODS

Guidelines like the Austrian RVS, the Swiss ASTRA and the German RABT demand the consideration of barometrical and wind pressures by evaluating a meteorological portal pressure difference. There is no detailed method how to compute the relevant meteorological pressure difference defined.

Table 2 lists portal pressure differences for the Arlbergtunnel in Austria that were calculated with different methods, which are all conform to the RVS and which still are used in different projects. The example shows the large margin in the evaluation of portal pressure differences in accordance with the RVS 09.02.31.

Table 2: Variation of portal pressure differences for diverse evaluation methods, Arlbergtunnel (13,972 m excl. gallery), Austria

98th-percentile of portal pressure differences [Pa]				
Direction-independent	216.6			
Direction-dependent	All values		Positive values only	
Transfer to portal altitude:	h_{east}	h_{west}	h_{east}	h_{west}
p_{east} - p_{west}	198.7	215.4	222.8	**241.1**
p_{west} - p_{east}	**109.0**	117.0	126.2	135.0

The method *direction-independent* evaluates the 98th-percentile of all hourly pressure values. The resulting portal pressure difference is used for both extraction directions (east to west and west to east). Within the *direction-dependant* method, portal pressure differences are evaluated separately. The portal pressure difference p_{east} - p_{west} is considered in the ventilation design, whenever the extraction direction is from west to east and v.v.

Due to the varying air column, different altitudes lead to different barometrical pressures. Therefore, prior to the evaluation of barometrical pressure differences, barometrical pressures at both portals have to be transferred onto a common altitude. The transfer from one altitude to the other depends on the prevailing vertical temperature gradient at the respective portal position. This gradient is mostly unknown. It can be estimated by evaluation of data from different measurement sites (see below) or e.g. by considering the typical temperature gradient of -0.0065 K m^{-1} as per DIN ISO 2533 norm atmosphere.

The RVS 09.02.31 neither defines temperature gradients, nor the common altitude (e.g. altitude of the lower portal). Thus, varying methods are possible. **Table 2** shows the spreading by transferring the measured barometrical pressure either to the altitude of the east portal (h_{east}) or to the altitude of the west portal (h_{west}). With consideration of an isentropic atmosphere with a linear temperature drop of -0.0065 K m^{-1}, differences of up to 19 Pa occur for the Arlbergtunnel.

Further potential for variations results from the consideration of all values either, or positive values only within the evaluation of the percentiles. The method *positive values only* restricts the data to positive values only, before the 98th-percentile is calculated. Therefore, the evaluation of *positive values only* results in higher pressure differences than the method *all values*.

The comparison in **Table 2** reveals that the resulting portal pressure difference p_{west} - p_{east} varies in a wide range of 109 Pa and 217 Pa depending on the calculation method.

4. CALCULATION METHODS

Up-to-date two general methods are common, to evaluate the typical meteorological conditions in the project area and to calculate the meteorological portal pressure difference. Either barometrical pressures, temperatures, wind direction and wind speed are measured at the (projected) portals, or the analysis of meteorological pressure differences is based on data of the local meteorological service. The Austrian meteorological service *Zentralanstalt für Meteorologie und Geodynamik* (ZAMG) for example delivers meteorological data for a representative year out of a period of ten years. Since the number of measurement stations of the ZAMG is limited, the nearest measurement station might be at a distance of several kilometers from the portal. Especially in mountainous regions, the local distance leads to uncertainties that are difficult to estimate.

On-site measurements at the (projected) portals avoid this problem. But in contrast to long-term measurements of the meteorological services, in the majority of projects on-site measurement periods of several years are not feasible.

The portal pressure differences in **Table 2** show a variance of up to 19 Pa depending on whether pressure data is transferred onto the altitude of the east portal or onto the altitude of the west portal. The reason for the variation is the necessity to approximate the vertical change of the atmosphere and thereby also the approximation of the vertical temperature gradient.

A common approximation is the barometric formula in equation (1), that allows to transfer the barometrical pressure from one altitude to the other. As mentioned before, the vertical temperature gradient a in equation (1) is unknown. A typical approximation is to consider a temperature gradient of -0.0065 K m^{-1} according to DIN ISO 2533.

$$p_{h1} = p_{h0} * \left(1 - \frac{a * \Delta h}{T_{h_0}}\right)^{\frac{M*g}{R*a}} \tag{1}$$

p_{h1} pressure at altitude h_1 [Pa]
p_{h0} pressure at altitude h_0 [Pa]
R universal gas constant for ideal gas [J mol^{-1} K^{-1}]
a vertical temperature gradient [K m^{-1}]
Δh vertical height between h_1 und h_0 [m]
g gravitational acceleration [m s^{-2}]
M molar mass air [g mol^{-1}]
T_{h0} temperature at altitude h_0 [K]

Equation (1) shows the barometric formula for a linear temperature trend in vertical direction of the atmosphere. The assumption of constant temperatures in vertical direction and thus of an isothermal atmosphere leads to the following equation:

$$p_{h1} = p_{h0} * e^{-\frac{M*g}{R*T}*\Delta h} \tag{2}$$

p_{h1} pressure at altitude h_1 [Pa]
p_{h0} pressure at altitude h_0 [Pa]
R universal gas constant for ideal gas [J mol^{-1} K^{-1}]
Δh vertical height between h_1 und h_0 [m]
g gravitational acceleration [m s^{-2}]
M molar mass air [g mol^{-1}]
T temperature [K]

Up-to-date, neither on site-measurements nor measurements of local meteorological services provide data that allow for a calculation of vertical temperature gradients at the tunnel portals. The consideration of two measurement sites at different altitudes allows for an approximation. In case of the Strenger Tunnel for example, the meteorological service ZAMG provided data of a measurement site in Landeck (809 m) and a second one in Ischgl/ Idalpe (2,312 m) to approximate a vertical temperature gradient at the east portal. For the west portal measurement data for St. Anton am Arlberg (1,300 m) and Galzig (2,079 m) were used. **Figure 1** shows the measurement sites. The meteorological service chose them with respect to the local geography.

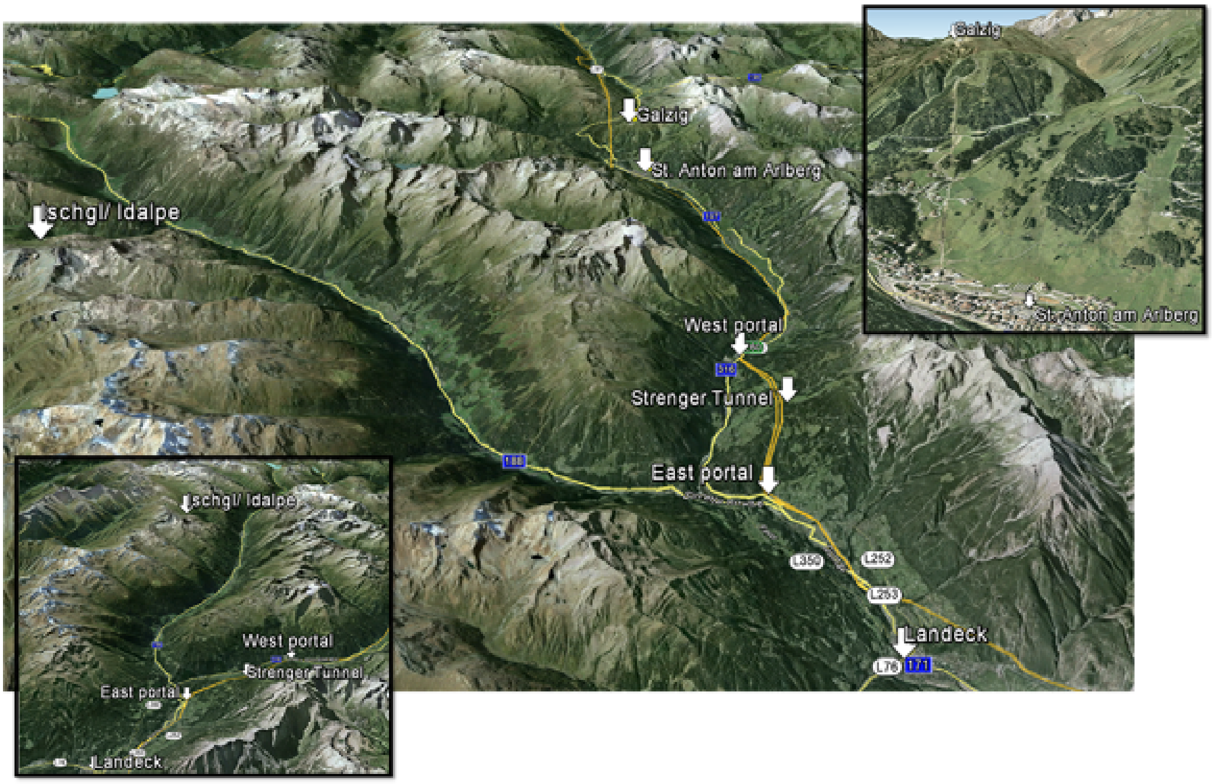

Figure 1: Measurement sites ZAMG data (Google Earth)

Figure 2 shows the vertical temperature gradients (hourly values in the course of one year) that were calculated with the data of each two measurement sites, compared to the vertical temperature gradients for the isothermal assumption (a = 0 K m^{-1}) as well as for the temperature gradient according to DIN ISO 2533 (a = -0.0065 K m^{-1}).

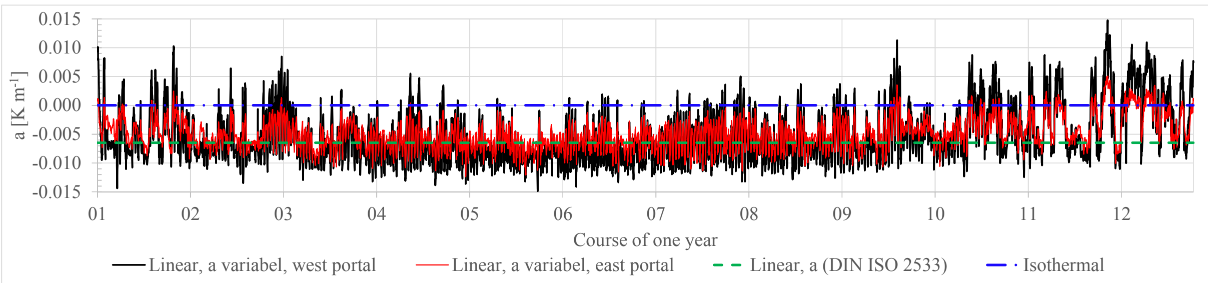

Figure 2: Vertical temperature gradient for different evaluation methods

The data allows to determine the influence of the vertical temperature gradient on the portal pressure difference. **Figure 3** and **Figure 4** show each average hourly value for the pressure difference of the relevant year including a straight line for the 95 percentile.

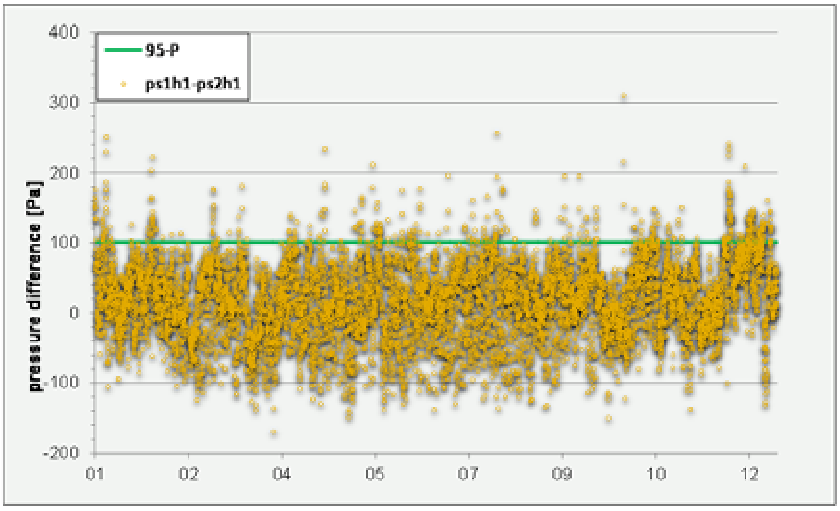

Figure 3: Pressure difference west – east

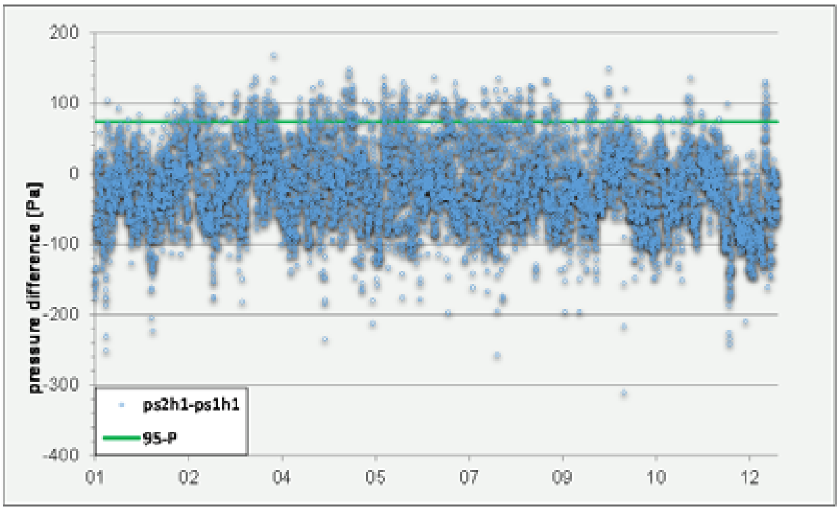

Figure 4: Pressure difference east – west

Figure 5 shows the variance of the pressure difference between west – east and east – west.

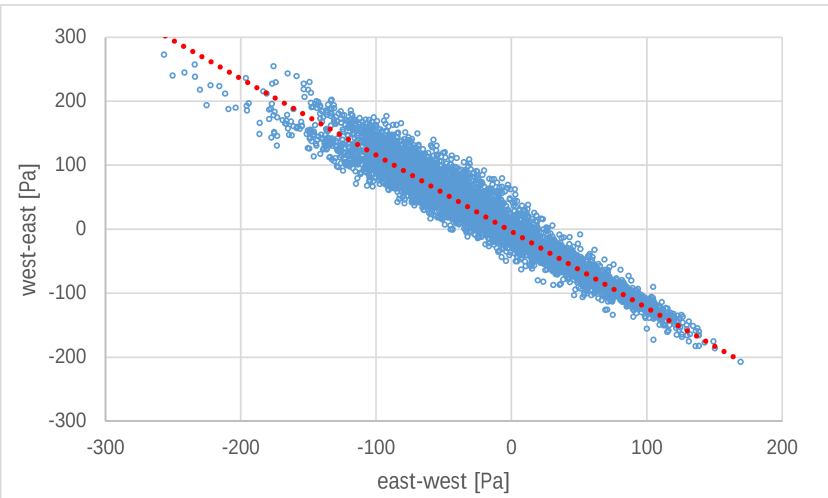

Figure 5: Variance of the pressure differences

Table 3 shows the results of different calculation methods for the Strenger Tunnel.

The calculation method is direction-dependent with consideration of either a varying vertical temperature gradient, a constant vertical temperature gradient of -0.0065 K m^{-1} according to DIN ISO 25 or an isothermal atmosphere.

Table 3: Variation of portal pressure difference for diverse evaluation methods, Strenger Tunnel (5,851 m), Austria

95th-percentile of barometrical portal pressure differences [Pa], direction-dependent								
Vertical temperature gradient (a):	All values				Positive values only			
	p_{east} - p_{west}		p_{west} - p_{east}		p_{east} - p_{west}		p_{west} - p_{east}	
	h_{east}	h_{west}	h_{east}	h_{west}	h_{east}	h_{west}	h_{east}	h_{west}
a = variable*	82.3	73.0	124.1	98.6	106.7	95.6	**135.6**	111.4
a = 0.0065 K m^{-1}	76.2	71.2	106.8	99.6	100.0	94.7	120.1	112.0
a= 0 K m^{-1} (isothermal)	**59.9**	75.8	123.8	94.8	90.2	96.9	132.7	108.4

*: east portal: -0.012 K m^{-1} ≤ a ≤ 0.005 K m^{-1} and west portal -0.015 K m^{-1} ≤ a ≤ 0.015 K m^{-1}

The comparison shows that the results differ in a range of 76 Pa (77% of the average value), from 60 Pa to 136 Pa. The major impact results from the direction-dependent evaluation (up to 64 Pa). The transfer from p_{east} onto the altitude h_{west} either, or p_{west} onto the altitude h_{east} results in a difference up to 29 Pa and the consideration of positive values only in the evaluation of the percentile leads to differences up to 30 Pa. A difference of up to 22 Pa occurs between the different models for the vertical temperature gradient.

5. CONCLUSION AND SUGGESTIONS

Using the examples of the Arlbergtunnel and the Strenger Tunnel in Austria, calculations demonstrated the possible influence of divergent calculation methods on portal pressure differences. In case of the Arlbergtunnel, the different methods - all in accordance with the regulations of the Austrian RVS 09.02.31 - result in variations of up to 121%. The reason for the variation is a lack of regulation in the following regards:

- Common altitude for the pressure transfer
- Character of the vertical temperature gradient for the pressure transfer to a common altitude
- Direction-dependent or –independent evaluation of portal pressure differences
- Consideration of all values or positive values only in the calculation of percentiles

The regulation of the ASFiNAG PlaPB [1] considerably improved the situation, as it states the evaluation method more precisely. As per PlaPB the averaged measurement data of total pressures at one tunnel portal (altitude h_1) is transferred onto the altitude of the second tunnel portal (altitude h_2) with help of the barometric formula (cf. equation (2)). The temperature is used as the average temperature between the two portals.

Up-to-date meteorological analysis base on on-site measurements or on measurement data of the meteorological services. On-site measurements mostly consist of data for only one year. Measurement data of the meteorological services often consider a representative year out of a period of ten years. This is an advantage, but on the other side, measurement sites of the meteorological services may be several kilometers away from the portal.

To achieve a well-founded assumption about the meteorological portal pressure differences, a combination of on-site measurements and ZAMG-data seems to be the best solution. Hereby, the advantages of both methods are combined.

In general, on-site measurements should include wind direction, wind speed, barometrical pressure and temperature. To receive additional data about the vertical temperature gradient at the (projected) portals, on-site measurements should consider two measurement altitudes for the temperature: one at the altitude of the portal and a second one about 100 m above if possible. This allows to calculate the vertical temperature gradient for each hourly or half-hourly data point.

Under consideration of the variable vertical temperature gradient, the barometric formula (equation (1), previous chapter) allows to transfer the measured pressure at the higher portal (hourly or half-hourly values) onto the altitude of the lower portal. The exact altitude of both portals (measurement sites) is essential to avoid errors in the pressure transfer from one altitude to the other.

Subsequently, the respective percentile can be calculated. The consideration of positive values only in the percentile-evaluation will lead to a more conservative value. Seeing the uncertainties within the calculation process as well as a measurement precision of about 30 Pa for common pressure measuring instruments, a conservative approach for the meteorological impact on the ventilation system seems to be justified.

If data of on-site measurements are not available for several years, a second evaluation ought to be done. The latter should base on measurement data of the meteorological service for the representative year. The comparison includes the aspect of time in the analysis of meteorological impacts.

This way reduces the risk of a designing mistake in the ventilation system because of the meteorology and should be considered in the tunnel ventilation guidelines.

A discussion about the variation of the wall friction between $\lambda = 0.015$ or 0.017 results for the 5.780 m long Strenger Tunnel in a change of 3.2 Pa for 2 m/s, which is nothing compared with the meteorological issue. The variation of the meteorology results in a difference of four jet fans. We sometimes talk about the wrong screws.

6. REFERENCES

[1] ASFiNAG, (January 2016) Technisches Planungshandbuch der ASFiNAG. PlaPB 800.542.1000 Tunnel – Lüftung (TLü). Technische Richtlinie. Version 3.00.

[2] Eidgenössisches Departement für Umwelt, Verkehr, Energie und Kommunikation UVEK, (2008) Richtline. Lüftung der Strassentunnel. Systemwahl, Dimensionierung und Ausstattung. ASTRA 13001. Bundesamt für Strassen ASTRA. Bern. Version 2.03.

[3] Forschungsgesellschaft für Strassen- und Verkehrswesen, workgroup "Verkehrsführung und Verkehrssicherheit", technical committee "Ausstattung und Betrieb von Straßentunneln", (May 2006) Richtlinien für die Ausstattung und den Betrieb von Straßentunneln RABT. FGSV Verlag GmbH. Cologne.

[4] Österreichische Forschungsgesellschaft Straße, Schiene, Verkehr, workgroup "Tunnelbau", technical committee "Betriebs- und Sicherheitseinrichtungen", (Juni 2014) Tunnel. Tunnelausrüstung. Belüftung. Grundlagen RVS 09.02.31. Vienna. Version 1.

PARTIALLY ENCLOSED STATIONS – KEY SAFETY CONSIDERATIONS

P.J. Gehrke, R. Nuttall; Mott MacDonald, Australia
S. O'Gorman; WSP|Parsons Brinkerhoff, United States
A. Purchase; WSP Sverige AB, Sweden

ABSTRACT

Underground/enclosed stations pose a challenging environment for passenger safety in the event of a fire. Regulations and analysis techniques have been developed that allow for confident design decisions based on precedents and performance engineering. However, decisions involving the configuration of new public transport facilities are driven by many factors. High capital and operating costs envisaged for completely underground or enclosed stations can make options where stations are open or connected to atmosphere attractive. Removal of ventilation systems for amenity and smoke management is seen as a great advantage of this strategy. Another facet for consideration is existing stations at grade or in cuttings with available air space that can be used for full or partial overbuild structures. Assessment of partially enclosed stations is not as developed and can pose unique challenges for designers.

The question for designers, especially at an early project stage, is what defines an enclosed station? Without knowing this, requirements for various disciplines cannot be accurately established creating risk at later stages. This paper proposes that ultimately the amenity and safety of passengers must be the determining factor rather than simple geometric guidelines around percentage of station enclosure. The assessment of passenger safety in this context uses many of the same tools developed for enclosed stations. However, there are a number of additional considerations that must be made.

This paper describes the significant elements that need to be considered. The impact of some of these elements is tested by analysis to provide guiding principles for designers. A description of what constitutes a partially enclosed station and when analysis is required is presented based on occupant safety, namely heat and smoke accumulation interacting with egress. These guidelines allow planners and engineers to make practical decisions on infrastructure configurations.

Keywords: station smoke management, partially enclosed station, natural ventilation

1. INTRODUCTION

The driver for this work was mainly from the project experiences of the authors during the front end development stages of passenger rail projects. During alignment development stages, many options can be produced that result in stations with varying depths. Options can develop where it is questionable to keep the stations fully underground/enclosed. Additionally, many rail facilities that are currently aerodynamically 'open' have available development space above. These are typically stations in cuttings but can also be stations at grade with multi-level buildings above. Grade separation projects can also result in having stations partially enclosed by a roadway. Often ventilation and fire safety practitioners are forced to make decisions in regards to system provisions (ultimately space-proofing) with limited information and time.

The different decisions between open and enclosed stations can include the need for: smoke exhaust ventilation systems, dedicated egress stairs, normal vertical transport provisions protected by smoke screens and barriers as well as a number of other mechanical and electrical provisions to aid egress and fire service intervention. By far the biggest impacts on the station's design are requirements related to mechanical exhaust systems, egress stairs and vertical transport.

This paper analyses the impact on available egress time under the covered section of a platform for a number of scenarios. The focus is on scenarios with no mechanical ventilation to identify the limitations of natural ventilation in a partially enclosed station. The objective is to provide a reference point for these decisions and highlight aspects that will need due consideration before decisions can be made. Ideally it would be advantageous to know the point where the platform enclosure (extent of cover) is not a fire safety design issue.

2. FIRE SAFETY ASSESSMENT

2.1. Existing definitions and requirements

Some countries/regions may have specific jurisdictional requirements that recognise and accommodate partially enclosed stations, however, it is expected that many wouldn't. For example, in Australia the station would need to be assessed under the National Construction Code [1]. Many aspects of a partially enclosed station would not fit with the intent and prescriptive provisions of this code - ultimately a performance assessment would be required.

In the United States NFPA 130 (2014) [2] would apply. It defines an open station as *"A station that is constructed such that it is directly open to atmosphere and smoke and heat are allowed to disperse directly into atmosphere."* The document then describes changes in provisions that can be made from that required for a closed station. There is no description or definition of what physically constitutes an open station. It is the responsibility of the designer to determine if smoke and heat will disperse as required (performance assessment).

The United Kingdom Statutory Instrument 1989 No 1401 [3], outlines the fire precautions that must be undertaken for sub-surface railway stations (enclosed underground platform). The document provides a definition of an enclosed platform as a platform situated wholly or mainly in a tunnel, or wholly or mainly within or under any building. Mainly is defined as more than half the length of platform (e.g. 50% coverage).

2.2. Current study – fire safety considerations

Regardless of varying global jurisdictional requirements, the typically accepted strategy for a train fire at a station is to enable occupants to reach a point of safety. In a fully underground station the platform 'compartment' would not typically be deemed a place of safety. When the station platform is only partially enclosed this consideration may change. If it can be shown that the open area remains tenable for an extended time period, it can be argued that this is a place of relative safety.

Protected station concourses above or below the platform as well as exit points to surface are typically considered places of relative safety. To reach these, egress paths must be provided that remain tenable for longer than it takes passengers to move through them. Acceptable times for tenability and egress vary depending on the jurisdiction and station configurations. For example, NFPA 130 [2] outlines a 4 minute (240 s platform evacuation) and 6 minute (360 s to point of safety) requirement to ensure a minimum standard of egress provisions. These requirements have become a benchmark in many countries, but are often varied based on the outcome of a performance assessment.

One of the main benefits of a partial station opening is that it can act as an effective natural ventilation path for smoke which can reduce the impact to egress paths. However, it does also mean the station aerodynamics and smoke movement are critically subject to meteorological affects such as wind. For a partially enclosed station the fundamental questions to be answered are:

- Can the open area be considered a place of relative safety (extended tenability)?
- Does natural ventilation through the opening reduce the accumulation of smoke and heat to allow egress or are protected/ additional egress elements required?
- Do the normal vertical transport paths provide sufficient egress capacity or are protected/additional egress elements required?

This study uses computational fluid dynamics (CFD) analysis to investigate these questions for an indicative partially covered station. For a completely open station the tenability along the platform and along the egress paths is expected to be significantly long. Issues may only occur at locations in the vicinity of the fire. For the partially enclosed station the time of tenability has been considered along the platform, between the fire and the open area, and where typical egress stair and vertical transport provisions would be located. This has been compared against the following egress benchmarks (baseline fire safety strategy):

- NFPA130 [2] 240 s platform clearance and 360 s to a point of safety requirements
- A required egress time estimate of 210 s: 120 s pre-movement time for one train car, 60 s detrainment time, and 30 s to clear 20 m of platform length (one train car length).

3. MODELLING DESCRIPTION

3.1. Geometry

To limit the scenarios studied, ensuring a refined focus on egress is met, the following overarching allowances have been made. Consideration is only given to a station fire, as the most likely scenario is a train on fire stopping at a station to allow passenger egress. Fire suppression provisions have not been considered as concern is only for the egress phase and typically automatic provisions are not included in rail facilities. Excessive fire sizes or rapid growth rates have not been allowed for (typical/probable fire scenarios only). A generic station geometry has been used that is considered to be ‘typical’ of a modern mass rapid transit system. A station length of 200 m to accommodate an 8 car train was adopted (20 m car length, 160 m train length). Lateral provision for two tracks has been allowed for with a station box width of 15 m. One platform end is open to atmosphere, whilst at the covered end a short length of tunnel was included to accommodate anticipated smoke spread. Station platforms are rarely sloping so a level track and ceiling (0% grade) was used.

Specific parameters that were modified included the amount of platform cover (2/4/6 train cars covered or 25/50/75% coverage), fire size (1.5/5/10 MW), platform depth (shallow 5 m/deep 10 m), fire location (car 1 covered/car 4 covered/car 6 uncovered) and the wind condition (no wind/2.5 m s^{-1} cross wind/2.5 m s^{-1} longitudinal wind). Depending on the extent of cover, openings in the platform roof have been included to emulate open vertical transport provisions. **Figure 1** shows an example of the model geometry (shallow trench, 50% cover).

3.2. Model parameters

This section provides a brief summary of the model inputs (refer **Table 1**) and methodology. The results are presented and discussed in Section 4. CFD modelling was undertaken using Fire Dynamics Simulator (FDS) version 6.2.0 [4]. FDS is a purpose built CFD modelling program for simulating fire and smoke dynamics, and has undergone rigorous verification and validation [5], [6], [7]. FDS default modelling methodology and parameters were used except as noted. The grid cell size varied for different models but was in the order of 0.25 m (in the vicinity of the fire) to 0.5 m (remote from the fire location). Grid sensitivities were also undertaken. Models with wind were started with negative time to allow the boundary condition to develop before the fire started at time zero. The different wind conditions were applied on the extents of the domain in the directions indicated on **Figure 1**. An increased domain was used to provide adequate spatial allowance to capture the wind effect and allow for dispersion of the products of combustion from the platform area.

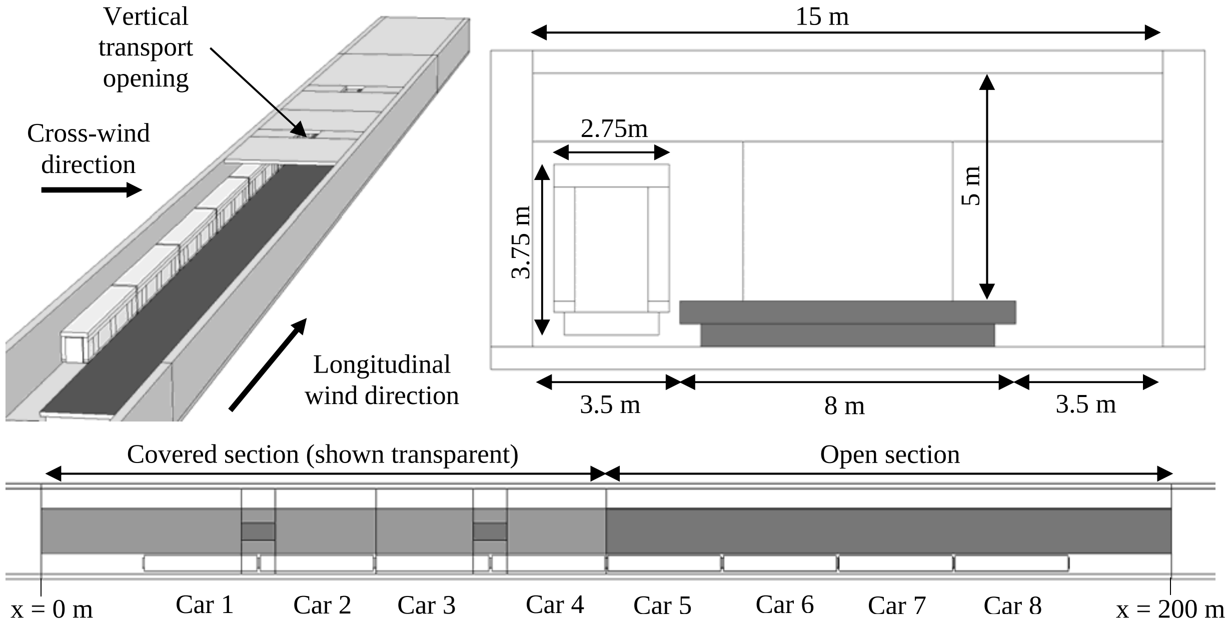

Figure 1: Example station geometry (shallow trench) – main dimensions and car numbering

Table 1: Main modelling inputs and assessment criteria

Parameter	Value	Units	Comment
Fire Parameters			
Type	Polyurethane, GM27	-	Typical for interior vehicle materials
Fire size	1.5/5/10	MW	Varies – refer Table 2
Heat of combustion	19.6	MJ kg^{-1}	Based on polyurethane (GM27) fire
Soot yield	0.2	kg kg^{-1}	Typical based on polyurethane (GM27) fire
CO yield	0.04	kg kg^{-1}	Based on polyurethane (GM27) fire
Radiative/convective	0.3/0.7	-	Typical
Growth rate	0.01172	kW s^{-2}	Medium t^2 growth, no decay modelled (conservative)
Boundary conditions			
Tunnel extension	Open	-	Open boundaries
Uncovered platform	Open	-	No forced boundaries with no wind
Wind	2.5	m s^{-1}	Application discussed in Section 3.2
Numerical parameters			
FDS defaults	Yes	-	Except as noted above for fire parameters
Assessment criteria – multiple considered, outcomes driven by visibility limit			
Tenability height	2	m	Above walking surface, consistent with grid size
Visibility limit	<10	m	NFPA 130 [2]. Considered conservative
Temperature	>60	ºC	NFPA 130 [2]
CO	255	ppm	NFPA 130 [2], 30 minute exposure

3.3. Scenarios

Table 2 lists the scenarios considered. These were selected in order to assess the effect of extent of cover, fire size, platform depth, fire location and wind. Any results denoted as 'not plotted' means that tenability outcomes were clearly better than for cases with the same geometry or impacts were only local to the fire. This enabled better clarity on result plots.

Table 2: Description of simulations

Case ID	Fire size [MW]	Fire Location [car]	Extent of cover [car]	Station depth [m]	Wind [direction/ m s^{-1}]	Frame on Figure 2 (or not plotted) / notes and brief comments on results
ENC-A-001	1.5	1	2	5	NA/0	Frame (a)/only local impacts
ENC-A-002	5	1	2	5	NA/0	Frame (a)/only local impacts
ENC-A-003	10	1	2	5	NA/0	Frame (a)/only local impacts
ENC-B-001	1.5	1	4	5	NA/0	Not plotted/better than ENC-B-003
ENC-B-002	5	1	4	5	NA/0	Not plotted/better than ENC-B-003
ENC-B-003	10	1	4	5	NA/0	Frame (b)/better than wind cases
ENC-B-007	10	1	4	5	Long/2.5	Not plotted/end only affected
ENC-B-009	10	1	4	5	Cross/2.5	Frame (b)/most impact on Car 1
ENC-B-011	10	4	4	5	Cross/2.5	Frame (b)/affects egress to opening
ENC-B-013	10	4	4	5	Long/2.5	Frame (b)/affects most of platform
ENC-B-014	1.5	4	4	5	Cross/2.5	Frame (b)/reduced buoyancy test
ENC-B-015	10	6	4	5	Cross/2.5	Not plotted/only local impacts
ENC-B-016	10	6	4	5	Cross/2.5	Frame (b)/only local impacts
ENC-C-001	1.5	1	6	5	NA/0	Frame (d)/affects open area
ENC-C-002	5	1	6	5	NA/0	Frame (d)/affects open area
ENC-C-003	10	1	6	5	NA/0	Frame (d)/affects open area
ENC-C-004	10	6	6	5	Cross/2.5	Frame (d)/affects egress to opening
ENC-D-001	10	4	4	10*	Cross/2.5	Frame (c)/better with high ceiling
ENC-D-002	10	4	4	10	Cross/2.5	Frame (c)/affects egress to opening
ENC-D-003	10	6	4	10	Cross/2.5	Not plotted/only local impacts
ENC-D-004	1.5	4	4	10	Cross/2.5	Frame (c)/affects egress to opening
ENC-D-005	1.5	6	4	10	Cross/2.5	Not plotted/only local impacts

*Double height (10 m) ceiling in platform. Other 10 m deep stations have 5 m platform ceiling height.

3.4. Sensitivities

A number of sensitivities were tested. This included checking the effects of the station smoke layer with the open boundary parameters modelled at the interface to the tunnel. This was done to check there was no significant bias with the simplifications adopted. Also the mesh size sensitivity was examined along with parameters and geometry used for the open platform boundaries. These tests increased the confidence in the results and conclusions formulated.

3.5. Limitations

A number of limitations apply. Holistically not every conceivable parameter and combination has been assessed due to obvious limits of time, computational capacity and presentation space. Wind cases were limited to a 2.5 m s^{-1} ground level velocity and two directions. Scenarios selected were based from experience on projects. Also there was no consideration of effects from the surrounding built environment. From an assessment perspective no consideration of radiation (from overhead smoke or walking past the fire) has been included. From experience this is typically not an issue except in the immediate vicinity of the fire.

4. RESULTS DISCUSSION

Figure 2 summarises the main study outcomes. Assessment criteria are listed in **Table 1**. As we are interested in the time when visibility tenability is lost, output is in the form of x-t plots (as opposed to timewise contour plots). For different cases the time t (s) when 10 m visibility is lost at a longitudinal platform location x (m) is presented. The results for the platform centreline are given. Other longitudinal positions were considered (incident and non-incident platform edge), however, it was found that the centreline is indicative of overall results. An indication of the ability for occupant egress was thus evaluated. It should be noted that visibility tenability alone is unlikely to result in fatal consequences but it is a convenient metric for comparing outcomes for this investigation.

Frame (a) shows the results for platform coverage of cars 1 and 2 (approx. 25%) with a fire in car 1 and no wind. Tenability is affected close to the fire for one case (200 s of tenability). However, the time of tenability is good for the remainder of the covered platform area, almost 600 s adjacent to car 2. Also tenability does not appear to be affected in the open area of the platform. Comparing to proposed egress benchmarks, it is considered likely passengers can egress from the fire car and the covered platform before tenability is lost in these scenarios.

Frame (b) shows the results for platform coverage of cars 1 to 4 (approx. 50%). A number of additional scenarios are analysed for this configuration. For the no wind case with a fire in car 1 the results are similar to frame (a) (marginally better adjacent to the fire at 400 s) with likely sufficient time of 500-600 s to egress to the uncovered platform area or through vertical transport before tenability is lost.

Frame (b) also shows scenarios with a 2.5 m s^{-1} cross or longitudinal wind. In these scenarios the time for tenability is greatly reduced. Although time of tenability varies across the platform, several areas lose tenability at 200 s or less. Passenger egress may be affected during these scenarios. It can also be seen that with a fire in car 4, tenability is lost near the start of the uncovered area, affecting the ability to egress to this area. The uncovered area remains largely tenable for extended time periods, even for fires in the uncovered area.

Frame (c) shows a deeper trench station with two platform ceiling heights of 5 m and 10 m. The results for the 5 m high cover in the 10 m trench are similar to the results of the 5 m trench, in that tenability is lost at various locations across the platform at approximately 200 s. For the higher cover height of 10 m, as expected the results are significantly better (400-500 s available).

Frame (d) shows results for a platform coverage of cars 1 to 6 (approx. 75%) with a fire in car 1 and no wind, and a car 6 fire with a cross wind. The no wind results are similar to the no wind cases described above, with tenability maintained for the majority of the platform for times in the order of 500-600 s. There are discrete sections of the platform with much shorter times for tenability which may affect egress to the open area. For the fire in car 6 with wind, it appears that the tenability is impacted more severely. Access to the open area is impacted at 200-300 s. The results collectively indicate a protected egress stair, or dedicated exit stair would be beneficial for this amount of platform coverage. Also for this limited open area it could be argued that extended tenability is not achieved and this area may not be considered a place of relative safety. Assessment of this would likely be subjective.

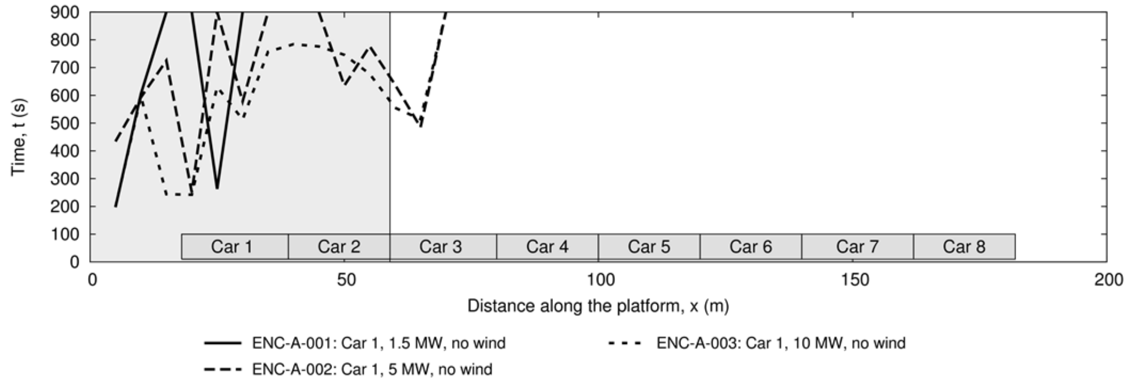

(a) Coverage over 2 cars (approx. 25%), 5 m deep trench

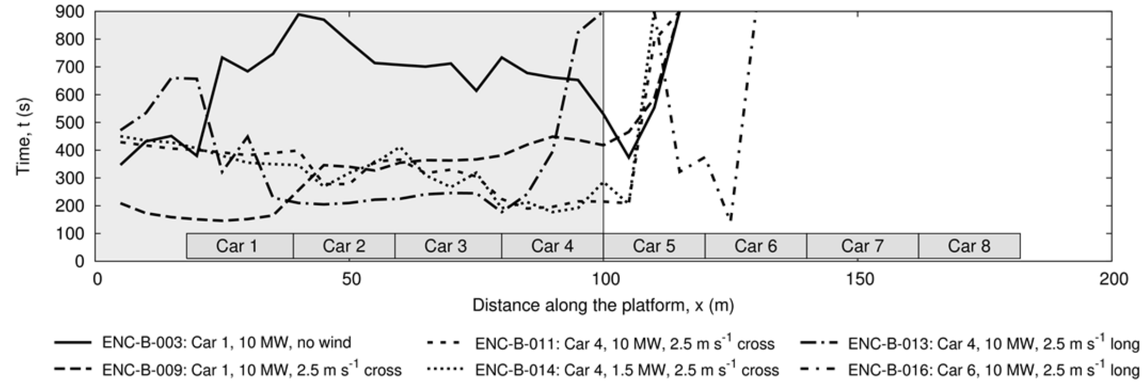

(b) Coverage over 4 cars (approx. 50%), 5m deep trench

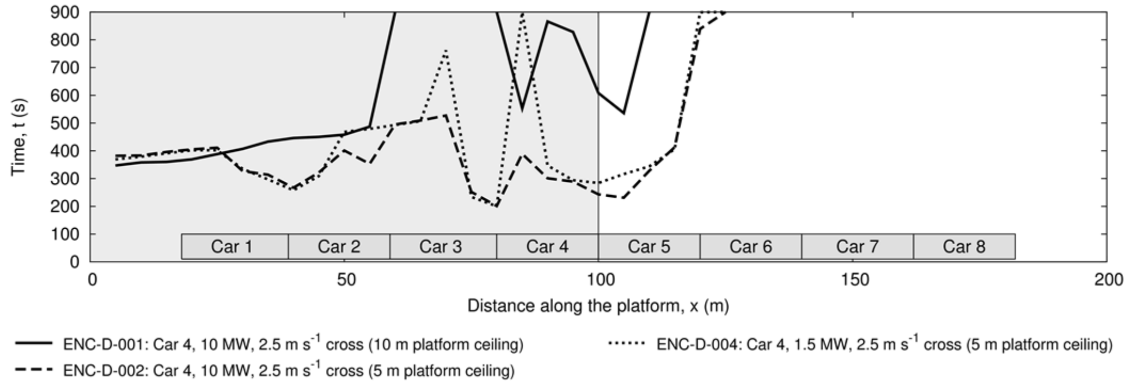

(c) Coverage over 4 cars (approx. 50%), 10 m deep trench

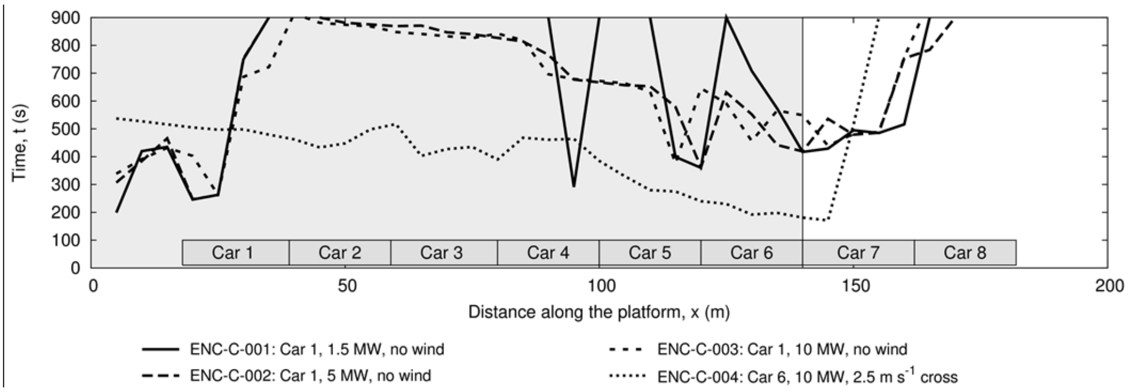

(d) Coverage over 6 cars (approx. 75%), 5 m deep trench

Figure 2: X-T plots for visibility (m) of less than 10 m – Along platform centreline

5. CONCLUSION

The results show that for the station configurations, fire sizes and wind conditions modelled:

- For cases with 25% platform coverage, tenability can be limited to 200 s local to the fire car, but with good access to the open area the station can likely be considered open. Wind impacts on this were not directly assessed, however, it is considered probable that acceptable outcomes would result.
- Generally the uncovered portion of the platform did not see significant accumulation of combustion products and remained tenable even with the potentially constraining effects of cross and longitudinal winds. The majority of smoke vented naturally from the covered section through the station opening. However, for some cases with 75% coverage it could be argued that the open area is impacted enough to not achieve broad acceptance of it as a place of relative safety. Based on this, and also given that the available area to hold passengers would be relatively small, dedicated egress from these areas may be required.
- For a platform coverage of 50% and 75% the effects of moderate cross and longitudinal winds, as well as possible fire locations adjacent to the opening, means passenger egress to the uncovered section of the platform may be impacted by the effects of the fire. This configuration cannot be deemed to be a fully open station and access to the open area cannot be relied upon. Dedicated egress stair/s or protected vertical transport would likely be required. Open areas of this size when coupled with possible wind effects, are not considered by the authors to provide sufficient natural ventilation benefits to enable fire safety provisions typically used in enclosed stations to be automatically discounted. Assessment of these provisions would be required.
- For deeper stations, raising the height of the cover has more impact on the results than the depth of the trench for the scenarios and configurations considered here. A higher roof may alleviate the tenability issues experienced for partially covered stations. Where space permits this should be considered an option in station designs if provision of egress elements are problematic.
- For uncovered area fires, tenability at platform level was predicted. Consideration must still be given to protecting egress elements above this level from smoke impacts.

6. REFERENCES

1. The National Construction Code (NCC) - The Building Code of Australia (BCA) Volume 1 and Volume 2 of the NCC, Australian Building Codes Board (ABCB)

2. NFPA 130 – National Fire Protection Association, Standard for Fixed Guideway Transit and Passenger Rail Systems, 2014 Edition

3. The Fire Precautions (Sub-surface Railway Stations) Regulations 1989, Statutory Instruments 1989, No. 1401

4. Fire Dynamics Simulator (Version 6) User’s Guide, NIST (National Institute of Standards and Technology, USA) Special Publication 1019

5. Fire Dynamics Simulator (Version 6) Technical Reference Guide, Volume 1 Mathematical Model, NIST, Special Publication 1018-1

6. Fire Dynamics Simulator (Version 6) Technical Reference Guide, Volume 2 Verification, NIST, Special Publication 1018-2

7. Fire Dynamics Simulator (Version 6) Technical Reference Guide, Volume 3 Validation, NIST, Special Publication 1018-3

CHOOSING A FIRE VENTILATION STRATEGY FOR AN UNDERGROUND METRO STATION

Wojciech Węgrzyński, Grzegorz Krajewski, Paweł Sulik
Fire Research Department, Building Research Institute (ITB), Poland

ABSTRACT

In Poland, a valid approach for fire ventilation of an underground metro station is to use a longitudinal system – similar to the ventilation systems used in tunnels. Such system may provide similar environmental conditions to transverse systems on the station platform, while maintaining smoke free access through the station galleries. In order to do so, designer must carefully balance the air flow into the station, through mechanical and natural means. In this papers authors present results of short numerical study, on how to achieve this balance, along with their reflections after 6 months of performing hot smoke tests in a large underground metro system.

Keywords: ventilation design, metro systems, longitudinal ventilation

1. INTRODUCTION

An underground public transport system is one of the most commonly used solution in modern, overfilled with road traffic, cities. The main advantage of such system is the ability to move a large amount of people from one point of traffic network to another. With this benefits, comes an increased risk of fire, thus special care on the field of fire protection of such facility has to be taken into consideration. The underground stations are very specific form of construction work – usually long compartments with low height and average of 2 – 3 escape routes. The fire scenarios connected to the fire of a train show, that growth of fire can be very fast and amounts of smoke produced big enough, to fill such a place in matter of minutes.

To keep the evacuation routes safe from smoke, a smoke exhaust systems are developed, based on different approaches and different strategies, varying from longitudinal to transversal solutions. What is especially difficult, these systems have to take into account not only the station itself, but also the possible air-streams coming from adjacent tunnel network – often difficult to assess at the design stage.

In Polish legislation, the design of ventilation system in a metro system is described in *Technical Guidelines for Metro Construction Works and Their Placement (Regulation no 859 D.U. 144, 17.06.2011)* [1]. In the appendix 1 of the Act, there is a requirement for provision of a functional ventilation system, that is protecting the station, exits and other critical infrastructure from heat and smoke. More to that, the tunnels longer than 300 m shall also be fit with mechanical ventilation. For the design, a minimum HRR value of 15 MW shall be used (unless determined otherwise with engineering analysis). The same act also provides the designer with acceptance criteria:

- temperature not higher than 60°C at a height of 1,80 m above evacuation route;
- radiated heat flux not higher than 2,50 kW/m², for an exposition time of 30 s;
- temperature of smoke and other combustion products not higher than 200°C at a height of 2,50 m above the evacuation route;
- visibility range not lower than 10 m, at a height of 1,80 m above the evacuation route;
- oxygen concentration not lower than 15%.

For the required safe evacuation time calculations, a minimum safety factor of 1,30 should be used. The evacuation route is considered safe, when the available safe evacuation time (ASET) is longer than the required safe evacuation time (RSET).

2. VENTILATION STRATEGY

Authors determine three types of ventilation of a station, which can fulfil the requirements of [1]:

- transverse ventilation system – designed according to the building regulations, following the axisymmetric or spill plume assumption and according laws of physics that apply;
- transverse ventilation system with compartmentation between the platform and a train, which can be used to limit the amount of smoke reaching the station;
- longitudinal system using points of exhaust within the tunnels and at the ends of the station.

Despite the fact these systems differ in their principles, all are able to provide sufficiently clear of smoke escape routes, limit the spread of smoke and heat through the station and its surroundings, and provide possibility for rescue services to operate within the station, as shown on figure 1. In the opinion of authors, the design of transverse systems, with and without comparmentation, is generally well described in the literature. References worth mention are [2], in which some general rules for building ventilation employing transverse smoke movement are presented, and [3, 4] in which results of various engineering analysis in this field are presented.

Figure 1: Hot smoke test in a Metro station, with transverse (left) and longitudinal (right) system

For a longitudinal station ventilation system, between many, this paper focuses on following three key aspects that have to be determined by the designer:

- division of the station into detection zones;
- points of smoke exhaust;
- points of supply and their capacity, usage of natural station exits as the supply points, technical provisions to keep them free of smoke (i.e. smoke barriers).

2.1. Separation of the station into detection zones

In most tunnel ventilation systems, typical metro station allows a bi-directional flow of smoke, towards either of its portals. This allows for a natural division of the station into two virtual smoke zones. The line of separation may be symmetrical in the middle of the station, which in general is advised in most applications, or asymmetrical – for example at one of the station entrances (Figure 2). If the portals of the station are equipped with ventilation points in each of tubes, and allow to operate them independently, it might be possible to always use the point of exhaust in the tube corresponding to the track, on which engulfed train is detected, but this may require further subdivision of the detection zones.

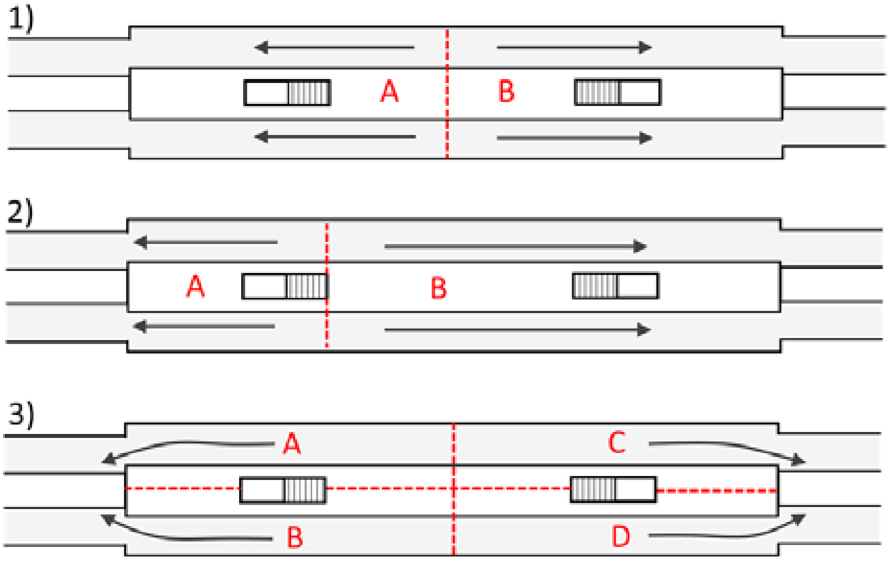

Figure 2: Bi-directional detection zoning – axisymmetric (1) and asymmetric (2) and four zone detection zoning (3)

The influence of separating the station smoke or detection zones should not be trivialised, as this design decision will determine the area of the station that may be filled with smoke in case of fire. This will be explained further in paragraphs 2.2 and 2.3. Designer must be also aware of possible detection methods:

a) point detection (heat, smoke);
b) linear heat or smoke detection;
c) flame detection.

In case of point detection, the fire location is pointed with great precision, unless the flow of smoke was affected or redirected away from the fire (in example by opening one door on other end of the burning metro car). In case of linear heat or smoke, or flame detection, the location is more an approximation within the detection area. In case of fire at the boundary of smoke detection zone, system is expected to operate in a way, that will provide necessary environmental conditions, despite the scenario that is activated. Physical barriers at the smoke zone boundaries could provide help, but may be impossible to fit within the architectural framework of a station.

2.2. Determination of points of exhaust location

Due to typical division of a metro system into stations connected with tubes, typical layout of ventilation system will usually consist of multiple tunnel and station exhaust points, in various combinations (Figure 3). Presence of an exhaust point in the middle of a tunnel, and two points at each of it ends may seem as safe design, but usually will not provide other benefits beside limiting the length of tunnel that is filled with smoke. On the other side, having at least two separate exhaust points within one tunnel (ie. middle of the tunnel and one of its ends) may be worth, due to possibility of altering the supply airflow, and overcoming natural flows that can occur in the system.

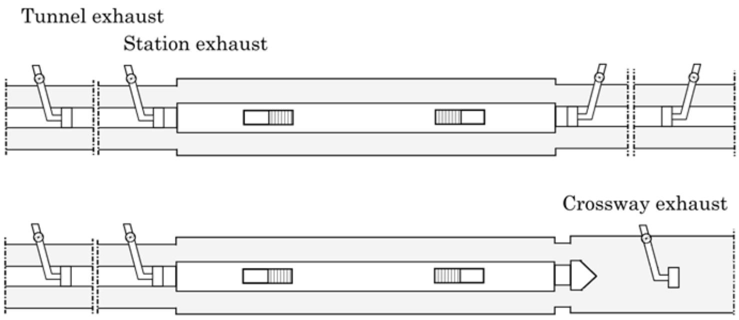

Figure 3: Possible exhaust points locations in a longitudinal approach of station ventilation connected to a tunnel (top) and a crossway (bottom)

The sizing of the exhaust points is out of the scope of this paper, although the designer has to acknowledge, that the combined efficiency of two exhaust points located in different parts of the system (portals, tunnel, ends of stations) may be worse than the efficiency of a single point with the same volumetric capacity.

2.3. Determination of supply air location and its balance

For stations protected with longitudinal systems, the provision of fresh air is the most critical aspect, that influences the flow pattern of smoke within the protected volume. Air may be provided through (figure 4):

- tunnel portals;
- tunnel air supply points (reversed exhaust points);
- station air supply points (reversed exhaust points);
- station entrances.

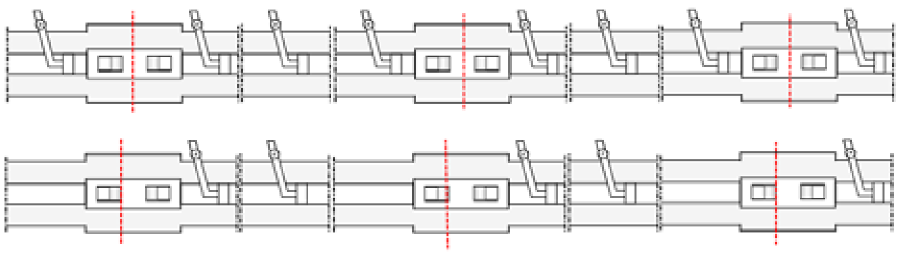

Figure 4: Possible supply points in axisymmetric (top) and asymmetric (bottom) longitudinal ventilation system

The location of supply points does not solely determine the strategy of air supply within a system – it may be different in stations at different depths or remote parts of metro system, as shown in the numerical study. This strategy should always be a result of an engineering approach – with at least a 1-D flow simulation. Authors of the paper for this task employ a 3-D model of complete metro system with its surroundings, solved with a CFD model.

The amount of air supplied into the system can be controlled by balancing the amount of air supplied and exhausted through mechanical points. Natural supply points, unless located in great depth, will act as free boundaries of the system, balancing the difference between the mechanical supply and exhaust. It must be noted, that in some cases natural flows may occur in the tunnel, that can strongly disturb the air balance in the ventilation system. In such case it is advised to use additional supply/exhaust points, even at great distance from the fire – just to control the air velocity in remote areas of the system. In some scenarios, same effect may be reached with use of air curtains [5, 6].

3. NUMERICAL STUDY

In order to visualize the importance of balancing supply and exhaust rates for different protection scenarios, authors have performed a series of numerical studies on an air flow in metro system in fire conditions, as shown in table 1. Scheme of the metro system with supply and exhaust points is presented on Figure 6. All of the stations of the system were connected to the exterior through a gallery, and were part of the same numerical domain. The numerical model is shown on Figure 7.

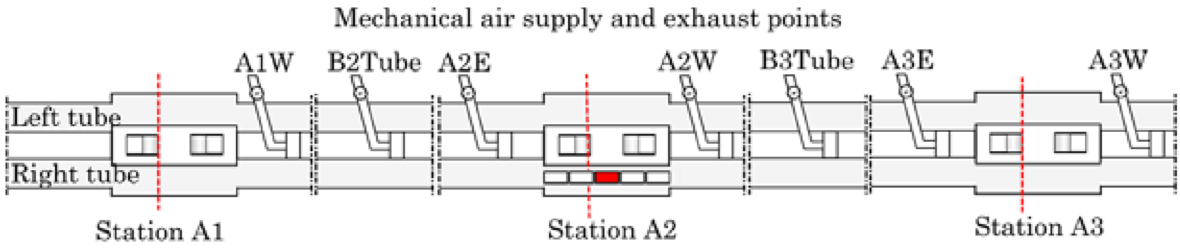

Figure 6: Simplified schematic of numerical model used in the research, with the reference names for exhaust and supply points.

Fire was located in the middle of station A2, that was assumed to be asymmetrically divided into two smoke zones. Three fire powers were analyzed – 5 MW, 15 MW and 25 MW, and the assessment was performed 5 minutes after the peak power was reached (steady state conditions). System capacity was chosen as 300 m^3/s, although some of the simulations were later rerun with capacity of 150 m^3/s (out of the scope of this paper). All calculations were performed using ANSYS Fluent CFD model, for transient conditions. K-ε turbulence model (standard) was used for the turbulent flow, and P1 model for radiation. Walls were made from concrete, while train was made with insulated steel.

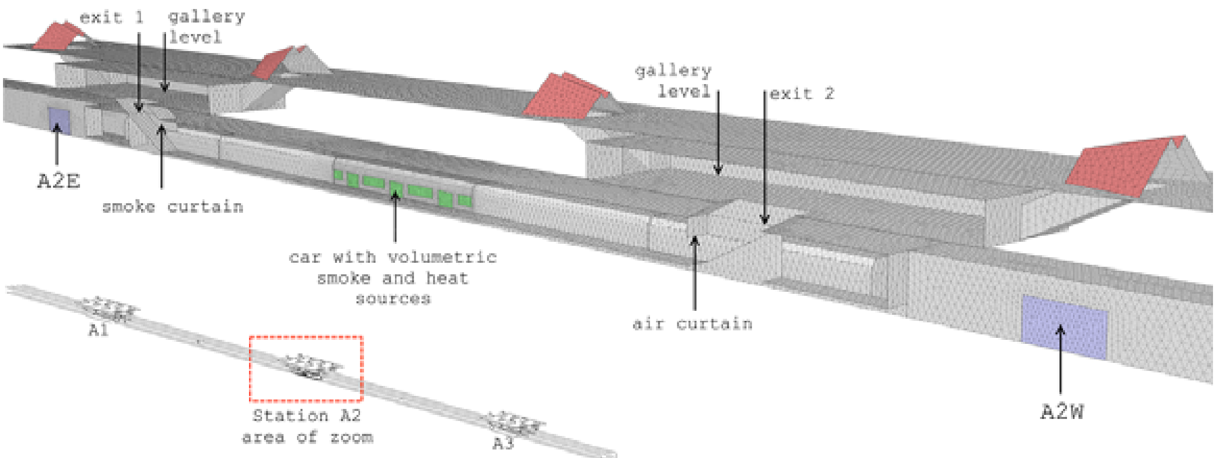

Figure 7: Part of numerical model used in the analysis (station)

Table 1: Scenario matrix

Scenario	Exhaust	Supply	Comment
1	A2W	B2T	50% of supply through station A2 entrance
2	A2W + B3T	B2T	50% of supply through station A2 entrance
3	B3T	B2T	50% of supply through station A2 entrance
4	A2W	B2T	10% of supply through station A2 entrance
5	B3T	A2E + B2T	50% of supply through station A2 entrance
6	A2W (L)	A2E + B2T	exhaust only through one tube
7	B3T (L)	A2E + B2T	exhaust only through one tube

4. RESULT ANALYSIS

In first three scenarios, Authors were investigating the influence of changing the exhaust point location, and combination of two different points, on the system performance. No difference on the system performance was observed in the station itself, although the flow within the adjacent tunnel tube and the galleries differed in each of the scenarios (Figure 8). In the scenarios using the tunnel exhaust point, the smoke did not move further than the exhaust point location, although in scenario 1 at fire power of 25 MW some smoke movement was observed into one of the tunnel tube. In all of the three compared scenarios, the gallery was free of smoke – the smoke did stop at the smoke screen, and was pushed away from the entrance due to large flow of incoming air (Figure 9). In scenario 4, in which 90% of air was supplied through mechanical supply, smoke penetrated gallery of the station after approx. 5 minutes of the study, as shown in Figure 10. This may be directly dangerous to life and health of occupants, as they may not be expecting hot smoke to appear in such distance from the fire. Similar effect was observed in hot smoke tests, when the air balance did not allow natural air supply through station entrances.

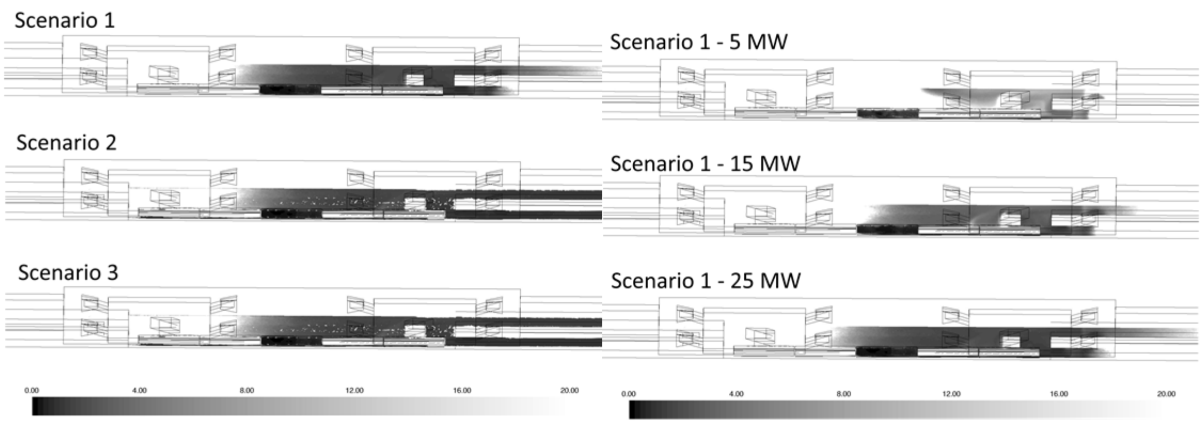

Figure 8: Comparison of local visibility of walls (0 – 20 m, and more) at height of 2,00 m above the platform for different scenarios, and different fire power within a chosen scenario

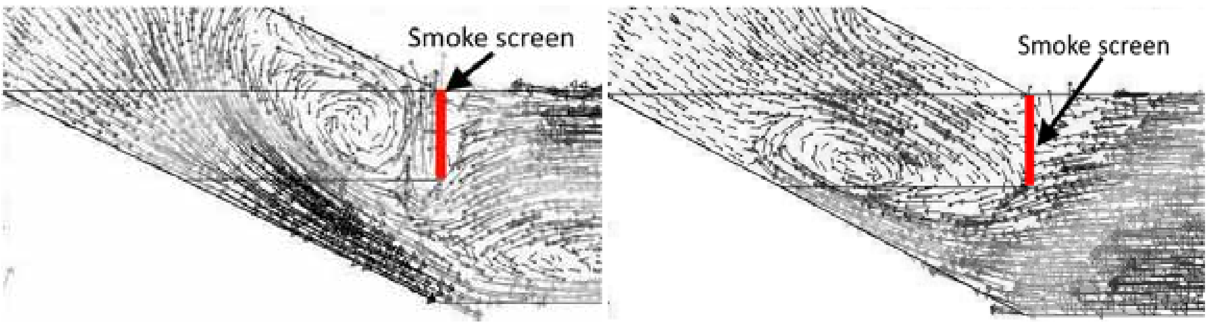

Figure 9: The influence of the smoke screen on the flow of air at supply point, at 5 MW fire (left) and 25 MW fire (right)

In scenario 5, the effect of incorrect fire detection was determined. As mentioned before in the text, the system is expected to cope with incorrect detection at the zone boundary, as it may be impossible to utilize physical comparmentation of the zones. In the simulation, for just the platform level, the system did remove the smoke through exhaust point B2T (Figure 11), although it must be noted that some smoke was observed at the gallery level for the fire of 25 MW. In this case, this might be accepted by the Authority, as the simulation did prove the robustness of the system design.

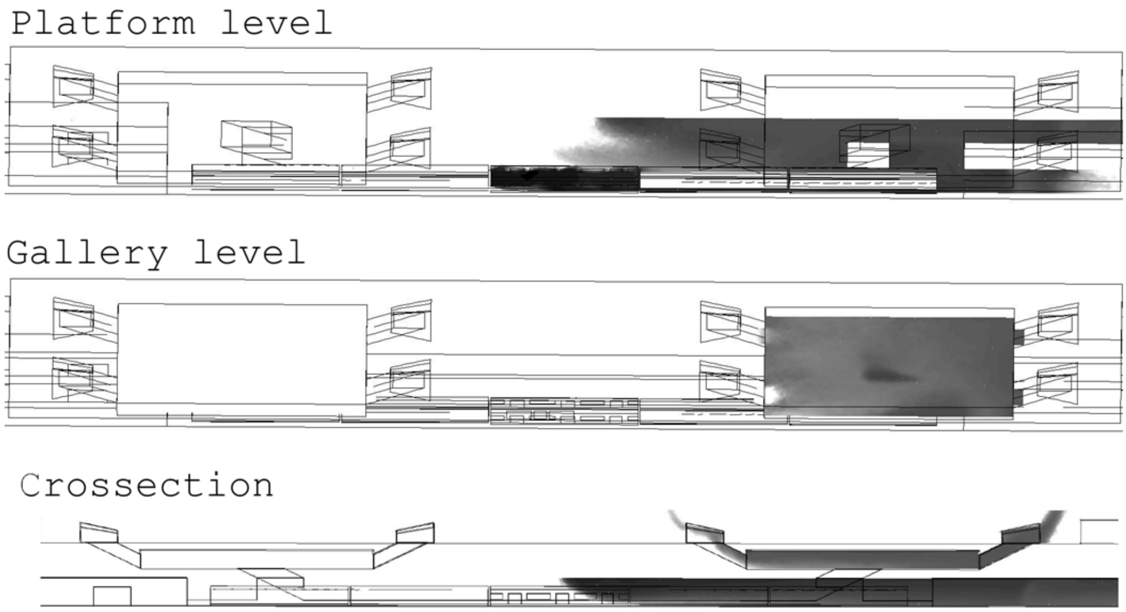

Figure 10: Smoke penetration of the station gallery in scenario 4 at 25 MW – effect of too strong mechanical air supply into the station

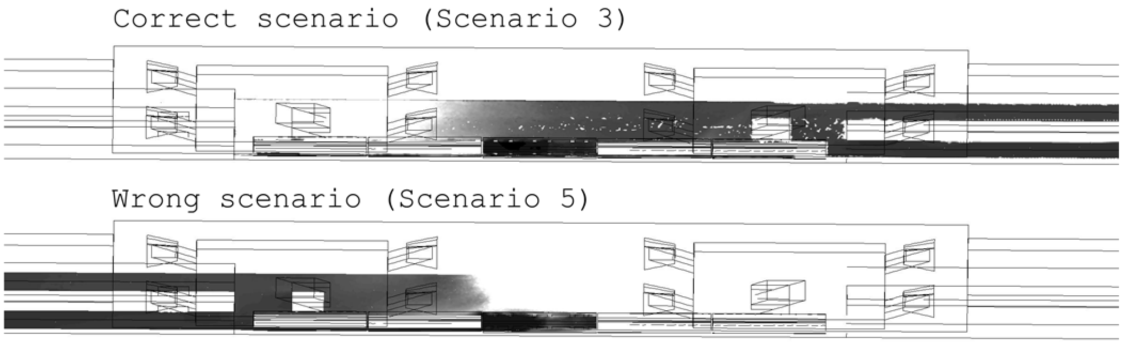

Figure 11: Effect of system starting in incorrect scenario mode

In scenarios with single point of exhaust (only left or right) tube the positive effect of smoke filling of only a quarter of the station was only observed for the 5 MW fire. In larger fires, this effect diminished. The positive effect observed in simulation is in line with authors observations during hot smoke tests, although in real scale fires larger than 2 MW were not tested, Figure 13. For larger fires, smoke movement in second tunnel tube was observed towards adjacent station – this was also observed in some of the full scale tests. In the simulation, after approx. 20 minutes of simulation, the smoke penetrated approx. 70% of the tunnel length (figure 12) – in the full scale test similar effect was observed in time of 15 to 25 minutes.

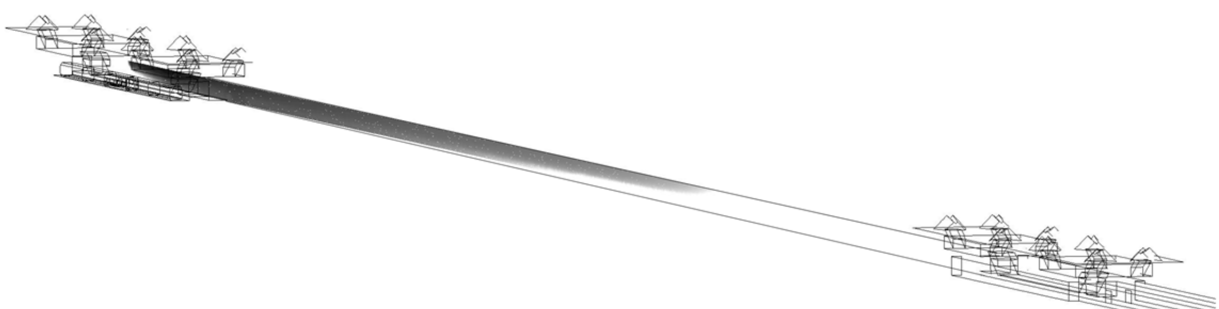

Figure 12: Upstream movement of smoke after 20 minutes of simulation (scenario 7)

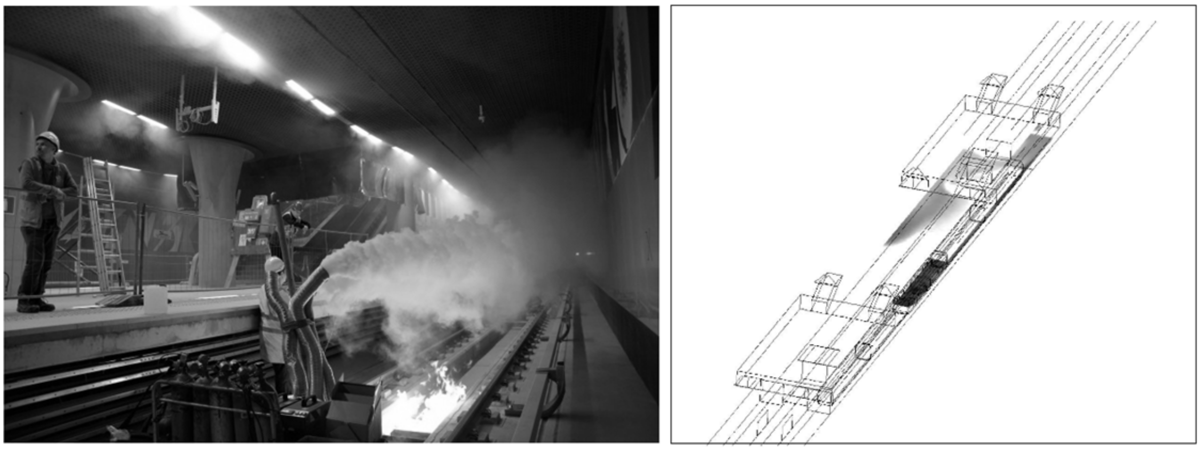

Figure 13: Smoke movement in one quarter of the station in a hot smoke test and in simulation (scenario 7)

5. CONCLUSIONS

Longitudinal system may be a valid solution in a simple metro station, although its design requires wide investigation of many system parameters – such as supply air location, air balance or usage of physical boundaries (like smoke barriers). Even at fires of 25 MW power, longitudinal system was able to provide both safe approach for firefighters, and smoke-free galleries of the metro station. This was possible mainly due to fact, that large amount of air was supplied into the station through the connection with the gallery – creating an air flow that prevented smoke movement into the gallery. This is consistent with observations of authors, done during full scale tests of complete metro system. The airflow pattern in the system, especially in the station galleries, changed with the growing HRR of the fire, which shows that just cold flow assessment is insufficient for this design task.

Literature

[1] Technical Guidelines for Metro Construction Works and Their Placement (Regulation no 859 D.U. 144, 17.06.2011)

[2] Milke A.J., Smoke Control by Mechanical Exhaust or Natural Venting, in SFPE Handbook of Fire Protection Engineering, 5th Edition, Springer 2016

[3] Na Meng, Longhua Hu, Long Wu, Lizhong Yang, Shi Zhu, Longfei Chen, Wei Tang, Numerical study on the optimization of smoke ventilation mode at the conjunction area between tunnel track and platform in emergency of a train fire at subway station, Tunnelling and Underground Space Technology Volume 40, February 2014, Pages 151–159

[4] R. Harish, K. Venkatasubbaiah, Effects of buoyancy induced roof ventilation systems for smoke removal in tunnel fires, Tunnelling and Underground Space Technology Volume 42, May 2014, Pages 195–205

[5] G. Krajewski, “Air barriers used for separating smoke free zones in case of fire in tunnel”, Proc. 7th International Conference “Tunnel Safety and Ventilation” Graz, 2014

[6] G. Krajewski, W. Węgrzyński, Air curtain as a barrier for smoke in case of fire: Numerical modelling, Bulletin of the Polish Academy of Sciences Technical Science, vol. 63, 2015

DEVELOPMENT OF AN ORIGINAL MEASUREMENT METHOD FOR THE TOULOUSE METRO (FRANCE)

Julien VEYET, Julien LEQUENNE
ENGIE Axima, France

ABSTRACT

The line A of the Toulouse metro is approximately 12km long and serves 18 stations. 60 million of passengers travel on the metro network yearly. This line went into service in June 1993, a second line was added in 2008 and later on between 2012 and 2015 the line A underwent a renovation by ENGIE Axima to upgrade the smoke exhaust system according to current regulations.

The renovation of ventilation shafts consisted in the replacement of all the fans and the installation of two new motorized doors to isolate the two metro lines. Afterwards, all fire scenarios had to be approved during a global test campaign.

Additionally, the regulations require the tunnel operator to run regular periodic performance reviews. The velocity measurements in the metro tunnels are one of the requirements, ensuring that shafts capacities are preserved during the lifetime of the system.

Considering the regulatory constraints and the performance tests, the tunnel department at ENGIE Axima designed an innovative solution to carry out these measurements: two measurement carts and the “SPEED’AIR” vehicle specifically tailored for the Toulouse metro.

Our design and test teams worked extensively on this project for many purposes:

- Defining a method for carrying out the measurements in metro tunnels.
- Verifying and validating the anemometer mesh using Computational Fluid Dynamics.
- Designing the measurement carts carrying the anemometers.
- Modifying an electrical vehicle for rail tracks compatibility.
- Working closely with the tunnel operator on preparing and implementing the complete measurements procedure.

We were confident in making the measurements procedure significantly more reliable, time-efficient and cost-efficient than usual methods. In order to do this we implemented a repeatable method thanks to a fixed mesh of high performance measuring devices. Our system gave the opportunity of a significant optimization of the on-site tests planning and the fan use.

Thanks to the “SPEED’AIR” we were able to take all the measurements for a total of 20 different measurement positions in the tunnel and 67 tested scenarios in only 7 nights of 4 hours. Up to five times faster than the initially planned method.

Keywords: Metro ventilation, full scale testing, measurements, innovation

1. PRESENTATION OF THE TOULOUSE METRO (FRANCE)

The line A of the Greater Toulouse area metro was opened in 1993, it is 12km long and serves 18 stations. It is comprised of underground and surface sections.

For efficient ventilation, platform screen doors are used to isolate the metro stations from the tunnel.

The Line A and the Line B are connected by a tunnel section called ‘service track’. This connection only serves for transferring the metro cars between the lines.

The Line A of Toulouse metro uses automatic light vehicles (“*Véhicule Automatique Léger*” in French abbreviated as VAL). The VAL concept is of rubber-tyred light-weight vehicles using a segregated fully automated guideway. It is characterized by its fully automatic operation, allowing it to reach top-quality service frequency and reducing running costs (No personnel aboard), remotely controlled from the Operation Control Center.

1.1. Principles of operation of the tunnel ventilation system

In case of fire in the tunnel, the smoke exhaust system of the tunnel extracts fumes using the shaft located in the affected station to confine the fumes and protect nearby stations and the tunnel.

Each ventilation shaft is equipped with a 100% reversible fan. Fans work in exhaust or supply mode depending on the location of the incident: Ventilation shafts of the affected part are used to exhaust smoke and nearby shafts are put in supply mode to create a defined air stream in order to obtain a smoke free zone for rescue. Back-layering (fumes going back to the station) of smoke in the tunnel will not occur if the velocity of the ventilating air moving toward the fire is equal to or exceeds a certain critical velocity.

1.2. Tunnel Ventilation System Upgrade (2013-2015)

1.2.1. Ventilation equipment

The Tunnel Ventilation System (TVS) was upgraded between 2013 and 2015 to enhance the smoke exhaust system performance to comply with the decree released on November 22nd 2005.

The main goal of the upgrade was to reach a critical velocity of 1.5m/s from both sides of the ventilation shaft to avoid back-layering. This objective was achieved with the installation of 12 new exhaust fans in a range from 250kW to 280kW, thus multiplying the ventilation airflow rate by 3.

We also had to isolate the two metro lines to avoid smoke propagation and enhance the performance of the ventilation system by reducing air leaks. To do so, we installed two motorized doors on the track. In normal operation these doors are closed. They are opened during metro cars transfer from one line to the other.

1.2.2. Operation modes

Currently, the tunnel ventilation works with predefined operation modes, which are defined as a likely operating arrangement of the TVS within a defined area, for a common purpose. The choice of the operation mode is determined depending on the area of the emergency event and the availability of the ventilation equipment.

As explained earlier, in fire emergency operating mode, the fans of the affected station are put into exhaust mode and nearby stations are put into supply mode. Considering all degraded modes, there are about 4 different ventilation modes for each station.

2. PERFORMANCE REVIEWS OF THE SMOKE EXHAUST SYSTEM

After the installation of the ventilation system, we had to run performance reviews in different operation modes to ensure the design criteria were met.

These tests consisted in velocity measurements on a given cross-section upstream and downstream of each ventilation shaft for each operation mode.

Considering that any intervention in the tunnel has to be performed at night, we only had 4 hours (from 1 am to 5 am) to carry out the measurements and to move in the tunnel from one measuring point to the next one.

This schedule led us to seriously consider the measurement method we had to apply.

2.1. Conventional Methods

Basically there are two common methods to measure the velocity:

- The first method is to manually move a vane anemometer across the section to get an average velocity of the airflow on the trajectory (or point by point); this is the scanning method.
- The second method is to use propeller anemometers mounted on a group of poles to form an anemometers mesh according to the log-Tchebycheff method.

Figure 1: Scanning method (left-hand side) and anemometers mesh (right-hand side)

To get the best results, these measurements have to be carried out according to the French standard: NF EN ISO 5802.

This standard recommends the Log-Tchebycheff method which consists in taking the measurements on several different points on the traverse plane (Minimum 5 points horizontally and 5 points vertically). The distance between two points depends on the cross-section.

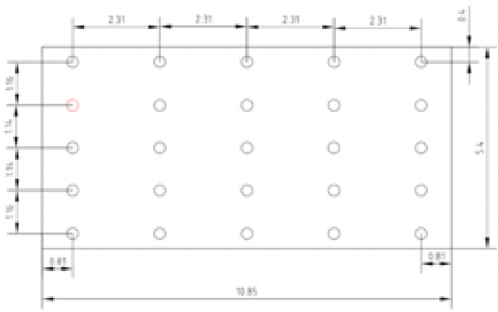

Figure 2: Example of Log-Tchebycheff distribution

2.1.1. Scanning method

The scanning method requires the operator holding the anemometer pole to scan a large cross-section (usually greater than 25m^2) at a steady rate and keeping the anemometer perpendicular to the airflow.

An alternative method would be to only aim the Tchebycheff method's points instead of scanning continuously the whole cross-section. However, it is very difficult to precisely respect the predefined points when taking the measurements.

In the case of metro tests, this method can be very challenging due to all the obstacles in the tunnel (Tracks, signs, cable-trays, duckboards, etc…). Moreover, these methods require a short time interval between measures because the velocity can fluctuate significantly in a few minutes, which could make this method unreliable.

With both methods, in the case of Toulouse Metro Reviews, we had to have two simultaneous measurements for each operating mode, causing risks of measure uncertainty. All the more, with two persons measuring simultaneously, it could be tricky to compare the plots.

2.1.2. Anemometers mesh method

The anemometers mesh method is fairly reliable. The anemometers have a fixed position for the whole measurements.

This kind of mesh provides reproducible results as long as the equipment is installed. So it is very efficient over a night of tests but may vary if the equipment is moved one night after another. The disassembling and reassembling operations are so long that it becomes incompatible with the night metro schedule. Indeed, the probes need to be installed carefully to ensure their accuracy. Another advantage of this method is the possibility to log each probe independently, allowing a much more complete post-processing, like plotting graphics over time or space for example.

2.1.3. Comparison

The radar-graph below shows 5 criteria used to qualify the quality of the method on a 0-10 scale (where 0, at the center, is the worst option and 10 is the best).

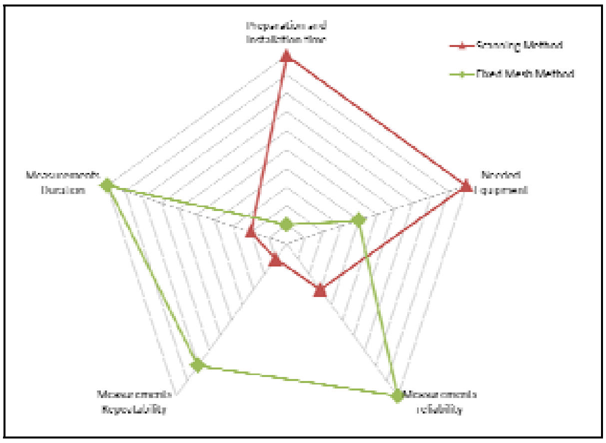

Figure 3: Comparison graph of conventional methods

As a result, these two methods have strong and weak points but they don't fit our needs for this project. The preparation time is highly disadvantageous on one side and the degree of uncertainty makes the results unreliable on the other side.

2.2. Improving the existing methods

2.2.1. Description of the process

Clearly, existing methods present serious drawbacks. That's why we needed to develop a new measurement system that is more reliable and can make repeatable measurements in a short delay. (Only 4 hours a night)

At first glance of the problem, we set out to build two light frames that can move easily throughout the tunnel with the same guiding chassis. One frame is used to measure the velocity upstream of the ventilation shaft and the second downstream. On this frame we would determine the places of the sensors depending on the tunnel cross-section.

The frames had to be equipped with 9 high accuracy anemometers, connected to a data-logging station. The station records values measured every second and then it displays real-time curves on the screen. Being able to analyze the results in real-time gives us the opportunity to check the validity of the results during the test and to identify the stabilization of the current mode.

Another crucial design criterion was to be able to move these frames easily and quickly on the tracks in order to minimize the intervention window as much as possible. To do so, we decided to modify a small electric vehicle by working closely with the manufacturer to make it compatible both on rail tracks and conventional roads. This vehicle would tow the two frames to the measuring site.

2.2.2. Benefits

This method has many advantages. It allows the reproducibility of the measuring mesh on the entire structure as the selected positions for the anemometers remain unchanged. The measuring devices have an identical position relative to the cross section from one measurement to another. Therefore, the measurements are more reliable and repeatable over time.

In addition, the mobility of the measuring system allows the achievement of a large number of tests in one night.

Finally, being able to considerably reduce the duration of measurements means the operating time of the fans during tests will be considerably reduced allowing us to significantly reduce energy consumption.

2.3. Implementation of the innovative solution

2.3.1. Development of the measurement method

The first step in developing this process was to determine the structure of the anemometers mesh. In parallel, we worked on the design of the frames. The data logging system and the traction vehicle were developed later.

2.3.1.1. Determining the positions of the sensors

We needed to determine the structure of the anemometers mesh that would allow us to get the best results, but that would also fit on the carrying frame. Besides, the meshes of anemometers needed to be compatible with the three different tunnel geometries.

All these different constraints led us to simplify the “Log-Tchebycheff” method. In order to make sure that the simplified method was acceptable, we used the Computed Fluid Dynamics (CFD) software ANSYS CFX, to run a 3D simulation of different tunnel segments. This method has already proven its worth in previous projects.

With CFD, we have determinated that the average airflow velocity of 25 points distributed according to the Log-Tchebychoff method is equal to the average face velocity in the whole tunnel segment with a margin of error lower than 0.5%. We had to found the error rate of the simplified mesh.

But in our case, we had to lower the mesh size due to geometric constraints: the mesh has to travel along the tunnels so we have to avoid anemometer outside of the metro size limit.

As we can see on **Figure 4**, a cross-section is occupied by plateform volume at stations and signalization panels all along the way. The rolling stock area limit is the only 100% safe area for placing our mesh.

Considering these areas in the cross-section, we have immedialy planned to design a foldable structure to cover both rolling stock areas.

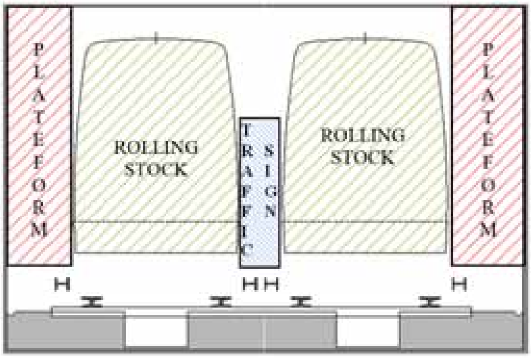

Figure 4: Cross-section occupation

At first, we tried to simulate a mesh fully included in the rolling stock area limit. By experience, we knew that we had to avoid a high concentration of anemometers in the center of the section.

The simulations allowed us to verify the placement of the anemometers in each of the 30 defined tunnel segments. The average error rate was slightly higher than 6%, more than expected. So we tried to move measurements closer to the walls to decrease the error below 5%. That allowed us to gain between 0.5 and 2% depending on the tunnel segment considered. Anyway, with the limitations on-site, we finally assumed that the error rate cannot be dropped more.

Figure 5 shows the position of the 9 anemometers needed for an average velocity equal to the measured velocity.

To ensure that these assumptions are realistic, the positions of the measurement points on site have been defined to get a uniform air flow. That means away from any significantly disruptive singularity.

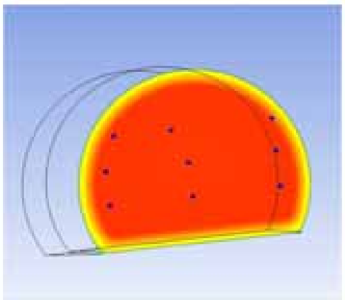

Figure 5: Simulation results in ANSYS CFX

2.3.1.2. Mechanical design of the measurements frame

The second challenge while implementing this method was the design of a lightweight frame with modular mounts allowing us to place the sensors freely on the frame.

We designed the frame using 3D Computer Aided Design (CAD) and chose to build the frame in aluminum because it's solid enough for our needs and lightweight.

As explained earlier, our frames needed to fit in the different tunnel geometries and keep the anemometers in the same relative position along the tunnel.

Considering the previous challenges, we designed and built a foldable frame, with telescopic parts allowing us to get a small transport volume but a large range of measure once deployed.

Figure 6: 3D design of the measurement foldable frame (left-hand side) and frame as-built in the tunnel (right-hand side)

2.3.1.3. Data logging (Data acquisition system)

In order to record and visualize data, we have built a standalone data logging station powered by batteries to receive signals transmitted from the anemometers.

2.3.1.4. Traction Vehicle

Once the measuring system was designed and built we focused on the traction vehicle. We chose to modify an electric vehicle to be able to run on metro tracks by working closely with the manufacturer. At the same time we needed the vehicle to operate both on rail tracks and conventional roads.

Initially built for industrial or farming transport, the modified electric vehicle has a range of 60km and a top speed of 30km/h, enough to cover the whole tunnel back and forth.

Figure 7: Traction vehicle and measurement frame

2.3.1.5. Conclusion

The Mobile Mesh method is added on the radar-graph shown on Figure 3 (where 0, at the center, is the worst option and 10 is the best):

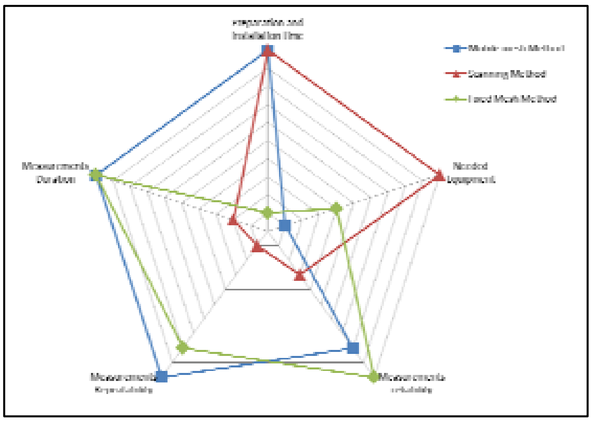

Figure 8: Comparison graph of all methods

The benefits of this system are clearly established even though it requires a large amount of equipment (Instrumentation, Frame, and Vehicle).

2.3.2. Tests and measurements

The measurements procedures were prepared by placing the anemometers on the frame, as shown on Figure 5. The fact that the frame can be moved with all the equipment mounted, allows the test team to prepare for the tests beforehand and not waste any time during the intervention window. The system "ready to use" can now be put on the tracks as soon as the tunnels are available.

Once in place, one of the two frames is put upstream and the second frame is put downstream of the ventilation shaft. After the system is ready and the conditions are stable, the concerned fans are put into the operation mode to be tested. Afterwards, there is a waiting period of approximately 10 minutes to wait for the airflow to re-stabilize.

The results recorded at the site have proven to be stable and precise. In fact, being able to analyze the diagrams and the results in real-time allowed us to adjust the sampling period necessary for each operation mode and gave us the best results.

After the measurements at one point are done, we can fold the frames and move on to the next point using the traction vehicle.

All the measurements of the Line A were achieved in only 7 nights, when 7 weeks were initially scheduled considering the conventional testing method, saving us a considerable amount of time on site.

3. CONCLUSION

This article describes an innovative method to test the performance of tunnel ventilation systems in the railway environment. This method has proved to be very reliable, accurate, fast and repeatable.

As a matter of fact, measuring velocity using this process is considered very efficient for many reasons:

- The position of the sensors was defined using computer simulation, which ensures an optimum placement within the allowed area of the cross-section.
- The design of the light frames allows to repeat the measurements for the exact same mesh on the cross-section for the whole tunnel.
- Recording data and being able to analyze results in real-time during the tests allow to adjust the sampling period on-site and get the best results.
- Repeatable measurement gives a real confidence in the results for Operators.

USE OF VENTURI JETS LOCATED OUT OF TUNNELS FOR THEIR VENTILATION DURING THE PERIODS OF TUNNELING COMPLETION OR AT THEIR RECONSTRUCTION

[1]S. G. Gendler, [2]E. A. Savenkov

[1]National mineral resource university "Mining", Russia
[2]Open joint stock company Scientific Research, Design and Surveying Institute "Lenmetrogiprotrans", Russia

ABSTRACT

The need to maintain the specified atmospheric parameters inside tunnels is still critical even during the closing stages of new tunnel construction or major overhauls of old tunnels, i.e. when through-flow ventilation is already in place. This task is becoming especially important when vehicles and equipment driven by internal combustion engines are used in mining and overhaul operations. Application of traditional ventilation schemes with fans located inside the tunnel does not seem rational as it decreases mobility of the mining and construction equipment. However, it is known that fans located at some distance from the tunnel portals and creating a free airflow directed perpendicular to the tunnel face are often used in tunnel fire tests. Various publications claim that the maximum efficiency of these fans will be achieved if they are located at such a distance to the tunnel portal that the cross-section of the jet expansion is equal to the portal section. However, they do not provide any justified methods to select parameters of such fans. The investigation included complex theoretical and experimental studies. The resulting dependences render it possible to select ventilating equipment parameters for the ventilation schemes with the draught source located outside of the tunnel.

Keywords: *venturi jets, jet fan, longitudinal ventilation, through underground workings, motorway tunnel, construction and installation activities, calculation method*

1. INTRODUCTION

Construction of transport tunnels involves three main stages that determine specific features of their ventilation. During the first stage when excavation is done with dead end headings, ventilation is arranged with ventilation tubes. Parameters of these ventilation systems are calculated using well-proven methods and do not pose any challenges.

The second stage, when tunnel driving is completed and through-flow ventilation is introduced, is characterized with difficulties in establishing of steady air movement due to significant impact of the natural draught [4] as well as inefficiency of traditional way of fan location inside the tunnels where they impede movement of vehicles and other equipment [3].

During the last third stage, which includes fire safety assessment of the competed tunnel, dedicated tests are performed to estimate the possibility to create critical air velocity that would prevent expansion of fire gases and smoke against the ventilation airflow [1].

Tasks similar to those arising during the second and third stages of a new tunnel construction are also typical of major overhauls associated with enlargement of the tunnel sections. Considering that the number of railroad tunnels in the Russian Federation that need major overhauls is steadily increasing, the task of maintaining the specified parameters of their atmosphere is becoming particularly critical especially when the overhaul is done using vehicles and equipment driven by internal combustion engines.

It is known that during the fire tests air is delivered into the tunnels using the so-called venturi jets, i.e. fans that are located at some distance from the tunnel portals and that create a free airflow directed perpendicular to the tunnel face. Various publications provide contradictory opinions regarding the distance between the venturi jet location and the tunnel portal that will create the maximum air velocity in the tunnel. Thus, a number of researchers claim that the maximum air velocity will be achieved with the venturi jets located so that the cross-section of the jet expansion is equal to the portal section.

Our research aimed to establish a functional relationship between the venturi jet performance curves and air velocity in the tunnels. For this task, we used physical and mathematical modelling of aerodynamic processes in tunnels with a venturi jet used as the draught source (**Figure 1**).

Figure 1: Location of venturi jet in front of tunnel portal

2. PHYSICAL MODELING

Physical modeling was preceded by analysis of factors that affect the air velocity in the tunnel (U_T) when a venturi jet located outside of the tunnel is used as the draught source. The following determining factors were established: internal diameter of the fan hole (d_f), output air velocity (V_f), tunnel length (L_T), distance from the venturi jet location to the portal (L_{loc}), hydraulic diameter of the tunnel (D_T), air density (ρ_a); full aerodynamic drag factor of the tunnel (ζ_T): $\zeta_T = (1 + \xi_{ext} + \lambda_T \frac{L_T}{D_T})$, where λ_T is the friction factor; ξ_{ext} is the local drag coefficient of the tunnel intake section.

The following similarity criteria were determined for physical modelling and processing of its results using the dimensional theory: $Z_1 = \frac{8}{\pi^2} \zeta_T \frac{d_f^4}{D_T^4}$; $Z_2 = D_T/d_f$; $Z_3 = L_{loc.}/d_f$ [5].

The dimensionless air velocity in the tunnel U_T/v_f as a function of these similarity criteria can be expressed in the following way:

$$U_T/V_f = F\,[(Z_1)^x \cdot (Z_2)^m \cdot (Z_3)^n] \quad (1)$$

The performed assessment showed that for conditions of real tunnels with the lengths from 1,000 to 3,000 m, the internal diameters of 7.5 – 8.4 m and the friction factors of 0.02 – 0.033, ventilated with a free airflow created by venturi jets with the diameter of 1.6 - 2 m and located 10 - 60 m from the portal, the similarity criteria will vary within the following ranges: Z_1= (0,013-0,07), Z_2 = (3 - 5), Z_3 = (5-30).

Geometrical dimensions of the bench model were defined based on the need to observe all the geometrical similarity principles and with due account for similar structural parts of the model and the prototype. The tunnel was modelled using an acrylic plastic tube with the length $L_{T,0}$=1.5 m and the cross-section of 0.0066 m^2. The friction factor determined for a similar tube was 0.029 [2]. Given these conditions for the model with the output diameters of the venturi jet of 0.027 m, 0.03 m and 0.035 m, values of Z_1, Z_2 and Z_3 will equal 0.012 – 0.050; 2.66 – 3.35; 1.48 – 22.22 respectively, i.e. they fall within the range of values measured in real tunnels. Impellors, that are used in aeromodelling and which design is similar to the venturi jets, were used in model experiments to imitate the venturi jets that are intended for use in real conditions. The impellors were fitted with frequency converters (**Figure 2**), which helped to change the impellor rotation speed and control the output air velocity within 8 - 40 m/s.

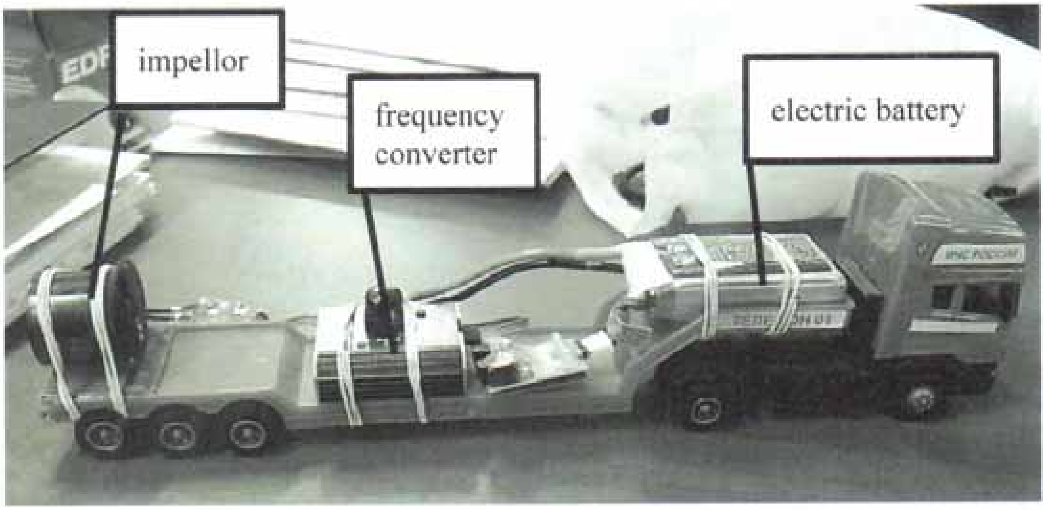

Figure 2: Layout and design of setup up for model experiments

Dependence of the air velocity at the output of each impellor type on the rotation speed was established by measuring the air velocity inside a pipe attached to the impellor and characterized with negligible aerodynamic drag.

To make sure that the similarity criteria of the model experiment match the similarity criteria of real tunnels, it was suggested that the model resistance is deliberately increased by fitting a flap at its output. Decreasing the effective section of the air flow at the model output helps to increase the full aerodynamic drag factor of the model ζ_T due to the local drag factor of the flap ξ_g, $\zeta_T = \frac{8\rho_a}{\pi^2 D_T^4}(1 + \xi_{ext} + \xi_g + \lambda_T \frac{L_T}{D_T})$.

Comparing correlations of full aerodynamic drag factor ζ_T of the models with and without flaps, we can easily derive an equation that would link the drag factor of the flap with

$$\xi_g = \frac{\lambda_T}{D_T}(L_{T,i} - L_{T,0}) \quad (2)$$

Thereby, each position of the flap at the output of the tunnel model will correspond to a specific tunnel length in terms of the aerodynamic drag.

As the air velocity in the model is essentially determined by its aerodynamic drag, we can use the model with the tunnel length $L_{T,0}$ to create air flow parameters typical of tunnels with unspecified length $L_{T,i}$ by setting the desired value of the model length and subsequently calculating value ξ_g using equation (2).

In order to find the local drag coefficient of the flap in its various positions with reference to the tunnel model cross-section, we performed simultaneous measurements of the mean air velocities in the tunnel model and loss of air pressure at the flap.

The physical modelling procedure consisted in impellor positioning at various distances from the tunnel portal in parallel with its axis and delivery of the air jet to the portal with air velocity measurement at its exit.

A heat-loss anemometer was used to measure changes in the air velocity in all experimental series, while measurements of the air pressure loss were made by a pressure differential gauge.

The measured data were processed using non-dimensional similarity criteria Z_1, Z_2 and Z_3 and were represented as a characteristic curve of the dimensionless air velocity $\frac{U_T}{V_f}$ versus argument $Y_{\text{phys.mod.}} = Z_1^x \cdot Z_2^m \cdot Z_3^n$. The x, m, n values were selected in such a way that secures the best approximation of experimental data (the correlation ratio at the statistical reliability of 0.95 was equal to 0.94) with an analytic dependence which curve is shown in **Figure 3.**

Upon transformation of this dependence with account for numerical values of the power of numbers Z_1, Z_2 and Z_3, the equation for calculation of the air velocity with a venturi jet installed in front of the tunnel portal and the air jet delivered to its cross-section will take the following form:

$$U_T / V_f = 0{,}31 \cdot Z_1^{-0{,}48} \cdot Z_2^{-1{,}63} \cdot Z_3^{-0{,}26} \qquad (3)$$

Based on the physical modelling results, a conclusion was also made that at a certain distance between the venturi jet location and the tunnel portal, the air velocity reaches its maximum. This maximum velocity decreases both with increasing or decreasing distance to the tunnel portal.

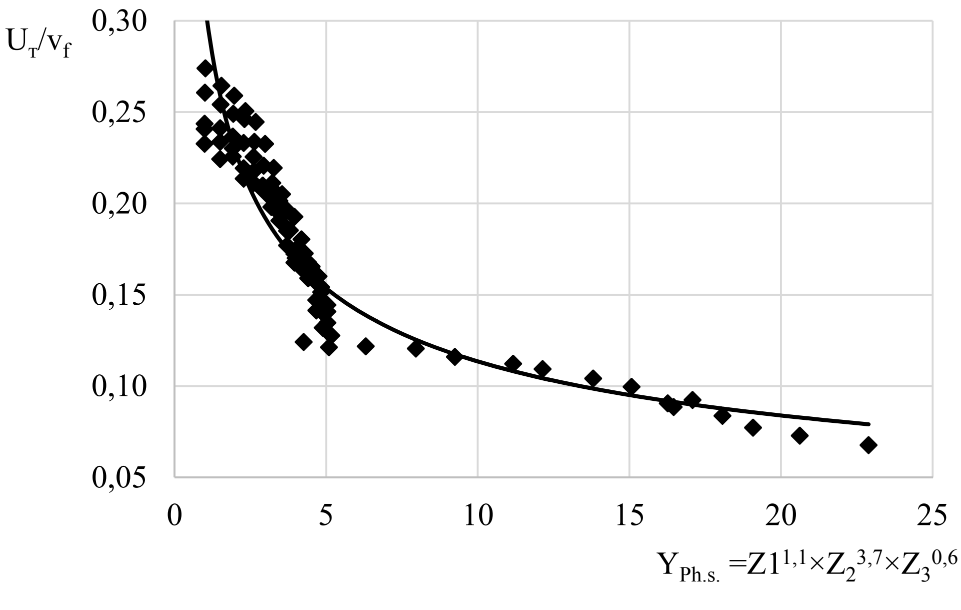

Figure 3: Dependence diagram of dimensionless air velocity versus argument $Y_{\text{ph.s.}}$

3. MATHEMATICAL MODELLING

In order to verify the physical modelling results as well as to account for the impact of natural draught ($h_{n.d.}$) that acts against the air movement, we performed mathematical modelling of aerodynamic processes taking place when a free air jet created by a venturi jet located at the tunnel portal is acting upon the air flow in the tunnel. Mathematical modelling of the aerodynamic processes was done with the Ansys CFX software package.

Similar to physical modelling, a number of scenarios were considered that take into account various aerodynamic and geometrical parameters of venturi jets located at various distances from the portal of tunnels that have different lengths.

The input data used in mathematical modelling are given in Table 1.

Table 1: Numerical values of aerodynamic and geometrical parameters used in mathematical modelling

Parameter	L_{loc}, m	L_T, m	d_f, m	V_T, m/s	$h_{n.d.}$, Pa
Numerical value	10; 25; 40	150; 320; 740; 1100; 2730	1.0; 1.6	35.6; 32.8	0; 10; 20

Calculation results for each of 64 various scenarios were presented as air velocity and pressure profiles at the tunnel entrance and during its movement through the tunnel.

Analysis of the mathematical modelling results demonstrated that moving the venturi jet closer to the tunnel portal decreases its operational efficiency due to an air recirculation zone that is created close to the portal (**Figure 4**).

The length of this recirculation zone is decreasing when the venturi jet is moved away from the tunnel portal, and tends toward zero at the distances exceeding 25 metres (**Figure 5)**. Complete stabilization and straightening of the air draught takes place at the distance of 100-120 m from the tunnel portal with the incoming air jet.

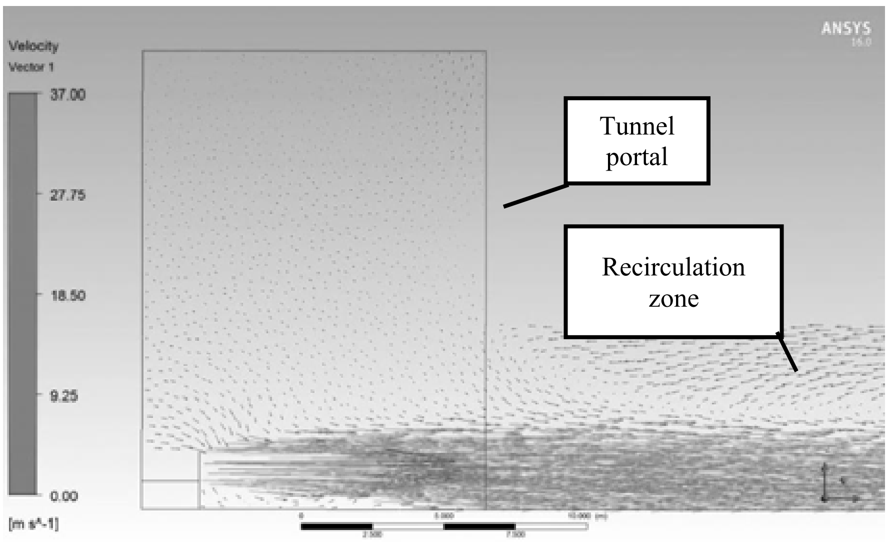

Figure 4: Air jet velocity vectors at tunnel entrance ($L_{loc.}$=10 m, d_f=1.0 m, V_f =35.6 m/s)

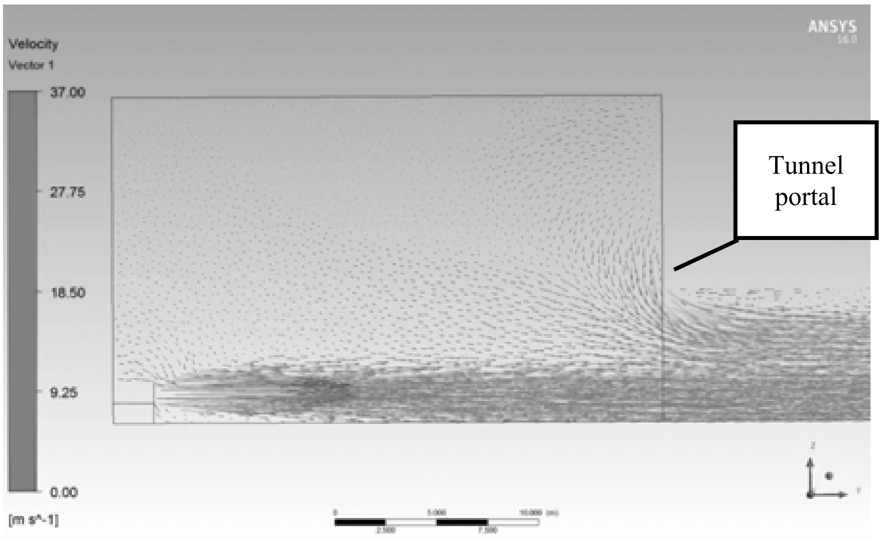

Figure 5: Air jet velocity vectors at tunnel entrance ($L_{loc.}$=25 m, d_f=1,0 m, V_f =35,6 m/s).

Results of mathematical modelling in the absence of the natural draught are given in the same format as the corresponding dependence (3) (**Figure 6**):

Their correlation with the physical modelling data (**Figure 3**) shows that the discrepancy does not exceed 15%.

$$U_T/V_B = 0{,}43 \cdot Z_1^{-0{,}60} \cdot Z_2^{-2{,}56} \cdot Z_3^{-0{,}06} \qquad (4)$$

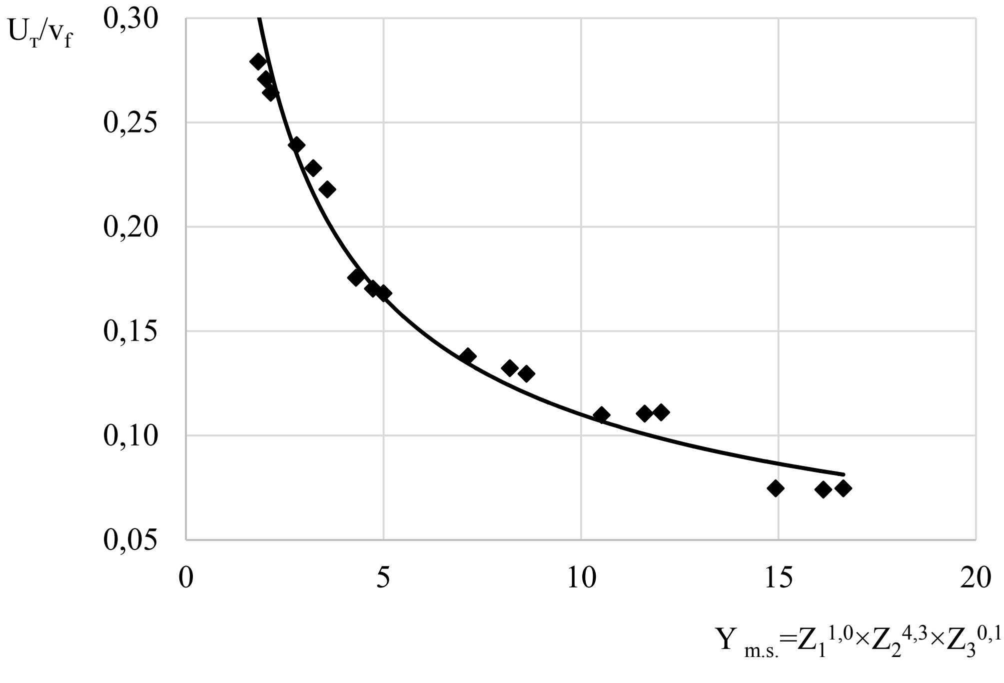

Figure 6: Dependence of dimensionless air velocity in the tunnel versus argument $Y_{m.s.}$. (in natural draught absence)

In order to assess the impact of natural draught ($h_{n.d.}$) on the air velocity in the tunnels, we performed additional mathematical modelling whereby the natural draught was taken as acting against the air stream created by the venturi jet and its value was changing within 0-20 Pa.

In processing of the mathematical modelling data, the natural draught impact on dimensionless air velocity in the tunnel was taken into consideration by introducing similarity criterion $Z_4 = h_{n.d.}/\rho_a \cdot v_f^2$.

Modelling results are given as a dependence diagram in **Figure 7**.

The dependence relative to the dimensionless air velocity in the tunnel and describing mathematical modelling results with the correlation ratio of 0.93 is as follows:

$$U_т/V_в = 0{,}087 \cdot Z_1^{-0{,}93} \cdot Z_2^{-4{,}00} \cdot Z_3^{-0{,}09} \cdot Z_4^{-0{,}47} \quad (5)$$

Use of dependences (4-5) provides a way to calculate air velocities in tunnels in a wide range of meteorological conditions as well as with account for mine technical and aerodynamic parameters of the tunnel when venturi jets located at the tunnel portal are used as the draught source.

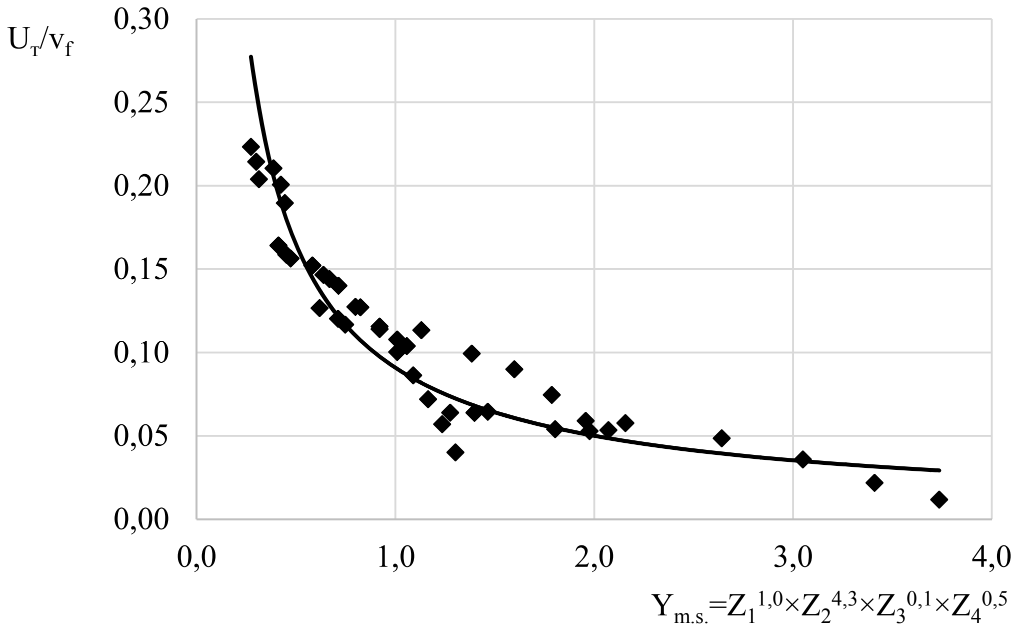

Figure 7: Dependence diagram of dimensionless air velocity versus argument $Y_{m.s.}$ (with account for natural draught)

4. CONCLUSIONS

The performed complex theoretical and experimental studies justified the possibility to use venturi jets located at the tunnel portal as the draught source for tunnel ventilation during construction and assembly operations provided a through air flow is present.

The obtained dependences render it possible to determine the aerodynamic parameters and rational location of the venturi jets with reference to the tunnel portals.

REFERENCE

1. Gendler S.G., Castañeda V.N., Belen A. G. Increasing tunnels fire safety due to use of jet fans and portal gates. See Tunnel. Promoting Tunneling in South East European Region. 41st General Assembly and World Tunnel Congress of International Tunneling and Underground Space Association ITA-AITES7 Dubrovnik. Croatia. May 22-28. 2015. pp. 240-241.
2. Gendler S.G. Peculiarities of control ventilation in the Kuznetsovsky railway tunnel. BHRg 15th International Symposium on Aerodynamics, Ventilation and Fire in Tunnels. 2013. Barcelona. Spain. pp. 309-323.
3. Gendler S.G., Sokolov V.A., Savenkov E.A. Usage pattern of jet fans for ventilation of railway tunnels. 6th International Conference «Tunnel safety and Ventilation – New Developments in Tunnel Safety. 23. – 25 April 2012. Graz University of Technology. pp. 116-123.
4. Gendler S.G., Castañeda V.N., Belen A. G. Control of natural air flow in road tunnels& International conference "Tunnel Safety Forum for Road and rail", Nice, France, 4-6 April 2011, pp. 155- 164.
5. Alabuzhev P.M., Geronimus V.B., Minkevitch L.M., Shekhovtsov B.A. Theory of Similarity and Dimensional Theory. Modelling. Moscow: Vysshaya Shkola, 1968, 206 p.

EFFECTIVENESS OF SMOKE EXTRACTION WITH SEMI-TRANSVERSE VENTILATION SYSTEMS IN SHORT ROAD TUNNEL

[1]Y. Mikame, [2, 3]M. Seike, [2]N. Kawabata
[1]Shutoko Engineering Company Limited, Japan
[2]Kanazawa University, Japan
[3]National Science and Technology Center for Disaster Reduction, Taiwan

ABSTRACT

This paper describes the effects of smoke extraction by semi-transverse ventilation systems in road tunnel fires. The adopted tunnel model was a U-shaped urban tunnel that was shorter than 500 m in length. The investigation used a CFD smoke simulation and evacuation simulation. At the Tunnel Safety and Ventilation–7th International Conference (2014), we presented factors affecting safety for users in the natural ventilation case in the same tunnel model when a tunnel fire occurred. One of the main factors was the smoke spread by natural wind at approximately 1.0 m/s, and another was the presence of a bus, which takes time to evacuate many passengers. In this paper, we determined the amount of smoke extraction needed for ensuring a safety area in a short road tunnel with semi-transverse ventilation systems. The conditions of smoke extraction volume were from 0.1 m^3/s·m to 0.5 m^3/s·m, which is based on existing tunnel extraction volumes in the Tokyo area. The results of examination in the case with a natural ventilation velocity of 1.2 m/s showed that more than 10 tunnel users were exposed to smoke from a tunnel fire. Moreover, in the case with over 0.3 m^3/s·m of smoke extraction by ventilation facilities, smoke propagation can be controlled even with existing natural ventilation, and the number of users exposed to smoke decreased from 3 persons to 0. For the case in which buses were included in the tunnel, a smoke extraction capacity of over 0.5 m^3/s·m was required to ensure a safety area in a short road tunnel. Therefore, it was confirmed that even in a short road tunnel, smoke extraction by ventilation facilities was necessary to ensure safe user evacuation from tunnel fires.

Keywords: road tunnel fire, short road tunnel, smoke extraction volume, bus

1. INTRODUCTION

At the Tunnel Safety and Ventilation–7th International Conference (2014), we described factors affecting the safety of users in the natural ventilation case and in the case of a short road tunnel fire. In this paper, we examined the effectiveness of smoke extraction in a short road tunnel and the smoke extraction volume that was necessary to ensure safe user evacuation. The adopted smoke extraction method was transverse ventilation, in which the smoke can exhaust directly to the outside. In the case of smoke extraction, ventilation method is the semi-transverse ventilation method.

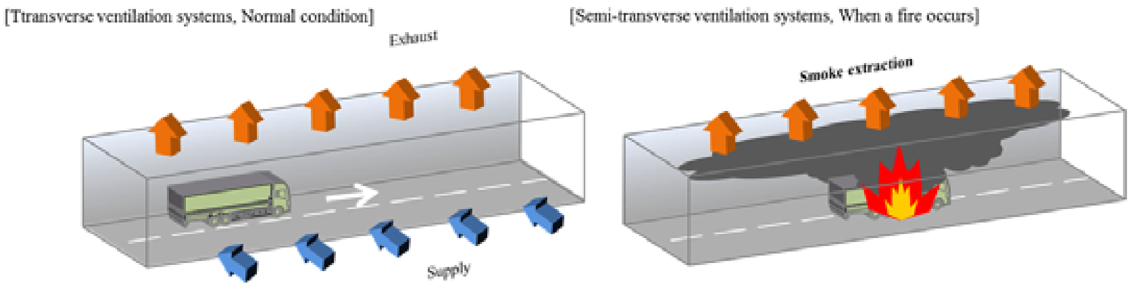

Figure 1: Smoke extraction method (semi-transverse ventilation systems).

2. EXAMINATION CONDITIONS

2.1. Simulation

The spread of smoke from a tunnel fire was simulated using an original three-dimensional simulation (fireless) [1]. This simulation was calculated partly by the authors, and the turbulence model was a large-eddy-simulation. The precision of this simulation was confirmed by comparing it with full-size tunnel experiment results [2]. This method is generally used to study road tunnel safety when a tunnel fire has occurred in Japan. To understand the simulation of the evacuation of tunnel users, this investigation used an evacuation simulation [3]. This simulation calculated the number of persons requiring help (NPRH), those who cannot evacuate for 10 minutes after the occurrence of the tunnel fire.

2.2. Specification of the model tunnel

• Tunnel length	450 m
• Cross section of the tunnel	rectangular (about 8.5 m W × 4.5m H)
• Longitudinal gradient	−4%–4%
• The computational grid sizes	0.33 m in the x-direction, 0.31 m in the y-direction, 0.23 m in the z-direction
• Number of divisions	1429 in the x-direction, 43 in the y-direction, 29 in the z-direction (includes area outside the tunnel)

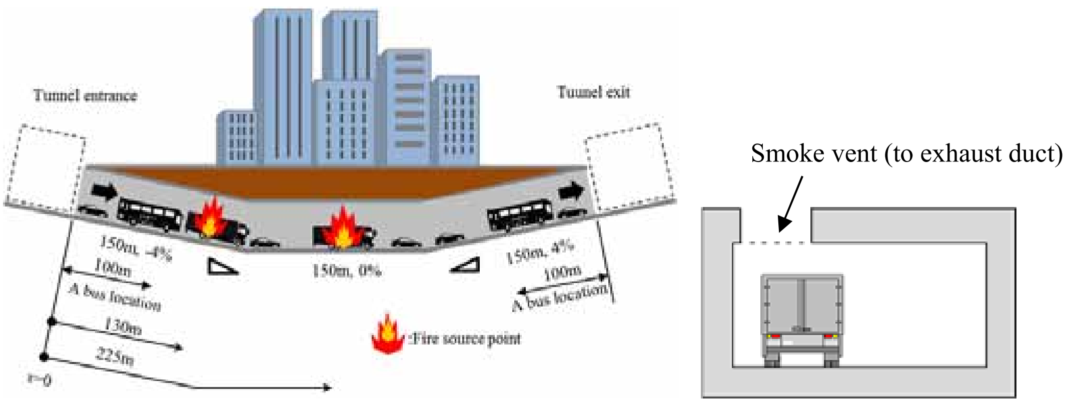

Figure 2: Outline of the tunnel model.

2.3. Tunnel fire conditions

When a fire occurs, the factors affecting the safety of tunnel users are fire source points, natural wind, and the arrangements and configuration of vehicles. The fire source points have an impact on smoke spread by the longitudinal gradient. Natural wind, which is the pressure difference between the tunnel entrance and exit for natural ventilation, causes the smoke to spread in the tunnel. The NPRH is related to the arrangement and configuration of vehicles. Table 1 shows the fire source points and pressure difference conditions. Vehicles were arranged from the tunnel entrance to the fire source point and from the fire source point to the tunnel exit. The arrangement of vehicles assumed only passenger vehicles, large-size vehicles comprised 10% of the total traffic, and a bus was included. In this paper, it was assumed that a single large-size vehicle caught fire in the tunnel. The adopted heat release rate was 30 MW, which changed over time to become constant after 480 seconds.

Table 1: Tunnel fire conditions

Category	Conditions
Fire source points	x=225 m (Sections of longitudinal gradient 0%) x=130 m (Sections of longitudinal gradient -4%)
Pressure difference between the tunnel entrance and exit for natural ventilation	0 Pa [0 m/s],5 Pa [0.85 m/s],10 Pa [1.2 m/s]

Table 2: Number of passengers (per vehicle)

	Number of passengers
Passenger vehicles	Average of 1.4 person
Large size vehicles	Average of 1.3 person
Bus	50 person

The conditions under which it is difficult for tunnel users to evacuate were defined as a smoke density greater than Cs 0.4 [1/m] and a smoke height less than 1.5 m from the road surface. The start of the evacuation of tunnel users was triggered by a smoke density of Cs 0.4 [1/m] reaching the ceiling. Users evacuated when they saw other tunnel users evacuating. The evacuation velocity distribution increased linearly from 0.9 m/s to 1.2 m/s, was constant from 1.2 m/s to 1.8 m/s, and linearly decreased from 1.8 m/s to 2.1 m/s. The direction of evacuation of tunnel users was assumed to be towards the tunnel portals.

2.4. Smoke extraction volume

The adopted maximum smoke extraction volume was 0.5 $m^3/s \cdot m$ and was based on the gradient section ventilation amount of urban road tunnels in the 1970s. In these simulation conditions, the smoke extraction volumes were at intervals of 0.1 $m^3/s \cdot m$. The smoke vents were installed in the ceiling of the travelling direction on the left lane of the vehicles. The installation interval of vents was 10 m, and their shape was rectangular (about 2.5 m × 2.0 m).

Table 3: Smoke extraction volume

Smoke extraction volume	Note
0.5 $m^3/s \cdot m$	225 $m^3/s \cdot$450 m, 500 $m^3/s \cdot$1 km
0.4 $m^3/s \cdot m$	180 $m^3/s \cdot$450 m, 400 $m^3/s \cdot$1 km
0.3 $m^3/s \cdot m$	135 $m^3/s \cdot$450 m, 300 $m^3/s \cdot$1 km
0.2 $m^3/s \cdot m$	90 $m^3/s \cdot$450 m, 200 $m^3/s \cdot$1 km
0.1 $m^3/s \cdot m$	45 $m^3/s \cdot$450 m, 100 $m^3/s \cdot$1 km

3. SIMULATION CASE AND RESUTS

3.1. Simulation case

The number of the simulation cases was 78. They consisted of a combination of the following conditions:

- Fire source point 225 m, 130 m
- Pressure difference 0 Pa, 5 Pa, 10 Pa
- Smoke extraction volume 0 $m^3/s \cdot m$, 0.1 $m^3/s \cdot m$, 0.2 $m^3/s \cdot m$, 0.3 $m^3/s \cdot m$, 0.4 $m^3/s \cdot m$, 0.5 $m^3/s \cdot m$

- Arrangement of the bus The case of no buses case and the case of including buses The bus is located 100 m from the tunnel entrance and exit.

3.2. Simulation results

Figure 3 shows the simulation results when the fire source point is 225m, in the case where a bus is included (pressure difference: 10 Pa). The left-side figure is 0.2 m^3/s･m, and the right-side figure is 0.5 m^3/s･m. For the 0.2 m^3/s･m case, the results show that there are NPRH from the 350 m section (with a bus) to the tunnel exit. The reason is that the smoke layer descends near to the road surface because of a decrease of the longitudinal flow velocity, although the smoke extraction system was operating. In the 0.5 m^3/s･m case, the results show no NPRH due to the effectiveness of smoke extraction.

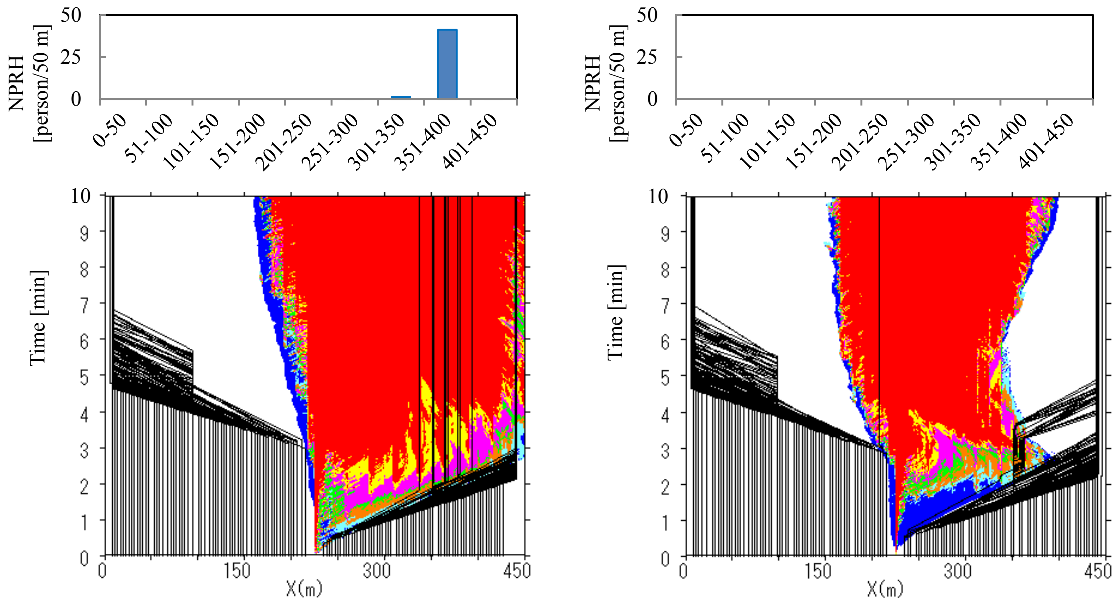

F225_10Pa_q0.2_bus F225_10Pa_q0.5_bus

Figure 3: The results of case F225, 10 Pa, q0.2, and q0.5 (cases in which a bus was included).

Table 4 and Figure 4 show a summary of the simulation results for the fire source point 225 m case. With a smoke extraction volume of 0 m^3/s･m (pressure difference 10 Pa and no bus), an NPRH of about 15 persons occurs. The NPRH is significantly reduced when the smoke extraction volume is more than 0.3 m^3/s･m. In the case where there is a bus, and the smoke extraction volume 0.3 m^3/s･m, the NPRH is about 40 persons. The NPRH is almost the same in situations in which there is smoke from a tunnel fire with and without a bus. There is little difference between the times to reach the smoke density to which the tunnel users are exposed at an arbitrary point in the tunnel. Therefore, when many passengers are riding the bus, it takes time to disembark during the evacuation, and many persons who are in the bus or getting off the bus are exposed to smoke. From these results, for the case with a bus in the tunnel and natural wind, it is effective to ensure a smoke extraction volume of more than 0.5 m^3/s･m.

Table 4: NPRH of fire source point 225m (Unit [person])

Smoke extraction volume \ Pressure difference	No bus case			Cases of including the bus		
	0 Pa (0 m/s)	5 Pa (0.85 m/s)	10 Pa (1.2 m/s)	0 Pa (0 m/s)	5 Pa (0.85 m/s)	10 Pa (1.2 m/s)
0 $m^3/s \cdot m$	0 (0 / 0)	0.537 (0 / 0.537)	14.135 (0 / 14.136)	0 (0 / 0)	26.646 (0 / 26.646)	52.432 (0 / 52.432)
0.1 $m^3/s \cdot m$	0 (0 / 0)	0.379 (0 / 0.379)	9.414 (0 / 9.414)	0 (0 / 0)	26.306 (0 / 26.306)	48.810 (0 / 48.810)
0.2 $m^3/s \cdot m$	0 (0 / 0)	0.120 (0 / 0.120)	6.169 (0 / 6.169)	0 (0 / 0)	23.985 (0 / 23.985)	42.682 (0 / 42.682)
0.3 $m^3/s \cdot m$	0 (0 / 0)	0.004 (0 / 0.004)	3.342 (0 / 3.342)	0 (0 / 0)	3.034 (0 / 3.034)	37.880 (0 / 37.880)
0.4 $m^3/s \cdot m$	0 (0 / 0)	0 (0 / 0)	1.210 (0 / 1.210)	0 (0 / 0)	0 (0 / 0)	32.503 (0 / 32.503)
0.5 $m^3/s \cdot m$	0 (0 / 0)	0.001 (0 / 0.001)	0.228 (0.124 / 0.104)	0 (0 / 0)	0.004 (0 / 0.004)	0.204 (0 / 0.204)

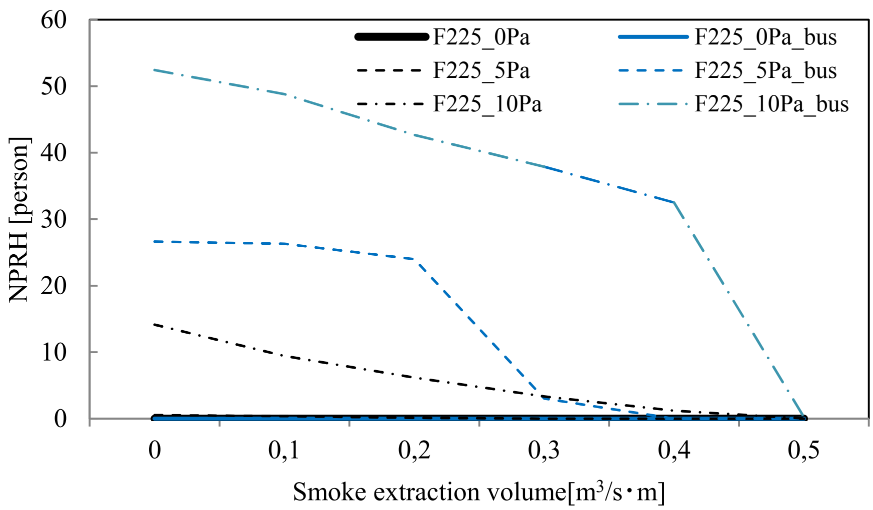

Figure 4: Results for fire source point 225m.

Figure 5 shows the simulation results for the fire source point in the 130-m case in which a bus is included (pressure difference: 10 Pa). The left-side figure is 0 $m^3/s \cdot m$, and the right-side figure is 0.5 $m^3/s \cdot m$. For the fire source point in the 130-m case, smoke backlayering and the presence of natural wind caused smoke to spread throughout the tunnel. For this reason, the people who are exposed to smoke break out on the left side of the fire source point and from the 300-m area to the tunnel exit. On the other hand, in the case with a smoke extraction volume of 0.5 $m^3/s \cdot m$, the results show the extraction volume effect on the decrease in NPRH according to the smoke extraction.

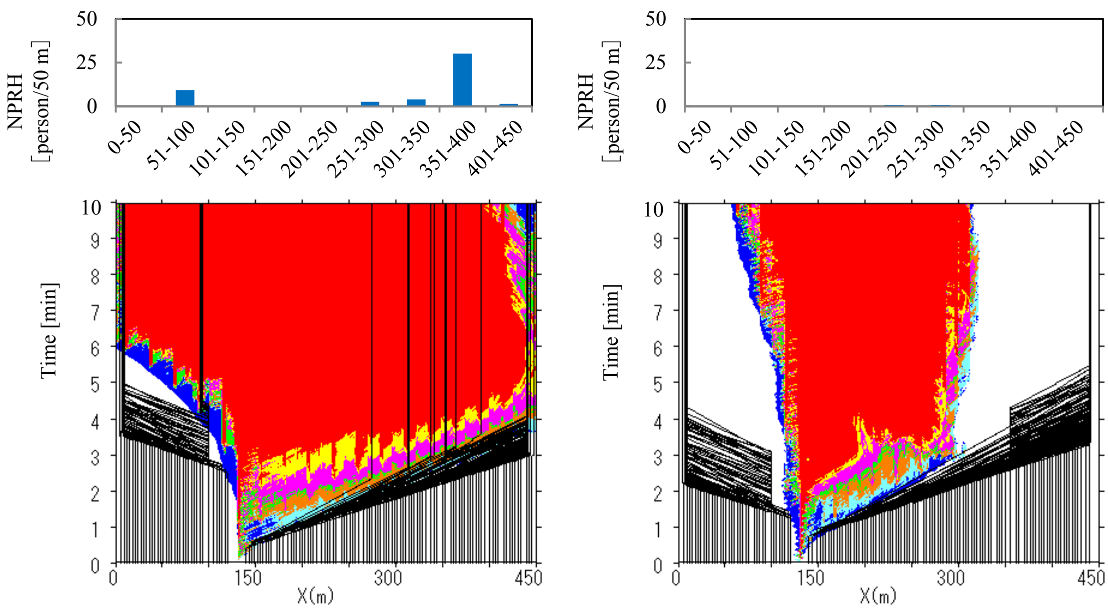

F130_10Pa_bus F130_10Pa_q0.5_bus

Figure 5: The results of case F130, 10 Pa, q0, and q0.5 (cases in which a bus was included).

Table 5: NPRH of fire source point (Unit [person])

Pressure difference / Smoke extraction volume	No Bus			Cases of including the bus		
	0 Pa (0 m/s)	5 Pa (0.85 m/s)	10 Pa (1.2 m/s)	0 Pa (0 m/s)	5 Pa (0.85 m/s)	10 Pa (1.2 m/s)
0 $m^3/s\cdot m$	0 (0 / 0)	0.032 (0 / 0.032)	10.480 (0 / 10.480)	27.661 (27.661 / 0)	24.022 (23.98 / 0.042)	47.454 (9.274 / 38.180)
0.1 $m^3/s\cdot m$	0 (0 / 0)	0.03 (0 / 0.03)	10.366 (0 / 10.366)	30.429 (30.429 / 0)	0.059 (0.024 / 0.035)	37.694 (0.009 / 37.685)
0.2 $m^3/s\cdot m$	0 (0 / 0)	0 (0 / 0)	3.277 (0 / 3.277)	30.352 (30.352 / 0)	0 (0 / 0)	20.390 (0 / 20.390)
0.3 $m^3/s\cdot m$	0 (0 / 0)	0 (0 / 0)	0.021 (0 / 0.021)	30.420 (30.420 / 0)	0 (0 / 0)	0.045 (0 / 0.045)
0.4 $m^3/s\cdot m$	0 (0 / 0)	0 (0 / 0)	0.036 (0 / 0.036)	17.084 (17.084 / 0)	0.0171 (0.0171 / 0)	0.036 (0 / 0.036)
0.5 $m^3/s\cdot m$	0 (0 / 0)	0.009 (0 / 0.009)	0.069 (0 / 0.069)	0.030 (0.030 / 0)	0.015 (0 / 0.015)	0.068 (0 / 0.068)

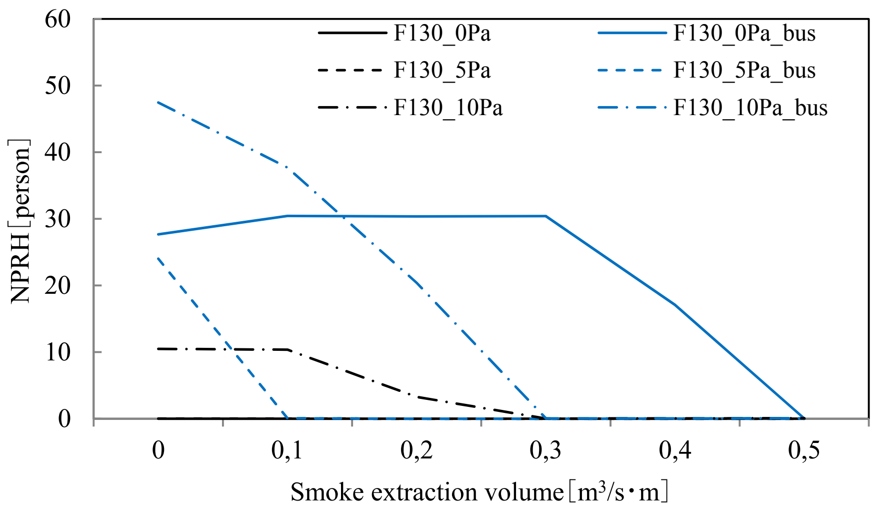

Figure 6: Results for fire source point 130m.

Table 5 and Figure 6 show the results of NPRH for the fire source point of 130 m. In these cases, the fire source point is on the tunnel entrance side. When the natural wind is weak, the NPRH increased due to factors of backlayering because of a falling gradient, and smoke extraction is in effect at smoke extraction volumes of 0.5 m^3/s・m or more. From the above results, in the case of including a bus in a short road tunnel, a smoke extraction volume of over 0.5 m^3/s・m is required to ensure safety during evacuation.

4. CONCLUSIONS

This paper derived the effects of smoke extraction in a short road tunnel fire. The users' evacuation environment was found to be much worse when natural wind (approximately 1.2 m/s) flows in the tunnel. This investigation confirmed that under such conditions, even in a short road tunnel, smoke extraction by ventilation facilities was necessary to ensure the safe evacuation of users from tunnel fires. This is especially true in the case of many passengers in a bus, in which a smoke extraction capacity of over 0.5 m^3/s·m was required to ensure a safety area in a short road tunnel.

5. REFERENCES

[1] Y.Kunikane, N.Kawabata, K.Takekuni, A.Shimoda, "Heat Release Rate Induced by Gasoline Pool Fire in a Large-Cross-Section Tunnel", 4th International Conference, Tunnel Fires, in Basel, p387-396, 2002.

[2] N.Kawabata, Y.Kunikane, K.Takekuni, A.Shimoda, "Numerical Simulation of Smoke Decent in a Tunnel Fire Accident", 4th International Conference, Tunnel Fires, in Basel, p357-366, 2002.

[3] M. Seike, N. Kawabata and M. Hasegawa, Study of Assessment of Fire Safety in a Road Tunnel by Evacuee's Behavior based on Smoke Behavior by 3-D CFD Analysis, Advanced Research Workshop Evacuation and Human Behavior in Emergency Situations, Santander, pp.111-125, 2011.

EXPERIMENT ON VELOCITY CONTROL BY A SHUTTER DEVICE INSTALLED ON TUNNEL PORTAL

K. Hatamoto, K. Horikoshi, K. Ajihara;
Hanshin Expressway Company Limited, Japan

SUMMARY

Hanshin Expressway, one of the road management companies in Japan, has been studying a system used for the purpose of reduction of longitudinal velocity and shutoff of traffic in case of a tunnel fire.

A long tunnel with longitudinal ventilation system needs a number of ventilators to suppress the longitudinal velocity to 0m/s quickly if smoke stratification generated by a fire has to be kept under control in heavy traffic or two-way traffic situations.

The presented system in this study, though a very simple method that involves closing the tunnel portal with a shutter at the entrance, would have an effect on not only the control of longitudinal velocity to 0m/s by suppression of the inertia force, but also reduction of initial and running costs with fewer ventilators.

To prevent damaging the shutter by the shock load associated with the huge inertia force, we took the measure to add a control damper system to absorb the shock load.

We confirmed through tests in an existing tunnel that the ability to suppress the inertia force on this system becomes four to five times faster than in the condition of no equipment.

In this paper, we describe the system outline and the detailed report of the performance tests.

1. INTRODUCTION

Fire operations in a long tunnel with longitudinal ventilation system in Japan usually involves one of two methods, depending on the traffic situation, to protect evacuees from fire smoke. One is a forward smoke ventilation method applied in normal traffic conditions to prevent backlayering of smoke as shown in Figure 1. The other is low velocity control(called “the zero-flow control”) applied in heavy traffic to keep the stratified flow of smoke from escaping upstream and downstream, as shown in Figure 2.

We installed the shutter device outlined in this paper on the southbound way of the Shin-Kobe tunnel measuring 8,055 meters(m) in length with a cross-section opening of 50 square meters(m^2). Hanshin Expressway operates this tunnel since January 2014 and it chronically has traffic jams of over 500 meters, due to a traffic signal near the exit portal and heavy traffic on ordinary roads connected with the tunnel. Therefore, innovative sophisticated zero-flow fire control method has been experimented on.

The conventional method of zero-flow control using ventilators such as jet fans often requires huge costs due to the installation of many sets of ventilators and large electrical power equipment. We therefore proposed a device of blockage of the airflow by a shutter-equipped inlet portal instead of a ventilator system. Although it's a very simple idea, it can reduce the airflow to 0 m/s more efficiently than with the ventilator system. In addition, the shutter will play a role in preventing secondary accidents by preventing further entries of vehicles. However, if the airflow of the tunnel is stopped suddenly, the huge inertia force would put an extra load on the shutter and there might be breakage. Hence, we introduced a control damper to the upper part of the device to regulate inlet flow as needed.

We tested this portal closing system by using a test model placed on the portal of the Shin-Kobe tunnel to examine the mitigating effect of inertia force to the shutter in the condition of controlling the damper, and we confirmed the capability of the system to reduce of longitudinal velocity in the tunnel.

In this paper, we report the schema of the portal closing system on the experimental stage, the experimental outline and the result in the field tests, and future tasks toward official operation.

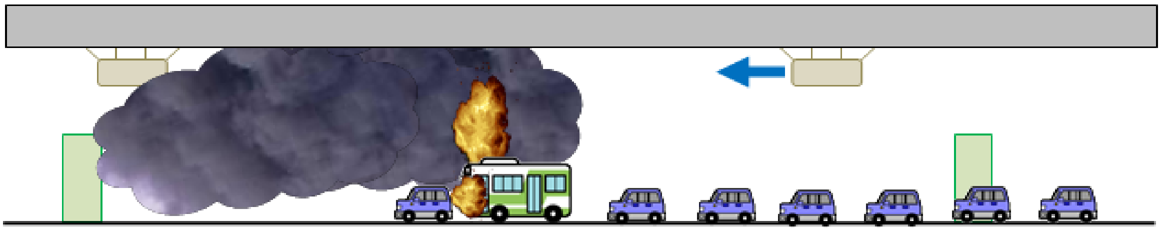

Figure 1: Outline of the forward smoke ventilation method

Figure 2: Outline of the zero-flow control

2. OUTLINE OF THE PORTAL CLOSING SYSTEM

2.1. System component

The outline of the portal closing system is shown in Figure 3.This system equipped on the inlet portal can shut off the inflow of the air and the traffic flow by the operation of closing as the situation demands. This system consists of four parts with respect to function.

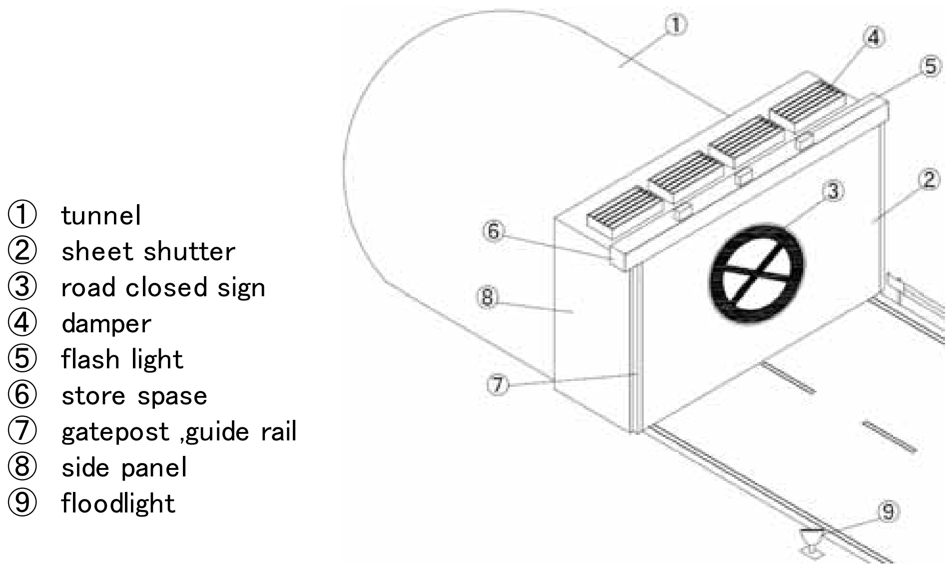

(Closed state)

Figure 3: The portal closing system

1) Opening and closing device

A rolling shutter made of a generic type of vinyl at the upper part of the system was introduced into the opening and closing device without new development. This is why we think this system can reduce cost and allow prompt provision in the event of a defect. The material of the rolling shutter is a flameproof flexible polyvinyl chloride, in consideration for impact relaxation of minor collisions, resistance to heat, lightweightness and non-adhesiveness over long duration.

The operation environment of the shutter is a longitudinal velocity of up to 8 m/s and a pressure acting on the surface of up to 80 Pa. Closing speed of the shutter can be selected from 0.3 m/s to 0.5 m/s in consideration of the safety of running vehicles and the huge inertia force.

2) Ventilation damper(Control damper)

The performance on resistance to wind is specified by wind pressure as mentioned above. However, the inertia force of air needs to be taken into consideration not only wind pressure, because the shutter is closed in the setting of longitudinal flow in the tunnel. When we consider that the tunnel has a cross section of 50 m^2 and a length of 8,000 m, the volume becomes 400,000 m^3 and the weight of the air becomes about 480 tons under the condition that the density is 1.2 kg/m^3 at 1 atmosphere and 20 degrees centigrade. Therefore, the shutter may be in danger of breaking down if the huge inertia force in the initial phase of closing loads on the shutter directly. To avoid that prospect, a ventilation damper was installed to the upper part of the device.

The damper must be operable under the velocity of 15 m/s as the specification of common ventilation dampers, be changeable according to the speed of opening and closing operation, and be operable remotely.

3) Side wall

The side space of the device between the portal and the shutter must be closed by a steel plate or a rigid concrete structure. In addition, sufficient strength is necessary to endure the huge inertia force mentioned above.

4) Alarm equipment

LED flashing lights installed on the top of the device are turned on just before closing for notifying caution to the running vehicles. Then, floodlighting that brings the closed shutter into clear view was installed as a measure to indicate the presence of the shutter to drivers at night.

2.2. Outline of operation

The operation of shutter and ventilation damper has three modes as shown in Table 1, and we choose the mode depending on the situation in the tunnel as shown in Table 2.

Table 1: Operation mode of the portal closing system

Mode	Shutter	Control damper
1	open	open
2	close	open
3	close	close

Mode 1 is a normal situation before a fire in the tunnel. If a fire breaks out in the tunnel with stationary vehicles ahead of the fire location, the system will make the shift to Mode 2 from Mode 1. This will enable us to prevent secondary accidents by the entry of vehicles, and the forward ventilation method by jet fans can be operated owing to the inflow from the ventilation damper.

When the vehicles are beyond the fire, the zelo-flow control will be activated. Although instantly changing to Mode 3 is preferable, we change to Mode 3 after changing to Mode 2, because the shutter can not close or there may be breakage by the shock load associated with the inertia force if the airflow of the tunnel is stopped suddenly by closing shutter. Therefore, we take a measure to suppress shock load to the shutter by opening the ventilation damper during the closing action of the shutter. After the shutter is closed, the ventilation damper is closed slowly. After completion of evacuation in the forward region from the fire, the mode is changed to Mode 2 from Mode 3, so that the smoke in the tunnel can be ventilated with the shutter closed.

Table 2: Operation outline of the portal closing system

state of inside of tunnel	front view	side view
Nomal time MODE1 	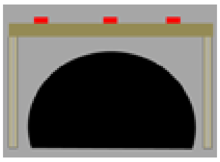	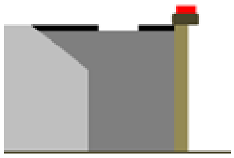
In case of fire (no traficc jam forward of the fire point) 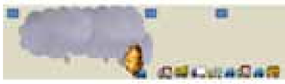	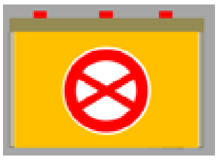	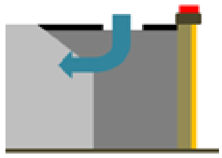
In case of fire (traficc jam forward of the fire point) MODE2 → MODE3 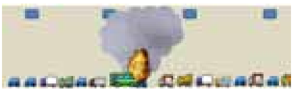	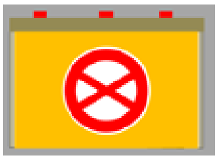	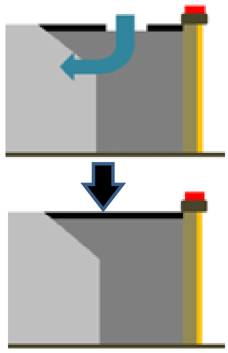
In case of fire (removed traffic jam and evacuation completed) MODE3 → MODE2 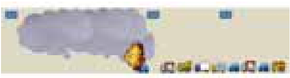	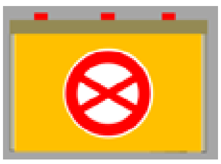	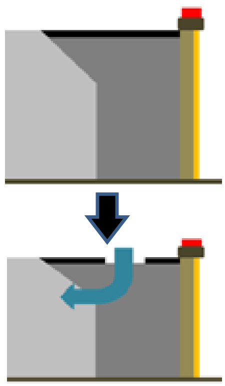
In case of fire (shutter closed at night) 	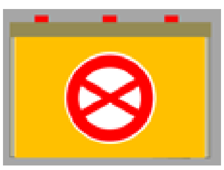	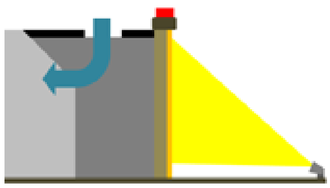

3. OUTLINE OF THE TEST

The purpose of this test is data collection to make a specification document by analyzing the velocity change, the operating conditions and the durability of the portal closing system.

3.1. Testing location

Although the portal closing system will be installed into the inlet portal of southbound on the Shin-Kobe tunnel, the system during the experimental stage was set temporarily at the exit portal of northbound on the tunnel with a 6,910 m length with a 58.8 m^2 cross-section by reason of long-term closing for construction work.

3.2. Experimental apparatus

The structure of the gate that was assembled by stock steel was tightly installed to the rigid concrete of the road shoulder of the tunnel, and the shutter was equipped on the structure of a gate. A space of the side surface of the apparatus was closed by a tough panel, and the ventilation damper was simulated by a manual control sheet that regulates opening space.

The opening space of the simulated damper was 10 m^2 while in fully open status. As for the shutter, we could not close it completely for the convenience of road structure. Consequently, about 5 of 58.8 m^2 of the cross section of the tunnel remained opened during the fully closed operation. The installed condition of the portal closing device is shown in Figure 4 ~ 6.

Figure 4: Tunnel portal(Before installation)

Figure 5: Portal closing device(Open)

Figure 6: Portal closing device(Close)

3.3. Experimental methodology

The test was conducted under the condition of mechanically-generated longitudinal velocity by six units of jet fan as shown in Figure 7.

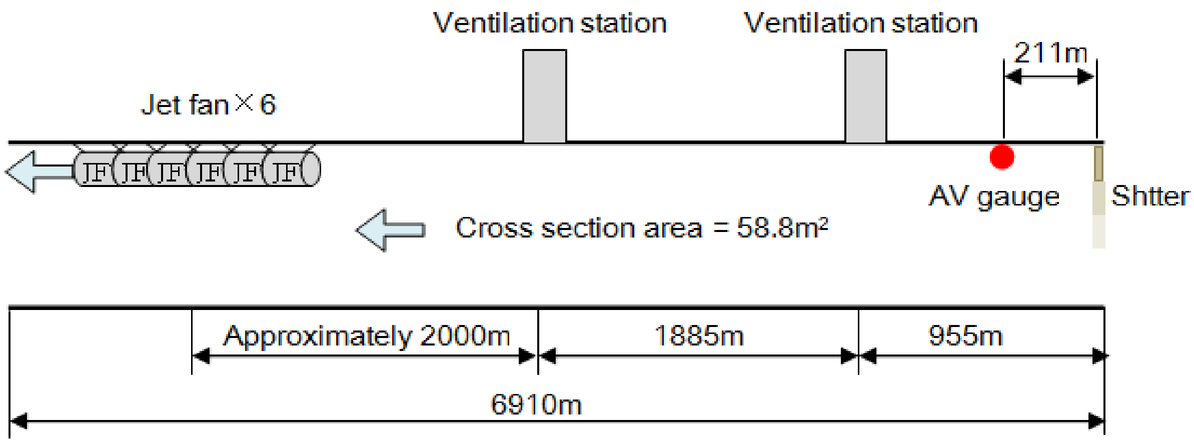

Figure 7: Schema of the test tunnel

The jet fans were stopped after checking numerical stability of the anemometer, and at this time was defined as the starting time of the test. We recorded the time variation of the longitudinal velocity on the 6 cases as shown in Table 3.

It should be noted that the closing speed of the shutter was 0.3 m/s(about 15 seconds until fully closed) in all cases. This speed was determined from the result of a study that shows that a driver can notice the shutter closing and avoid collision to the shutter.

The simulated damper started closing after the shutter closed completely except in CASE 1, CASE 2 and CASE 6. CASE 1 measured natural decrease of the longitudinal velocity without closing the shutter and the simulated damper as the comparison with the case operating the system. CASE 2 is the case that the longitudinal velocity is suppressed by the shutter only. In CASE 6, the simulated damper is closed before the starting time of the test and it is the heaviest load to the shutter.

Table 3: Test cases

Test case	State of component		Remarks
	Shutter	Damper	
CASE 1	open	open	natural decrease
CASE 2	closed at 15s	open	closed only shutter
CASE 3	closed at 15s	closed at 120s	
CASE 4	closed at 15s	closed at 60s	
CASE 5	closed at 15s	closed at 30s	
CASE 6	closed at 15s	closed	

4. TEST RESULTS

Initial velocity of the tunnel before the starting time of the test was different in all cases because of meteorological conditions and so on. Therefore, we examined the decrease rate of the velocity by using velocity ratio to the initial velocity.

The time to reach each velocity ratio in each case is shown in Table 4, and the decrease rate in each case is shown in Figure 8.

Table 4: The time that reached each velocity ratio

Test case	State of component		Velocity ratio				
	Shutter	Damper	0.8	0.6	0.4	0.2	0
			unit[sec]				
CASE 1	open	open	63	122	233	448	858
CASE 2	closed at 15s	open	33	62	117	218	411
CASE 3	closed at 15s	closed at 120s	26	49	93	177	335
CASE 4	closed at 15s	closed at 60s	25	45	80	143	255
CASE 5	closed at 15s	closed at 30s	33	52	83	132	210
CASE 6	closed at 15s	closed	25	46	83	151	273

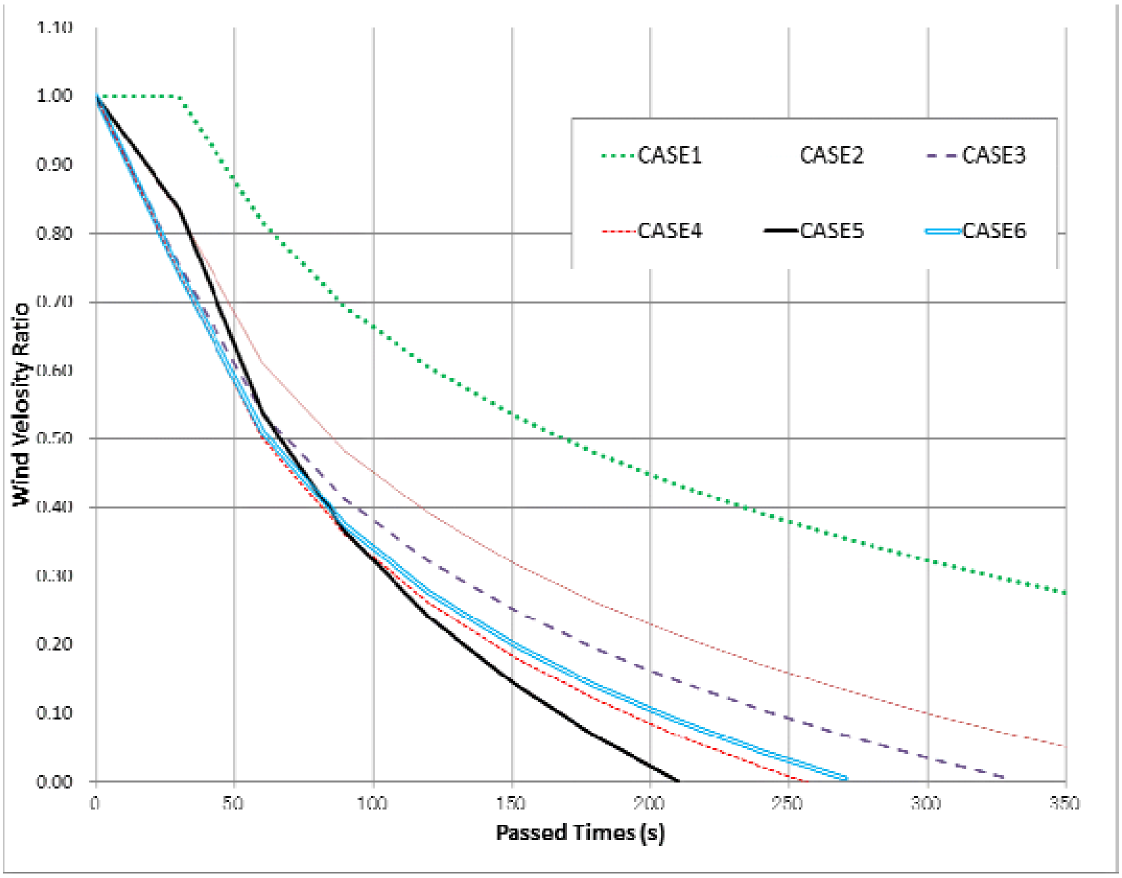

Figure 8: The decrease rate of the velocity

5. DISCUSSION OF RESULTS

5.1. Decrease trend of the velocity

In CASE 2, with the damper left open, velocity reached 0 m/s in less than half the time compared with the natural decrease as in CASE 1. From this result, the system has enough ability to reduce inertia force even with a space of 10 m^2 in the upper part the damper and 5 m^2 under the shutter test conditions.

Once the shutter was closed, the sooner the simulated damper was closed,the quicker longitudinal velocity decreased. The time to reach the ratio of 0.20, that becomes approximately 0.5 m/s in real velocity, for CASE 4 (damper closed 60s after shutter closure)and CASE 5(closed after 30s) is almost same time. The velocity decrease varied to some extent by the space of 5 m^2 under the shutter, and external factors like meteorological conditions and manual control damper need activation.

The target velocity of the zero-flow control by the ventilator is considered in the range of +/- 0.5 m/s so that the longitudinal velocity doesn't have a negative impact on the smoke layer. In addition, the standard completion time of zero-flow control by ventilators in Japan is sometimes set within 3~4 minutes as the goal. From this test result, therefore, the control of longitudinal velocity below 0.5 m/s within 3 minutes with the portal closing system would be possible when the dampers is closed within 120 seconds.

5.2. Durability of the shutter

The decrease rate in CASE 6, with the simulated damper is closed while lowering the shutter, was slow in comparison to CASE 4 and CASE 5. The reason is that the total closing speed of the shutter was slowed down by a stop in the middle of closing due to the high load caused by the inertia force acting on the sheet. Due to its materials, the shutter can resist to pressures of up to 82 Pa in normal conditions. This is too close to the operation conditions should the damper be shut from the start of the shutter closing. There is nothing wrong with the performance of the shutter in the case of CASE 2 ~ CASE 5 when the damper was opened once the shutter closed.

5.3. Installation condition of the ventilation damper

The installations conditions and the operation method of the damper are important to operate the shutter within the wind pressure of the operating limit, because a generic vinyl shutter will be introduced in the closing device.

The velocity ratio just behind the closed shutter was about 0.8, that becomes 2.2 m/s in real velocity. So, the initial velocity through the damper might reach about 8.6 m/s in consideration of the flow rate of 129 m^3/s(2.2 m/s * 58.8 m^2) and the total opening area of 15 m^2(10 m^2+5 m^2). This velocity satisfies the operational condition of the damper at less than 15 m/s.

The longitudinal velocity of the southbound in the Shin-Kobe tunnel under normal conditions is estimated to be 6 m/s. If the opening space under the shutter was 5 m^2 just like the test, the velocity just behind the closed shutter should decrease to 4.8 m/s(6.0 m/s * 0.8). In this situation, the total opening area (damper and bottom) must be over 16 m^2 (11 m^2+5 m^2) in consideration of the flow rate of 240 m^3/s(4.8 m/s * 50 m^2) and the operational condition of the damper at less than 15 m/s.

6. FUTURE TASKS

The present system can suppress the velocity ratio to 0.2(0.5 m/s in real velocity) within 120 ~ 150 seconds from the start of operation. However, time could to be shortened according to the circumstances. In addition, air tightness of the device must be improved against the longitudinal velocity caused by residual traffic flow in the tunnel after the completion of closing.

A combined use of the portal closing system and the jet fans installed for forward smoke ventilation would have a beneficial effect on the earlier suppression of the velocity.

These tasks mentioned above might be impossible to examine in the field tunnel because of decreasing chances of tunnel closures. Therefore, we will examine the suitable specifications of the system for each tunnel with the aid of numerical simulations. Also, we have to prepare the input conditions such as traffic, installation, and the opening-closing characteristics relevant to the device.

ON THE SPECIFICATION OF OPERATION MODES FOR TUNNEL VENTILATION

I. Riess, U. Welte,
Amstein + Walthert Progress AG,
Zurich, Switzerland

ABSTRACT

Tunnel ventilation systems are designed to specific goals for normal and emergency operation. The ventilation goals and the required capacity of the ventilation system are well defined. A control concept is usually within the scope of the ventilation designer, limited to the description of normal and emergency ventilation.

Depending on the complexity of the tunnel, there may be additional operation modes required inside and outside normal and emergency operation. Furthermore, in the ventilation designer's technical report, transitions between operation modes are usually not defined. If certain functionality is to be included in the control system, but not clearly defined, design decisions will be made by the software developer.

The paper gives some examples for consequences of undefined transitions between operation modes. It also demonstrates how additional operation modes (automated equipment test, dew-point ventilation, and fire with unknown location) can be handled and how transitions between the operation modes can be defined.

Keywords: tunnel ventilation, control system design, TVCS, operation mode, ventilation mode, functional specification

1. INTRODUCTION

Tunnel ventilation systems are designed to specific goals: In normal operation, adequate visibility and pollution levels must be maintained. In emergency operation, smoke propagation must be controlled in order to ensure minimum exposure and safe egress of tunnel users. After self-egress is completed, the ventilation system shall assist emergency services for assisted rescue and firefighting.

In general, the required capacity of the ventilation system and the operation both in normal and emergency mode are defined either in national design codes (e.g. RVS 09.02.31, FEDRO 13001, RABT-2015) or in project specific technical requirements.

A ventilation control concept is usually within the scope of the ventilation designer. It is part of the detailed design. It may be limited to the description of normal and emergency ventilation. Typically, this is a section of the design report that describes the operation in terms of flow rates and velocities.

In our work as designers and as specialists for integral system tests prior to tunnel opening, we find that

- depending on the complexity of the tunnel or ventilation system, there usually are additional operation modes inside and outside of normal and emergency ventilation; and
- transitions between operation modes are rarely defined.

If operation modes and transitions between them are not defined in detail, design decisions will be made during software development. In extremis, the operation of the ventilation system may not meet the design intent.

2. DESIGN CODES

2.1. Austria

The design code RVS 09.02.31 describes the requirements for normal operation and emergency operation: selection of ventilation concept, flow rate and air velocity, various boundary conditions to be applied to ventilation design. Section 7 of the code is dedicated to operation and control. The RVS requires an automated ventilation control system for normal operation and emergency operation. It shall always be possible to control the ventilation system by manual override of the automated system.

The RVS refers to the following operation modes: Normal Automatic, Normal Semi-Automatic, Emergency Automatic, Manual Operation, Maintenance Operation, and Revision. Some transitions between operation modes are specified: For the transition between Normal Automatic to Manual Operation, the settings of fans and dampers are frozen until a new manual control signal is sent.

For the transition from normal ventilation to emergency, a time limit is defined: 5 min (longitudinal ventilation) or 10 min (smoke extraction) from alarm, the air flow in the tunnel has to be as required according to the ventilation concept.

2.2. Switzerland

The design code FEDRO 13001 also gives the requirements for normal and emergency ventilation: flow rate, air velocity and boundary conditions for the design. More details on ventilation control are given in the FEDRO 23001 documentation of operation and safety equipment. The ventilation system is controlled automatically in normal and emergency ventilation. It shall be possible to change the ventilation operation by manual intervention.

For new or refurbished tunnels in the Swiss national road network, the ventilation control system functional specification forms part of the detailed design documentation. Without this document, a tunnel project will not be approved by the Federal Road Administration.

2.3. Germany

The design code RABT-2015 describes the ventilation requirements for normal and emergency ventilation: selection of ventilation concept, flow rate and air velocity, various boundary conditions to be applied to ventilation design. In general, the ventilation system is controlled automatically.

In normal ventilation, a time/date-program shall be included. In emergency ventilation, it shall be possible to change the ventilation operation by manual intervention according to the requirements of emergency services.

For the transition from normal ventilation to emergency, a time limit is defined: 60 s from alarm, all fans and dampers have to operate as required by the emergency ventilation.

3. OBSERVATIONS

3.1. Undefined transition

Operation modes for normal and emergency ventilation are clearly defined, but the transition from automatic fire location to manual override by the operator remains undefined.

Prior to tunnel opening, the functionality of the tunnel ventilation control system is being tested from the tunnel control centre. The fire alarm is simulated coming from the fire detection system. The normal ventilation is stopped. Emergency ventilation is started; jet fans are selected correctly according to their priority. Within the required period of 5 min, the longitudinal air flow is controlled to the required air flow velocity.

Then, the operator changes the fire location from one fire sector to the adjacent one. The change is minor, it is expected that the new fire section is visualised on the screen, but the ventilation system continues to operate, possibly changing the operation of a single jet fan.

Surprisingly, the ventilation is switched off completely. When all the jet fans are off, the emergency ventilation starts again, jet fan by jet fan, until the same setting of jet fans is reached as before the manual intervention. Within the required period of 5 min, the longitudinal air flow is controlled to the required air flow velocity.

What went wrong?

The emergency ventilation program includes the transition:

fire alarm > stop normal ventilation > start emergency ventilation > control air velocity

Without detailed requirements, the software engineer developed the code by the procedure that requires minimum effort: copy and paste. As a consequence, a change from any operation mode into emergency ventilation causes the ventilation to switch off and then to re-start.

Following the tests, the control system is adjusted to the new requirement for the transition and tested again. Now following a manual selection of the fire sector, the transition is limited to the differential of the current state and the new operation mode. This way, a fast and smooth transition is ensured. The software change is minor. The system passes the second test and the tunnel is opened on schedule.

3.2. Operation mode added to defined specifications

The ventilation engineer defined the modes for normal and emergency ventilation including transitions, but later a manual switch panel is added. The panel is located at the tunnel portal, available to emergency services. It has highest priority, with or without fire alarm.

As a design requirement, the switch panel allows the manual change from any operation mode into the ventilation program for emergency operation (automatic control or pre-defined settings) without issuing a general fire alarm. A fire alarm would cause the tunnel to be closed for traffic. The functionality is requested by the emergency services in order to match their fire intervention plan. Furthermore, it allows manual ventilation tests and training while the tunnel is open to traffic.

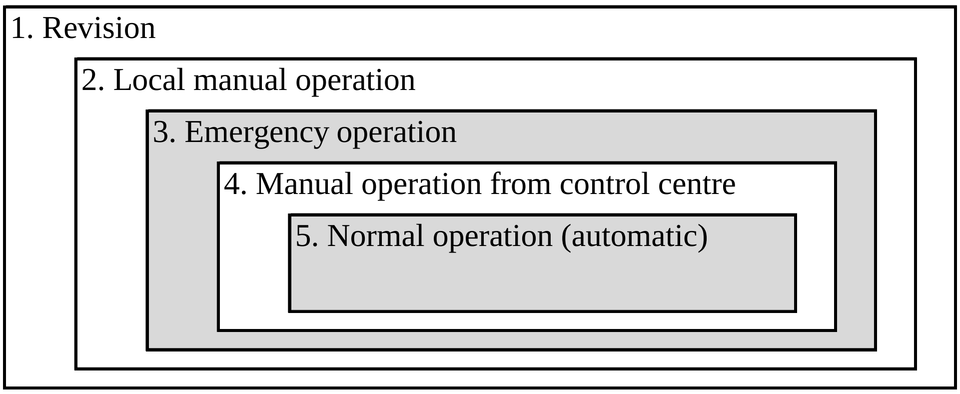

Figure 1: Simplified definition of operation modes with priority

Figure 1 shows the priorities of the ventilation operation modes. In the ventilation control specification, the operation modes were defined with the relevant transitions. The interface with the switch panel was not included.

The switch panel allows an immediate change from operation mode 5 into mode 3 without fire alarm.

However, the ventilation control specification requires a reset of the fire alarm issued from the control center, before the transition from mode 3 to mode 5 is possible. As the emergency operation has been started from the switch panel, there is no fire alarm. Without the reset, the control system remains stuck in emergency ventilation - a dead end.

The issue can be solved by introducing a new operation mode above mode 3 with similar functionality but different requirements for the transition to operation modes 3 to 5. The software is developed to match the ventilation designer's and the emergency services' functional requirements.

3.3. General specifications

The ventilation control system must be realised according to…

For a tunnel project, the design is verified and approved by the authorities. There is a tender for the safety equipment delivery and installation. For pricing, the detailed design documentation is included as an appendix to the tender documents. The ventilation design report is provided including a brief description of ventilation operation in normal and emergency modes.

And there is a separate report with the functional specification of the ventilation control system. It includes one sentence:

> "The ventilation control system must be realised according to *Design Code XY*."

We do not know if and how the control system is developed and how it is tested during commissioning. After contract award, the supplier has to employ a ventilation specialist for the definition of the required functionality - hopefully.

4. OPERATION MODES

The definition of operation modes depends on project requirements (e.g. design code, safety concept, alarm plan, intervention strategy), on the available information (air-quality and air-flow monitors, detection systems for traffic and fire) and on actors (fans, dampers). Each operation mode is described in detail in the control system specification.

Figure 2 gives an example of how operation modes for a road tunnel can be summarised with their priorities. The priority defines which ventilation operation takes precedence in a certain situation. For example, if an egress door is opened, operation mode 6 is started. Then, an increased CO level will not cause additional jet fans to start as required under operation mode 12.

The figure serves only as an example. A tunnel may require the definition of additional operation modes. Some modes shown here may not be required elsewhere.

In normal operation, it is useful to include a time/date program (mode 10 in Figure 2) for automated tests of ventilation equipment, especially when fans and dampers are rarely used under normal traffic conditions.

Dew-point ventilation (mode 11) is a special operation mode that aims at avoiding wind-screen fogging for vehicles entering the tunnel under certain temperature-humidity conditions.

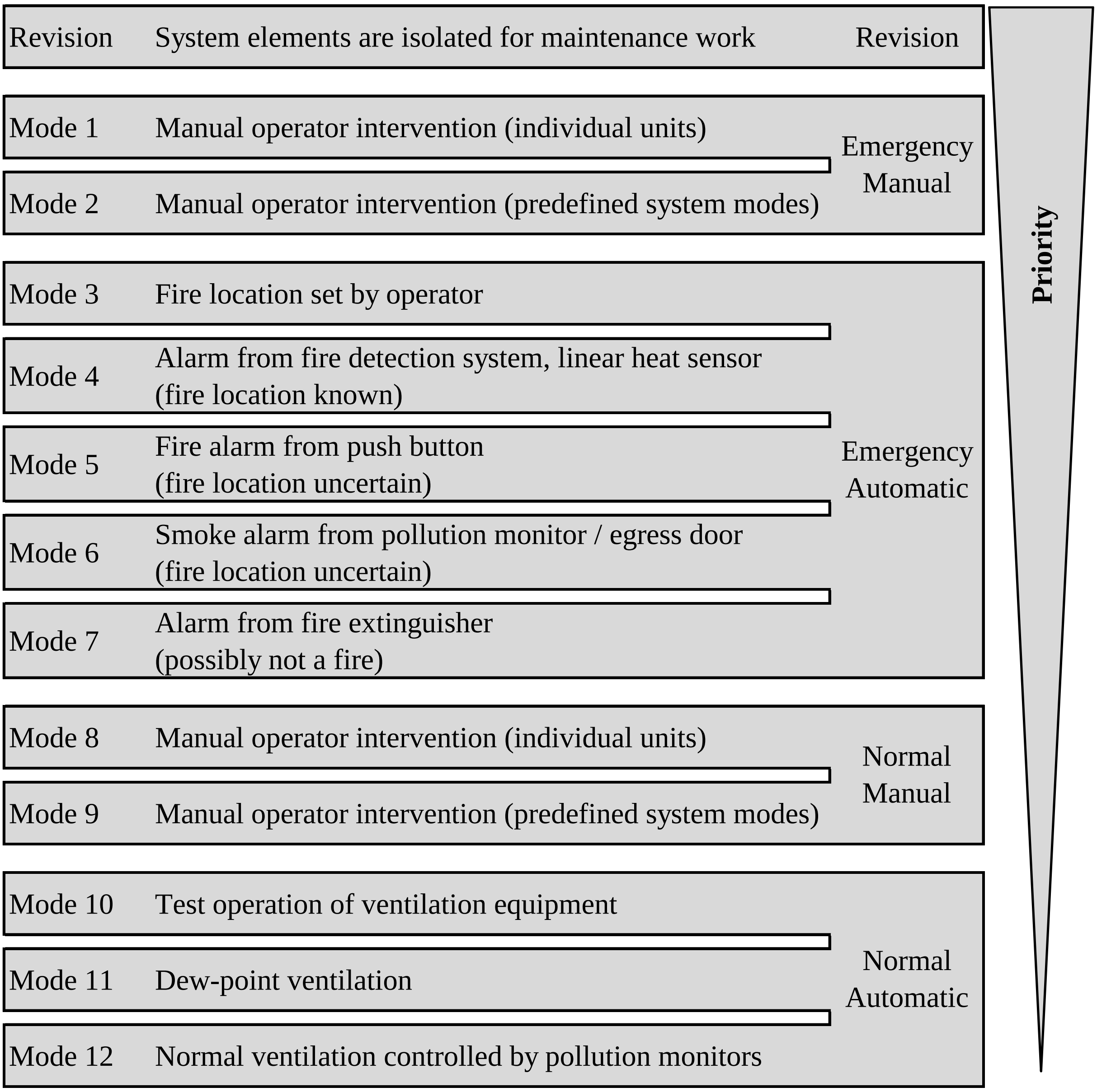

Figure 2: Operation modes for normal and emergency ventilation with priority

It is reasonable to give a dew-point ventilation higher priority than normal ventilation (mode 12). It usually requires very large air-flow rates, thereby ensuring sufficient pollution dilution.

However, it can be argued to give system tests (mode 10) lowest priority. The way it is described in Figure 2, during system tests some ventilation equipment may not be available for pollution dilution and for dew-point ventilation.

In all modes of Normal Automatic and Normal Manual, the system is prepared to switch into Emergency Automatic or Emergency Manual (higher priority).

In Emergency Automatic, several operation modes are defined. For some ventilation concepts, the system reaction depends on the available information. Past experience has shown: when an alarm is issued that a fire extinguisher is removed from the SOS box, it is likely that there is no fire at all. Probably, the extinguisher is about to be stolen. But still the control system has to respond as there is a pedestrian in the tunnel - and there might be a broken down vehicle or a fire.

For a local smoke extraction, the fire location is an important parameter. When a fire push button is triggered, the fire location is uncertain. For fire extinguisher removal and for a push button alarm, it may not be useful to start smoke extraction immediately. However, the system shall not remain in normal operation, possibly requiring an increased longitudinal air flow.

Most operation modes are defined for the ventilation system. In this example, modes 8, 1 and revision are defined for individual fans or dampers. The ventilation system remains in the operation mode at lower priority.

It is not the intention to go into more detail here on operation modes and their priorities. The point is; the definition of the ventilation operation requires design decisions. If the decisions are not made by the ventilation designer, they will be made by the software developer. And design decisions shall be made during detailed design or with the control system specification. They shall not be made during software development - or during system commissioning.

5. TRANSITIONS BETWEEN OPERATION MODES

Table 1 gives an example of how the transition between operation modes can be defined. Again, the table shall only serve as an example. If the operation modes (revision and mode 1 to mode 12 in Figure 2) require different transitions, the table could be extended to include all possible transitions.

Table 1: Transitions between operation modes

Transitions	Revision	Emergency Manual	Emergency Automatic	Normal Manual	Normal Automatic
Revision		Type C	Type C	Type C	Type C
Emergency Manual	Type D		Type 0	Type 0	Type C[1]
Emergency Automatic	Type D	Type A		Type 0	Type C[1]
Normal Manual	Type D	Type 0	Type B		Type C
Normal Automatic	Type D	Type 0	Type B	Type A	

1: The transition requires a reset of the fire alarm

Type 0	The transition is not possible
Type A	The actor or the actors remain in the current state, until the new ventilation regime requires a change.
Type B	The operation of the actor or the actors is defined in the detailed description of the operation mode, see section x.x
Type C	The actors are switched off before the new operation mode becomes active.
Type D	When being switched into "revision", the actors are isolated from power supply. The remaining actors continue to operate according to the current operation mode.

In this example, some transitions have been excluded (Type 0). For example: the operator shall not be allowed to switch directly from Emergency Manual into Emergency Automatic. It is expected that the control algorithm for the longitudinal air flow in Emergency Automatic modes requires stable initial conditions. If there is a project requirement that any transition shall be possible, this will lead to a different control system design.

The specification in Table 1 does not allow a transition from Normal Automatic into Emergency Manual. Such a transition would be similar to the requirement of the switch panel described in section 3.2. For a real fire scenario, it is preferred to have the operator switch into Emergency Automatic by selecting a fire section.

Some transitions may be too complex to be specified as a generic transition in this table. Then, the table may include a reference to a more detailed description elsewhere in the document.

Again, the definition of the transitions between operation modes requires design decisions. These shall be made during detailed design or with the control system functional specification. They shall not be made as part of the software development.

6. VENTILATION CONTROL SYSTEM FUNCTIONAL SPECIFICATION

As a minimum, the tunnel ventilation control system functional specification shall include the following items:

1. Brief description of tunnel and ventilation concept
2. Summary of actors (fans, dampers) with data points
3. Summary of sensors (air-flow and air-quality monitors, smoke detection if connected to the ventilation control system) with data points
4. Interface to other sub-systems (data points, reference to tunnel reflexes)
5. List of operation modes including their priority (see Figure 2)
6. Table and description of transitions between operation modes (see Table 1)
7. Detailed functional description of each operation mode
8. Functional description of each type of actor including alarms ("How to start a fan.")
9. Evaluation methodology for sensor data ("How to check air-flow measurements for plausibility.")

In order to assess the required level of detail, we recommend the reference reports (Musterlastenheft) published by Asfinag (2016 a, b).

7. CONCLUSIONS

The observations can be summarised:

- For the functionality of the ventilation system, the control system is just as important as the correct selection and installation of air-quality and air-flow monitors, fans and dampers.
- The specification of operation modes and of transitions between operation modes requires design decisions.
- If the control system functional specification is ambiguous or if something is not specified, design decisions will be made during software development, with or without involvement of the ventilation designer.

As a tunnel owner, you will get what you're asking for. It is preferable to take care that the "Tunnel Ventilation Control System Functional Specification" forms part of the ventilation designer's scope for the detailed design.

There are different ways to ensure that the design is developed as required:

- The Austrian approach: Requirements for the tunnel ventilation control system are specified in the design code RVS 09.02.31. This requires significant detail to a section dedicated to the control system. And the definition in a design code may not be suitable for all tunnel projects.
  We believe the RVS will require further detail on the control system. And we recommend a review by an independent expert. Today, the review of the ventilation control system is done with the safety evaluation just before the tunnel opening. This may be too late for significant improvements.
- The Swiss approach: The "Tunnel Ventilation Control System Functional Specification" is required as part of the detailed design documentation. Therefore, it is subject to the project approval.
  Currently, there appears to be no procedure defined for the review of the ventilation design. In some projects, a review is done by an independent expert. But it is still within the responsibility of the authority's project director if an external reviewer shall be appointed.

8. REFERENCES

Asfinag, (2016 a) Tunnel-Lüftung, Musterlastenheft Lüftungssteuerungskonzept Längslüftung, PLaPB 800.542.1602

Asfinag, (2016 b) Tunnel-Lüftung, Musterlastenheft Lüftungssteuerungskonzept Querlüftung, PLaPB 800.542.1603

FEDRO, (2008) Richtlinie Lüftung der Strassentunnel, Systemwahl, Dimensionierung und Ausstattung, Bundesamt für Strassen, 13001, Ausgabe 2008

FEDRO, (2015) Betriebs- und Sicherheitsausrüstungen, Fachhandbuch BSA, 23001, Februar 2015

FGSV, (2015) RABT - Richtlinien für die Ausstattung und den Betrieb von Strassentunneln, Forschungsgesellschaft für Strassen- und Verkehrswesen, Entwurf Juni 2015

FSV, (2014) Richtlinie Tunnelausrüstung, Belüftung, Grundlagen, RVS 09.02.31

MODEL BASED DYNAMIC FEEDFORWARD CONTROL OF LONGITUDINAL TUNNEL VENTILATION

[1]N. Euler-Rolle, [1]C. Bammer, [2]M. Reinwald, [1]S. Jakubek

[1]TU Wien, Austria
[2]ASFINAG Bau Management GmbH, Austria

ABSTRACT

When a fire is detected in a road tunnel with longitudinal ventilation, a predefined air flow velocity has to be achieved by adequately controlling the installed jet fans. As a non-linear extension of common linear feedback control strategies, in this paper a model based dynamic feedforward control law is proposed. The design of the feedforward control part is based on feedback linearization of an analytical non-linear zero-dimensional model of the air flow in the tunnel. By its incorporation an improved closed loop behaviour is achieved. In the initial transient phase after detection of a fire in the tunnel, the flow velocity is required to be brought into its target range without significant overshoot and within a required time interval. As the dynamics of the air flow in road tunnels strongly depend on the tunnel length, short tunnels with longitudinal ventilation systems pose a challenging control task even if the jet fans are equipped with frequency converters. Application results of the St. Ruprecht tunnel on the Austrian Semmering motorway S6 are shown to demonstrate the practical applicability.

Keywords: non-linear control, tunnel ventilation, feedforward control, jet fan control

1. INTRODUCTION

In the course of new constructions or refurbishments of road tunnels, increasingly tight safety requirements have to be satisfied in terms of equipment, but also with respect to its operation. Nearly all of the safety facilities are designed to protect life and health of the tunnel users. Particularly in the event of an incident with fire and smoke spreading in the tunnel, adequate safety measures have to be taken without delay. For this purpose, tunnels exceeding a certain minimum length are equipped with ventilation systems to reduce the concentration of toxic fumes and guarantee a minimum amount of time for persons in the tunnel to safely follow the escape routes with sufficient visibility available. However, since the spread of smoke in the tunnel cannot be measured, a simplifying assumption is used to control the ventilation system. In tunnels with longitudinal ventilation only, a safe condition is achieved by maintaining an average air flow velocity in the tunnel, which is high enough to convey smoke out of the tunnel, but not too high not to destroy the naturally occurring smoke layering. Especially the latter is less a question of technical equipment, but rather a feedback control task.

In the literature, contributions dealing with advanced control methodologies for tunnel ventilation control are scarce. Furthermore, the focus is mainly on normal operation, where objectives for air quality criteria have to be achieved or an energy and wear-optimal control of fans is required. Bogdan et al. [1] developed a static feedforward control for the number of necessary jet fans and combined it with fuzzy control to meet the air quality limits. Another contribution to the refinement of a tunnel model used for control is made by Jang and Chen [2]. They examine the effect that the momentum on the air flow is not only determined by the number of vehicles alone, but also by their clustering pattern. A grouping algorithm was developed to detect traffic patterns and their effect on the flow velocity.

In contrast, in this manuscript a dynamic flatness-based feedforward control approach is presented. Feedback linearization is applied to the analytic zero-dimensional model of tunnel air flow and the resulting input transformation is used as model inverse to feedforward control the rotational speeds of the jet fans. Originally, the concept of feedback linearization has been introduced by Byrnes and Isidori [3] for the first time. Basically, a non-linear differentially flat system is linearized exactly by using a non-linear coordinate transformation such that the resulting transformed system consists of an input transformation and linear external dynamics.

Usually, classic linear feedback controller design is merely based on an operating point linearization of non-linear differential equations, which result from physical whitebox modelling of the plant. However, to improve the dynamic closed-loop behaviour especially in the initial transient phase of the emergency ventilation program, non-linear control methodologies can be applied beneficially. As such, a dynamic flatness-based feedforward control is designed as a non-linear extension of common feedback control strategies.

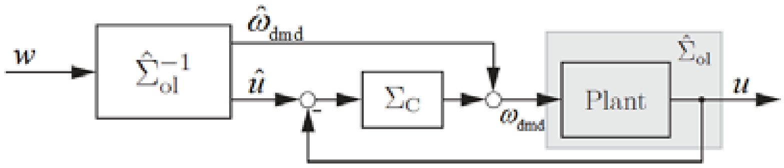

Figure 1: Two-degrees-of-freedom control scheme

In **Figure 1** the so called two-degrees-of-freedom control scheme is depicted. It combines feedback Σ_C and feedforward control $\hat{\Sigma}_{ol}^{-1}$ so that requirements on the reference trajectory tracking can be separated from requirements on robustness and disturbance attenuation. Thus, the design of the feedforward part and the feedback part are independent of each other. In the combined control scheme, based on the desired trajectory $w(t)$ of the flow velocity $u(t)$ (controlled variable), the feedforward part generates a model-based required control signal $\hat{\omega}_{dmd}(t)$ denoting the normalized demanded rotational speed of the jet fans. This feedforward control signal is added to the control signal of the correcting feedback control. Additionally, that feasible flow velocity trajectory $\hat{u}(t)$, which will be achieved by applying the feedforward control signal $\hat{\omega}_{dmd}(t)$ to the jet fans, is calculated and passed to the control loop as reference. If parameter uncertainties or model errors occur in the open loop plant model $\hat{\Sigma}_{ol}$ and in the feedforward control $\hat{\Sigma}_{ol}^{-1}$, respectively, the feedback part will still track the desired trajectory, try to compensate for the inaccuracies and improve control performance.

After a short description of the used model in the next section, the basic concept of feedback linearization and its application to the tunnel model is shown in Section 3. Finally, the proposed feedforward control has been implemented and tested in the Semmering motorway tunnel St. Ruprecht in Austria. The results are presented in Section 4.

2. MODEL OF TUNNEL AIR FLOW

In the literature, different approaches to the modelling of the air flow in road tunnels exist. These models usually do not focus solely on an event with fire and smoke, but in many cases treat the normal tunnel operation. Both situations impose special requirements on the ventilation system, which are regulated by [4] and [5] in Austria. Also the concepts of control usually focus either on one or the other case, and are specifically designed for their intended application. In general, the same fact holds for the underlying models. A brief introduction into modelling can be found in [6], where an overview of possible methods for the design and validation of tunnel models is given.

Since in ventilation control the average flow velocity is considered only and spread of smoke or heat release are not treated directly, the application of a zero-dimensional model is sufficient. Thus, the tunnel is considered as concentrated system without spatial extension. All quantities must represent average values, either over the cross section (such as e.g. the flow velocity) or the length of the tunnel (such as e.g. the density). In this modelling approach all the relevant sources and losses of momentum can be taken into account. A density change due to pressure differences is not considered, whereas a density change due to the temperature can be included in the model. From the zero-dimensional approach, it follows that the density of the air in the tunnel is only a mean value, which represents a severe limitation in case of fire. It should therefore be further assumed that the considered model applies to a cold state with moderate temperature gradients only, although temperature differences could be incorporated into the model e.g. by buoyancy. There exist approximation formulas how the average temperature can be determined during a fire [4].

The dynamic behaviour of the flow velocity $u(t)$ is described by the incompressible unsteady Bernoulli equation yielding a non-linear ordinary differential equation of first order

$$\frac{\mathrm{d}u(t)}{\mathrm{d}t} = \sum_{i}^{n_{\mathrm{JV}}} k_{\mathrm{JV},i} v_{\mathrm{JVmax},i}^2 \,|\,\omega_i(t)\,|\,\omega_i(t) \left(1 - \frac{u(t)}{\omega_i(t) v_{\mathrm{JVmax},i}}\right) - k_{\mathrm{Fric}} u(t)\,|\,u(t)\,| + \sum_{j} \frac{\Delta p_j(t)}{\rho L}\,. \tag{1}$$

The first sum describes the effect of the jet ventilators on the flow velocity. Each ventilator with index i is characterised by its maximum average outlet velocity $v_{\mathrm{JVmax},i}$ and by the factor

$$k_{\mathrm{JV},i} = \frac{1}{L} \frac{A_{\mathrm{JV}}}{A_{\mathrm{Tunnel}}} k_{\mathrm{e}} \tag{2}$$

with L describing the tunnel length, A_{JV} the cross sectional area of the ventilator, A_{Tunnel} the cross sectional area of the tunnel and k_e a correction factor considering the installation situation of the ventilator. The dimensionless rotational speed $\omega_i(t)$ of jet fan i represents the ratio of the momentary to the maximum rotational speed. If a frequency converter is available, $\omega_i(t)$ can take any value between zero and one, otherwise only zero and one exactly.

The second term in (1) characterizes the wall friction as well as flow losses decelerating the air flow. The factor

$$k_{\mathrm{Fric}} = \frac{1}{2L} \left[\frac{\lambda L}{D_{\mathrm{hydr}}} + \zeta_{\mathrm{E}} + 1 \right] \tag{3}$$

incorporates the hydraulic diameter D_{hydr} of the tunnel, the wall friction coefficient λ and the factor ζ_{E} describing influx losses. Any additional influences such as the stack effect, vehicle movement, wind load on the portal or metrological pressure differences are included in the last sum term in (1) in form of equivalent pressure differences $\Delta p_j(t)$. Therein, the air density in the tunnel is denoted by ρ.

To represent the dynamic relation between the control signals of the jet ventilators $\omega_{\mathrm{dmd},i}(t)$ and the momentary dimensionless rotational speeds $\omega_i(t)$, which determine the momentary thrust, a first-order low-pass behaviour with appropriate time constant τ_{JV} is assumed

$$\frac{\mathrm{d}\omega_i(t)}{\mathrm{d}t} = \frac{1}{\tau_{\mathrm{JV}}} (\omega_{\mathrm{dmd},i}(t) - \omega_i(t))\,. \tag{4}$$

Although measurement dynamics are not considered in the feedforward controller design, their consideration is necessary when designing the feedback controller. Otherwise, a dead time or any other delays could significantly deteriorate the closed loop performance. For further considerations, (1) and (4) are formulated as non-linear state space system of the form

$$\begin{aligned}\frac{\mathrm{d}\boldsymbol{x}(t)}{\mathrm{d}t} &= \boldsymbol{f}(\boldsymbol{x}(t)) + \sum \boldsymbol{g}_i(\boldsymbol{x}(t))\omega_{\mathrm{dmd,i}}(t) \\ y(t) &= h(\boldsymbol{x}(t))\end{aligned} \tag{5}$$

with state vector $\boldsymbol{x}(t)$, inputs $\omega_{\mathrm{dmd,i}}(t)$, output $y(t)$, smooth vector fields $\boldsymbol{f}(\boldsymbol{x}(t))$ and $\boldsymbol{g}_i(\boldsymbol{x}(t))$ as well as a smooth function $h(\boldsymbol{x}(t))$. The state vector is defined as

$$\boldsymbol{x}(t) = \left[u(t), \omega_1(t), \ldots, \omega_{n_{JV}}(t)\right]^{\mathrm{T}}. \tag{6}$$

Then the first line in the non-linear state space system (5) yields

$$\dot{x}_1(t) = \sum_{i=1}^{n_{\mathrm{JV}}} k_{\mathrm{JV},i}\; v_{\mathrm{JVmax},i}^2 \,|\, x_{i+1}(t) \,|\, (x_{i+1}(t) - \frac{x_1(t)}{v_{\mathrm{JVmax},i}}) - k_{\mathrm{Fric}}\; x_1(t) \,|\, x_1(t) \,| + \sum_j \frac{\Delta p_j(t)}{\rho L}. \tag{7}$$

The remaining $(n_{JV} - 1)$ entries corresponding to the states $x_2(t)$ to $x_{n_{\mathrm{JV}}+1}(t)$ describe the start-up characteristic of the jet fans according to (4) as

$$\dot{x}_i(t) = -\frac{1}{\tau_{\mathrm{JV}}} x_i(t) + \frac{1}{\tau_{\mathrm{JV}}} \omega_{\mathrm{dmd},i-1}(t). \tag{8}$$

3. METHODOLOGY

3.1. Feedback Linearization

By feedback linearisation [3] a system transformation of a non-linear system (5) into an equivalent linear system through a change of variables and a suitable control input is performed such that it renders a linear input-output map between a new (virtual) input $v(t)$ and the output. An outer-loop control strategy for the resulting linear control system can then be applied. Although the theory also applies to very general non-linear state space systems, in this manuscript only non-linear affine input systems are considered. Initially assume that only one jet fan exists, so that an single input, single output system can be considered. To obtain the required transformation, the system output $y(t)$, which represents the flow velocity $y(t) = u(t) = x_1(t) = h(\boldsymbol{x}(t))$ in case of the tunnel model, is derived repeatedly with respect to time along a solution trajectory of the state space system (5) until the control signal $\omega_{\mathrm{dmd}}(t)$ appears explicitly. The first derivative yields

$$\dot{y} = \frac{\partial h}{\partial \boldsymbol{x}} \frac{\mathrm{d}\boldsymbol{x}(t)}{\mathrm{d}t} = \frac{\partial h}{\partial \boldsymbol{x}} \left(\boldsymbol{f}(\boldsymbol{x}(t)) + \boldsymbol{g}(\boldsymbol{x}(t))\omega_{\mathrm{dmd}}(t) \right) = \mathrm{L}_{\boldsymbol{f}} h(\boldsymbol{x}(t)) + \mathrm{L}_{\boldsymbol{g}} h(\boldsymbol{x}(t))\omega_{\mathrm{dmd}}(t). \tag{9}$$

The expressions $\mathrm{L}_{\boldsymbol{f}} h(\boldsymbol{x}(t))$ and $\mathrm{L}_{\boldsymbol{g}} h(\boldsymbol{x}(t))$ in (9) are the Lie derivatives of the scalar function $h(\boldsymbol{x}(t))$ along the vector fields $\boldsymbol{f}(\boldsymbol{x}(t))$ and $\boldsymbol{g}(\boldsymbol{x}(t))$, respectively. The Lie derivative $\mathrm{L}_{\boldsymbol{f}}^k h(\boldsymbol{x}(t)), k \in \mathrm{N}$ is defined recursively

$$\mathrm{L}_{\boldsymbol{f}}^k h(\boldsymbol{x}(t)) = \mathrm{L}_{\boldsymbol{f}} \left(\mathrm{L}_{\boldsymbol{f}}^{k-1} h(\boldsymbol{x}(t)) \right), \qquad \mathrm{L}_{\boldsymbol{f}}^0 h(\boldsymbol{x}(t)) = h(\boldsymbol{x}(t)). \tag{10}$$

Using this definition, the relative degree r of a system (5) at $\bar{\boldsymbol{x}}$ is determined by

$$\begin{aligned}&\mathrm{L}_g \mathrm{L}_f^k h(\boldsymbol{x}(t)) = 0, \quad k = 0,\dots,r-2, \quad \forall\, \boldsymbol{x} \text{ in a neighbourhood of } \overline{\boldsymbol{x}} \\ &\mathrm{L}_g \mathrm{L}_f^{r-1} h(\overline{\boldsymbol{x}}) \neq 0.\end{aligned} \tag{11}$$

Thus, the relative degree equals the number of differentiations of the output $y(t)$ which have to be applied before the input $\omega_{\mathrm{dmd}}(t)$ appears in the resulting equation for the first time explicitly. This leads to the relation

$$\begin{aligned} y(t) &= h(\boldsymbol{x}(t)) \\ \dot{y}(t) &= \mathrm{L}_f h(\boldsymbol{x}(t)) \\ &\vdots \\ y^{(\mathrm{r}-1)}(t) &= \mathrm{L}_f^{r-1} h(\boldsymbol{x}(t)) \\ y^{(r)}(t) &= \mathrm{L}_f^r h(\boldsymbol{x}(t)) + \mathrm{L}_g \mathrm{L}_f^{r-1} h(\boldsymbol{x}(t)) \omega_{\mathrm{dmd}}(t). \end{aligned} \tag{12}$$

Using the state vector feedback control law with virtual input $v(t)$

$$\omega_{\mathrm{dmd}}(t) = \frac{v(t) - \mathrm{L}_f^r h(\boldsymbol{x}(t))}{\mathrm{L}_g \mathrm{L}_f^{r-1} h(\boldsymbol{x}(t))}, \tag{13}$$

leads to a linear input-output behaviour in form of an integrator chain of r integrators

$$y^{(r)}(t) = v(t). \tag{14}$$

The system (14) is called external dynamics and the control law (13) is also referred to as input transformation. Particularly interesting is the case, if $r = n$. Then, the system is said to have full relative degree and a differentially flat system is present. However, in general a relative degree less than the system dimension n might appear. By applying the state feedback (13), a partially linear system is obtained. The resulting transformed system is decomposed into the external dynamics of dimension r as a linear subsystem and a possibly non-linear subsystem of dimension $n-r$, which is referred to as internal dynamics [3].

3.2. Flatness-based feedforward control

If the system (5) has full relative degree, i.e. is differentially flat, the required control signal $\hat{\omega}_{\mathrm{dmd}}(t)$ can be found directly from the desired output trajectory $w(t)$ and its derivatives up to order r. The input transformation (13) is used to evaluate the required control signal

$$\hat{\omega}_{\mathrm{dmd}}(t) = \frac{w^{(r)}(t) - \mathrm{L}_f^r h(\boldsymbol{w}(t))}{\mathrm{L}_g \mathrm{L}_f^{r-1} h(\boldsymbol{w}(t))}. \tag{15}$$

If the plant model was exact with no parameter uncertainties or disturbances on the plant, the dynamic feedforward control law (15) would drive the system such that it exactly fulfils $v(t) = w^{(r)}(t)$, thus $y(t) = w(t)$ holds along the whole trajectory. Disturbance attenuation is achieved by the feedback part in the two-degrees-of-freedom control scheme of **Figure 1**.

3.3. Design for the tunnel ventilation system

The derivation of the feedforward control law for the tunnel ventilation incorporates the differential equations describing the air flow and the start-up characteristic of the jet fans. Whereas the feedback control part unconditionally requires the incorporation of the measurement dynamics, in the feedforward control the actual flow velocity can be used directly although it is not accessible as a measurement.

Technically speaking, the considered system (5) is an over-actuated multiple input, single output system, as multiple control variables (jet fans) are available. However, due to the purely additive structure of their effect in the momentum balance, the overall structure remains simple and facilitates the application of the described approach. In the evaluation of the feedforward control law (15), an additional algorithm is required to determine the individual control signals out of a cumulated sum. It is merely this cumulated term, which can be determined by the feedforward control. By considering the Lie derivatives of the treated state space system, the relative degree is determined to be two, because the mixed derivative

$$\mathrm{L}_{\boldsymbol{g}_i}\mathrm{L}_{\boldsymbol{f}}h(\boldsymbol{x}(t)) = \mathrm{sign}(x_{i+1}(t))\frac{k_{\mathrm{JV},i}\ v_{\mathrm{JVmax},i}^2}{\tau_i}\left(2x_{i+1}(t) - \frac{x_1(t)}{v_{\mathrm{JVmax},i}}\right) \tag{16}$$

is the lowest one not being equal to zero. According to the general methodology, in this case the feedforward control law reads as

$$\sum_{i=1}^{n_{\mathrm{JV}}}\mathrm{L}_{\boldsymbol{g}_i}\mathrm{L}_{\boldsymbol{f}}h(\boldsymbol{w}(t))\hat{\omega}_{\mathrm{dmd},i}(t) = \frac{\mathrm{d}^2 w(t)}{\mathrm{d}t^2} - \mathrm{L}_{\boldsymbol{f}}^2 h(\boldsymbol{w}(t)), \tag{17}$$

where the second order Lie derivative is

$$\mathrm{L}_{\boldsymbol{f}}^2 h(\boldsymbol{x}(t)) = \boldsymbol{f}^{\mathrm{T}}(\boldsymbol{x}(t))\begin{bmatrix} -2k_{\mathrm{Fric}}\left|x_1(t)\right| - \sum_{i=1}^{n_{\mathrm{JV}}} k_{\mathrm{JV},i}\ v_{\mathrm{JVmax},i}\left|x_{i+1}(t)\right| \\ \vdots \\ \mathrm{sign}(x_{i+1}(t))k_{\mathrm{JV},i}\ v_{\mathrm{JVmax},i}^2\left(2x_{i+1}(t) - \frac{x_1(t)}{v_{\mathrm{JVmax},i}}\right) \\ \vdots \end{bmatrix}. \tag{18}$$

From (17) the control signals $\hat{\omega}_{\mathrm{dmd},i}(t)$ have to be determined by a segmentation algorithm in such a way that the term $\sum \mathrm{L}_{\boldsymbol{g}_i}\mathrm{L}_{\boldsymbol{f}}h(\boldsymbol{w}(t))\hat{\omega}_{\mathrm{dmd},i}(t)$ equals the right hand side in (17). In this algorithm, also application relevant information such as a ventilator priority matrix could be incorporated for example.

In (17) the state vector $\boldsymbol{x}(t)$ has been replaced by the vector $\boldsymbol{w}(t)$. It includes those states and their derivatives, which in case of differential flatness result directly from the desired trajectory. In terms of the flow velocity and its derivatives, this is found directly from the trajectory itself. If there were one single jet fan, also the trajectory of its rotational speed could be determined from the desired velocity trajectory, as the system would be differentially flat. However, when considering multiple jet fans, their rotational speeds have to be found by a co-simulation, in which the momentary speeds are simulated.

3.4. Discretisation

To be able to implement the two-degrees-of-freedom control scheme, a discrete-time representation of equations is required. However, this task is directly achieved by applying the Euler method. Due to the large time constants of the plant, no stability issues or excessive errors arise by using an adequately short step size of 0.5 s or 1 s.

4. RESULTS

The proposed non-linear dynamic feedforward control has been implemented and tested in November 2015 in the southern tube of the St. Ruprecht motorway tunnel on the Austrian Semmering motorway S6 in course of a complete tunnel refurbishment and modernization. A schematic drawing of the considered tube is shown in **Figure 2**. The longitudinal flow velocity is measured by two independent measurement locations consisting of three measurement devices each. Three jet fans are installed along the tunnel. Except of that one in the centre of the tunnel, the other two jet fans are equipped with a frequency converter (FC).

In case of fire detection, that jet fan located nearest to the triggering fire area (denoted AS to FS), remains switched off permanently. Thus, at least one jet fan with FC remains available.

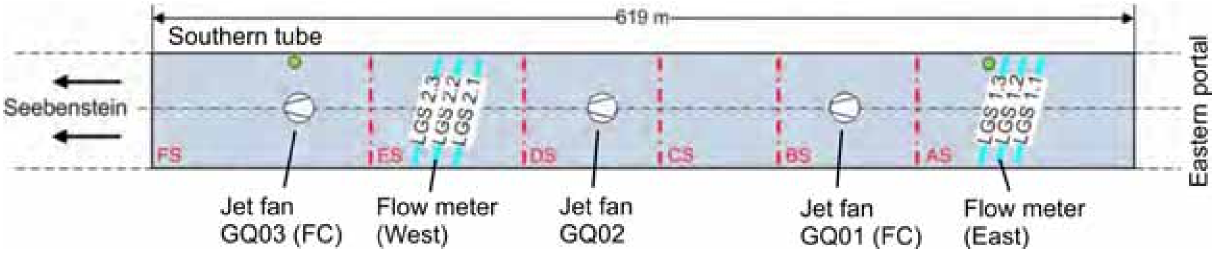

Figure 2: Installation layout of the southern tube of the St. Ruprecht tunnel on motorway S6

The parameters of the non-linear equations used to feedforward control the flow velocity in the tunnel are given in **Table 1**. They have been validated by open loop experiments and yield a good model fit in the required operating range. To test the feedforward control in a two-degrees-of-freedom control scheme, experiments in the empty tunnel without an actual fire have been carried out. As feedback controller a standard linear PI controller has been used for disturbance rejection. Its parameter tuning has been carried out using an operating point linearization of the non-linear plant in combination with linear design methodologies. A phase margin of 53 degrees has been used as design target. In **Figure 3** and **Figure 4** results are shown for a one-way traffic (flow velocity target range 1.5-2 m/s) and a two-way traffic situation (target range 1-1.5 m/s), respectively. In the upper panels, the measurements of the eastern flow meters are shown as solid lines together with the desired reference trajectory $\hat{u}$

Table 1: Model parameters

v_{JVmax}	27.4 m/s	k_{JV}	2.9018e-5 m^{-1}	τ_{JV}	22 s
k_{Fric}	2.5e-3 m^{-1}	ρ	1.15 kg/m³	L	619 m

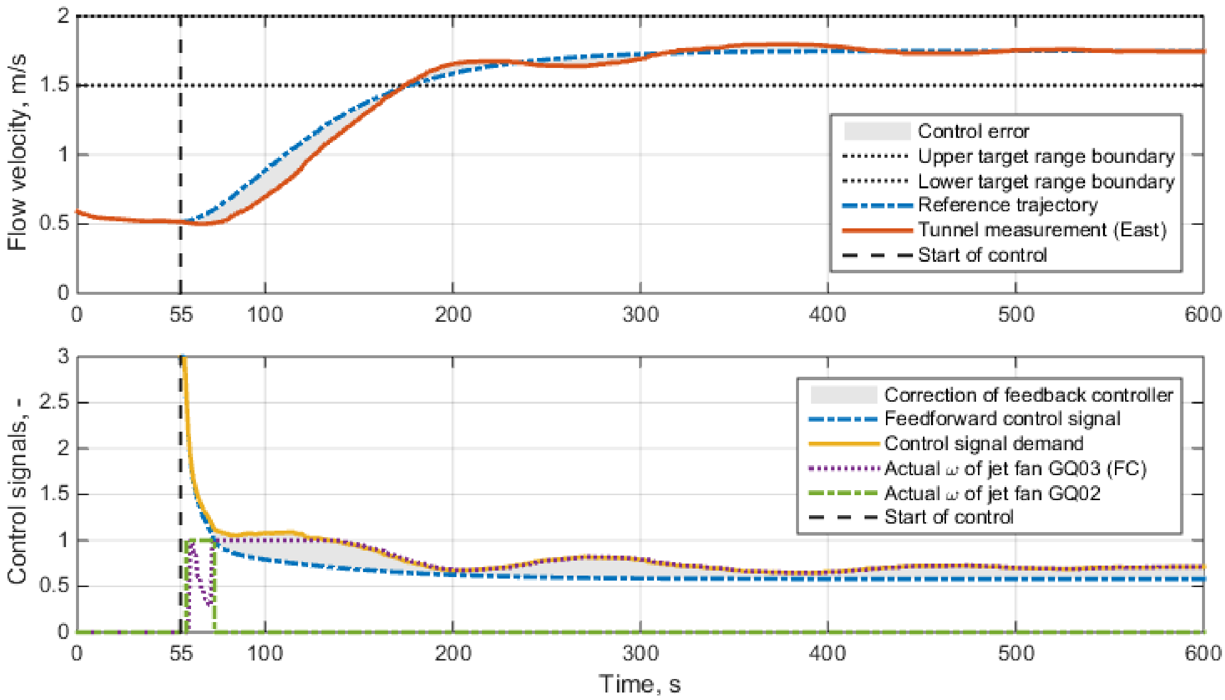

Figure 3: Start up of fire ventilation program for one-way traffic in the tunnel St. Ruprecht

determined by the feedforward control as dashed/dotted lines. The fire detection is assumed to occur in fire area AS, thus the jet fans GQ03 (with frequency converter) and GQ02 are available for control. In the lower panels of **Figure 3** and **Figure 4**, the control signals are shown. The overall control signal ω_{dmd} (solid line) is comprised of the feedforward control signal $\hat{\omega}_{\mathrm{dmd}}$ (dashed/dotted line) and the feedback control signal added up. The actual rotational speeds of the two jet fans are shown in addition. The distribution of the overall demanded control signal to the individual jet fans was achieved under consideration of the ventilator priority matrix.

Altogether, the achieved results are satisfying. The air flow velocity reaches the desired target interval in less than two minutes without any overshoot. Required feedback controller corrections are minimal also. However, when stronger disturbances are acting on the tunnel, also the required controller action increases.

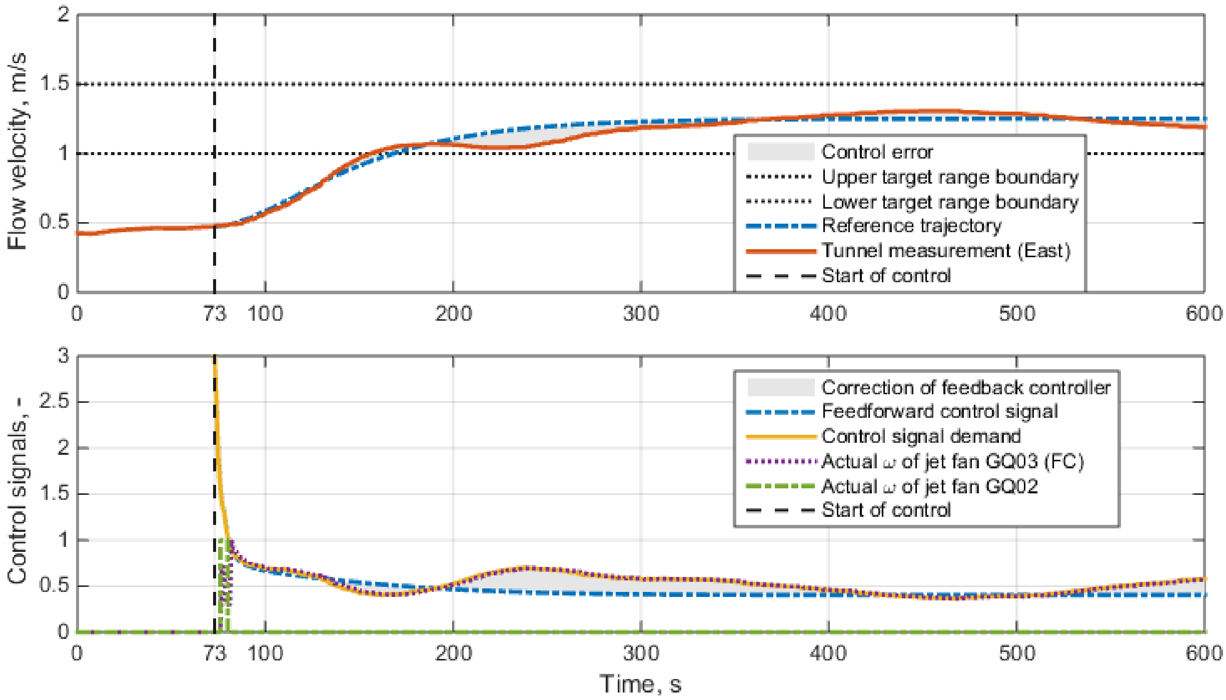

Figure 4: Start up of fire ventilation program for two-way traffic in the tunnel St. Ruprecht

5. REFERENCES

[1] S. Bogdan, B. Birgmajer and Z. Kovacić, “Model predictive and fuzzy control of a road tunnel ventilation system,” *Transportation Research Part C,* vol. 16, pp. 574-592, 2008.

[2] H. Jang and F. Chen, “A novel approach to the transient ventilation of road tunnels,” *Journal of Wind Engineering and Industrial Aerodynamics,* vol. 86, pp. 15-36, 2000.

[3] A. Isidori, Nonlinear Control Systems, Berlin: Springer-Verlag, 1995.

[4] „RVS 09.02.31 Belüftung - Grundlagen,“ Juni 2014.

[5] „RVS 09.02.32 Belüftung - Luftbedarfsberechnung,“ Juni 2010.

[6] P. Sturm, M. Bacher, G. Schmölzer and M. Beyer, “Ventilation design tools and validation,” in *5th Int. Conf. on Tunnel Safety and Ventilation*, Graz, Austria, 2010.

VENTILATION CONTROL IN THE CASE OF FIRE: A PRACTICAL APPROACH TO THE IMPLEMENTATION OF PI CONTROLLERS

[1]G. Schmölzer, [1]P. Sturm, [2]D. Zettl, [3]W. Koppensteiner, [3]A. Wierer
[1]Graz University of Technology, [2]Austria, Dürr Austria GmbH, [3]ASFiNAG BMG

ABSTRACT

The aim of the study is to find a simple, transparent and generally applicable procedure for configuration and commissioning of PI controllers in tunnel ventilation systems. The experimental determination of the transmission behavior of the system can be done with the inflection tangent method or the time percentage value method. The initial parameterization of the controller is done on the basis of empirical setting rules. Numerous tests are performed in order to find out which of the known setting rules is best for initial parameterization of ventilation systems. Control-related measures allowing for general usage of a PI controller, regardless of tunnel design are also devised. Finally, two examples are used to illustrate application of the method developed.

Keywords: PI-controller, higher order lag elements, tuning rules, command and disturbance response, physical tests, ventilation control

1. INTRODUCTION

In the case of fire, the control of the air speed in a tunnel is of the utmost importance since it is a key factor in facilitating self-rescue conditions for tunnel users [Sturm, Beyer, & Rafiei, 2015]. Closed loop controlled ventilation systems are nowadays state of the art. Various possibilities for controlling tunnel air speed have been developed over the last few years. These range from simple on/off switching procedures to complex PI or PID controller applications. In the majority of cases fan operation, and control of longitudinal air velocity, are achieved by threshold switching (a simple form of multistep controller). However, such procedures often result in inacceptable oscillations in air speed and in undesirable smoke propagation. In contrast, more sophisticated applications are now based on the usage of PI controllers in combination with variable speed controlled jet fans.

PI controllers provide considerable advantages compared to threshold switching. These are:

- The setpoint can be achieved and maintained more easily
- The control behavior is much less dependent on external conditions
- Adjustment of control performance and reaction to disturbances can be significantly improved

To gain the full benefits of a PI controller the latter’s parameters have to be adjusted to suit the specific tunnel system under consideration. Currently, the setting of controller variables is very often undertaken during system installation by ‘trial and error'. However, experience shows that in most cases a poorly tuned PI controller performs considerably less effectively than a well-configured threshold switching system.

Although detailed investigations in this area have been undertaken in Switzerland [Altenburger, Riess, & Brandt, 2013], feedback from system integrators reveals that, with respect to ventilation systems at least, more simple and robust methods are still required.

The purpose here is thus to describe a simple, transparent and generally applicable procedure for the configuration and commissioning of PI controllers in tunnel ventilation systems, which enables targeted initial configuration and subsequent optimization for an appealing control and disturbance behavior. The final procedure must also be applicable in systems with fans without speed-control (fans which may be switched on or off).

Since sensible configuration and optimization of the controller is not possible until the ventilation system is fully working, and this is normally very late in the course of the system integration and commissioning work, the proposed procedure needs to be executable directly on site and thus to demand very little time and effort.

2. STEP RESPONSE / SYSTEM IDENTIFICATION

To configure a controller appropriately it is essential that the transmission behavior of the controlled system be well known. This means that an accurate mathematical model of the essential physical processes in the tunnel (capable of mapping pressure effects of the jet fans, flow losses, inertia of the air, etc.) is required. Such a model has to be configured to suit each individual tunnel.

However, transmission behavior can also be determined experimentally via the response of the system (i.e. air velocity) to a step change in a reference variable, e.g. a sudden increase in air speed as a result of fan activation (i.e. a step response). The advantage of this method is that the characteristics of the tunnel and its response to fan activation are determined automatically. To do this, however, first requires that such step response behavior be observed and recorded

When recording the step response of a tunnel the following requirements have to be complied with:

- The tunnel must be absolutely free of any traffic.
- Before the start and termination of the recording, a steady state condition of the longitudinal air velocity has to be ensured.
- The jet fans have to be activated as quickly as possible, and any safety locks and delays (e.g. minimum running time or reverse rotation) have to be deactivated during the testing.
- Since the course of the step response depends, among other things, on the natural base flow in the tunnel, recording must always be carried out for both directions of air flow

The step response of a tunnel is always s-shaped, this means it first has an inflection point, and then approaches a new steady-state value (with final speed at $t \rightarrow \infty$). This is the characteristic behavior of a higher order lag element. The dynamic behavior (transfer function) of the controlled system can therefore be approximated by a so called PT_n element (series of n 1^{st} order lag elements with the same time constant T_S. See **Figure 1**).

The required parameters of the controlled system are provided by the step response. For the analysis of the step response either the inflection tangent method or the time percentage value method proposed by SCHWARZE may be used [Lutz & Wendt, 2014]. Since the inflection tangent method entails a number of inaccuracies the time percentage value method is normally to be preferred.

Irrespective of their degree of accuracy, both methods are capable of providing, quickly and simply, the five characteristic parameters of the controlled system. These are:

- Static gain, K_S
- Delay time, T_u
- Compensation time, T_g
- Order of the system, n
- Time constant of the PT_n element, T_S

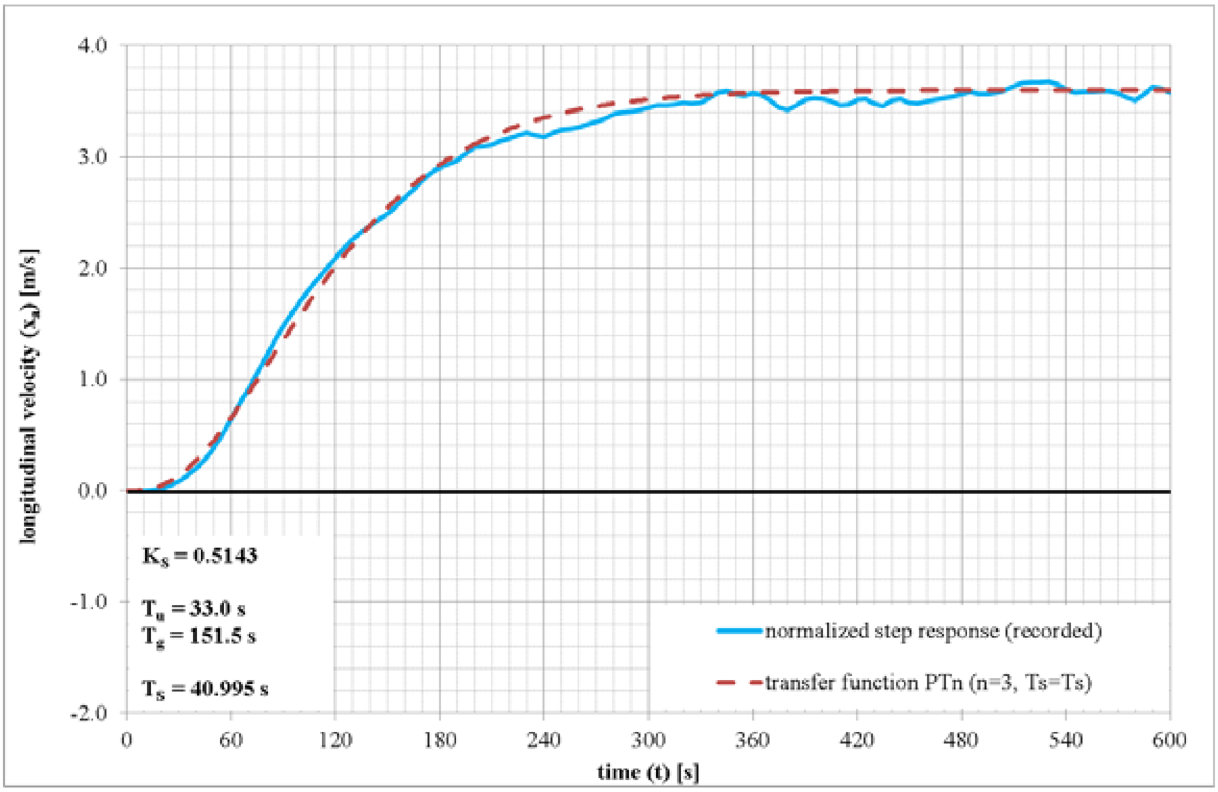

Figure 1: Comparison recorded step response / transfer function PT_n

Since in the majority of cases the step responses for the two flow directions can vary significantly, an average value of both parameter sets must be used so that the controller set-up is as 'neutral' as possible.

3. DESIGN OF THE CONTROLLER / CONTROL RELATED MEASURES

The controller, used for all subsequent studies, is basically a classic PI controller in parallel structure.Since only a restricted number of jet fans are available in a tunnel, the manipulated variable has to be limited accordingly (saturation). In the presence of such saturation, the integral part of the controller would still keep accumulating the remaining control error, but no more fans would be activated. To prevent this, in the case of saturation the integral part of the controller has to be stopped (anti-windup).

In an emergency, fans close to the location of the fire must not be activated (in order to preserve the smoke layer). The maximum number of actually available fans thus depends on the specific fire zone. This means that for the anti-windup to work properly, the maximum number of available jet fans has to be dynamically adjusted by the control system so as to match the needs of the actual fire location.

In addition, a PI controller also provides a continuous control signal. However, many tunnels are either not equipped, or are only partially equipped, with speed-controlled fans. This then means that the system reaction is sometimes stepwise in that single fans have to be turned on or off. It is thus essential that a control solution be found which is also applicable to systems with fixed-speed fans, i.e. a system which overcomes the need for frequent on/off fan operation (which may lead to fan failure). In the tests described here, the implementation of a system entailing switching hysteresis proved to be extremely effective:

Example:

A switching hysteresis of +/- 0.6 means, that only for a control signal value > 1.6, is a second fan switched on, and that vice versa, the same fan is only switched off for a control signal value < 1.4.

This switching hysteresis, in combination with the inertia of the system, prevents (even under unfavorable conditions) ‘unnecessary’ switching operations or limit-cycles and thus helps minimize the risk of fan overload or fan failure.

Since actual velocity values, and for transverse ventilation systems, set point values are provided by air velocity sensors which, depending on the measurement principle employed, may be quite sensitive to disturbance, a moving average (averaging over the period configurable) needs to be calculated for the controller input (control error).

In order to avoid unnecessary switches due to larger proportional-action coefficients K_P and sudden fluctuations in actual values (longitudinal velocity), the usage of a moving average for the controller output (manipulated variable) is also recommended.

For transverse systems one must also ensure that the controller is not activated until the air flow on both sides of the extraction point is in steady state. Otherwise the controller, which is set on the basis of initial conditions, may react incorrectly and the resulting error is carried through over time due to the integral part of the controller. This problem can be easily fixed by configuring a time delay with respect to controller start after emergency triggering, or by arranging for the controller start to be dependent on the flow rate of the axial fan(s).

4. INITIAL ADJUSTMENT / SETTING RULES

A PI controller has two control (set) parameters: proportional gain K_P and reset time T_N. For their initial parameterization a variety of practical setting rules is available, which provide empirical rules for the calculation on the basis of the parameters determined by the inflection tangent method or the time percentage value method.

As part of research work carried out at Graz University of Technology, Institute for Internal Combustion Engines and Thermodynamics, a total of 6 well-known tuning rules for PT_n transfer behavior were tested on a real ventilation system, in order to assess their respective command and disturbance behavior. These rules comprised:

- ‚second’ setting rule by ZIEGLER and NICHOLS [Lutz & Wendt, 2014]
- 4 setup options by CHIEN, HRONES and RESWICK [Lutz & Wendt, 2014]
- Rules, specifically derived for the time percentage value method by LATZEL [Zacher & Reuter, 2011]

The profiles of the controlled variable (longitudinal velocity) and the switching status of the jet fans were recorded during the tests and then subsequently evaluated and compared. The following evaluation criteria were considered:

- control rise time (t_{CRT})
- overshoot
- setting time (t_{ST})
- number and frequency of switching operations

With respect to the ventilation systems examined, the settings by CHIEN, HRONES and RESWICK, optimized for disturbance response with limited overshoot (see **Table 1**) delivered the best results:

Table 1: setting rules CHIEN, HRONES and RESWICK, optimized for disturbance response and limited overshoot [Lutz & Wendt, 2014]

CHIEN, HRONES and RESWICK		*Optimized for disturbance response, limited overshoot (20%)*
PI controller	K_P	$0.70 \cdot \frac{T_g}{K_S \cdot T_u}$
	T_N	$2.30 \cdot T_u$

5. APPLICATION TO DIFFERENT VENTILATION SYSTEMS

The above described procedure was applied to two tunnels along the S10 Mühlviertler expressway. The tunnels differ in terms of their respective lengths (2000m and 4500 m), regular cross-sections (53 m² and 67 m²), and ventilation design (longitudinal ventilation with speed-controlled fans, and semi-transverse ventilation with fixed speed jet fans). The results of the tests are presented in the following sections.

5.1. Longitudinal ventilation and speed-controlled jet fans

The Neumarkt tunnel (driving direction Linz) is a twin bore 2-lane road tunnel (regular cross-section approximately 53 m^2) with a length of 2007 m. The, in total, 7 jet fans are (with the exception of one fan) arranged pairwise under the tunnel roof. The two outermost fan couples are equipped with a frequency converter, while the other jet fans are switched directly on/off. All fans are reversible, each with a static thrust of 880 N (based on a density of 1.2 kg/m^3).

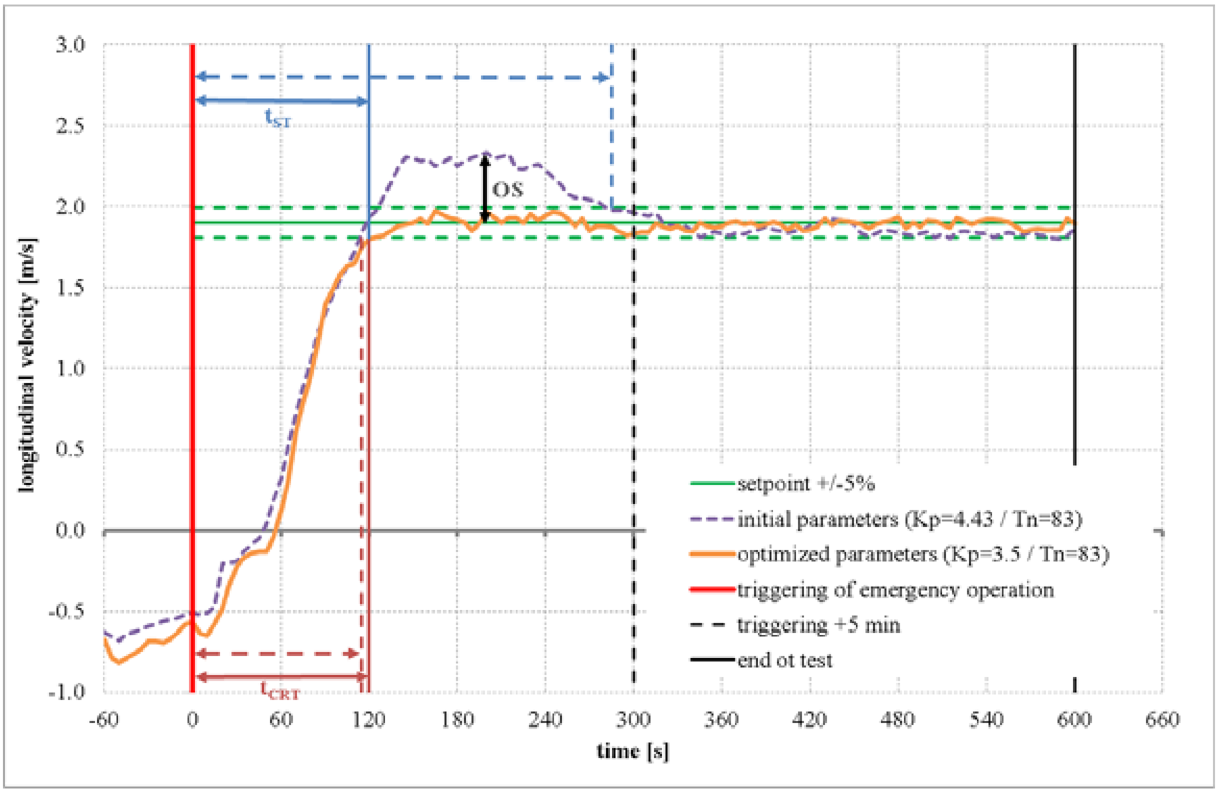

Figure 2: command response, initial / optimized parameters, tunnel Neumarkt, S10 (LV)

Initial parameter setting was done in accordance with the rules of CHIEN, HRONES and RESWICK based on the data (on K_S, T_u, T_g, n and T_S) obtained through the inflection tangent method or time percentage value method from the recorded step responses. Subsequent to this, a test of the command behavior was performed for the setpoint 1.9 m/s. The result is shown in **Figure 2** (the violet dashed line). The control rise time t_{CRT} (i.e. the time elapsing before the controlled variable reaches the tolerance range of +/-5% for the first time) of 115 s is quite short, although there is an overshoot here of 21%, i.e. up to 2.30 m/s. The control variable then finally falls back to within the tolerance range after a total of 285 s have elapsed (this is the setting time t_{ST}).

The observed overshoot can be avoided or reduced by decreasing the proportional gain K_P (in this case from 4.4 to 3.5). Compared to the initial parameterization, the reset time T_n was not changed. The second test with the reduced proportional gain is also shown in **Figure 2** (orange line). While the adjustment results in a slight increase in control rise time from 115 s to 120 s, the overshoot is avoided entirely, thus leading to a significant reduction in setting time from 285 s to 120 s. The command behavior is now almost optimal.

Subsequently, the disturbance response of the controller was checked for the adjusted parameters. After triggering emergency operation, counter-pressure was generated by using a mobile axial fan with 2660 N static thrust as soon as the longitudinal velocity stabilized in the target range. The response of the controlled variable to these external impacts is shown in **Figure 3**. The achieved control rise time and setting time is 175 s (disturbance ON) and 200 s (disturbance OFF) with no post-oscillations. The velocity overshoot is -28 or + 26% compared to the nominal value of 1.9 m/s. The observed disturbance behavior can therefore be described as very good.

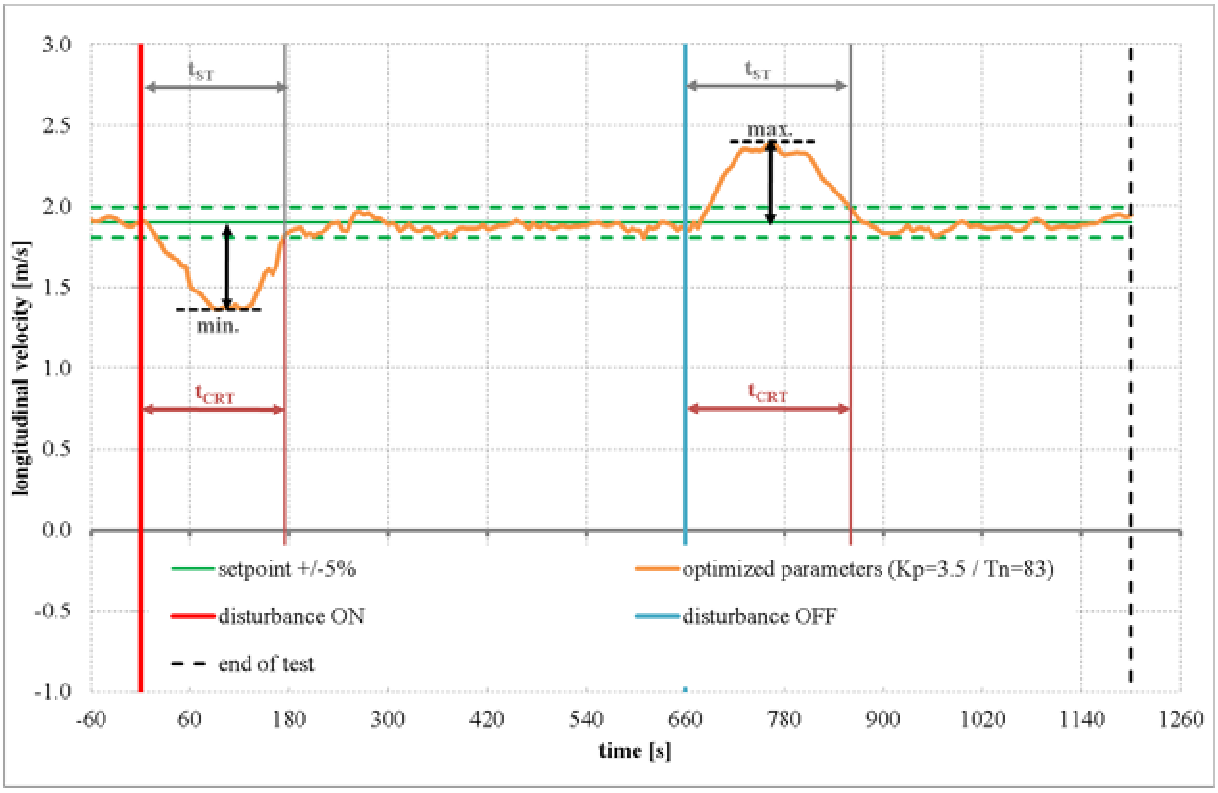

Figure 3: disturbance response, optimized parameters - tunnel Neumarkt, S10 (LV)

5.2. Semitransverse ventilation and line-controlled jet fans

In addition to the tests in the Neumarkt tunnel , the method described above was also tested in the Götschka tunnel. The two tunnels are entirely different. The latter is a 4500 m long, twin tube tunnel with 3-lanes (with a regular cross-section of about 67 m^2) and has a semi-transverse ventilation system. The extracted air volume in the case of a fire is approximately 250 m^3/s. The inflow from both sides to the extraction point can be controlled by 16 jet fans, which are installed in side niches below the false ceiling. All jet fans are reversible with a static thrust of 880 N each (based on a density of 1.2 kg/m^3). All fans are simply switched either on or off, and are not equipped with frequency converters.

Again, as a first step, the command behavior with initial settings according to CHIEN, HRONES and RESWICK (optimized for disturbance response and limited overshoot) was tested for longitudinal ventilation only (WITHOUT any air extraction). The result is shown in **Figure 4** (the violet dashed line). The initial dynamic response is very good, and is followed by a noticeable flattening as the set point is approached. The control rise time (in this case identical with the setting time) is 450 s and therefore quite long. This indicates that the reset time, T_n, was slightly too high. Hence the reset time was decreased from 128 s to 90 s. The result of the repeated test with adjusted parameters is also shown in **Figure 4** (orange line). The good initial dynamic behavior was maintained and the flat convergence was completely eliminated. The control rise time and setting time were reduced to 195 s (a little more than 3 minutes) which is very good for a 4.5 km long tunnel with such a large cross-sectional area.

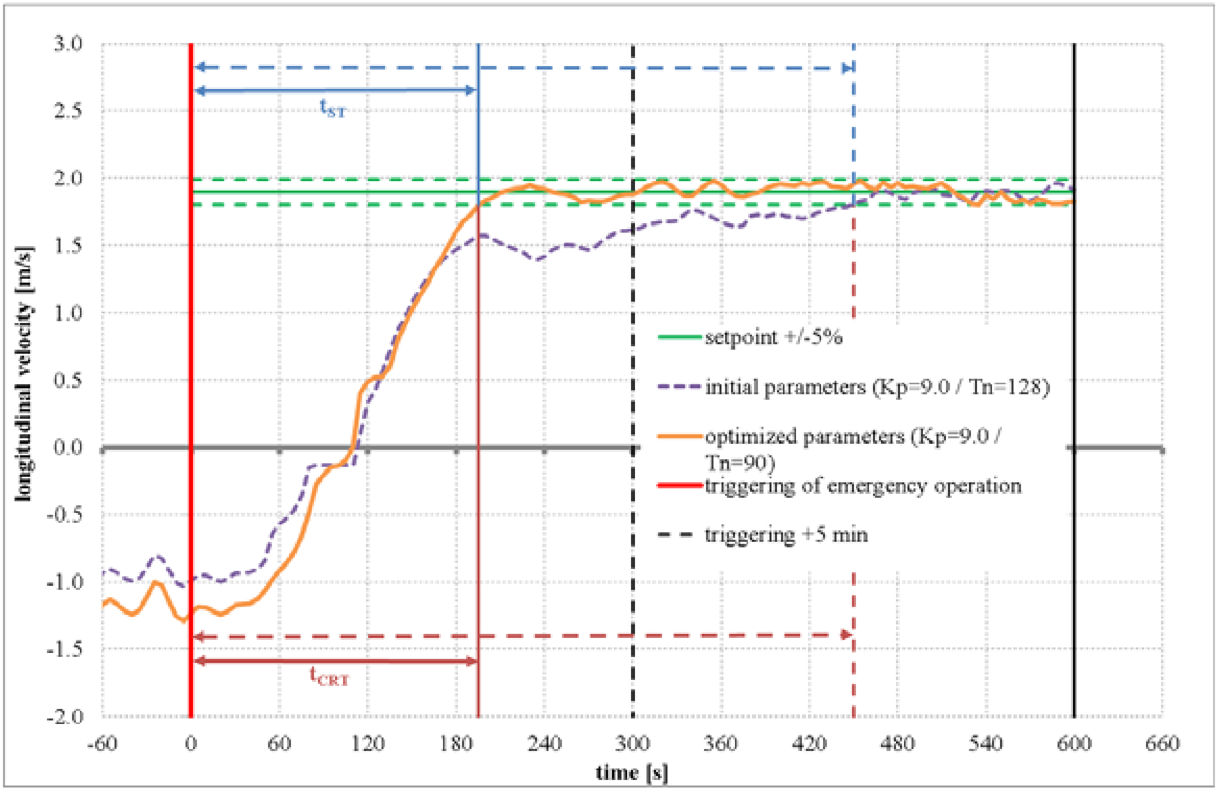

Figure 4: command response, initial / optimized parameters - tunnel Götschka (LV)

In order to check the quality of the adjusted setting with respect to transverse ventilation another test using the optimized parameters was then carried out, i.e. with activated air extraction fans (semi-transverse). The result is shown in **Figure 5**. The point of extraction (location of the fire) was chosen so as to be as unfavorable as possible for the prevailing starting conditions (i.e. close to the portal, and with a natural base flow over the short branch of the tunnel). The rise time achieved is 335 s (about 5.5 minutes) which is quite short for a 4.5 km long tunnel with semi-transverse ventilation. Furthermore, no overshoot or undershoot was observed. The course described by the longitudinal velocity helps illustrate why the controller requires a start delay (as mentioned in section 3). For example, we can see that within the first 30 seconds after activation of the fire program (the red line) there was no change in longitudinal air velocity in the tunnel. This was because the air dampers for extraction had to be opened / closed and the exhaust fans had to be started. Additionally it took almost 30 seconds to stabilize the air flow in the two tunnel branches. So for a total of nearly 60 seconds the controller would (if it had started immediately after the triggering of the fire) be responding to an incorrect reference value. This would probably result in an initially wrong reaction and, due to the integral component of the controller, to a long-term distortion of the manipulated variable.

Finally, disturbance behavior with respect to the optimized controller setting was also reviewed. As disturbance creator, 4 of the 16 jet fans installed were used, with in total approximately 3520 N static thrust. These 4 jet fans were taken out of the control system and temporarily made separately manually switchable. The test was performed during an ongoing fire test as soon as the set point value was reached and maintained. The result is shown in **Figure 6**.

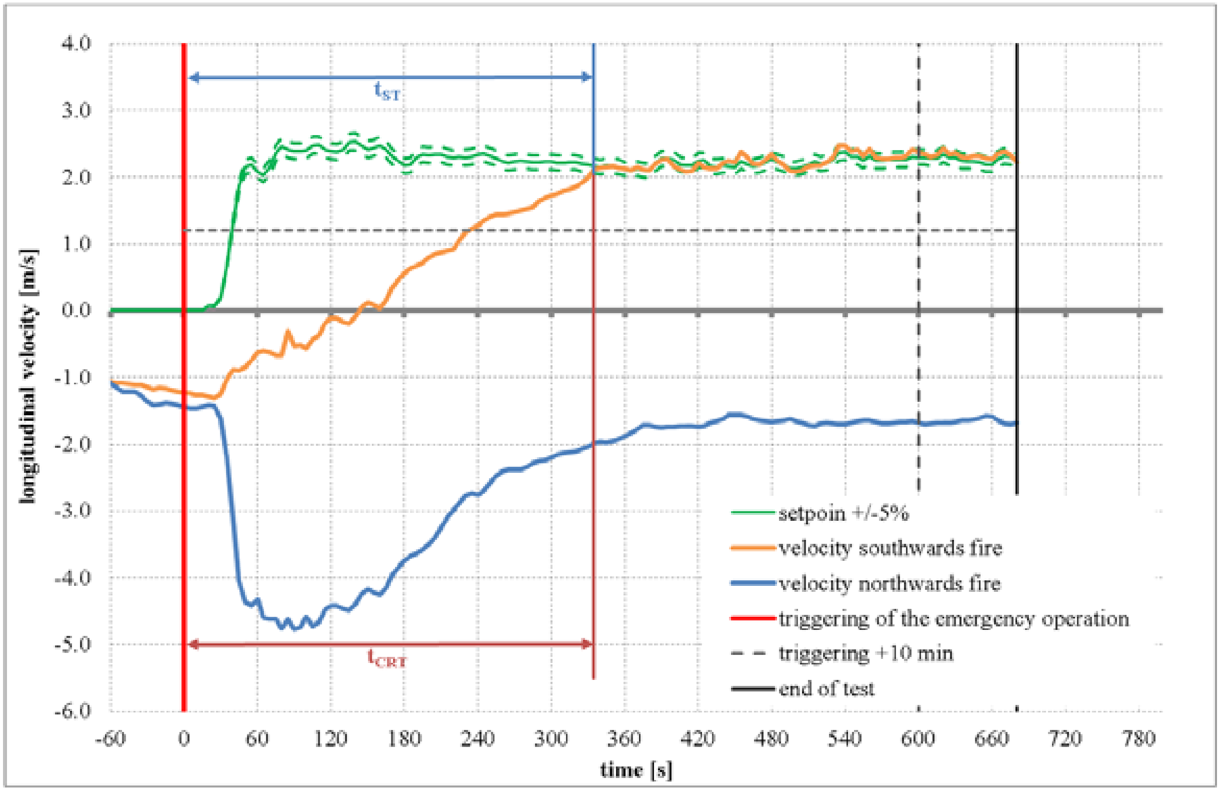

Figure 5: command response, optimized parameters – tunnel Götschka, S10 (STV)

The achieved control rise and setting time is 235 s (disturbance ON) and 170 s (disturbance OFF). The observed velocity overshoot is -25% and +18%. The control behavior in the case of the disturbance can be judged to be very good, particularly for such a relatively slow and inert system such as a semi-transverse ventilation system.

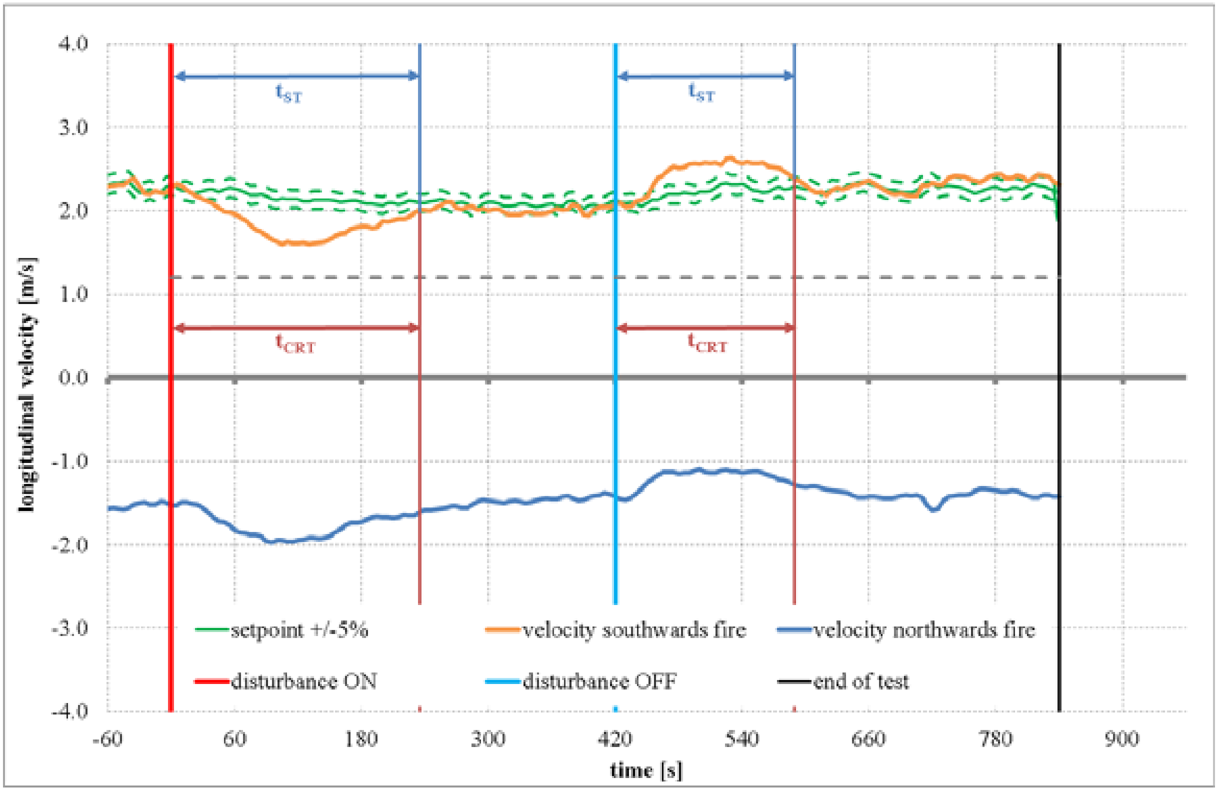

Figure 6: disturbance response, optimized parameters – tunnel Götschka, S10 (STV)

6. SUMMARY AND CONCLUSIONS

The aim of this study was to find a simple, fast and generally applicable procedure for parameterization and optimization of PI controllers during commissioning. The following sequence of work steps has proved to be very effective in numerous tests:

- Recording of step response (ALWAYS for both directions)
- Evaluation of step responses with the help of inflection tangent method or time percentage value method (determination of K_S, T_u, T_g, n and T_S)
- Checking the obtained values by comparison of the recorded step responses (in the tunnel) and the achieved PT_n transfer function
- Calculation and implementation of the initial controller parameters based on the setting rules of CHIEN, HRONES & RESWICK (optimized for disturbance response and limited overshoot)
- Test of command behavior. This test should always be carried out for longitudinal ventilation regardless of the ventilation system.
- Test results show whether there is a need for optimization.
- If necessary: adjust parameters to optimize the control performance
- If necessary: final test of command behavior with adjusted parameters
- For systems with air extraction: test of command behavior for transverse ventilation
- Test for disturbance behavior (e.g. using a mobile fan)

The controller should always be fitted with appropriate anti-windup measures to prevent unnecessary delays in the case of saturation.

In addition to the PI controller the following basic arrangements should be provided in fan control:

- Dynamic saturation limit for the anti-windup
- Configurable moving averaging at the controller input (control error)
- Configurable moving averaging at the controller output (manipulated variable)
- Configurable switching hysteresis (especially for fans without speed-control)
- For systems with air extraction: delayed start of the controller (configurable time delay, or controller dependency on the flow rate of the axial fan(s))

The above procedure facilitates uniform and transparent commissioning and also allows for good and attractive control behavior (command behavior as well as disturbance behavior) to be achieved with relatively little effort.

7. BIBLIOGRAPHY

Altenburger, P., Riess, I., & Brandt, R. (2013). *Control of longitudinal airflow in road tunnels in case of fire.* Bundesamt für Strassen (ASTRA).

Lutz, H., & Wendt, W. (2014). *Taschenbuch der Regelungstechnik* (ergänzte Auflage, 10. Ausg.). Haan-Gruiten, Deutschland: Verlag Europa-Lehrmittel.

Sturm, P., Beyer, M., & Rafiei, M. (2015). On the problem of ventilation control in case of a tunnel fire event. *Case Studies in Fire safety, CSFS 22, Elsevier publishing, doi: 10.1016/j.csfs.2015.11.001*.

Zacher, S., & Reuter, M. (2011). *Regelungstechnik für Ingenieure* (überarbeitete und erweiterte Auflage, 13 Ausg.). Vieweg + Teubner Verlag / Springer Fachmedien Wiesbaden GmbH.

CONTROL OF LONGITUDINAL AIRFLOW VELOCITY DURING FIRE SITUATIONS IN THE TUNNEL COMPLEX BLANKA

[1]J. Šulc, [2]J. Zápařka, [2]J. Pořízek, [3]J. Cigler and [4]L. Ferkl
[1]CTU in Prague, Faculty of Electrical Engineering, Department of Control Engineering
[2]Satra, spol. s r.o.
[3]Feramat Cybernetics, spol. s r.o.
[4]CTU in Prague, University Centre for Energy Efficient Buildings

ABSTRACT

The Blanka Tunnel Complex, which is a part of the Prague City Ring, was opened to traffic in September 2015. It is the longest road tunnel in the Czech Republic and the longest city tunnel in Central Europe, with the total length of 5.5 km and several connected grade separated junctions. The system of fire ventilation in the tunnel complex Blanka is a combination of semi-transverse exhaust in driven sections and massive exhaust in cut and cover sections. The paper presents design and implementation of the PI controller of the longitudinal airflow velocity during fire situations in the tunnel complex Blanka. The design of the PI controller was performed using two different methods – Ziegler Nichols and Root locus. The paper includes comparison of these methods as well. The paper also presents results from complex examinations in the tunnel complex Blanka, which were held before opening of the tunnel to traffic.

Keywords: tunnel complex Blanka, PI controller, mathematical model, road tunnel, Ziegler-Nichols, Root locus, airflow velocity

1. THE BLANKA TUNNEL IN PRAGUE

1.1. SHORT INTRODUCTION

Construction of the tunnel complex Blanka in Prague started in 2007 and the tunnel was opened to traffic and put into the trial operation in September 2015. The total length of the tunnel complex, including connected ramps in parallel is more than 6 km. The tunnel consists of three tunnels, which can be operated independently – Bubeneč tunnel, Dejvice tunnel and Brusnice tunnel. The aerial map of the tunnel complex Blanka is shown in Figure 1. It is a double tube tunnel with traffic intensity about 60 000 vehicles per day and there are three entrances and exits in both tubes [4].

1.2. SYSTEM OF VENTILATION

Ventilation in the tunnel complex Blanka can operate in two different modes – normal mode and fire mode. The normal mode of operation ensures good environmental quality in the tunnel, i.e. admissible values of pollutant concentrations – NO_x, CO and opacity in the tunnel. The aim of the fire mode is described in Section 1.3. We are focused only on the fire ventilation mode in this paper.

The fire ventilation system of the tunnel complex Blanka is combined. In driven sections, there is a semi-transverse extraction with controllable dampers and in cut and cover sections, the smoke is extracted by massive point extraction. Portal sections and ramps are ventilated longitudinally. The longitudinal flow is controlled in the sense of jet fans. The major part of jet fans is controlled by soft-starters and the only possibility to control these jet fans is in the way of start/stop. However, there is at least one jet fan with variable speed drive in each ventilation section of the tunnel, which allows the continuous regulation.

Figure 1: The aerial map of the Blanka tunnel, a route of the tunnel passes the urban development and partially the historical center as well [4].

The ventilation system comprises of five ventilation machine rooms for smoke extraction – Trója, Letná, Prašný most, Špejchar and Strešovice. The ventilation rooms Prašný most and Špejchar are intended for the fire ventilation only, whereas the other ventilation rooms are used for both normal and fire operation.

The ventilation machine rooms are equipped with axial flow fans. They are bigger and have higher power in comparison with jet fans. There are 20 axial flow fans in the machine rooms (in both tubes together) used for the fire ventilation mode. For the fire ventilation purpose, only outlet ventilation rooms are in operation, in order to extract smoke from the tunnel.

1.3. FIRE VENTILATION MODE IN THE TUNNEL COMPLEX BLANKA

In tunnels with unidirectional traffic the common strategy during fire is to maintain the direction of airflow in the direction of traffic [1]. Because of occurrences of traffic congestions, there might be, in the case of fire, persons trapped downstream from the fire as well, therefore a two-stage smoke control, has been used [2].

The first stage, evacuation stage, consists of maintaining the lower longitudinal airflow velocity, approximately 1.0-1.6 m/s, in order to create conditions for stratification, and thus extend the time for evacuation on both sides of fire [3]. In the second stage, fire-fighting stage, a critical velocity about 2.2-3.6 m/s, is required, which preserves smoke propagation only in the direction of traffic and allows access for emergency services to the fire location. The PI controller has been used for the control of the longitudinal airflow velocity during fire situations in the tunnel complex Blanka.

Fire in the tunnel complex can be detected using three different sensors. Required linear heat detector was supplemented with smoke detectors and video detection, in order to localize emergency situations. There are 125 sections corresponding to 125 smoke detectors (in both tubes together), placed after circa 80 meters, where fire can be localized. The camera system uses a real-time video to identify smoke in images from analyzing changes such as brightness or contrast. On the other hand, the camera system is, similarly as smoke detector, sensitive to nuisance alarms [5]. The camera system in the Blanka tunnel involves together 180 cameras.

There are three ways for smoke extraction in the Blanka tunnel. In driven parts, the extraction of smoke through fire canal is used. There is a fixed value of extraction capacity and PI controllers using jet fans for controlling the desired airflow velocity. In cut and cover tunnels, the massive point extraction of smoke through ventilation machine rooms with fixed extraction capacity is used and PI controllers are in operation as well. In sections near to exit portals, there it is more effective to extract smoke from the tunnel through portals, thus ventilation machine rooms are not in operation in this case.

The PI controller is in operation for both phases of fire ventilation state above. Each fire section has the list of following parameters:

- Proportional and integral constants of the PI controller,
- Setpoint value of the airflow velocity in the first and second phase,
- Allowed band of airflow velocity,
- Sensors of airflow velocity, which are used for the control,
- Specific list of jet fans, which are to be used for the control.

Moreover, all these parameters can differ for different fire sections.

2. MATHEMATICAL MODEL OF AIRFLOW VELOCITY

In recent years, there have been several groups dealing with mathematical modeling of airflow dynamics in road tunnels. We are inspired by A.Bring, whose group verified the modeling approach on real measured data from Söderledstunneln in 1997 [7]. Ferkl, et al. used similar approach to verify the mathematical models on the Czech highway tunnels [8]. We have not to forget on the Spanish group of Del Rey [9], which used these models for fire ventilation design.

All these groups used simplified models based on Newton’s law, continuity equations and Bernoulli’s equations. They did not model the airflow dynamics in three dimension using CFD simulations, either due to inability to calculate the results within a reasonable time or, since this approach cannot be applied for the design of the controller during fire situations.

The airflow dynamics in road tunnels is influenced by many factors, especially air friction, piston effect of vehicles, chimney effect and effect of running jet fans. We should not also omit the effect of airflow extraction thanks to ventilation machine rooms, which strongly influences the airflow velocity in the tunnel. We will not state the computational formulas for the effects stated above in our paper, as they can be found in the literature [7,8,9]. The aim of the paper is to show, how is possible to use the mathematical model of airflow dynamics for the design of the PI controller for longitudinal airflow velocity in case of fire. The only important thing differs our model from the models described above, namely, our model is dynamic and not steady state. The dynamic model can be derived from the steady state model and vice versa. The dynamic model describes the time progress of airflow velocity and can be used for simulation of the airflow velocity control in case of fire and for the design of the PI controller as well.

Our mathematical model describes the time progress of airflow velocity in all tunnel sections. See Figure 2, there are depicted all sections of the Blanka tunnel, while each section has a time dependent airflow velocity. The sections are marked as v1-v34. Figure 2 involves entrance and exit ramps of the tunnel and ventilation machine rooms for smoke extraction as well.

As stated above, the dynamic mathematical model can be derived via Bernoulli equations, continuity equations and Newton’s law. Equation (1) describes the general structure of the mathematical model for airflow dynamics:

$$\frac{dv_i}{dt} = v^T A_i v + B_i v + f_i u + g_i Q + d_i \tag{1}$$

where v_i (m/s) represents airflow velocity in the respective section of the tunnel and v is a vector of airflow velocities, i.e. $v=[v_1, v_2, \ldots v_{34}]$.

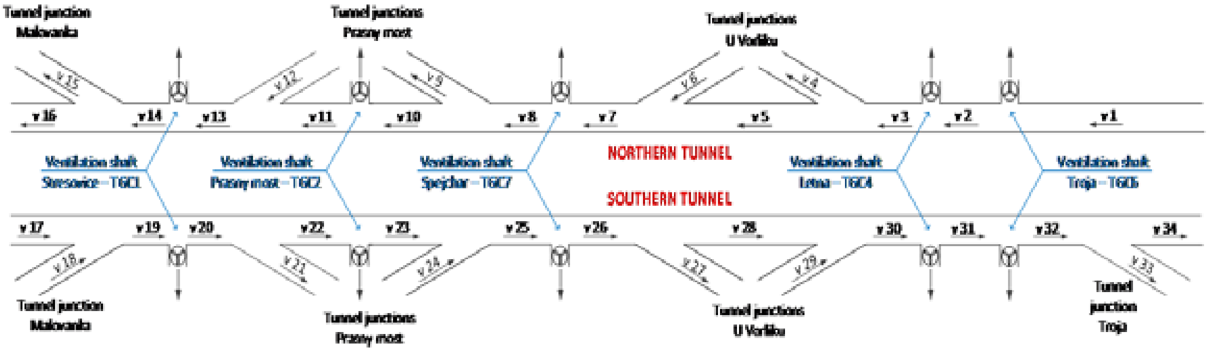

Figure 2: Blanka tunnel scheme including exits, entrances, ventilation machine rooms (ventilation shafts) and unknown variables – airflow velocities in the respective tunnel sections.

A_i, B_i, f_i, g_i are matrices of known coefficients, which depend on current conditions in the tunnel during fire – vehicles leaving the tunnel and vehicles that remained blocked in the tunnel, number of running jet fans, pressure conditions during fire, etc.

The vector $u=[u_1, u_2, \ldots u_{34}]$ represents vector of running jet fans in different tunnel sections, i.e. u_1 represents jet fans, which are running in the tunnel section 1, etc. The vector $Q=[Q_1, Q_2, \ldots Q_m]$ denotes volumetric airflow rate, the extracted amount of air in case of fire, given by ventilation machine rooms. The vector d_i represents disturbances, which are given by piston effect of vehicles, pressure loss during fire, measurement noise and errors, etc.

3. DESIGN OF PI CONTROLLER FOR LONGITUDINAL AIRFLOW VELOCITY

Once the mathematical model in the form of (1) is created, one can proceed to the design of the PI controller of longitudinal airflow velocity. Although the PI controller has only two independent parameters, it is not an easy task to tune the P – proportional and I – integral constant properly. As can be seen in practice, the most of engineers still use trial/error methods to tune the PI controller, partly because of lack of time to use any advanced method to design the controller and secondly due to poor knowledge of process dynamics to be controlled. In often cases, it tends to poor performance of designed controllers.

A lot of tuning methods of PI controllers have been introduced in last seventy years. In this paper, we show two different methods to design the PI controller for the longitudinal airflow velocity in case of fire in road tunnels:

- Ziegler-Nichols method
- Root locus method

For practical use we consider the PI controller in the discrete form, which can be easily implemented into the Programmable logic controllers (PLC):

$$u(k) = K_p e(k) + K_i \sum_{i=0}^{k} e(i) \Delta T \tag{2}$$

Where *u(k)(-)* is the control input at time step *k*– desired jet fans to be run, *e(k)(m/s)* is the control error – difference between desired airflow velocity (setpoint value) and currently measured airflow velocity, K_p is the proportional constant and K_i is the integral constant of the PI controller and ΔT(s) is the sampling period of the controller.

3.1. ZIEGLER-NICHOLS METHOD

It is probably the oldest tuning method, which was introduced in 1941 and is still relatively popular, especially for designers, which do not have basics from control engineering. This method does not require any knowledge of process dynamics. It has never been proven that this method works fine for all type of processes, the resulting controller based on the Ziegler-Nichols can destabilize the controlled process. Finding of parameters K_p and K_i can be performed via step response. The Ziegler-Nichols tuning rule consists of the following steps [10]:

1. Determine and measure your step response, as depicted in Figure 3.
2. Find the inflection point of the step response and draw tangent at this inflection point.
3. Find parameters A, L, which are shown in Figure 3.
4. Parameters K_p and K_i are given as

$$K_p = \frac{0.9}{A}, K_i = \frac{K_p}{3L} \tag{3}$$

Although this method does not require a knowledge of process dynamics, as the step response can be performed on the real system, if the model of process dynamics (airflow dynamics in our case) is available, it is strongly recommended to perform simulations with the PI controller tuned via Ziegler-Nichols method to verify the performance of the designed controller because of the facts stated above.

3.2. ROOT LOCUS METHOD

The root locus method requires some basics from the branch of control engineering. This method works with the linearized model of process dynamics. This method is very useful with the help of computational tools like MATLAB, which provide graphical interface to design PI control using Root locus method. The original, nonlinear model of airflow velocity can be usually approximated as the first (or second order) linear dynamic system with the following transfer function

$$\frac{\Delta v}{\Delta u} = \frac{K}{\tau_1 s + 1} \tag{4}$$

where Δv denotes difference of airflow velocity from some operating point, Δu denotes difference of control input from some operating point. The approximation (finding of parameters K and τ_1) can be performed in many ways. The most used method is based on the step response and the approximation procedure is shown in Figure 3. The parameters of the linearized model are given as

$$K = \frac{\Delta v(\infty)}{\Delta u(\infty)}, \tau_1 = L + T \quad (5)$$

where $\Delta v(\infty)$ is the steady state value of airflow velocity in the step response, $\Delta u(\infty)$ is the steady state value of control input in the step response (jet fans, which are running during the experiment with the step response).

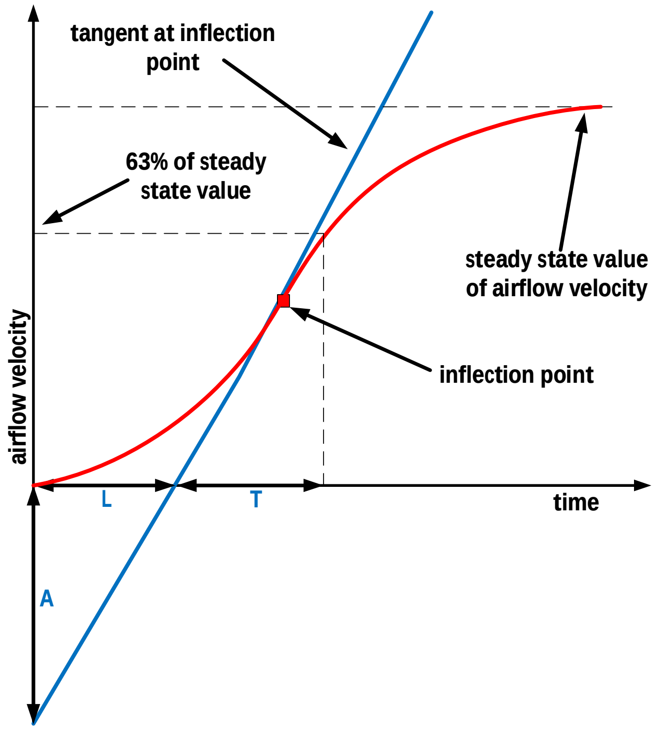

Figure 3: Finding of parameters *A, L* for the design of PI controller from the step response using Ziegler-Nichols method. Finding of parameters *K* and τ_I to obtain the linearized model of airflow dynamics.

Once the linearized model in form (4) is obtained, the PI controller can be tuned using Root locus method. In MATLAB, there are commands like *rltool* or *sisotool*, where the parameters of the PI controller can be found. One can draw the step response and observe, how it looks like with changing of the parameters K_p and K_i. Moreover, Root locus also enables automatic tuning for both – fast or slow, more robust response. More information can be found at [11].

4. EVALUATION AND COMPARISON OF DESIGNED PI CONTROLLERS

In this section we evaluate and compare both designed PI controllers using Ziegler-Nichols and Root locus method. The comparison was performed on simulations using our developed mathematical model. We show the result from the fire section, which is marked as SM59 and is located in the Brusnice tunnel (at the end of the northern tunnel). The longitudinal extraction of smoke through tunnel portal Malovanka is used in this case, i.e. transverse extraction using ventilation machine rooms is not used in this case. In Figure 4 we compared PI controllers tuned using both of the methods – Ziegler-Nichols (blue line) and Root locus (red line). The simulation of airflow velocity control was performed for the first stage of the fire ventilation, while the setpoint of airflow velocity was 1.6 m/s. As you can see, the Ziegler-Nichols tuning method led to rather aggressive settings of the controller, which caused overshoot in our simulation. This behavior is undesirable, as it can cause instability of the controlled system and allows reverse of airflow direction against blocked vehicles in the tunnel. Against that, the PI controller designed by Root locus method fulfilled all requirements on the airflow velocity control, since it kept airflow velocity in desired range without any overshoot.

A part of Figure 4 is a comparison of the mathematical model and real measured data from fire section SM35 during complex examinations. The controller was tuned using Root locus method in this case. As can be seen, the performance of the PI controller was satisfactory in both stages of the fire ventilation.

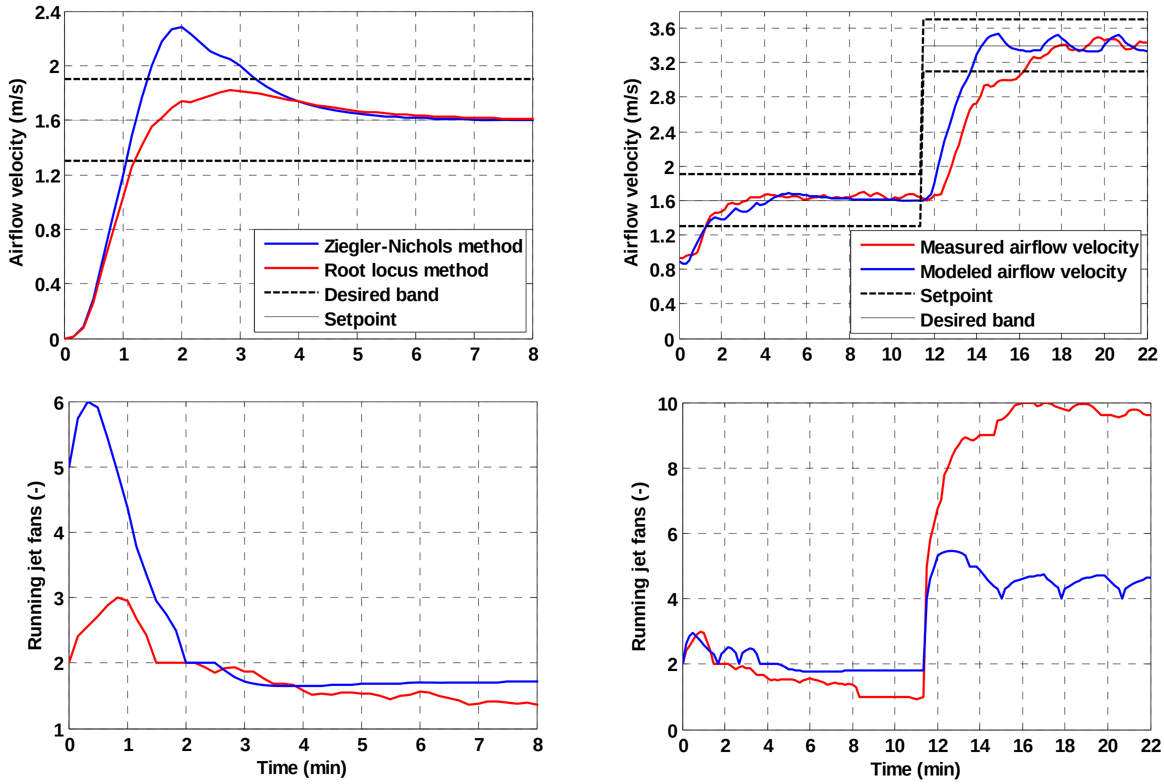

Figure 4: Left side: Comparison of two different methods for PI controller tuning – Ziegler-Nichols and Root locus method. Right side: Comparison of the mathematical model and real measured data during complex examinations.

5. CONCLUSION

The paper described a design of the PI controller of the longitudinal airflow velocity during the fire ventilation mode in the tunnel complex Blanka. Two methods were used for the design of the PI controller – Ziegler-Nichols method and Root locus method. The design was based on the mathematical model of airflow dynamics and PI controllers were tuned for all sections of the tunnel. The tuning and verification of the controller was executed through simulations, which significantly saved time with the controller tuning and detected potential errors, which can occur during the real operation.

6. ACKNOWLEDGEMENTS

The paper was supported by the project of University Centre for Energy Efficient Buildings of CTU in Prague and further financed by the Grant Agency of CTU in Prague as a grant no. SGS16/232/OHK3/3T/13 and Norway grants as the project number NF-CZ07-INS-5-118-2015.

7. REFERENCES

[1] R. Stosch, M. Wehner, R. Brandt, Optimisation of Ventilation in the Case of Fire in Road Tunnels, International Conference „Tunnel Safety and Ventilation" 2004, Graz.

[2] I. Espinosa, S. Fernández, I. Del Rey, E. Alarcón, Experiences on the Specification of Algorithms for Fire and Smoke Control in Road Tunnels, International Conference „Tunnel Safety and Ventilation" 2010, Graz.

[3] P. Sturm, M. Beyer, M. Rafiei, On the Problem of Ventilation Control in Case of a Tunnel Fire Event, Case Studies in Fire Safety, Article in Press, 2015.

[4] Brusnický, Dejvický a Bubenečský tunel (in Czech). Retrieved from: http://www.tunelblanka.info/aktualni-informace/. (Tunel Blanka info, 2016).

[5] Moore, I. "Taking a view on Tunnel Smoke Detection", Retrieved March 3, 2016, from http://www.sourcesecurity.com/companies/micro-site/ad-group/news/co-58-ga-co-2248-ga.2115.html

[6] NCHRP, Design Fires in Road Tunnels, National Academy of Sciences, 2011.

[7] A. Bring, T. Malmström, C. Boman, Simulation and Measurement of Road Tunnel Ventilation, Tunnelling and Underground Space Technology 12 (3), 417-424, 1997

[8] L. Kurka, L. Ferkl, O. Sládek, J. Pořízek, Simulation of Traffic, ventilation and exhaust in a complex road tunnel, Proceedings of the 16th IFAC World Congress, Prague, 2005

[9] I. Del Rey, S. Fernández, A. Fraile, I. Espinosa, Simplified Method for Longitudinal Ventilation System Design in Fire Situations, International Conference „Tunnel Safety and Ventilation" 2012, Graz.

[10] M. Šebek, Lecture Notes for the course Automatic Control, Department of Control Engineering, Faculty of Electrical Engineering of CTU in Prague, available on: http://www.polyx.com/_ari/slajdy/Bas-ARI-11-Controllers.pdf, 2015

[11] Introduction: Root Locus Controller Design, available on: http://ctms.engin.umich.edu/CTMS/index.php?example=Introduction&section=ControlRootLocus

INTELLIGENT SENSOR FUSION IN ROAD TUNNEL OBSERVATION FOR FALSE ALARM REDUCTION USING SUPERVISED MACHINE LEARNING AND UNSUPERVISED UNUSUAL EVENT DETECTION.

*J. Traxler, **G. Mayer, ***M. Obst, ****T. Heinrich, *M. Bommes

* TB-Traxler GmbH, Austria
** PTV Transport Consult GmbH, Germany
*** Baselabs GmbH, Germany
**** Transver GmbH, Germany

ABSTRACT

Infrastructure safety requirements are becoming more important because of road traffic increase, especially for potentially high-risk spots like road tunnels. Tunnels can be equipped with a multitude of different sensors like inductive loops, video detection, audio detection, CO2, Nox and others to provide information to tunnel operators who have to react adequately to incidents, for example by adjusting traffic signals. Sensors typically analyse their own raw data to only deliver meaningful information like alarm messages in case of a detected incident. Because of the independent character of different sensors, false alarms sum up and become a real problem for observers. Big number of false alarms decreases reliance in automatic incident detection, increasing the risk of inappropriate or delayed reaction to a real incident alarm. This work focuses on creating a higher level information layer to combine the information of different independent sensors, so-called sensor fusion, to reduce false alarms without losing sensor sensitivity. Probabilistic fusion methods are discussed in terms of applicability. Supervised machine-learning approaches are used to classify global sensor information by feature training from labelled data. In addition, an unsupervised learning approach to detect unusual events is presented.

Keywords: sensor fusion, video detection, audio detection, smoke detection, supervised learning, unsupervised learning, unusual event detection, false alarm reduction

1. INTRODUCTION

Increasing road traffic is demanding more and more safety requirements for road infra-structure. The detection of safety-critical situations is becoming very important. Recent development concerning incident detection systems have increased the amount of information on traffic situation and road condition provided for the operator. Each of these systems is a useful tool and shortens the reaction, thus decreasing the risk of damage for the following drivers. Since the process control systems communicate independently with so many different systems (inductive loops, CO2, NOx, video detection, audio detection, etc.), each additional sensor increases the false alarm rate. The efforts for the operator to even quit even the on-coming alarms makes it very difficult for him to keep the overview.

Therefore, the issue nowadays is to make the final messages for the operator more reliable. This was the reason why the Austrian highway undertaking ASFINAG, as one of the worldwide leading highway tunnel operator with more 150 tunnel and 2.700km length, did trigger the research project “tunnel sensorfusion” in 2013. This project was fundet by the “Verkehrsinfrastrukturforschung 2013” initiative from ASFINAG and BMVIT.

Using simple logical linkage between different sensor systems is generally not sufficient. For example, a vehicle detected by a video incident detection system and an inductive loop using a logical AND would increase the false positive [FP] rate, but also the false negative [FN] rate because the sensitivity of both systems would reduce the sensitivity of the result. If an OR linkage is used, the sensitivity increases (i.e. FN decreases) but also both false detections would lead to a false alarm (i.e. FP increases).

One of the most promising ways to solve this problem is to use “probabilistic” reasoning methods, i.e. the solution is using the probability theory to combine different sensor values in one combined sensor model which represents the dependencies between the different system states. Using that technique, the FP rates for video systems caused by light changes or for inductive loops by rain or snow can be minimized. The probabilistic data fusion models recognize individual probabilities for each sensor system and are able to keep the false positive rate very low while reducing the false negative rate significantly.

2. SENSOR INFORMATION IN ROAD TUNNELS

Road tunnel monitoring uses a wide variety of sensors to be able to react appropriately to incidents since risk potential is strongly increased in that special environment. Typical types of incidents in tunnels and the ways to detect them will be described.

2.1. Incident types and sensors in road tunnels

Several kind of incidents that have influence on the road users’ safety can occur in road tunnels. They require appropriate reaction by tunnel monitoring operators. The tables 1, 2 and 3 below list different types of incidents and show the sensors or measurement devices which can detect or help to detect such incidents. The below matrices have been compiled by tunnel experts during the requirements phase for the TSFu project. Based on these matrices the superposition of the incident types with the sensors or resp. detectors reveals the sensor fusion potential.

Within the framework of the research project ASFINAG’s Kirchdorf tunnel on the S35 in Styria was chosen as study tunnel, on the one hand, because it was easily accessible and, on the other hand, because it has been the first tunnel in the world which was equipped with AKUT, the acoustic incident detection system. This system was particular interesting with regard to the fusion possibilities between the subsystems, assuming that the different sensor modalities may increase regarding the relevance for the incident information.

The safety systems installed in ASFINAG Kirchdorf tunnel can detect the following types of incidents: Stopped (individual) vehicles, wrong-way or backwards driving/turning manoeuvres, accidents/collisions with involvement of hazardous goods, smoke emissions from vehicles, vehicle fires. Hereby, stopped vehicles, accidents and collisions will be detected by the video detection system VBTC installed and by the AKUT system. Wrong-way or backwards driving/turning manoeuvres will equally be detected by the video detection system, whereas smoke will be detected by the video detection system and by the devices measuring opacity, CO concentration and NOx. The linear fire detector detects the actual fire.

In this context, it was primarily examined in how far the relevance of the incidents, i.e. relationship between the number of actual (positively detected) incidents compared to the total number of incidents detected can be increased without considerably deteriorating the detection times.

Table 1: Sensor-incident matrix A: Traffic incidents.

Sensor \ Incident	Speed violation	Traffic density	Traffic congestion.	Slow moving vehicle	Stopped vehicle	Emergency bay	Wrong way driver	Lost object on road
Traffic counts	x	x	x	x		x	x	
Traffic surveillance	x							
Video detection	x	x	x	x	x	x	x	x

Table 2: Sensor-incident matrix B: Emergency incidents.

Sensor \ Incident	Pedestrian / animal on road	Emergency call	Fire / smoke	Hazardous good transport	Visual range threshold	CO threshold	NOx threshold
Fire detection system	x	x	x				
Contact sensors	x	x	x	x			
Video detection	x		x	x	x		
Emergency station		x		x			
Opacity measurement			x		x		
CO detector			x			x	
IR camera			x				
Hazardous goods plate reader				x			
WIM sensor				x			
Laser-scanner				x			
NOx measurement							x

Table 3: Sensor-incident matrix C: Other events.

Sensor \ Incident	Height violation	Slippery road	Crash / collision	Overheated vehicle	Air ventilation failure	Lighting system failure	Power supply failure
Height control	x						
Video detection			x	x		x	x
Environmental data acquisition		x					
Emergency station			x				
AKUT Acoustic tunnel monitoring			x				
Laser scanner				x			
IR camera				x			
Sonometer					x		
Luminance camera						x	

2.2. Sensor quality evaluation

A precondition for the improvement of the quality of incident detection by fusion of different data sources is the knowledge of the quality of each data source. Therefore, the quality of the traffic data delivered by the inductive loop detectors and the qualities of the video and noise based incident detections have been checked in advance.

The quality of the traffic data delivered by the inductive loop detectors has been checked by use of more than 20 quality indicators defined by FGSV Workgroup 3.5.20. The analysis has shown that the quality of the traffic data delivered by the traffic loop detectors is very good except from small deviations in vehicle counting at neighbourhood measurement cross sections. These deviations could be caused by lane changing manoeuvres.

For the identification of situations (e.g. congestions) that could be interesting for the development and test of the data fusion algorithms, the traffic state over space and time has been reconstructed by use of local traffic data from stationary inductive loop detectors and a traffic model (anisotropic smoothing method) that estimates the traffic state in between the local measurements.

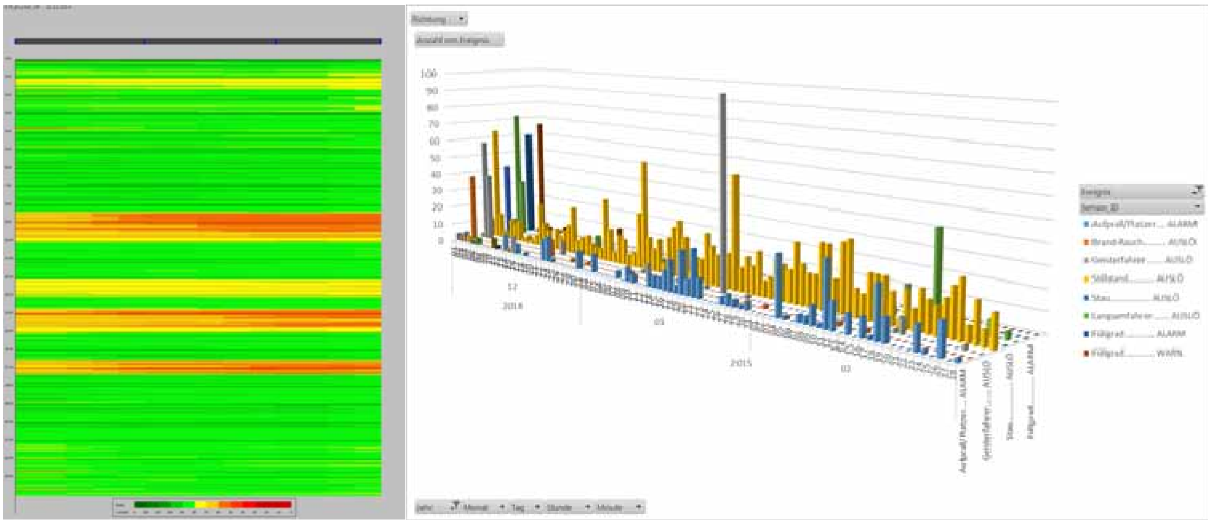

Figure 1: Traffic state reconstruction (left) and accumulation of alerts (right)

For probabilistic sensor fusion, quality information in kind of sensitivity and specificity of each sensor has to be known or assumed. For supervised machine learning techniques, labelled sensor alarm event data are required. During the TSFu project, sensor data has been collected during three months between December 2014 and March 2015 as shown in Figure 1.

This data has been annotated manually by sighting event videos. Each of 1113 events has been classified as either being TP or FP including a comment. Information about false negative [FN] and true negative [TN] events could not be evaluated, since such events are undetected and unrecorded, and therefore can’t be read from offline data.

3. SENSOR FUSION

Typically, road tunnels are equipped with several heterogeneous sensors as introduced in section two. Initially, each individual sensor was foreseen to detect a particular event or incident such as a wrong way driver or smoke. However, practice reveals that solely using one sensor system or technology does not always results in the expected performance. Especially when considering the criteria of false alarm rates, a demand for further improvement becomes visible. One potential solution to address the aforementioned problem is to combine the information from several sensor systems by *data fusion* techniques. For example, in the automotive domain data fusion among *perception sensors* (e.g. radars, lidar and computer vision) is a well-known and established approach to increase robustness and accuracy. In the following section two different data fusion schemes, an *object-based* and a *feature-based* approach, will be introduced.

3.1. Object-based data fusion with BASELABS Create

The exteroceptive sensors used in the automotive domain typically emit several independent detections at one cycle. For example, a long range radar—as used for an *adaptive cruise control* (ACC) function—provides the distance and the bearing (i.e. in polar coordinates) of detected objects relative to the position of the ego vehicle. Similarly, a smart camera system, which is typically mounted behind the windshield, provides the longitudinal and lateral position (i.e. in Cartesian coordinates) of other road users inside the sensor's field of view. Additionally, the sensor measurements, often also coined *object detections*, comprise further information such as velocity, heading or object extension.

According to the exemplarily mentioned sensor setup of a camera and a radar, an object-based data fusion would require serval task to be realized in order to fuse sensor information over time: First, as both sensors are independent, the data fusion has to synchronize the sensor measurements to a common time basis. Furthermore, as the sensors use different measurements principles and, thus, also distinct coordinate systems, the data fusion has to perform an appropriate transformation to a common reference frame. Typically, this task is achieved by implementing a so-called observation/measurement model. Besides describing the transformation from one coordinate system to another, the measurement model usually also accounts for the potentially different mounting positions of the perception sensors. Finally, the data provided by the sensors is subject to different errors like sensor noise, latencies or calibration error. Also sensors may fail to detect objects at all or falsely report objects that are not present in the environment.

For a practical implementation of an object-based multi-sensor data fusion system, all of the aforementioned tasks have to be carried out. In Figure 2 the architecture of a multi-sensor data fusion for environmental perception as proposed by BASELABS Create is depicted. Although, object-based data fusion by probabilistic filtering is a powerful and proven technique, it obviously requires a high and accurate amount of information regarding sensor specification, mounting position as well as physical measurement principles and direct access to the sensor data.

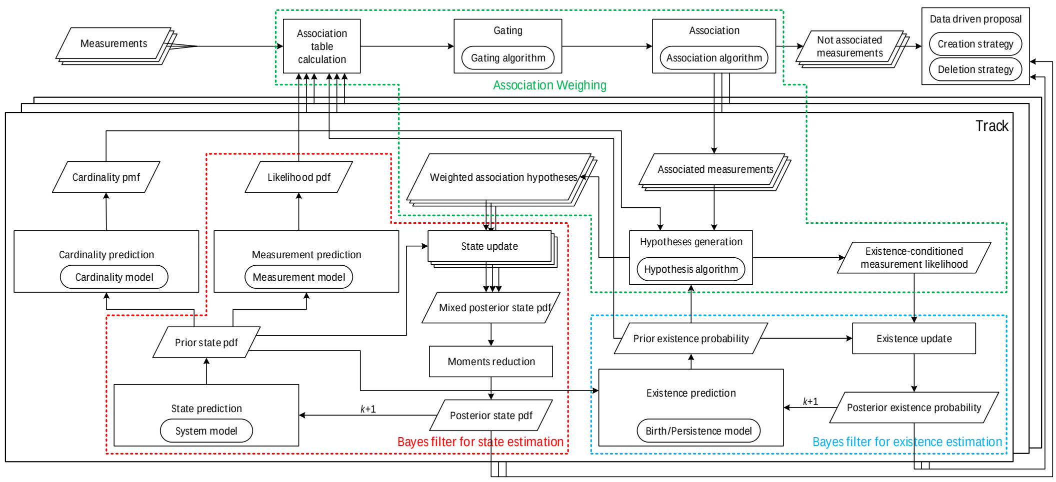

Figure 2: General structure of multi-sensor data fusion for an object-based approach as <

3.2. Feature-based data fusion by supervised machine learning

After carefully analyzing the provided measurements of the sensor systems installed in the road tunnels under investigation in the TSFu project, we concluded that an object-based data fusion approach as outlined in section 3.1 might not be an optimal choice. For example, a practical implementation would require the following perquisites: 1) Sensor mounting positions are accurately known (including tilt and pan parameters) in order to implement the physical measurement models. 2) Details of the sensor statistics are available, e.g. this would include measurement noise. As the sensor do not directly detect objects but events, this information cannot be reconstructed. 3) The sensor measurements are required to have accurate and consistent timestamping in order to realize the synchronization task.

Unfortunately, these requirements were not fulfilled to the required extend for the selected road tunnel configuration. Hence, another data fusion technique, based on the fusion of dedicated features or events, has been investigated. In general, this technique utilizes several classification algorithms from robotics and machine learning. For the sake of completeness, the evaluated candidates are briefly described in Table 4.

Table 4: Description of evaluated classification algorithms for road tunnel data fusion [1]

Algorithm	Description
Nearest Neighbor	Classification algorithm which does not require any parameters. A class detection is based on a distance measure (e.g. Euclidian).
Linear Support Vector Machine	An SVN tries to estimate so-called hyper planes in order to efficiently classify and separate data samples.
Decision Tree	A tree-based approach which answers the questions whether a sample belongs to a particular class.
Random Forest	Parallel usage of multiple decision trees.
AdaBoost	Adaptive boosting combines multiple weak classifiers in order to provide a more powerful classifier.
Naïve Bayes	A probabilistic classifier which assumes the quantities of the feature vector to be independent.
Linear discriminant analysis	The LDA identifies representatives parameters of the feature vector in order to separate the classes.

3.2.1. Feature Vector

For the realization of a feature-based data fusion, an n-dimensional feature vector $x \in \mathbb{R}^n$ has to be composed from the available sensors. In general, it is not required at this stage to consider whether the individual sensor systems provide correlated or significant observations. An inherent task of the learning step in classification is to estimate exactly theses underlying correspondences by identifying appropriate mechanisms for separation of the sensor samples. As the evaluated classification algorithms from Table 4 are based on different ideas, different learning strategies are expected as well.

We chose a sliding window approach to accumulate the number of alarms/events of each single sensor system. By that, one particular dimension of the feature vector represents the number of detected alarms within one sensor (e.g. wrong way driver) during the considered time. Hence, the final feature vector $x \in \mathbb{R}^n$ was identified:

$$x = [\, WrongWayDriverCount\,, SlowVehicleCount, SmokeCount, StoppedCount\,]^T$$

For example, for the event of a wrong way driver within the road tunnel with a sliding window of t = 30s, one observed feature vector sample was:

$$x_{t=30s} = [\, 2, 3, 0, 0\,]^T$$

This means, that within an observation time of 30 seconds two *wrong way driver* alarms as well as three *slow vehicle* alarms have been fired. Obviously, the remaining sensor system did not detect any event. This is already a first indication, that the alarms *smoke* and *stopped vehicle* are not relevant in order to reliably detect the event of a wrong way driver. Of course, this decision has to be robustified by a large number of observations during the learning phase.

3.2.2. Event Classification

The event classification was realized by implementing the classification algorithms from **Table 4** by using the open source library *scikit-learn*[1]. All the available measurement data from the road tunnel has been annotated in order to have a ground truth and was separated in a training and test set according to machine learning best practices. Afterwards, a supervise learning with randomly selected training data (60% of the available data has been used for learning) was applied. In this stage, positive as well as negative samples have been used. This process was repeated for each event to be classified (e.g. wrong way driver or smoke in tunnel) as well as for each classification algorithm.

After the learning phase, each classifier was tested and evaluated with unknown measurement samples. This result of the classification step is an answer to the questions whether the to be tested event was present or not. Dependent on the particular classifier approach, this answer could be either *yes* or *no* or a *probability* value.

4. UNUSUAL EVENTS DETECTION

In the previous section specific classifier for particular events were introduced. The basic idea was to implement a supervise learning based on labeled measurement data. Although, this approach allows identifying particular events with improved robustness regarding false alarms, it also requires a large amount of consistent measurement data including class annotations for the learning step.

In the course of the TSFu project another probabilistic learning approach, which does not require annotated measurement data, has been evaluated. It is based on the same feature vector as introduced in section 3.2.1. However, the general idea was to detect whether the situation in the road tunnel, as observed by the sensors, deviates from a typical *normal* situation. Hence, we coined the method the *Unusual Event Detection* (UED).

Instead of providing labeled measurements during the learning phase, the UED only requires a parameter that describes the app. percentage of measurement data contained within the whole samples which represents a normal situation. In our evaluation, we chose a value of 95%, which is in line with the ground truth data we got from analyzing the tunnel data during the project.

5. EXPERIMENTS AND RESULTS

In this section, results regarding the event classifiers as well as the UED are presented.

5.1. Classification Results

For each of the investigated events, a performance indicator in the range from 0.0 to 1.0 was calculated. A value of 1.0 indicates that the classifier was able to assign the sensor data to the right class in all performed tests. This value is compared to a straightforward heuristic which is applied to a single sensor system for event detection (i.e. without no event detection). Here, each time, a single sensor raises an event at least twice; we count this as an event alert which is to be reported to the road tunnel operator. The results are summarized in **Table 5**. For the sake of compactness, only the performance of the Nearest Neighbor algorithm is depicted.

[1] http://scikit-learn.org/

Table 5: Classification results

Event	Single Sensor Heuristic	Classifier result (Nearest Neighbor)
Slow vehicle	0.029	0.97
Smoke in tunnel	0.93	0.93
Stopped vehicle	0.29	0.93
Wrong way driver	0.22	0.98

5.2. Unusual Event Detection

In **Table 6** the results for the UED for the time range from December 2014 till January 2015 are shown. Obviously, an unusual events count >=2 already indicates that the tunnel is in an abnormal mode. For example, the UED reported 95 unusual events on 22.1.2015. After a manual inspection, it was figured out, that exactly at this time, a real wrong way driver was present within the tunnel due to construction works.

Table 6: Results of Unusual Event Detection

Date	Usual Events	Unusual Events	Comment
2014-12-01	23	1	No real event
2014-12-02	482	3	Fire in tunnel
2014-12-21	61	2	Traffic jam in tunnel
2014-12-30	17	1	No real event
2015-01-22	73	95	Wrong way driver in tunnel

6. SUMMARY AND CONCLUSIONS

We have surveyed the needs and abilities to add intelligent sensor fusion mechanics in road tunnels. Sensor raw data and incident notifications were extracted from “Kirchdorf” tunnel in Styria, Austria on the Highway S35 in a duration of three months between December 2014 and March 2015. Sensor and incident types were analyzed and classified by experts. Traffic data provided by inductive loop sensors was analyzed by FGSV quality assurance methods and anisotropic smoothing method, showing an excellent quality of most of the traffic data. Sensor incident notifications were manually investigated and labeled to reveal real events and false alarms. Labeled data was used to train classifiers with supervised learning methods, while unsupervised learning was used for an “unusual event detection” mechanism.

Supervised trained classifiers could improve the incident detection accuracy up to more than 93% for different incident types, reducing the number of false alarms to increase tunnel observer’s trust in sensor- and automatic incident detection systems.

Unusual event detection could detect unsupervised and automatically unusual events in scenarios like traffic congestion, wrong way driver occurrence and rainfall which might help a tunnel system to guide an observer’s attention to corresponding cameras, screens or tunnels.

Summarized, intelligent sensor fusion by both, supervised and unsupervised learning techniques looks very promising, while additional experiments with more data have to be performed and more experience with a system implementation in a tunnel has to be gained.

7. REFERENCES

[1] S. Russell, P. Norvig, (2010) Artificial Intelligence. Third Edition, pp. 738 - 850

RELIABLE DETECTION OF ABNORMALITIES WITHIN TRAFFIC FLOW IN TUNNELS

P.J.C. Maessen, H.M. Hendrix, - Rijkswaterstaat, the Netherlands
P.L. Böhnke - ave Verkehrs- und Informationstechnik GmbH, Germany

ABSTRACT

This paper will give an overview about the latest investigation of Rijkswaterstaat (RWS) in the field of reliable detection of abnormalities within traffic flow in tunnels. It will draw a comparison between local measurements (current state-of-the-art technology) and an incident detection system based on measured travel-times (alternative system).

The reason behind the new investigation was an internal RWS report showing that the operational incident detection systems used in the RWS tunnels produce many false alerts and sometimes miss alerts resulting in tunnel operators not trusting the system. This could lead to a late reception and action in case of a real incident. This situation is not acceptable for RWS.

In the first quarter of 2015, an alternative incident detection system for tunnels based on intelligent induction loops (measuring section based data) was tested by RWS in the A2 Leidsche Rijn Tunnel near Utrecht. This alternative system operated in parallel to the actual implemented incident detection system and independent from any tunnel safety system. The required induction loops for the alternative system were already present in the tunnel but had not been used before. During the test period both systems were tested extensively with normal traffic flow as well as with special test scenarios. Due to the topics of the test scenarios (wrong-way driver, stopped vehicles etc.) these tests were done during maintenance work when there was no traffic in the tunnel.

The result of the test is, that the alternative incident detection system is much more reliable (no false alerts and no alerts missed during the test period) and in addition, the response time was a lot shorter than the current system. Based on the test results RWS is now looking to update their requirements for future incident detection systems.

Keywords: incident detection system, reliability, traffic tunnel, induction loops, testing, requirements

1. INTRODUCTION

Rijkswaterstaat, the executing organ of the Dutch ministry of transport and the environment, is the client and owner for the majority of the tunnels in the Dutch motorway network. To provide a safe tunnel according to the Dutch building code and the Dutch tunnel law, all tunnels are equipped with several tunnel safety systems, for example: ventilation, lighting, a safe escape route and an automated incident detection system to recognise abnormalities in the traffic flow. In this paper, the last mentioned tunnel safety system – incident detection – will be described more in detail. The automated incident detection systems which are currently used in the Dutch highway tunnels generally report too many errors. Regardless of whether these errors are missing or false alarms (so called “false negatives” or “type 1 failures” and “false positives” or “type 2 failures”). This may lead to the fact, that the operators don’t trust and therewith don’t use those systems which is not acceptable while operating a tunnel.

The present paper is divided into different parts. In the first part the current problems are described more in detail, as well as the steps that were taken to perform a test. The second part gives a brief description about the tested incident detection system of the ave called MAVE®-tun (hereafter the tested incident detection system) and its functionality. After that, the performed test is described and finally some conclusions are drawn in the last part of the paper.

2. STATUS QUO - PROBLEMS WITH CURRENT INCIDENT DETECTION SYSTEM

Most Dutch motorway tunnels are controlled and operated through bundled traffic centrals, i.e. in one traffic central, several tunnels and/or sections of motorway are being watched by traffic controllers or operators. To provide a safe operation of tunnels, it is essential that the operator can rely on a correct, consistent and complete interaction with the tunnel safety systems. For some time, operators complained about the number of false positives and occasional false negatives errors of the implemented incident detection systems. The automated incident detection systems are critical safety systems, as they are designed to alert the operators on abnormalities in traffic flow in the tunnel, for instance a broken-down car or an accident. All such incidents can lead to a calamity in a tunnel and should be detected quickly and reliably.

In Dutch motorway tunnels, the currently applied automated incident detection system is based on local measurements of traffic flow by induction loops. The number of passing vehicles is counted as well as the speed of passing vehicles at the location of the induction loops. For an acceptable resolution of the local measurements in the tunnel, the induction loops should be placed at a short center-to-center distance (in the Leidsche Rijn tunnel every 60 meters). This is quite costly and, as it will be described further on, not as effective as foreseen.

On top of that, the necessary sensitivity and reliability numbers of the system are not prescribed in requirements. This leads to the problem that a *critical* safety system can neither be designed properly nor can it be adjusted in a satisfactory way to meet the owner's and user's requirements.

To determine the proper requirements for the incident detection system, it is important to determine which functionalities the incident detection system should fulfil:

1. Reliability of the detection signal is essential. Many false positive errors will lead to operators not trusting and therefore not using the systems. Opposite to that, a false negative error is even more undesirable, as this may lead to a calamity while a signal was never triggered by the system. If at all, there are only very few false negative and false positive failures acceptable.
2. Detection of abnormal traffic behaviour is a reliable and detectable parameter for the tunnel operator, for instance:
    a. Traffic detection: compared to the normal surrounding traffic flow conspicuously slow driving or even standstill vehicles
    b. Wrong-way driver: vehicle driving against the allowed driving direction

    These examples are incidents which can lead to a traffic accident and should therefore be detected with the highest possible reliability.
3. Detection of too large relative speed differences is no longer required in the Dutch tunnel standard, although it is a much more accurate way of detecting abnormalities.
4. Reliability should allow max. 2 false negative and max. 4 false positive alarms per 100 given alarms.

The tested incident detection system has been developed outside the Netherlands and is successfully implemented and operational in several tunnels in Europe. Tunnel owners are very pleased with the system as it is a reliable incident detection system. In the next paragraph it will be explained more in detail.

3. DESCRIPTION OF THE TESTED INCIDENT DETECTION SYSTEM

To operate the tested incident detection system the tunnel has to be divided into different adjacent measuring sections. Each measuring section (MQi till MQi+1) is limited by its entrance (MQi) and exit (MQi+1) cross section (**Figure 1**). The length of a measuring section is variable, more or less free eligible but still has an important impact on the alarm latency. Typically a length of about 300m is chosen.

Road traffic flow is measured at these cross-sections by Intelligent Inductive Loop in real time, this comprises locally and section-related traffic data. The generated traffic data characterise the traffic situation in the tunnel at any time. Furthermore the loops measure an electro-magnetic pattern of every single vehicle, which passes the loops. This allows tracking by re-detection of the vehicle e.g. at the next cross section downstream. The section-related measurement also determines the current collective and individual travel time. If a vehicle has passed a cross-section it will be expected at the next cross-section within a travel time which is roughly around the current travel time of the previous vehicles.

Intelligent Inductive Loops deliver high-quality traffic data. Furthermore special know-how could be developed concerning the loop installation even in armoured concrete road surfaces.

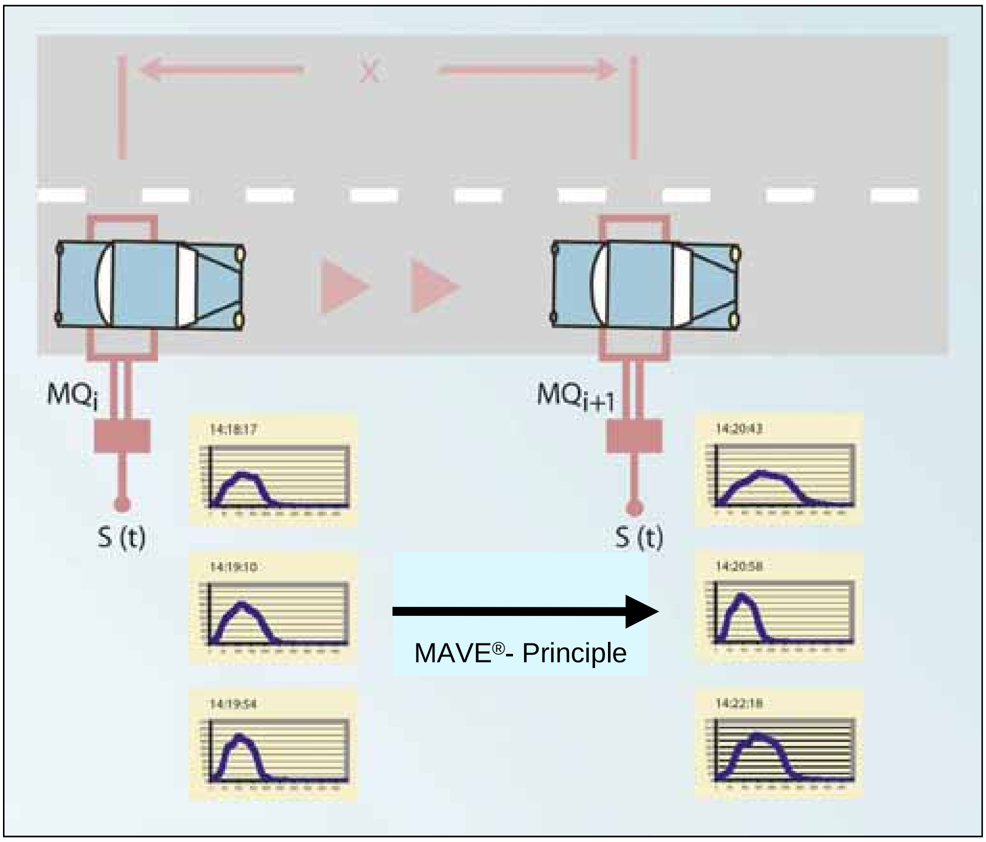

Figure 1: Basic mechanism of vehicle recognition for incident detection

For the detection of incidents, the system permanently measures local and section-related traffic flow data. Irregularities in traffic flow are determined in real-time. The system automatically discovers abnormal behaviour of single vehicles in comparison with the general traffic flow.

The system assumes an incident situation if one or more vehicles do not arrive at the next loop cross-section during the expected time interval and will react automatically with an alert. Different kind of alerts can be defined like for example slow driving or standstill vehicles. Furthermore the system is able to detect vehicles driving in the wrong direction.

Generally the generated alerts are given to a tunnel control centre including the actual incident measuring section (**Figure 2**). Depending on the real distance between the cross-sections, the location of the incident within the measuring section and on the speed of the general traffic flow this will usually be the case within a couple of seconds. Via conventional video monitoring subsystem, which is mandatory in most of the tunnels, the tunnel operators are able to analyse the situation of the incident cause in detail. Possibly necessary rescue or assistance measures can be started immediately after the incident.

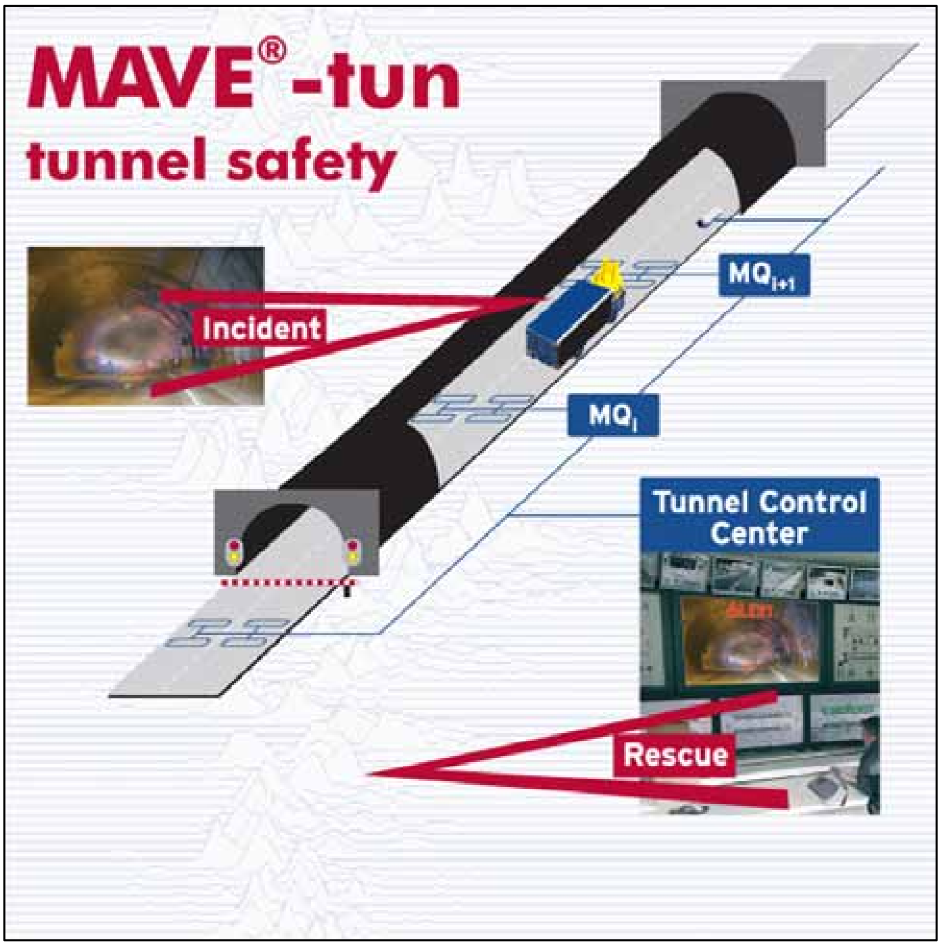

Figure 2: General principle of the incident detection system

4. TESTING IN THE A2 LEIDSCHE RIJN TUNNEL

To gain information about the achievable requirements for incident detection systems, some comparative research (between the conventional incident detection systems and the tested incident detection system) needed to be done. Goal of the research was to perform a test to compare both systems, to determine achievable reliability numbers for automated incident detection systems. The A2 Leidsche Rijn tunnel – opened in 2012 - proved to be a suitable location for the test, because the tunnel was already equipped with TLS-2 induction loops which were not in use but which fit the requirements of the tested system (Figure 3). Furthermore the Leidsche Rijn tunnel is also a major tunnel with a high traffic density (up to 230,000 vehicles per day) which is also important for a reliable and significant system test.

In the Netherlands, the usual type of automated incident detection systems is based on local speed measurements based on RWS standard induction loops (Figure 4). These systems use each single induction loops to determine the speed of vehicles passing the induction loops.

The test itself was – thanks to the already available induction loops – quite easy to initiate. Only the roadside stations and a data connection to the central data processing unit needed to be installed and the test could take place without any interference with the operational tunnel systems whatsoever.

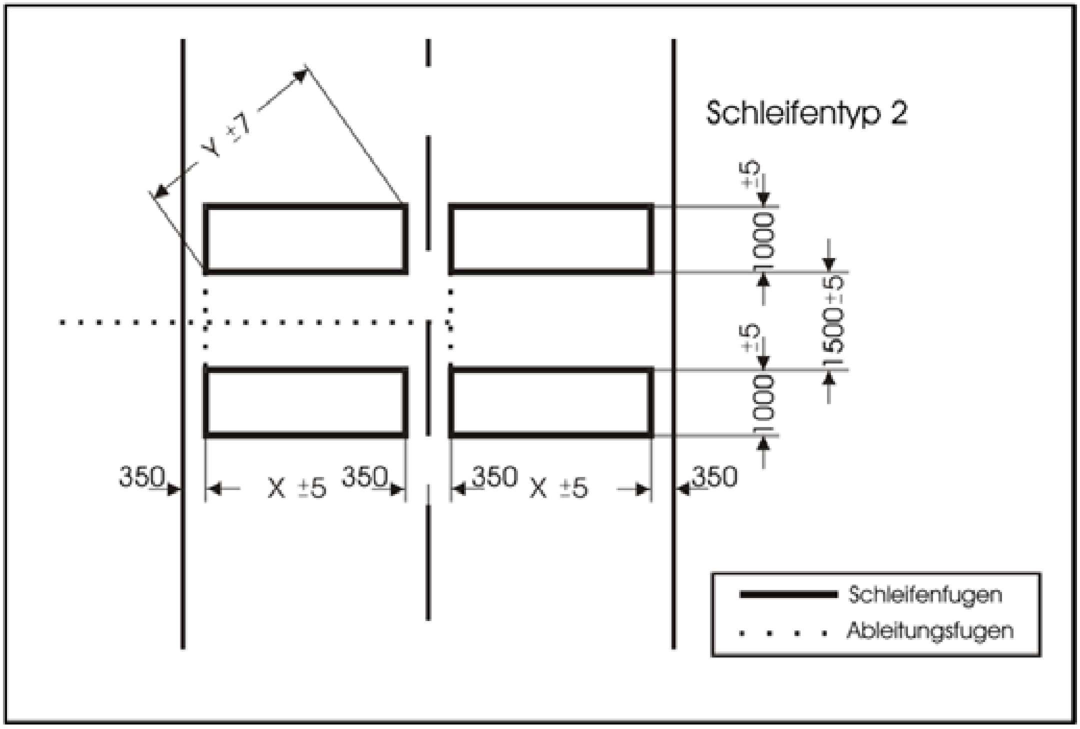

Figure 3: TLS-2 induction loop geometry, as required by the tested incident detection system [2]

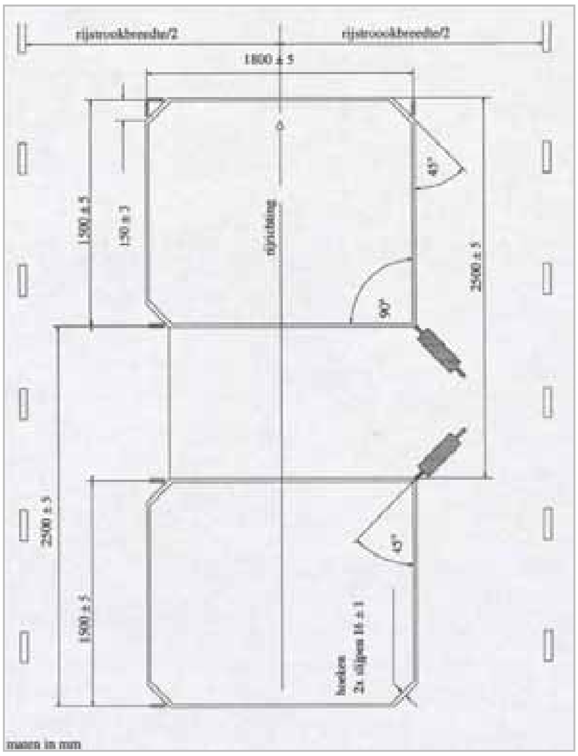

Figure 4: RWS standard induction loop geometry [2]

4.1. The A2 Leidsche Rijn tunnel

The A2 Leidsche Rijn tunnel is located on the West side of Utrecht in the A2/E35 motorway just north of traffic junction Oude Rijn. In the A2 Leidsche Rijn tunnel, traffic is separated between transit traffic and local or diverging traffic, which is the reason for having 4 tunnel tubes: 2 transit tunnel tubes in the middle for 3 lanes + shoulder and 2 local tunnel tubes for 2 lanes + shoulder on the outside, see also Figure 5.

Together with the operational management of the A2 Leidsche Rijn tunnel, it was decided to perform the test in the local traffic tube in northern direction. ave GmbH was commissioned to perform the test.

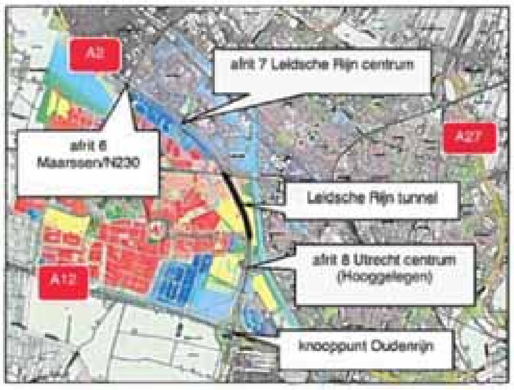

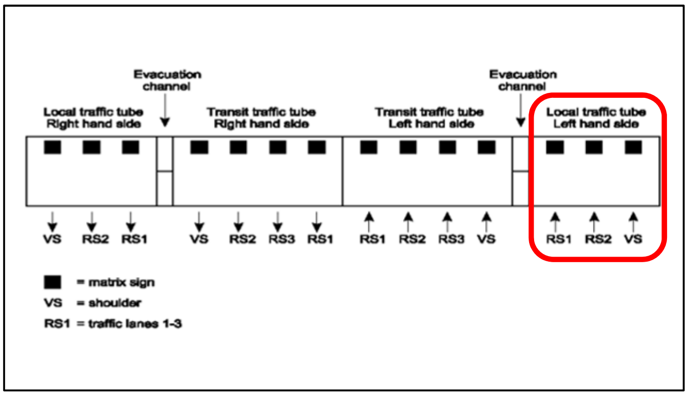

Figure 5: Location and cross-section of A2 Leidsche Rijn tunnel

4.2. Test environment, test duration & test night

For automatic incident detection in traffic flow in the A2 Leidsche Rijn tunnel there is a Motorway Traffic Management system (MTM) implemented according to current Dutch RWS tunnel standard. To verify the detections by the tested incident detection system, the log files from the tunnel operators were required, as well as the log files from the MTM system. The test period was limited to 25 days because of the limited availability of the MTM log files. In the parallel tube, a section of 1210m., containing 4 pairs of induction loops per lane, was used for the test. The test was split in 2 parts: a long time test in normal traffic and a test night. During a maintenance night, which takes place every 4 weeks for each tunnel tube, a test procedure was run to perform 3 different scenarios to verify the functionality of the ave system. During the whole test period, including the test night, and up to the moment at which ave handed over their test results to RWS, ave had no information about the performed test scenarios during the test night, MTM or tunnel operating loggings, loggings from operators, video data or things like that. All available information for ave was generated by the used intelligent induction loops.

4.3. Results & findings

The data for the test, usable for analysis, were the following:

- Log files by the operators;
- Log files from the tunnel operating system and the MTM system;
- Log files from the tested incident detection system
- Registration of observations from the test scenarios during the test night.

During the test period, which lasted from April 6th until April 30th of 2015, about 34,000 motor vehicles per day passed the equipped local tunnel tube. During that period in time, the MTM logging system reported 451 incidents in the test section to the operator (average 20 alarms per 24 hours). Reports varied from slow driving vehicles and standstill vehicles to wrong-way drivers. The tested system reported 16 incidents in the test section during the test period. All of these reports were related to slow driving and standstill vehicles.

Finding 1:

The current incident detection system reports wrong-way driving vehicles. But during the test period, the reports from the MTM belonging test section were often false and inconsistent. Verification of this finding has been done during the test night, when an actual wrong-way driver scenario was performed. The reports from the current incident detection system were significantly different from the ones logged by the tested incident detection system, which proved to be correct.

Finding 2:

Follow-up alarms are not suppressed by the current incident detection system. If the current incident detection system is triggered by a slow driving vehicle on one loop, the system should suppress all alarms generated by the following slow driving vehicles on the same loop, to avoid an overload of alarms for the operator. Also, the alarms triggered by a slow driving vehicle on adjacent induction loops should be suppressed. The tested incident detection system was working correctly.

Finding 3:

The currently implemented RWS incident detection system did not report all incidents in the test section which leads to false negative failures. This kind of failure is a potential safety hazard and is not acceptable for a reliable incident detection system. All of these incidents were reported by the tested system.

During the test night, four different test scenarios were performed in two-fold.

1. Scenario of a standstill vehicle in the test section
2. Scenario of a slow driving vehicle in the test section
3. Scenario of a vehicle driving on the left shoulder with 80 km/h, changing to the overtaking lane (left lane) after the first pair of induction loops and slowing down to 20 km/h before the last pair of loops in the test section.
4. Reversing in the tunnel by 3 cars.

All of the tests were 100% accurately detected by the tested incident detection system of ave GmbH. The current incident detection system reported several inaccurate or incorrect incidents.

5. CONCLUSIONS AND RECOMMENDATIONS

The currently implemented incident detection system in the A2 Leidsche Rijn tunnel does not meet the requirements as stated by Rijkswaterstaat. It informs the operator too late or with inaccurate information which might lead to unwanted incidents or to the fact, that the operators don’t use/trust those systems. Based on the experiences with implemented RWS incident detection systems also from other tunnels it is assumed that this is not a single failure of the system in Leidsche Rijn Tunnel but rather a general problem.

The main goal for the test – gaining information about the possible reliability numbers for automated incident detection systems – is reached, which allows Rijkswaterstaat to change and set up additional requirements for new automated incident detection systems.

6. REFERENCES

[1] Böhnke, P. (2011), Automatical incident detection in tunnels based on loop sensors, Tunnels and ITS Symposium Bergen, Norwegian Public Roads Administration; Norway (http://www.vannforeningen.no/ikbViewer/Content/821207/15-1200%20Peter%20Bohnke%20Tunnelkongress%20Bergen%202011%20AID%20in%20Tunnels%20with%20Loop%20Detectors.pdf)

[2] Maessen, P. Et al. (2016), Betrouwbare detective van afwijkingen in de verkeersstroom in RWS tunnels, Utrecht, The Netherlands

[3] TLS (2012); Technische Lieferbedingungen für Streckenstationen, Bundesministerium für Verkehr, Bau und Stadtentwicklung (D), Germany

HIGH PERFORMANCE LIGHTING - ON THE ROAD FOR ENERGY EFFICIENCY IN TUNNELS

[1]J. Vercammen
[2]A. Audenaert
[1]Agency for Roads and Traffic, Flemish government, Belgium
[2]Departement of Applied Engineering: Construction, University of Antwerp, Belgium

ABSTRACT

In the last decade, improving energy efficiency has taken a prominent role in energy policies throughout the world. One of the large energy consumers in road tunnels is tunnel lighting. Nevertheless, the literature related to energy efficiency of road tunnel lighting is scarce. This paper helps in filling this gap by providing insight in how the tunnel design phase might impact energy efficiency of tunnel lighting. To this end, the different types of influencing tunnel lighting factors in the tunnel design phase are highlighted: the entrance design and related entrance lighting, the reflection properties of pavement and tunnel wall materials, the lighting material (bulbs, luminaire and driver) and the maintenance of the tunnel lighting. At the same time, empirical studies, examples of recent renovation projects and international guidelines are provided for these influencing factors. The paper clearly demonstrates the benefit of involving all stakeholders right from the tunnel design phase to reach high performance lighting in road tunnels.

Keywords: road tunnel; tunnel lighting; efficiency maximization; tunnel design phase; entrance lighting

1. INTRODUCTION

It is well-known that light plays an important role in maximizing the safety and comfort of tunnels. The total energy use of a road tunnel can amount to several GWh per annum, which is equivalent to the energy use of several hundreds of households. The energy used for tunnel lighting equals 50 % of the total energy consumption of a tunnel. This means that increasing the efficiency of tunnel lighting gives rise to large potential energy savings. Moreover, as in many tunnels in Flanders the electromechanical equipment (of lighting, ventilation,…) has exceeded its useful life-time, the renovation of the tunnels are an opportunity for large energy savings. The goal of this paper is to provide insight in how the road tunnel design phase and the tunnel lighting design itself: maximize the energy efficiency of tunnel lighting, thus minimize (electric) energy use. Note that the impact of the choices in these design stages are mostly irreversible. Hence, it is of utmost importance to carefully take decisions in each stage. To provide evidence on the content of each of these stages, empirical studies, recent renovation projects and international guidelines are included. The projects were set up by the Flemish government and executed under the supervision of the Agency for Roads and Traffic.

The paper is organized as follows. Section 2 starts with the terminology used for tunnel lighting. In the next four sections, the different design stages and the specific factors influencing tunnel lighting efficiency are discussed. Section 3 focuses on the entrance design and the related entrance lighting. Section 4 highlights the impact of the reflection properties of road and tunnel wall materials on the whole lighting installation. Thereafter Section 5 discusses the lighting material used and zooms in on LED as new lighting technology. Finally, Section 6 discusses maintenance management of the tunnel lighting. Section 7 concludes the paper with the most important insights generated from the four design stages.

2. TERMINOLOGY

The requirements for a lighting installation of a tunnel are influenced by several critical factors which determine the ultimate visibility: characteristics of the driver, the physical condition of the road, the access to and the length of the tunnel, the atmospheric conditions, the traffic density, the volume, the speed and type of vehicles in transit, the architectural aspect of the tunnel opening in terms of visual guidance (i.e., safety), comfort and overall maintenance of the installation. There are also the photometric characteristics of tunnel lighting: the level of luminance of the road and the lower parts of the tunnel walls, the uniformity and distribution of the luminance of the road surface and walls, the limitation of glare caused by light sources, the limitation of the flicker effect, the visibility level of possible obstacles and the visual guidance.

Note that apart from these factors, the lighting requirements of a tunnel differ for day and night times. At night, the decision is relatively simple, i.e., provide luminance levels inside the tunnel that at least equal those outside the tunnel. On the contrary, the design of day time lighting is more complex due to the human visual system. A driver outside the tunnel cannot simultaneously perceive details on the road with a highly illuminated exterior and a relatively dark interior (i.e., transient adaptation). That is because the adaptation of the human eye takes a certain time, depending on the amplitude of the reduction. The greater this amplitude is, the longer the adaptation time is. Therefore, entrance lighting in the tunnel must ensure that the contrast between road and objects in the tunnel as to allow the driver to observe the object in time [1].

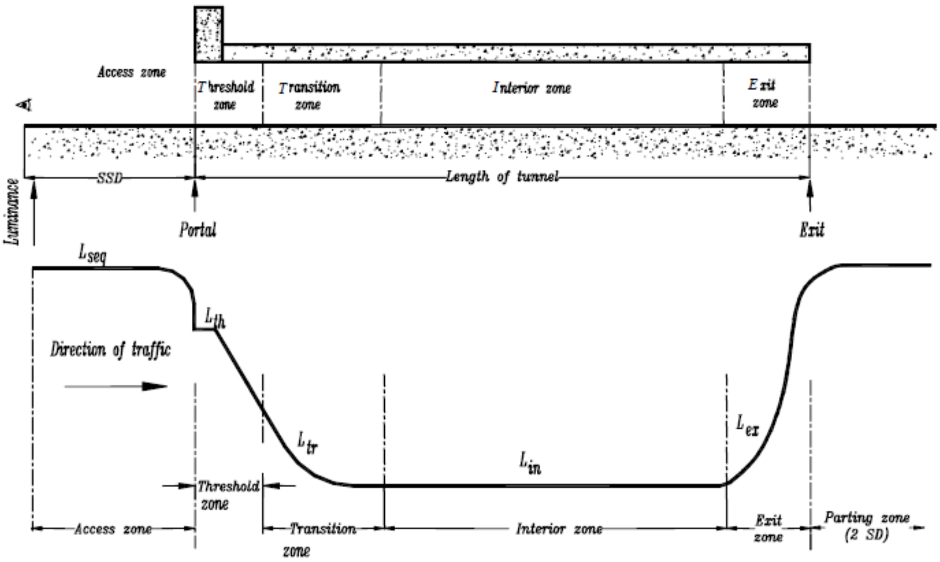

Figure 1: The different zones in a tunnel [1]

As human behaviour is known to be a major contributor to fatalities in road tunnels [2], it is e.g., key to help the driver's eye adapt easily and quickly. Therefore, the tunnel is divided in different zones (upper part of Figure 1) having different luminance levels (L) (lower part of Figure 1). The zone before the tunnel portal is defined as the access zone (seq). It starts at a distance ahead of the portal equal to the (safe) stopping distance (SD) [1]. This distance covers the reaction time and the braking time, for an approaching driver to see in the tunnel. The first part of the tunnel is called the threshold zone (th), starting at the portal. It is at least equal to the stopping distance (SD) (note that this is not clearly visible in Figure 1). The luminance level over the first half of this distance (Lth) must be equal to the luminance level at the beginning of this threshold zone. Then the level is gradually and linearly decreased to a level which equals 0.4 times the level in the first half of this zone. The threshold zone is followed by the transition zone (tr) in which the level of luminance is gradually reduced, over a distance determined by the speed limit, to the level of the interior zone. This adaptation process allows the (eyes of the) driver to drive safely through the (first part of the) tunnel. After the entrance lighting (i.e., the lighting in the threshold zone and transition zone), only the base lighting remains in the interior zone (in). The exit zone (ex) is less critical in terms of visual perception. It is lit in such way as to prepare the drivers for return to external luminance and the perception of obstacles in the exit zone. The Flemish government has since many years opted to light the exit zone the same manner as the interior zone, called tunnel zone. The parting zone starts after the exit portal of the tunnel and is advised to cover two times the SD. The base lighting consists of a night regime and a day regime, in Flanders always designed as a continuous light line through whole the tunnel length (all zones) [1],[3].

3. ENTRANCE LIGHTING

The first stage in the tunnel lighting design decides on the entrance lighting [1]. Figure 1 shows the gradual decrease of the entrance lighting to the lighting level in the interior zone, this avoids the "black hole" effect of driving in an under-lit tunnel.

As the energy use of the entrance lighting is 50-60 % of the energy use of the whole tunnel lighting installation, it is key to focus on this entrance lighting when aiming at energy savings. Indeed, the lower the level of entrance lighting is, the lower the energy use will be. To decrease this lighting level, we give insight in the influencing factors of this entrance lighting.

The level of Lth is calculated using the L20 method. L20 is defined as the outside luminance created by natural light in the access zone at stopping distance from the tunnel portal in a 20° wide circular field and can be approximated by a weighted average of the luminance values of sky, road and environment as can be seen in Figure 2 [1]:

$$L20 = \gamma \, Lc + \rho \, Lr + \varepsilon \, Le \qquad (1)$$

with $\gamma+\rho+\varepsilon$ smaller than one. Lc, Lr and Le represent respectively the luminance of the sky, road and environment and γ, ρ and ε respectively the % sky, road and environment in the 20° field. Note that τ Lth, with entrance luminance Lth and τ the % of the tunnel entrance is omitted from Eq. (1) as this term is negligible. τ as well as Lth are very small as compared to the other percentages and luminance values.

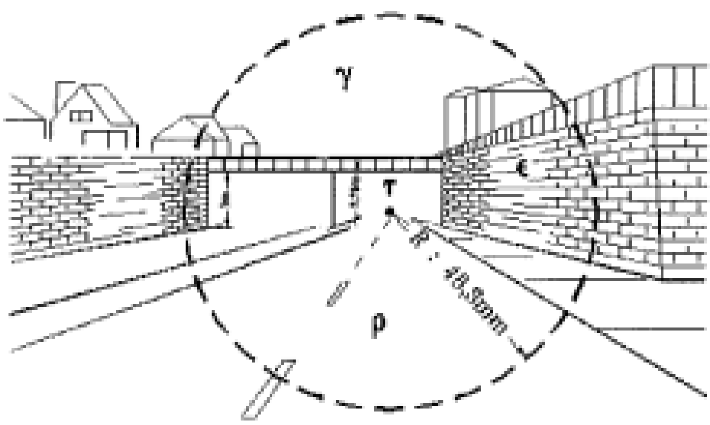

Figure 2: The perspective view of tunnel entrance with superimposed 20° subtended circle [1]

The level of entrance luminance (Lth) can now be calculated as follows:

Lth = k L20 (2)

with k the fraction of Lth as compared to L20 [1]; k depends on the speed and is represented in Table 1. It is worth to notice that the lower the speed, the lower the level of entrance lighting is.

Table 1: The Lth / L20 ratio's for various speeds [1]

Speed (km/h)	k
<=60	0.05
80	0.06
120	0.10

The entrance lighting is made up of different regimes. The entrance lighting is designed as discrete lighting. The timing of changing to one of the different entrance lighting regimes depends on the L20 value. This value is constantly measured (luminance meter) and triggers the lighting system which adapts the entrance lighting accordingly. Note that a good alignment of this luminance meter is important to avoid wrong lighting levels in the tunnel, and related energy use.

The stopping distance is determined by the friction coefficient tire-pavement, the speed, the gravity acceleration and the mass of the vehicle. A shorter stopping distance means a lower sky percentage in the L20 calculation (see Eq. (1)), resulting in a lower level of entrance lighting. Minimizing the sky percentage and as such decreasing L20 and Lth can be accomplished by thoughtful design as:

- making the tunnel gable around the road big enough;
- putting trees on the gable: the leaves of the tree in the summer lower the sky percentage;
- having careful geographic implantation of the tunnel;
- minimizing the stopping distance. Also, with a shorter SD the threshold zone (Lth) is shorter, what results in less installed and consumed power.

Also the tunnel's orientation influences the values of the luminance levels in Eqs. (1) and (2).

4. IMPACT OF REFLECTION PROPERTIES OF ROAD AND WALL

The importance of the entrance lighting in terms of energy saving potential and safety has already been discussed in the previous section. Yet the design of the whole lighting installation depends strongly on the reflection properties of the road (pavement) and the walls. Optimization of the reflection of the road and the walls increases the efficiency, decreases the power required from the lighting installation and as such can lead to important potential savings. The road and wall materials are thus crucial because the reflection properties result from it. The impact of the reflection will be examined based on empirical studies and a new type of "clear asphalt" along with international guidelines.

In general, the reflection characteristics of a road are determined by the following three factors in order of importance: nature of the road surface, physical state and the direction in which the road surface is irradiated and viewed by the driver. The uniformity determines the quality of lighting and specific levels are recommended: a longitudinal uniformity of 0.6 and an overall uniformity of minimum 0.4 [4]. The calculation of tunnel lighting has some additional aspects relative to road lighting: walls, contrast, luminaire spacing, etc. [4].

The effect of different materials for wall and road will be examined based on an empirical study in cooperation with the Flemish government. The study is related to the Bevrijdingstunnel in Antwerp. This tunnel was opened in 1978. The lighting installation, the ventilation, the energy distribution and the emergency lighting were renewed in 2013. The apparatus (lighting) were installed above the lanes. The calculation below highlights different scenarios. These scenarios illustrate the impact of different reflection properties (i.e., reflection coefficient) of road and wall on the required power and flux for a constant lighting level within a specific regime (luminance) in the tunnel. Note that although other results would be obtained when using other tunnel geometries, lighting installations, …, the relationships that result from this study remain indicative. The results are represented in Table 2.

Table 2: The impact of road and wall reflection on additional required flux and power for having a constant lighting level [5]

Fixed	Change in	Extra required flux	Extra required power
R3008 (asphalt)	Wall reflection: from 0.5 to 0.3	36% - 39%	36% - 39%
R1010 (concrete)	Wall reflection: from 0.5 to 0.3	39% - 44 %	36% - 39 %
Wall reflection=0.3	Road pavement: from R1010 to R3008	6% - 10%	6% - 8%
Wall reflection=0.5	Road pavement: from R1010 to R3008	4% - 6.5%	6.5% - 8%

The lowest values in column 3 and 4 of Table 2 refer to the whole lighting installation (i.e., the LED and the entrance lighting), the highest value refers to the LED line only (base lighting).

When the wall and road reflection decreases, the power and flux needed increases respectively approximately 40 % and with 4% till 10%. Note that this represents a huge impact in terms of energy use as compared to a rather small investment in infrastructure.

From the study, we can conclude that the optimal material choices are those with high reflection coefficients: clear pavement and white walls. The Bevrijdingstunnel is equipped with concrete (R1010) and white walls (reflection factor = 0,5). These reflection properties are the general goal of the Flemish government. Note: Reflection factors of walls higher than 0,5 are common nowadays.

Installation of luminaires above the lane is the most effective way of installation, this implies maximal direct light on the road and less through reflection.

There exists a special type of very clear pavement, called “clear asphalt”. With clarity values about 0,3 – 0,4. There remain important questions to be answered on the use of clear asphalt before the Flemish government can decide on using it on a long-term basis: e.g., more experience is needed, the maintenance team will have to be trained and we will have to discuss new types of contracts and prices [6].

5. CHOICE OF THE LIGHTING MATERIAL AND NEW TECHNOLOGIES

The total efficiency of the lighting installation is determined by the efficiency of the luminaire (apparatus), bulbs (lamps) and the driver. The efficiency of the luminaire mainly depends on the material of the outer glazing (this will be discussed in Section 6). We will describe three recent Flemish tunnel projects where the effect of renewing tunnel lighting with different kinds of lamps on energy use is measured: the Craeybeckxtunnel, the Rupeltunnel and the Bevrijdingstunnel. The driver will not be considered as a parameter because there is opted for the most optimal electronic driver, i.e., with cos φ larger than 0.95. For each of the three projects one could also make the (historical) step to LED lighting instead of choosing these high efficient T5 lamps. The advantages of LED are obvious: it is 100 % dimmable, it has a good color rendering index (CRI), it makes a colour temperature of 4000K for tunnel lighting easily feasible, it has a long lifetime and requires fewer replacements of lamps. In Table 3, we represent the tunnel characteristics.

The old and new apparatus were installed above the lanes. In the Craeybecktunnel the 65 W bulbs (night regime) were replaced by a fluorescent 28 W (T5), in the Rupeltunnel by a fluorescent 14 W (T5). For both tunnels the 110 W bulbs (low luminance levels) were replaced by a fluorescent 54 W (T5). Some of the low pressure sodium 180 W bulbs (high luminance levels) were replaced by low pressure sodium 91 W bulbs (SOX). The Bevrijdings-tunnel is equipped with a whole new lighting installation: a continuous LED line for base lighting: 3 (night) and 12 (day) cd/m2, the entrance lighting consists of NaHP (SON-T).

Table 3: The tunnel characteristics for the three renewal tunnel lighting

	Craeybeckxtunnel	Rupeltunnel	Bevrijdingstunnel
Opening date	1981	1982	1978
City	Wilrijk	Boom	Antwerp
Length	1600 m	600 m	340 m
Width of tube	20 m	14,25 m	9,5 m
Number of tubes	2	2	2
Lanes per tube	4 and 1 verge	3	2
luminaire renewal date	2009	2012	2013
Annual saving	2,2 GWh	1,1 GWh	0,7 GWh

The annual savings in the three tunnels are considerable, approximately 50 % reduction of the installed power of the lighting installation. In the Bevrijdingstunnel the reduction is near to 66%, because of the whole new installation: LED and NaHP. The luminance level, at night, in the Rupeltunnel and Bevrijdingstunnel is half of the level in the Craeybeckxtunnel.

The payback time of the investment of LED lighting is 6 years, approximately 1/2 to 1/3 of the lifetime of a LED. This is a very interesting driving factor. After the renewal of the Bevrijdingstunnel the first LED road tunnel in Flanders had become a reality. This is the tipping point from fluorescent to LED. The next step in the future is to apply LED for the entrance lighting.

6. MAINTENANCE OF LIGHTING INSTALLATION

The importance of the impact of maintenance on energy saving is largely overlooked. This means cleaning, maintenance feasibility, degradation of materials with less transparency of the luminaire. The losses of light output are a result of environment, operating and age conditions. The “Maintenance factor (MF)” [7] describes this reduction. Initially a new installation will be oversized with the MF due to the fact of having enough light after a certain period. Figure 3 gives a clear view of the effect of periodic maintenance.

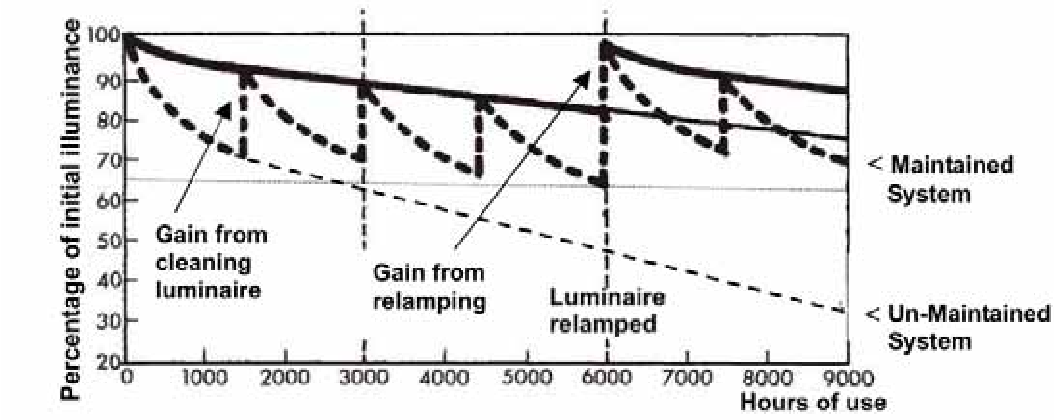

Figure 3: The effect of periodic maintenance [7]

The initially oversizing can be minimized with "constant lumen output" (CLO), due to the fact the lighting installation regulates itself during lifetime. This means the decrease of lighting output during lifetime is continuously compensated by increasing of illuminance of the luminaire (flux) with increased steering current (of the driver).

The impact of cleaning and (the material of) the outer glazing is described based on an original test in the tunnel Cointe-Kinkempois at Liège. R-tech made the set-up in close cooperation with the government.

Test: Tunnel Cointe-Kinkempois in Liège [8]:

- Two types of apparatus – IP66 devices equipped with LED – were examined. One closed by a glass protector (flat and smooth), the other "closed" by the PMMA lenses;
- Three fixtures of each type were installed for three months (winter 2011-2012) in the tunnels of the E25-E40 link in Liège (Cointe & Kinkempois). These were installed at the ceiling, in different areas of the tunnel. The apparatus are not electrically connected to eliminate all possible influences due to the variation of the flow of sources over time.

Measurements of the devices by photometers (results in Table 4):

- Before installation. This is a reference value 100;
- After disassembly, not cleaned;
- After manual cleaning.

Table 4: Measurement results of total efficiency

with outer glazing of glass				
	Entrance Cointe	Body Cointe	Body Kinkempois	Average
new (clean)	100	100	100	**100**
dirty	93,3	92	95,9	**93,7**
cleaned	100	100	100	**100**
without outer glazing (PMMA lenses)				
	Entrance Cointe	Body Cointe	Body Kinkempois	Average
new (clean)	100	100	100	**100**
dirty	86,4	81,2	87	**84,8**
cleaned	97,9	96,8	97,9	**97,5**

The devices with a flat glass were dirty, normal and uniform. The average depreciation because of dirty is 10 % lower than that of devices without an outer glazing (cover).

The luminaires without an outer glazing have a considerable irreversible decrease of efficiency and luminance. The apparatus were foul, uneven and unbalanced. The unbalanced fouling was in flow direction on the lenses (‘asymmetric fouling”): pro beam.

A glass protector increases the maintenance factor. Nevertheless, cleaning stays just as important. The Flemish government opts for luminaires with an outer glazing of transparent (hardened) glass.

7. CONCLUSION

Tunnel lighting is crucial for the tunnel safety and comfort of the drivers in a road tunnel. The potential energy savings of the whole lighting system are considerable and depends on the design of the tunnel and the lighting installation.

The influencing factors for lowering the level of entrance lighting are speed, stopping distance and design of the entrance portal. The efficiency of the whole lighting installation depends strongly on the reflection properties of the road (pavement) and the walls, efficiency of the luminaires, efficiency of the bulbs and maintenance.

Through the whole building process – from concept to realization and maintenance – all interdisciplinary stakeholders must be involved. They must be aware of the importance and impact of the influencing factors. Only that way the integral project (design) succeeds in minimizing the energy use of tunnel lighting and optimizing the tunnel design. We are on the road.

8. REFERENCES

[1] International Commission on Illumination, 2004, CIE 88:2004: Guide for the lighting of road tunnels and underpasses, 32 p.

[2] Alan Beard and Richard Carvel, Handbook of Tunnel Fire Safety, London, ICE Publishing, 2012, 694 p.

[3] Bureau voor Normalisatie, 2001, NBN L18 – 003: Regels van goed vakmanschap voor verlichting van wegtunnels en ondergrondse doorgangen, 29 p.

[4] International Commission on Illumination, 2010, CIE 189:2004: Calculation of tunnel lighting quality criteria, 2010, 10 p.

[5] Schréder s.a., Tunnels: Vergelijkende studie reflectiecoëfficiënten wanden en wegdek, 2015, 1 p.

[6] Shell Bitumen, 2010, Clear asphalt for tunnels & underpasses: a clear way to improve safety & savings in tunnels with Shell Mexphalte C., 31 p.

[7] CIE 154, The Maintenance of outdoor lighting systems, 2003, 18 p.

[8] R-Tech (R-Tech is Schréder’s European Research & Development Centre at Liège), Analyse du salissement des luminaires dans un tunnel (research project), 2012, 7 p.

RELIABILITY AND AVAILABILITY PREDICTION CALCULATIONS IN THE GOTTHARD BASE TUNNEL – WATER SUPPLY AND DRAINAGE SYSTEM

D.P. Huber, M. Steiger
Pöyry Switzerland Ltd, Switzerland

ABSTRACT

The Gotthard Base Tunnel (rail tunnel) is in the final phase of its construction. Different mechanical and electromechanical systems will ensure a high level of safety for people underground. One of these is the water supply and drainage system. To secure a high degree of reliability and availability, targets values for different scenarios were defined.

During the RAMS process according to SN EN 50126, the reliability and availability levels for the system have been examined to determine whether or not the target values have been met. To check for target compliance, the examined system was modelled using a software-based reliability block diagram (RBD).

It was shown that the given targets have been fulfilled. However, the review of such theoretical values will take place as part of the operation of the tunnel.

The work presented here has been carried out on behalf of AlpTransit Gotthard Ltd (ATG), a wholly owned subsidiary of the Swiss Federal Railways (SBB) and the constructor of the Gotthard Base Tunnel as part of the New Rail Link through the Alps. [1]

Keywords: Rail tunnel, SN EN 50126, RAMS, reliability, availability, reliability block diagram (RBD), water supply, drainage system

1. INTRODUCTION

As part of the New Rail Link through the Alps, the 57 km long Gotthard Base Tunnel (GBT) was built. The GBT consists of two single track tunnels (STT east and west), but also includes 176 cross passages (CP), two multi-function stations (MFS) as well as several vertical and horizontal shafts, technical stations and a variety of other structures built outside the tunnel. [1]

Since 2011, the installation of the railway systems and the mechanical and electromechanical systems (MES) has been undertaken. Since October 2015, test operations have been taking place and, in June 2016, the first commercial trains will pass through the GBT as part of the trial operation. Scheduled commercial trains will not pass through the tunnel before December 2016. [1]

The MES are subdivided into different systems / lots such as tunnel ventilation, ventilation and air conditioning systems for auxiliary structures and buildings, cranes, doors, technical floors, metal structures, etc. and also water supply and drainage which will be discussed in more detail in this paper with respect to RAMS. The work regarding the RAM studies for the tunnel ventilation of the GBT has been published recently [2].

The water supply and drainage system has several functions: water is provided for the cooling of different technical rooms and to ensure a constant amount of water is present in the foul water part of the drainage system in order to reduce the extent of damage in case of an explosion in the tunnel. The drainage system ensures the removal of tunnel ground water and, in a separate pipe, the removal of foul water from the tunnel. The foul water is examined when leaving the tunnel and processed if necessary. [3]

Each MES ensures the safety for people in the tunnel in its way. Based on the project requirements, targets have been defined for the railway systems and for the MES in general. As a function of the importance of an individual MES, it was either subjected to the RAMS process according to SN EN 50126 or not. The general target values for all MES have been broken down to the individual MES systems with RAMS relevance [4].

2. RAMS PROCESS

Due to the importance of a variety of MES regarding the safety for people underground, a RAMS process was implemented based on SN EN 50126 in addition to the “standard” building process (development, submission, construction, commissioning, operation). The norm was applied for MES even though it was originally developed for railway applications.

The RAMS process consists of 14 phases starting with the Concept phase (1) and ending with the Disposal phase (14). The RAMS phases are typically represented in the V-model which shows the RAMS phases 1-7 on the left (descending branch of **Figure 1**), the RAMS phases 7-10 on the right (ascending branch of **Figure 1**) and the RAMS phases 11-14 (right side of **Figure 1**).

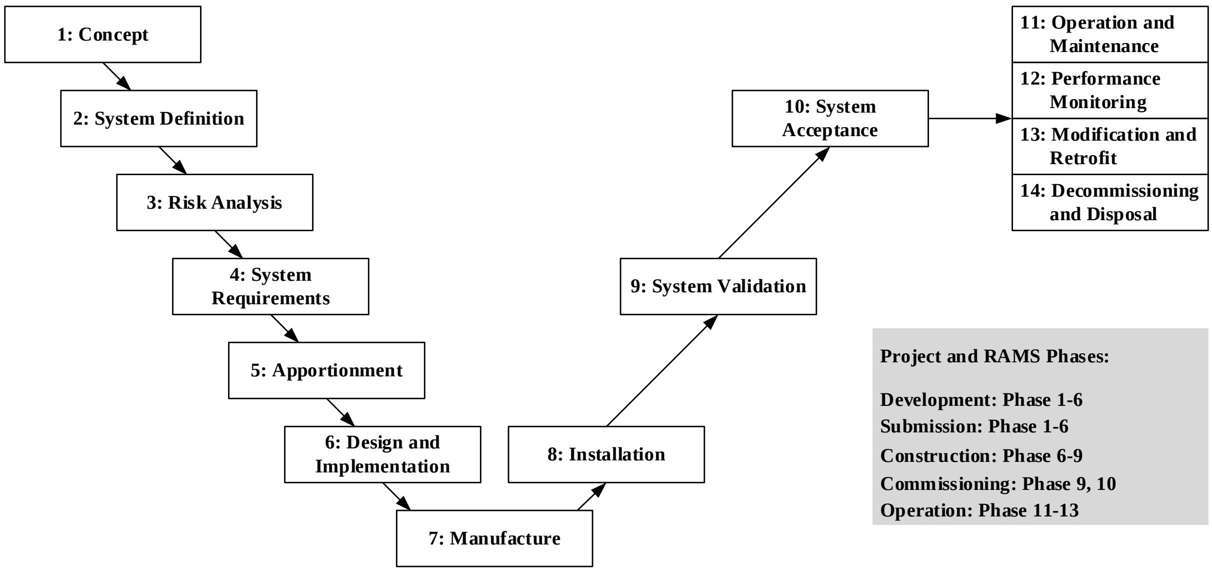

Figure 1: The RAMS phases 1 to 14 in the V-model representation according to SN EN 50126.

It should be noted that, despite the fact that **Figure 1** shows arrows between RAMS phases, the RAMS process should be regarded more as an iterative than a linear process. The correlation of the RAMS phases to the building process is not unambiguous because the RAMS phases are repeated to some extent in different building phases (see **Figure 1**). [2]

Each RAMS phase requires a defined extent of work which was performed under the responsibility of the various stakeholders of the project such as the ATG (client), the representatives of the client (IG GBTS, Interessensgemeinsachft Gotthard Basistunnel Süd), the contractors and the approval authority (Swiss Federal Office of Transport, FOT). Selected tasks along the RAMS or building process will be discussed in more detail below.

The following chapters follow the design and building process.

3. DEVELOPMENT

The development includes the RAMS phases 1-6. As part of this paper, the focus lies on the concept (RAMS phase 1), the system description (RAMS phase 2) and the system requirements (RAMS phase 4). The risk analysis (RAMS phase 3) relies mainly on the quantitative risk analyses (QRA) which was not part of this work [5]. The apportionment of the system requirements (RAMS phase 5) as well as the design and implementation (RAMS phase 6) will be discussed in chapter 4 (Submission).

The system water supply and drainage is a complicated system because it runs throughout the whole length of both STT and also a large part of the vertical and horizontal shafts Sedrun and Faido (**Figure 2**). Furthermore the system is in operation all the time and for all operational modes such as normal tunnel operation, maintenance and incident.

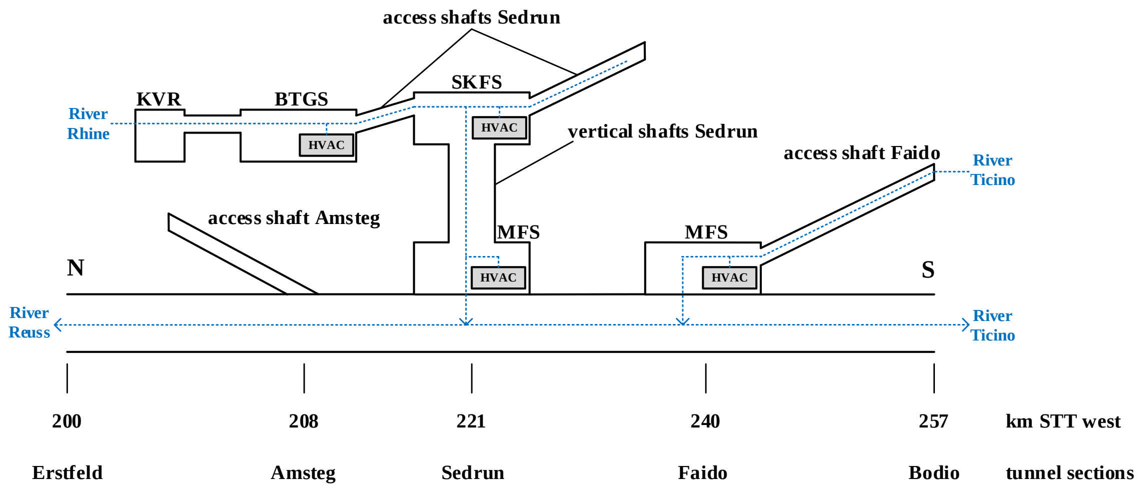

Figure 2: Overview water supply and drainage system of GBT.

Water is needed for all heating, ventilation and air conditioning (HVAC) systems which are present at the MFS Faido and Sedrun as well as the shaft head Sedrun (SKFS) and the technical building Sedrun (BTGS) (**Figure 2**). As mentioned before the other important function is to secure a constant amount of water in the foul water part of the drainage system of the two STT. The entrance point of the water into the STT is at the MFS Sedrun because it is at the highest point of the tunnel. A substantial amount of water is available naturally via the access shafts Sedrun (shaft head Sedrun). In case of a shortage, additional water can be supplied by the power station on the river Rhine (KVR) at Sedrun or the drinking water supply of the village Sedrun via the technical building Sedrun (BTGB) and the shaft head Sedrun (SKFS). The transport from KVR to SKFS involves two pumping steps (KVR → BTGS and BTGS → SKFS). The difference of height from SKFS to the MFS Sedrun of approx. 800 m is used to generate electricity. The water passes via a generator or as an alternative via two possible by-passes in case of maintenance or a disturbance. In the MFS Sedrun, the water is then distributed into the two STT and the two directions north and south (distribution station). At the portals North and South (Erstfeld, Bodio), the amount of water ($5\ l\ s^{-1}$) and its quality are checked, the water is collected in basins to cool down and is then discharged to the river Reuss or Ticino respectively.

General RAMS target values were defined for the lot water supply and drainage system for the following scenarios [4]:

Reliability (R): No water running in the foul water part of the drainage system of the STT (i.e. no transport of liquid hazardous cargo allowed) (MTBF, mean time between failure): **4 years**.

Availability (A): No water running in the foul water part of the drainage system of the STT (i.e. explosion protection not ensured) (%): **97.5%**.

This availability target value addresses the fact, that it ought to be known at all times whether water is running in the drainage system or not when a liquid hazardous cargo is being transported in the STT. The availability target above represents a safety relevant requirement. However, within the project of the GBT, a safety (S) target was only defined when a system is capable to cause fatalities directly on its own.

No specific RAMS target values have been defined for this system regarding maintenance (M) and/or safety (S). However it is important to note that the contractor was required to set up the system to be as maintenance free as reasonably possible.

Additionally, some general considerations regarding MTTR (mean time to restoration) are given: The MTTR includes the time for a team to be ready at the location needed and the time for the repair itself. As part of the project, it was demanded that repair work should start on average within 15 h after the outage when the functionality of a system is affected and within an average of 72 h when it is not. The 72 h period is connected to the scheduled weekly maintenance periods. The length of a working shift should not exceed 6.5 h due to the limited accessibility within the tunnel. The time for preventive maintenance is not part of MTTR and is therefore not considered to influence the system's availability. [3]

4. SUBMISSION

The submission is based on the development phase and includes again the RAMS phases 1-6. As mentioned above, the focus of this chapter lies on RAMS phase 5 and 6. The given general RAMS target values for the system water supply and drainage (RAMS phase 4) [4] were subdivided to different sub-systems, main components and components in a tree-like structure. [2] [3]
Sub-systems represent different locations throughout the tunnel system but also the data processors (see also **Figure 2**). Main components are given in brackets.

- Erstfeld (power supply, control, communication, components and sensors)
- Shaft head Sedrun (KVR, drinking water supply Sedrun, BTGS, SKFS)
- MFS Sedrun (reservoir, pumping and distribution stations, side shafts, control, etc.)
- Faido (basins)
- Bodio (service chamber, basins)
- Processors (data processors)

Main components may represent locations within the sub-systems (e.g. shaft head Sedrun) or other units such as communication, electrical power supply, control (e.g. Erstfeld). Main components consist in general of a number of components which can be arranged in a serial and/or a parallel manner. The same holds true for the main components themselves. Single components represent the actual devices used such as pumps, valves, power supply units, circuit breakers, sensors, etc.

The described subdivision of the system was also the basis of the structure of the reliability block diagram (RBD) models and, as a consequence, allowed the apportionment of the general target values to target values for each main component. A commercial software was used for the calculations. The target values which were assigned to each main component were the basis for the generation of the forecast values for the contractor during submission but also during construction. More details regarding RAMS phase 6 is given in the following chapter.

5. CONSTRUCTION

The construction includes the RAMS phases 7-9 but also 6 since the forecast values of the contractor from their submission were rendered more precisely before the start of construction. MTBF and MTTR values were provided by the contractor for each main component. Generally, but also in case of project changes, it was the challenge of the IG GBTS to verify these forecast values to ensure the system's compliance with its general target values from RAMS phase 4. To check this, an updated overall RBD model from the submission was used. If the contractor exceeded a given MTBF target value, no issue arose. However, in several cases, the given target value was not met and a more careful evaluation was necessary. The resulting mixture of met and not met target values was implemented into the updated RBD model and the calculated values obtained were checked for compliance. Parts of the updated RBD model used for the calculation are presented below [3]:

5.1. General assumptions

For the calculation of the RAMS forecast values, a number of general assumptions were made:

- Focus on technical failures
- Constant failure rate during the life time of the component
- MTBF / MTTR values of contractor are used for components and/or main components
- MTBF values include forecasted real environmental conditions
- Interfaces to the railway's systems are fully available (data and power supply)
- The requirements of the contractor regarding maintenance are met

The top level of the RBD model (6 blocks) is based on the list of sub-systems in chapter 4 (Submission): All sub-systems were arranged in a serial manner and will be discussed in more detail in the following sub-chapters:

5.2. Sub-system Erstfeld

Within the sub-system Erstfeld the following main components were defined during the submission phase: power supply, control, communication, other components and sensors. However, during construction, it became evident that the planned separation of the main components power supply and communication based on a serial arrangement was no longer useful. One such example is given in the following **Figure 3**.

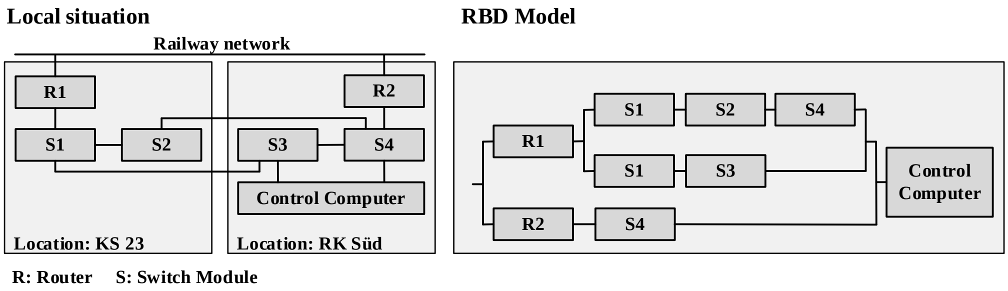

Figure 3: Power supply and communication of sub-system Erstfeld.

The communication from the network of the railway systems to the control computer of the water supply and drainage system relies on two routers 1 and 2 which are located at different locations (KS 23 and RK Süd). Depending on the location, one to several switch modules are involved (**Figure 3**, left). This set up was converted into the corresponding RBD model (**Figure 3**, right). The components with respect to power supply are omitted in **Figure 3** for clarity.

5.3. Sub-system shaft head Sedrun

Within the sub-system shaft head Sedrun four main components were defined (see also **Figure 2**). The KVR as well as the drinking water supply Sedrun are redundant whereas the main components BTGS and SKFS are arranged in a serial manner. The contractor was obliged to calculate the reliability of these main components which each include components regarding power supply, control, communication and other components. In the case of sub-system shaft head Sedrun, the RBD model from submission did not need any adaptations.

5.4. Sub-system MFS Sedrun

The original RBD model from submission showed the following main components: reservoir MFS, pumping station MFS, distribution station, side shafts, power supply, control, communication and other components (sensors, valves, etc.). Several of these required an update of the original RBD model due to major changes regarding connectivity. Similar to the sub-system Erstfeld, the communication chain from the router to the control computer involved a number of different locations with different power supply and also a series of different switch modules.

Another change to the original RBD model was the fact that the amount of water in the four pipes going east and west in the two STTs is measured three times: once after separation of the four pipes (distribution station) and twice shortly before the water enters the STT (side shafts) (see **Figure 4**).

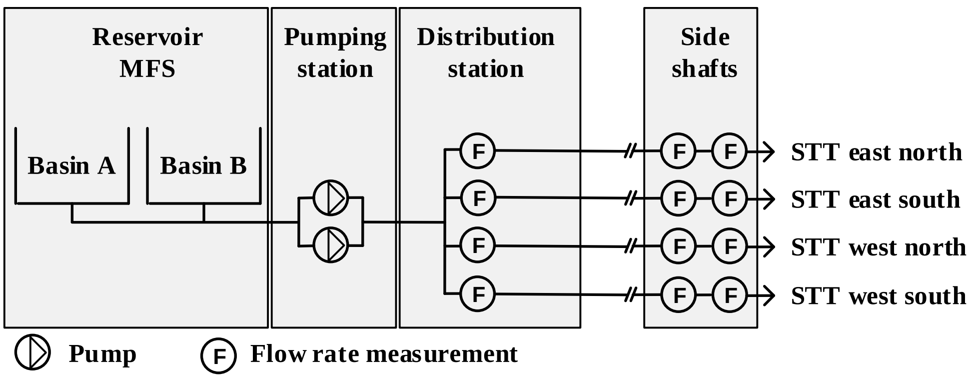

Figure 4: Flow rate measurement in sub-system MFS Sedrun (locations).

The local situation shown in **Figure 4** was translated to a RBD model shown below in **Figure 5.**

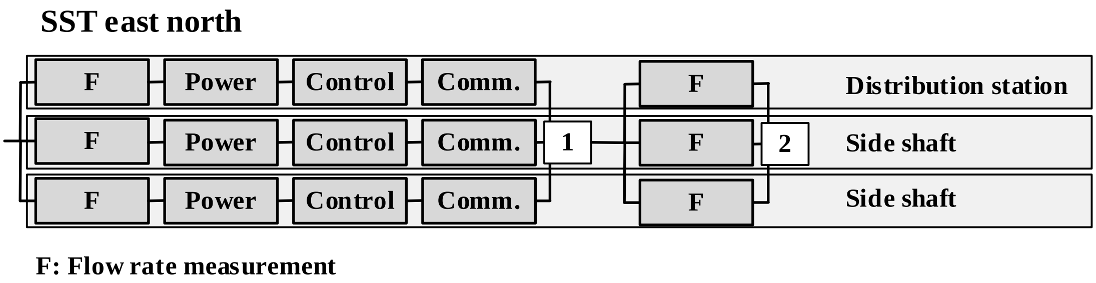

Figure 5: Flow rate measurement in sub-system MFS Sedrun (RBD model)

Regarding outage a one out of three redundancy (1oo3) was modelled (**Figure 5**, left). With respect to the consistency of the measured flow rates the more conservative redundancy of two out of three (2oo3) was implemented (**Figure 5**, right).

5.5. Sub-system Faido

Based on the target definition (RAMS phase 4) [4], the sub-system Faido has no direct influence on the general target values. However, as part of the RAMS process it was decided to implement an additional reliability target for sub-system Faido to ensure a comparable quality of its components. This work is not included within the scope of this paper.

5.6. Sub-system Bodio

Within the sub-system Bodio two main components were defined: the service chamber and the basins. The contractor provided forecast values of these serially arranged blocks which each includes all components regarding power supply, control, communication and other components present. With regard to the RBD model from submission, no changes were necessary.

5.7. Sub-system Processors

The sub-system processors represents two redundant data processors at Sedrun and Faido plus the corresponding communication components to the data net of the railway system. The situation with regard to the RBD model from submission did not change.

5.8. Results

Based on the forecast values provided by the contractor and the RBD model as partially shown above with a total of 84 blocks, a reliability of approx. 6 years and an availability of approx. 99.9% were obtained. Both values outperform the required target values (see chapter 3, RAMS phase 4). [3]

6. COMMISSIONING AND OPERATION

The commissioning phase includes the RAMS phases 9 and 10. As part of the RAMS process, all requirements which have been placed towards water supply and drainage were collected in a database and validated during construction and commissioning. For the validation of a single requirement it was defined whether documentation or a test was required. A series of tests were performed throughout the construction and commissioning process: factory acceptance and field tests (tests of isolated areas), tests of integration into the data net of the railway system and also tests of the complete system including its interacting systems. The status of each requirement was regularly checked, particularly before the beginning of the next project phase of the GBT (i.e. test operation, trial operation). [6]

The forecast reliability and availability values for the water supply and drainage system are based on the information provided by the contractor. During operation, a maintenance management tool will be implemented to allow verification of the calculated values (RAMS phase 11 and 12): Relevant failures will be collected and analysed. This will then allow comparison of the forecast values with the real RAMS performance in the future.

7. SUMMARY & OUTLOOK

The RAMS process has been carried out based on SN EN 50126. Based on the general target values for the system water supply and drainage and a RBD model, sub-target values for main components have been defined for the contractor. During submission and in more detail during construction, the contractor provided MTBF forecast values for main components which were then used as base information for the updated RBD model to calculate the forecast values for reliability and availability for the whole system. The theoretical values obtained fulfill the required general target values. During operation of the GBT, the real RAMS performance will be determined and a review of the forecast theoretical values will be possible. [3]

It was observed that the necessary changes of the RBD model from submission involved main components which described functions (power supply, control, communication). From this it was concluded that the verification of general target values should be more straightforward / requires less changes if target values for locations are defined.

Currently, the system water supply and drainage is in its final stage. Some final work and testing is still going on. Due to this, the validation is not yet 100% complete [6] and also the forecast values of the contractor still need some minor adaption at one location. However, no major impact on the overall forecast value is expected [3].

8. REFERENCES

[1] AlpTransit Gotthard Ltd, (2015) www.alptransit.ch (31.03.2015).

[2] Podofillini L. et al. (Ed.), (2015) Safety and Reliability of Complex Engineered Systems, pp. 320. CRC Press/Balkema. London.

[3] Huber D., Steiger M., (2016) RAM- und Sicherheitsnachweis Los G/K, Phasen 1-10 (Endzustand) (Version C, 22.01.2016, LZ01-422007) unpublished (report on behalf of ATG).

[4] Kost M., (2014) Elektromechanische Ausrüstung Zuteilung RAM- und Sicherheitsziele (Version 1.0, 08.10.2014, LZ01-341334) unpublished (report on behalf of ATG).

[5] Gerber P., Kost M., Hegglin R., (2015) Quantitative Risikoanalyse Gotthard-Basistunnel – QRA GBT (Version 1.1, 08.05.2015, LZ01-344301) unpublished (report on behalf of ATG).

[6] Freudiger J., Huber D., (2016) Verifikations- und Validierungsplan inkl. Validierungsbericht Los G (Endzustand) (Version B, 22.01.2016, LZ01-356401); Pinotti M., Huber D., (2015) Verifikations- und Validierungsplan inkl. Validierungsbericht Los K (Testbetrieb) (Version 0, 27.02.2015, LZ01-404540); Huber D., Pinotti M. (2016) Anmerkungen zum Verifikations- und Validierungsplan inkl. Validierungsbericht Los K (Version A, 22.01.2016, LZ01-510042) all unpublished (reports on behalf of ATG).

EVACUATION SPEED DISTRIBUTION BY FULL-SCALE TUNNEL EXPERIMENTS

[1, 2]M. Seike, [1]N. Kawabata, [1]M. Hasegawa, [1, 3]Y. Lu
[1]Kanazawa University, Japan

[2]National Science and Technology Center for Disaster Reduction, Taiwan
[3]Chiayi County Fire Department, Taiwan

ABSTRACT

In tunnel fires, smoke by fire forms stratified flow and diffuses inside the long and enclosed space. Therefore, evacuation, rescue and fire extinguishing activities in fire incidents in tunnels are difficult and even small incidents have a high possibility to cause the huge losses. To evaluate tunnel fire safety quantitatively, especially regarding evacuation behaviour, walking speed of evacuee in tunnel fire needs to elucidate. Hence the experiments [1] conducted in December 2013 at the test tunnel of National Institute for Land and Infra-structure Management, Japan. Emergency evacuation speed become information speed to other passengers in tunnel fires, hence maximum evacuation speed is one of the most important components on assessment for tunnel fire safety. Normal walking speed and emergency evacuation speed during the tests in imitation smoke using full-scale tunnel was experimentally investigated. Additionally, normal walking speed were also calculated as the probability distribution in a smoke density to install in the evacuation simulation [2].

Keywords: *smoke density, evacuating walking speed, imitation smoke, full scale tunnel experiment*

1. INTRODUCTION

The authors have proposed the tunnel evacuation simulation model, in which each evacuee influenced by smoke is analyzed using CFD based three dimensional smoke behavior [2], and the number of evacuees who cannot evacuate in a smoke-filled tunnel are calculated to assess tunnel fire safety [3].

In the evacuation model proposed in the paper [3], people start to evacuate when they see smoke or other people evacuating or hear emergency announcements, and after recognizing that they must evacuate, they evacuate at a constant walking speed. Hence walking speed during evacuation is not just the moving speed of evacuees but affects the speed of information exchange, which alerts people to the need for evacuation. Thus, the maximum evacuation speed is one of the most important factors to consider to assess tunnel fire safety. Jin etc. [4] has measured the walking speed in corridors filled with smoke, and reported that walking speed decreased rapidly at smoke optical density, Cs = 0.4 m^{-1} in irritant smoke produced by burning wood. These results are generally used in Japanese road tunnel fire disasters prevention, to assess fire safety as the inability of evacuees to evacuate at evacuee face height, which is 1.5 m high from the floor, at smoke optical density higher than 0.4 m^{-1} [5]. Regarding walking speed in a tunnel, there have been a few experimental instances [6-8]. However, the evacuation simulation has so far used normal outside walking speed, not the walking speed in smoke, to give probability distribution function of walking speed. It is necessary to clarify the evacuation behavior in a tunnel fire and to perform a high quantitative assessment to use evacuation speed in diffusing smoke. Hence, the objective of the present study is to clarify simple walking speed in smoke and evacuation speed in smoke measured using a full-scale experimental tunnel as a method of investigating the basic evacuation performance characteristics during a fire.

In the present study, normal walking speed and emergency evacuation speed during the tests in imitation smoke using full-scale tunnel was experimentally investigated. Additionally, using these results, evacuation speed curve and normal walking speed curve were calculated.

2. EXPERIMENT

The experiments conducted in December 2013 at the test tunnel of National Institute for Land and Infrastructure Management, Japan, which is 700 m long, 9.8 m wide and 6.9 m high, and is horseshoe shaped. A 400 m section of the tunnel whose both ends were shuttered was used. Subjects were directed in advance to walk at normal speed during the tests.

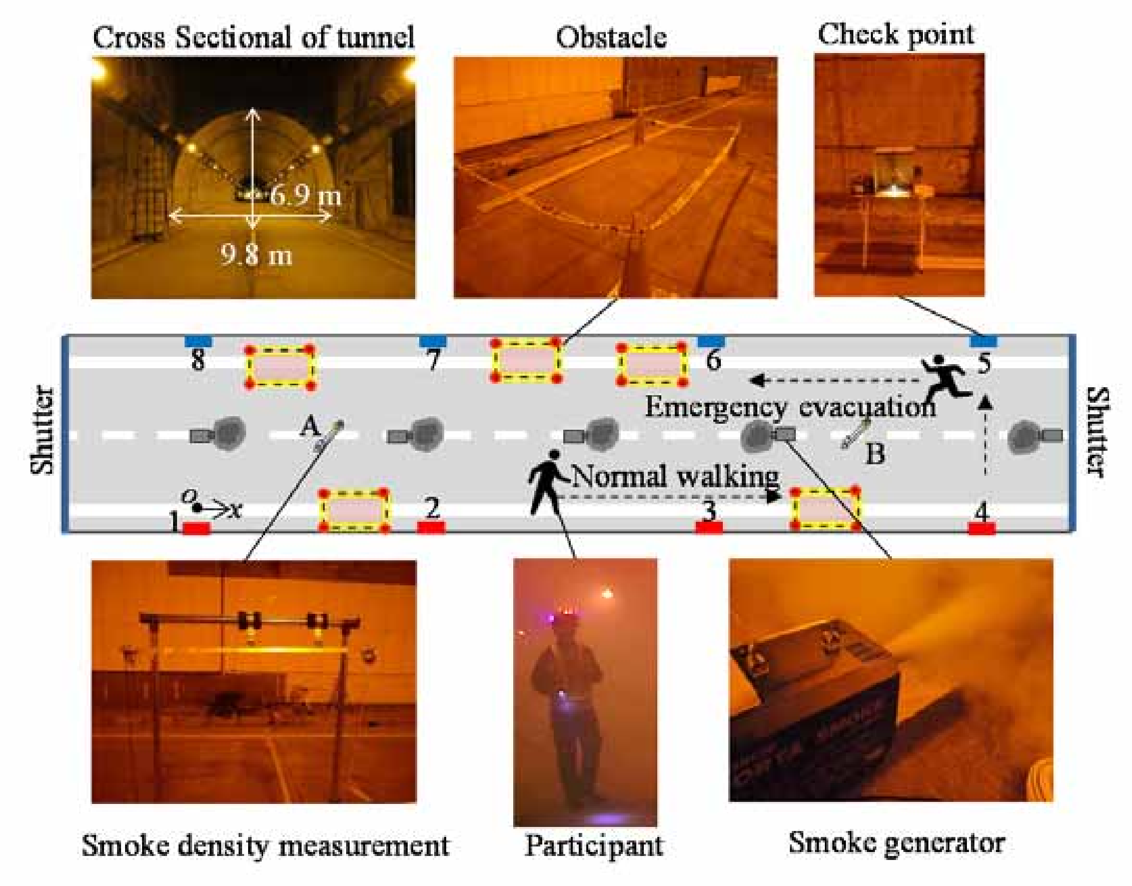

Figure 1: Evacuation experiments in the full-scale tunnel [1]

Evacuation speed and normal walking speed were derived from the elapsed time between checkpoints along the longitudinal direction. Four checkpoints were installed in the tunnel at an interval of 100 m. Obstacles were put on the route of subjects and were relocated randomly during the experiments to prevent the subjects from memorizing those locations. The numbers (averaged ages) of subjects were 40 (30.9), 40 (30.6) and 50 (31.5) for cases with the Extinction coefficient *Cs* set value 0.4 m^{-1}, 0.6 m^{-1} and 0.8 m^{-1}, respectively. All subjects were male. Subjects wore a safety vest, a mask and a helmet, and held a stopwatch and a flashlight simulated the flashlight function of smart phones.

Extinction coefficient was measured by laser sensor (KEYENCE LV-NH100) and was determined by the Lambert-Beer equation,

$$Cs = -(1/l) \ln (I/I_0)$$

where, I: intensity of transmitted light, I_0: intensity of incident light (or transmitted light in non-smoke condition), and l: the light path length. In the present study, the light path length was 0.8 m, and wavelength was 660 nm. The sensor output was calibrated with ground glasses whose transmittances are 0, 10, 20, 30, 40 and 50%.

The explanation to participants was given as follows.
Normal walking (normal walking speed): "Please walk in the tunnel as you normally walk."
Emergency evacuation (evacuation speed): "Fire occurs in the tunnel and the present situation is considerably serious that an explosion could occur or the fire might spread, so please decide to evacuate, and do extremely urgently."
Additional explanations were given in earlier experiments. For example, "Smoke used for the experiments is not toxic. Please suppose that you enter the smoke the first time and evacuate in actual smoke."

3. EXPERIMENTAL RESULTS

Figure 2 shows the results of evacuation speed as triangle markers and the range of evacuation speed, red line of maximum, minimum and mean values in experiments I, II and III normal walking speed as blue dotted lines.

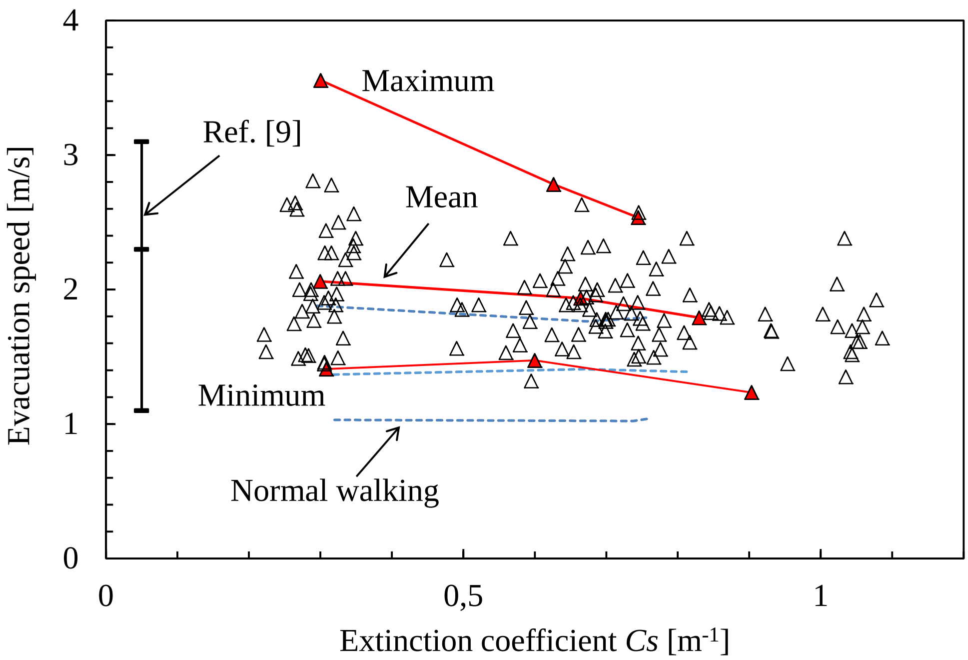

Figure 2: Evacuation speed and normal walking speed with smoke density [1]

Focusing on the maximum distribution of the emergency evacuation speed in the figure, emergency evacuation speed at *Cs* = 0.30 m^{-1} reached a running speed of 3.55 m/s, however at *Cs* = 0.63 m^{-1} the emergency evacuation speed fell rapidly to semi-jogging speed of 2.78 m/s. Moreover the emergency evacuation speed at *Cs* = 0.75 m^{-1} decreased to 2.53 m/s. Thereby, the maximum distribution of emergency evacuation speed has dropped rapidly according to smoke density. Meanwhile, the minimum distribution was 1.41 m/s at *Cs* = 0.30 m^{-1}, and later 1.47 m/s at *Cs* = 0.60 m^{-1} and 1.24 m/s at *Cs* = 0.90 m^{-1}, hence although the impact is small, the minimum distribution decreases close to *Cs* = 1.0 m^{-1}. The mean smoke densities were also calculated in Experiments I, II and III corresponding to the mean emergency evacuation speed as the same normal walking speeds. Mean emergency evacuation speeds were almost 2.06 m/s at *Cs* = 0.30 m^{-1}, 1.93 m/s at *Cs* = 0.66 m^{-1} and 1.79 m/s at *Cs* = 0.83 m^{-1} which is about semi-jogging speed. Therefore the mean emergency evacuation speed is not influenced very much by smoke density. Boer [9] conducted experiments to investigate drivers' evacuation activity using a full-scale tunnel in 2001.

Participants were explained that they must save their own lives by leaving their vehicles because of the presence of toxic gas and danger of an explosion. And their evacuation speed was measured assuming it was an emergency evacuation. The range of Boer's emergency evacuation speed [9] is also shown by black line in Fig. 2. In Boer's evacuation experiment, there was no smoke Cs = 0 m^{-1} but tiny smoke density Cs = 0.05 m^{-1} is shown to simplify the comparison. Emergency evacuation speeds in Boer's experiments are reported as maximum 3.1 m/s, minimum 1.1 m/s and mean 2.3 m/s. Comparing the present experiments to Boer's, emergency evacuation speed in the present experiments results in the low smoke density, emergency evacuation speed in the present experiment becomes a little larger than Boer's results, but the mean emergency evacuation speed becomes a little smaller than Boer's reported mean speed.

4. CALCULATION OF EVACUATION SPEED CURVE

In the present evacuation model [3], giving a distribution of evacuation speeds has been indicated the individual differences. Here an evacuation speeds distribution was defined evacuation speed v as horizontal axis and probability distribution S as vertical axis, and normalized an integral calculus S by v. In the present chapter, evacuation speed distribution was calculated by the present experimental results (see Figure 3).

To show the probability distribution of evacuation speed in a range, the evacuation speed distribution is indicated. The range of smoke density was determined as becoming same the number of samples. The probability distribution was calculated as follows. The breadth between evacuation speeds was 0.25 m/s, at first, the numbers of participants every 0.1 m/s were calculated ex. from 0.75 to 1 m/s, 0.85 to 1.1 m/s. A number of participants in an evacuation speeds breadth as P_i, a total numbers of participants in a breadth as P_{total}, a supremum of an evacuation speeds breadth as v_{ui}, an infimum of an evacuation speeds breadth as v_{di}, probability distribution of participants in an evacuation speed S_i is following equation (1).

$$S_i = \frac{P_i}{P_{total} \cdot |v_{ui} - v_{di}|} \times 100 \qquad (1)$$

In the present paper, a supremum of an evacuation speeds breadth as v_{ui} and an infimum of an evacuation speeds breadth as v_{di} have the following equation relations (2).

$$\begin{aligned} v_{ui+1} &= v_{ui} + 0.1 \\ v_{ui} - v_{di} &= 0.25 \end{aligned} \qquad (2)$$

In the present paper, normal walking speed were also calculated as the probability distribution in a smoke density. Furthermore, smoke density range of normal walking speed was same as the evacuation speed.

5. DISCUSSION

Regarding evacuation speed and normal walking speed, smoke density divided at a boundary value evacuation distribution curves were calculated each low and high dense of smoke. The boundary value was adopted Cs = 0.7 m^{-1}, that is the number of participants in emergency evacuation and normal walking becoming around same in each smoke density, moreover maximum evacuation speed became slower than around 2.5 m/s. In Cs = 0 to 0.7 m^{-1} there were 69 participants in normal walking speed, 73 in the case of evacuation speed, in over Cs = 0.7 m^{-1}, 61 participants in normal walking speed, 57 in the case of evacuation speed.

In the range of Cs = 0 to 0.7 m^{-1}(see Fig. 3(i)), a probability distribution of normal walking speed increased from 0.875 m/s (0.75-1.0 m/s) rapidly, 156 %/(m/s) at 1.175 m/s (1-1.25 m/s), the maximum rate became 214 %/(m/s) at 1.375 m/s (1.25-1.5m/s), after that decreased to 40.6 %/(m/s) at 1.575 m/s (1.45-1.7 m/s), 0 %/(m/s) at 2.025 m/s (1.95-2.2 m/s). Meanwhile, in the evacuation speed, the probability distribution increased from 1.275 m/s (1.15-1.4 m/s) rapidly, 93.2 %/(m/s) at 1.575 m/s (1.45-1.7 m/s), the maximum rate became 132 %/(m/s) at 1.975 m/s (1.85-2.1m/s), and became temporarily 0 %/(m/s) at 2.975 m/s (2.85-3.1 m/s). However, the participants who evacuate 3.55 m/s existed, so that the propagation distribution raised at 5.5 %/(m/s) temporarily and then decreased to 0 %/(m/s) at 3.775 m/s (3.65-3.9 m/s).
Over Cs = 0.7 m^{-1}(see Fig. 3(ii)), the propagation distribution of normal walking speed increased from 0.875 m/s (0.75-1.0 m/s) rapidly as same as the range of Cs = 0 to 0.7 m^{-1}, the maximum rate became 203 %/(m/s) at 1.375 m/s (1.25-1.5m/s), after that decreased rapidly to 0 %/(m/s) at 1.875 m/s (1.75-2.0 m/s). Meanwhile, in the evacuation speed, the probability distribution increased from 1.175 m/s (1.05-1.3 m/s), the maximum rate became 182 %/(m/s) at 1.775 m/s (1.65-1.9 m/s), and became 0 %/(m/s) at 2.775 m/s (2.65-2.9 m/s).

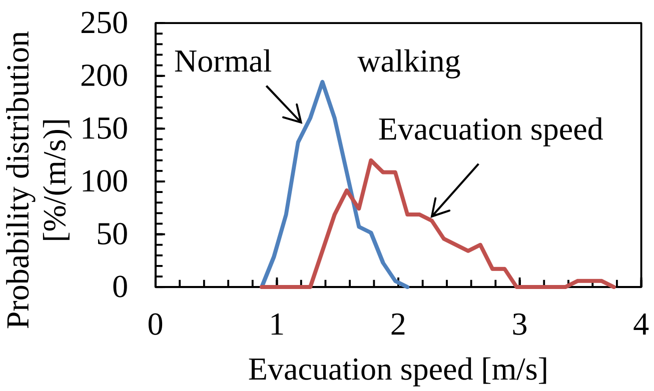

(i) Extinction coefficient Cs = 0 - 0.7 m^{-1}

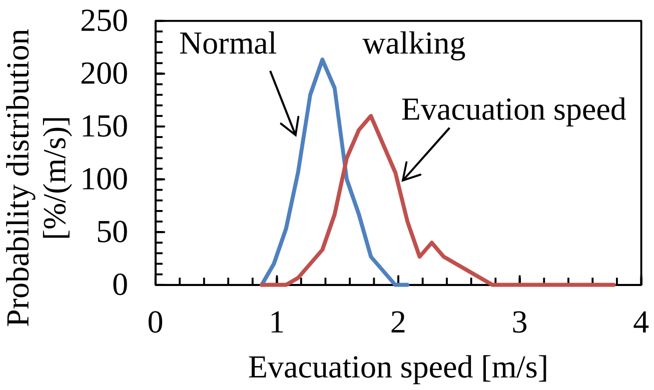

(ii) Extinction coefficient Cs over 0.7 m^{-1}

Figure 3: Evacuation speed curve and normal walking speed curve

Consequently, the range of normal walking speed is almost same though smoke denser, however, the range of evacuation speed becomes narrow by denser smoke. In the evacuation model proposed in the paper [3], almost people start to evacuate when they see other people evacuating. Hence it is considerable that the maximum evacuation speed becoming slow affects the speed of information exchange, which alerts people to the need for evacuation.

6. CONCLUSIONS

As the aim to clarify the relation between smoke density normal walking and emergency evacuation speeds, walking experiments in smoke using a full-scale experimental tunnel by participants were performed to investigate of basic evacuation performance characteristics in fire. Consequently, in the condition during the present experiments following results are obtained.

1. Maximum, minimum and mean of normal walking speed became almost constant.
2. Maximum of emergency evacuation speed has large influence by smoke density, decreased rapidly from 3.55 m/s at Cs = 0.30 m^{-1} to 2.53 m/s at Cs = 0.75 m^{-1}.
3. Regarding evacuation speed and normal walking speed, smoke density divided at a boundary value evacuation distribution curves were calculated each low and high dense of smoke.
4. The range of normal walking speed is almost same though smoke denser, however, the range of evacuation speed becomes narrow by denser smoke.

REFERENCES

[1] Seike, M., Kawabata, N., Hasegawa, M., 2016.
Experiments of Evacuation Speed in Tunnel Filled Smoke, Tunnelling and Underground Space Technology, Vol. 53, pp. 61-67.

[2] Kawabata, N., Wang, Q., Yagi, H., Kawakita, M., 1998.
Study of Ventilating Operation during Fire Accident in Road Tunnels with Large Cross Section, Proceedings of the Fourth KSME-JSME Fluid Engineering Conference, Pusan, pp. 53-56.

[3] Seike, M., Kawabata, N., Hasegawa, M., 2011.
Study About Assessment of Fire Safety in a Road Tunnel by Evacuee's Behavior Based on Smoke Behavior by 3-D CFD Analysis, Advanced Research Workshop Evacuation and Human Behavior in Emergency Situations, Santander, pp. 111-125.

[4] Jin, T,. Yamada, T., 1985.
Irritating Effects of Fire Smoke on Visibility, Fire Science & Technology, 5:1, pp. 79-89.

[5] Mikame, Y., Kawabata, N., Seike, M., Hasegawa, M., 2014.
Study for Safety at a Relatively Short Tunnel when a Tunnel Fire Occurred, 7th International Conference 'Tunnel Safety and Ventilation', Graz, pp. 133- 139.

[6] Frantzich, H., Nilsson, D., 2003.
Utrymninggenomtätrök: beteendeochförflyttning [Evacuation in Dense Smoke: Behaviour and Movement], Department of Fire Safety Engineering and Systems Safety, Lund University, Report 3126, p. 75.

[7] Frantzich, H., Nilsson, D., 2004.
Evacuation Experiments in a Smoke Filled Tunnel, Proceedings of the 3rd International Symposium on Human Behaviour in Fire, Interscience Communications Ltd., London, pp. 229-238.

[8] Fridolf, K., Andree, K., Nilsson D., Frantzich, H., 2013.
The impact of smoke on walking speed, Fire and Materials, Vol. 38, pp. 744-759.

[9] Boer, L.C., 2002.
Behaviour by motorists on evacuation of a tunnel, TNO Report, TM-02-C034, p. 23.

CONSIDERATIONS ON THE APPLICATION OF WATER MIST IN ROAD TUNNELS

ir. E.W. Worm; retired Safety Officer of the
Dutch State owned road tunnels The Netherlands.

ABSTRACT

Following analysis shows that application of water mist in the situation with one-way traffic and longitudinal ventilation, together with the other Dutch usual safety features doesn´t appear to be the obvious solution. Reducing escape door distances, reducing the risk of traffic congestion and influencing the quantity of transport of dangerous substances appear to be much more efficient and effective.

Keywords: tunnel safety; water mist; quantitative risk analysis

1. INTRODUCTION

The Dutch Minister of Transport has formulated two prerequisites regarding the application of additional (not explicitly required by law) safety measures such as water mist. It concerns the status of proven / non proven technology and cost-effectiveness / proportionality. These two preconditions are analysed in relation to the application of water mist as a safety measure.

2. ANALYSIS

2.1. Definitions

Proven technology is assumed to be the result of nine steps, defined as Technology Readiness Levels from TRL 1: description of the basic principle through description, analysis, experiments, validation and demonstration to TRL 9: The system has proven itself through a relevant number of successful operations.
The *cost effectiveness* represents the degree to which the stated objective is achieved , given the used resources. Likewise the *safety effectiveness* reflects the degree to which the stated safety improvement is achieved.
The higher the cost-effectiveness and the safety-effectiveness , the better the use of resources.

2.2. Tunnel safety in a nutshell

Assessing tunnel safety is about finding the balance between four basic considerations:

- Avoid unsafe situations and reduce the probability of unsafe situations (prevention)
- Should an unsafe situation occur nonetheless, do not allow it to extend (mitigation)
- Should a dangerous situation arise, that cannot be limited sufficiently, enable safe evacuation of the tunnel-users (self-rescue)
- Ensure that assistance can be provided (emergency response)

The above balance may be achieved in different ways, by technical and organizational measures. Ultimately in the chosen solution:

- the necessary technical measures should be applied
- they should operate reliably and be available on demand
- the organizations of the operator and emergency services should be able to perform their tasks.

2.3. European / Dutch tunnel safety

A strict translation of the EU Directive No. 2004/54/EC into Dutch legislation would have meant a decrease of the safety of the Dutch tunnels. The Dutch tunnel law therefore has some more strict prescriptions:

- The regulation is applicable for all tunnels irrespective of ownership
- The Dutch regulations hold for road tunnels longer than 250m (instead of 500m)
- Exclusively unidirectional traffic in tunnel tubes
- Control centre for tunnels longer than 500 m (instead of 3000m)
- Mechanical ventilation in tunnels longer than 500m (instead of 1000m)
- Distance between the emergency exits <250m (instead of 500m)
- Distance between the fire extinguishing connections <100m (instead of 250m)

For the Dutch state owned road tunnels the aforementioned policy has been implemented by formulating a mandatory standard package of measures. With this package, not including water mist or sprinkler almost always all requirements of the regulations are met. Compliance is checked by means of a quantitative risk analysis (obliged for all Dutch road tunnels longer than 250m), in which the social risk should not exceed $p=10^{-1}/N^2$ per km tunnel tube per year with N=number of fatalities (N>10).

2.4. Fire as a disaster scenario for tunnels

The application of one-way traffic in combination with longitudinal ventilation, which is the basic principle of the Dutch safety philosophy for road tunnels, in general means that there's no direct threat for the tunnel user in case of a fire. The traffic upstream is stopped and people upstream are safeguarded from exposure to smoke and heat through longitudinal ventilation. However: due to the enormous increase in traffic intensity, there is an increased risk of traffic congestions, which in case of fire upstream suddenly makes the use of longitudinal ventilation not evident anymore. In those cases a fire can have disastrous consequences for the people downstream of the fire, especially when escape doors are not reached quick enough. For those situations an active firefighting system, or in particular: water mist, could be a good solution. Application of water mist may have the following advantages:

- A usually small developing fire is easy to control and in several cases even to be extinguished, so that fire growth is avoided
- The risk of fire spread to other vehicles is significantly reduced
- The structure might be protected against further damage
- The tenability conditions downstream might be positively affected
- In case of fires in the tail of a traffic jam, road users downstream get the opportunity to escape, because the tenability conditions do not significantly deteriorate (longer fire development time and thus longer evacuation time available). It should however be kept in mind that situations first get worse before they get better. Indeed, there is fire!
- The possibilities to come close to the fire are significantly better
- In category A tunnels (transport bulk LPG allowed) the probability of a hot BLEVE is significantly reduced

Looking at all those arguments many may wonder why such a system is not applied in all tunnels. That now is entirely related to the status of proven / non proven technology and cost effectiveness considerations as mentioned in the introduction.

2.5. Water mist as part of the overall safety concept

To the opinion of the author water mist as such passed through all the steps of the proven technology definition. Water mist however cannot operate of its own account. It is linked to a method of activation, which in turn would be coupled to one or other method of detection. And it is precisely this combination of detection, activation and effective extinguishing, that ultimately determines the effectiveness of the water mist system (WMS). As far as the author is aware the coherence, reliability and functionality of the entire sequence has never been studied satisfactorily up to now and all tests publically available are based solely on the activation by the researchers themselves. Regarding proven technology of the system as a whole, there still are some questions to be answered:

- How does the integrated detection, activation and extinguishing system respond? On one single or possibly multiple detections?

- Does it concern a fully automated system and if so, on what built-in default values? (One or more temperature limits, time lag between detection and activation, otherwise?)
- Or does it include human/manual actions and if so, based on which considerations?
- Are the right sections activated?
- Will the system be activated, while people (evacuating) are still present in the tunnel?
- If yes, to what extent does this affect the evacuation process?
- Is there any realistic evidence?
- What is the risk of activation of the system, when this is not at all desirable?

Even when all those questions will be answered satisfactorily and water mist justifiably can be said to be a proven technology, for the author it's still not evident to apply it, due to the second boundary condition: the cost effectiveness (safety effectiveness).

2.6. The cost effectiveness

Consider a tunnel 2000m long with three lanes per tunnel tube in each direction; Category A; 40 million vehicles in two directions, 14% goods/freight transport, 1% buses.
This tunnel is equipped with the standard safety measures as defined for the Dutch state owned tunnels .[1]
What will be the effect of a possible application of water mist in this example? Table 1 below mentions the effects of water mist in the context of the safety chain.

Table 1: Influence of water mist on the different phases of the safety chain

Safety Phase	Influence application WMS	Important parameter
prevention	No difference. Probabilities of an accident are not affected by WMS, except for the (unknown) probability that a WMS unwantedly starts up and thus has a negative influence!	None
mitigation	Improvement as a result of fire control / fire extinguishment, reducing the probability of a hot BLEVE; reducing probability of flashover / fire spread	The larger the fire load and the amount of hazardous substances, the more useful the WMS
self-rescue	Especially in case of fire near the tail of a traffic jam, improvement of the tenability conditions may be possible allowing for longer evacuation times	The larger the probability of stopped traffic and the distance between the exit doors, the more useful the WMS
emergency response	Better possibilities to get close to the fire.	Amount of damage

Three variables seem eminently decisive when analysing the safety situation. In particular we have to regard here as a result of a traffic jam the locked up tunnel users downstream of a fire (as a result of a ignited hazardous substance) who are at risk (depending on the distances to be bridged to the emergency exits). For this tunnel therefore calculations have been carried out for situations with and without WMS with the (very conservative) QRA model, prescribed in the Dutch tunnel law. Herein the probability of congestion, the quantity of dangerous goods and the distances between the emergency exits are varied. (These calculations could only be made thanks to essential delivery of data by ing. R. Mante; head of the centre for tunnel safety at RWS; the Netherlands). The effectiveness of a WMS is taken into account by increasing the probability of extinguishing as shown in Table 2 (flammable gases and liquids excluded).

[1] See: http://www.rijkswaterstaat.nl/zakelijk/werken-aan-infrastructuur/bouwrichtlijnen-infrastructuur/aanleg-tunnels/landelijke-tunnelstandaard/gewijzigde-tunnelwet.aspx

Table 2: Effect applying water mist on the probability of extinguishing the fire, as input variable

Probability of extinguishment (P_e)	**Default-value (without WMS)**	**Adjusted value (with WMS)**
P_e slowly developing fire with a car	0,25	0,95
P_e slowly developing fire with a truck or bus	0,1	0,95
P_e quickly developing fire with a car	0	0,95
P_e quickly developing fire with a truck or a bus	0	0,95

So in 95% of the cases:

- The WMS is in full operation shortly after the start of the fire, so the fire does not grow
- The appropriate sections of the WMS are enabled
- No additional casualties occur

By increasing the probability of extinguishment, in the QRA model automatically the probability of a hot BLEVE is reduced. The assumed effectiveness of the WMS (95%) does not seem unreasonably low; rather optimistically high. In practice the WMS has to be initiated either automatically or manually by the tunnel operator. Both options take time, and it is still questionable as to whether or not the system is in operation quickly enough. This apart from the question if initiating should be done only after road users are already in a safe position, because activating the system will definitely destroy any smoke stratification (if not already destroyed by the ventilation) with all associated negative consequences. Additionally this assumption does not take into account a possible application of the wrong sections or not completely extinguishing a fire with solid combustibles as a result of which poor tenability conditions occur locally.

Fires with flammable liquids (pool fires) and with flammable gases are assumed to occur so quickly that all the fatalities arise prior to the WMS operation.
The possible effect of WMS on reducing fatalities in incidents involving discharges of toxic liquids is not included either, because this effect as yet is not clear.

The following Table 3 summarizes the different situations, and the results in terms of so-called f-N curves (8 in total) are shown in Figure 1.

Table 3: Summary QRA model variants with and without WMS

	Distance between the emergency exits	**Dangerous goods**	**Traffic jam frequencies**
Variant 1	100m	average	low
Variant 2	100m	average	high
Variant 3	100m	high	low
Variant 4	100m	high	high
Variant 5	250m	average	low
Variant 6	250m	average	high
Variant 7	250m	high	low
Variant 8	250m	high	high

The next Figure 1 shows the social risk per km tunnel tube/year (frequency as a function of the number of fatalities) for 8 variants: red line indicates the legal risk criterion; blue line the situation without WMS; the yellow line with WMS.

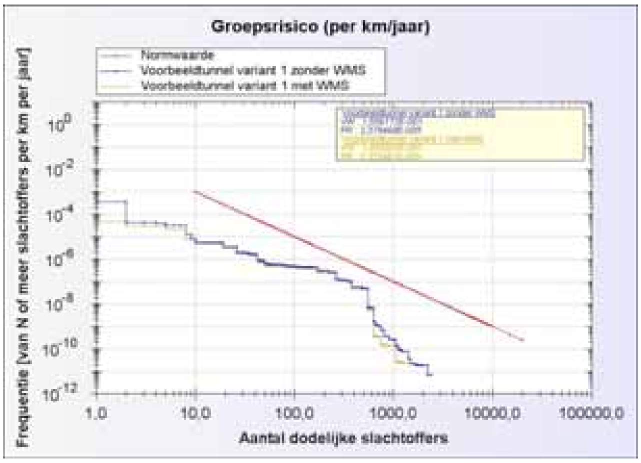

Variant 1:
Vluchtdeurafstand 100m; aandeel gevaarlijke stoffen gemiddeld; filekans laag

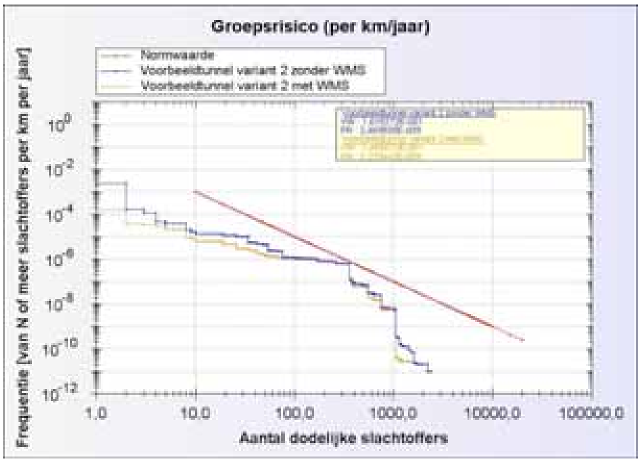

Variant 2:
Vluchtdeurafstand 100m; aandeel gevaarlijke stoffen gemidd

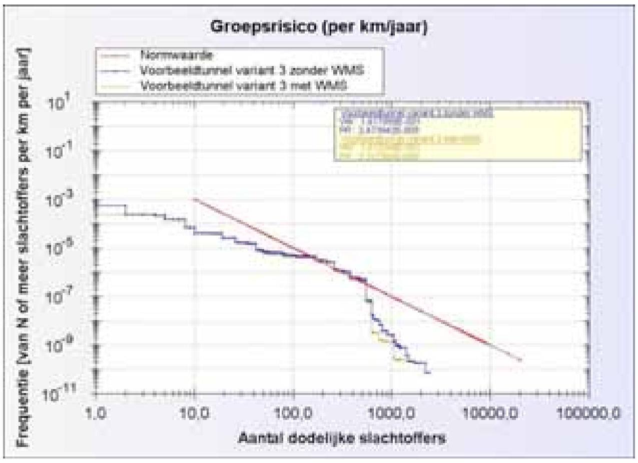

Variant 3:
Vluchtdeurafstand 100m; aandeel gevaarlijke stoffen hoog; filekans laag

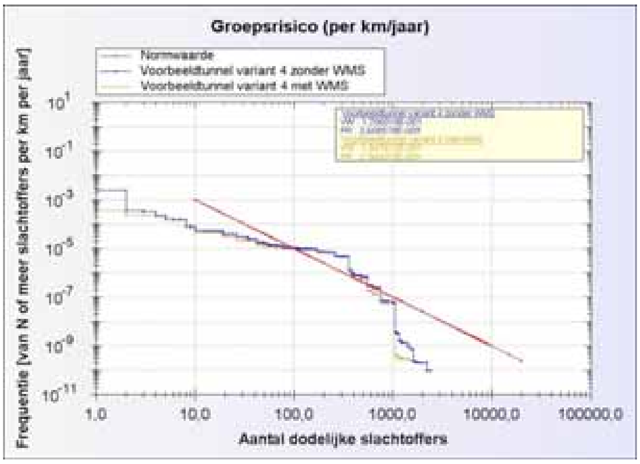

Variant 4:
Vluchtdeurafstand 100m; aandeel gevaarlijke stoffen hoog; filekans hoog

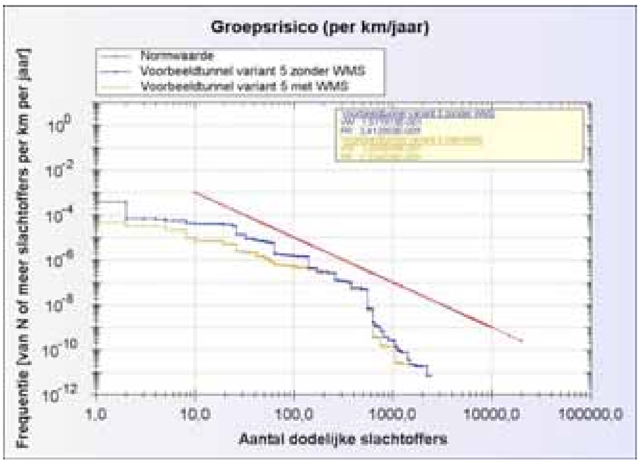

Variant 5:
Vluchtdeurafstand 250m; aandeel gevaarlijke stoffen gemiddeld; filekans laag

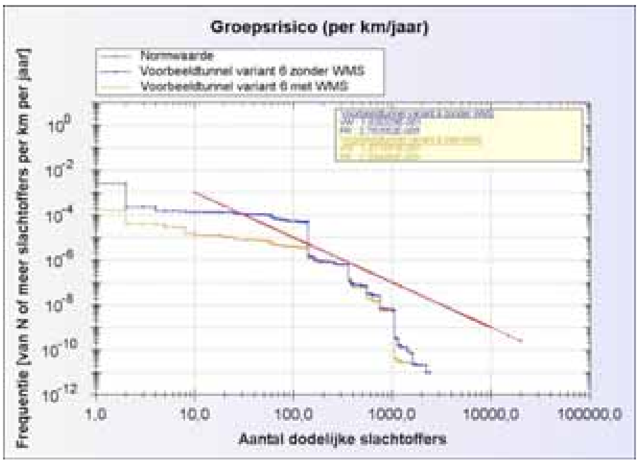

Variant 6:
Vluchtdeurafstand 250m; aandeel gevaarlijke stoffen gemiddeld; filekans hoog

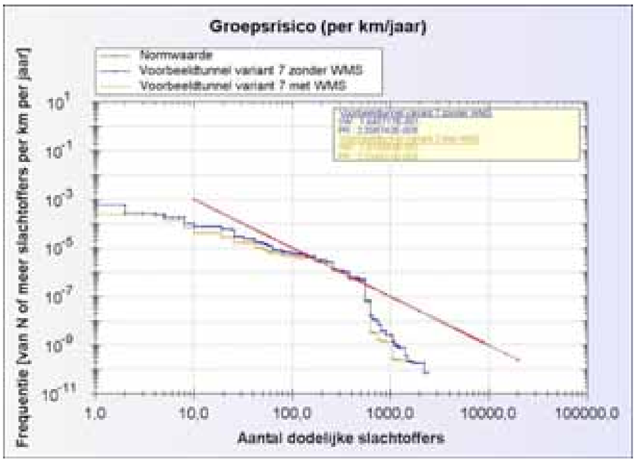

Variant 7:
Vluchtdeurafstand 250m; aandeel gevaarlijke stoffen hoog; filekans laag

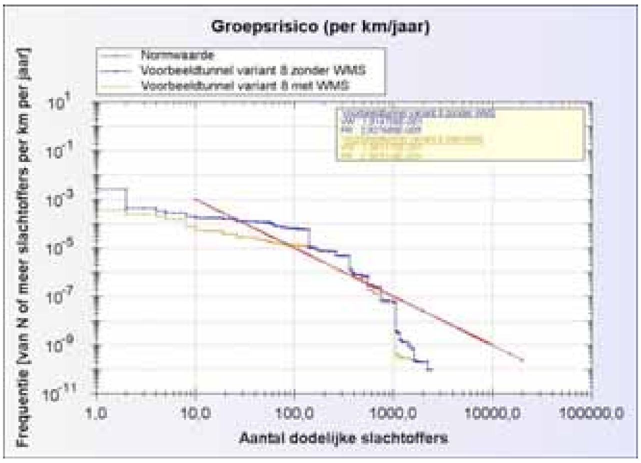

Variant 8:
Vluchtdeurafstand 250m; aandeel gevaarlijke stoffen hoog; filekans hoog

From the analysis the following conclusions can be drawn:

- In a tunnel with small distances between the emergency exits (100m in variants 1 up to 4) water mist has very little effect on the social risk! The exception is variant 2 with a significant influence, but the variant without water mist already meets the risk standard.
- with small distances between the emergency exits (100m) and a high percentage of hazardous goods the social risk is too high in the case of traffic jams (variants 3 and 4) WMS shows no solution however, i.e. no significant effect!
- In a tunnel with maximum distances between the emergency exits (250m) and low congestion frequency (variants 5 and 7) it turns out that with an average quantity of dangerous goods (variant 5) there is a substantial effect of WMS. A situation however where a solution without WMS already meets the standard. For larger quantities of dangerous goods (variant 7) the standard is exceeded and again application of WMS does not offer a solution for the exceeded risk!
- In a tunnel with maximum distances between the emergency exits (250m) and high congestion frequency, the social risk is exceeded in the case of high quantities of dangerous goods (version 8). Application of WMS shows a strong reduction factor, but does not turn out to be the solution to the problem!(still too high social risk)
- In a tunnel with maximum distances between the emergency exits (250m) and high congestion frequency in combination with an average amount of dangerous goods (variant 6), the social risk standard is exceeded if only the standard safety measures are applied. Application of WMS shows a strong reduction in the social risk and compliance with the standard.

Formulated in another way:

- In tunnels where we can keep small distances between the emergency exits (immersed tunnels and land tunnels) WMS has little added value to safety! There is a very low safety effectiveness (see definition).
- In tunnels with large emergency exit distances (generally for bored tunnels) WMS provides a substantial contribution to the reduction of the social risk (except in variant 7). With average quantities of hazardous goods and low risk of congestion, the system is not needed to meet the standard. In the case of a high proportion of dangerous goods regardless of congestion, the application of the system is not enough to comply with the standard. Despite a high safety effectiveness, the system is not necessary (variant 5) or it ultimately cannot yield satisfactory results (variant 8)

The chosen example (in fact an existing tunnel where application of water mist was heavily discussed but not implemented) was relatively short (2 km). Therefore additional calculations were made with the same quantitative risk model for 4 km and 6 km length, without changing any other variable in order to determine whether or not the tunnel length is of importance. It turned out that conclusions, formulated for a tunnel at 2000m length do not vary a lot for the variants 4000m and 6000m length.

Independent of the tunnel length the same 3 parameters remain decisive for safety considerations: the amount of tunnel users (*as a consequence of traffic congestion*) trapped downstream of a fire (*as a result of a fire involving dangerous goods*) which need to find their way out (*covering a certain distance to an escape door*). With increasing tunnel length, depending on the fire location, the traffic queue length can vary. Assuming escape door distances to be constant over the tunnel length, the amount of tunnel users seeking refuge per escape door does not vary when the traffic queue increases. In other words: regardless of the traffic queue length, the situation (in terms of people trying to escape through the escape doors) does not vary. In total however, the number of fatalities will increase and this can be seen especially at the end of the spectrum of the risk curve, for a very high number of fatalities and related to extreme low probabilities of 10^{-8}.

The final conclusion then is that WMS is not a good solution? No, definitely not.

WMS might bring added value for sure, but not in tunnels with a high level of standard safety measures as obliged in The Netherlands, being well above the EU minimum requirements. As mentioned before, a sufficient level of safety can be reached in several ways. With the Dutch “standard measures package”, which does not include water mist, almost always all requirements of the regulations are met. Where in extraordinary situations the standard is not met, managing the main factors of influence (distance between the emergency exits, quantity of dangerous goods and probability of congestion) is the preferred improvement option.

Regarding the ***distance between the emergency exits*** , in the Netherlands it has been the standard already for long in immersed and land tunnels to apply a distance of approximately 100m. For bored tunnels the maximum is 250m. Compared to the EU directive, in which the upper bound for this distance has been set at 500m, this represents a significant increase in safety levels and consequently a largely reduced attractiveness of WMS as an additional safety measure.

Regarding the ***quantity of dangerous goods*** the use of the category classification for the transport of dangerous goods is the possibility to be influenced. The Dutch policy is focused on the Dutch highways always being available for all transport of dangerous goods. So in that case influencing this main influence factor (quantity of dangerous goods) is not on the agenda and consequently in the tunnels under consideration, the distance between the escape doors and the probability of traffic congestion are the remaining head targets to be influenced. This then concerns land tunnels, which are classified in category A and where no restrictions apply.

The only exception in this general policy for the main road network is the transport of flammable gases through underwater tunnels. This exception does not so much apply to safety in the strict meaning of the word (the use of the tunnel and the risk for road users, in the case such transport would lead to a fire and / or explosion). A social risk analysis addressing exactly that particular aspect, shows that transport of flammable gases might be permitted: refer to the f-N curves of the variants 1 and 2. However, this is more an economic consideration. As a consequence of an explosion, evidently the river crossing would be out of order for many years if not completely destroyed, which is considered to be unacceptable. This therefore concerns availability and economy (asset protection), rather than safety (of road users).

Regarding the ***probability of congestion*** it seems obvious to try to limit the traffic jam frequency. This can be achieved with the upstream Motorway Traffic Management System

(MTM) or downstream of the tunnel using physical space (more traffic lanes). The idea behind is that the tail of a traffic jam is avoided to grow into the tunnel. These solutions are relatively easy to achieve and also greatly reduce the attractiveness for a much more complex WMS.

However, there are cases where WMS might be an interesting option:

- In situations where it is not possible from cost perspective to decrease the distance between the escape doors.
- In special cases like f.i. the bidirectional Felbertauern tunnel in Austria, where new emergency exits have been built up to the ventilation area above the road. The costs associated with an additional separate evacuation tunnel, with cross-passages each 500m to the main tunnel would have been considerably more expensive.
- The double deck tunnel in the A86 around Paris. Water mist was not prescribed but applied at own request of the operator. In this case it fulfils economical requirements, which in itself is ok but if not explained properly leads to incorrect and diverging safety discussions.

In the examples mentioned above, economic considerations have emerged apart from the safety considerations. This may be stretched a bit further towards a purely economic consideration. Thus in situations where safety is basically well regulated, the question might arise as how to safeguard the availability of the tunnel. For the Netherlands the governmental policy on the transport of dangerous goods through underwater tunnels f.i. provides answers to these questions. Flammable gases are unacceptable in underwater tunnels, because damage or even collapse of the tunnel would cause an economic disruption of proportions of many years.

In that case, life safety is not the main driver any more, but economy.

Indeed, one can estimate what the loss of a tunnel (entirely or partially) means in terms of direct and indirect costs to the society. Similarly, the contribution of water mist to the reduction of the probability of these consequences can be approximated. Establishing the investment and maintenance costs of a water mist system allows comparison to the expected savings in tunnel loss. When extended over the lifecycle of the tunnel such analysis reveals if the investment in water mist makes sense or not.

Finally the question arises, whether savings are possible on the standard measures, when applying water mist.

In terms of *prevention* (reference is made to Table 2), water mist has no influence, hence no savings are possible.

Looking at *mitigation*, where water mist generally has a positive influence on controlling the fire size, the question arises whether or not passive fire protection could be reduced and e.g. also hand extinguishers for the tunnel users.

Which tunnel manager or owner however, would trade the reliable passive and ever-present heat-resistant cladding against the active, but not 100% certain WMS system? Which manager will rely entirely on water mist and leave out extinguishing tools for the road user?

Which fire brigade officer will reduce on fire protective clothing and other firefighting equipment, when tunnels are equipped with WMS?

Considering *self-rescue*, water mist in general provides longer times to escape (despite negative effects on stratification), possibly allowing for longer distances between escape doors, within the legal framework. (In the Netherlands generally <250m, in particular when it concerns new land and underwater tunnels ≤ 100m)

All in all there appears to be little opportunity for saving in other safety measures and consequently (the non-mandatory) WMS needs to be considered as an **additional** measure.

To the opinion of the author in discussions it is not so much the difference in opinion about the benefits of the system, but much more how to judge situations in which the system can provide substantial added value.

In the Dutch situation with its high level of basic measures in most cases WMS will provide little added value regarding increasing the safety level (low safety- and cost-effectiveness).

EFFECT OF AUTOMATIC FIXED FIRE FIGHTING SYSTEMS ON TUNNEL SAFETY

Andreas Mühlberger, Prof. Dr., Universität Regensburg, Regensburg, D

Anne Lehan, Dipl.-Wirt.-Ing., Bundesanstalt für Straßenwesen, Bergisch Gladbach, D

Alexander Wierer, , Dipl.-HTL-Ing. Mag.(FH) ASFINAG, Innsbruck, A

AndreasPlab, , MSc Psych., Universität Regensburg, Regensburg, D

ABSTRACT

Measures applied for the safety of tunnels are intended to ensure the protection objectives (1) self-rescue of the tunnel user, (2) support of the rescue by emergency personnel, and (3) protection of the structure. The prioritization of protection objectives may vary by country, but synergy effects between the protection objectives are always desirable. While in Austria decisions regarding the additional application of automatic Fixed Fire Fighting Systems (FFFS) may be taken with regard to the protection of the structure and as a consequence of the availability, the installed systems in Germany are primarily to support the rescue by the emergency personnel. The self-rescue of tunnel users must not thereby be affected.

Regarding the use of FFFS in tunnels, different studies have been carried out by the Federal Highway Research Institute of Germany (BASt) concerning the effectiveness and efficiency of FFFS. It has been shown that the efficiency of using a FFFS is more given, the more protection objectives are incorporated in the analysis. In addition to the technical effectiveness, the effect of FFFS on the human behavior regarding the evacuation behavior of tunnel users in case of an incident is another essential aspect to the safety assessment**.**

Therefore, several studies were conducted concerning the effect of installed FFFS (type compressed air foam and water mist) on the reaction and escape behavior of the tunnel users. These experiments with tunnel occupants were conducted in virtual reality (VR) and in real tunnels, and analyses were focused on the behavior of the participants during an evacuation situation. In all experiments, behavior with and without activated FFFS were compared. The results of a study carried out in 2014 in the Tunnel Jagdberg (Germany) regarding the influence of compressed air foam-based systems, as well as the results of a study carried out in 2015 analyzing the effect of water mist systems in the Bregenz City Tunnel (Austria) are presented. By comparing the results of studies in real tunnels and in VR important insights with regard to the interpretation of the results can be generated.

The results show that the decision of using FFFS has to be made by taking into account the different protection objectives and the interaction with other safety infrastructure (e.g., evacuation instruction). A critical view is essential to achieve an optimized solution with consideration of safety-related and economically perspective.

Keyword: tunnel, FFFS, Human Behaviour, Virtual Reality, Field Test

1. INTRODUCTION

Compliance with a defined level of safety with the focus on the user safety is a top priority in the evaluation of tunnel safety. The measures for tunnel safety are used to ensure the safety objectives self-rescue of the tunnel users, support of the rescue by emergency personnel and protection of the structure. The prioritization of protection objectives may vary by country, but synergy effects between the protection objectives are always desirable. The focus, however, is basically to ensure efficient self-rescue. It is the first phase after an event and the behavior of tunnel users often decide on the consequences arising from the event. The serious tunnel accidents in the Alpine countries have shown this in particular.

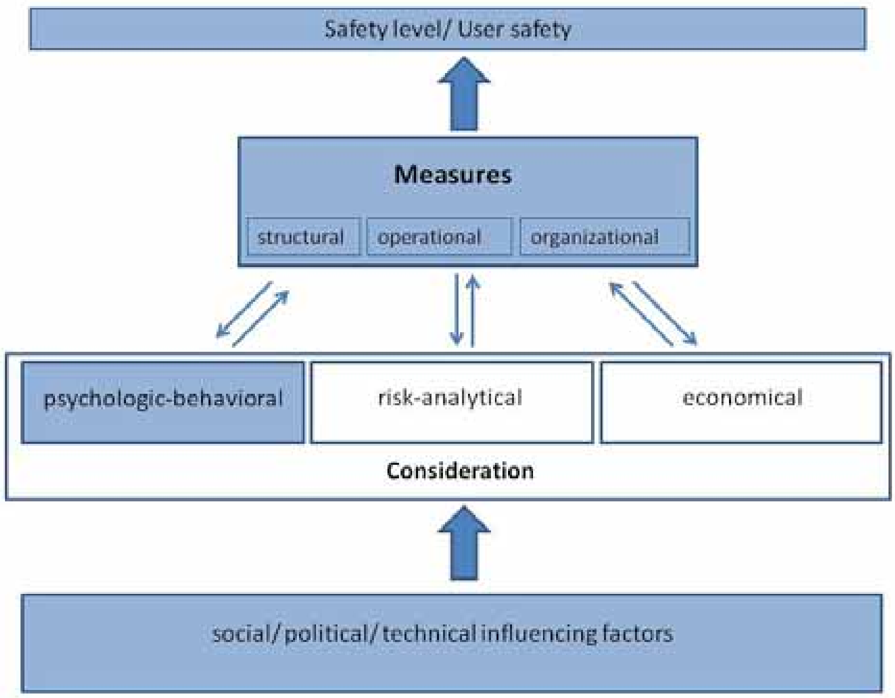

Figure 1: Classification of psychologic-behavioral investigation in the context of the evaluation of safety devices in road tunnels

If conditions change or new factors have to be considered, which affect the level of safety of a tunnel or the self-rescue of users, these have to be evaluated holistically. In addition to risk-analytical and economic issues, the psychological evaluation of the tunnel user in its entirety, especially in relation to his behavior is an essential object of investigation (see Fig. 1). This applies equally to technical innovations as well as for changes in the composition of the users-collective (e.g. demographic changes). If the level of safety cannot be adhered by the new environment or a change in the user-collective, hereinafter measures have to be taken subsequently to ensure the highest protection objectives.

The main objective of safety measures in tunnels is to ensure and to further enhance the self-rescue of the road users in case of events of an incident. To understand the behavior of road users in the event of an incident and to support self-rescue, it is necessary to consider various aspects of human information processing. A central component is the perception because of the various sensory channels the necessary information is included, which first include an understanding of the current situation as well as the perception of opportunities and goals of behavior. Major channels for communication of safety-related information are the visual and the acoustic channel. In addition to perception, the evaluation of the information and the decision making are of particular importance. Also motivational and emotional processes have be taken in consideration. Several models attempt to integrate the relevant processes in case of an incident [1,2].

2. FIXED FIRE FIGHTING SYSTEMS

Automatic fixed fire fighting systems (FFFS) in road tunnels are ment to ensure the containment of a vehicle fire in a road tunnel as early as possible to prevent the development of a major fire. They are used to limit the development of a fire and the fire spread and thus the effective fire power. Thereby the conditions for foreign rescue and also for firefighting should be supported as well as the protection of the structure from high temperature stress.

Regarding the installation of FFFS the envisaged support of the protection objectives for each country varies, even if synergy effects between the protection targets are detected. For example, while in Austria decisions for the additional use of FFFS are conductive to the structural protection and thus to availability, in Germany the installed FFFS serve primarily to support the foreign rescue.

In Germany, to date there are two tunnels with installed FFFS from the type foam, the Pörzbergtunnel and the Tunnel Jagdberg (both in Thuringia). In Austria, the City Tunnel in Bregenz, the Mona Lisa Tunnel in Linz and the Felbertauerntunnel feature a FFFS of the type high-pressure spray system. The equipment of the Arlberg tunnel and the Tunnel Liefering in Salzburg are in implementation.

In Germany, there is a tendency with the updating of the guidelines *Richtlinien für die Ausstattung und den Betrieb von Straßentunneln (RABT)* [3], that when there are certain criteria (e.g. a tunnel length greater than 3000 meters (unidirectional traffic) or length greater than 1200 m in case of two-way traffic tunnels and a designed heat release rate major 100 MW), in individual cases and in addition to the safety systems the use of FFFS can be taken in consideration. Other criteria are also that a strengthening of the structure or operational safety systems does not bring sufficient benefits or they are uneconomical. There has to be done an evidence about the expediency of FFFS for the defined specific protection objectives in a holistic evaluation.

In Austria's regulations, there are no defined guidelines for the use of FFFS, depending on certain criteria tunnel. However, in the case of the establishment of FFFS the *RVS 09:02:51 - Fixed firefighting systems* [4] gives detailed requirements which technical and operational criteria are to be observed. The protection objectives are similar to those of the RABT and are solely expanded to the reduction of contamination of equipment and construction of fire products, as well as to the reduction of environmental impact expanded. However, only high-pressure spray equipment has been authorized in Austria.

For a holistic consideration of the effects of a FFFS on the safety level, the interaction of the tunneling equipment to each other and their influence on user behavior must be validated. It should be noted that on the one hand an early activation of a FFFS brings the best chance of controlling the fire, on the other hand in case of a previous activation, tunnel users may be in the effective range of the system. For a review of the safety level, the criteria that make up the respective protection objectives have to be known.

However, so far there were no systematic studies of the effect of an activated FFFS on the behavior of tunnel users, because a FFFS is currently activated only after the self-rescue phase. Therefore several controlled randomized studies were carried out on the initiative of the Federal Highway Research Institute (BASt).

BASt devoted himself primarily the study of the influence of an activated FFFS to the self-rescue of tunnel users. Particular attention was directed to the investigation of the effects of the FFFS in terms of perception and the evacuation behavior of tunnel users. The important parameters here are the response- and escape velocity, which were considered in relation to the case "without" FFFS.

Different investigations were conducted: one study about the influence of water mist systems in Virtual Reality as well as two field studies in real tunnels to investigate both types of FFFS (water mist and compressed air foam). It was expected that an activated FFFS possibly delaying the evacuation behavior or even prevented because the visibility can be seriously impaired and people avoid leaving their vehicle in the area of the activated FFFS, due to the water or foam.

3. VIRTUAL REALITY RESEARCH

Besides examining tunnel user self-rescue behavior in real trials with limited possibilities and high availability requirements – it is only possible during maintenance periods – "virtual reality" (VR) offers an increasingly popular alternative. VR strongly evolved as a research method in recent years and offers multiple advantages like repeated presentation of standardized scenes and presentation of dangerous situations, which wouldn't be researchable in reality due to both ethical and logistical reasons [5]. Thus experimental approaches to various questions can be conducted with reasonable effort. In a first attempt within a research project the influence of an activated FFFS on tunnel users was examined („Wirksamkeit automatischer Brandbekämpfungsanlagen in Straßentunneln" (15.0563/2012/ERB)).

Within this study 50 participants randomly divided in two groups were examined. One group was presented the activated FFFS (water mist), the other group was not. All participants took part in a virtual tunnel drive entering a tunnel as driver and encountering an accident involving a burning truck, three cars stuck behind it and smoke slowly spreading towards the participant. After stopping the vehicle an announcement instructed the participants to evacuate the tunnel. In the activated FFFS group, the FFFS was activated during the announcement playing for the first time. Virtual cars of participants came to hold directly in the FFFS's area of influence and the car was entirely covered in water mist (see image 3). Measurements were taken on whether participants left the vehicle or not and on latencies occurring until participants got out of the car. After they left the vehicle the experiment was paused. Upon resuming the simulation, participants had the opportunity of continuing their escape via gamepad until they reached an escape goal. Goal and duration of the escape were measured, too. This research was conducted in a 3D multisensory laboratory (Cave System) [6].

Figure 2: The participants view immediately upon the end of the announcement in the FFFS condition (on the left) and in the no-FFFS condition (on the right) [7]

This VR experiment provides first valuable insights on how a FFFS affects experience and behavior of tunnel users. While the activated FFFS had distinct impact on the participant visual perception, hence a considerable reduction of vision inside and outside the car, the FFFS activation had only little effect on escape behavior. Both, participants with activation and those without activation of the FFFS left their vehicle within half a minute upon the beginning of the announcement and mostly chose the nearest by safety infrastructure as escape goals. Participants however differed in their escape routes to the emergency exit. Whereas participants in the FFFS condition kept rather close to the tunnel walls, those in the no-FFFS condition evacuated right through to the middle of the tunnel. The announcement, which asked to leave the tunnel, was equally well understood in both conditions and was not drowned out by the sound of the FFFS.

4. RESEARCH IN REAL TUNNELS WITH FFFS

To gain further insights considering humidity and cold, (real life) trials with test participants and both types of FFFS (high pressure foam and water mist) were conducted. Even if the basis for the decision on usage of FFFSs differ in both countries (Austria and Germany), the studies at hand provide clues on how to improve their application.

Objective of this first of two research project (Einfluss einer aktivierten Brandbekämpfungs-anlage (DLS) auf das Reaktions- und Fluchtverhalten der Verkehrsteilnehmer (FE 89.0299/2014)) was to determine the influence of an activated, water mist based FFFS on behavior and experience of tunnel users in respect to haptic stimuli like humidity and cold (which can’t be simulated in VR) in a field study and to validate the findings of the VR experiment. This study was conducted in the Jagdberg tunnel (A4 near Jena), which was mostly completed when the study was done but not yet opened to the public. In a randomized, controlled design in the Tunnel Jagdberg the escape behavior of the participants inside and outside the car was measured. Participants drove a car into the tunnel and were confronted with a simulated accident with smoke proliferation. After stopping the vehicle in front of the accident an announcement asked them to evacuate. Additionally the FFFS was activated for one half of the participants (see figure 3, on the left). A special focus was put on analysis of the participants’ reaction and escape behavior and also on the choice of the escape goals [7].

Figure 3: Car immediately after activation of the FFFS, Foam (on the left) and Water mist (on the right)

In accordance to the VR experiment's findings participants in the FFFS condition report restricted vision due to the foam (especially when sitting in the car without activating the windshield wiper). Compared to the VR experiment the loudspeaker announcement in the tunnel was less well comprehensible. Participants hardly feared any negative effects of the foam and reported no irritations on mucous membranes. They felt slightly influenced in their escape behavior, because they assumed the foam to be slippery and thus had watched their step. Behavior analysis shows most participants to have left their vehicle even with the FFFS activated. Both groups did not show any meaningful differences respective to escape goal and required time to exit the car. In both groups most participants evacuated to the nearest emergency exit. This finding suggest that most participants complied with the loudspeaker announcement's request to leave the tunnel.

After the study of the foam based FFFS a second research project about the "analysis of tunnel users' reaction and escape behavior upon activation of a water mist based FFFS in realistic conditions (FE 15.0607/2014)" was conducted. The objective was similar to the previous study changing the FFFS type to water mist. With support by the ASFINAG, this study took place in the Citytunnel in Bregenz, which was closed to the public during the research period (nighttime). Here too the escape behavior of the participants inside and outside the vehicle was analyzed in a randomized, controlled study. In the same way as in the study conducted in the Tunnel Jagdberg, participants drove a car into the tunnel and encountered a simulated accident with smoke proliferation. After stopping their car next to the accident a loudspeaker announcement asked them to evacuate. One half of the participants additionally experienced activation of the FFFS (see image 4, on the right). Again, a special focus was put on analysis of reaction and escape behavior of the participants as well as on the choice of escape goals. Within this study the amount of participants was further extended to 64 to conduct additional couple tests to determine tendencies concerning the interaction of passengers and possible delays or improvements regarding the escape behavior.

In accordance to the previous findings participants in the FFFS condition report the water mist based FFFS to considerable restrict their vision inside and outside the vehicle. As seen in the Tunnel Jagdberg study, loudspeaker announcements were less well comprehensible due to the FFFS activation. A particularly meaningful finding of this study concerned about 40% of the participants in the FFFS condition not disembarking their vehicle. As a result the number of participants reaching the emergency exit was considerably smaller whereas the number of other escape goal choices did not seem to be influenced (see figure 4, on the right). The couples, which entered the tunnel together, showed a tendency towards faster and more consequent reactions in comparison to individual drivers. This becomes especially apparent considering none of the couples stayed in the vehicle.

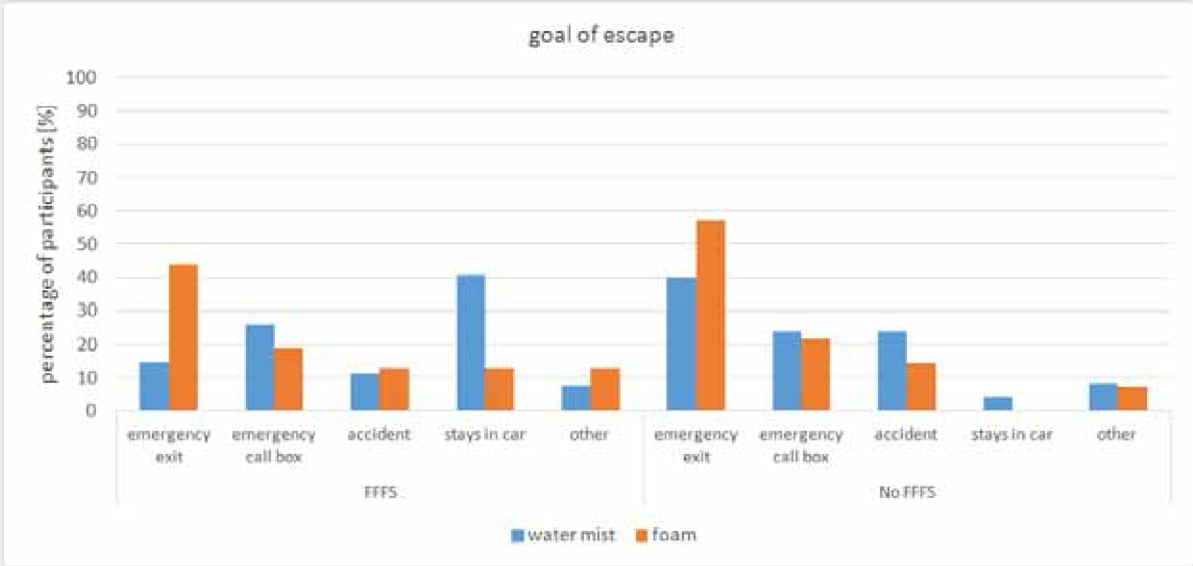

Figure 4: Behavior of participants and goals of escape behavior in %. Numbers over the boxes indicate absolute numbers

5. SUMMARIZING EVALUATION

Even though these three FFFS studies only covered one possible scenario and although the transfer of the findings at hand on real fire scenarios has to be handled very carefully, it seems that activating a FFFS in a tunnel might indeed limit vision considerably, but has no decisive negative impact on tunnel users, as long as relevant parts of tunnel infrastructure are being adjusted to the FFFS activation appropriately. In doing so, a well comprehensible announcement, when indicated with reference to the FFFS activation, is very important, so tunnel users finding themselves in the FFFS's immediate area of influence can understand the announcement and disembark their vehicle.

Interestingly in all studies at hand a considerable percentage of participants, which also got prompted to evacuate via loudspeaker announcements (real and VR), initially located an emergency call system. In the case of fire and strong smoke production, in which appropriate authorities are already informed, this is no constructive behavior. Having heard the announcement, tunnel users should be able to deduct that authorities are already involved. This raises the question of whether measures should be taken to change this behavior. Moreover, the VR and field study comparison suggests that virtual reality research is an appropriate means for researching behavior of tunnel users in case of an incident and gaining valuable insights on infrastructure requirements for tunnels with specific safety systems. Furthermore these findings show the importance of researching user behavior from psychological perspective to extensively evaluate safety standards of tunnels. Psychological user studies should be established as a fundamental pillar for evaluation of tunnel safety, especially with regard to a synchronized overall safety concept.

REFERENCES

[1] Kinateder, M., Ronchi, E., Nilsson, D., Kobes, M., Müller, M., Pauli, P., & Mühlberger, A. Virtual, Reality for fire evacuation research. Proceedings of the 2014 Computer Science and Information Systems (FedCSIS), 2. 313–321, 2014.

[2] Kuligowski, E., The process of human behavior in fires: US Department of Commerce, National Institute of Standards and Technology, 2009.

[3] Forschungsgesellschaft für Straßen- und Verkehrswesen: Richtlinien für die Ausstattung und den Betrieb von Straßentunneln (RABT), Entwurf 2015, unveröffentlicht

[4] Österreichische Forschungsgesellschaft Straße-Schiene-Verkehr: Richtlinien und Vorschriften für das Straßenwesen 09.02.51 – Ortsfeste Brandbekämpfungsanlagen, Ausgabe 1. Juli 2014

[5] Kinateder, M., Ronchi, E., Nilsson, D., Kobes, M., Müller, M., Pauli, P., & Mühlberger, A. Virtual, Reality for fire evacuation research. Proceedings of the 2014 Computer Science and Information Systems (FedCSIS), 2. 313–321, 2014.

[6] Kinateder, M., Ronchi, E., Gromer, D., Müller, M., Jost, M., Nehfischer, M., Mühlberger, A., & Pauli, P. (2014). Social influence on route choice in a virtual reality tunnel fire. Transportation Research Part F-Traffic Psychology and Behaviour, 26, 116-125.

[7] Lehan, A., Mühlberger, A., Gast, P., Pauli, P.: Selbstrettung der Verkehrsteilnehmer: Menschliches Verhalten in Wechselwirkung mit der Tunnelausstattung [Self-Evacuation of Road Users: Human Behaviour interacting with the Tunnel Furnishings], Tagungsband zur STUVA-Tagung 2015, Stuttgart, 321-325.

TESTING OF COMPLEX TUNNEL SYSTEMS

T.T. Aralt, K.S. Kvinge

Multiconsult ASA, Norway

ABSTRACT

Tunnel safety is a topic that is highly relevant in modern traffic planning. With the introduction of new technology, tunnel systems and equipment are increasing in complexity. This development presents a need for more thorough testing, and sets demands both for designer, supplier and tunnel owner. This article will present the method used for testing the Knappetunnel, as well as challenges faced during testing. Preparing for testing in the design documents and description of the tunnel, proved to be of great value for the testing.

Keywords: SAT, UAT, Design control systems

1. INTRODUCTION

The Knappetunnel, located in Bergen, is a 6.4 km long highway tunnel with six tunnelled slip roads and a total of 10 tunnel portals. North of the Knappetunnel, lies the 1.2 km long Lyderhorntunnel. The exiting left lane of the Knappetunnel leads directly to the slip road into the Lyderhorntunnel. Due to this, the control systems of both tunnels are connected into one joint system. In total the system consist of 2730 objects, and all together 756 variable message signs (VMS), lane signals and automatic barriers in the two tunnels. An overview of the tunnel is given in **Figure 1**.

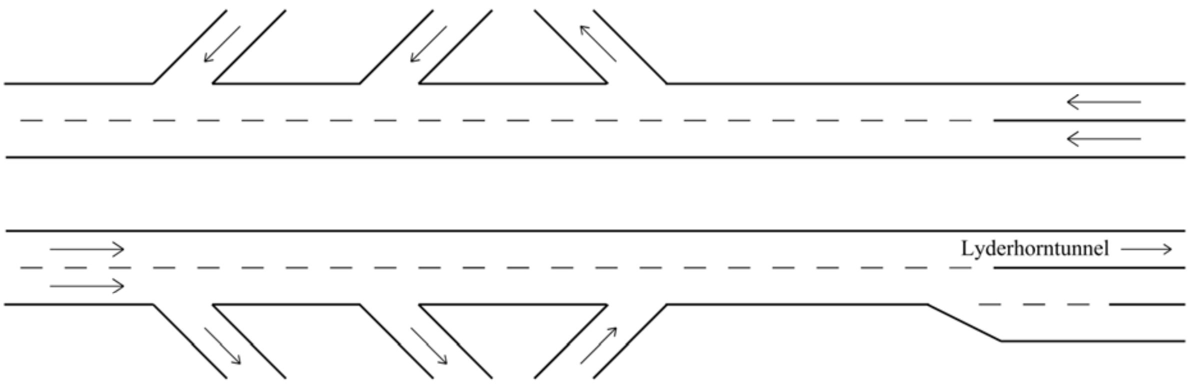

Figure 1: The Knappetunnel with slip road leading to the Lyderhorntunnel.

The majority of the system is considered critical to traffic safety and availability for the public, which sets high demands to the reliability of the system. It should also be taken into consideration that the road traffic centre in Bergen supervises nearly 250 tunnels, hence there is a very low tolerance for incoming alarms. This requires thorough testing of the tunnel, where both components and functions are tested in detail. The testing of the Knappetunnel has been performed over a period of five months, and adjustments of the control system have been implemented during this period.

Chapter 2 of this article will discuss how preparations for testing were made already in the design and contract phase of the project. Factory Acceptance Test (FAT) is a good precaution to ensure that the products meet the requirements set in the contract early in the process, and to avoid delays. Chapter 3 discusses this topic. After the supplier has tested and approved the tunnel, the Norwegian road administration have two tests the tunnel has to pass. Site Acceptance Test (SAT) and User Acceptance Test (UAT). The process for these two tests are presented in chapter 4 and 5.

2. DESIGN AND CONTRACT

Creating a plan for testing early in the design process, can be conductive to assuring quality of the delivery. During preparations of tender documents for electrical installation, covering all equipment using electricity, it is important to consider how you are going to verify that the contractor delivers according to the specification. The road authority needs a way to confirm that the final product is in accordance with the designers intent.

Two documents that are essential in this work are “Requests for programming” and the “List of objects”. “Requests for programming” consists of a detailed description of the functionality of the system. The main objective for this description is to ensure that the functionality is implemented as the designer planned, and to define a response to any combination of statuses and commands. “Requests for programming” consists of some scenario descriptions, combined with tables with numbered and specific requirements. **Table 1** presents an extract from one of these tables, describing requirements for variable speed signs. This document is also structured with testing in mind. Numbering the requirements, and providing a column for signing when the requirement is fulfilled, is done with the purpose to make the follow-up and control of the programming easier, for both supplier and owner.

Table 1: Example of requests for variable speed signs

Request No.	Request	Approved	Deadline
5.3.1	The routine in the last PLS before the speed limit sign should have the highest priority.		XX
5.3.2	Position “3” has priority over position “2” which has priority over position “1”. “60” has priority over position “80” which has priority over position “off”.		XX

The “List of objects” is based on the Norwegian road administrations standardized description for process interface. Herein every object is described, and a bit is assigned to every status or command the object can use to communicate with the Man Machine Interface (MMI). An example of such an object is an emergency cabinet, presented in **Table 2** and **Table 3**. Every object has similar tables, and these can be used to get an overview of which functions should be tested.

Table 2: Status bit assignment for an emergency cabinet

Status Bit	High	Low	Ok / Comments
0	Door open	Door closed	
1	Door Blocked	Door enabled	
2	Telephone receiver lifted	Telephone receiver in place	
3	Fire extinguisher removed	Fire extinguisher in place	
4	Fire extinguisher blocked	Fire extinguisher enabled	
5	Telephone receiver blocked	Telephone receiver enabled	
6	Telephone error	Telephone ok	
7	Error on telephone blocked	Error on telephone enabled	

Table 3: Command bit assignment for an emergency cabinet

Command Bit	High	Ok / Comments
0	Block alarm for door open	
1	Enable alarm for door open	
2	Block alarm for fire extinguisher removed	
3	Enable alarm for fire extinguisher removed	
4	Block alarm for telephone receiver lifted	
5	Enable alarm for telephone receiver lifted	
6	Block alarm for telephone error	
7	Enable alarm for telephone error	

These tables are used to describe every object in the “List of objects”. Herein, every object is listed in a table with tag, command and status bits, parameters, analogue values, reference to switchboard room PLS, control cabinet and a brief description. This is used as a test-list, where the supplier sign that all objects work end to end.

3. FACTORY ACCEPTANCE TEST

For large projects with several electrical power distributions, and close to 300 minor control cabinets a complete FAT will be expensive, and delay production. FAT of prototypes for minor control cabinets and all main electrical switchboards will often give necessary results. The extent of the FAT, and time schedule for when different parts should be tested, were described in the contract.

4. SITE ACCEPTANCE TEST

For the purpose of SAT and UAT we made a control room equipped as a small traffic central, with access to all systems. During testing, the central control system was running on a test server, where only new tunnels under construction are active. The tunnel is at this time not actively connected to the traffic operator’s central server. The «List of objects» was used by the supplier to document that every object was tested, and to leave comments where there were shortcomings in either testing or performance. Given the confirmation that all objects are tested end to end by the supplier, a selection of objects and functions were chosen for SAT, depending on the impact on safety. The following chapters presents testing procedure for different types of objects.

4.1. Control cabinets and VMS signs

Outdoors, 10 % of the control cabinets with underlying VMS signs were tested. Alarms and feedback from the cabinets were tested by disconnecting fuses and fibres. Commands were issued, to confirm expected results, with and without faults in the cabinets. Blocking the alarms from the control system, verified that the expected response was given. In order to simplify testing of the VMS signs, a test button is installed in the control cabinet. By activating the button, the signs in the current control cabinet, will run through every position. Feedback from the signs are then verified with visual control of the physical sign, combined with monitoring the status from the control system. The same procedure was used for testing signs and control cabinets in the tunnel, but here 100 % of the objects were tested.

4.2. Emergency cabinets

Every emergency cabinet was tested thorough. Testing the telephones included incoming calls, outgoing calls to the road traffic central and sound check. Fire extinguishers were removed to test that the road traffic central received an alarm, and that the correct fire ventilation program started automatically.

4.3. Switchboard rooms

For every switchboard room, a random selection of fuses were disconnected, and the response in the top system were observed. The UPS was activated and tested over time with a realistic load, to ensure an acceptable performance.

4.4. Road barriers

Road barriers were tested in combination with the red lights. The bar should not be able to close when the red light is off. Detection loops are installed in the road covering the bars working area. Tests were performed on every barrier point with a car in the detection zone, to ensure that the bar is prevented from closing, and an alarm is sent to the road traffic central, when the bar is prevented to close due to a vehicle in the detection area.

4.5. Emergency panels

Manually controlled barriers, lighting and ventilation, as well as emergency closing of the tunnel, were tested from every emergency panel. A ranking was described for commands between the emergency panel, automatic responses and the road traffic central. Local controlling from the emergency panel should have the highest priority, and the panel needs to be set in automatic mode before the road traffic central can regain control. Combinations of commands from the emergency panel and MMI system were tested, to ensure that the procedure for closing behaved as expected.

4.6. Ventilation

4.6.1. Ventilation system

The ventilation in the Knappetunnel is divided into 12 sections, where each section is controlled as a ventilation object. Depending on the number of ventilators in a section, a number of steps with a predefined number of active ventilators is defined by the use of parameters for the ventilation object. This makes the ventilation system very flexible, and gives opportunity for a number of predefined ventilation plans. The Knappetunnel has sensors for detection of CO, NO, NO_2 and dust. During normal operation, they control the ventilation in the tunnel.

4.6.2. Single objects

Every ventilator was tested to ensure that the control and feedback from the top system performed as expected. Verification of the direction of the air flow was performed by tests with a flag indicating the direction. Delay time when reversing the direction were also observed in the tunnel.

4.6.3. Fire plans

In case of fire, a predefined fire plan can be activated, either by removing a fire extinguisher or manually from the road traffic central. A fire plan includes emergency closing of the tunnel, as well as activation of a predefined ventilation plan. The Knappetunnel has seventeen different ventilation plans, where each plan is adjusted to address a different location of fire. There are a few conditions that should be met when tuning in the ventilation system. Ventilators located close to the fire should not be activated, in order to keep the smoke close to the ceiling in the area of the fire. The airflow should always follow the traffic direction in the area of the fire. Air velocity should always be above 3.5 m/s. A starting criterion is defined for each fire plan, and based on air velocity measurements, the ventilation will increase until an acceptable speed is reached.

As previously mentioned, each section of ventilators has an object in the MMI, where a set of parameters can be defined in order to set the start criterion for each fire plan. Every plan was tested, and tuning of the ventilation was done by observing the measured values of the air velocity, and adjusting the parameters to meet the requirements.

Based on previous experiences, some scenarios that have caused problems in other projects were studied. Automatic ventilation can be started either by activation of a fire plan, or by measured traffic pollution. While traffic ventilation was running, a fire plan was activated to ensure that the fire ventilation would overrule the commands from the pollution sensors. Changing between different active fire plans was tested, to verify that the ventilation plan changed while the tunnel kept closed. Removing a fire extinguisher will activate the fire plan for the area. When a fire plan is activated, removing another fire extinguisher should not change which plan is active. A probable scenario would be that in the case of a fire, fire extinguishers will be removed in different locations not only for the purpose of putting out the fire. Removing several extinguishers in different locations, verified that this functionality was implemented.

4.7. AID and automatic response

The Knappetunnel has full video coverage, with automatic incident detection. Detection with alarm is implemented for stopped vehicles. Detection of queues and wrong-way-drivers gives both an alarm and an automatic response. A wrong-way-driver will cause the tube to close, and uses lane signals to close the left lane. Detection of a queue activates warning signs with queue notice in a predefine zone.

Stopped vehicle detection and camera coverage were tested by driving a car through the tunnel, stopping to receive an alarm for every camera. Automatic response for wrong-way-drivers was tested for each tube in a couple of locations. Extended calibration of the AID system during a six month period after opening, was described in the contract.

4.8. Traffic plans

The Knappetunnel has 81 different predefined traffic plans which can be activated with one command closing parts of the tunnel, lanes or part of lanes. Every traffic plan was tested, as well as combinations of different plans. Certain combinations of plans can not be active simultaneously, and the graphic interface of the top system should indicate when a plan is not a legitimate option. Depending on what plan is active, the status of every traffic plan will change, indicating whether it is a valid option. The transaction between plans was tested, and also combinations of different active plans. The Lyderhorntunnel lies north of the Knappetunnel, and is connected directly to the exiting left lane. Closing the Lyderhorntunnel, means that the exiting left lane of the Knappetunnel should also be closed. Hence, the two tunnels should be tested together. Several tests were performed to stress the system, with swift changes between traffic plans, both legal and illegal combinations of different traffic plans as well as closing of the tunnel.

4.9. Practical challenges during SAT

4.9.1. Delays

A well known problem that occurs in many projects, is the fact that due to delays in the project, the time left for testing is less than what was originally planned. Testing will then be on a very strict time schedule to meet the opening date. For the Knappetunnel, testing started while there was ongoing works in the tunnel, and with a list of defects that were being corrected. In addition, the SAT started before the suppliers tests were complete, and parts of the UAT were performed in collaboration with the SAT. This complicated the testing process. One may discuss whether or not postponing the start of SAT and giving the supplier access priority to the tunnel to finish repairs and testing, would have been a better approach. Based on experience from the testing in the Knappetunnel, we would recommend that suppliers test, SAT and UAT are carried out separately.

4.9.2. Two construction stages

The Knappetunnel was built in two construction stages. This means there was traffic on half of the tunnel during testing of the final construction stage. During the Norwegian general staff holiday, the entire tunnel was closed for traffic. After this period, testing that could affect the traffic or required a closed tunnel, could only be performed at night or during a limited time period during the day. This resulted in an inefficient testing period. Building the tunnel in one construction stage would have reduced the total time for both execution and testing.

4.9.3. Communication

Testing started before the cell phone coverage was established in the tunnel. Ensuring that this is installed before testing starts, will make the process more efficient, as it simplifies communication between the operator at the test central, and the people located in the tunnel. Emergency phones were used for communication during testing in this project.

5. USER ACCEPTANCE TEST

When the SAT has been approved, the tunnel needs to pass a user acceptance test. The user of the Knappetunnel is the road traffic central in Bergen, who monitor and control approximately 250 tunnels. Every week there are upgrades in their tunnels. They also receive several new tunnels each year. Before UAT can start, faults discovered during SAT should be corrected. UAT focuses mainly on scenario testing, changing between different situations. Parts of the scenario testing were also performed during SAT, but nothing can replace an experienced operator when carrying out this kind of testing. The UAT uncovered faults that occurred when executing specific routines or typical responses from operators, which we did not discover during SAT which was based on the designers mindset.

6. CONCLUSION

Preparing for testing when working out the design documents and specifications for the tunnel, proved to be valuable for testing of the Knappetunnel. Design documents were used to keep track of what should be tested, and helped during the follow-up of faults that were discovered. Planning the testing in advance, and supplying the contractor with documentation that shows the extent of what is expected from the suppliers test, resulted in a thorough testing during which the majority of the faults were discovered and corrected before the start of the SAT. During testing of the Knappetunnel, construction stage two, the amount of faults discovered were significantly less than the amount observed in construction stage one. In construction stage one “Requests for programming” was not separated into one document, and the requests were far less detailed.

EVALUATION OF JET FAN PERFORMANCE IN TUNNELS

Beyer M., Sturm P.J., Saurwein M., Bacher M.
Graz University of Technology, Austria

ABSTRACT

This paper deals with the analysis of jet fan efficiency in road tunnels. Jet fans are often used for tunnel ventilation and due to lack of space they are commonly installed close to the wall. However, as a result of the increased wall shear stress around the jet, thrust effectiveness is significantly reduced. In addition, diffusion losses which occur when transferring momentum from a high jet velocity to the surrounding secondary flow in the tunnel can be noted. In this paper an installation efficiency coefficient is employed in order to account for such thrust losses. The coefficient describes the ratio of the thrust provided by the jet fan and the momentum received in the tunnel.

Two full-scale measurements of different jet fan applications in existing road tunnels in Austria were performed in order to analyse installation efficiency. Based on these measurements a numerical model was then developed and validated. The validated numerical model was then used to analyze installation efficiency under several scenarios. Investigations showed that apart from wall clearance, jet fan size, etc. the installation efficiency is strongly dependent on the air velocity in the tunnel. It was also found that the thrust losses were consistently higher than expected.

Keywords: ventilation design, jet fan, installation efficiency, tunnel ventilation

1. NOTATION

Δp_{mt_theo}	(Pa)	Theoretical pressure rise caused by a jet fan
ρ	(kg/m³)	Air density
ρ_0	(kg/m³)	Reference air density = 1.2 kg/m³
A_s	(m²)	Free cross section area of a jet fan
A_t	(m²)	Tunnel cross section area
u_s	(m/s)	Jet velocity at fan exit
u_t	(m/s)	Tunnel air velocity
L	(m)	Measurement length for pressure difference
η	(-)	Installation efficiency coefficient
η_{op}	(-)	Efficiency coefficient owing to a shift of jet fan's operating point
Δp_{mt}	(Pa)	Effective pressure rise in the tunnel due to running jet fans
n	(-)	Number of running jet fans
Δp_{12}	(-)	Measured / simulated pressure rise in the tunnel due to running jet fans
λ	(-)	Friction coefficient of the tunnel
ζ_{12}	(-)	Resistance coefficient
F_s	(N)	Jet fan thrust
F_0	(N)	Static thrust of a jet fan at ρ_0
F_{mt}	(N)	Effective thrust in the tunnel due to running jet fans
d_i	(m)	Free inner jet fan diameter
d_o	(m)	Outer jet fan diameter
Δp_{dyn}	(Pa)	Dynamic pressure difference
T_t	(°C)	Air temperature
p_{abs_t}	(Pa)	Absolute pressure in the tunnel

d_t	(m)	Hydraulic tunnel diameter
u_{s_ref}	(m/s)	Jet velocity for a known installation efficiency

2. INTRODUCTION

Jet fans play an important role in tunnel ventilation. As discussed in [12], they may be used to influence tunnel air velocity so as to conform to a specific ventilation philosophy, or so as to comply with international and national guidelines. The advantages of jet fans derive from their relatively low construction costs and from their ability to allow for relatively simple control of the air/smoke movement inside the tunnel. For transverse ventilated systems other methods, such as Saccardo type fresh air injection, might also be used, especially in cases of tunnel refurbishment. Relevant discussion concerning the application of ventilation systems can be found in [15] and [16].

Owing to lack of space, jet fans are usually installed very close to the tunnel wall or in fan niches. As a result of the short distance between the tunnel wall and the fan jet, the jet flow tends to remain attached to the tunnel surface (Coanda-effect). This causes high wall shear stresses around this region and thus results in a considerable reduction of the acting jet fan thrust. For jet fans mounted in niches, additional momentum losses due to the required deflection of the jet flow also arise.

Jet flow friction losses on walls have already been analysed in many small-scale tests [8], [2], [3], [4], [10] and [5]. However, it seems that the efficiency values thus derived are too optimistic. To overcome the associated level of uncertainty, full scale tests were realised. The investigations described here were carried out in two existing road tunnels in Austria. One tunnel has a longitudinal ventilation system with jet fans mounted on the tunnel ceiling. The other tunnel is equipped with a semi-transverse ventilation system where the jet fans are mounted in niches on both side walls.

Based on the measurements a numerical model was then applied and validated. In a further step, an extensive investigation was realised, implying different jet fan types, tunnel profiles, air velocities inside the tunnel, distances between jet fans and tunnel wall as well as double and single fan arrangements. The analysis was carried out at Graz University of Technology and is described in detail in two master theses [7], [14].

2.1. Physical Backround

Jet fans in road tunnels are used to control the air velocity in the tunnel by transferring the momentum of the jet fan to the surrounding tunnel air flow. From the outlet of the jet fan the momentum along the jet flow decreases and is transferred to the airflow in the tunnel. This causes a pressure rise downstream of the jet fan. The momentum of the jet fan is fully transferred where the pressure reaches its highest level. At this point, the velocity profile has returned to that of a fully-developed pipe flow. Depending on the tunnel profile and the jet fan type this occurs 80 m to 160 m downstream of the jet fan (see also [11], [8], [17]). The mathematical description of the momentum transfer of a jet fan in a tunnel was introduced by Meidinger [9], followed by Rohne [10] and Kempf [8] and is now summarised below.

With respect to Figure 1, and according to [9] and [17], the maximal theoretical achievable pressure rise in the tunnel owing to a running jet fan is given by eq. 1.

$$\Delta p_{mt\_theo} = \frac{\rho}{2} u_s^2 \cdot \left[\left(2\frac{A_s}{A_t} - 2\frac{A_s}{A_t}\frac{u_t}{u_s} \right) + \frac{\left(\frac{A_s}{A_t}\right)^2 - 2\left(\frac{A_s}{A_t}\right)^3 + 2\left(\frac{A_s}{A_t}\right)^3 \frac{u_t}{u_s} - \left(\frac{u_t}{u_s}\right)^2 \left(\frac{A_s}{A_t}\right)^2}{\left(1 - \frac{A_s}{A_t}\right)^2} \right] \quad \text{eq. 1}$$

However, in practical applications it is common to simplify equation eq. 1 by neglecting the second term in the square brackets (see also [9], [10] and [13]). This leads to following equation:

$$\Delta p_{mt\_theo} = \rho u_s^2 \frac{A_s}{A_t} \cdot \left(1 - \frac{u_t}{u_s}\right) \quad \text{eq. 2}$$

This equation is similar to that relating to an impeller in a free stream [17]. As discussed in [5], [9], [10] and [13] the difference between equations 1 and 2 is due to the pressure and velocity change surrounding the jet flow as a result of the confining influence of the duct. The error is given by the second term in the square brackets of eq. 2 and mainly depends on the area ratio $\left(\frac{A_s}{A_t}\right)$. However, even when this is dropped, the simplified equation still underestimates the pressure difference by between 2% to 4%, and is therefore a more conservative approach.

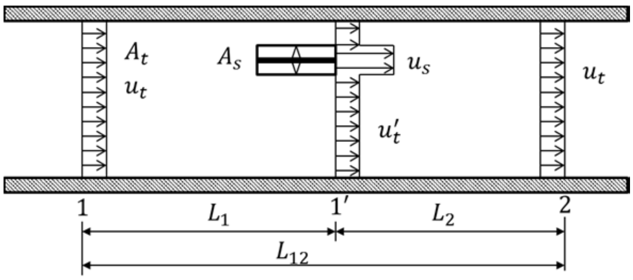

Figure 1: principal sketch of a jet fan in a tunnel

The equations above consider the theoretical momentum transfer into the tunnel flow in the absence of losses. However, all losses of the thrust by installing a jet fan in the tunnel can be accounted for by introducing an installation efficiency coefficient in eq. 2. Thus:

$$\Delta p_{mt} = \frac{\eta}{100} \cdot n \cdot \rho u_s^2 \frac{A_s}{A_t} \cdot \left(1 - \frac{u_t}{u_s}\right) \quad \text{eq. 3}$$

It is essential to combine the right efficiency coefficient with the right equation. For instance, Kempf [8] introduces an efficiency coefficient into an equation in which the volume flow ratio between the jet fan and the tunnel has been taken into account. This formulation lies between eq. 1 and eq. 2 and provides results similar to those derived by means of the more exact formulation (eq. 1). However, the use of the efficiency coefficient suggested by Kempf [8] in combination with eq. 2, results in an error in the same scale like that between eq. 1 and eq. 2. A similar problem arises when the efficiency coefficient defined by Armstrong [5] (which is evaluated with eq. 1) is used in combination with eq. 2.

The installation efficiency η as defined in eq. 3 for multiple fans (n) captures all losses occurring between the effective jet fan thrust F_s and the effective momentum transferred to the tunnel airflow (pressure rise in the tunnel) which result from installation configuration and differences arising from simplification of eq. 1. In the present context, two main types of loss can be analysed, i.e. that relating to momentum diffusion, and that relating to increased wall shear stresses.

A relatively high velocity gradient can be identified between the core of the jet flow and the surrounding airflow in the tunnel. Along the jet flow the radial velocity gradient decreases due to the momentum transport between the jet and the surrounding tunnel air until a fully-developed velocity profile is once more attained. This momentum transfer is caused by viscous stress and is accompanied by a loss in jet momentum. Depending on fluid properties, shape of the jet, and the velocity gradient, such losses can reduce the effective momentum by between 8% and 24% [7], [14].

In addition to diffusion of momentum, losses in effective momentum relating to the proximity of the jet fan to the tunnel wall, also need to be accounted for. As discussed and highlighted in [5] the short distance between jet and tunnel wall reduces the area available for momentum transfer. Moreover, the high velocity gradient of the jet flow next to the tunnel wall causes high wall shear stresses and therefore frictional losses. The momentum losses of a jet fan induced by the tunnel wall have been extensively analysed in [2], [3], [4], [5], [10] and [8]. However, additional losses exist relating to geometry (shape of the tunnel cross section, niche installations, etc.), to momentum transport between the jet and the surrounding tunnel air, to installation parameters, to tunnel air velocity etc. All of these need to be taken into consideration too.

It needs to be noted that two issues are particularly important when applying an efficiency coefficient to jet fans. First, the nature of the losses to be captured by the efficiency coefficient, and second, the nature of the equation used in the definition of the efficiency coefficient.

The pressure difference Δp_{12}, needed for deriving the installation efficiency was measured with respect to those points upstream and downstream of the jet fan position, where the velocity profile in the tunnel was fully developed. This was done in order to determine the entire pressure rise caused by the jet fan and to obtain repeatable flow conditions at the positions where the pressure was measured. As can be seen in Figure 2, the pressure rise due to the effective momentum transferred to the tunnel airflow Δp_{mt} is higher than the evaluated or measured pressure difference Δp_{12}. This is due to the friction losses between point 1 and 2 and is treated as follows:

$$\Delta p_{mt} = \Delta p_{12} + \left(\frac{\lambda \cdot L_{12}}{d_t} + \zeta_{12}\right)\frac{\rho}{2}u_t^2 \qquad \text{eq. 4}$$

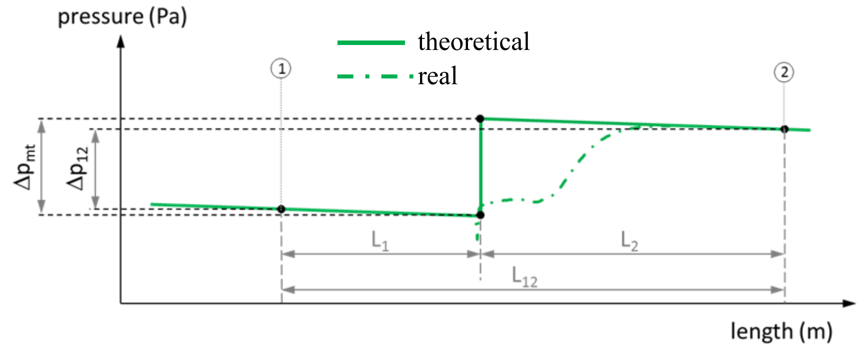

Figure 2: Theoretical and real pressure rise in the tunnel owing to a running jet fan

On the basis of eq. 3 and eq. 4, the installation efficiency is given by eq. 5 and represents the ratio between the theoretically achievable pressure rise in the tunnel owing to running jet fans and the actual pressure rise in the tunnel.

$$\eta = 100 \cdot \frac{\Delta p_{12} + \left(\frac{\lambda \cdot L_{12}}{D} + \zeta_{12}\right)\frac{\rho}{2}u_t^2}{n \cdot \rho u_s^2 \frac{A_s}{A_t} \cdot \left(1 - \frac{u_t}{u_s}\right)} \qquad \text{eq. 5}$$

For practical applications, normally only the static thrust of the jet fan, as provided by the manufacturer, is known. In general, the static thrust of a jet fan is already slightly reduced or increased upon installation due to a shift in the jet fan's operating point. In order to take account of the impact of such a shift in operating point the efficiency coefficient η_{op} is introduced. For example, in the case of a deflection of the jet, static thrust is reduced by the higher resistance impinging on the jet when leaving the fan. Measurements undertaken in the Bosruck tunnel revealed that the shift in the jet fan's operating point reduced the static thrust by up to 9% (see η_{op} in Table 3). In contrast, in the case of a paired (or greater) jet fan arrangement, static thrust may be slightly increased due to the mutual support provided by the fans (see η_{op} in Table 4). One also needs to note that static thrust may vary by up to 5% as a result of jet fan construction tolerances.

Thus, the ratio between the static thrust and the available effective thrust (based on the reference density ρ_0) of a jet fan installed in a tunnel can be determined using eq. 6.

$$F_s = \rho u_s^2 A_s = \frac{\rho}{\rho_0} \cdot \frac{\eta_{op}}{100} \cdot F_0 \qquad \text{eq. 6}$$

This then implies that the effective thrust in the tunnel can be calculated based on the static thrust of a jet fan by means of the following equation:

$$F_{mt} = \frac{\Delta p_{mt} \cdot A_t}{n} = F_S \frac{\eta}{100} \cdot \left(1 - \frac{u_t}{u_s}\right) \qquad \text{eq. 7}$$

During the full-scale measurements the effective jet fan thrust Fs was determined by measuring the dynamic pressure $\frac{\rho}{2} u_s^2$ with a kind of a pitot tube mounted in the jet fan upstream the fan blade.

3. MEASUREMENTS AND NUMERICAL MODEL VALIDATION

In order to determine the installation efficiency and to validate the numerical model for a deep case study, full-scale measurements were carried out in the Bosruck tunnel [18] and in the Niklasdorf tunnel [14]. Figure 3 shows the fan installations in the Bosruck tunnel (left) and in the Niklasdorf tunnel (right).

3.1. General Tunnel Parameters

The Bosruck tunnel has two tubes, a length of approx. 5.5 km and is equipped with a semi-transverse ventilation system. Jet fans are installed in five niches on both sidewalls of the tunnel. Due to the fact that these niches have orthogonal front walls the jet fans are equipped with deflection blades with a blade angle of 13.5°. The jet fans are mounted in the upper third of the wall (the vertical distance between outer jet fan surface and side walk is 2.6 m). The minimum distance between the tunnel ceiling or tunnel side wall and the outer surface of the jet fan is 0.3 m. The horizontal distance between the jet fan outlet and the end of the niche is 12 m.

The Niklasdorf tunnel also consists of two tubes, and has a length of approx. 1.4 km. It is equipped with a longitudinal ventilation system. Measurements were carried out in the south tube, which is equipped in total with 8 jet fans (3 pairs and 2 single fans). The minimum distance between the outer surface of the jet fan and the tunnel ceiling is 0.2 m. In the pairwise installation the distance between the jet fan axes is 2.8 m ($2 \cdot d_o$). An overview of the relevant tunnel and jet fan parameters for both tunnels can be found in Table 1. Figure 3 shows the position of the jet fan in the Bosrucktunnel (left) and in the Niklasdorftunnel (right).

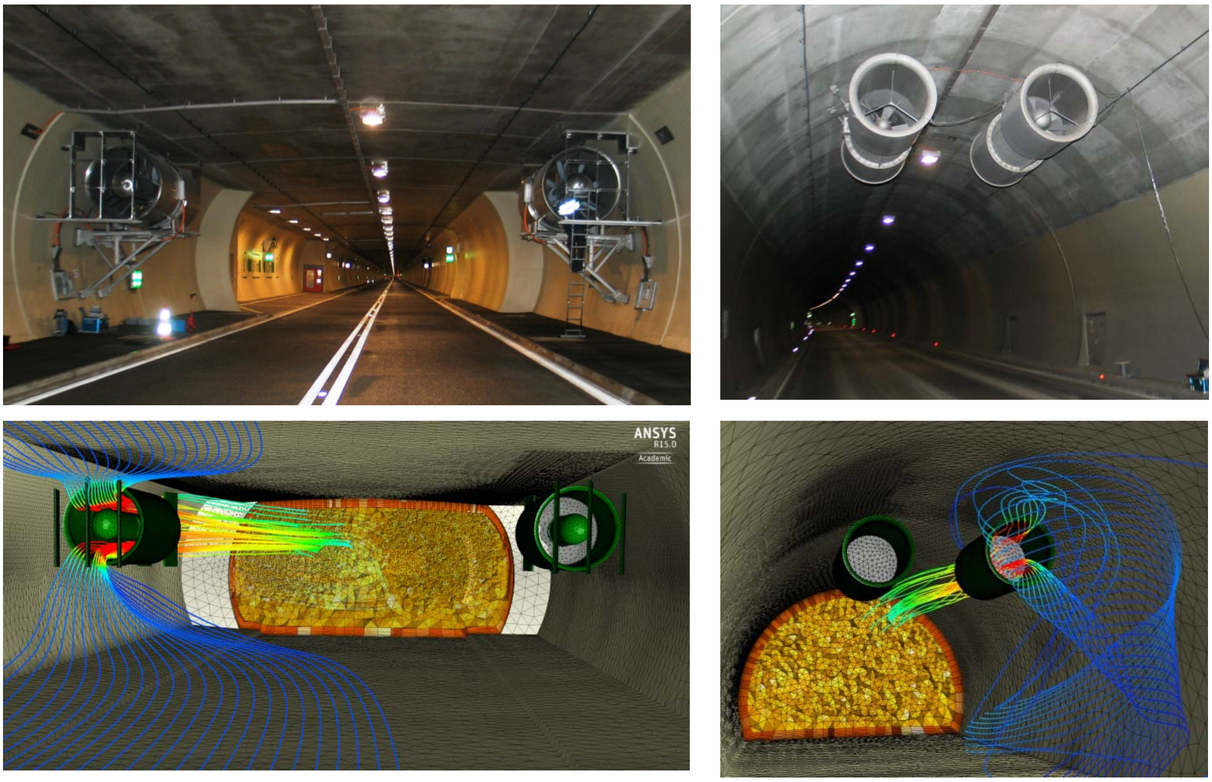

Figure 3: Picture of the Bosruck tunnel - east tube (left) and the Niklasdorf tunnel - south tube (right) as well as the corresponding numerical model (below), and depicting velocity streamlines

Table 1: Relevant tunnel and jet fan parameters of the on-site measuremnts.

Parameter	Bosruck tunnel	Niklasdorf tunnel
Regular tunnel cross section, A_t	51.21 m²	51.0 m²
Hydraulic tunnel diameter, d_t	7.92 m	7.89 m
Static thrust, F_0	2826 N	884 N (SVS4.1) and 899 N (SVS4.2)
Reference density, ρ_0	1.2 kg/m³	1.2 kg/m³
Inner diameter, d_i	1.6 m	1.12 m
Outer diameter, d_o	1.8 m	1.4 m
Free cross section area of fan, A_s	1.658 m²	0.985 m²
Length of jet fan	4.1 m	4.1 m
Deflection blade angel	13.5°	no defection blades

3.2. Measurement Set-up

The measurements were carried out in accordance with the requirements necessary for defining the installation efficiency η. All the parameters were recorded at locations upstream and/or downstream of the fans, where the velocity profile of the tunnel air was fully developed, i.e. the effect of the jet of active fans was no longer noticeable. The real thrust of the installed jet fans F_s was determined by measuring the dynamic pressure $\frac{\rho}{2} u_s^2$ with a kind of a pitot tube device mounted in the jet fan upstream of the fan blades. Without this information validation of the numerical model and the derivation of the installation efficiency coefficient would not have been possible, i.e. it was necessary to ascertain the boundary condition of the jet fan. The static thrust cannot be used for the boundary condition due to the non-negligible difference between the static thrust and the real thrust of an installed jet fan. The measurement device used for the determination of real thrust was tailor-made for each jet fan (see Figure 4) and calibrated in the wind tunnel of the Institute of Fluid Mechanics and Heat Transfer at Graz University of Technology.

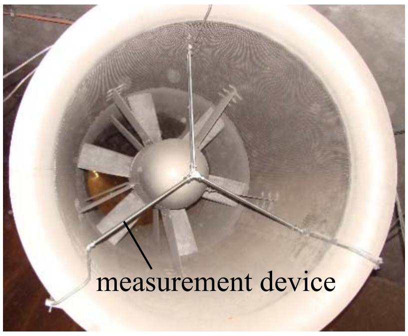

Figure 4: Measurement device for thrust measurement at the fan

Figure 5 shows a sketch of the tunnel section with the installed jet fans in the niches and the measurement set-up for the on-site measurement in the Bosruck tunnel. Figure 6 shows the same for the Niklasdorf tunnel. The basic measurement set-up was equal for both tunnels. Compared to the measurement set-up in the Bosruck tunnel, one additional pressure difference was considered in the Niklasdorf tunnel in order to analyse the installation efficiency for each group of pairwise mounted jet fans separately, as well as for all four jet fans together with one and the same set-up. An overview of the measurement devices employed and their main specifications can be found in Table 2.

In order to determine the friction coefficient of the tunnel, the pressure difference over a distance of 500 m (with no lay-bys, fan niches, or cross section changes) was measured in both tunnels.

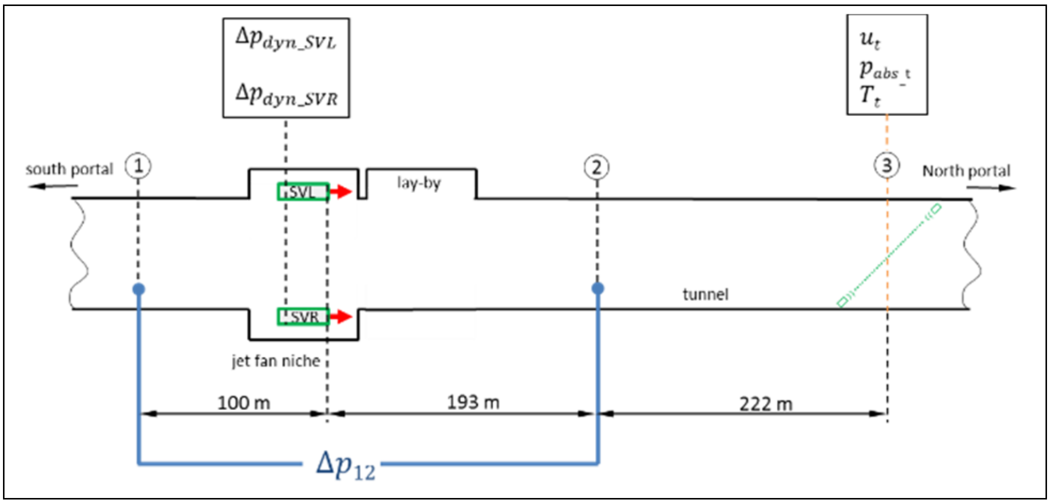

Figure 5: Measurement set-up of the Bosruck tunnel)

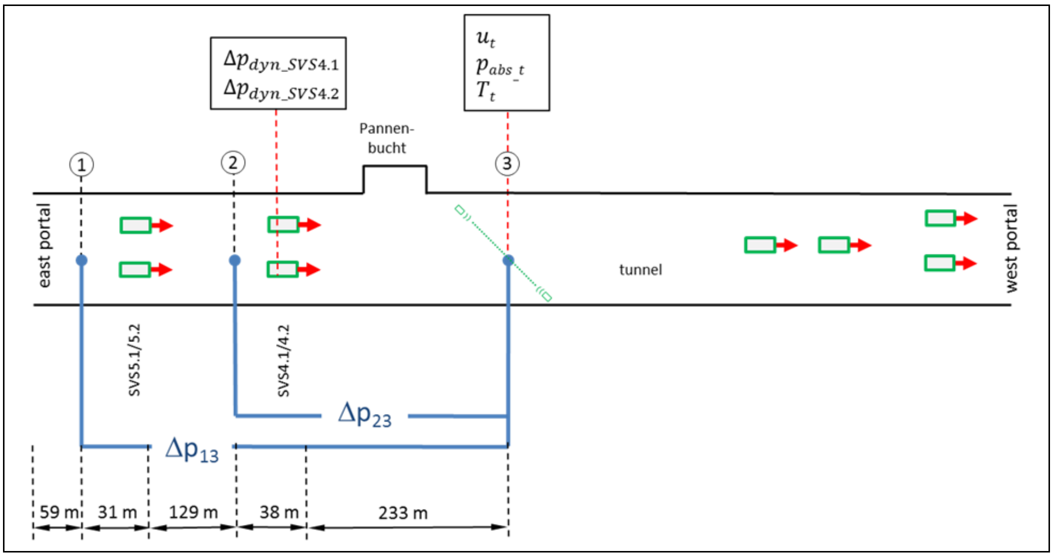

Figure 6: Measurement set-up of the Niklasdorf tunnel

Table 2: Main specification of the measurement devices used.

Value	Measurement device	Range	Precision
u_t	Sick (Flowsic 200)	-20 to +20 m/s	± 0.3 m/s
Δp_{12} and Δp_{23}	Halstrup & Walcher (P26)	+500 to -500 Pa	± (0.5 % + 0.3 Pa)
Δp_{13}	Halstrup & Walcher (P26)	0 to +500 Pa	± (0.5 % + 0.3 Pa)
Δp_{dyn_SVL} and $_{SV1}$	Halstrup & Walcher (P92)	0 to +5000 Pa	± (0.5 % + 0.3 Pa)
$\Delta p_{dyn_SVR}$$and$ $_{SV2}$	Jumo 4304	0 to +5000 Pa	± (0.5 % + 0.3 Pa)
T_t	Testo (177-T2)	-40 to +70 °C	± 0.4 °C
p_{abs_t}	Kroneis (Barogeber Type 315 K)	850 to 1050 hPa	± 0.5 hPa

In order to determine the friction coefficient of the tunnel, the pressure difference over a distance of 500 m (with no lay-bys, fan niches, or cross section changes) was measured in both tunnels.

3.3. Measurement Program

The measurement in the Bosruck tunnel was performed for all of the 5 jet fan niches in three steps. In the first step the pressure difference over one jet fan niche (Δp_{12}) with deactivated jet fans in this region was recorded for a time interval of 20 minutes after reaching steady state conditions, in order to define the resistance coefficient of the tunnel section under consideration and in order to subsequently be able to determine the effective momentum transferred into the tunnel airflow (Δp_{mt}) (see Figure 2). In order to gain reliable measurements, the relatively high air velocity in the tunnel was achieved by means of the remaining jet fans, i.e. those outside of the measurement location. In the next step one jet fan of the niche under investigation was started and the pressure difference recorded. The same procedure was repeated with both fans of the niche activated.

In order to evaluate the effect of the deflection blades the measurements with two active fans were repeated again after the deflection blades had been removed. The measurement values for each of these tests were recorded for at least 10 minutes after reaching steady state conditions. In order to have comparable test results for each of the fan niches the overall air speed in the tunnel was kept at a value of 1.5 m/s by activating those fans which were outside of the measurement domain.

The measurement procedure for the Niklasdorf tunnel was similar to that employed in the Bosruck tunnel, except – as already mentioned above – for the additional pressure difference measurement covering two pairs of jet fans. First of all, pressure differences over the jet fans (Δp_{13} and Δp_{23}), with the fans remaining inactive, were recorded for 20 minutes. After this the pressure differences for 2 active fans and then for 4 active fans, were measured in order to evaluate the efficiency coefficient as a function of the base tunnel air velocity. Each of these tests was repeated at three different tunnel air velocities. In total, 6 test cycles with running jet fans were performed. The duration for each test cycle was 10 minutes.

Table 3 and Table 4 show a summary of the results of all measurements performed.

3.4. Numerical Model

ANSYS Fluent software was used for the numerical study. Turbulence was modelled using the realizable k-e model [19] with a logarithmic wall function. This turbulence model was chosen due to its good prediction of turbulence behaviour for both planar and round jets (see also [1] and [6]). The logarithmic wall function satisfies the requirements for the boundary layer and works reasonably well for wall-bounded flows. For the discretization of the 3d geometry analysed, a hybrid mesh comprising a few million elements was applied. In compliance with the requirements of the turbulence model and the logarithmic wall function, the region in close proximity to the wall was discretized with prism layers as well as with pyramidal and tetrahedral elements. Near to the jet fans and in regions where high velocity and pressure gradients were predicted, a fine mesh with tetrahedral elements was chosen. Beyond this region, at nearly constant flow conditions, a coarser discretization with hexahedral elements was applied. For the numerical computation of the conservation equation a method with second order accuracy was selected.

In order to have the same flow conditions as those measured during the on-site tests and to evaluate the installation efficiency coefficient at different tunnel air velocities, an air velocity boundary condition was set for the inlet, as was a pressure boundary condition with a gauge pressure of 0 Pa for the outlet. The boundary condition for the jet fans was applied by using a fan model (pressure rise across the fan depending on the magnitude of the local air velocity normal to the fan) given in Fluent. This model was adjusted in order to obtain exactly the same jet fan thrust as recorded during the on-site measurements. The roughness of the tunnel wall was defined in relation to the measured friction coefficient. Details about the mode can be found in [7] and [14].

3.5. Results of On-site Measurements and Numerical Model Validation

Table 3 shows the results of the measurements with deflection blades for the jet fan niche N-05 in the Bosruck tunnel in the case of one (test M2) and two running jet fans (test M1), as well as for no deflection blades in the case of two running jet fans (M3). The measured pressure difference was evaluated according to eq. 4 and corresponds to the effective momentum transferred to the tunnel airflow Δp_{mt}. In the case of two active jet fans with deflection blades (test M1) a pressure rise of 74.0 Pa was recorded, whereas with no deflection blades, a pressure rise of 47.9 Pa (test M3) was recorded. This shows that the deflection blades have a considerable impact, increasing efficiency by more than 35%. On comparing the results for M1 and M2 it can be observed that the installation efficiency also depends on the number of active jet fans. The reason for this is the induced change in the flow pattern (an asymmetric flow around the jet fan niche results in additional vorticities and losses) and the fact that all the losses corresponding to the jet fan niche are attributed to only one jet fan instead of two. Compared to the static thrust given in Table 1 the measured thrust is up to 9% lower (represented by η_{op}) as a result of the shift in the jet fans's operation point.

Table 3: Result of the measurements in the Bosruck tunnel and the simulations

Jet fan niche		Jet fans		tunnel air velocity (m/s)	density (kg/m³)	Δp_{mt} (Pa)	F_{mt}* (N)	F_S (N)*		η (-)	η_{op} (-)
		SV-1005	SV-2005					SV-1005	SV-2005		
Results of measurements											
N-05	F	off	off	4.46	1.12	evaluation of the resistance coefficient					
	M1	on	on	1.46	1.12	74.00	1895	2522	2627	**76.6**	**97.2**
	M2	on	off	1.43	1.12	32.46	1662	2414	off	**71.7**	**91.3**
N-05 n.d.	M3	on	on	1.36	1.14	47.86	1225	2588	nm	**49.2**	**96.4**
Results of simulations											
N-05	S1	on	on	1.50	1.12	71.43	1829	2545	2518	**75.3**	**1.7%#**
	S1.1	on	on	2.00	1.12	69.22	1772	2534	2624	**72.6**	5.2%#
	S1.2	on	on	5.08	1.12	55.25	1415	2521	2612	**63.9**	16.6%#
N-05 n.d.	S3	on	on	1.36	1.14	47.04	1204	2465	2548	**48.0**	**2.4%#**

n.d. … no deflection blades; nm… not measured; *… corresponds to the measured density; M… measured; S… simulated; F… friction measurement; #... deviation between simulation and measurement

This lower value results from the restriction of the exit jet flow and also mainly depends on the number of jet fans running and on the installation configuration itself (niche, deflection blades, distance to the wall etc).

As can be seen, the efficiency coefficient η_{op} of two active jet fans with deflection blades is slightly higher than that of two active jet fans without deflection blades. This indicates that the interference of the jet flow due to the jet fan niche (niche with orthogonal front wall) is higher than that due to the deflection blades.

The tests served for the validation of the numerical model. The simulation set-up and evaluation was done on the basis of the measurements. The corresponding parameters are listed in Table 3. In the case of the two active jet fans with deflection blades (M1 and S1), the deviation between measurement and simulation concerning the installation efficiency coefficient is 1.7%. With no deflection blades the production of vorticity near the jet fan niche is higher and in general more difficult to predict in the numerical simulations. As a result, the deviation in this case (S3) is 2.4% and slightly higher compared to the simulation with deflection blades (S1). Nevertheless, the correlation between measured and modelled values was still found to be good. Concerning model validation, two more simulations with higher tunnel air velocities (2.00 m/s and 5.08 m/s) were performed. Based on these simulations, it was found that installation efficiency strongly depends on tunnel air velocity. This may be explained by the associated change in the flow pattern (see Figure 7). With increasing tunnel air velocity, the jet flow is attached to the wall for a longer distance (see Figure 7, middle picture). This produces more losses due to the increased region of high wall shear stress. As a consequence of this, the installation efficiency deteriorates (this is apart from the thrust reduction due to the difference between jet exit velocity and tunnel air velocity).

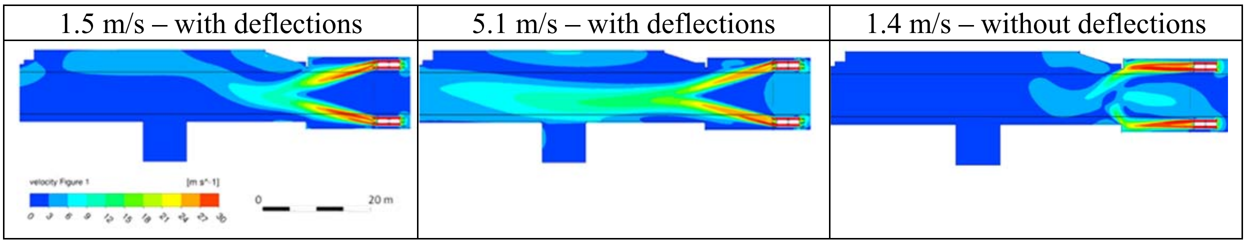

Figure 7: Top view of the velocity distribution for two active jet fans with deflection blades at a tunnel air velocity of 1.5 m/s (left) and of 5.1 m/s (middle), as well as for 1.4 m/s without deflection blades (right) – 3d simulation Bosruck tunnel.

Based on this finding, additional measurements in the Niklasdorf tunnel were performed in order to confirm the dependency of the installation efficiency on the tunnel air velocity. Moreover, the Niklasdorf tunnel measurements served to provide an additional sample of installation efficiency coefficients for jet fans which are not installed in a niche.

Table 4 represents the results of all measurements performed and the corresponding 3d-simulations. The values of the simulations were derived from the case study (see section 4) by interpolation and extrapolation with respect to the efficiency values for a tunnel air velocity of 1.0 m/s, 2.0 m/s and 3.0 m/s. The measurements reveal that the installation efficiency varies between 69.1% and 89.8% and strongly depends on the tunnel air velocity. Hence, these measurements corroborate the influence of the tunnel air velocity on installation efficiency. However, one needs to note that the influance of the effective thrust by the relative velocity between jet exit velocity and tunnel air velocity have already been considered in the derivation of installation efficiency (see eq. 3).

In addition, the installation efficiency also depends on the number of jet fans in operation and is in general better as the number of active fans increases.

Table 4: Result of the measurements in the Niklasdorftunnel and the performed simulations

	Jet fans		tunnel air velocity (m/s)	density (kg/m³)	Δp_{mt} (Pa)	F_{mt}* (N)	F_S (N)*		η (-)	η_{op} (-)
	SVS-4.1/4.2	SVS-5.1/5.2					SVS-4.1	SVS-4.2		
Results of measurements										
F	off	off	3.89	1.20	evaluation of the resistance coefficient					
M1	on	off	3.82	1.20	23.69	604	944	1088	**69.1**	**112.4**
M2	on	off	2.32	1.20	26.29	670	950	1041	**73.9**	**110.3**
M3	on	off	1.35	1.20	31.39	801	943	991	**87.8**	**107.3**
M4	on	on	3.08	1.20	49.15	627	941	1019	**72.4**	**108.6**
M5	on	on	1.91	1.20	56.61	722	940	1031	**79.2**	**109.2**
M6	on	on	0.88	1.20	62.85	801	892	970	**89.8**	**103.1**
Results of simulations										
S1	on	off	3.82	1.20	8.40	489	835	835	**69.2**	**2.2%#**
S2	on	off	2.32	1.20	9.92	577	835	835	**76.3**	**4.7%#**
S3	on	off	1.35	1.20	10.86	632	835	835	**80.1**	**6.2%#**
S4	on	on	3.08	1.20	9.14	532	835	835	**72.7**	**2.1%#**
S5	on	on	1.91	1.20	10.36	603	835	835	**78.2**	**0.3%#**
S6	on	on	0.88	1.20	11.31	658	835	835	**81.7**	**7.9%#**

*… corresponds to the measured density; #... deviation between simulation and measurment; M… measured; S… simulated; F… friction measurement;

In addition, the installation efficiency also depends on the number of jet fans in operation and is in general better as the number of active fans increases.

Evaluation of the measurements revealed that the measured thrust F_s of the jet fans increases with tunnel air velocity. An increase of the tunnel air velocity leads to a reduction of the entrance losses of the jet fans. This in turn leads to a 'positive' shift in the jet fan's operating point and enhances the thrust of the jet fan compared to its related static thrust by up to 4% (see F_s of SVS-4.2 in Table 4). The values η_{op} represents the differences between the static thrust and the measured thrust and also include the impact of construction tolerances.

These measurements were compared with the simulations obtained from the case study. The simulations were performed with the jet fan type JF835 (see Table 5) with a static thrust of 835 N. This value differs slightly from the measured thrust. Nevertheless, the values of the simulated installation efficiency coefficient correspond very well to those measured. The higher deviation at lower tunnel air velocities can be explained with respect to the accuracy of the velocity measurement device (see Table 2), the impact of which is stronger on low air velocities.

4. NUMERICAL CASE STUDY

4.1. Case descriptions

As the numerical model was validated by the actual measurements it proved possible to perform an extensive numerical case study in order to obtain a collection of installation efficiency coefficients for typical installation configurations [14]. For this purpose, a standard rectangular tunnel profile (2 lanes, cross section 57.5 m², hydraulic diameter 7.92 m) and a horseshoe tunnel profile (2 lanes, cross section 58.2 m², hydraulic diameter 7.41 m) as shown in Figure 8 were used. In combination with the horseshoe profile, two types of jet fan (JF2000 and JF835, see Table 5) with a single and paired arrangement for different tunnel air velocities, and various distances between tunnel wall and jet fan (a_v), as well as between the jet fans themselves ($x \cdot d_o$) were analysed. The installation efficiency was examined, for both arrangements (single and paired) and for all jet fan positions, in which the jet fans were located close to the tunnel wall, and with deflection blades for various deflection angels (α and β). The rectangular tunnel profile was analysed for one jet fan type (JF763, see Table 5) in a paired arrangement and for various distances horizontal (y_v) and vertical (a_v) with respect to the tunnel wall, as well as for different tunnel air velocities. In total, more than 170 different configurations (simulations) were examined within the scope of the case study. An overview of all cases, together with the evaluated installation efficiency coefficients can be found in section 6.

Table 5: Types of jet fans used for the numerical case study

Description	**d_o (m)**	**d_i (m)**	**u_s (m/s)**	**F_0 (N)**
JF2000	1.66	1.40	32.90	2000
JF835	1.40	1.20	24.80	835
JF763	0.88	0.71	40.07	763

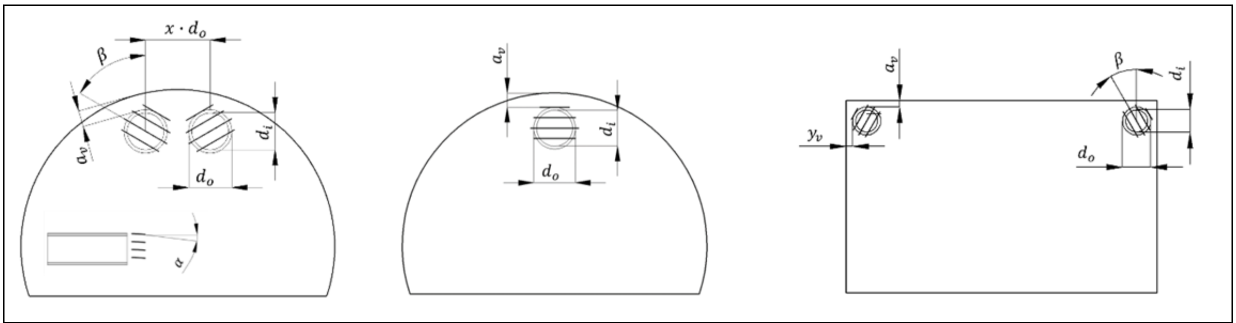

Figure 8: Geometrical configurations used for the numerical case study. Horseshoe tunnel profile with a paired jet fan arrangement (left) and a single jet fan arrangement (middle) both with deflection blades, and a rectangular tunnel profile with a paired jet fan arrangement in the corners and deflection blades (right).

4.2. Results and Findings

The calculated installation efficiency coefficients for all simulations performed are presented in tabular form in section 6. A separate table is provided for each configuration, and the respective efficiency coefficients are expressed in dependency of the tunnel air velocity and the distance to the wall. In the case of a configuration with deflection blades the dependency on the deflection angle is added.

Dependency of efficiency values on tunnel air velocity was confirmed by the measurements undertaken in the Niklasdorf tunnel. A similar relationship was also found in the simulations, regardless of the configuration analysed (e.g. paired or single jet fans, with or without deflection blades, horseshoe or rectangle profile, high or small distance to the wall). The reason for this is that a higher tunnel air velocity always causes an enlargement of the jet in the flow direction and thus induces higher wall friction. Moreover, a higher tunnel air velocity supports the Coanda effect and the jet remains attached to the tunnel surface for a longer period (see Figure 9).

A paired jet fan arrangement improves the installation efficiency especially for horseshoe profiles. The two jet flows band together in flow direction, so that the area with higher wall shear stress per jet fan is lower than for a single jet fan arrangement.

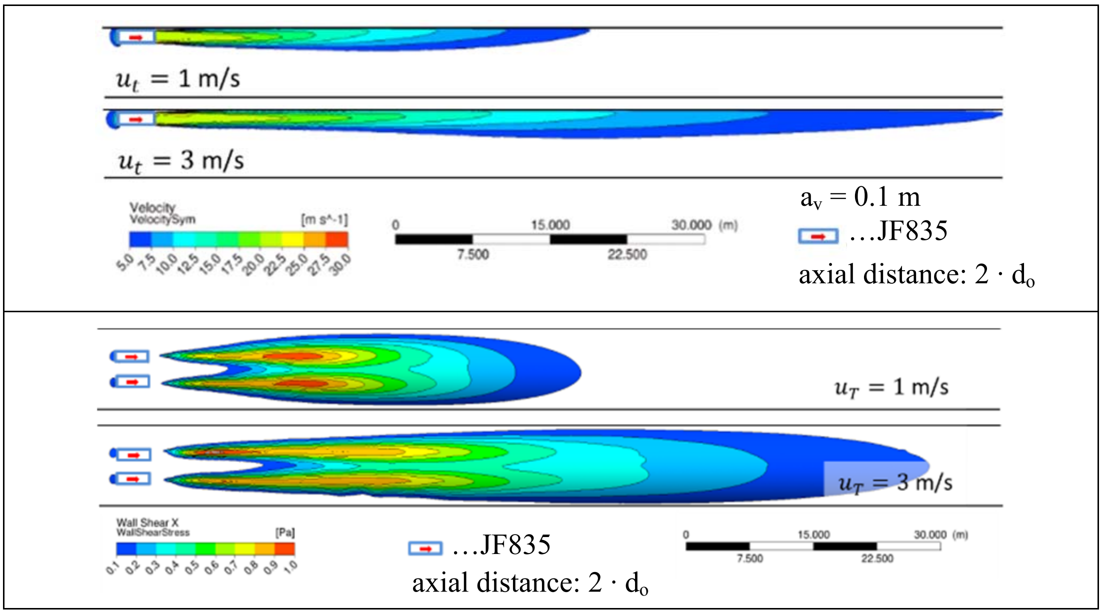

Figure 9: Velocity distribution (above) and distribution of the wall shear stress at the tunnel ceiling (below) for different tunnel air velocities – paired jet fan arrangement with an axial distance of $2 \cdot d_o$ and a distance between fan and tunnel wall of $a_v = 0.1$ m

In the case of a single jet fan arrangement (middle of the tunnel, ceiling) the impact of the tunnel wall on jet flow is greater due to the convex shape of the horseshoe tunnel profiles. On average this effect leads to a deterioration in the installation efficiency by 1.5% compared to that of a single jet fan arrangement in a rectangular tunnel profile [14].

It thus appears that the commonly used installation efficiency coefficients derived from Kempf [8] lead to an underestimation of the real losses caused by the momentum transfer and the high wall shear stress. Compared to the values obtained from the measurements and the simulations, these deviations can be up to 20%. Figure 10 shows the efficiency coefficient derived from Kempf [8] related to the values obtained from the 3d – simulation (configuration with one jet fan of the type JF835, without deflection blades in the horseshoe profile). For this illustration the simulation was evaluated as proposed by Kempf [8] and not according to eq. 3 or eq. 5 .

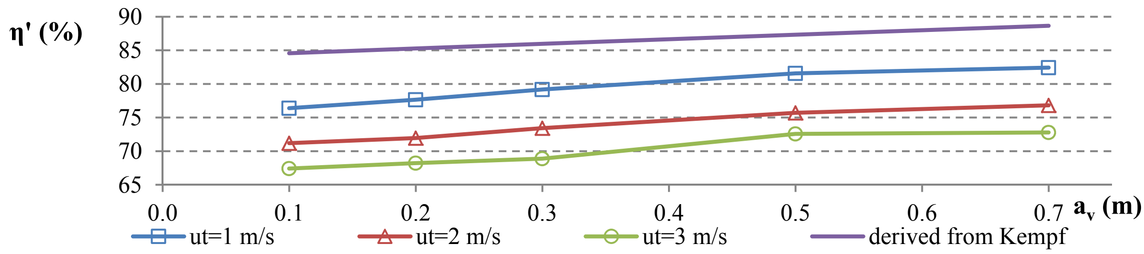

Figure 10: Installation efficiency coefficient as a function of the wall distance (a_v) derived from Kempf [8] compared with the values obtained from the 3d – simulations. Efficiency coefficient values η' are calculated as proposed by Kempf [8]

Irrespective of tunnel profile and distance to tunnel wall, bigger jet fan sizes in general improve the installation efficiency. In addition, it was observed that for a given jet fan size the installation efficiency improves in accordance with the increase in jet flow velocity. The relationship between the change in installation efficiency and the change in velocity is approximately linear. Amstrong [5] identified this relationship and presented the following velocity correction equation for a given jet fan size:

$$\Delta\eta = 2.2 \cdot (u_s - u_{s\_ref}) \cdot \frac{d_i}{d_t}$$ eq. 8 [5]

The validity of this equation was also confirmed by the simulations (see section 6). This relationship can be very useful where the installation efficiency for a given installation and jet velocity u_{s_ref} is known and needed for any other jet velocities u_s.

In addition, the results of the case study show, as expected, that the installation efficiency for all configurations analysed decreases as the jet fans approach the wall. This deterioration can be offset to some extent by the use of deflection blades. However, establishing the correct blade angle is essential in order to achieve an optimal effect. The best results were obtained in the case of tunnels with a rectangular profile and a paired jet fan arrangement installed at the outmost corners, with angles of $\beta = 60°$ and $\alpha = 19°$. This led to an improvement in installation efficiency by up to 20 %. For horseshoe tunnel profiles and a single jet fan arrangement an improvement of 8 % (optimum angle $\alpha = 7°$), and for paired jet fan arrangements of 5 % (optimum angle $\alpha = 10°$ and $\beta = 120°$) were also attained.

Analysis also revealed that varying the distance between the fan axles ($x \cdot d_o$) had no impact on installation efficiency for distances between 1.3 and $4.0 \cdot d_o$. However, a distance less than $1.3 \cdot d_o$ is not to be recommended since in addition to the adverse effect on the installation efficiency this may also lead to problems due to lack of air at the suction side of the jet fan during operation.

5. REFERENCES

[1] Zhou X., Sun Z., Durst F., Brenner G.: Numerical Simulation of Turbulent Jet Flow and Combustion. In “Pergamon. Computers and Mathematics.” Vol. 38, 1999, pp 179-191.

[2] Rohne E.: The Friction Losses on Walls Caused by the Jet Flows of Booster Fans. In “Aerodynamics and Ventilation of Vehicle Tunnels”, 3rd International Symposium, BHR Group, 1979, pp 57-70.

[3] Rohne E.: The Friction Losses on Walls Caused by a Row of Four Parallel Jet Flows. In “Aerodynamics and Ventilation of Vehicle Tunnels”, 6th International Symposium, BHR Group, 1988, pp 151-164.

[4] Rohne E.: Friction Losses of a Single Jet Due to its Contact with Vaulted Ceiling. In “Aerodynamics and Ventilation of Vehicle Tunnels”, 7th International Symposium, BHR Group, 1991, pp 679-687.

[5] Armstrong J., Bennett E.C., Matthews R.D.: Three-Dimensional Flows in a Circular Section Tunnel Due to Jet Fans. In “Aerodynamics and Ventilation of Vehicle Tunnels”, 8th International Symposium, BHR Group, 1994, pp 743-756.

[6] Bardina J.E., Huang P.G., Coakley T.J.: Turbulence Modeling Validation, Testing and Development. NASA Ames Research Center, 1997.

[7] Galehr J.: Effektivität der Schubeinbringung durch Strahlventilatoren in Tunneln. Diplomarbeit. Technische Universität Graz, 2012.

[8] Kempf J.: Einfluss der Wandeffekte auf die Treibstrahlwirkung eines Strahlgebläses. Ein Beitrag zur Aerodynamik der Tunnellüftung. In „Schweizerische Bauzeitung“, Vol. 4, 1965, Zürich, pp 47-52.

[9] Meidinger U.: Längslüftung von Autotunneln mit Strahlgebläse. In „Schweizerische Bauzeitung“, Vol. 28, 1964, Zürich, pp 498-501.

[10] Rohne E.: Über die Längslüftung von Autotunneln mit Strahlventilatoren. In „Schweizerische Bauzeitung“, Vol. 48, 1964, Zürich, pp 840-844.

[11] Betta V., Cascetta F., Musto M., Rotondo G.: Numerical Study of the Optimization of the Pitch Angle of an Alternative Jet Fan in a Longitudinal Tunnel Ventilation System. In ”Tunneling and Underground Space Technology”, Vol. 24, 2009, pp 164-172.

[12] Sturm P., Beyer M., Mehdi R.: On the Problem of Ventilation Control in Case of a Tunnel Fire Event. In ”Case Studies in Fire Safety”, 2015, pp 1-8.

[13] Tarada F., Brandt R.: Impulse Ventilation for Tunnels – A State of the Art Review. In “Aerodynamics and Ventilation of Vehicle Tunnels”, 13th International Symposium, BHR Group, 2009.

[14] Saurwein M.: Beurteilung der Effektivität der Schubeinbringung durch Strahlgebläse in Tunneln mit Hilfe numerischer Modelle und Messungen. Masterarbeit. Technische Universität Graz, 2014

[15] Sturm P., Beyer M., Bacher M., Schmölzer G.: The influence of pressure gradients on ventilation design – special focus on upgrading long tunnels, Proceedings of the 6th Symposiumon Tunnel Safety and Ventilation, Graz, Austria, 23–25 April, 2012, pp. 90–99 ISBN:978-3-85125-210-1.

[16] Bacher M., Sturm P.: Upgrading Existing Road Tunnels in the TERN to Current Needs, Taking the Arlbergtunnel as an example, Proceedings of the 7th Symposium Tunnel Safety and Ventilation, Graz, Austria, 12-13 May, 2014, pp. 28-37.

[17] Truckenbrodt E.:, Fluidmechanik, Band 1: Grundlagen und elementare Strömungsvorgänge dichtebeständiger Fluide, 4. Auflage 1996, Nachdruck in veränderter Ausstattung, Leipzig, 2008, Springer-Verlage, ISBN 978-3-540-79017-4.

[18] FVTmbH, Beyer, M.: Vermessung der Schubeinbringung der Strahlventilatoren im Bosrucktunnel – Neubauröhre, Version 3, Graz am 18.10.2013, Dokument-Nr.:FVT-47/13/BE V&U 2008/33/6400 V3.0.

[19] T.-H. Shih, W. W. Liou, A. Shabbir, Z. Yang, and J. Zhu. A New k-Eddy-Viscosity Model for High Reynolds Number Turbulent Flows - Model Development and Validation. Computers Fluids, 24(3):227{238, 1995.

6. APPENDIX – INSTALLATION EFFICIENCY COEFFICIENTS

Table 6: Installation efficiency ceofficients of a horseshoe tunnel profile with a paired jet fan arrangement

	JF835			JF2000		
	$1.3 \cdot d_o$ - $4.0 \cdot d_o$					
	u_t (m/s)					
a_v (m)	1.0	2.0	3.0	1.0	2.0	3.0
0.1	*81*	*77*	*73*	*82*	*81*	*78*
0.2	*81*	*78*	*73*	*82*	*82*	*78*
0.4	*82*	*80*	*76*	*83*	*82*	*81*
0.7	*84*	*81*	*76*	*85*	*84*	*81*

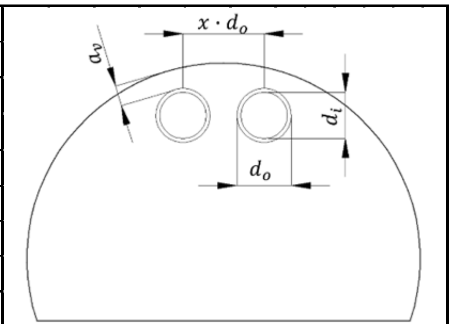

	JF835								
	$1.0 \cdot d_o$			$1.5 \cdot d_o$			$2.0 \cdot d_o$		
	u_t (m/s)								
a_v (m)	1.0	2.0	3.0	1.0	2.0	3.0	1.0	2.0	3.0
0.1	*77*	*72*	*68*	*81*	*77*	*73*	*81*	*77*	*72*
0.2	-	-	-	*81*	*78*	*73*	-	-	-
0.4	*82*	*79*	*76*	*83*	*80*	*76*	*83*	*81*	*76*
0.7	*85*	*81*	*76*	*84*	*81*	*76*	*84*	*81*	*77*

Table 7: Installation efficiency ceofficients of a horseshoe and a rectangular tunnel profile with a single jet fan arrangement

	JF835			JF2000		
	single arrangement					
	u_t (m/s)					
a_v (m)	1.0	2.0	3.0	1.0	2.0	3.0
0.1	*77*	*72*	*68*	*81*	*78*	*75*
0.2	*78*	*73*	*69*	*82*	*79*	*75*
0.3	*80*	*74*	*69*	*83*	*81*	*77*
0.5	*82*	*76*	*73*	*83*	*81*	*78*
0.7	*83*	*78*	*74*	*86*	*83*	*80*

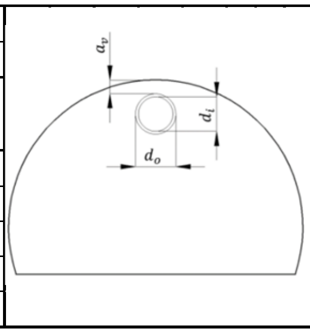

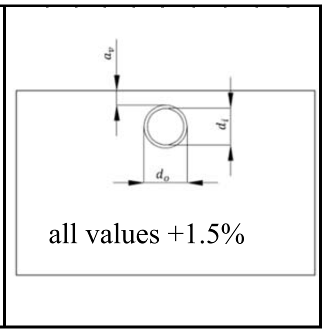

Table 8: Installation efficiency ceofficients of a horseshoe tunnel profile with a paired jet fan arrangement and deflection blades

			JF835	
			1.0 · d_o	
a_v	α	β	u_t (m/s)	
(m)	(°)	(°)	2.0	3.0
0.1	X	X	*77*	*73*
0.1	15.8	90	-	*72*
0.1	10.0	90	*81*	*79*
0.1	10.0	60	*81*	*78*
0.1	10.0	120	*82*	*78*
0.2	X	X	*82*	*79*
0.2	10.0	90	*81*	*73*
0.2	10.0	60	*80*	*79*
0.2	10.0	120	*82*	*79*

X… without deflection blades

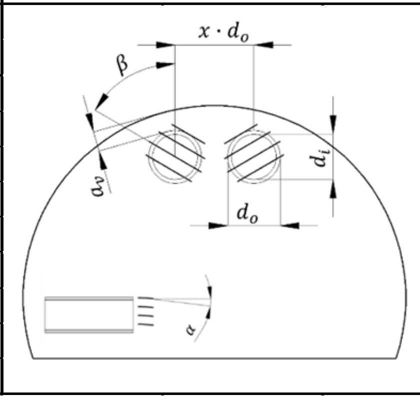

			JF2000	
			1.0 · d_o	
a_v	α	β	u_t (m/s)	
(m)	(°)	(°)	2.0	3.0
0.1	X	X	*81*	*78*
0.1	15.8	90	-	*78*
0.1	10.0	90	*82*	*81*
0.1	10.0	60	*81*	*83*
0.1	10.0	120	*84*	*83*
0.2	X	X	*81*	*79*
0.2	10.0	90	*83*	*81*
0.2	10.0	60	*82*	*80*
0.2	10.0	120	*84*	*81*
0.1	7.0	90	*81*	*82*
0.1	7.0	60	*77*	*78*
0.1	7.0	120	*82*	*80*

Table 9: Installation efficiency ceofficients of a horseshoe tunnel profile with a single jet fan arrangement and deflection blades

		JF835		JF2000	
		single arrangement			
		u_t (m/s)			
a_v (m)	α (°)	2.0	3.0	2.0	3.0
0.1	X	*72*	*68*	*78*	*75*
0.1	10.0	*80*	*74*	-	-
0.1	7.0	*81*	*79*	*83*	*81*

X… without deflection blades

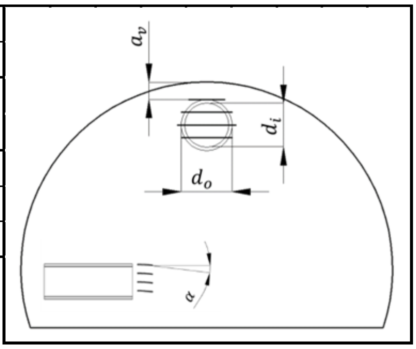

Table 10: Installation efficiency ceofficients of a rectangular tunnel profile with a paired jet fan arrangement with and without deflection blades

		JF763	
		u_t (m/s)	
y_v (m)	a_v (m)	2.0	3.0
0.1	0.1	*61*	*57*
0.1	0.2	*62*	*58*
0.1	0.3	*64*	*60*
0.1	0.5	*67*	*62*
0.2	0.1	*63*	*59*
0.2	0.2	*64*	*60*
0.2	0.3	*66*	*61*
0.2	0.5	*68*	*63*
0.3	0.1	*64*	*60*
0.3	0.2	*66*	*61*
0.3	0.3	*67*	*62*
0.3	0.5	*69*	*65*
0.5	0.1	*66*	*62*
0.5	0.2	*67*	*63*
0.5	0.3	*68*	*64*
0.5	0.5	*71*	*66*
1	0.1	*71*	*67*
2	0.1	*76*	*71*
3	0.1	*77*	*72*
2	0.2	*77*	*71*
2	0.5	*81*	*76*
2	0.7	*84*	*79*

				JF763	
				u_t (m/s)	
y_v (m)	a_v (m)	β (°)	α (°)	2.0	3.0
0.1	0.1	X	X	*61*	*57*
0.1	0.1	0.0	19.0	*75*	*72*
0.1	0.1	0.0	14.0	*74*	*72*
0.1	0.1	45.0	19.0	*80*	*78*
0.1	0.1	60.0	19.0	*81*	*79*
0.1	0.1	30.0	19.0	*68*	*64*

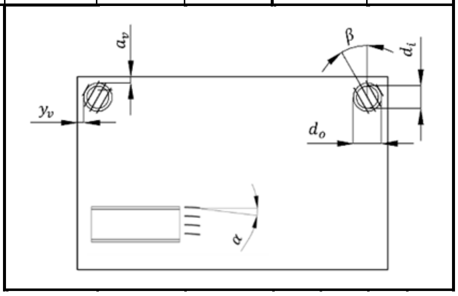

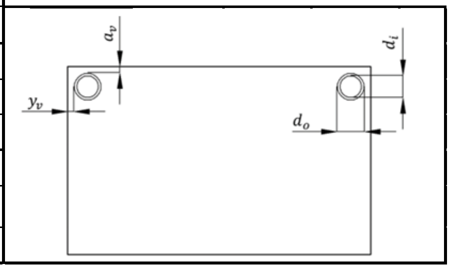

X… without deflection blades

COMISSIONING OF THE VENTILATION CONTROL OF THE E4 STOCKHOLM BYPASS

R. Brandt; HBI Haerter, CH
L. ELERTSON; Swedish Transport Administration, S

ABSTRACT

56 km of tunnel tubes compose the road tunnel E4 Stockholm Bypass. The main line is 17 km long and the twelve connecting ramps have lengths of up to about 2 km.

Frequent traffic congestion of the 140 000 vehicles daily cannot be excluded. Considering, the very onerous air-quality criteria, longitudinal ventilation of such a network is a challenge. Air-quality requirements have to be met in the tunnel and for the portals at minimum energy consumption. It is not trivial to decide using the fresh-air stations or to take in the not entirely fresh air via the entry ramps.

In case of fire, active ventilation control based on measurements of flow velocities is being used. Detailed descriptions of the control principles including data treatment and system-selection priorities have been elaborated. Equipment failures are catered for and plausibility tests of the flow-velocity measurements carried out.

In the tunnel-ventilation simulations, the control procedures are mimicked. In this manner, all possible as well as less realistic scenarios have been simulated in order to test the robustness of the ventilation-control routines.

For test purposes and the commissioning (FAT and SAT), a tunnel-ventilation simulator is being developed that links the genuine tunnel-ventilation controller (soft- and hardware) with the simulation tool. In this simulation mode, the tunnel-ventilation simulator receives the fan settings from the external control program and computes the resulting values of flow speed, air quality, temperatures etc.

Keywords: ventilation control, commissioning, tunnel-ventilation simulator

1. INTRODUCTION

1.1. E4 Stockholm Bypass

56 km of tunnel tubes compose the road tunnel E4 Stockholm Bypass, see overview in Figure 1. The main line is 17 km long and the twelve connecting ramps have lengths up to about 2 km. As traffic congestion of the daily 140 000 vehicles cannot be excluded, a fixed fire-fighting system (FFFS) will be installed.

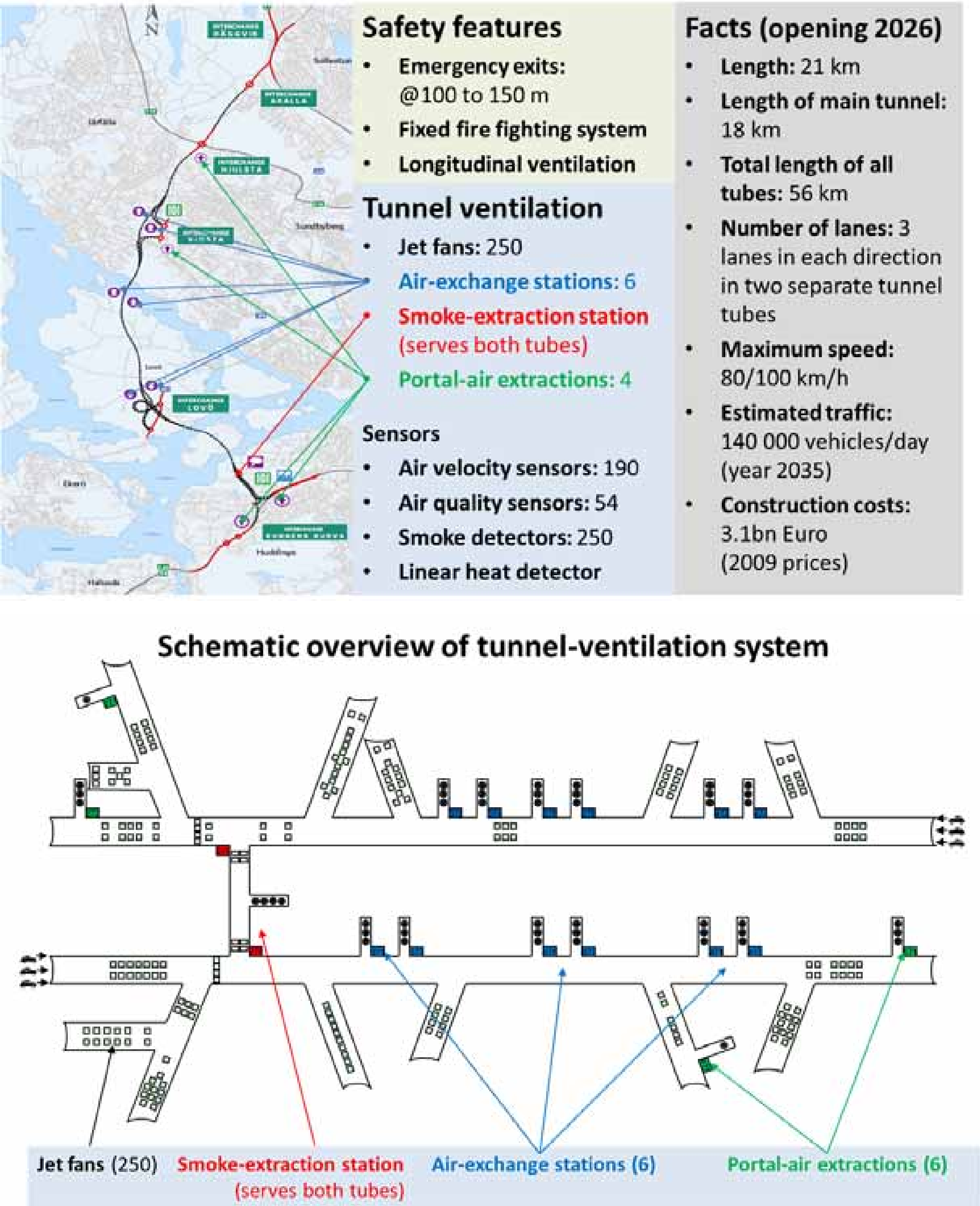

Figure 1: Overview of E4 Stockholm Bypass

1.2. Ventilation system

The longitudinal ventilation system encompasses 250 jet fans operated by frequency converters enabling them to give full thrust in both directions. Moreover, 48 identical axial fans each with a nominal flow rate of 200 m^3/s are being installed.

As shown for the northbound tube in the schematic below (Figure 2), each main line has three air-exchange stations each with a capacity to extract 600 m^3/s of vitiated air and subsequently to supply the same amount of fresh air. The fans in the fresh-air stations can be reversed to be used for smoke extraction.

Moreover in order to reduce the length with smoke in case of fire, a smoke extraction station that has a fourth redundant fan is envisaged. This is the only ventilation station that serves both main-line tunnels. The design smoke-extraction capacity is 600 m^3/s.

Four of the exit portals have portal-air extractions with the purpose to be able to minimise the impact of vitiated tunnel air on the environment.

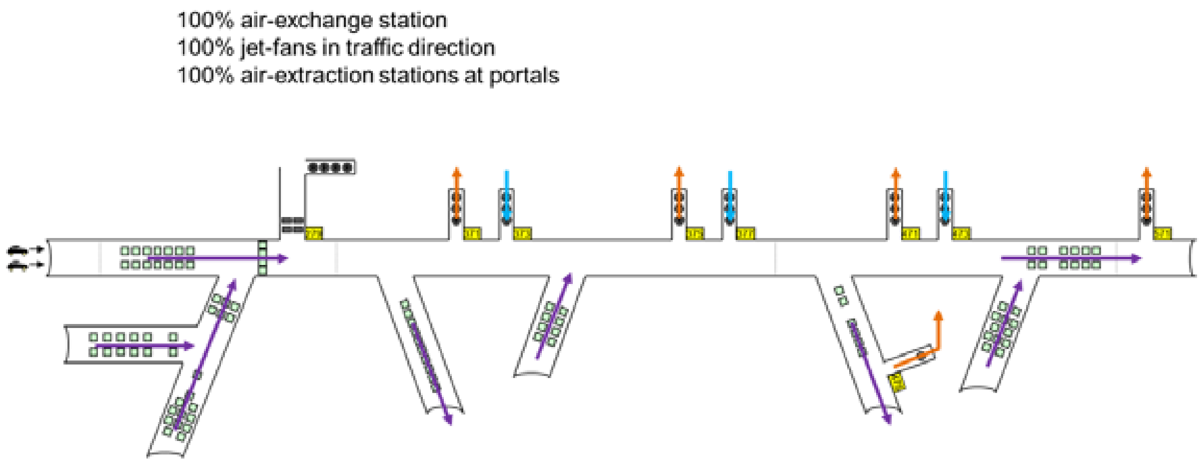

Figure 2: Northbound tube: maximum ventilation mode during normal operation

The in-tunnel air quality is monitored by 54 air-quality sensors that are placed on strategically important locations though maximum 1 km apart. Each sensor measures visibility as well as concentrations of NOx and CO.

In particular for the active control of the longitudinal flow in case of fire, the 62 positions with anemometers are of paramount importance. Consequently, they are tripled in order to enable automatic plausibility checks. Fire detection is conducted with linear heat sensors and smoke detectors.

Brandt et al. [4] offer a more elaborate description of the ventilation system and its control.

2. NORMAL VENTILATION

2.1. Internal air-quality challenges

Considering, the very onerous air-quality criteria, longitudinal ventilation of such a network is a challenge. Air-quality requirements have to be met in the tunnel and for the portals at minimum energy consumption. It is not trivial to decide between using the fresh-air stations or to take in the not entirely fresh air via the entry ramps.

2.2. Controller principle for internal air quality

It was found that a step-wise controller would be the most appropriate control principle as this is robust and yet flexible.

The tunnel is divided into logical ventilation technical sections (VTS). For the ventilation during normal operation, the VTS are combined to larger normal operation sections (NOS). Each NOS has at least one triple air-quality sensor and ventilation equipment assigned to it. The same ventilation equipment can be assigned to several NOS with the priorities of their usage depending on the specific section NOS.

Each ramp and each portal-air extraction has its own sub-controller, see Figure 3. The input comes from the air-quality and air-flow sensors. In total, the main controller of the northbound tunnel consists of 11 sub-controllers.

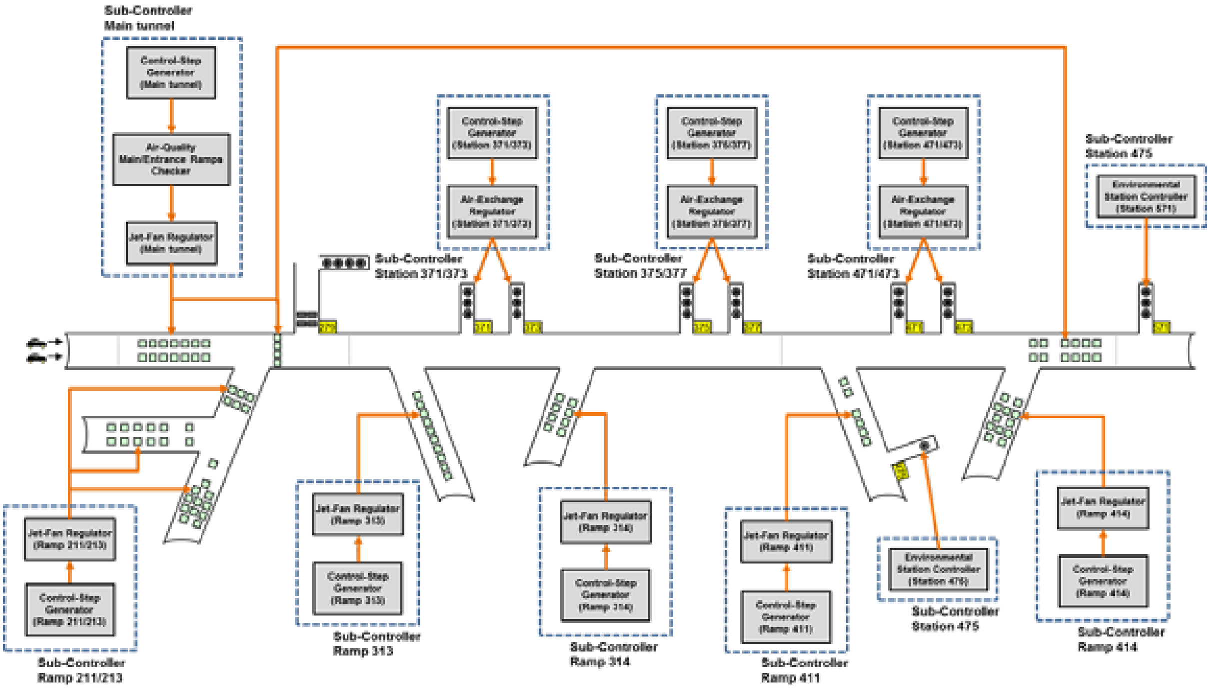

Figure 3: Overview of controllers for normal operation

Each sub-controller reacts and works independently of other sub-controllers and has its unique Control-Step Generator (CSG). The consequence of this is that for certain ventilation equipment, different steps i.e. different ventilation capacities could be required. The dilemma is that different sensors could give diverging instructions to the same actuators (fans). In order to resolve this, it was decided to assign the control to the sensors with the highest value. The combinations of sub-controllers may also result in conflicts that therefore have been identified and rules for their resolution defined.

In the main tunnel, the controller automatically assesses whether it is best to improve the air quality by increasing the flow rate or by using air from the ramp.

For a simple tunnel, it can be ensured that the step-wise controller provides maximum ventilation capacity when the highest control step is engaged. Due to the interdependencies, this is somewhat more complex in this type of configuration. Consequently, in case a control step higher than the maximum would be desired, the maximum ventilation capacity is engaged for the main line and all connecting ramps, as shown in Figure 2. In this manner, the risk of undesired tunnel closure caused by too bad in-tunnel air quality is minimised.

2.3. Minimising impact on ambient air

As a result of the analysis of the impact on the environment (Swedish MKB: Miljökonsekvensbeskrivning), vitiated tunnel air can be extracted at four exit portals. Here, the strategy is at most to extract the air that flows towards the portal-air extraction. In fact, only a certain pre-set fraction of the flow approaching the air-extraction station is being extracted. Moreover, measurements of the air quality outside the portal are used to assess whether or not it is worthwhile extracting the vitiated tunnel air at all.

3. SMOKE MANAGEMENT

In case of fire, the smoke is always ventilated in direction of traffic and extracted at the first possible downstream location. If this station is out of order, the subsequent one is engaged.

Due to the different objectives compared to normal operation, smoke management sections called SMS have been defined. Except for the first SMS at the entry sections of the tunnel, all boundaries line up with those of the ventilation technical sections (VTS). In case of fire in the main line, following principles are applied:

- the smoke is always extracted from a ventilation station or blown out of the exit portal i.e. smoke management of the main tunnel is never occurring over a ramp.
- All non-incident ramps protect themselves by having a controlled flow velocity of 1 m/s towards the main tunnel.

An example of the smoke management is shown in Figure 4. A longitudinal flow velocity of 3 m/s in direction of traffic is specified. The smoke is extracted at the smoke-extraction. All ramps have their own control lops ensuring a velocity of 1 m/s towards the main line.

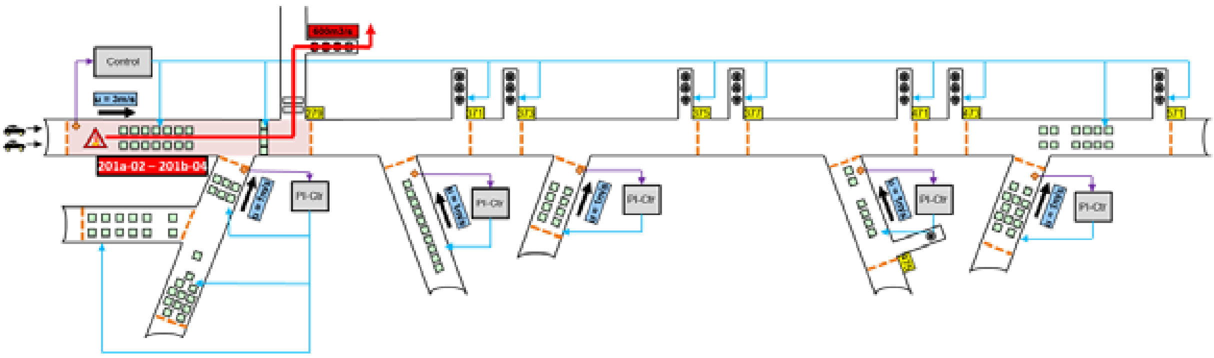

Figure 4: Example of smoke management control loops for sector

Similarly, in case of fire in a ramp, smoke is always blown in direction of traffic and extracted at the first possible extraction point respectively blown out of an exit portal. The other ramps and connecting sections of the main tunnel protect themselves by ensuring a velocity of 1 m/s.

Automatic plausibility checks of the quality of the flow velocity measurements by the anemometers are being carried out using logical rules. If the flow measurements are judged of inadequate quality, the second set of anemometers is selected; and if they are also judged to be of inadequate quality, the velocity is calculated based on the measurements in the other tunnel sections and the air-extraction rates.

In case of fire, one of the following ventilation programs is automatically selected

- Standard Fire Ventilation with an air velocity of approx. 3 m/s
- Minimal Fire Ventilation with an air velocity of approx. 1.5 m/s; which is automatically selected, if the FFFS does not function and there is congested traffic.

The set points of the flow velocities are parameters used in the active control loops and if at a later stage other values are preferred, these can easily be changed by an authorised person.

The operator, typically on request by the fire brigade, can also select following programs:

- Forced Fire Ventilation i.e. maximum possible air velocity
- Adjustable Fire Ventilation: initially freezing all control settings and then manually changing set points of velocities or operating individual fans.

It is essential to engage the ventilation system quickly in case of fire. Therefore, the fire ventilation plan is initiated already in case of a pre-alarm. The tunnel portals are not closed to traffic at pre-alarm and evacuation is not initiated. Pre-alarm can be detected by a smoke detector or the linear heat detector and can be selected by the operator. If subsequently an alarm is raised, the fire zone corresponding to the alarm is applied and the full emergency plan including tunnel closures and evacuation is engaged.

4. SIMULATION TOOL: IDA RTV

4.1. Introduction

The design of the tunnel-ventilation system and the testing of the control routines were carried out using the software Road Tunnel Ventilation (IDA RTV) from the company EQUA (www.equa.se). This one-dimensional instationary flow simulation program also enables specifying control loops using logical libraries. It has therefore been possible to test all possible scenarios varying e.g. traffic, external winds and temperatures as well as the heat-release rate of fires. Moreover, system failures can be mimicked.

4.2. Tunnel simulator

The IDA RTV program will be at disposition for the contractor that is awarded the contract to build the tunnel-ventilation control system.

The contractor will be requested to interface the IDA RTV model with his software-development environment in order to be able to conduct software factory tests. Here, the IDA RTV program will mimic the responses from the tunnel such as flow velocities and air qualities (i.e. the sensors) but also the actuators (i.e. the fans), see Figure 5.

Example: Application logic orders a jet fan to start, orders are sent to the simulator. The simulator calculates, with the aid of a mathematical model, the airflow in the tunnel which also has effect on the traffic flow. The simulated air flow gives the response caused by the jet fan that is sent back to the application logic from the simulator.

The tunnel-ventilation system is very complex and extensive. The client and the contractor need reasonable time to try to cover all requirements in the appropriate software. To minimize the risks to tunnel ventilations, logic errors and/or problems detected until the SAT (Site Acceptance Test), a tunnel simulator is used as a testing tool during the FAT (Factory Acceptance Test).

This, however, only verifies that the software of the control system functions as planned. Site testing (SAT) will finally be conducted in order to confirm that the control of the tunnel-ventilation system fulfils the design objectives.

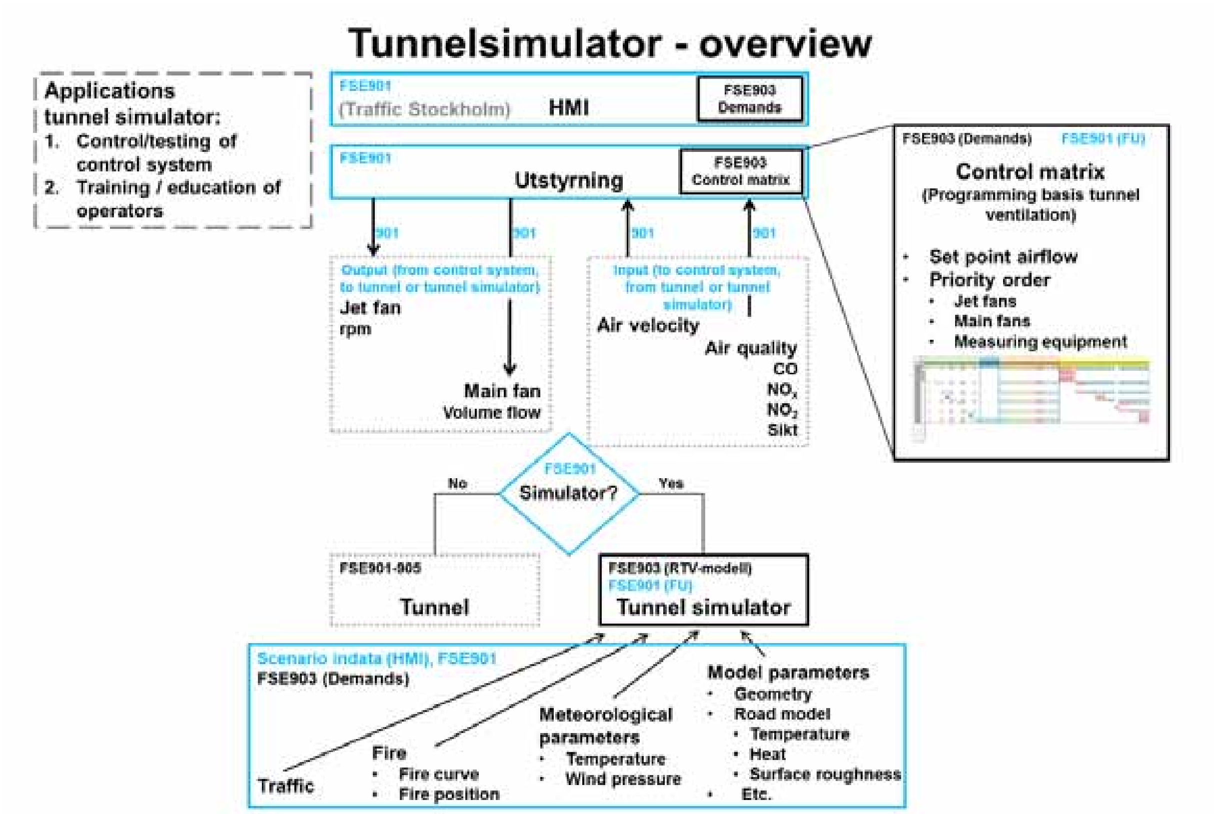

Figure 5: Overview of tunnel simulator

4.3. Work process for the contractor

The contractor shall implement the IDA RTV model (without the IDA RTV control routines) to produce a real-time tunnel simulator, which can handle IDA RTV files. The tunnel simulator will mimic the tunnel and its sensors physical response to the same accuracy as the simulator in IDA RTV.

The contractor shall then implement all control functions in a hardware solution (PLC), which is the real control system with its software solution called Real-time Tunnel Simulator. The Real-time Tunnel Simulator is then linked to the Model Tunnel Simulator.

From the HMI, authorized users can view the current status for all variables and parameters that have an impact on the simulation. Also from the HMI, it shall be possible from authorised personnel to edit all variables and parameters that have an impact on the simulation.

This system of tunnel simulator, documentation, courseware and other support functions allows for useful operator training. The approved version of the control system and the final version of the tunnel simulator will be implemented in an operation simulator.

The additional effort required for the tunnel simulator lies in the development of the interface between the dynamic software model of the tunnel and the PLC. Often, the implementation of this interface can be based on the Open Process Control (OPC) standard. This reduces the need for manufacturer-dependent coding. The interface of IDA-RTV has to manage the time step of the numerical model and alarms. For instance, the simulation model lags too far behind physical time. The numerical model sometimes has to negotiate system discontinuities using elaborate and time consuming methods, so that exceptions may occur even if the average progress of the simulation model is considerably faster than real time.

Further details of the testing of the tunnel-ventilation control system and its development is described in Elertson [1].

5. CONCLUSION

The E4 Bypass Stockholm is a large road tunnel complex with in total 56 km of tunnel tubes. The main line is 17 km long and has several entry and exit ramps. The longitudinal ventilation of such a long and complex tunnel is a challenge for normal and smoke management operation.

For normal operation, a step controller was developed that is composed of several sub-controllers. A methodology has been found to select the determining air-quality sensors. Although several sub-controllers rely on the same fans (actuators), a method to resolve potential control conflicts ensuring adequate ventilation in all tunnel sections has been found.

The longitudinal smoke management uses closed loop feedback to reach the specified flow velocity. Based on a priority system, alternative sensors (anemometers) as well as actuators (fans) are automatically engaged if required

During the FAT, the contractor verifies the tunnel-ventilation simulator for his own benefit and ensures for the client that the implemented functions in the control system for the tunnel ventilation meets the requirements in the contract. In this way, application logic for tunnel ventilation is tested cost-effectively in an office environment. Doing this, systems, design errors, discrepancies and risks of application logic can be identified and corrected before the SAT begins.

In previous tunnel projects, the time for testing tunnel ventilation has been shortened because of pressure to open early considering the economic advantages for the public. We have concluded that the money invested on a simulator is well worth in order to reduce time and to ensure quality. In a global context, our goal is to act in a smart manner.

BE SMART = Be Exceptional - Save Money And Reduce Time

6. REFERENCES

[1] Elertson, L. Swedish Transport Administration, Ventilation simulation of a large and complex Road Tunnel, A safe journey - E4 The Stockholm bypass Project, 16th International Symposium on 'Aerodynamics and Ventilation of Vehicle Tunnels', Seattle, USA, 15-17 September 2015

[2] Nakahori, I.; Ato, T.; Murakami K.; Araki, D; Kanatani, T.; Vardy, A. The use of inverter-driven jet fans to reduce tunnel ventilation costs, BHR, 13th International Symposium on Aerodynamics and Ventilation of Vehicle Tunnels, New Brunswick (USA), 13 -15 May 2009, Edited by Ian Sweetland, ISBN: 978 1 85598 107 2

[3] Contracts for the Installation of Mechanical and Electrical Systems, E4 The Stockholm Bypass, Trafikverket, Swedish Transport Administration, 100661, November 2013, www.trafikverket.se

[4] Brandt, R; Engman, E.; Lucchini, S. Elertson, L.; Berg, C. Malmros, U. Ventilation of the E4 Stockholm Bypass, 16th International Symposium on 'Aerodynamics and Ventilation of Vehicle Tunnels', Seattle, USA, 15-17 September 2015

COMPLEX COMMISSIONING AND QUANTITATIVE TESTING OF THE GOTTHARD BASE TUNNEL VENTILATION SYSTEM

M. Viertel, Ch. Brander, J. Badde, M. Poloni
Pöyry Switzerland Ltd., Switzerland

ABSTRACT

The new Gotthard Base Tunnel will be opened to train traffic mid-2016. As part of the ventilation concept proofing and thermodynamic tunnel system modelling, as well as the commissioning process of the system, an ongoing series of measurement campaigns was carried out within the course of 3 years.

These commissioning and measurement campaigns include initial start-up of the fans, combined functional tests, leakage and airflow measurements as well as pressure measurements. These tests were carried out for various types of structures within the tunnel. The aim was to provide the proof or validate the assumptions made in the concept phase which are crucial for the dimensioning of the ventilation system and surrounding structures.

The focus in this publication is placed on leakage measurements in exhaust ducts as these tests require the combination of low error volume flow measurements in ducts, CFD analysis as well as data modelling to produce plausible results.

Following the different phases of the commissioning of the ventilation system, the applied measurement concepts and strategies, results and lessons learned within the multidisciplinary field of fluiddynamic, thermodynamic and process control validation testing are discussed.

Keywords: *ventilation design, commissioning, measurement approach, volume flow measurement in ducts, leakage measurement*

1. INTRODUCTION

The Gotthard Base Tunnel (GBT) is the longest railway tunnel in the world and is soon to be opened (June 2016). Before opening the general operation approval has to be given by the FOT (Federal Office of Transport). Part of the approval process are the tests involving all the components and interfaces of the ventilation system.

The commissioning and testing of the ventilation system consists of several phases. The following phases are discussed in this paper:

- Commissioning stages such as
  - Factory acceptance tests before installation
  - Initial start-up of the ventilation system
  - Combined functional tests
- Measurement and validation of climate and ventilation goals

The goal of this paper is to give an overview of measurement and proofing concepts and strategies, results and lessons learned within the broad field of commissioning and testing this system. An especially challenging and innovative concept of the leakage measurements in exhaust ducts during the first start-up of the Faido ventilation station is presented in detail in the case study below.

2. THE GBT VENTILATION SYSTEM

The ventilation system of the GBT consists mainly of the following parts:

- Underground ventilation central Sedrun with two fresh air fans (1.5 MW each) and two exhaust fans (2.4 MW each). Each axial fan has a diameter of 2.8 m. Every fan's speed blade angle is controllable
- Aboveground ventilation central Faido (analog to the station in Sedrun)
- 28 smoke extraction vents with ventilation dampers (4.3 x 5 m)
- 12 jet fans at the portal Erstfeld and 12 jet fans at the portal Bodio
- An array of sensors in the tunnel tubes and in the emergency stations

3. COMMISSIONING STAGES OF THE GOTTHARD BASE TUNNEL VENTILATION SYSTEM

The commissioning and testing of the Gotthard Base Tunnel ventilation system was a challenging task especially due to the large distance between the ventilation stations and the other components of the ventilation system. The ventilation station Faido is located above ground and connected to the tunnel with a 2.7 km long access gallery, sucking and blowing air through dampers located near the tunnel itself. The Sedrun ventilation station is located in an underground cavern, connected by two 800 m deep vertical shafts to the tunnel. The jet fans, also part of the ventilation system, are located at the portals of the tunnel. In total the different components and stations spread over the entirety of the 56 km tunnel, and are connected over hundreds of kilometers of cables.

Furthermore, during all the ventilation tests, construction and commissioning work was carried out throughout the tunnel. To provide sufficient ventilation and cooling of the construction site, the temporary ventilation system was still active and had to be deactivated for the test phases of the permanent ventilation. When testing operation points of the fans all air ways blocked by the temporary ventilation system and extra leakages had to be accounted for.

Several electromechanical components are not functionally associated with the ventilation system, but are essential to the functioning of the ventilation system. For example, the doors to the emergency stations serve as air dampers for the ventilation of both station and tunnel. The doors and gates, the elevator in the vertical shaft in Sedrun, the HVAC ventilation systems of the underground facilities and the cross sections and the energy supply system have their own master controller which communicates via cross-connections with the master controller of the ventilation system. These systems have to be controlled remotely by the ventilation system master or at least monitored to ensure the proper functioning of the ventilation as a whole.

The above mentioned challenges made the commissioning and validation testing especially demanding and thematically broad. The general approach to testing and validation of technical components and systems, or better the measurement of the underlying physical processes, is a feedback loop. It starts with the modelling of the system and the establishment of the measurement goals. Once these have been sought out, different measurement concepts are weighed up against each other. The heaviest weighting in commercial testing is typically placed on feasibility, cost and expected measurement error. Especially cost and achievable measurement precision are somewhat in stark contrast.

After the measurement concept has been established, sensors and data acquisition units are put in place and the data can be sampled. Most of the time, then, since the sought after quantity cannot be measured directly, the data has to be analyzed, filtered and fit to a previously derived model. Fitting a model to the data is especially useful for extrapolation to other conditions or operating points, which could not be tested.

With the best fit model at hand the feedback loop closes with the formulation of conclusions and/or requirements for the tested systems. This approach was implemented for every testing and validation task of the GBT ventilation system.

3.1. First test phase: Initial start-up of the ventilation stations and stand-alone tests

Before installation, most of the components had to undergo factory acceptance tests. The interaction between the functional units was tested with emulations of the GBT ventilation control system. These emulated tests, including MMI and functional tests, served as the main platform for last optimizations to be done to the equipment. The ventilation stations with 4 fans each were initially started in January 2015. Before the initial start-up, the exhaust ducts were commissioned and integrated into the master controller, so that the airways could be opened by remote control. The emergency doors, which act as fresh air dampers, had to be opened manually during the first start-up. In this phase, the control system of each axial fan and its auxiliary systems such as external cooling and hydraulic fan blade adjustment was tested.

During the first start-up of the Faido fans precautious high frequency pressure measurements were done to establish the exhaust duct loading. Results showed differential pressure peaks approx. 35% above stationary conditions but still below model predictions. These measurements were also used to establish whether the time between the staggered start-up of fresh air and exhaust air fans could be shortened.

At the end of this intense test phase the proper stand-alone function of all systems such as axial fans, jet fans, tunnel climate measurement and fire detection systems was proven and analysed. Feedback from the measurement campaigns, which were run in parallel, helped fine tune operational points or operating control modes of the system.

One of the most challenging test cases involved the measurement of leakage flow through the exhaust air duct boundaries along the Faido gallery during the first start-up of the Faido ventilation station. This quantity is relevant in the setting of the operating points of the fans, as it has to be added on top of the flow rate required in the emergency station, at the beginning of the duct.

3.1.1. System modelling and uncertainty of the leakage flow measurement

As described above, first a model has to be derived. According to [2] ducts can be treated as ventilation ducts for underground mining. In essence a porous duct in which air flows and which through static pressure differences draws (or expels) extra air mass from or to the surrounding environment. The exhaust air duct and measurement setup is shown in Figure 1.

A minimum of two mass flow measurements are necessary to calculate the leakage of the duct. As well as the flow, the differential and absolute pressure, temperature and humidity have to be sampled.

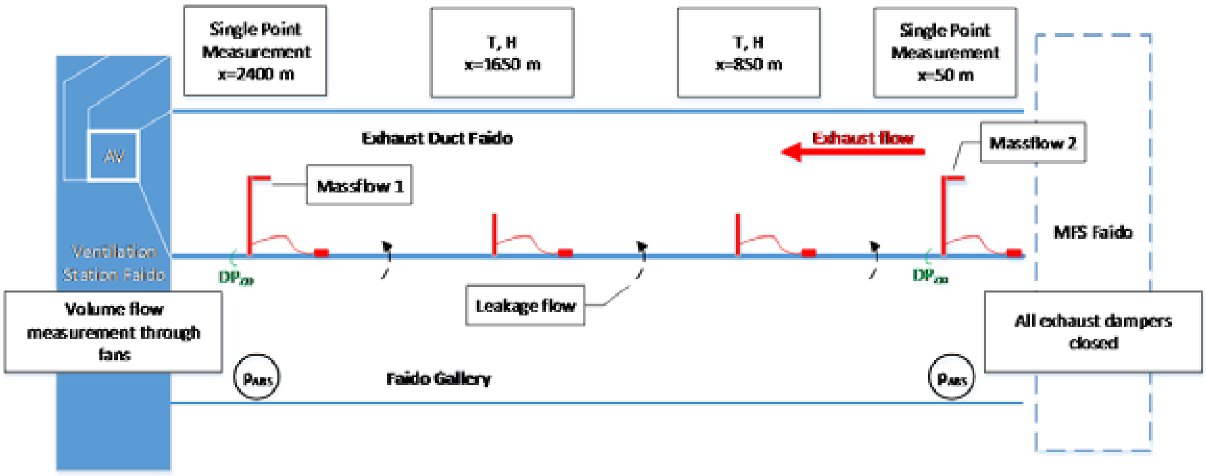

Figure 1: Measurement setup of the leakage measurement

The quantity we are interested in is the leakage mass flow rate $\Delta\dot{m}$:

$$\Delta\dot{m} = \int_0^L \rho(x)\frac{d\bar{u}}{dx}Adx = \dot{m}|_L - \dot{m}|_0 = \dot{m}|_{x=2400m} - \dot{m}|_{x=50m} \qquad (1)$$

Where $\bar{u}$ denotes the local mean air flow velocity in the duct, L is the duct length, A is the cross section area of the duct, assumed to stay constant in this formula. $\dot{m}$ represents the mass flow rate. When measuring this quantity at least 2 synchronous measurements k are necessary at the ends of the duct (see Figure 1). Hence the measurement uncertainty of the leakage $\Delta\dot{m}$ becomes:

$$\partial\Delta\dot{m} = \sqrt{\sum_i^n \left(\frac{\partial\dot{m}}{\partial a_i}\Delta a_i\right)^2} = \sqrt{2} * \partial\Delta\dot{m}|_k \qquad (2)$$

Where a_i denotes an independent variable for the computation of $\dot{m}$ and $\partial\Delta\dot{m}|_k$ is the uncertainty of the measurement in one of the 2 cross sections.

Unsurprisingly, the uncertainty of the measurement is a strong function of Δu, our ability to measure the mean velocity as certain as possible. Of course, $\partial\Delta\dot{m}$ also depends on variables such as absolute pressure, temperature and the area of the duct, all of which have a smaller influence on $\partial\Delta\dot{m}$.

From the equations which govern $\partial\Delta\dot{m}$ we notice the following statements (see also [2]):

- $\partial\Delta\dot{m}$ grows with higher $\bar{u}_k$
- $\partial\Delta\dot{m}/\Delta\dot{m}$ should be as low as possible

The above statements lead us to make measurements of $\Delta\dot{m}$ with $\bar{u}_k$ as small as possible and $\Delta\dot{m}$ as high as possible. $\Delta\dot{m}$ grows with increasing distance L between the measurement cross sections and increasing differential pressure from the duct to its environment. $\bar{u}_k$ is as small as possible when the only flow flowing in the duct is $\Delta\dot{m}$ itself, achievable, in our case, when the fans draw air against closed exhaust dampers in the emergency station.

To be able to parametrize the duct to later be able to extrapolate to different operating points we need to model the left hand side of equation (1). According to [2], 2 models can describe the flow through porous ducts:

$$\frac{du}{dx} = \frac{U}{A} f_{turb}^{*} \sqrt{\frac{2\Delta p}{\rho}} \qquad (3)$$

Or:

$$\frac{du}{dx} = \frac{U}{A} f^*_{lam} \frac{\Delta p}{\mu} \quad (4)$$

The turbulent model (3) assumes that with growing Δp (mean differential pressure between 0 and L) the increment in leakage decreases (square root function). The laminar model (4), also known as the Darcy law, predicts a proportional increase of leakage with growing Δp (linear function). The derivation of these models can be found in [2].

By measuring the differential pressure between the duct and its environment, we are able to fit parameters to the data, and use these to track leakage over operating time or establish massflow rates in conditions which might occur in the future.

Having established what we would like to measure and what the consequences of uncertain measurements are, we proceed to defining the measurement strategy and tools.

3.1.2. Measurement strategy and CFD-Analysis

Referring to Figure 1 and equations (1) through (4) we need to measure the following quantities:

- Volume flow $\dot{Q}_k = \bar{u}_k A_k$ [m^3/s]
- Temperature T_k [K]
- Absolute pressure $p_{abs,k}$ [Pa]
- Differential pressure Δp_k [Pa]

A large variety of methods exist to measure $\dot{Q}_k$ ([1],[2],[3]). Table 1 weighs the pros and cons of the most popular measurement strategies.

Table 1: Methods for measurement of $\dot{Q}_k$

Method	Description	Pros	Cons
Equal area methods, Log Chebychev Grid [3]	Measurement grid with a minimum of 20 sensors in the cross section of interest. Sub-area weighted integral to find average $\dot{Q}_k$ flowing through A_k.	• Low measurement error • Standard, well known technique for precise measurement of confined volume flow	• Time consuming setup • Costly measurement equipment (20 Sensors!) • Duct blockage • Tends to overestimate the volume flow
Tracer Gas measurements [3]	Measure the concentration of a tracer gas from source to measurement	• No knowledge of geometry of duct needed • Independency of flow velocity profile	• Costly, non- portable measurement equipment • Not environmentally friendly • Homogenous mixing required • Only few suppliers
Ultra Sound Measurements	Measurement of average $\bar{u}_k$ over measurement path via ultra sound emitter and receiver	• Direct measurement of average u_k <u>along sound wave path</u> • Very precise measure-ment devices readily available on the market • Standard and reliable measurement for normal operation in Tunnels	• Costly, usually non-portable, sensitive measurement equipment • Several measurement paths needed for non-standard geometry measurement of $\dot{Q}_k$ • Time consuming setup

Method	Description	Pros	Cons
Single point measurements	Measurement of $\bar{u}_k$ with previous hypothesis of velocity profile.	• Very Cost effective measurement (only 1 Sensor) • Standard measurement technique • Low duct blockage	• Previous knowledge of velocity profile is imperative for calculation of $\dot{Q}_k$ • No redundancy

Feasibility, cost and measurement uncertainty are therefore the main decision factors for which strategy to go for. As the geometry and resistance coefficients of the duct were well known beforehand and do not change within our measurement path L we opted for a single point measurement in combination with CFD-Analysis. This strategy is cost and time efficient.

The scopes of the CFD-Analysis includes:

- Compute stationary velocity profiles in the duct for different volume flows
- Establish the measurement location to minimize the error of the measurement of u_k

The results of the CFD-Analysis should give a factor $B_{CFD} = f(u_k)$ such that:

$$\dot{Q}_k = A_k * \bar{u}_k = B_{CFD}(u_k) * u_k \tag{5}$$

u_k here denotes the measured local velocity and $\bar{u}_k$ is the mean flow velocity in the measurement cross section. The mean flow velocity $\bar{u}_k \sim u_k$ influences the velocity profile shape. Therefore B_{CFD} is a function of u_k.

Using the CFD results the optimal measurement location can be chosen to be at the height z, distance from the centre of the profile y, so that the profile at this height z is as flat as possible for as wide of a range of z as possible. Mathematically:

$$\min_{y,z} \frac{du_k}{dydz} \tag{6}$$

For fully developed flow this is mostly at the point where $u_k = \max(u_k)$. In this way, the systematic error of positioning the probe can be reduced to a minimum as the profile is presumed to be as flat as possible.

3.1.3. Data analysis and results

The measurement setup is the result from sections 3.1.1 and 3.1.2. They can be seen in Figure 1. The two single-point measurements (u_k) were placed at $x = 50\,m$ and $x = 2400\,m$ from the fans in the centre of the duct ($y = 0\,m$) and at a height $z = 1.05\,m$ above the false ceiling.

The fans were operated at 12 different points. Once stationary conditions were reached at least 4 minutes worth of data was sampled. Computing $\Delta\dot{m}$ from the raw data with equation (1) and applying the derived models (3,4) we can approximate the leakage massflow. The laminar model (3) is conservative at high Δp_{mean} in the duct (linear increase of leakage with Δp_{mean}). The turbulent leakage model (4), is conservative at low Δp_k in the duct. A mixed model was therefore assumed, which sums the laminar and turbulent leakages to give total leakage. This model lies between laminar and turbulent leakage, accounting for changes in flow turbulence with changing Δp_{mean}. f^*_{Turb} in our case resulted to be 1.922 $[\frac{mm^2}{m^2}]$ and f^*_{Lam} is in the order of 3.197×10^{-12} $[m]$, which according to [2] is a very sealed duct. Figure 2 illustrates the obtained results.

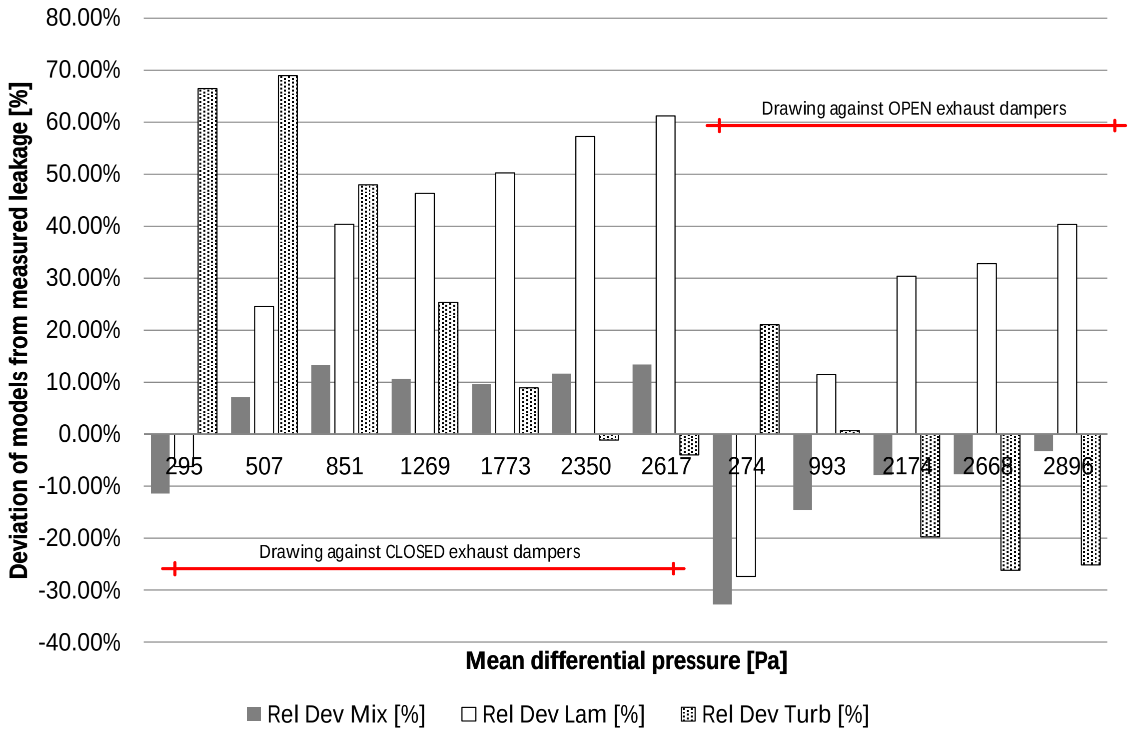

Figure 2: Comparison of leakage flow models. Relative deviation [%] of predicted to measured leakage flow [kg/s] as a function of mean differential pressure in the duct.

The fitted model can now be used to calculate leakage for conditions that were not directly measured. Also, quantitative conclusions can be made by comparing the tested object to others. The feeback loop closes with the fine tuning of operating points of the fans. After this phase, the stand-alone components had to be integrated into the tunnel control system.

3.2. Second commissioning phase: Combined tests including the train control system and auxiliary electromechanical systems

From August to September 2015, the ventilation system was tested for the first time as a complete system. Before these tests could start, relevant electromechanical systems master controllers such as the train control system, emergency doors, the HVAC of technical rooms, doors and gates were integrated into the tunnel control system and their cross connections to the ventilation master controller were setup and commissioned. Several major test cases proved the proper automated response of the ventilation system to an incident detection of the train control system e.g. in case of fire on a train. Immediate smoke extraction in the predicted tunnel emergency station and fresh air supply to the escape ways is needed in that case.

During the planning of the system 44 ventilation strategies were defined for every conceivable scenario. Each strategy includes a control scheme for the ventilation and its surrounding systems. Most ventilation strategies include the two ventilation stations. When a ventilation strategy is initialized, the ventilation ducts are prepared and all dampers, doors and gates are brought into the necessary positions in several consecutive steps. These actions are performed and supervised by the dedicated redundant master controller. Local functions such as start or redundancy switches were previously successfully tested during the initial start-up phase.

In the end of the combined commissioning phase, every single ventilation strategy had been activated and all volume flows of the axial fans, in the airways and in the tunnel as well as pressure differences between the tunnel tubes were measured. The measurement of these previously defined reference values were used to validate computational models used in the dimensioning of the system and iteratively tune operating points. For example, exhaust dampers were adjusted to achieve a homogenous exhaust flow through all 7 exhaust vents of each emergency station. Previous CFD analysis established the damper blade opening angles which were then hard coded into the control of the dampers. Volume flow measurements allowed the validation of the made assumptions.

Immediately after the combined tests, the test operation of the tunnel including electric driven rail tests with a maximum velocity of 275 km/h started. During this test phase from October 2015 until May 2016, a total of 37 tests with realistic operation conditions and train traffic, smoke and heat generators were done to verify the validation for operation approval by the FOT.

4. CONCLUSION

In this publication commissioning and testing methods applied to the Gotthard Base Tunnel are discussed. The general structure of its ventilation system, the interfaces and different components are outlined. Especially the large distances between components of the system and ongoing construction work from third party lots during commissioning work proved to be challenging.

Following a case study of one of the many tests performed during the 3 year commissioning period the general methodology of testing is explained. A comparison between several methods of measuring volume flow in ducts is given. Drawing on this comparison, a new method is introduced, which is based on the combination CFD analysis and single-point measurements. The relative uncertainty in the outlined leakage measurement varies between 15% and 20% for the very sealed duct which was tested (small leakage flow). Furthermore, a mix of turbulent and laminar leakage flow models is used to predict this flow within a margin of 10% in the relevant operating points.

The commissioning and testing phase of the complex GBT ventilation system required an early and accurate planning and coordination. Time slots for the tests had to be reserved with a special focus on the contractual situation of all other contractors of the tunnel.

Volume flow in all emergency stations and open doors, smoke propagation and the recirculation on the portals were measured to provide proof of defined targets and ensure the safety of future train passengers as well as operators of the tunnel.

5. ACKNOWLEDGEMENTS

The authors would like to thank the AlpTransit Gotthard Ltd for kindly authorising to publish of the content of this paper.

6. REFERENCES

[1] Strömungs- und Durchflussmesstechnik, O. Fiedler, Oldenbourg, 1992
[2] Quantification of the leakages into exhaust ducts in road tunnels with concentrated exhaust systems, Pöyry Infra AG, R. Buchmann & S. Gehrig, Research for ASTRA, Dec. 2010
[3] Comparative Study of Flow Measurement Methods in Road Tunnel Exhaust Ducts, T. Melchior, R. Ruckstuhl, R. Buchmann, Pöyry Switzerland Ltd, Zürich, Switzerland, Proceedings ISTSS 2014, Marseille, France, March 12-14, 2014
[4] AVR121: Enhancing ADC resolution by oversampling, Application Note, Atmel Coorporation, San Jose, CA 95131, USA, 2005

Reports of the
Institute of Internal Combustion Engines and Thermodynamics

HEFT NR.	VERFASSER	TITEL	ERSCHIENEN	PREIS in ATS
77		Der Arbeitsprozess des Verbrennungsmotors The Working Process of the Internal Combustion Engine Tagung / Symposium 18. und 19. Oktober 1999	1999	950,--
78	SCHLAG S.	Biodiesel im realen Motoreinsatz	2001	490,--
79		Der Arbeitsprozess des Verbrennungsmotors The Working Process of the Internal Combustion Engine Tagung / Symposium 27. und 28. September 2001	2001	950,--

HEFT NR.	VERFASSER	TITEL	ERSCHIENEN	PREIS in €
80	STURM P.J.	Sicherheit und Belüftung von Tunnelanlagen Tunnel Safety and Ventilation Tagung/Symposium 8.-10. April 2002	2002	50,--
81	STURM P.J.	Verkehr und Umwelt Transport and Air Pollution Tagung/Symposium 19.-21. June 2002	2002	50,--
82	HAUSBERGER St.	Simulation of Real World Vehicle Exhaust Emissions Transport and Air Pollution	2003	40,--
83		Der Arbeitsprozess des Verbrennungsmotors The Working Process of the Internal Combustion Engine Tagung / Symposium 25. und 26. September 2003	2003	70,--
84	STURM P.J.	Sicherheit und Belüftung von Tunnelanlagen Tunnel Safety and Ventilation Tagung/Symposium 19.-21. April 2004	2004	50,--
85	STURM P.J.	Verkehr und Umwelt Transport and Air Pollution Tagung/Symposium 1.-3. June 2005	2005	50,--
86		Der Arbeitsprozess des Verbrennungsmotors The Working Process of the Internal Combustion Engine Tagung / Symposium 22. und 23. September 2005	2005	70,--
87	STURM P.J.	Sicherheit und Belüftung von Tunnelanlagen Tunnel Safety and Ventilation Tagung/Symposium 15.-17. Mai 2006	2006	50,--
88		1st International Symposium on Hydrogen Internal Combustion Engines 28. und 29. September 2006	2006	50,--

89		Der Arbeitsprozess des Verbrennungsmotors The Working Process of the Internal Combustion Engine Tagung / Symposium 20. und 21. September 2007	2007	70,--
90	STURM P.J.	Sicherheit und Belüftung von Tunnelanlagen Tunnel Safety and Ventilation Tagung/Symposium 21.-23. April 2008	2008	60,--
91		Verkehr und Umwelt Transport and Air Pollution Tagung/Symposium 16.-17. June 2008	2008	60,--
92		Der Arbeitsprozess des Verbrennungsmotors The Working Process of the Internal Combustion Engine Tagung / Symposium 24. und 25. September 2009	2009	70,--
93	STURM P.J.	Sicherheit und Belüftung von Tunnelanlagen Tunnel Safety and Ventilation Tagung/Symposium 3.-4. Mai 2010	2010	70,--
94		Der Arbeitsprozess des Verbrennungsmotors The Working Process of the Internal Combustion Engine Tagung / Symposium 22. und 23. September 2011	2011	100,--
95	STURM P.J.	Sicherheit und Belüftung von Tunnelanlagen Tunnel Safety and Ventilation Tagung/Symposium 23.-25. April 2012	2012	70,--
96		Der Arbeitsprozess des Verbrennungsmotors The Working Process of the Internal Combustion Engine Tagung / Symposium 24. und 25. September 2013	2013	100,--
97	STURM P.J.	Sicherheit und Belüftung von Tunnelanlagen Tunnel Safety and Ventilation Tagung/Symposium 12.-13. Mai 2014	2014	100,--
98		Inter-Regional Air Quality Assessment Bridging the Gap between Regional and Kerbside PM Pollution Results of the PMinter Project Authors: U. Uhrner, B.C. Lackner, R. Reifeltshammer, M. Steiner, R. Forkel, P.J. Sturms	2014	30,--
99		Der Arbeitsprozess des Verbrennungsmotors The Working Process of the Internal Combustion Engine Tagung / Symposium 24. und 25. September 2015	2015	100,--
100	STURM P.J.	Sicherheit und Belüftung von Tunnelanlagen Tunnel Safety and Ventilation Tagung/Symposium 25.-26. April 2016	2016	100,--